ACTA RADIOLOGICA

FOUNDED IN 1921 BY GÖSTA FORSSELL

OFFICIAL ORGAN OF THE RADIOLOGICAL SOCIETIES OF DENMARK, FINLAND NORWAY AND SWEDEN

THERAPY PHYSICS BIOLOGY

INDICES to Vol. 14 (1975)

February April June August October December

Contents of Volume 14 — THERAPY-PHYSICS BIOLOGY

ACTA RADIOLOGICA

OFFICIAL ORGAN OF THE RADIOLOGICAL SOCIETIES OF DENMARK FINLAND NORWAY AND SWEDEN

Vol 14 Fasc 1 — THERAPY PHYSICS BIOLOGY — 1975 February

TURNOVER OF ^{65}Zn AND ^{85}Sr IN GROWING RATS

A comparative investigation

KENNETH R WING

The turnover of ^{65}Zn in the mammalian body has been the subject of many investigations using either whole body autoradiography (BERGMAN & SÖREMARK 1968) microautoradiography (HAUMONT 1961, HAUMONT & MCLEAN 1966, JOWSEY & ORVIS 1967) or quantitative scintillation techniques (BALLOU & THOMPSON 1961, CZERNIAK et coll 1962 STRAIN et coll 1964, BERGMAN 1970, MCINTOSH & LUTWAK-MANN 1972) These investigations have shown ^{65}Zn to be rapidly taken up and lost by such viscera as kidney, pancreas, liver and spleen and by the gastrointestinal tract It is moderately rapidly taken up by the skeleton and the activity remains in bone for a very long time The rate of the uptake and loss in the central nervous system is slow and in skeletal and heart muscle it is intermediate

In preparation for a comparison of the turnover of ^{65}Zn in rats fed a zinc deficient diet with and without a zinc supplement, it was necessary to obtain more complete knowledge of how ^{65}Zn turnover reflects the turnover of zinc in various tissues and organs particularly in bone For this purpose the present attempt was made to analyze quantitatively the turnover of ^{65}Zn in the tissues of growing rats using the model of BAUER et coll (1955 a) Two isotopes, ^{65}Zn and ^{85}Sr, were injected simultaneously into the same animals in order that direct comparisons could be made between the calculated parameters for zinc and those for calcium (^{85}Sr)

From the Biophysical Laboratory and the Department of Oral Roentgenology University of Umeå S-901 85 Umeå Sweden Submitted for publication 4 April 1974

Materials and Methods

Forty-eight female, albino rats of the Sprague-Dawley strain were used The animals were raised in our laboratory from 3 weeks of age, just after weaning They were housed in cages of acrylic resin with stainless steel covers They had access to ordinary tap water and were fed a conventional pellet *diet ad libitum* (210 Anticimex, Anticimex, Stockholm)

At six weeks of age the rats were injected intraperitoneally with both ^{65}Zn and ^{85}Sr The ^{65}Zn, *as zinc chloride in 0 1 N HCl, had a specific activity of 118* mCi ^{65}Zn/mg zinc, and the ^{85}Sr, as strontium chloride in aqueous solution, had a specific activity of 9 2 mCi ^{85}Sr/mg strontium (the Radiochemical Centre, Amersham) The injection solution was prepared by mixing portions of the two stock solutions and diluting with physiologic saline to final concentrations of 40 μCi ^{65}Zn and 25 μCi ^{85}Sr per ml of injection solution The injected doses were 0 2 μCi ^{65}Zn and 0 125 μCi ^{85}Sr per gram body weight

Four rats, randomly selected, were killed at 0 25, 0 5, 1, 1 5, 2, 3, 4, 6, 8, 12, 16 and 24 days following the injection The animals were lightly anaesthetized with ether and killed by decapitation The sampling techniques and preparation of samples for the determinations have been described previously (BERGMAN 1970) Samples of serum, whole kidney, pancreas, spleen, liver, heart, incisors (pulpless crowns), mandibular condyle, mandibular bone (ramus and part of corpus), tibia epiphysis and tibia diaphysis (bone marrow removed) were taken using polyethylene or polyethylene-covered instruments, placed in weighed Pyrex tubes and weighed immediately Thereafter, the samples were dried in an oven for 4 to 6 hours at 100 C and then overnight at 150°C They were transferred to a muffle oven and the temperature was slowly raised and maintained at 550°C for a second night When they had cooled to room temperature, the ash weights were recorded and the ash dissolved in 0 5 ml HCl 10 5 % overnight All samples were then diluted with 2 0 ml 3x-distilled water (BERGMAN et coll 1974)

As 49 % of the disintegrations of ^{65}Zn result in the emission of 1 116 MeV γ-rays and 100 % of the disintegrations of ^{85}Sr in the emission of 0 514 MeV γ-rays (LEDERER et coll 1968), a 7 6 cm × 7 6 cm NaI(Tl) well scintillation detector with a two channel analyzer (Picker Dual Channel Analyzer), one channel calibrated to count at each of these two energy levels, was used to measure the ^{65}Zn and ^{85}Sr activities *in* the samples Known amounts of ^{65}Zn, ^{85}Sr and the injection solution in separate tubes were diluted to the same volume, 2 5 ml, to assure comparable counting geometry and were measured as references on each occasion The background counting rate was also measured on each occasion and subtracted from the counting rate for each sample and reference As the annihilation γ-rays (0 511 MeV) and some of the Compton-scattered 1 116 MeV γ rays from ^{65}Zn are also counted in the 0 5 MeV channel, the counting rate in this channel due to the ^{85}Sr γ-rays must be separated from the ^{65}Zn counting rate The counting rate (cpm) in the 0 5 MeV channel due

to the ^{85}Sr in a tissue ash or injection solution sample was calculated using the ratio (R) of the cpm in the 0 5 MeV channel to the cpm in the 1 1 MeV channel for the ^{65}Zn reference sample

$$\text{sample } ^{85}\text{Sr cpm at 0 5 MeV} = (\text{sample total cpm at 0 5 MeV}) - R\ (\text{sample total cpm at 1 1 MeV})$$

The ^{85}Sr in the samples was not sufficient to cause a significant counting rate above background in the 1 1 MeV channel

After the ^{65}Zn and ^{85}Sr activities had been measured, the samples were further diluted with HCl 2 2 % as needed and the zinc concentrations determined by atomic absorption spectrophotometry using a Unicam SP 90 spectrophotometer at 213 9 nm with a zinc lamp For each of the mineralized tissue samples a further absorption measurement was made at 210 nm using the same lamp and subtracted from that at 213 9 nm in order to correct for the absorption due to the high calcium concentration (BERGMAN et coll 1974)

The relative activities (RA) of ^{65}Zn and ^{85}Sr in the samples were defined and calculated as follows

$$RA = \frac{\text{cpm/g fresh weight of the sample}}{\text{cpm injected/g body weight}}$$

In the presentation of the data, these values are multiplied by 100 to obtain the RA in per cent The ^{65}Zn specific activity (SA) in each sample was obtained by dividing the ^{65}Zn RA by the zinc concentration (mg Zn/mg fresh weight of the sample) The ^{85}Sr SA in serum, viscera and heart were obtained by dividing the ^{85}Sr RA by the respective average calcium concentrations (g Ca/g fresh weight of the sample) obtained in a separate investigation of four female rats of the same age using the same sample preparation as above and operating the SP 90 at 422 7 nm with a calcium lamp The ^{85}Sr SA in the mineralized tissue samples were calculated by dividing the ^{85}Sr RA in each sample by its ash weight/fresh weight ratio and by the average ash weight calcium concentrations (g Ca/g ash) obtained from these same four rats

The calculations of the RA and SA and the means and standard deviations for all data as well as the variance and least squares analyses were performed on an electronic computer (Control Data 3200, Umeå Datacentral) or a programmable calculator (Canon Canola 167P) using standard programs In the presentation of the results of statistical tests, the following levels of significance are used

$0\,05 < p$	not significant	
$0\,01 < p \leq 0\,05$	nearly significant	*
$0\,05 < p \leq 0\,01$	significant	**
$p \leq 0\,001$	highly significant	***

where p is the probability of incorrectly rejecting the null hypothesis

Results

The means and standard deviations of the fresh weight zinc concentrations in the eleven samples from all 48 rats are presented in Table 1 For the concentrations in serum, viscera and heart, the coefficients of variation (100 SD/$\bar{x}$) within the individual groups (n = 4) averaged 9 per cent and were largest for pancreas and liver and least for spleen These concentrations were quite stable between 6 and 9 5 weeks of age and the analysis of variance on the mean concentrations in these samples from the twelve groups was significant only for those in the liver, the mean concentration in which was relatively low at 6 days following injection The coefficients of variation for the concentrations in the mineralized tissues also averaged 9 per cent and were highest for mandibular condyle The zinc concentrations in mandibular condyle and mandibular bone increased slightly and that in tibia epiphysis moderately with increasing age The analyses of variance were significant or highly significant for the concentrations in these three samples but not for those in the incisors or tibia diaphysis

The means and standard deviations of the ash weight/fresh weight ratios and the *ash weight zinc concentrations in the mineralized tissues are also presented in Table* 1 The coefficients of variation for the ash weight/fresh weight ratios averaged 6 per cent and were greatest for mandibular condyle In the bone samples but not the incisors, the ratios increased with increasing age and the analyses of variance were significant or highly significant The coefficients of variation for the ash weight zinc concentrations averaged 8 per cent and were largest for mandibular condyle and incisors These concentrations were stable throughout the experimental period and the analyses of variance were nearly significant only for those in tibia epiphysis

The body weights of these rats increased with increasing age during the experimental period They averaged 130 g (SD – 11 g, n = 48) at the time of injection (6 weeks old) and the last group killed 24 days later weighed 194 g (SD – 12 g, n = 4) The analysis of variance on the mean body weights of the individual groups (n = 4) was highly significant (F – 13 06***)

The mean ^{85}Sr relative activities (RA) in the serum, viscera, heart and mineralized tissue samples at twelve different times following injection are presented in Fig 1 The groups at 0 25, 1, 6, 12 and 16 days following injection are composed of only three rats because both the ^{85}Sr and ^{65}Zn activities in all eleven samples from the rat which was eliminated were very low compared to those in the remaining rats in the group, indicating that an error had been made in the injection The coefficients of variation for the ^{85}Sr RA in the serum averaged 40 % (range 10 to 133 %) and were greatest for the data from later post-injection times The coefficients of variation for the ^{85}Sr RA in viscera and heart were very large, due to the low amount of ^{85}Sr activity in these tissues relative to the ^{65}Zn activity, and largest for the RA from later times post-injection The activities in these tissues beyond 3 days following injection are not presented as the coefficients of variation were greater than 100 per cent and a

Table 1

The fresh weight zinc concentrations in ppm (μg/g) in the eleven samples from 6 to 9½ week old females rats killed in groups of four at twelve different times after injection with ^{65}Zn at 6 weeks of age The ash weight/fresh weight ratios and the ash weight zinc concentrations in the mineralized tissue samples are also given The means are those for all 48 rats and the standard deviations are those for the individual groups (within) and for all 48 rats (total) obtained in the analysis of variance on the twelve sacrifice groups, the results of which are presented under F with the levels of significance To the right are given the average calcium concentrations obtained in a separate experiment and used in the calculation of the ^{85}Sr specific activities (SA)

	$\hat{x}$	S D within	S D total	F	$\bar{x}$
	Zn ppm fresh weight				10^3 g Ca/g fresh weight
Serum	1 34	0 14	0 15	1 61	0 1035
Kidney	23 0	1 3	1 3	0 97	0 0692
Pancreas	22 4	3 5	3 4	0 75	0 1131
Spleen	22 2	0 6	0 6	1 42	0 0451
Liver	28 0	3 0	3 9	3 68**	0 0389
Heart	17 6	1 4	1 4	0 59	0 0404
Incisors	89 8	7 3	7 7	1 47	
Mand condyle	117 2	13 8	16 6	2 92**	
Mand bone	135 2	10 4	12.7	3 12**	
Tib epiphysis	100 1	7 5	18 5	22 50***	
Tib diaphysis	161 9	14 0	15 2	1 76	
	Ash weight/fresh weight				
Incisors	0 679	0 031	0 030	0 71	
Mand condyle	0 289	0 027	0 035	3 91***	
Mand bone	0 439	0 020	0 033	8 83***	
Tib epiphysis	0 218	0 016	0 034	15 43***	
Tib diaphysis	0 524	0 028	0 035	3 39**	
	Zn ppm ash weight				g Ca/g ash weight
Incisors	132 3	11 6	11 2	0 71	0 345
Mand condyle	406	40	41	1 16	0 369
Mand bone	308	20	21	1 64	0 369
Tib epiphysis	459	23	27	2 49*	0 366
Tib diaphysis	309	24	23	0 91	0 376

large number of the calculated activities were negative, which is possible with the method used for separating the ^{85}Sr from the ^{65}Zn activity The coefficients of variation averaged 17 per cent for the RA in the incisor crowns (range 5 to 51 %) and 11 per cent for those in the bone samples (range 3 to 36 %) The bar in Fig 1 and subsequent figures represents a coefficient of variation of 10 per cent

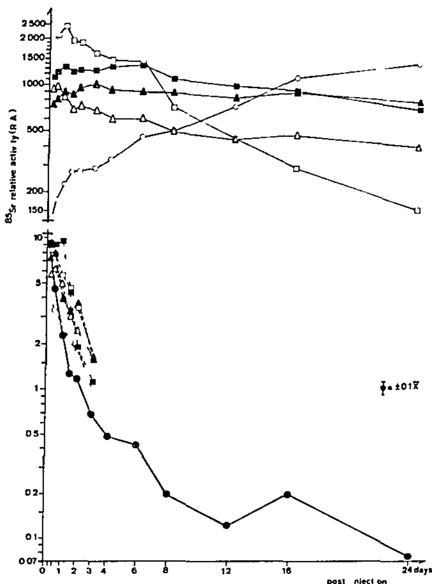


Fig 1 The mean ^{85}Sr relative activities (n 4 for 0 25 1 6 12 and 16 days n 3) for the 11 samples from 6 week old rats The bar represents a coefficient of variation (100 SD/x) of 10 per cent
●—● serum □ □ kidney ■ ■ pancreas △ △ spleen ▲ ▲ liver ○ ○ heart □—□ mandibular condyle ■—■ mandibular bone △—△ tibia epiphysis ▲—▲ tibia diaphysis ○—○ incisors

The means of the estimated ^{85}Sr specific activities in these samples are presented in Fig 3 The coefficients of variation for the SA in serum viscera and heart were necessarily the same as those for the RA in the respective samples The coefficients for the SA in incisor crowns averaged 19 per cent and those for the bones averaged 12 per cent, thus slightly higher than the coefficients of variation for the corresponding RA

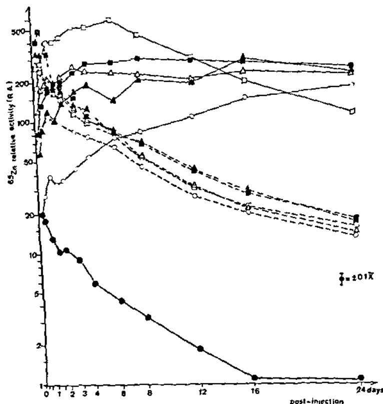


Fig 2 The mean ^{65}Zn relative activities (n = 4 for 0 25, 1, 6, 12 and 16 days, n 3) for the 11 samples from 6-week old rats The bar represents a coefficient of variation (100 SD/$\bar{x}$) of 10 per cent (Symbols as in Fig 1)

The ^{85}Sr RA in serum was relatively low and the SA high at 0 25 day The activity decreased extremely rapidly during the first 1 5 days following injection and much more slowly thereafter The course of the serum SA during the short period from 0 25 through 1 5 days (Fig 3) may be approximated by the straight line $SA_t = 1089$ $e^{-1\,54t}$ Plotting the serum activity on log – log scales (Fig 5) reveals a straight line course from 0 25 through 4 days, $SA_t = 205\,4\ t^{-1\,041}$ The line best fitting the data from 0 25 through 24 days has a slope (exponent) of −0 991 These and subsequent lines were obtained by the least squares method on the logarithms of the data from the time period against the time post-injection or the logarithm of the time

The ^{85}Sr RA in the viscera were less than that in serum at 0 25 day following injection and the SA, except for that in pancreas, were greater than the SA in serum The activities in these organs decreased more slowly than that in serum during the next few days The SA in pancreas was nearly equal to that in serum at 0 25 day and,

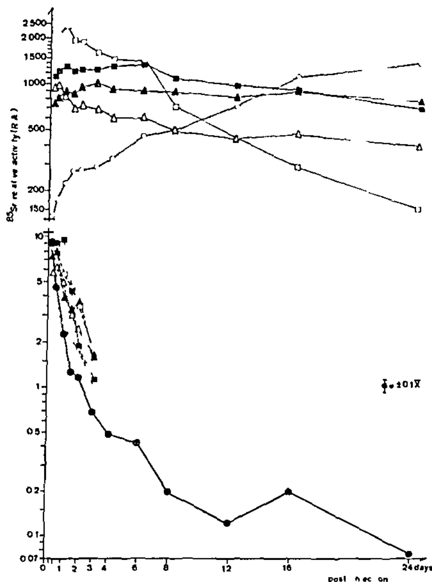


Fig 1 The mean ^{85}Sr relative activities (n 4 for 0 25 1 (12 and 16 days n = 3) for the 11 samples from (week old rats The bar represents a coefficient of variation (100 SD/$\bar{x}$) of 10 per cent
●—● serum □ □ kidney ■ ■ pancreas △ spleen ▲ ▲ liver ○ ○ heart □—□ mandibular condyle ■—■ mandibular bone tibia epiphysis ▲—▲ tibia diaphysis ○—○ incisors

The means of the estimated ^{85}Sr specific activities in these samples are presented in Fig 3 The coefficients of variation for the SA in serum viscera and heart were necessarily the same as those for the RA in the respective samples The coefficients for the SA in incisor crowns averaged 19 per cent and those for the bones averaged 12 per cent thus slightly higher than the coefficients of variation for the corresponding RA

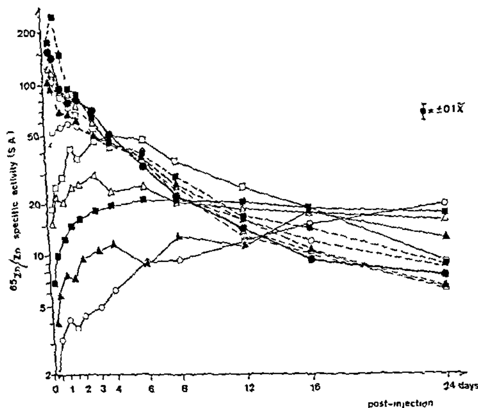


Fig. 4 The mean ^{65}Zn specific activities (n = 4 for 0 25 ...
from 6-week old
tion The means
The bar represen

periods of smaller increases, the RA and SA in mandibular bone and tibia diaphysis decreased very slowly The activity in the incisor crowns was the lowest of those in the mineralized tissues at 0 25 day and increased exponentially from the third day onward

The means of the ^{65}Zn RA in these same serum, viscera heart and mineralized tissue samples are presented in Fig 2 The coefficients of variation averaged 11 per cent for all samples and killing times (range 1 to 37 %) The individual sample zinc concentrations were used to calculate the SA, the means of which are presented in Fig 4 The coefficients of variation for the SA averaged 11 per cent for all samples and killing times or the same as the average coefficient of variation for the RA

At 0 25 day, the serum ^{65}Zn RA was lower than all but that in incisors and the serum SA was higher than all but that in pancreas The serum activity decreased at a moderately rapid rate through 1 5 days, increased slightly at 2 days and then

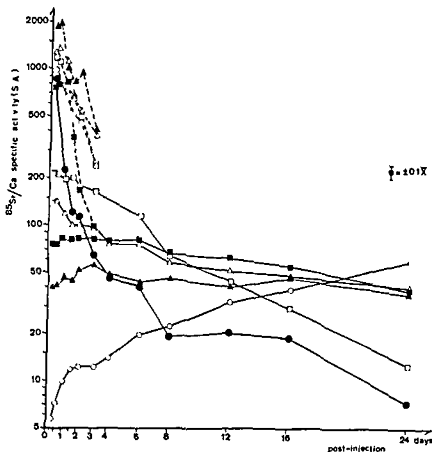


Fig 3 The mean ^{85}Sr specific activities (n = 4, for 0 25, 1, 6, 12 and 16 days, n = 3) *for the 11 samples from 6-week old rats For serum, viscera and heart,* the SA were obtained by dividing the RA (Fig 1) by the mean fresh weight calcium concentrations in Table 1 For the mineralized tissue samples, the RA were divided by ash weight/fresh weight ratio in the sample and the appro priate mean ash weight calcium concentration given in Table 1 The bar represents a *coefficient of variation (100 SD/$\bar{x}$) of 10 per cent (Symbols as in* Fig 1)

beginning at 1 day, decreased as rapidly as the activity in serum decreased shortly earlier

For each of the bone samples, the ^{85}Sr RA and SA curves differ somewhat at the earlier times following injection The initial rises in the RA were not present in the SA curves except that for tibia diaphysis The mandibular condyle SA decreased exponentially from 0 25 through 6 days with a slope (exponent) of 0 113 Between *6 and 8 days the rate of loss of activity was accelerated and then returned to ap-* proximately the original rate (0 102) After an initial period of rapid loss, the RA and SA in tibia epiphysis decreased more slowly through 8 days post-injection and even more slowly through the remainder of the experimental period The later rate of decrease was greater for the SA than for the RA in tibia epiphysis After initial

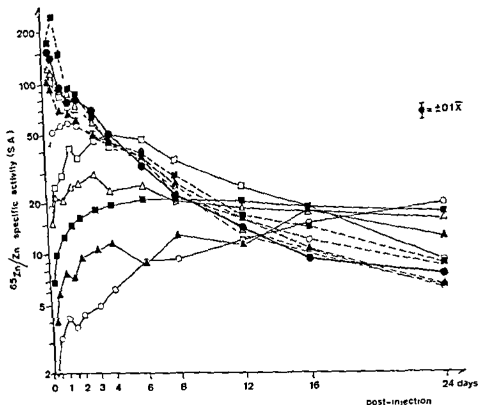


Fig. 4 The mean ^{65}Zn specific activities (n = 4 for 0 25, 1, 6 12 and 16 days n = 3) for the 11 samples from 6-week old rats The SA in each sample was obtained by dividing the RA by the zinc concentration The means of the zinc concentrations used to calculate these values are presented in Table 1 The bar represents a coefficient of variation (100 SD/$\bar{x}$) of 10 per cent (Symbols as in Fig 1)

periods of smaller increases, the RA and SA in mandibular bone and tibia diaphysis decreased very slowly The activity in the incisor crowns was the lowest of those in the mineralized tissues at 0 25 day and increased exponentially from the third day onward

The means of the ^{65}Zn RA in these same serum, viscera, heart and mineralized tissue samples are presented in Fig 2 The coefficients of variation averaged 11 per cent for all samples and killing times (range 1 to 37 %) The individual sample zinc concentrations were used to calculate the SA, the means of which are presented in Fig 4 The coefficients of variation for the SA averaged 11 per cent for all samples and killing times or the same as the average coefficient of variation for the RA

At 0 25 day, the serum ^{65}Zn RA was lower than all but that in incisors and the serum SA was higher than all but that in pancreas The serum activity decreased at a moderately rapid rate through 1 5 days, increased slightly at 2 days and then

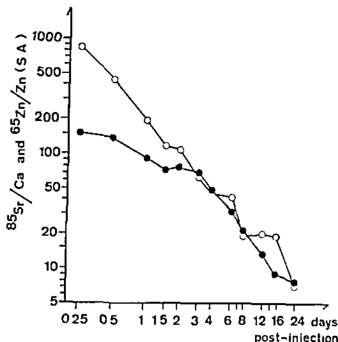


Fig 5 The mean ^{85}Sr ○ and ^{65}Zn ● specific activities in the serum Both the SA and the time axes are logarithmic The data are the same as those in Figs 3 and 4 respectively

decreased at a rate slower than the initial rate The coefficients of variation at 2, 3 and 4 days were relatively large The course of the serum SA during the periods from 0 25 through 1 5 and from 2 through 8 days (Fig 4) may be approximated by two straight lines $SA_t - 183\ 7\ e^{\ 0\ 613\ t}$ and $SA_t = 125\ 7\ e^{\ 0\ 223\ t}$, respectively Plotting the serum SA on log – log scales (Fig 5) reveals a straight line course between 3 and 24 days, $SA_t - 228\ 5\ t^{\ 1\ 118}$ or a slightly faster rate of loss than for ^{85}Sr

The RA in the viscera were on the average 15 times that in serum at 0 25 day The SA in pancreas was slightly greater than that in serum and, after increasing to an even higher level at 0 5 day, decreased approximately parallel to the serum SA from 1 5 day The SA in kidney, spleen and liver were slightly below the serum SA at 0 25 day and, decreasing, slowly approached the serum SA and were equal to it at 5 days after injection The RA in heart is one half and the SA one fourth of the RA and SA, respectively, in serum at 0 25 day and increasing The SA in heart reached a peak at 1 5 days and, decreasing, slowly approached the serum SA After 4 days, the SA in the heart behaved much the same as those in the viscera, following the serum SA in its downward course

For each of the bone samples, the ^{65}Zn RA and SA differ only in that the RA rose slightly more rapidly or decreased more slowly than the SA For the mandibular condyle this difference was very small while the difference in the rate of decrease of the RA and SA in tibia epiphysis at later times was most marked The SA in mandibular condyle was highest of those in the mineralized samples at 0 25 day and increased until it crossed the serum SA curve at 4 days After a short period with a high rate of decrease between 6 and 8 days, the SA decreased exponentially

($e^{-0\ 0855\ t}$) at a rate less than that for serum The SA in tibia epiphysis reached a peak by the third day and, while decreasing at a rate slower than that for the serum SA, crossed this curve at 9 days and decreased at a very slow rate thereafter The mandibular bone SA reached its peak between 8 and 12 days, at which time it crossed the serum SA curve, and then decreased exponentially at a very slow rate The SA in tibia diaphysis had an irregular course at times The SA appeared to increase through 6 to 8 days and then stabilize at the 8 day level The SA in incisors was initially the lowest and increased exponentially from the sixth day onward

At later times the courses of the ^{65}Zn RA in the bone samples approached those of the ^{85}Sr RA In incisors, the courses of the ^{85}Sr and ^{65}Zn RA were very much alike, the major difference occurring at early times post injection when the ^{65}Zn RA increased more rapidly than the ^{85}Sr RA

Estimates of the exchangeable pool sizes E and the accretion rates A for both ^{85}Sr and ^{65}Zn in the bone samples have been made using the equation of BAUER et coll (1955 a)

$$R_t = E\ S_t + A \int_0^t S_t\ dt,$$

where R_t is the retention of activity (RA) in the sample and S_t is the specific activity (SA) in serum at time t The serum activities are assumed to decrease exponentially through 1 5 days, $S_t = S_0\ e^{\ K_s\ t}$, thus

$$R_t = S_0 \left[E\ e^{\ K_s\ t} + \frac{A}{K_s}\ (1 - e^{\ K_s\ t})\right]$$

The E and A values were calculated using each of the six possible pairs of data from 0 25, 0 5, 1 0 and 1 5 days and solving two simultaneous equations The calculated value for E increases and that for A decreases as much as two- or three fold as data from the later of these times are used in the equation In Table 2 are presented the calculated values for the data from 1 0 and 1 5 days as they give the highest value for E and the lowest for A The values are based on 1 gram fresh weight of bone The data point at 1 day for ^{65}Zn in mandibular condyle and at 1 5 day for ^{65}Zn in tibia diaphysis were not used as they give values which are very much different from the remaining points and they appear to be extreme points compared to the general trend in these samples

As it is believed that the retention in the bone samples by 6 days reflects almost exclusively the accretion phase as it is estimated by the equation of BAUER et coll and that little resorption should have occurred by this time, the equation may be simplified to

$$R_t \simeq A \int_0^t S_t\ dt$$

A further estimate of the value for A may be made by dividing the retention at 6 days by an estimate of the integral of the serum curve from 0 to 6 days obtained

Table 2

The values for the exchangeable pool size E and the accretion rate A for calcium (^{85}Sr) and zinc (^{65}Zn) in the bone samples calculated using the equation of BAUER *et coll (1955a) and the data from 1 and 1 5 days The retention R_6 in the sample at 6 days has been divided by the graphically estimated time integral of the serum specific activity S_t as a further estimate of A The values in per cent are obtained by dividing by the appropriate calcium or zinc concentrations All values are based on 1 gram fresh weight of bone sample*

	BAUER et coll				$R_6/\int_0^6 S_t\,dt$	
	E	*A*	*E*	*A*	*A*	*A*
^{85}Sr	g Ca	g Ca day^{-1}	% Ca	% Ca day^{-1}	g Ca day^{-1}	% Ca day^{-1}
Mand condyle	0 0533	0 0205	54 6	16 0	0 0145	13 9
Mand bone	0 0191	0 0156	12 4	10 1	0 0141	9 0
Tib epiphysis	0 0162	0 0079	23 1	11 3	0 0064	8 8
Tib diaphysis	0 0083	0 0121	1 2	6 3	0 0093	4 8
^{65}Zn	mg Zn	mg Zn day^{-1}	% Zn	% Zn day^{-1}	mg Zn day^{-1}	% Zn day^{-1}
Mand condyle[a]	0 0089	0 0191	7 4	15 9	0 0135	11 7
Mand bone	0 0076	0 0071	5 8	5 4	0 0065	5 0
Tib epiphysis	0 0087	0 0075	10 1	8 7	0 0054	6 0
Tib diaphysis[b]	0 0023	0 0072	1 4	4 5	0 0043[c]	2 7

[a] data from 0 5 day replaces 1 day
[b] data from 0 5 day replaces 1 5 days
[c] data from 8 and 0–8 days respectively

graphically These values are also presented in Table 2 Each of the values for *E* and *A* in Table 2 has been divided by the appropriate average calcium or zinc concentration to obtain the value in per cent

The *A*-values for both ^{85}Sr and ^{65}Zn as calculated by the equation of BAUER et coll were between 10 and 60 per cent higher than the corresponding *A*-values estimated graphically The *E*- and *A*-values in per cent for both isotopes in the cortical bone of the tibia diaphysis and the predominantly cortical bone of the mandible were less than the corresponding values for the endochondral bone of the mandibular condyle or the calcifying cartilage of the tibia epiphysis The fraction of the zinc which was rapidly exchangeable (E%) was in each case less than the fraction of calcium, the difference between the two in mandibular condyle being the greatest The relative rates of 'accretion' (A%) of zinc in the bone samples were in each case less than the respective relative rates of accretion of calcium, and in the cortical bone samples they were much less

Due to the effects of eruption and attrition on the data from the incisors, the *E*- and *A*-values cannot be calculated using the equation of BAUER et coll The reten-

tion at 6 days divided by the time integral of the serum SA from 0 to 6 days was 0 0048 for ^{85}Sr and 0 0018 for ^{65}Zn Dividing these values by the calcium and zinc concentrations, respectively, in incisors gave values of 2 05 (% day^{-1}) for calcium and 2 00 for zinc

Discussion

The methods and method errors have been discussed at length previously (BERGMAN et coll 1974, BERGMAN 1970) The coefficients of variation (100 SD/$\bar{x}$) for the wet weight and ash weight zinc concentrations and ash weight/fresh weight ratios in most samples are less than 10 per cent (Table 1) as they were in the report of the zinc concentrations during growth (BERGMAN et coll 1974) The coefficients of variation for the ^{85}Sr activities in serum and bones average 40 and 13 *per cent*, respectively The coefficients of variation for the ^{65}Zn relative and specific activities (RA, SA) average 11 per cent

While the major source of random error may be the biologic variation, other sources are also important The size of the sample taken can affect its relative morphology, due to the heterogeneity of several of these tissues, and may affect the zinc, ash (calcium) and nuclide concentrations The relative success of the injection will dramatically effect the RA and SA in all samples This is apparent in some rats in which both the ^{85}Sr and ^{65}Zn activities in all eleven samples were much lower than in those from the remaining rats in the same sacrifice group These data were eliminated Smaller errors in the injections may go undetected and thus increase the total random error The large errors in the ^{85}Sr activities in the viscera were anticipated from the method used for separating the ^{85}Sr from the total activity in the 0 5 MeV channel The relative amounts of the nuclides injected were chosen in order to make the relative concentrations in the serum and mineralized tissues as favorable as possible at the expense of those in the viscera The ^{85}Sr RA and SA in the viscera are sufficiently reproducible at early times following injection such that a pattern can be discerned, and this is sufficient to the present purposes

The fresh weight and ash weight zinc concentrations and the ash weight/fresh weight ratios in these 6 to 9 5 weeks old rats (Table 1) compare well with those for 6 and 8 weeks old rats in the previous report on the variation of the zinc concentrations with age (BERGMAN et coll 1974) The relationship of the zinc concentration to the mineral concentration in the tibia epiphysis during active mineralization found was confirmed by the present data

That these animals were in an active growth period is indicated by the increase with increasing age in both the body weights and the ash weight/fresh weight ratios in the mineralized tissue samples While the fresh weight zinc concentrations in the serum, heart and the viscera, with the exception of the liver, and the ash weight zinc concentrations in the mineralized tissues do not vary significantly during the experimental period, the ash weight/fresh weight ratios (fresh weight calcium concentrations) and fresh weight zinc concentrations do increase in most of the mineralized

samples causing the concentrations of calcium and zinc in the animals as a whole to increase These increases are the cause of the divergence of the RA and SA curves for each mineralized tissues at later post-injection times

In order to test the validity of the nuclide retention data and to be able to interpret them, a separate experiment was made on a 7-week old female rat The fresh weight and ash weight concentration of calcium and zinc as well as the ash weight/fresh weight ratio in the animal as a whole were determined (10 4 mg Ca, 29 6 μg Zn and 37 2 mg ash per g body weight, and 280 mg Ca and 795 μg Zn per g ash) As well over 99 per cent of the calcium in the body is located in the bones and teeth and the ash weight calcium concentrations in these tissues appear to be relatively stable (a value of 0 37 g Ca/g ash was used which is representative for the values in cortical bone given in Table 1 obtained by the same method as was used in this experiment), the calculated part of the total body ash representing bones and teeth is 75 per cent If the ash weight/fresh weight ratios in mineralized tissues of rats of this age average 0 40, approximately 7 per cent of the rat's body weight is mineralized tissue Thus, if losses to excretion were negligible and all the ^{85}Sr was accumulated in the mineralized tissues, the maximum average expected ^{85}Sr RA in per cent would be 1 400, or fourteen times that injected per gram body weight The observed RA in the bone samples at 0 25 day range from 773 to 1 967 per cent If, instead, the bones and teeth of rats of this age were to comprise 10 per cent of the body weight, a generally accepted value, the observed ^{85}Sr RA would be too high as they should not, with very few exceptions, exceed 1 000 per cent

The expected ^{65}Zn RA were much lower due to the more even distribution of zinc in the body If the 7 per cent of the body which is mineralized tissue contains an average of 135 ppm (μg/g) zinc, then approximately one third of the zinc in the rat is located in the bones and teeth, and the remaining tissues of the body should have an average fresh weight zinc concentration of 22 ppm If all zinc were equilibratable and excretion negligible, the average expected RA in per cent in the mineralized tissues would be 470 per cent and the average in the remaining tissues would be 70 per cent The RA in the bones at 0 25 day are between 50 and 200 per cent and only the RA in mandibular condyle reaches as high as 470 per cent If the zinc in bones and teeth were unavailable for exchange, the average expected RA in the samples other than bone should not exceed 150 per cent or 1 5 times that injected per gram body weight The average RA in the viscera is twice this value at 0 25 day despite the fact that the bones had accumulated significant activity by this time Thus a sizable fraction of the zinc in some of the tissues of the body in addition to that in bone must exchange slowly with the ^{65}Zn in serum if the RA in viscera are to be as large as 300 per cent If the heart can be used as approximately representative for skeletal muscle as well in this respect (BERGMAN & SÖREMARK 1968), then the approximately one third of the total body zinc in the skeletal muscle may be a large part of this slowly exchanging fraction The relatively large fraction of the body's zinc located in the hair also accumulates ^{65}Zn at a very slow rate (BERGMAN & SÖREMARK 1968)

The accuracy of the ^{85}Sr and ^{65}Zn SA in serum are very important to the accuracy of the calculated E and A values as both values vary inversely proportionally to the respective serum SA The average serum calcium concentration used in calculating the ^{85}Sr SA is 0 000104 g Ca/g serum which is approximately equivalent to 10 mg % and close to the generally accepted value This concentration is expected to be very stable The zinc concentrations in serum may be 15 to 20 per cent too low due to losses of zinc to the glass tubes during ashing (BERGMAN et coll 1974) This systematic error would cause the serum ^{65}Zn SA to be approximately 20 per cent too high and the E- and A-values to be 15 to 20 per cent too low Thus the E- and A-values should be multiplied by a factor of 1 2 to obtain more accurate values

The A-values for mandibular condyle are 16 per cent for both calcium (^{85}Sr) and zinc (adjusted value for zinc 19 per cent) which indicate that the isotope fronts should reach the resorption zone in 5 to 7 days The marked decreases in the activities of both isotopes between 6 and 8 days indicate that the activity fronts have reached the resorption zone by this time The ^{85}Sr RA decreases relatively more than the ^{65}Zn RA at this time As the specific activity of the ^{85}Sr in the bone which is being accreted at the time of the injection should be higher relative to the remainder of the retention than the specific activity of the ^{65}Zn front is in relation to the remainder of the ^{65}Zn in the condyle this may be the cause of the difference in the relative loss of the two isotopes between 6 and 8 days The agreement of the RA in the incisors divided by the time integral of the serum SA and the concentration of the element also indicates that zinc (^{65}Zn) is being accumulated at the same relative rate as calcium (^{85}Sr) These values cannot be used as accretion rates as the eruption rate dominates the shape of the retention curves Both these observations appear to support the hypothesis that zinc is being 'accreted' in bones and teeth

The similarities in the courses of the ^{85}Sr and ^{65}Zn RA in the bone samples at later times post-injection may indicate that similar processes dominate the loss of both isotopes Resorption is expected to play a dominant role at these times This might be interpreted as further indicating that zinc, like calcium and strontium, is being 'accreted' or moved from an exchangeable pool to one which is relatively unavailable for exchange It is as yet unknown whether or not zinc replaces calcium in the lattice of the apatite crystals in bones and teeth, but zinc may be 'buried' in newly accreted bone and tooth mineral even if it is located in the organic matrix or the hydration layer of the crystals (BRUDEVOLD et coll 1963, HAUMONT & MCLEAN 1966 JOWSEY & ORVIS 1967) It was on this assumption that the equation of BAUER et coll was applied to the ^{65}Zn as well as the ^{85}Sr data

The increasing E values and decreasing A-values as data from later times post-injection are used in the calculations have been observed previously by many authors (MARSHALL 1969) Comparing the lowest A-values calculated using the equation of BAUER et coll with those obtained by dividing the retention at 6 days by the integral of the serum SA to 6 days, the A-values are expected to decrease even more if data from times later than 1 5 days are used in the equation In an effort to quantitatively

describe the behaviour of ^{65}Zn in heart muscle and to calculate E- and A-values which obtain at all times post-injection, an equation was derived to describe the retention with time in a slowly exchanging compartment (see Appendix), incorporated in the equation of BAUER et coll and used with this data This 3-compartment equation has its parallel in the analogue technique used by WENDEBERG (1965) and others for ^{47}Ca and ^{85}Sr and the digital equivalent used by McINTOSH & LUTWAK-MANN (1972) for ^{65}Zn

The equation for the retention R_{L_t} in a slowly exchanging compartment, assuming that the course of the serum SA is initially exponential, $S_t = S_0\, e^{-K_s t}$, is

$$R_{L_t} = S_0\ L\ \frac{K_L}{K_L - K_s}\ (e^{-K_s t} - e^{-K_L t})$$

where S_0 is the initial serum SA (extrapolated), L is the size of the slowly exchanging compartment, and K_s and K_L are the rate constants of the serum and compartment respectively As the earlier courses of the serum SA for both ^{85}Sr and ^{65}Zn in the data presented here can be approximated by single exponentials through 1 5 days post-injection, the full equation for the retention R_t in a sample containing rapidly exchanging (E), more slowly exchanging (L) and accreting (A) fractions becomes

$$R_t = S_0 \left[E\ e^{-K_s t} + L\ \frac{K_L}{K_L - K_s}\ (e^{-K_s t} - e^{-K_L t}) + \frac{A}{K_s}\ (1 - e^{-K_s t})\right]$$

Unfortunately this equation cannot be solved directly for E, L, K_L and A using simultaneous equations Under certain circumstances, as for example when the accreted fraction of the activity in a sample can be assumed to be very small relative to the activity in the exchangeable pools E and L, K_L can be solved directly using the ratios of the sample and serum SA from the times when the sample activity is at its peak and after it has assumed a constant ratio to the serum SA (see Appendix) If accretion is likely to be playing a dominant role in the retention of activity, as it does for ^{85}Sr and ^{65}Zn in the bone samples, it is still possible to solve the full equation by making successive approximations to K_L and then solving three simultaneous equations for E, L and A This method was applied to the same data as were used in the equation of BAUER et coll A programmable calculator (Canon Canola 167P) was used to solve the equations

The results of the method of successive approximations on the data from the bone samples are presented in Table 3 When K_L is chosen such that the E component is insignificantly small, that is, only the more slowly exchanging compartment L and accretion A are operative, the accretion rates calculated using the data from three of the four killing times between 0 25 and 1 5 days are with few exceptions at least as small as the smallest calculated with the equation of BAUER et coll, and thus closer to the values obtained graphically at 6 days, and the predicted retention at the fourth point falls within the range $\bar{x} \pm 2$ SE_x of the observed RA for both nuclides in each of the bone samples

Table 3

The values for the size of the slowly exchanging compartment L with an exchange rate K_L and either the accretion rate A or the size of the rapidly exchangeable pool E for calcium (⁸⁵Sr) and zinc (⁶⁵Zn) in the bone samples calculated using the modified equation for retention and the data from 0.25, 1 0 and 1.5 days The values to the left were obtained when the rapidly exchangeable pool E was of insignificantly small size and those to the right when the accretion rate A was at or near 0 All values are based on 1 gram fresh weight of bone sample

	E inoperative					*A* inoperative				
	K_L	L	A	L	A	E	K_L	L	E	L
⁸⁵Sr	day⁻¹	g Ca	g Ca day⁻¹	% Ca	% Ca day⁻¹	g Ca	day⁻¹	g Ca	% Ca	% Ca
Mand condyle	2 3	0 0408	0 0154	40 3	15 2	0 0073	0 96	0 0740	7 2	73
Mand bone	4 1	0 0136	0 0153	8 8	9 9	0 0071	0 44	0 0591	4 6	38
Tib epiphysis	5 3	0 0120	0 0078	17 3	11 3	0 0082	0 52	0 0302	11 9	44
Tib diaphysis	7 9	0 0067	0 0120	3 5	6 2	0 0061	0 11	0 1304	3 2	68
⁶⁵Zn	day⁻¹	mg Zn	mg Zn day⁻¹	% Zn	% Zn day⁻¹	mg Zn	day⁻¹	mg Zn	% Zn	% Zn
Mand condyle[a]	4 0	0 0099	0 0180	8 8	16 1	0 0032	0 52	0 0648	2 9	58
Mand bone	2 0	0 0089	0 0056	6 8	4 3	0 0011	0 64	0 0275	0 8	21
Tib epiphysis	4 6	0 0079	0 0074	9 4	8 8	0 0041	0 52	0 0267	4 9	32
Tib diaphysis[b]	5 6	0 0023	0 0070	1 5	4 5	0 0011	0 48	0 0212	7 1	14

[a] data from 0 5 day replaces 1 0 day
[b] data from 0 5 day replaces 1 5 day

In effect what is done by allowing the *E*-value to approach 0 is to replace the rapidly exchanging compartment *E* with the less rapidly exchanging compartment *L* The equation used for the retention is then

$$R_t - S_0 \left[L \frac{K_L}{K_L - K_s} (e^{-K_s t} - e^{-K_L t}) + \frac{A}{K_s} (1 - e^{-K_s t})\right]$$

The equation of BAUER et coll is a simplification of the above equation, the assumption having been made that K_L is so much larger than K_s that

$$L \frac{K_L}{K_L - K_s} (e^{-K_s t} - e^{-K_L t}) \approx L e^{-K_s t}$$

The results indicate that this assumption may not be valid Assuming that the retention equation above is a more accurate description of retention than the equation of

BAUER et coll, the A-value calculated by solving this equation for two unknowns ($E = L \cdot K_L/(K_L - K_s)$ and A) will decrease and become more accurate at later times, while the E-value will increase and will eventually be over-estimated by a factor of $K_L/(K_L - K_s)$

MARSHALL (1969) uses the decreasing A-values as evidence for the existence of very slowly exchanging or expanding compartments and argues that the straight line course of the serum activities on log–log scales with a slope near -1 (Fig 5) is further evidence of the existence of such compartments In an attempt to detect whether or not the existence of very slowly exchanging compartments was consistent with the present data, further approximations to K_L were made for each of the bone samples and isotopes Using the same data, the K_L-values were decreased until the accreted fraction was no longer operative (Table 3) The predicted value for the data point not used in the calculation in each case falls within the range $\bar{x} \pm 2$ SE_x of the measured RA For ^{85}Sr, the fit to the data is improved by decreasing the K_L-value and a perfect fit is obtained for the RA in tibia epiphysis with a K_L of 2 32·day^{-1} (*E*=0 0067 g Ca, *L*=0 0073 g Ca *and A*=0 0070 g Ca *day*$^{-1}$) *For* ^{65}Zn, the fit to the RA in mandibular bone and tibia epiphysis is poorer than with larger approximations to K_L However, the K_L-value for mandibular bone in the calculation in which E was inoperative is already quite low (2 0 day^{-1}) compared to those for the other bones The fit to the curve drawn for mandibular condyle is poorer and the fit to the curve for tibia diaphysis improved by replacing the accreted fraction with a slowly exchanging compartment

While it is not plausible that accretion of ^{85}Sr is non-existent, the true accretion rate is likely to be even less than the low value determined graphically and almost any value between these values and 0 is consistent with the data Again, the values for E, L and A for zinc may be too low due to the ^{65}Zn SA in serum having been overestimated Multiplying these values by 1 2 should correct for this error None of the sums of the E- and L-values for zinc (Table 3), when corrected, exceed 75 per cent of *the element in the sample and most are well below this figure It is difficult to explain how the remainder of the zinc could come into a fraction which is un-*available for exchange when accretion is not operative in the model Further, the SA *curve for* ^{65}Zn *in* mandibular condyle reaches its peak as it meets the serum SA curve which indicates that, if accretion is negligible, all the zinc in the condyle should be in the slowly exchangeable pool The L-value is only 58 per cent (corrected value 70 per cent)

The straight line courses on log log scales for the ^{85}Sr SA in serum throughout most of the experimental period and that for ^{65}Zn from 3 days may give an indication of the relative sizes of these slowly exchanging compartments Their relative importance to the course of the serum SA may be quite different for ^{65}Zn and ^{85}Sr as only one third of the zinc and almost all of the calcium in the body is located in bone The exchange with the zinc external to bone may dominate the serum ^{65}Zn SA course *for a long time until the* two have almost fully equilibrated while the ^{85}Sr

SA in serum is from the outset dominated by exchange with and accretion in bone As the fit to the ^{85}Sr data from all four samples is improved by the inclusion of a slowly exchanging compartment and the serum ^{85}Sr SA curve behaves as it does from 0 25 day, it appears that a relatively large portion of the ^{85}Sr in bone is slowly exchanged and not accreted The inclusion of very slowly exchanging compartments is consistent with the retention data even at later times as these compartments gain activity until they attain the serum SA, which may take a very long time, and are resorbed along with the accreted activity and returned to the exchangeable pool The ^{65}Zn data from mandibular condyle and tibia epiphysis is not improved by the inclusion of such a compartment, which may indicate that accretion is dominating in the late retention of ^{65}Zn in these samples The A-values in per cent for ^{65}Zn in cortical bone were approximately 60 per cent of those for ^{85}Sr and, in endochondral bone and calcifying cartilage, approximately 80 per cent of those for ^{85}Sr (corrected values 72 and 96 per cent, respectively) It may be that the ^{65}Zn data is more accurately reflecting the accretion of bone, particularly cortical bone, the ^{85}Sr data generally giving an over-estimate due to the accumulation in the slowly exchanging compartments The observation that the hot spot to diffuse retention ratio for ^{65}Zn in cortical bone is several times that for ^{45}Ca (JOWSEY & ORVIS 1967) is consistent with this hypothesis The retention of ^{85}Sr is expected to be very similar to that of ^{45}Ca in this respect (BAUER et coll 1955 b) It is possible that isotopes of zinc will be used as tracer nuclides for measurement of parameters of bone anabolism in man The short half life and γ-emission of ^{69}Zn^{m} are well suited to this purpose (LORBER et coll 1970)

One of the large depots of zinc which appears to affect the course of ^{65}Zn activity in serum is that in muscle (using heart muscle as representative) The same model used above was applied to the RA in heart and a perfect fit was obtained for the first four data points when $K_L = 0\ 92$ day^{-1} $E = 0\ 0024$ mg Zn, $L = 0\ 0087$ mg Zn and $A = 0\ 0010$ mg Zn day^{-1}, the corrected zinc values being 20 per cent larger According to the corrected values, the zinc which is relatively unavailable for exchange is 4 3 ppm of 17 6 ppm total and it is 'accreted' or made unavailable for exchange at the rate of 1 2 ppm day $^{-1}$ The alternative is to eliminate accretion from the model Two methods are available The equations derived in the Appendix may be used to directly solve for K_L, E and L from the peak and late ratios of the SA in the sample to that in serum Using the corrected serum SA (0 83 SA), the values obtained are $K_L = 0\ 69$ day $^{-1}$, $E = 0\ 0013$ mg Zn and $L = 0\ 0163$ mg Zn When these values are used in the [illegible]

more th [illegible]

the fit is [illegible] following values $K_L = 0\ 76$ day^{-1}, $E = 0\ 0024$ mg Zn and $L = 0\ 0117$ mg Zn Multiplying E and L by 1 2, the total exchangeable zinc is approximately 16 9 ppm, which is very close to the total zinc in heart, 17 6 ppm Using these values the predicted retention in the model reaches a peak at approximately 1 5 days and the predicted limit of the ratio of the heart to serum ^{65}Zn SA (K_L/

$(K_L - K_s))$ is 1.30 in the time period between 2 and 8 days ($K_s = 0.223$ day^{-1}) which agrees fairly well with observed ratios at 6 and 8 days of approximately 1.4 (serum SA corrected). Each of the three models is dominated by a large, slowly exchanging compartment with a turnover time ($1/\lambda_L$) of between 1.1 and 1.4 days.

The zinc in the viscera, with the exception of pancreas, appears to be relatively rapidly exchangeable as the SA follow the serum SA (corrected) at a slightly higher level. These results agree with those of GILBERT & TAYLOR (1956). The SA in pancreas increases between 0.25 and 0.5 day even after having exceeded the serum SA level. This may indicate that zinc is in some way being actively accumulated in pancreas in a fraction which is relatively unavailable for exchange. Further data on the turnover of zinc in pancreas is presented in a subsequent article (BERGMAN & WING 1974).

Appendix

The derivation of the equation for the retention in a slowly exchanging pool and subsequent equations used to determine its size and rate of exchange.

If R_{Lt} is the amount of activity in the pool at time t, dR_{Lt}/dt is the change in the amount of activity in the pool per unit time and

$$\frac{\partial R_{Lt}}{\partial t} = K_L \cdot L \left(S_t - \frac{R_{Lt}}{L}\right), \tag{1}$$

where λ_L is the fraction of the pool moving out (= in: it is assumed that steady state conditions apply) per unit time, L is the pool size (g, mg), $\lambda_L \cdot L$ is the amount of the element moving out (= in) per unit time, and S_t and R_{Lt}/L are the specific activities in the serum and pool respectively. If it can be assumed that the serum activity decreases exponentially, that is $S_t = S_0 \cdot e^{-K_s t}$, then

$$\frac{\partial R_{Lt}}{\partial t} = K_L \cdot L \cdot S_0 \cdot e^{-K_s t} - \lambda_L \cdot R_{Lt} \tag{2}$$

The activity in the pool at time t is derived by first rearranging and multiplying both sides by $e^{K_L t}$

$$\frac{\partial R_{Lt}}{\partial t} + \lambda_L \cdot R_{Lt} = \lambda_L \cdot L \cdot S_0 \cdot e^{-K_s t} \tag{3}$$

$$\left(\frac{\partial R_{Lt}}{\partial t} + K_L \cdot R_{Lt}\right) \cdot e^{K_L t} = K_L \cdot L \cdot S_0 \cdot e^{-(K_s - K_L) t} \tag{4}$$

$$\frac{\partial(R_{Lt} \cdot e^{K_L t})}{\partial t} = \lambda_L \cdot L \cdot S_0 \cdot e^{-(K_s - K_L) t} \tag{5}$$

Integrating both sides with respect to t,

$$R_{Lt} \cdot e^{K_L t} - R_{L0} = \lambda_L \cdot L \cdot S_0 \cdot \frac{1}{\lambda_s - \lambda_L} \cdot (1 - e^{-(K_s - K_L) t}) \tag{6}$$

and, as $R_{L0} = 0$, the activity in the pool at time t is

$$R_{Lt} = S_0 \cdot L \cdot \frac{K_L}{\lambda_L - K_s} \cdot (e^{-K_s t} - e^{-K_L t}) \tag{7}$$

A special case arises when the rate constants K_s and K_L are equal. Substituting K_s for K_L in equation 1, equations 5 and 7 become

$$\frac{\partial(R_{L_t}\, e^{K_s t})}{\partial t} = K_s\, L\, S_0 \tag{8}$$

and

$$R_{L_t} = K_s\, L\, S_0\, t\, e^{-K_s t} \tag{9}$$

The activity in this pool increases until it meets the serum specific activity on its downward course. After this time the pool must begin to lose activity (equation 1), the loss of activity depending on the size of K_L in relation to K_s. If $K_L > K_s$, the specific activity in the pool approaches a constant ratio to that in serum as t becomes large

$$\frac{R_{L_t}/L}{S_t} = \frac{S_0 \dfrac{K_L}{K_L - K_s}\,(e^{-K_s t} - e^{-K_L t})}{S_0\, e^{-K_s t}} = \frac{K_L}{K_L - K_s}\,(1 - e^{-(K_L - K_s) t}) \tag{10}$$

$$\lim_{t\to\infty}\left(\frac{R_{L_t}/L}{S_t}\right) = \frac{K_L}{K_L - K_s} \tag{11}$$

In cases in which $K_L < K_s$ the ratio of the specific activities (equation 10) increases without limit. When $K_L = K_s$ the ratio is equal to $K_s\, t$ and also increases without limit. However, if $K_L < K_s$ the retention should decrease exponentially at later times and approach $R_{T+t} = R_T\, e^{-K_L t}$

The equation for the retention in the pool becomes more complex if the serum activity cannot be represented by a single exponential over a long period of time. If the serum activity can be expressed as the sum of weighted exponentials, $S_t = S_0 \sum_{i=1}^{n} K_i\, e^{-K_{si} t}$, equation 7 becomes

$$R_{L_t} = S_0\, L \sum_{i=1}^{n} K_i \frac{K_L}{K_L - K_{si}}\,(e^{-K_{si} t} - e^{-K_L t}) \tag{12}$$

If $K_L > K_{sn}$ the ratio of the pool to serum specific activities will become constant at later times

$$\lim_{t\to\infty}\left(\frac{R_{L_t}/L}{S_t}\right) = \frac{K_L}{K_L - K_{sn}} \tag{13}$$

pe [illegible]
B[illegible] ... to a retention in the rapidly exchanging and accreted fractions

$$R_t = E\, S_t + A \int_0^t S_t\, dt$$

can be expanded to include the slowly exchanging pool

$$R_t = S_0 \left[E \sum_{i=1}^{n} K_i\, e^{-K_{si} t} + L \sum_{i=1}^{n} K_i \frac{K_L}{K_L - K_{si}}\,(e^{-K_{si} t} - e^{-K_L t}) + A \sum_{i=1}^{n} \frac{K_i}{K_{si}}\,(1 - e^{-K_{si} t})\right] \tag{14}$$

The four unknown quantities E, L, K_L and A cannot be found by solving four simultaneous equations In many cases it may be necessary to use analogue techniques It is also possible to use successive approximations to K_L and solve three equations in A, L and E In some cases, *explicit solutions can be derived if certain assumptions can be made If the retention* of activity in the sample at later times follows a course parallel to the course of the serum activity, one might assume that little or none of the element is accreted and use a model in which only rapidly and slowly exchanging pools are present

$$R_t = S_0 \left[E \cdot \sum_{i=1}^{n} K_i \; e^{-K_{si} t} + L \cdot \sum_{i=1}^{n} K_i \; \frac{K_L}{K_L - K_{si}} \cdot (e^{-K_{si} t} - e^{-K_L t})\right] \tag{15}$$

When a stable ratio has been achieved,

$$\lim_{t\to\infty} \left(\frac{R_t}{S_t}\right) = E + L \cdot \frac{K_L}{K_L - K_{sn}} \tag{16}$$

where R_t/S_t is the ratio of the retention in the sample to the serum specific acitvity At the time of peak activity in the pool, t_p,

$$R_{t_p} = S_0 \left[E \; \sum_{i=1}^{n} K_i \; e^{-K_{si} t_p} + L \; \sum_{i=1}^{n} K_i \; \frac{K_L}{K_L - K_{si}} \; (e^{-K_{si} t_p} - e^{-K_L t_p})\right] \tag{17}$$

and

$$\left(\frac{\partial R_t}{\partial t}\right)_{t_p} = S_0 \cdot \left[E \; \sum_{i=1}^{n} K_i \; (-K_{si}) \; e^{-K_{si} t_p} + L \; \sum_{i=1}^{n} K_i \; \frac{K_L}{K_L - K_{si}} \; (-K_{si} \; e^{-K_{si} t_p} + K_L \; e^{-K_L t_p})\right] = 0 \tag{18}$$

Multiplying 17 through by K_L and adding it to 18, the $e^{-K_L t}$ term is eliminated The resulting equation in E and L can be simplified by substituting S_{t_p} for $S_0 \sum_{i=1}^{n} K_i \; e^{-K_{si} t_p}$ and $-K_{sp} \; S_{t_p}$ for $S_0 \sum_{i=1}^{n} K_i \; (-K_{si}) \; e^{-K_{si} t_p}$, the slope of the serum specific activity curve at t_p

$$E = \left(\frac{R_{t_p}}{S_{t_p}} - L\right) \frac{K_L}{K_L - K_{sp}} \tag{19}$$

where R_{t_p}/S_{t_p} is the ratio of the retention in the sample to the serum specific activity at the peak Equations 16 and 19 can be solved for K_L, E and L in terms of the total amount of the element in both pools, $T = L + E$ (if none of the element is accreted then none should be inaccessable and T can be assumed equal to the total concentration)

$$K_L = \frac{K_{sn} \; K_{sp} \; \lim_{t\to\infty} \left(\frac{R_t/T}{S_t}\right)}{K_{sn} \left(1 - \frac{R_{t_p}/T}{S_{t_p}}\right) + K_{sp} \left(\lim_{t\to\infty} \left(\frac{R_t/T}{S_t}\right) - 1\right)} \tag{20}$$

where the ratios are those of the specific activity in the sample to that in serum at the peak and after equilibration E and L can then be solved using either equation 16 or 19 and $L = T - E$ Note that, if the specific activity ratio at the peak is 1, that is the two specific activity curves meet at the peak, then $E = 0$, $L = T$ and

$$K_L = \frac{\lim_{t\to\infty} \left(\frac{R_t/T}{S_t}\right)}{\lim_{t\to\infty} \left(\frac{R_t/T}{S_t}\right) - 1} \; K_{sn}$$

Acknowledgements

I wish to thank Dr Jack Higby, presently of the Department of Physics, University of Queensland, Australia, for helping me with the equations, and Rolf Sjostrom, laboratory engineer, for helpful discussion and a technical assistance This investigation was supported by a grant from the Swedish Medical Research Council (Project No B73-24X-3342-02)

SUMMARY

Analysis of bone retention data using 2- or 3-compartment models gives nearly equal relative accretion rates for zinc and calcium (^{85}Sr) in endochondral bone and calcifying cartilage The rate for zinc in cortical bone is 70% of that for calcium As the existence in cortical bone of large, slowly exchanging compartments imitating accretion is consistent with the data, the relative accretion rate for zinc may more closely reflect the relative accretion rate of cortical bone

ZUSAMMENFASSUNG

Analysen der Knochen Retentionsdaten unter Verwendung von 2 oder 3 Compartment-Modellen ergaben beinahe gleiche Werte fur die relativen Anstiegsgeschwindigkeiten von Zink und Calcium (^{85}Sr) im endochondralen Knochen und dem verkalkendern Knorpel Die Geschwindigkeit fur Zink im cortikalen Knochen betragt 70% der Geschwindigkeit fur Calcium Da das Vorkommen von grossen, sich langsam umsetzenden Compartments, die die Ansammlung nachahmen, mit den Daten übereinstimmt, mag die relative Ansammlungsgeschwindigkeit fur Zink die relative Ansammlungsgeschwindigkeit des cortikalen Knochens eher wiedergeben

RESUMÉ

L analyse des mesures de rétention osseuse par des modeles à 2 ou 3 compartiments donne des taux relatifs d accretion à peu près égaux pour le zinc et pour le calcium (^{85}Sr) dans l'os enchondral et dans le cartilage en voie de calcification Le taux pour le zinc dans l os cortical est de 70% de celui du calcium Comme l'existence dans l os cortical de grands compartiments à échange lent imitant l accretion est compatible avec les resultats, le taux relatif d accrétion pour le zinc pourrait refléter plus fidèlement le taux relatif d accretion de l os cortical

REFERENCES

BALLOU J E and THOMPSON R C Metabolism of zinc 65 in the rat Consideration of permissible exposure limits Hlth Phys 6 (1961), 6

BAUER G C H, CARLSSON A and LINDQUIST B (a) Evaluation of accretion, resorption and exchange reactions in the skeleton Kungl Fysiogr Sallskap Lund Forhandl 25 (1955) 3

— — — (b) A comparative study on the metabolism of Sr^{90} and Ca^{45} Acta physiol scand 35 (1955) 56

BERGMAN B Comparative study of distribution of injected zinc 65 in the mandibular con-

dyle and other tissues in rat as determined by gamma scintillation Acta radiol Ther Phys Biol 9 (1970) 577

— SJÖSTRÖM R and WING K R The variation with age of tissue zinc concentrations in albino rats determined by atomic absorption spectrophotometry Acta physiol scand 92 (1974) 440

— and SÖREMARK R Autoradiographic studies on the distribution of zinc 65 in mice J Nutr 94 (1968) 6

— and WING K R The turnover of ⁶⁵Zn in rats fed a zinc deficient diet Acta physiol scand 92 (1974) 451

BRUDEVOLD F STEADMAN L T SPINELLI M A AMDUR B H and GRON P A study of zinc in human teeth Arch oral Biol 8 (1963) 135

CZERNIAK P NAHARIN A and ALEXANDER N Turnover rate of zinc in the body as determined by the study of ⁶⁵Zn in rats Int J appl Radiat 13 (1962) 547

GILBERT I G F and TAYLOR D M The behaviour of zinc and radiozinc in the rat Biochim biophys Acta 21 (1956) 545

HAUMONT S Distribution of zinc in bone tissue J Histochem Cytochem 9 (1961) 141

— and MCLEAN F C Zinc and the physiology of bone In Zinc metabolism p 169 Edited by A S Prasad Charles C Thomas Springfield Ill 1966

JOWSEY J and ORVIS A L Comparative deposition of ⁴⁵Ca ⁶⁵Zn and ⁹¹Y in bone Radiat Res 31 (1967) 693

LEDERER C M HOLLANDER J M and PERLMAN I Table of isotopes 6th ed pp 199 220 J Wiley & Sons New York 1968

LORBER S A GOLD F M MAGLIONE A A and RUBENFELD S ⁶⁹ᵐZn chloride—a new scanning agent a study of its dosimetry and biological fate J nucl Med 11 (1970) 699

MARSHALL J H Measurements and models of skeletal metabolism In Mineral metabolism Vol III p 1 Edited by C L Comar and F Bronner Academic Press New York 1969

MCINTOSH J E A and LUTWAK MANN C Zinc transport in rabbit tissues Some hormonal aspects of the turnover of zinc in female reproductive organs liver and body fluids Biochem J 126 (1972) 869

STRAIN W H HUEGIN F LANKAU JR C A BERLINER W P MCEVOY R K and PORIES W J Zinc 65 retention by aortic tissue of rats Int J appl Radiat 15 (1964) 231

WENDEBERG B Bone salt accretion and exchangeable calcium spaces in man measured with ⁴⁷Ca and ⁸⁵Sr Clin Orthop 40 (1965) 162

FROM THE GENERAL AND SURGICAL DEPARTMENTS, THE NORWEGIAN RADIUM HOSPITAL, MONTEBELLO, OSLO, NORWAY.

COMBINED SURGERY AND RADIATION THERAPY VERSUS SURGERY ALONE IN PRIMARY MAMMARY CARCINOMA

I The effect of orthovoltage radiation

HERMAN HØST and IVAR O BRENNHOVD

Although carcinoma of the breast is the most common malignancy in women, there is no general agreement as to the best treatment of an early case This uncertainty relates not only to the type of surgery, but also to the value of radiation therapy as an adjunct to surgery Figures have been published suggesting that radical mastectomy combined with postoperative irradiation produces the best treatment results (GUTTMANN 1967, HARRINGTON 1952, LEWISON & SMITH 1963, MARSHALL & HARE 1947, WATSON 1967) However, the results from Manchester (EASSON 1968) and from the National Surgical Adjuvant Project (FISCHER et coll 1968) give little support to radiation therapy after radical mastectomy as it did not affect survival Data from the latter reports even indicate that postoperative irradiation may increase the risk of and the rate of growth of distant metastases

Radical mastectomy with axillary lymph node dissection and prophylactic postoperative irradiation has been widely used in the treatment of early carcinoma of the breast in Norway for many years The present investigation, started a decade ago was intended to evaluate postoperative irradiation as an adjuvant to surgery

Submitted for publication 27 May 1974

dyle and other tissues in rat as determined by gamma scintillation Acta radiol Ther Phys Biol 9 (1970), 577

— SJÖSTRÖM R and WING K R The variation with age of tissue zinc concentrations in albino rats determined by atomic absorption spectrophotometry Acta physiol scand 92 (1974), 440

— and SÖREMARK R Autoradiographic studies on the distribution of zinc 65 in mice J Nutr 94 (1968), 6

— and WING K R The turnover of ^{65}Zn in rats fed a zinc deficient diet Acta physiol scand 92 (1974), 451

BRUDEVOLD F, STEADMAN L T, SPINELLI M A, AMDUR B H and GRON P A study of *zinc in human teeth Arch oral Biol 8 (1963), 135*

CZERNIAK P, NAHARIN A and ALEXANDER N Turnover rate of zinc in the body as determined by the study of ^{65}Zn in rats Int J appl Radiat 13 (1962), 547

GILBERT I G F and TAYLOR D M The behaviour of zinc and radiozinc in the rat Bio chim biophys Acta 21 (1956), 545

HAUMONT S Distribution of zinc in bone tissue J Histochem Cytochem 9 (1961), 141

— and MCLEAN F C Zinc and the physiology of bone *In* Zinc metabolism, p 169 Edited by A S Prasad Charles C Thomas, Springfield Ill 1966

JOWSEY J and ORVIS A L Comparative deposition of ^{45}Ca, ^{65}Zn and ^{90}Y in bone Radiat Res 31 (1967), 693

LEDERER C M, HOLLANDER J M and PERLMAN I Table of isotopes 6th ed pp 199, 220 J Wiley & Sons New York 1968

LORBER S A, GOLD F M, MAGLIONE A A and RUBENFELD S ^{69m}Zn chloride—a new scanning agent a study of its dosimetry and biological fate J nucl Med 11 (1970) 699

MARSHALL J H Measurements and models of skeletal metabolism *In* Mineral metabolism Vol III p 1 Edited by C L Comar and F Bronner Academic Press, New York 1969

MCINTOSH J E A and LUTWAK MANN C Zinc transport in rabbit tissues Some hormonal aspects of the turnover of zinc in female reproductive organs liver and body fluids *Biochem J 126 (1972), 869*

STRAIN W H, HUEGIN F, LANKAU JR C A, BERLINER W P MCEVOY R K and PORIES W J Zinc 65 retention by aortic tissue of rats Int J appl Radiat 15 (1964) 231

WENDEBERG B Bone salt accretion and exchangeable calcium spaces in man measured with ^{47}Ca and ^{85}Sr Clin *Orthop 40 (1965), 162*

defined as occurrence of the disease in the axilla or supraclavicular fossa, while distant metastasis has been defined as disease occurring elsewhere

Results

The patients in stage I amounted to 345, of these 173 belonged to the irradiated group and 172 to the control group Of 201 patients in stage II, 109 received postoperative irradiation, while 92 were allocated to the control group

Survival rates according to the life table method have been calculated (Fig 1) It will be observed that there is no difference between the irradiated group and the control group either in patients stage I or in those stage II Five years after treatment 91 3 per cent of the irradiated patients in stage I were living, compared to 89 9 per cent of the control groups In stage II the 5-year survival rates were 71 4 and 71 7 per cent, respectively

The disease free survival for patients stage I and stage II according to initial treatment appears in Fig 2 No difference was found

Although no differences have been demonstrated either in crude or in the disease-free survival, a comparison of the spread of the disease in the different treatment groups might be of interest

Local recurrence has always been confirmed histologically except in cases with widespread distant disease at the same time The rate of local recurrence in the two groups is given in Table 1 In stage I local recurrence was observed at the same rate in the irradiated patients as in the controls, whereas in patients with stage II disease local recurrence appears to be almost twice as frequent in the control group as in the irradiated group This difference is, however, not statistically significant

In the majority of cases the local recurrence appeared as part of widespread disease In the remaining patients the local recurrence preceded later regional or distant metastases in 10 cases (8 controls and 2 irradiated patients) while in 6 patients (4 controls and 2 irradiated) further spread has not been observed

Regional metastases to the axillary or supraclavicular nodes were mainly based on clinical examination The frequency of regional spread appears in Tables 2 and 3 Homolateral axillary metastasis was observed in only 10 out of 546 patients (Table 2) Table 3 shows that postoperative irradiation reduced significantly the occurrence of later supraclavicular lymph node metastasis ($p < 1\ ‰$) in patients in stage II A similar but less evident trend is seen in cases in stage I

Distant metastasis The number of patients with distant metastasis and the time of appearance after primary treatment may be seen from Table 4 No difference existed between the two groups either in stage I or in stage II, and postoperative irradiation had no influence on the time when distant metastasis appeared in patients stage I In patients stage II the data suggest that distant metastasis occurred earlier in the irradiated group than in the control group It should be stressed, however, that 4 patients stage I in the control group had distant metastases within one year, while

In Part I, which is presented here, a conventional roentgen therapy unit was used, and in Part II a ^{60}Co unit, with considerably increased dosage and altered treatment plan The results from Part II are not yet available

Material and Methods

Only women considered operable according to the criteria laid down by HAAGENSEN (1949) have been included in the material Surgery, in principle, has been Halsted's standard radical mastectomy, consisting of an en bloc removal of the breast, pectoral muscles and axillary contents The distinction between stages I and II was made on the basis of histology of the axillary nodes Ovarian irradiation was also carried out as part of the primary treatment (NISSEN-MEYER 1965)

The trial was started in January 1964 and completed in December 1967 This report concerns 546 cases or about two-thirds of the total number of patients with carcinoma of the breast (stages I and II) admitted to the Norwegian Radium Hospital during this period In its surgical department 383 patients were operated upon, while the remaining 163 patients had a radical mastectomy at another hospital

Out of the patients with mammary carcinoma, stage I or II, admitted to the hospital during the period 263 were excluded for the following reasons (1) A standard mastectomy of the Halsted type had not been performed, (2) the criteria for operability laid down by HAAGENSEN had not been followed, or (3) evidence of residual malignancy within the operation area existed

The patients included in the trial were divided by randomization into two groups (1) postoperative irradiation (irradiated group), and (2) no postoperative irradiation (control group)

Irradiation data were 200 kV with a half-value layer of 1 5 mm Cu The internal mammary lymph node chain, the ipsilateral axilla, the supraclavicular fossa and the skin flaps were irradiated by two tangential opposing beams to the anterior chest wall with supporting beams to the supraclavicular fossa and the axilla

The doses to the supraclavicular fossa and the axilla were respectively 3600 R and 1800 R, measured as skin dose The tangential opposing fields were each irradiated with 2600 R, measured as free air dose in the centre of the beam The actual dose to the skin of the chest wall was from 2500 R to 3100 R Dose measurements performed on an Alderson phantom have revealed a rapid decrease of the dose in the depth The latter is caused by absence of scatter as most of the beams from the tangential fields projects beyond the skin of the patient

All patients have been followed up at close intervals for at least 5 years If local recurrence or metastasis was detected, hormones, roentgen irradiation or both combined were given as indicated in the individual case

Local recurrence was defined as reappearance of disease within the area of operation, which means the operation scar and the chest wall Regional metastasis has been

Table 1

Frequency of local recurrences

	Irradiated	Controls
Stage I	6/173 (3 5 %)	7/172 (4 0 %)
Stage II	9/109 (8 2 %)	14/92 (15 2 %)
Total	15/282 (5 7 %)	21/264 (8 0 %)

Table 2

Frequency of homolateral axillary metastases

	Irradiated	Controls
Stage I	2/173 (1 2 %)	1/172 (0 6 %)
Stage II	2/109 (1 8 %)	5/92 (5 4 %)
Total	4/282 (1 4 %)	6/294 (2 3 %)

Table 3

Frequency of homolateral supraclavicular lymph node metastases

	Irradiated	Controls
Stage I	1/173 (0 6 %)	5/172 (2 9 %)
Stage II	3/109 (2 8 %)	13/92 (14 1 %) $p < 1$ %
Total	4/282 (1 4 %)	18/264 (6 8 %) $p < 1$ %

Table 4

Time from primary treatment to appearance of first distant metastasis

Treatment group	Months following the primary treatment			Total number of patients with distant metastasis
	−11	12–23	24–	
Stage I				
Irradiated	2	5	17	24
Controls	4	5	14	23
Stage II				
Irradiated	9	10	27	46
Controls		16	24	40

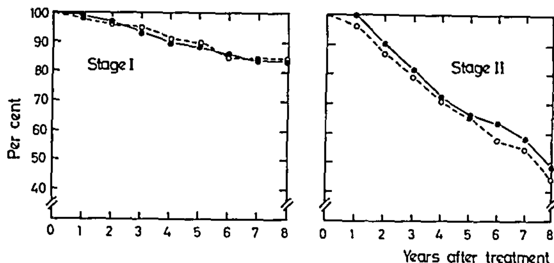


Fig 1. Survival rates according to primary treatment ○ Surgery and irradiation (n = 173 in stage I and 109 in stage II) ● Surgery alone (n = 172 in stage I and 92 in stage II)

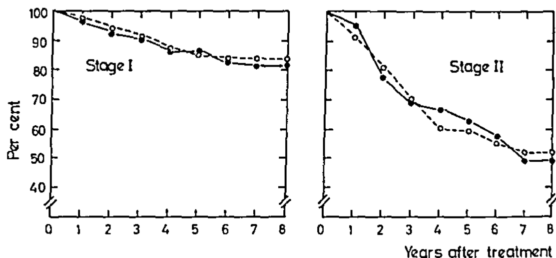


Fig 2 Proportion of patients free from disease according to primary treatment ○ Surgery and irradiation (n = 173 in stage I and 109 in stage II) ● Surgery alone (n 172 in stage I and 92 in stage II)

among patients stage II in the control group, no distant metastases were observed within the first year after the primary treatment

Discussion

Postoperative irradiation may be administered by different methods with variation of treatment fields and dosage This may explain possible differences in the results Evidence to support the value of postoperative irradiation as an adjuvant to radical mastectomy with axillary lymph node dissection is tenuous and only based

lymphopenia mainly affects the thymus dependent (T-) lymphocytes Previous results (EASSON, FISCHER et coll) also suggest that postoperative irradiation may increase the risk of distant metastases In the present material distant metastases occurred in 9 irradiated cases in stage II within the first year against none in the control group, which might suggest that postoperative irradiation enhances the risk of distant metastases However, in the controls stage I during the same period distant metastases occurred in 4 patients, i e twice as frequently as in the irradiated group This impairs the significance of the findings in the stage II patients Taken together, the results in stage I and stage II concerning time of occurrence of distant metastases *are confusing and difficult to explain* The results in stage II patients may support the hypothesis that postoperative irradiation may suppress the immunologic defence and thereby increase the risk of distant metastases

In the present material orthovoltage irradiation material only has been used and the dose to the skin and regional nodes has been rather small Even though postoperative irradiation with this technique decreased the incidence of local recurrence and regional metastasis, it had no influence on the proportion of disease free patients nor on the survival rate Only every fifth of the controls in stage I and every second in stage II needed radiation at a later date because of recurrent disease By giving up routine postoperative radiation with the employed technique particularly in stage I and using it later if need arises many patients with mammary carcinoma could be spared unnecessary radiation However, different results may possibly be obtainable by other treatment fields and by increasing the dose, which will be discussed in Part II

Acknowledgements

The authors are indebted to dr phil Knut Magnus for statistical advice and to Ashton Miller, M D, F R C S for reviewing the manuscript

SUMMARY

The effect of routine postoperative irradiation in the treatment of carcinoma of the breast has been evaluated Postoperative irradiation had no effect on the proportion of patients free of disease nor on the survival rate, but the incidence of local recurrence and homolateral supraclavicular lymph node metastasis was reduced In stage II patients homolateral axillary lymph node metastases were also encountered less frequently *in the irradiated group* Distant metastases occurred earlier in stage II patients with postoperative irradiation as compared with controls

ZUSAMMENFASSUNG

Der Effekt der routinemässig vorgenommenen postoperativen Bestrahlung bei der Behandlung des Brustkarzinoms wurde festgestellt Die postoperative Bestrahlung hatte keinen Effekt auf den Anteil der Patienten, die frei von der Erkrankung waren oder auf die

upon data obtained retrospectively (HARRINGTON 1952, LEWISON & SMITH 1963, WATSON 1967) The results of two randomized prospective clinical trials (EASSON 1968, FISCHER et coll 1968) did not indicate benefit from postoperative irradiation in terms of survival In the Manchester trial two different types of radiation therapy were applied with the object of comparing the effect of irradiation administered immediately after surgery with that administered only when recurrences appeared No significant difference in survival between the groups was encountered Immediate postoperative irradiation reduced the incidence of local recurrence, but at the time of death the percentage of patients with uncontrolled local recurrence was almost identical in the two groups A possible increase in the incidence of liver metastases was observed in the irradiated patients Since only one-third of the controls required treatment at a later time for local recurrence, two-thirds of these patients were spared unnecessary irradiation

In the National Surgical Adjuvant Project Protocol (NSABP), a randomized clinical trial (FISCHER et coll) designed to evaluate the value of postoperative irradiation to parasternal, axillary and supraclavicular fields a minimum of 3 500 rad in no more than 3 weeks or 4 500 rad in no more than 5 weeks was required About 75 per cent of the patients received supervoltage irradiation and the remainder were given orthovoltage irradiation This therapy reduced the number of regional metastases, but was without influence on disease-free and crude survival The data suggested, however, that distant metastases occurred earlier in the irradiated group than in the control group

The present results have clearly demonstrated that it is essential when discussing the value of postoperative irradiation in carcinoma of the breast to differentiate between patients in stage I and stage II No effect of postoperative radiation in stage I as regards crude survival, disease-free survival, local recurrence, axillary lymph node or distant metastases was demonstrated Homolateral supraclavicular lymph node metastases were, in fact, more frequent in the control group (2 9 %) than in the irradiated group (0 6 %)

In stage II postoperative irradiation significantly reduced the incidence of homolateral supraclavicular lymph node metastases

Moreover, the proportion of patients with homolateral axillary lymph node metastases was less in the irradiated group (1 8 %) than in the control group (5 4 %) Local recurrence also occurred less frequently in the irradiated group (8 2 %) than in the control group (15 2 %), but postoperative irradiation had no influence on the incidence of distant metastases or on survival

The effect of postoperative irradiation on the immunologic defence of patients with malignancy is not fully understood Local radiation therapy could impair the cell-mediated immune response in patients with carcinoma of the breast by destroying lymphocytes STJERNSVARD et coll (1972) have demonstrated that irradiation of parasternal and supraclavicular fields in patients with carcinoma of the breast not only resulted in general lymphopenia of longstanding duration, but also that this

FROM THE RADIUM CENTRE, ODENSE HOSPITAL, DK-5000 ODENSE, DENMARK

NEUROLOGIC COMPLICATIONS AFTER IRRADIATION OF THE CERVICAL SPINAL CORD FOR MALIGNANT TUMOUR OF THE HEAD AND NECK

ULLA BRITT BÆKMARK

Serious, irreversible transverse lesions of the cervical spinal cord after irradiation of tumours in the head and neck have been reported (AHLBOM 1941, BODEN 1948, JACOBSSON 1951, VAETH 1965, VAN DEN BRENK et coll 1968) Neurologic deficits developed as a result of radiation myelitis in 103 out of 4 365 patients from 15 treatment series who had received irradiation of the cervical, thoracic or lumbar spinal cord (survey by PALMER 1972) In addition to transverse spinal lesions milder transient neurologic symptoms such as parasthesias and weakness of the extremities were also reported Taken together, the total incidence for mild and severe complications was 2 4 per cent

The total dose to the spinal cord, the treatment time, and the area of the field are some of the physical factors of significance in the development of radiation myelitis There is, however, no agreement regarding the significance of the dose-time relation (BODEN, VAETH) or of the treatment volume (PALLIS et coll 1961, JONES 1964) A review of the available reports reveals that in the majority of cases radiation myelitis occurs in patients treated with very high doses, with large doses over a short period, with large fields, or with an irradiation technique that produces a 'hot spot' in the spinal cord

In view of these observations special consideration to the dose to the spinal cord

Submitted for publication 5 July 1974

Überlebensrate, jedoch war das Vorkommen lokaler Recidive und homolateraler supra clavikularer Lymphknoten-Metastasen geringer Bei Grad II Patienten wurden homolaterale Lymphknoten-Metastasen der Axilla ebenfalls weniger haufig in der bestrahlten Gruppe angetroffen Fernmetastasen traten bei Grad II Patienten mit postoperativer Bestrahlung im Vergleich zu den Kontrollen haufiger auf

RÉSUMÉ

Les auteurs ont étudié l'effet d'une irradiation post-opératoire systématique dans le traitement du cancer de sein L'irradiation post-opératoire n'a pas d'effet sur la proportion de *malades guéries ni sur le taux de survie, mais elle réduit la fréquence des récidives locales* et des métastases ganglionnaires lymphatiques susclaviculaires homolatérales Chez les malades du stade II les métastases ganglionnaires lymphatiques axillaires homolatérales ont aussi été moins fréquentes dans le groupe de malades irradiées Les métastases à distance se sont produites plus tôt chez les malades du stade II ayant reçu une irradiation post opératoire que chez les témoins

REFERENCES

Easson E C Postoperative radiotherapy in breast cancer *In* Prognostic factors in breast cancer, p 118 Edited by A P Forrest and P B Kunkler, E & A Livingstone, Edin burgh 1968

Fischer B, Slack N H, Cavanaugh P J, Gardner B and Ravdin R G Postoperative radiotherapy in the treatment of breast cancer results of the NSABP clinical trial Ann Surg 168 (1968), 337

Guttmann R J Radiotherapy in locally advanced cancer of the breast Adjunct to stan dard therapy Cancer 20 (1967), 1046

Haagensen C D The treatment and results in cancer of the breast at Presbyterian Hospital, New York Amer J Roentgenol 62 (1949), 328

Halsted W S The results of operations for the cure of cancer of the breast performed at the Johns Hopkin's Hospital from June, 1889, to January, 1894 Johns Hopk Hosp Rep 4 (1894–95), 297

Harrington S W Results of surgical treatment of unilateral carcinoma of the breast in women J Amer med Ass 148 (1952) 1007

Lewison E F and Smith R I Results of breast cancer treatment at Johns Hopkins Hos pital 1946–1950 Surgery 53 (1963), 644

Marshall S F and Hare H F Carcinoma of the breast Results of combined treatment with surgery and roentgen rays Ann Surg 125 (1947), 688

Nissen-Meyer R Castration as part of the primary treatment for operable female breast cancer Acta radiol (1965) Suppl No 249

Stjernsvärd J, Jondal M, Vanky F, Wigzell M and Sealy R Lymphopenia and change in distribution of human B and T lymphocytes in peripheral blood induced by irradiation for mammary carcinoma Lancet (1972), 1352

Watson T A Carcinoma of the breast Stage II—radiation range Can survival be increased by postoperative irradiation following radical mastectomy? J Amer med Ass 200 (1967), 136



Fig. 2. Drawing and control film of field arrangement for irradiation with a mantle field

Standard treatment of carcinoma The volume of tumour tissue consisting of the primary tumour and the regional lymph nodes on the sides of the neck was treated as a rule through 2 opposing lateral fields with a safety margin of 2 to 3 cm (Fig 1) The area of the field varied as a rule within a range of 10 cm × 16 cm A dose of 5 700 rad in 6 weeks was used as the standard dose, and for postoperative irradiation the dose was reduced to 5 300 to 5 500 rad because of the risk of fibrosis

Standard treatment of malignant lymphomas Of 103 patients with malignant lymphomas 93 were irradiated via a mantle field All supradiaphragmatic lymph node groups were irradiated through opposing anteroposterior fields from the base of the cranium to Th 10 (Fig 2) A dose of 3 700 to 4 300 rad was given in the course of 28 to 30 days In 83 patients, the field was undivided, and the treatment distance 130 to 140 cm, in the 10 earliest cases, anteroposterior fields bordering on one another were used, which involved a possibility of over- and underdosage corresponding to the borderline No neurologic complications developed in these patients however

In 10 patients with localized lymphomas on the sides of the neck, opposing lateral fields were irradiated as in carcinoma, with a dose of 4 000 to 4 500 rad in 28 to 32 days

Neurologic symptoms and signs

The material was estimated from the aspect of the occurrence of all neurologic symptoms or signs arising after irradiation, including mild complications such as parasthesias in the fingers and toes

The observation time after completion of radiation appears in Table 1 As the more severe neurologic complications described in the literature occurred mainly in the period from 1 to 1½ years following treatment, the patients with an observation time of less than one year were evaluated separately The material was also

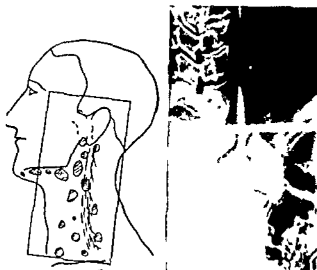


Fig 1 Drawing and control film of arrangements for irradiation to the neck with 2 opposing lateral fields

has not been paid at the Radium Centre since 1965, in the treatment of malignant tumours in the head and neck During the period February 1965 to December 1971, 165 patients with such tumours received irradiation which included the cervical spinal cord The records for these patients have been evaluated with reference to neurologic complications

Material The material consisted of 55 women and 110 men ranging in age from 6 weeks to 88 years, with the average age at 52 years The lesions in 62 cases were solid tumours in the head and neck and in 103 malignant lymphomas

All the patients were given high energy irradiation, the entire cervical cord was included in all cases, and the thoracic segment as well in 93 cases The observation time was in all cases at least 1½ years after completion of irradiation, except for those who died of their illness before the end of this time

Technique of irradiation

Simple treatment arrangements with 2 opposing fields, 'standard fields', were mostly used The patients were irradiated with photons from ^{60}Co (6 000 Ci) or a 6 MeV linear accelerator The treatment distance varied between 80 and 130 cm

In order to achieve homogeneous dose distribution in irradiated areas with differing tissue thicknesses, individually prepared compensation filters of aluminium blocks have been used since 1966 In most cases, the irradiation was given daily to both fields, 5 days a week The general aim was to give a weekly tumour dose of 1 000 rad During irradiation, the patients were immobilized in a plaster or plastic cast The field adjustments were performed under fluoroscopy, and control films of the field arrangements were obtained

Table 4

Distribution of tumour dose and neurologic symptoms in 113 patients under observation for more than 1 year

	Dose (rad)					Total
	<3 000	3 000–3 999	4 000–4 999	5 000–5 999	6 000–6 200	
No of patients	4	56	30	21	2	113
Neurologic complications	0	13	6	0	0	19

In one patient who had not received cytostatic treatment, slight weakness in both legs developed three months after irradiation The patient was a man of 43 with carcinoma of the epiglottis, T3 N2 M0, who was irradiated through 2 opposing lateral fields with a tumour dose of 5 700 rad in 42 days The symptoms disappeared within one month Three months later, he died of his original disease without any neurologic deficits

Observation time of 1 to 6 years A total of 113 patients were observed for 1 to 6 years after completion of irradiation, 46 were observed for more than 2 years and 61 for more than 3 years (Table 1) The neurologic complications in relation to the size of the dose to the spinal cord and the use of cytostatic compounds are given in Tables 4 and 5

Mild, transitory neurologic deficits, in the form of hypoesthesias or paresthesias in the peripheral parts of the extremities, were observed in 19 patients, all of whom had been irradiated via mantle fields and with a dose varying from 3 000 rad to 4 400 rad in 3 to 4½ weeks In 12 of these patients, the symptoms arose in connection with cytostatic therapy and disappeared within a few months after this was discontinued one of them also had temporary weakness in the right arm, which arose after an exploratory laparotomy and was probably caused by an incorrect position

Table 5

Occurrence of neurologic symptoms in relation to cytostatic treatment in 113 patients observed for more than 1 year

	Cytostatic agents		Total
	Given	Not given	
Without complications	73	21	94
With complications	7	12	19
Total	80	33	113

Table 1

Observation time after radiation therapy in 165 patients

Observation time (years)	0–1	1–2	2–3	3–4	4–5	5–6	Total
No of patients	52	27	25	36	11	14	165

Table 2

Distribution of tumour dose and neurologic symptoms in 52 patients under observation for less than 1 year

	Dose (rad)					Total
	<3 000	3 000–3 999	4 000–4 999	5 000–5 999	6 000–6 200	
No of patients	3	11	17	17	4	52
Neurologic complications	1	1	1	1	0	4

divided up according to the size of the dose to the spinal cord and whether cytostatic agents had been used during the observation period The cytostatic treatment included in all cases vincristine (oncovin), which is known to be neurotoxic (WHITELAW et coll 1963)

Observation time of less than 1 year Fifty-two patients died within 1 year after completion of treatment The neurologic complications in relation to the size of the dose to the spinal cord and the use of cytostatic agents are given in Tables 2 and 3

Mild, transitory paresthesias in the fingers and toes occurred in 3 of the 14 patients who received cytostatic therapy after the primary irradiation These symptoms arose immediately after the treatment with cytostatic agents and they were attributed to those agents The dose varied in these patients between 3 000 and 4 000 rad in 3 to 4 weeks

Table 3

Occurrence of neurologic symptoms in relation to cytostatic treatment in 52 patients under observation for less than 1 year

	Cytostatic agents		Total
	Given	Not given	
Without complications	37	11	48
With complications	1	3	4
Total	38	14	52

Table 6

Review of possible causes of some of the neurologic complications following irradiation of the cervical spinal cord reported in the literature

Reference	No of patients treated	No of cases with cervical myelitis	Dose	Ret	Possible cause			
					Over-dosage (1 700 ret)	Over-lapping of fields	No compli-cations	Other comments
AHLBOM (1941)	235	4/4						Dose not reported
BODEN (1948)	161	10/10	2 000 R/1 day –5 200 R/17 days	1 090–2 080	4			
BUSCHKE (1963)	125	6/6	7 000–8 000 rad/ 50 days	1 950–2 220	6			
DYNES & SMEDAL (1960)	800	3/10	4 350 R/18 days –6 750 R/69 days	1 740–2 300	1	5	3	1 rotation therapy
JACOBSSON (1951)	322	13/13	5 000 R/20 days –6 000 R/30 days	1 710–1 780	13			Dose not reported especially for patients who developed complications
PALMER (1972)	Not reported	4 12	3 920 rad/30 days –7 700 rad 59 days	1 500–1 925	1	2	4	
REAGAN et coll (1968)	1 018	8/10	4 000 rad/10 days –6 900 rad 43 days	1 350–1 900	5	1	3	
VAETH (1965)	166	3/3	4 800 rad/27 days –6 000 rad/56 days	1 520–1 580				

estimated to 5 000 rad (FLETCHER et coll 1962, RUBIN & CASARETT 1968) Our results suggest, however, that with fields of an area corresponding to about 10 cm × 16 cm a dose of up to 6 000 rad may be given to the spinal cord without serious complications, if the irradiation is extended over 6 weeks It should be pointed out, however, that only 23 of the patients who received more than 5 000 rad to the cord have been under observation for longer than one year

A tolerance level of 5 000 rad to the spinal cord presents a therapeutic dilemma in the majority of cancer forms, when irradiation is to be applied An attempt to

of the arm during narcosis In 7 patients, the neurologic complications could be attributed to the irradiation A common characteristic for these 7 patients was that they were all cases of Hodgkin's disease, and were irradiated with a mantle field, in two instances supplemented with an inverted Y field; the dose was in all instances 3 500 to 3 700 rad in 28 to 29 days

Discussion

The clinical symptoms and signs in radiation myelitis can be divided into 2 main types, reversible and irreversible (PALMER) The milder, transient cases, with paresthesias in the extremities, usually arise three to six months after completion of irradiation (DYNES & SMEDAL 1960) If the symptoms are aggravated by flexion or extension of the cervical portion of the vertebral column the designation L'Hermitte's sign is often used These symptoms disappear as a rule within a few months The irreversible type manifests itself as symptoms and signs of varying severity, up to total para- or tetraplegia with paralysis of the sphincter The latent period before the appearance of these complications varies, in different reports, but the average time stated is 1 to 1½ years The present material differs from other series in which radiation myelitis was mentioned through the fact that many of the patients received cytostatic treatment, including vincristine (oncovin), in addition to irradiation As this drug often gives rise to neurologic complications that may be confused with radiation myelitis the patients given vincristine were evaluated separately Neurologic deficits occurred in 15 (30 per cent) of 47 who received the drug, whereas only 8 (6 8 per cent) out of 118 not given vincristine developed such symptoms (Tables 2, 5) In the vincristine-treated patients, the nature of the deficits and their close time-relationship to the cytostatic therapy excludes the likelihood that they could reasonably be interpreted as being signs of radiation myelitis

In 8 patients, the neurologic complications could be attributed to the radiation treatment, 7 were patients with Hodgkin's disease who had received mantle treatment Both the cervical and thoracic parts of the spinal cord were included in the treatment field This suggests that the risk of neurologic complications increases appreciably with increasing area of the field The eighth patient was the one mentioned with an observation time less than one year

A total of 69 patients were treated by a mantle field, and signs of radiation myelitis arose in 7 of them, corresponding to a frequency of 10 per cent, 63 of these patients had Hodgkin's disease All the complications were mild and reversible, and were probably due to affection of the nerve roots (No electromyography was carried out)

Neurologic complications similar to those in the present material have been described in connection with the active form of Hodgkin's disease, but an accumulation of 7 active case of Hodgkin's disease in a total of 63 cases is hardly likely Doses to the spinal cord of over 5 000 rad were given to 44 patients (Tables 2, 4), most of them received 5 700 rad in 6 weeks Only 1 of these 44 patients developed mild transitory signs of radiation myelitis The spinal cord tolerance limit has been

de maladie de Hodgkin qui avaient reçu jusqu'à 3 700 rad par des champs en mantelet Une revue des publications sur les lesions transverses de la moelle provoquées par les radiations a montré la possibilité d'un surdosage dans plusieurs cas, c est pourquoi les limites tolérance de dose mentionnées auparavant devraient etre appliquees avec precaution

REFERENCES

AHLBOM H E The results of radiotherapy of hypopharyngeal cancer at the Radiumhemmet, Stockholm 1930-1939 Acta radiol 22 (1941), 155

BODEN G Radiation myelitis of the cervical spinal cord Brit J Radiol 21 (1948), 464

of cancers of the oral cavity and oropharynx Charles C Thomas Springfield, Ill 1962

HUNG T P Myelopathy following radiotherapy of nasopharyngeal carcinoma Proc Aust Ass Neurol 5 (1968), 421

JACOBSSON F

Radium

JONES A

paresthesias) Brit J Radiol 37 (1964) 727

PALMER J J

PALLIS C A, L

REAGAN T J

pathy J Amer med Ass 205 (1968), 106

RUBIN P and CASARETT G W Clinical radiation pathology Vol II W B. Saunders, Philadelphia 1968

VAETH J Radiation induced myelitis *In* Progress in radiation therapy Vol III, p 16 Grune & Stratton, New York 1965

VAN DEN BRENK H A S, RICHTER W and HURLEY R H Radiosensitivity of the human oxygenated cervical spinal cord based on analysis of 357 cases receiving 4 MeV X rays in hyperbaric oxygen Brit J Radiol 41 (1968), 205

WHITELAW D M COWAN O H, CASSIDY F T and PATTERSON T A Clinical experience with vincristine Cancer Chemother Rep 30 (1963), 13

avoid including the spinal cord in the irradiation involves a risk of underdosage of tumour-affected areas, this has to be *weighed against the risk of producing radiation* myelitis

A review of the materials describing serious irreversible neurologic complications (Table 6) reveals without *question in several cases the possibility of direct overdosage* (defined here as a dose larger than 1 700 ret) overdosage to the cord as a result of irradiation via fields bordering on one another with the concomitant risk of a 'hot spot' at the border, or overdosage because a *compensation filter was not used in* connection with varying surface levels and different tissue thicknesses These materials can thus only be used with reservation as an indication of the limit of tolerance of the spinal cord to *irradiation In the present material, in which a simple treatment* technique, undivided fields, and the use of a compensation filter were applied, the dose homogeneity may be considered reasonable

SUMMARY

A total of 165 patients with tumours of the head and neck were irradiated via fields including the entire cervical portion of the spinal cord Eight patients (4 8 per cent) developed mild reversible signs of radiation myelitis Only one of these cases was found among the 44 patients who received a dose to the spinal cord of over 5 000 rad via fields of less than 16 cm in length, 7 cases were patients with Hodgkin's disease who were given up to 3 700 rad via mantle fields A survey of previous reports on transverse spinal lesions provoked by irradiation revealed a possibility of overdosage in several cases, and dose tolerance limits mentioned previously should accordingly be applied with caution

ZUSAMMENFASSUNG

Insgesammt wurden 165 Patienten mit Tumoren des Kopfes und Nackens mit Feldern bestrahlt, die den gesamten cervikalen Teil des Ruckenmarks umfassten Acht Patienten *(4,8 %) entwickelten leichte reversible Zeichen einer Strahlenmyelitis Es wurde* unter den 44 Patienten, die eine Ruckenmarks-Dosis von uber 500 rad durch Felder von weniger als 16 cm in der Lange erhalten hatten, nur ein Fall gefunden, 7 Fallen waren Patienten mit Hodgkin'scher Ekrankung, denen bis zu 3 700 rad durch Mantelfelder gegeben worden war Eine Übersicht alterer Berichte uber Querschnittslahmungen, hervorgerufen durch Bestrahlung, liess die Moglichkeit der Überdosierung in verschiedenen Fallen erkennen, und fruher genannte Dosis Toleranz-Grenzen sollten entsprechend mit Vorsicht verwendet werden

RÉSUMÉ

Un total de *165 malades atteints de tumeurs de la tête et du cou* ont été irradiés par des champs comprenant la totalité de la moelle cervicale Huit malades (4 8 %) ont présenté des signes de myélite radiothérapique peu sévère et réversible Parmi les 44 malades qui avaient reçu une dose à la moelle de plus de 500 rad par des champs de moins de 16 cm de long un seul a présenté des signes de myélite, *les 7 autres cas étaient des malades atteints*

Table 1

Distribution by clinical stage of patients with radiation therapy only

Clinical stage	No of patients	5 year cure	
		No	%
IA	35	35	100
IB	60	53	88
IIA	60	39	65
IIB	53	21	40
III	38	6	16
IV	19	2	(11)
Total	265	156	59

therapy and followed up for 5 years The distribution by stage is presented in Table 1 Free of symptoms 5 years after the treatment were 156 patients (59 per cent) while 109 developed recurrence during the follow up period

Methods

Primary radiation therapy The individualized Stockholm technique (KOTTMEIER 1964 a) was used for patients given irradiation only The doses delivered by intracavitary irradiation were estimated by direct measurement in the bladder and rectum to reduce the frequency of complications (KOTTMEIER & GRAY 1961) In most cases the treatment was started with two intracavitary applications of radium at an interval of 3 weeks, the amount in the uterus as well as in the vagina varying between 45 and 100 mg and the treatment time between 20 and 27 hours for each course The rectal dose was usually about 4 500 rad, sometimes below the bladder dose was less than 5 000 rad External irradiation was given to all patients except 35 in clinical stage IA to increase the dose to the lateral parametria and pelvic walls to 5 000 rad or 6 000 rad in more advanced cases The total dose to the rectum did not exceed 5 000 rad and that to the bladder not 6 000 rad A few patients were first given external irradiation followed by intracavitary applications of radium in the uterus and vagina the total dose delivered and the dose distribution were the same

The external irradiation was usually delivered by two opposing fields with central shielding blocks and sometimes with 1 frontal and 2 lateral fields, using ^{60}Co as the radiation source the weekly tumour dose was 800 rad, given in 5 daily fractions The pelvic dose distribution with this technique has been reported by KOTTMEIER (1964 a) RANLOD (1966) and JOELSSON (1970)

The patients given combined therapy by radiation and surgery received 2 intracavitary applications of radium by the same technique and with the same dose as those treated by irradiation alone this was followed by radical surgery by the Wertheim Meig method In 4 patients where lymph node metastases were found during

FROM THE DEPARTMENT OF GYNECOLOGY (DIRECTOR B TJERNBERG), RADIUMHEMMET, KAROLINSKA SJUKHUSET, S-104 01 STOCKHOLM, SWEDEN

FREQUENCY OF SEVERE COMPLICATIONS AFTER RADIATION THERAPY FOR CERVICAL CARCINOMA

NINA EINHORN

A determination of the frequency of late complications of primary radiation therapy for cervical carcinoma constitutes a complex problem, it may be difficult to distinguish early symptoms produced by a recurrence from those due to radiation injury Moreover, the clinical picture may be confused by complications arising from *additional irradiation or surgery for the recurrence This report is a retrospective* analysis of the frequency of severe complications following radiation therapy for cervical carcinoma in patients with and without recurrence manifested during a long follow-up period

Material

The material comprised 321 patients treated at Radiumhemmet for cervical carcinoma during 1967 and followed up for 5 years Of these, 38 were given combined irradiation and surgical treatment and were analysed separately Fifteen patients receiving irradiation as the only primary treatment died from intercurrent disease within 5 years and 3 residing abroad were not followed up Since the aim was to analyse the frequency of complications, rather than the cure or survival rate, the main analysis was performed on the remaining 265 patients with primary radiation

Submitted for publication 1 August 1974

Table 1

Distribution by clinical stage of patients with radiation therapy only

Clinical stage	No of patients	5-year cure	
		No	%
IA	35	35	100
IB	60	53	88
IIA	60	39	65
IIB	53	21	40
III	38	6	16
IV	19	2	(11)
Total	265	156	59

therapy and followed up for 5 years The distribution by stage is presented in Table 1 Free of symptoms 5 years after the treatment were 156 patients (59 *per cent*) while 109 developed recurrence during the follow-up period

Methods

Primary radiation therapy The individualized Stockholm technique (KOTTMEIER 1964 a) was used for patients given irradiation only The doses delivered by intracavitary irradiation were estimated by direct measurement in the bladder and rectum to reduce the frequency of complications (KOTTMEIER & GRAY 1961) In most cases the treatment was started with two intracavitary applications of radium at an interval of 3 weeks, the amount in the uterus as well as in the vagina varying between 45 and 100 mg and the treatment time between 20 and 27 hours for each course The rectal dose was usually about 4 500 rad, sometimes below, the bladder dose was less than 5 000 rad External irradiation was given to all patients except 35 in clinical stage IA to increase the dose to the lateral parametria and pelvic walls to 5 000 rad or 6 000 rad in more advanced cases The total dose to the rectum did not exceed 5 000 rad, and that to the bladder not 6 000 rad A few patients were first given external irradiation, followed by intracavitary applications of radium in the uterus and vagina the total dose delivered and the dose distribution were the same

The external [illegible]

shielding [illegible]

radiation [illegible] weekly tumour dose was 800 rad, given in 5 daily fractions The pelvic dose distribution with this technique has been reported by KOTTMEIER (196[illegible]

T[illegible] received 2 intracav[illegible] of radium by the same technique and with the same dose as those treated by irradiation alone, this was followed by radical surgery by the Wertheim-Meig method In 4 patients, where lymph node metastases were found during

Table 2

Frequency of severe complications in patients without and with recurrence within 5 years primary radiation therapy only

Clinical stage	No recurrence			Recurrence		
	Total	Complications		Total	Complications	
		No	%		No	%
IA	35	1	2 8	0	—	—
IB	53	0	0	7	1	14
IIA	39	1	2 6	21	6	29
IIB	21	0	0	32	7	22
III	6	1	(17)	32	9	28
IVA	2	0	0	17	2	(11)
Total	156	3	1 9	109	25	23

operation, external radiation therapy was delivered, again with the same technique and dose as were used in the patients treated by irradiation only

Follow-up If no recurrence was indicated or the patients displayed no symptoms they were followed at intervals of 2 months during the first year after treatment, and then at increasing intervals of 3 to 6 months Only 3 patients, residing abroad, were lost to follow-up None of the 15 patients who died from intercurrent diseases during the follow-up had developed symptoms or signs of any severe complication

Treatment of recurrences Recurrence occurred in 109 patients after irradiation only, of these 17 were treated by electrosurgery, the unipolar fulguration technique (KOTTMEIER 1954) was used In 15 cases supplementary external irradiation was delivered, usually unilaterally, as a palliative measure to alleviate symptoms from metastases on the lateral pelvic wall The majority of the remaining 77 patients, as well as the 7 patients with recurrence after combined treatment, were given chemotherapy, some had no specific treatment aimed at influencing the tumour growth

Definition of complications It is always difficult, particularly in retrospect, to define and demarcate the more severe complications Since the main purpose of the present analysis was to establish the relative frequency of such complications in different groups of patients, those complications were considered severe which required surgical intervention, this provided a well defined group However, fairly severe manifestations, such as anorexia, loss of weight and intermittent diarrhoea, do not motivate surgery

Results

Primary mortality None of the patients died during the first 3 months after primary treatment

Table 3

Severe complications in patients with recurrence Distribution according to treatment

Treatment for recurrence	No of patients	Severe complications	
		No	%
Supplementary irradiation	15	5	(33)
Electrosurgery	17	4	(23)
Other treatment	77	12	14
Total	109	20	18

Irradiation only Severe complications that motivated surgical intervention were observed within 5 years in 28 of the 265 patients, i e a frequency of 11 per cent The distribution in relation to clinical stage is given in Table 2 Severe complications were found in only 3 of the 156 patients without recurrence (1 9 per cent) The remaining 25 were among the 109 with recurrence, i e a frequency of 23 per cent for this group (Table 2)

The recurrence was treated by electrosurgery in 17 patients, 4 developed severe complications, radiation therapy was administered to 15, 5 developed such complica tions i e a frequency of about 28 per cent for those two groups combined Of the 77 patients treated neither by electrosurgery nor by irradiation for the recurrence, 14 per cent developed symptoms or signs considered as a severe complication requiring surgical intervention (Table 3)

Three patients presented severe complications requiring surgery but had no known recurrence during the follow up period Rectovaginal fistula occurred in 2 and rectal stenosis in one, manifest from 7 months to 4 years after the primary treatment Colostomy was performed in 2 of the patients, one fistula and the rectal stenosis healed spontaneously

Combined therapy Thirty-eight patients were subjected to intracavitary radium and radical surgery, severe complications occurred in 5, 3 being in the group of 31 cured patients and in 2 in the group of 7 patients with recurrences All 4 patients with supplementary external irradiation for lymph node metastases were among the 5 patients with severe complications (Table 4) Only 1 of the 34 patients without this supplementary treatment developed such complications

Discussion

A tendency for a higher frequency of severe complications existed in those patients with initially more advanced tumours as may be expected (Table 2), this may be due to the higher radiation doses and the larger treatment fields used in more advanced tumours However, rectovaginal fistula developed in 1 of 35 patients in stage IA, who were given intracavitary applications of radium only

Table 2

Frequency of severe complications in patients without and with recurrence within 5 years primary radiation therapy only

Clinical stage	No recurrence			Recurrence		
	Total	Complications		Total	Complications	
		No	%		No	%
IA	35	1	2 8	0	—	—
IB	53	0	0	7	1	14
IIA	39	1	2 6	21	6	29
IIB	21	0	0	32	7	22
III	6	1	(17)	32	9	28
IVA	2	0	0	17	2	(11)
Total	156	3	1 9	109	25	23

operation, external radiation therapy was delivered, again with the same technique and dose as were used in the patients treated by irradiation only

Follow-up If no recurrence was indicated or the patients displayed no symptoms they were followed at intervals of 2 months during the first year after treatment, and then at increasing intervals of 3 to 6 months Only 3 patients, residing abroad, were lost to follow-up None of the 15 patients who died from intercurrent diseases during the follow-up had developed symptoms or signs of any severe complication

Treatment of recurrences Recurrence occurred in 109 patients after irradiation only, of these 17 were treated by electrosurgery, the unipolar fulguration technique (KOTTMEIER 1954) was used In 15 cases supplementary external irradiation was delivered, usually unilaterally, as a palliative measure to alleviate symptoms from metastases on the lateral pelvic wall The majority of the remaining 77 patients, as well as the 7 patients with recurrence after combined treatment, were given chemotherapy, some had no specific treatment aimed at influencing the tumour growth

Definition of complications It is always difficult, particularly in retrospect, to define and demarcate the more severe complications Since the main purpose of the present analysis was to establish the relative frequency of such complications in different groups of patients, those complications were considered severe which required surgical intervention, this provided a well defined group However, fairly severe manifestations, such as anorexia, loss of weight and intermittent diarrhoea, do not motivate surgery

Results

Primary mortality None of the patients died during the first 3 months after primary treatment

Table 3

Severe complications in patients with recurrence Distribution according to treatment

Treatment for recurrence	No of patients	Severe complications	
		No	%
Supplementary irradiation	15	5	(33)
Electrosurgery	17	4	(23)
Other treatment	77	12	14
Total	109	20	18

Irradiation only Severe complications that motivated surgical intervention were observed within 5 years in 28 of the 265 patients, i e a frequency of 11 per cent The distribution in relation to clinical stage is given in Table 2 Severe complications were found in only 3 of the 156 patients without recurrence (1 9 per cent) The remaining 25 were among the 109 with recurrence, i e a frequency of 23 per cent for this group (Table 2)

The recurrence was treated by electrosurgery in 17 patients, 4 developed severe complications, radiation therapy was administered to 15, 5 developed such complications, i e a frequency of about 28 per cent for those two groups combined Of the 77 patients treated neither by electrosurgery nor by irradiation for the recurrence, 14 per cent developed symptoms or signs considered as a severe complication requiring surgical intervention (Table 3)

Three patients presented severe complications requiring surgery but had no known recurrence during the follow up period Rectovaginal fistula occurred in 2 and rectal stenosis in one, manifest from 7 months to 4 years after the primary treatment Colostomy was performed in 2 of the patients, one fistula and the rectal stenosis healed spontaneously

Combined therapy Thirty eight patients were subjected to intracavitary radium and radical surgery, severe complications occurred in 5, 3 being in the group of 31 cured patients and in 2 in the group of 7 patients with recurrences All 4 patients with supplementary external irradiation for lymph node metastases were among the 5 patients with severe complications (Table 4) Only 1 of the 34 patients without this supplementary treatment developed such complications

Discussion

A tendency for a higher frequency of severe complications existed in those patients with initially more advanced tumours as may be expected (Table 2), this may be due to the higher radiation doses and the larger treatment fields used in more advanced tumours However, rectovaginal fistula developed in 1 of 35 patients in stage IA, who were given intracavitary applications of radium only

Table 4

Frequency of severe complications in patients with combined treatment

Clinical stage	No of patients	No recurrence			Recurrence		
		Total	Complications		Total	Complications	
			No	%		No	%
IA	1	1					
IB	15	13			2		
IIA	21	16	3*	18	5	2**	(40)
IIB	1	1					
Total	38	31			7		

* Two patients were given supplementary external irradiation postoperatively
** Both patients were given supplementary external irradiation postoperatively

The risk of complications in connection with radiation therapy may be reduced to some extent by careful dose planning and continuous observation of the patient during the irradiation. A certain frequency of complications must, however, be considered an inevitable consequence of curative irradiation for tumours of the pelvis. An increase in the radiation dose in cervical carcinoma has improved the survival rate, but has also produced a higher rate of severe late complications (KOTTMEIER 1961, 1964 b, JOELSSON et coll 1971). The radiation dose and the size of the volume to be irradiated constitute a dilemma: a more agressive approach will result in a higher survival and cure rate, but involves a greater frequency of complications. Extensive personal experience including knowledge of the frequency of complications and their management are mandatory.

Eleven per cent severe complications requiring surgery might seem discouraging, but it should be noted that for the patients remaining free of recurrence the frequency was less than 2 per cent. The figure is much higher for patients treated by electrosurgery because of recurrence (more than 20 per cent) or by additional radiation therapy (more than 30 per cent in a small material, Table 3). It is doubtful whether these forms of supplementary treatment are at all justified. It is notable, however, that 10 out of 17 patients treated by electrocoagulation for histologically or cytologically verified residue of local recurrence still presented no sign of recurrence 3 to 4 years afterwards.

Cytostatic therapy would seem to offer an alternative to the supplementary radiation therapy given to alleviate symptoms in the case of recurrence or metastases on the pelvic wall (EINHORN 1967). In experienced hands this therapy involves a lower frequency of severe complications.

The greatest interest, however, attaches to those patients that received radiation

therapy as the only primary treatment and developed severe complications motivating surgery In this group symptoms initially considered due to radiation complications in several of the patients were found in retrospect to be caused by recurrence of the tumour In addition, in the 156 patients remaining free of recurrence during the 5 year follow-up period the frequency of severe complications requiring surgical intervention was 1 9 per cent only

Complications after radiation therapy can occasionally be manifested after more than 5 years, even after more than 25 years (KOTTMEIER & GRAY 1961, YOUSSEF 1961) However, evidence of rectal injury usually appears 6 to 9 months after the initial irradiation, though the delay may be longer (KOTTMEIER 1964 b) Radiation injury to the colon and small bowel becomes manifest, on average, 13 months after treatment, but in about 4 per cent of cases with severe complications there is a lapse of 10 years or more (FABRIKANT et coll 1959) Radiation complications from the bladder, although on average appearing after a somewhat greater lapse of time, are usually manifested within 5 years after the treatment (KOTTMEIER 1961, 1964 b, BUCHLER et coll 1971) Thus, in the present series, severe complications may appear later on It will, however, probably be only in a few cases, and the number of complications observed during the 5-year follow-up period is to be considered as quite close to the actual final rate of complications

SUMMARY

An analysis of a material of 265 patients treated by radiation therapy for cervical carcinoma was performed with respect to severe complications The complication rate in patients free of recurrence was 1 9 per cent and in those with recurrence 23 per cent, which indicates that severe complications are often caused by recurrence of the tumour

ZUSAMMENFASSUNG

Es wurde eine Analyse eines Materials von 265 Patienten, die wegen eines Cervix Karzinoms Strahlentherapie unterzogen worden waren, hinsichtlich schwerer Komplikationen vorgenommen Die Komplikationsfrequenz bei Patienten, die frei von einem Rezidiv waren, betrug 1 9% und bei denen mit einem Rezidiv 23%, was darauf hindeutet dass schwere Komplikationen oft durch ein Rezidiv des Tumors verursacht werden

RÉSUMÉ

L auteur a analysé au point de vue des complications sévères une série de 265 malades traitées par les radiations pour un cancer d

REFERENCES

BUCHLER D A, KLINE J C, PECKHAM B M, BOONE M L and CARR W F Radiation reactions in cervical cancer therapy Amer J Obstet Gynec 111 (1971), 745

EINHORN N Effect of cyclophosphamide on pain in advanced carcinoma of the cervix Acta radiol Ther Phys Biol 6 (1967), 417

FABRIKANT J I, ANLYAN W G and CREADICK R N The management of radiation injuries to the intestines Sth med J 52 (1959), 1186

JOELSSON I Radiotherapy of carcinoma of the uterine cervix with special regard to external irradiation Acta radiol (1970) Suppl No 302

— RAF L and SÖDERBERG G Stenosis of the small bowel as a complication in radiation therapy of carcinoma of the uterine cervix Acta radiol Ther Phys Biol 10 (1971) 593

KOTTMEIER H L The treatment by fulguration of recurrent cancer of the cervix following radiation *In* Surgical treatment of cancer of the cervix Edited by J V Meigs Grune *& Stratton, New York 1954*

— (a) Erfahrungen des Radiumhemmet in Stockholm mit Hochvolttherapie beim Collumcarcinom Arch Gynäk 202 (1964), 305

— (b) Complications following radiation therapy in carcinoma of the cervix and their treatment Amer J Obstet Gynec 88 (1964), 854

— and GRAY M J Rectal and bladder injuries in relation to radiation dosage in carcinoma of the cervix Amer J Obstet Gynec 82 (1961), 74

RANUDD N E Dose distribution studies in external irradiation of carcinoma colli uteri Acta radiol Ther Phys Biol 4 (1966), 353

YOUSSEF A F Gynecological urology Charles C Thomas publisher, Springfield 1961

FROM THE RADIUM CENTRE (DIRECTOR SIGVARD KAAE) AND THE E N T. DEPARTMENT (DIRECTOR H C ANDERSEN), MUNICIPAL HOSPITAL, UNIVERSITY OF ÅRHUS, DK-8000 ÅRHUS, DENMARK

CARCINOMA OF THE LARYNX

IV Recurrences more than 5 years after primary treatment

KARSTEN JØRGENSEN

During the period January 1944 to August 1968 400 patients with carcinoma of the larynx were treated at the Municipal Hospital, Århus In 366 (91 5 per cent) of the cases the primary treatment was irradiation and in 34 (8 5 per cent) surgery The material has been analysed and the results of treatment reported previously (JØRGENSEN 1970, 1974, JØRGENSEN & SELL 1971) The present report concerns recurrences appearing more than 5 years after the primary treatment and the survival after 10 years of observation

Recurrences The great majority of recurrences appeared during the first 2 years of observation During the period August 1963 to August 1968 152 patients were treated and 53 displayed recurrences during the first 2 years, but only five altogether during the third, fourth and fifth years

The number of recurrences during the period 5 to 10 years of observation appears in Table 1 This table was designed to estimate the annual recurrence rate which (in per cent) was calculated from the formula $\frac{G \times 100}{E + ((A + C)/2)}$ (The factors G, E, A and C are defined in Table 1) The formula is intended to elucidate that the rate is dependent

---

This investigation was supported by a grant from the Danish Anti Cancer League Submitted for publication 11 September 1974

Table 1

The fate of 261 patients with carcinoma of the larynx during the period from 5th to 10th year of observation The table is used for cumulative survival rate calculation and evaluation of frequency of late recurrences

	Year of observation					
	6th	7th	8th	9th	10th	11th
A Number of deaths from other causes than carcinoma of the larynx during year	8	9	8	8	8	
B Number of deaths from carcinoma of the larynx during year	1	3*	0	0	0	
C Withdrawn alive recurrence free during year	14	28	16	21	13	
D Withdrawn alive with recurrence during year	0	0	0	1	1	
E Alive at beginning of year without recurrence	256	234	196	172	143	122
F Alive at beginning of year	261	238	198	174	144	122
G Number of recurrences during year	3	1	2	1	3	0
H Recurrence rate during year (%)	1 2	0 5	1 1	0 6	2 3	0 0

* This group includes the patients dying from a late recurrence

on the number of patients exposed to the risk of developing a recurrence in a certain year All cases with recurrences had been irradiated primarily However, the 34 primary operated patients were also included in the recurrence rate calculations Hence, the late recurrence rates for patients with primary irradiation are slightly higher

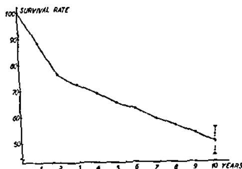
Ten patients developed recurrences, on average, a little more than 1 per cent a year, all of them in loco or in the marginal area of the location of the original tumour Only 2 recurrences occurred after more than 10 years One was almost certainly a new tumour, the original one being a T1N0M0 (UICC 1972) on the left vocal cord and the new tumour appearing in the right ventricular band In the second case the recurrence occurred in loco

The regional lymph nodes were not involved in any of the patients The treatment of these 12 cases (11 recurrences and one new tumour) appears in Table 2 Two pi-

Table 2

Treatment of 12 cases of recurrences appearing more than 5 years after primary treatment

Partial laryngectomy	6 patients
Partial laryngectomy Later total laryngectomy	2 patients
Total laryngectomy	3 patients
Palliative irradiation	1 patient
Total	12 patients



Survival rate (per cent) for 400 patients with carcinoma of the larynx Twice standard error is marked on the curve

tients had a partial laryngectomy made total, and in one of them 8 years had passed between the two operations One patient, old and feeble, had palliative irradiation Apart from this patient, no patients had died from or with recurrence after surgery No surgical complications appeared

The survival was calculated per August 1973 when 248 patients had been observed for more than 10 years and 152 for 5 to 10 years The crude 10-year survival rate for the former group was 49 per cent (122/248), the group of 152 patients had a 5-year crude survival rate of 68 per cent (104/152) A cumulative 10-year survival rate of all 400 patients was calculated after dividing the material as in Table 1 The mortality coefficient Q for the individual year of the follow up period was calculated and the corresponding survival coefficient was 1 – Q The cumulative 10 year survival was 50 4 per cent The survival rates of the individual years of observation are plotted in the Figure Standard error of the 10-year result was calculated using Greenwood's formula and twice standard error was found to be 5 23 per cent (For further information as to mode of calculation, see JØRGENSEN & SELL)

Discussion

The frequency of late recurrences was low In a series of 414 cases of carcinoma of the larynx all primarily irradiated, RYGAARD & HANSEN (1966) reported 11 cases of recurrences appearing 5 to 13 years after treatment, i e a frequency of the same order as the present one

It has been discussed whether late recurrences were to be considered as new, independent tumours possibly irradiation induced (SVANE KNUDSEN 1960, FALBE-HANSEN & JAZBI 1966) Apart from one case, all recurrences appeared at the site of the primary tumour or its immediate vicinity which indicates that late recurrences in the present material were almost exclusively ordinary recurrences and not new independent tumours MARKS et coll (1973) in a retrospective analysis of 134 cases of early glottic carcinoma, came to the same result However, late recurrences differ from early ones, viz half of the cases could be treated by partial laryngectomy It is

likely that also their histology differs and the result of a histologic grading, following the rules of JAKOBSSON (1973) not only the primary tumours but also of the recurrences would be most interesting

The low frequency of late recurrences and their benign behaviour indicate that there is no need for frequent follow up examinations of patients free of recurrence more than 5 years after the primary treatment In the present material these patients were examined once a year up to 10 years, which seems rational as only 2 recurrences occurred more than 10 years after the primary treatment

The declination of the survival curve in the Figure depends on two factors, the mortality from laryngeal carcinoma and from other causes The latter factor is the most important one after the 5th year of observation (Table 1), i e the declination of the last part of the survival curve is determined mainly by mortality from causes other than carcinoma of the larynx

SUMMARY

The annual frequency of recurrences appearing during the 5th to 10th year of observation was a little more than 1 per cent a year A formula is described for calculating this frequency Apart from one case all 12 late recurrences were ordinary recurrences and not new independent tumours Mortality was almost exclusively attributable to causes other than carcinoma of the larynx

ZUSAMMENFASSUNG

Die jahrliche Frequenz von Ruckfallen, die wahrend des 5 bis 10 Jahres der Untersuchung auftrat, betrug etwas mehr als 1 Prozent im Jahr Abgesehen von einem Fall waren alle spaten Ruckfalle gewohnliche Rezidive und nicht neue unabhangige Tumoren Die Mortalitat war beinahe ausschliesslich anderen Ursachen als dem Laryngx-Karzinom zuzuschreiben

RÉSUMÉ

La fréquence annuelle de récidive de cancer du larynx apparaissant de la cinquième à la dixième année d observation a été un peu supérieure à 1 % par an L auteur donne une formule pour calculer cette frequence A l'exception d un cas les 12 récidives tardives étaient des récidives ordinaires et n'étaient pas de nouvelles tumeurs indépendantes La mortalité a éte presque exclusivement due à d'autres causes que le cancer du larynx

REFERENCES

FALBE-HANSEN J and JAZBI B Late recurrences of laryngeal cancer which had been treated exclusively by Coutard irradiation or by operation plus irradiation Acta otolaryng (Stockh) (1966) Suppl No 224, p 492

JAKOBSSON P Glottic carcinoma of the larynx Thesis Stockholm 1973

JORGENSEN K Carcinoma of the larynx I Treatment mainly by primary irradiation Acta radiol Ther Phys Biol 9 (1970) 401

— Carcinoma of the larynx III Therapeutic results Acta radiol Ther Phys Biol 13 (1974) 446

— and SELL A Carcinoma of the larynx II Treatment by ^{60}Co supervoltage irradiation Acta radiol Ther Phys Biol 10 (1971) 161

MARKS J E, LOWRY L D, LERCH I and GRIEM M L Glottic cancer An analysis of recurrences as related to dose time and fractionation Amer J Roentgenol 117 (1973), 540

RYGAARD J and HANSEN H S Five year symptom free survival rate of 414 consecutive cases of laryngeal cancer referred to the Radium Centre Copenhagen Acta oto-laryng [illegible]

[illegible] penhagen 1960

FROM THE DEPARTMENTS OF RADIATION THERAPY AND OF RADIATION PHYSICS, AKADEMISKA SJUKHUSET, THE UPPSALA UNIVERSITY DATA CENTER AND THE DEPARTMENT OF COMPUTER SCIENCE, UNIVERSITY OF UPPSALA, S-750 14 UPPSALA, AND SIEMENS ELEMA, S-171 95 SOLNA, SWEDEN

CELL KINETIC APPROACH TO OPTIMISING DOSE DISTRIBUTION IN RADIATION THERAPY

S GRAFFMAN, T GROTH, B JUNG, G SKÖLLERMO and J-E SNELL

The results of tumour treatment by irradiation is, among other things determined by the distribution of tumour cells, the sensitivity of tumour and healthy tissue and *the distribution of radiation dose in space and time*

Before an optimum treatment can be selected it is necessary to be able to predict the effect of different dose distributions on a tumour of given type and extent There is little hope that controlled clinical trials will provide an understanding of the conditions in detail (GRAFFMAN & JUNG 1970), but the problem may be approached by using models

The tumour response models in current use might be classified in three categories To the first category belong the mental models used in ordinary clinical work These are based on principles regarding e g the importance of an even dose distribution over the tumour region, the value of dose to stations with possible lymphatic spread, and tolerable doses to critical organs or tissue These models have gradually devel oped from clinical experience and have been under clinical test for tens of years However, they often call for an intuitive evaluation and are often spiced with local believes They are not well documented and not amenable for an analytical approach with algorithms giving a quantitative measure of goodness of treatment

Submitted for publication 11 July 1974

Another approach has been to give a mathematical description of parameters considered by a set of clinicians in their mental evaluation of dose distributions and to derive heuristic score functions yielding verdicts as close as possible to the physician's judgements (HOPE et coll 1967) Whenever the treatment strategy changes, the parameter values have to be changed so that the model again agrees with the therapists

The models in the third category are based on cell kinetics They consider the tumour (and sometimes also healthy tissue) as a population of cells which is influenced by the radiation dose and by the temporal distribution of dose delivery during radiation therapy Such models often use, or easily include, biologic concepts such as shoulder curves, oxygen effect, tumour cell density, rate of cell division, re-oxygenation etc (ELLIS 1966, FISCHER 1969, COHEN 1971, KIRK *et coll* 1971, NIEDERER & CUNNINGHAM 1972, PREWITT 1972)

Cell kinetic models have often been strongly, and probably also correctly, criticized as being too crude and not in accord with clinical experience (cf e g SUIT et coll 1967) It might be expected, however, that the models will gradually approach reality and that, in the meantime, they may be used as a tool in selecting the best set of field parameters (beam widths, weights, and angles etc) from the multitude of alternatives which may be taken into account with computer techniques

The present investigation aims at an evaluation of a simple, tumour-cell radiation-response model which gives a simple figure of merit for selecting the best dose distribution in external radiation therapy The behaviour of this figure, when the weights, widths and angles of the radiation beams and the total dose are varied under different assumptions regarding density, oxygenation, sensitivity and distribution of tumour cells has been analysed as well as the limits on the treatment parameters imposed by a tolerable, dose-volume relationship in healthy tissue

Methods

Local tumour response It appears to be a reasonable inference from radiation biology that tumour cells are sterilized mainly by the dose received by the cells and that the risk of recurrence is depending on the number of vital tumour cells remaining after treatment

The surviving fraction of tumour cells, S, after a dose, D, was calculated from the formula

$$S = 1 - (1 - \exp(-D/D_0))^n \quad (1)$$

where D_0 is the mean lethal dose, and n is the extrapolation number (FISCHER 1969)

Measure of goodness of treatment The measure of goodness was taken as a probability, C, that no tumour cells survive the irradiation This quantity was calculated according to the formula

$$C = \exp\left(-\int S^m \zeta dv\right) \quad (2)$$

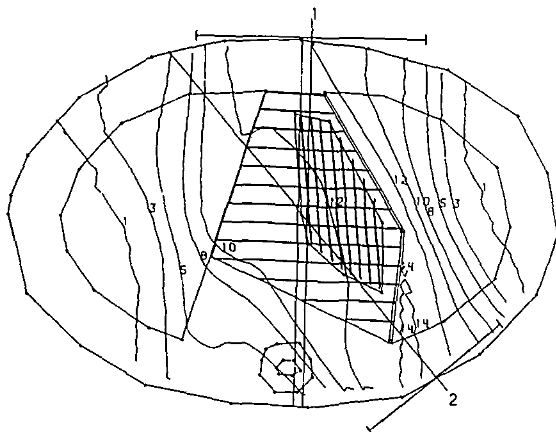


Fig 1 The simulated therapeutic situation The inner and outer regions of the tumour are indicated by shaded areas

where ζ is the local tumour cell density, m the number of fractions and the integration is carried out over all tumour tissue

Measure of tolerance The radiation effect on healthy tissue limits the dose that may be given to tumour tissue The consequence of irradiation may be related to the fraction of an organ that is irradiated above a certain critical dose (cf e g RUBIN & CASARETT 1973)

The measure of tolerance was therefore defined by a factor, T, which approaches unity when less than X′ per cent of the organ receives more than the critical dose and is almost zero when more than X″ per cent receives more than the critical dose Between the limits X′ and X″ the tolerance factor decreases in a sigmoidal way For each organ, or part of an organ, which should be given special consideration, the limits X′ and X″, as well as the corresponding critical accumulated doses, have to be defined Several critical dose levels with corresponding limits X′ and X″ may be defined for each organ

The simulated therapeutic situation A simplified case, simulating bronchial carcinoma (Fig 1) was considered The body outline and the outline of the lungs were

described by ellipses The tumour was divided in an inner region of constant cell density and an outer region, in which the density of tumour cells decreased radially from the tumour centre in a sigmoidal fashion Two different subpopulations, one euoxic and one hypoxic were assumed in the two tumour regions The mean lethal doses for euoxic and hypoxic tumour cells and the associated extrapolation numbers were chosen so (Table) that C approached a clinically reasonable local cure level (≈ 0.5) under conventional treatment conditions, i e 30 fractions with a total mean dose of about 6 000 rad (Bloedorn 1966) and a reasonable estimate of initial tumour cell density

Dose calculations were performed in two dimensions using a subroutine in UASDOS, a program used for automatic dose planning at the University Hospital This subroutine utilizes curved decremental lines and corrects for build up effects, oblique incidence and heterogeneities (cf GRAFFMAN et coll 1975)

The dose distributions were normalized so that the maximum accumulated dose in any point in the body cross section was 6 960 rad for the reference case

Computation methods The numerical computation of formulas (1) and (2) was performed as follows The cross section of the body at the tumour site was covered with a rectangular grid with gridpoints (i, j) $i = 1, 2, \ldots, K$, $j = 1, 2, \ldots, L$ The dose calculation program gave the relative dose $D(i, j)$ in these points A relationship between this distribution and the actual dose was given by the maximum dose, M rad, to any of the gridpoints A constant α was determined such that

$$\alpha \max_{\substack{1 \leq i \leq K \\ 1 \leq j \leq L}} D(i, j) = M$$

The absolute dose values were then recalculated from $D(i, j) = \alpha\ D(i, j)$ Eq (1) determined the fraction $S(i, j)$ of cells surviving the dose $D(i, j)$ After m fractions $(S(i, j))^m\ N_0(i, j)$ cells remain in the point (i, j) $N_0(i, j)$ stands for the initial number of tumour cells associated with the point (i, j)

Summation over all points gave the total number of surviving cells $= N_s$ With the assumption that the probable number of surviving cells obeys a Poisson distribution with the expected value N_s, the probability for zero survivors equals $C = \exp(-N_s)$

The number of cells per gridpoint in the outer region of the tumour was given by

$$N_0(i, j) = a(i, j)\ N_0 \tag{4}$$

with

$$a(i, j) = \int_{-\infty}^{x(i, j)} \frac{6}{b(i, j)\sqrt{2\pi}} \exp\left(-\frac{36\ (t - b(i, j)/2)^2}{2\ b(i, j)^2}\right) dt \tag{5}$$

Table

Parameter values in the reference case

Tumour data

Initial cell surface density 10^9 cells/cm^2
Initial fraction of hypoxic cells,
inner region 10 %
outer region 5 %
Mean lethal doses and extrapolation numbers
euoxic cells $D_0 = 88$ rad, $n = 3$
hypoxic cells $D_0 = 264$ rad, $n = 1$

Treatment data

	anterior	posterior field
Beam direction	0°	226°
Weight	1 00	1 00
Width	11 5 cm	9 5 cm

Number of fractions 30
total maximum dose $30 \times 232 = 6\,960$ rad

where N_0 is the constant initial number of tumour cells per gridpoint in the inner tumour region; *b(i, j) is the distance between the inner and outer tumour boundaries* as measured along a straight line through the point of computation (i, j), and x(i, j) is the distance from the outer boundary to the same point

The calculations were performed for each subpopulation of euoxic and hypoxic tumour cells with appropriate values of D_0, n and $N_0(i, j)$ The total curability was calculated as the product of the curabilities for the subpopulations It should be noted that the euoxic and the hypoxic populations were kept apart in the computations, which means that no reoxygenation was taken into account

The measure of tolerance was calculated as

$$T = \int_{X}^{100} \frac{6}{(X'' - X')\sqrt{2\pi}} \exp\left(-\frac{1}{2}\,\frac{(t - (X' + X'')/2)^2\; 36}{(X'' - X')^2}\right) dt \tag{6}$$

where X′ and X″ have been defined above and X is the percentage of the organ which has received a dose greater than the critical dose

The choice of a proper grid size is dependent on how large the dose changes are that occur over a small area Particularly for the computation of the measure of tolerance the grid size is of importance since two or three points receiving a dose just above or just below the critical dose may mean great changes in function value The choice of the limits X′ and X″ should take this into account The curability function will also depend on the grid size, with a finer grid the local effects are better taken into account and do not give undue merit to overkill This should not, however —for a reasonable choice of grid—mean any significant changes in the optimum setting of the field parameters

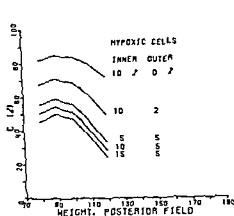


Fig 2

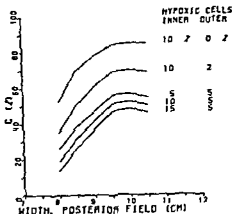


Fig 3

Fig 2. The curability function for variations of the weight of the posterior field The various curves correspond to various percentages of hypoxic cells in the inner and outer tumour region The other parameters are kept at their reference values

Fig 3 The curability function for variations of the width of the posterior field The various curves correspond to various percentages of hypoxic cells in the inner and outer tumour region The other parameters are kept at their reference values.

Results

The variations in the analysed parameters were centred around a *reference case*, for which the parameter values are given in the Table This reference case, selected after trial and-error calculations with the model, was chosen as an optimum from conventional clinical considerations taking into account injury to healthy critical organs

The effect of variation in the weight of the anterior and posterior fields on the curability appears in Fig 2, under five assumptions regarding the fractions of hypoxic cells in the inner and outer tumour regions

The effect of variation in the width of the posterior field on the curability under five assumptions regarding the oxygenation of the inner and outer tumour region is given in Fig 3

The effect on the curability of a variation in posterior field direction from 219° to 229° appears in Fig 4, for various assumptions regarding the maximum dose delivered per fraction, the number of fractions being kept constant equal to 30

The changes of the tolerance factor of the healthy lung with regard to various directions of the posterior field are illustrated in Fig 5 The three curves refer to three critical dose levels and three corresponding percentages of lung tissue describing the marginal zone between no and maximum risk

Table

Parameter values in the reference case

Tumour data

Initial cell surface density 10^9 cells/cm^2
Initial fraction of hypoxic cells,
inner region 10 %
outer region 5 %
Mean lethal doses and extrapolation numbers
euoxic cells $D_0 = 88$ rad, $n = 3$
hypoxic cells $D_0 = 264$ rad, $n = 1$

Treatment data

	anterior	posterior field
Beam direction	0°	226°
Weight	1 00	1 00
Width	11 5 cm	9 5 cm
Number of fractions 30		
total maximum dose 30 × 232 = 6 960 rad		

where N_0 is the constant initial number of tumour cells per gridpoint in the inner tumour region, $b(i, j)$ is the distance between the inner and outer tumour boundaries as measured along a straight line through the point of computation (i, j), and $x(i, j)$ is the distance from the outer boundary to the same point

The calculations were performed for each subpopulation of euoxic and hypoxic tumour cells with appropriate values of D_0, n and $N_0(i, j)$ The total curability was calculated as the product of the curabilities for the subpopulations It should be noted that the euoxic and the hypoxic populations were kept apart in the computations, which means that no reoxygenation was taken into account

The measure of tolerance was calculated as

$$T = \int_X^{100} \frac{6}{(X'' - X')\sqrt{2\pi}} \exp\left(-\frac{1}{2} \frac{(t - (X' + X'')/2)^2 \, 36}{(X'' - X')^2}\right) dt \qquad (6)$$

where X' and X'' have been defined above and X is the percentage of the organ which has received a dose greater than the critical dose

The choice of a proper grid size is dependent on how large the dose changes are that occur over a small area Particularly for the computation of the measure of tolerance the grid size is of importance since two or three points receiving a dose just above or just below the critical dose may mean great changes in function value The choice of the limits X' and X'' should take this into account The curability function will also depend on the grid size, with a finer grid the local effects are better taken into account and do not give undue merit to overkill This should not, however —for a reasonable choice of grid—mean any significant changes in the optimum setting of the field parameters

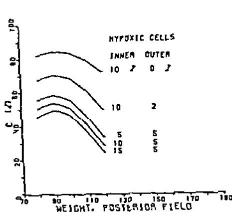


Fig 2

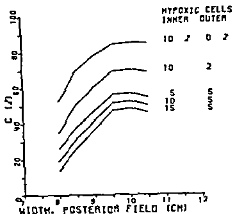


Fig. 3

Fig 2. The curability function for variations of the weight of the posterior field The various curves correspond to various percentages of hypoxic cells in the inner and outer tumour region The other parameters are kept at their reference values

Fig 3 The curability function for variations of the width of the posterior field The various curves correspond to various percentages of hypoxic cells in the inner and outer tumour region The other parameters are kept at their reference values

Results

The variations in the analysed parameters were centred around a reference case, for which the parameter values are given in the Table This reference case, selected after trial and-error calculations with the model, was chosen as an optimum from conventional clinical considerations taking into account injury to healthy critical organs

The effect of variation in the weight of the anterior and posterior fields on the curability appears in Fig 2, under five assumptions regarding the fractions of hypoxic cells in the inner and outer tumour regions

The effect of variation in the width of the posterior field on the curability under five assumptions regarding the oxygenation of the inner and outer tumour region is given in Fig 3

The effect on the curability of a variation in posterior field direction from 219° to 229 appears in Fig 4, for various assumptions regarding the maximum dose delivered per fraction, the number of fractions being kept constant equal to 30

The changes of the tolerance factor of the healthy lung with regard to various directions of the posterior field are illustrated in Fig 5 The three curves refer to three critical dose levels and three corresponding percentages of lung tissue describing the marginal zone between no and maximum risk

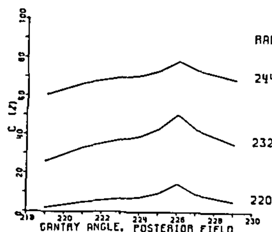


Fig 4

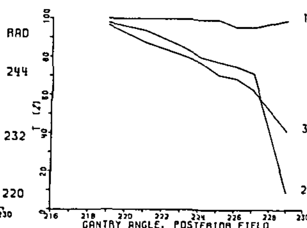


Fig 5

Fig 4 The curability function for variations of the direction of the posterior field The various curves correspond to various values for the maximum dose delivered per fraction The other parameters are kept at their reference values

Fig 5 The tolerance factor for variations of the direction of the posterior field (1) critical dose 3 000 rad, percentages X′ = 25 % and X″ = 60 %, (2) critical dose 4 000 rad, X′ = 20 % and X″ = 40 %, (3) critical dose 5 000 rad, X′ = 10 % and X″ − 26 %

Discussion and Conclusions

The optimum setting of the posterior beam angle, the weight of the anterior and posterior fields and the width of the posterior field are much independent on various assumptions regarding the maximum dose to the tumour area, and the fraction of hypoxic cells in the inner and outer tumour region (Figs 2–4) The general behaviour of the curability function is rather smooth and suboptima are not frequent or accentuated From these viewpoints the type of model applied here may suitably be used in an automatic optimisation procedure

The behaviour of the tolerance factor is critically depending on the assumptions regarding radiation effect on healthy tissue (Fig 5) The sharp decrease in one of the curves (No 2) may indicate a forbidden sector The tolerance factor may, alternatively, be included directly in the objective function for the optimisation procedure

Obviously the curability is critically depending on the assumption regarding the distribution of tumour tissue in the patient At present, the model does not allow the clinical judgement of the patient with respect to tumour cell spread to be included in a probabilistic way This possibility might be of value and should be tested when the necessary techniques and basic information are available

In the calculations the larger part of the computer time was spent on dose calculation and only a small fraction (about 10 %) on calculation of curability Also rather complicated models for estimating the goodness of a treatment therefore seem to be practical

The technique applied here is similar to that introduced by COHEN (1971) with regard to tumour tissue effect. It is extended, however, from single points to an area, approximating a three-dimensional volume. COHEN applied cell kinetic techniques also for estimating probable radiation effects in normal tissue. The approach taken here allows a similar treatment of the local effects on healthy tissue.

The validity of the tumour model and especially the measure of curability is, however, highly questionable. Curability is here only used as a technical term and should not be related to cure in the clinical sense. It is believed, however, that a treatment giving a higher curability is more probable to cure the patient than a treatment giving a low curability. It might also be hoped that the selection of optimum field parameters is not critically depending on the detailed characteristics of the applied cell model and that all reasonable models (and hence also the correct one) yield effectively the same set of optimum field parameters. This question has not been analysed in the present report, but will be thoroughly investigated. It also remains to apply cell models of the present type to a number of clinical situations and compare the model predicts with the judgements by clinicians.

SUMMARY

A simple tumour-cell radiation response model was coupled to a dose-calculation routine and applied to a clinical situation in radiation therapy. The dose distributions resulting from various settings of two radiation fields, as well as the tumour response under various assumptions regarding sensitivity and distribution of tumour cells, were calculated automatically. The probability of zero surviving tumour cells after 30 fractions was taken as a measure of goodness of the dose distributions and was found to vary rather smoothly over the param[illegible]

ZUSAMMENFASSUNG

Es wurde ein einfaches Tumor-Zell Strahlen-Respons-Modell einer Dosis Berechnungsroutine zugeordnet und [illegible]
Dosisver[illegible] Die
Respons[illegible] mor-
Tumorze[illegible] der
nach 30 Fraktionen überleben, wurde als Gütem[illegible]
sich als ziemlich gleichmässig über die gewäh[illegible]
wurde ebenfalls ein Toleranzfaktor für das gesun[illegible]
[illegible]
[illegible]Gesichtspunkt realistisch sein kann

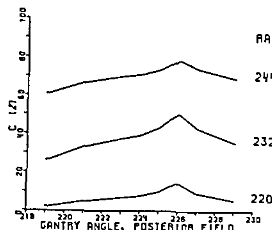


Fig 4

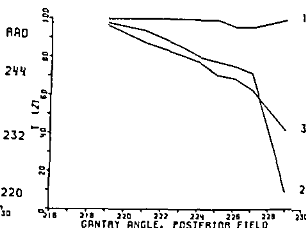


Fig 5

Fig 4 The curability function for variations of the direction of the posterior field The various curves correspond to various values for the maximum dose delivered per fraction The other parameters are kept at their reference values

Fig 5 The tolerance factor for variations of the direction of the posterior field (1) critical dose 3 000 rad, percentages X' = 25 % and X" 60 %, (2) critical dose 4 000 rad, X' = 20 % and X" = 40 %, (3) critical dose 5 000 rad, X' = 10 % and X" = 26 %

Discussion and Conclusions

The optimum setting of the posterior beam angle, the weight of the anterior and posterior fields and the width of the posterior field are much independent on various assumptions regarding the maximum dose to the tumour area, and the fraction of hypoxic cells in the inner and outer tumour region (Figs 2–4) The general behaviour of the curability function is rather smooth and suboptima are not frequent or accentuated From these viewpoints the type of model applied here may suitably be used in an automatic optimisation procedure

The behaviour of the tolerance factor is critically depending on the assumptions regarding radiation effect on healthy tissue (Fig 5) The sharp decrease in one of the curves (No 2) may indicate a forbidden sector The tolerance factor may, alternatively, be included directly in the objective function for the optimisation procedure

Obviously the curability is critically depending on the assumption regarding the distribution of tumour tissue in the patient At present, the model does not allow the clinical judgement of the patient with respect to tumour cell spread to be included in a probabilistic way This possibility might be of value and should be tested when the necessary techniques and basic information are available

In the calculations the larger part of the computer time was spent on dose calculation and only a small fraction (about 10 %) on calculation of curability Also rather complicated models for estimating the goodness of a treatment therefore seem to be practical

ROM THE INSTITUTE OF RADIATION PHYSICS, KAROLINSKA INSTITUTET, THE DEPARTMENT OF OTOLARYNGOLOGY, KAROLINSKA SJUKHUSET, S-104 01 STOCKHOLM, AND THE DEPARTMENT OF RADIATION PHYSICS, SÖDERSJUKHUSET, S-100 64 STOCKHOLM, SWEDEN

OBJECTIVE SYMMETRY DETECTOR METHOD FOR GAMMAENCEPHALOGRAPHY

I. Physical characteristics

STIG LARSSON, MAGNUS LIND and BERNDT SÖDERBORG

Various methods have been used to measure and evaluate the distribution of isotope tracers in the skull. Digital recording of the count rate, obtained from measurements with a single detector and a low resolution collimator placed at different positions around the head, was the first method used in gammaencephalography (MOORE 1948). High diagnostic accuracy was reported when the symmetry of isotope distribution in the skull was analysed (PLANIOL 1959, 1966, MUNDINGER & ASAI 1967).

However, detector positioning over symmetrically located regions of the skull was found to be intricate, implying a source of error difficult to evaluate. The interpretation of the results was time consuming. Nowadays, therefore, symmetry methods are only in use in a few hospitals in the world (PLANIOL 1966, BURROWS 1972).

Conventional image producing methods have improved during recent years, having benefited from technical progress including computer processing, high resolution collimators and short lived isotopes, all in order to obtain more detailed information on the isotope distribution. This has promoted the development of more

Submitted for publication 15 January 1974

RÉSUMÉ

Un modèle simple de réponse des cellules tumorales aux radiations a été associé à un calcul de dose de routine et appliqué aux conditions cliniques *en traitement par les radiations* Les auteurs ont calculé automatiquement les distributions de dose résultant de differentes dispositions de deux champs d'irradiation ainsi que la réponse de la tumeur dans diverses hypothèses concernant la sensibilité et la distribution des cellules tumorales La probabilité d'une survie nulle de cellules tumorales après 30 fractions a été prise comme une mesure de la qualité de la distribution de dose Les auteurs ont constaté qu'elle varie de façon assez *faible et régulière dans les intervalles de paramètres étudiés Pour certains paramètres on a* trouvé un optimum net, assez peu sensible aux différentes hypothèses concernant la reponse des cellules Les auteurs ont aussi étudié un facteur de tolérance du tissu sain, basé sur une relation entre la dose et la volume Les auteurs concluent qu'une approche par la cinétique cellulaire de l'optimisation automatique des paramètres de champs dans le traitement par l'irradiation externe pourrait être réaliste aussi bien du point de vue économique que du point de vue calcul par ordinateur

REFERENCES

BLOEDORN F G Rationale and benefit of preoperative irradiation of lungcancer J Amer med Ass 9 (1966), 340

COHEN L A cell population kinetic model for fractionated radiation therapy I Normal tissues Radiology 101 (1971), 419

ELLIS F The relationship of biological effect to dose-time fractionation factors in radiotherapy *In* Modern trends in radiotherapy Vol 1 Edited by T J Deeley and A P Wood Butterworths, London 1966

FISCHER J J Theoretical considerations in the optimisation of dose distribution in radiation therapy Brit J Radiol 42 (1969), 925

GRAFFMAN S and JUNG B Clinical trials in radiotherapy and the merits of high energy protons Acta radiol Ther Phys Biol 9 (1970), 1

— GROTH T, JUNG B, SKÖLLERMO G and SNELL J-E Errors and uncertainties in external radiation therapy A system analysis with a cell kinetic model To be published in Acta radiol Ther Phys Biol 14 (1975)

HOPE C S, LAURIE J and ORR J S Optimisation of X ray treatment planning by computer judgement Phys in Med Biol 12 (1967), 531

KIRK J, GRAY W N and WATSON E R Cumulative radiation effect Part I Fractionated treatment regimes Clin Radiol 22 (1971), 145

NIEDERER J and CUNNINGHAM J R A mathematical model for cellular response to radiation Digest of the 3rd International Conference on Medical Physics in Gothenburg, 1972

PREWITT J M S A radiobiological model for optimising radiation treatment *In* Proceedings from the Fourth International Conference on the Use of Computers in Radiation Therapy, Uppsala, 1972

RUBIN P and CASARETT G W Concepts of clinical radiation pathology in medical radiation biology Edited by Dalrymple et coll Saunders, Philadelphia 1973

SUIT H, WETTE R and LINDBERG R Analysis of tumour-recurrence times Radiology 88 (1967), 311

FROM THE INSTITUTE OF RADIATION PHYSICS, KAROLINSKA INSTITUTET, THE DEPARTMENT OF OTOLARYNGOLOGY, KAROLINSKA SJUKHUSET, S-104 01 STOCKHOLM, AND THE DEPARTMENT OF RADIATION PHYSICS, SÖDERSJUKHUSET, S-100 64 STOCKHOLM, SWEDEN

OBJECTIVE SYMMETRY DETECTOR METHOD FOR GAMMAENCEPHALOGRAPHY

I Physical characteristics

STIG LARSSON, MAGNUS LIND and BERNDT SÖDERBORG

Various methods have been used to measure and evaluate the distribution of isotope tracers in the skull. Digital recording of the count rate, obtained from measurements with a single detector and a low resolution collimator placed at different positions around the head, was the first method used in gammaencephalography (MOORE 1948). High diagnostic accuracy was reported when the symmetry of isotope distribution in the skull was analysed (PLANIOL 1959, 1966, MUNDINGER & ASAI 1967).

However, detector positioning over symmetrically located regions of the skull was found to be intricate, implying a source of error difficult to evaluate. The interpretation of the results was time consuming. Nowadays, therefore, symmetry methods are only in use in a few hospitals in the world (PLANIOL 1966, BURROWS 1972).

Conventional image producing methods have improved during recent years, having benefited from technical progress including computer processing, high resolution collimators and short lived isotopes, all in order to obtain more detailed information on the isotope distribution. This has promoted the development of more

Submitted for publication 15 January 1974

RÉSUMÉ

Un modèle simple de réponse des cellules tumorales aux radiations a été associé a un calcul de dose de routine et appliqué aux conditions cliniques en traitement par les radiations Les auteurs ont calculé automatiquement les distributions de dose résultant de différentes dispositions de deux champs d'irradiation ainsi que la réponse de la tumeur dans diverses hypothèses concernant la sensibilité et la distribution des cellules tumorales La probabilité d'une survie nulle de cellules tumorales après 30 fractions a été prise comme une mesure de la qualité de la distribution de dose Les auteurs ont constaté qu'elle varie de façon assez faible et régulière dans les intervalles de paramètres étudiés Pour certains paramètres on a trouvé un optimum net, assez peu sensible aux différentes hypothèses concernant la réponse des cellules Les auteurs ont aussi étudié un facteur de tolérance du tissu sain basé sur une relation entre la dose et la volume Les auteurs concluent qu'une approche par la cinétique cellulaire de l'optimisation automatique des paramètres de champs dans le traitement par l'irradiation externe pourrait être réaliste aussi bien du point de vue économique que du point de vue calcul par ordinateur

REFERENCES

BLOEDORN F G Rationale and benefit of preoperative irradiation of lungcancer J Amer med Ass 9 (1966), 340

COHEN L A cell population kinetic model for fractionated radiation therapy I Normal tissues Radiology 101 (1971), 419

ELLIS F The relationship of biological effect to dose time fractionation factors in radio therapy *In* Modern trends in radiotherapy Vol 1 Edited by T J Deeley and A P Wood Butterworths, London 1966

FISCHER J J Theoretical considerations in the optimisation of dose distribution in radiation therapy Brit J Radiol 42 (1969), 925

GRAFFMAN S and JUNG B *Clinical trials in radiotherapy and the merits of high energy* protons Acta radiol Ther Phys Biol 9 (1970) 1

— GROTH T, JUNG B, SKÖLLERMO G and SNELL J-E Errors and uncertainties in external radiation therapy A system analysis with a cell kinetic model To be published in Acta radiol Ther Phys *Biol 14 (1975)*

HOPE C S, LAURIE J and ORR J S Optimisation of X-ray treatment planning by computer judgement Phys in Med Biol 12 (1967), 531

KIRK J, GRAY W N and WATSON E R Cumulative radiation effect Part 1 Fractionated treatment regimes Clin Radiol 22 (1971), 145

NIEDERER J and CUNNINGHAM J R A mathematical model for cellular response to radiation Digest of the 3rd International Conference on Medical Physics in Gothenburg 1972

PREWITT J M S A radiobiological model for optimising radiation treatment *In* Proceedings from the Fourth International Conference on the Use of Computers in Radiation Therapy Uppsala, 1972

RUBIN P and CASARETT G W Concepts of clinical radiation pathology in medical radiation biology *Edited by Dalrymple et coll Saunders Philadelphia 1973*

SUIT H, WETTE R and LINDBERG R Analysis of tumour recurrence times Radiology 88 (1967) 311

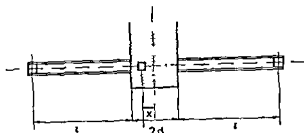


Fig 1 Phantom system and detector arrangement

mental modelling has been performed The skull was represented by a lucite box, containing a homogeneous solution of $^{99}Tc^{m}$-pertechnetate and water (Fig 1)

Theory Let the two detectors be located over the right (R) and left (L) side of a subregion of the skull phantom If the two detection-units are assumed to be identical, the results obtained will be the same for both and hence, only one of the detectors has to be considered for the following calculation

The count rate from a thin sheet of homogeneously distributed activity is approximately independent of the distance in air from the sheet to the collimator aperture, as long as the sheet extends outside the 'field of view' of the detector (MAYNEORD 1950, BROWNELL 1959, BECK 1964) The degree of approximation depends mainly on the relationship between the length and the aperture of the collimator

If the thickness of the walls (5 mm) of the phantom is neglected, the phantom may be described as consisting of a stack of thin sheets, each of them with a thickness Δx Hence, assume a sheet located at a distance $(d+x)$ from the collimator aperture From geometrical considerations, each point of the detector area can be shown to view approximately an area A_w of the sheet given by

$$A_w = \frac{A(l+d+x)^2}{l^2} \tag{1}$$

where A is the area of the collimator aperture and l, the length of the straight collimator (Fig 1) ΔQ (μCi) is the activity of the amount of isotope in the volume $\Delta V = A_w \Delta x$, which is recorded by the detector and can be expressed

$$\Delta Q = C\Delta V = CA_w\Delta x \tag{2}$$

where C (μCi/cm³), the activity per cm³, represents the concentration of isotope in the phantom If scattering and penetration effects are neglected, the fraction G(x), of photons (generated within ΔV) which can reach the detector, can be calculated according to the inverse square law

$$G(x) = \frac{A}{4\pi(l+d+x)^2} \tag{3}$$

complicated recording systems For economic reasons, however, these are often designed to suit a wide range of requirements It is therefore not always possible to take full advantage of the improvements in special clinical applications, since the choice of measuring and evaluation parameters may be restricted by the equipment A system specially designed for a specific purpose may thus be less expensive while still offering more relevant parameters

A further development of the gammaencephalographic methods, originally described by PLANIOL and MUNDINGER, based on the symmetrical isotope distribution in the skull therefore seemed desirable The diagnostic accuracy (obtained by MUNDINGER and PLANIOL) is difficult to evaluate because of the unknown selection of patients and a partly subjective interpretation of results which involved added clinical information The different sources of error, influencing the reproducibility, were not reported in detail but the results must have been influenced by large uncertainties from the counting statistics and from the positioning of the detectors (PLANIOL 1966, MUNDINGER & ASAI)

The measuring performance and the evaluation of the results of the method now described can be standardized in order to obtain an objective classification of the clinical results with high accuracy The significance of a deviation from the normal mean should be used as the basis for diagnosis, thus avoiding subjective interpretation of results (LARSSON & LIND, LIND et coll)

The equipment has been designed to be simple to handle and inexpensive, and the standardization of the measuring performance should make the method well suited to routine clinical work, including screening of large materials, even outside large medical centres (GOTTSCHALK 1971) The purpose of this report is to describe the physical characteristics of the equipment and the method

Principles of the method The method is principally based on a precise determination of the relative isotope distribution in different predetermined parts, 'subregions', of the skull, following intravenous administration of $^{99}Tc^{m}$-pertechnetate

Two equally collimated NaI-detectors, directed towards each other on a common axis and arranged symmetrically on the right and left sides of the skull, measure the γ radiation emitted from the isotope in a subregion A complete examination of the whole skull necessitates measurements in turn over each of several different subregions, having the same size (lateral projection), determined by the collimator design Their locations, in relation to the length and height of the skull, are made reproducible both within and between individuals by means of the detector movement By this means, the results obtained can be compared both between the right and left parts of each subregion, and also between different subregions of the same individual The relative evaluation parameters obtained permits objective comparisons between individuals

In order to illustrate the characteristics of the different evaluation parameters and the influence on the results of different physical factors, theoretical and experi-

assuming that the activity $Q_t = V_t(C_t - C)$ (μCi) of the local accumulation can be approximated by a point-source of the same activity N_{tR} and N_{tL} may be related to N_R and N_L, the values obtained without this brain lesion phantom V_t in the subregion and increase ratios, I_R and I_L, and a difference ratio D may be defined

$$I_R = \frac{N_{tR} - N_R}{N_R} \quad (10a)$$

$$I_L = \frac{N_{tL} - N_L}{N_L} \quad (10b)$$

$$D = \frac{N_{tR} - N_{tL}}{(N_R + N_L)/2} \quad (10c)$$

The ratios I_R, I_L and D are to be the evaluated results for each subregion of the standardized pattern of subregions of the skull

Ideally, if no local increase of isotope in a subregion is present, the ratios I_R, I_L and D obtained from this subregion should be zero If however a local accumulation of isotope with the activity Q_t, is located within the subregion, these ratios should deviate from zero The sensitivity S' to such a local accumulation of isotope located within a subregion and at a position (d+x) from one of the collimator apertures may be defined as a function of the location x *for the parameter D and a parameter defined as the maximum of* I_R and I_L, (max (I_R, I_L))

$$S_D(x) \quad \frac{D \; 100}{Q_t} = \frac{D \; 100}{V_t(C_t - C)} \text{ percental units}/\mu\text{Ci} \quad (11a)$$

$$S_I(x) = \frac{\max(I_R \; I_L) \; 100}{Q_t} = \frac{\max(I_R, I_L) \; 100}{V_t(C_t - C)} \text{ percental units}/\mu\text{Ci} \quad (11b)$$

if the local increase of activity Q_t *is expressed as the* product of the volume V_t of the accumulation and the increase of isotope concentration ($C_t - C$) in that volume

However, concentration ratios are of greater interest in clinical application of the method than absolute determination of accumulations of isotope

Therefore, the concentration differences (C_t C) is related to the homogeneous concentration C in the skull *phantom, thus giving*

$$\frac{C_t - C}{C} = \frac{C_t}{C} - 1 = c_0 - 1$$

where c_0 is the concentration *ratio between* the local accumulation and the surrounding homogeneous concentration

Corresponding to the definitions of $S_I(x)$ and $S_D(x)$, sensitivity functions $S_I(x)$ and $S_D(x)$ can be defined using the concentration ratio C_0 instead of the concentration difference (C_t C)

The symbol A in eq (3) represents the area of the detector, which in the case of a straight collimator, equals the area of the collimator aperture

When the attentuation of photons, the limited detector efficiency ε_d and the data-transfer efficiency ε_{dt}, are taken into account, the number of registered events/s ΔR, from the activity ΔQ, can be expressed, assuming k_1 γ-photons to be emitted per decay

$$\Delta R = 3.7 \cdot 10^4 k_1 \varepsilon_d \varepsilon_{dt} \Delta Q G(x) \exp(-\mu(d+x)) \tag{4}$$

By setting the results of eqs (1), (2) and (3) into eq (4) the following result is obtained

$$\Delta R = \frac{3.7 \cdot 10^4 k_1 \varepsilon_d \varepsilon_{dt} A^2 C}{4\pi l^2} \exp(-\mu(d+x)) \Delta x \tag{5}$$

By setting the thickness of the whole skull phantom = 2d and the location variable x = 0 in the median plane, the total number of registered events/s R, from all the activity within one subregion is obtained by integration of eq (5) from x = −d to x = +d

$$R = \frac{k_0 A^2 C}{l^2} \int_{-d}^{+d} \exp(-\mu(d+x))\,dx = \frac{k_0 A^2 C}{\mu l^2}(1 - e^{-2\mu d}) \tag{6}$$

where

$$k_0 = \frac{3.7 \cdot 10^4 k_1 \varepsilon_d \varepsilon_{dt}}{4\pi}$$

When a measurement is assumed to be performed during a time T, much shorter than the half-life of the isotope used, the mean number of registered events N from the detector, may be approximated by

$$N \approx RT = \frac{k_0 A^2 CT}{\mu l^2}(1 - e^{-2\mu d}) \tag{7}$$

As $\varepsilon_d \varepsilon_{dt}$ is assumed to be about the same for both the detectors, the number of counts N_L obtained from the left detector will be approximately equal to N_R, the number of photons registered by the right detector

A small volume V_t, representing a brain lesion with increased isotope concentration C_t, may be considered to be located within one subregion (d + x) cm from one of the collimator apertures The total number of counts from this subregion registered in the right (R) and left (L) detectors respectively, could approximately be expressed

$$N_{tR} \approx N_R + \frac{k_0 T(C_t - C) V_t A \exp(-\mu(d+x))}{(l+d+x)^2} \tag{8}$$

$$N_{tL} \approx N_L + \frac{k_0 T(C_t - C) V_t A \exp(-\mu(d-x))}{(l+d-x)^2} \tag{9}$$

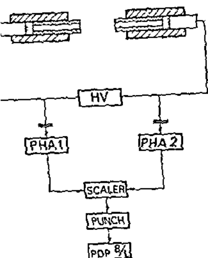


Fig. 2 Block diagram of the detection system. PHA = Pulse height analyser HV = High voltage supply PDP 8/L = Computer

The phantoms A lucite vessel, length 20 cm, height 20 cm, width 15 cm and wall thickness 0 5 cm, was used as a skull phantom Three cylindrical lucite containers with thin walls and volumes of 6 3, 21 and 33 cm^3 were used as brain lesion phantoms The diameter of each cylinder was approximately equal to its length The lesion phantoms were movable to different distances from the median plane of the skull phantom and always directed with their central axes along the central axis of the collimators (Fig 1)

Pulse height discrimination Two different pulse-height discrimination levels are frequently used in photon counting methods The upper discrimination level can be set high enough to accept most of the pulses from primary photons in the upper part of the total-absorption peak, if the background radiation level is low compared to the level to be measured The lower discrimination level is commonly set somewhere below or within the lower part of the total-absorption peak, in order to optimize the detectability by compromizing between two counteracting effects, rejection of scattered radiation and good counting statistics The problem of finding a suitable lower discrimination level for the measuring performance previously described might be important and was therefore analysed

For this purpose, assume the counting statistics to be the only or the most dominant source of variation, and that a large number of measurements is performed over a subregion of the skull phantom, all of them with measuring times of the same length and with the same homogeneous concentration of isotope in the phantom From the population of values obtained, $\{N_s\}$, the mean value $\overline{N}_s$, and the standard deviation SD may be calculated If however, $N_s \gg 1$, the measuring values obtained approach a normal distribution with an expected mean, η_s, and standard

$$S_D(x) = \frac{D}{V_t(c_0 - 1)} \cdot 100 \text{ percental units/cm}^3 \text{ of lesion volume} \qquad (12a)$$

$$S_I(x) = \frac{\max(I_R, I_L)}{V_t(c_0 - 1)} \cdot 100 \text{ percental units/cm}^3 \text{ of lesion volume} \qquad (12b)$$

Normally, $N_R \approx N_L$ (LIND et coll) and hence, by setting $N_R = N_L$ it is obtained from eqs (10 a), (10 b) and (10 c)

$$\max(I_R, I_L) > I_R - I_L \approx \frac{N_{tR} - N_R}{N_R} - \frac{N_{tL} - N_L}{N_L} = \frac{N_{tR} - N_{tL}}{(N_R + N_L)/2} = D$$

As max $(I_R, I_L) > D$, it is evident from eqs (12 a) and (12 b) that $S_I(x) > S_D(x)$ which indicates that the parameter D is less sensitive than the maximum of I_R and I_L

However, for the choice of clinical evaluation parameters, the figure of greatest interest is that for the detectability which is determined by the sensitivity in relation to the normal range (including the measuring error of the parameter) Therefore, as the normal range of a parameter is not known, it is not possible to exclude one parameter as being less valuable than another because of its lower sensitivity (LARSSON & LIND)

As no biologic effects can influence the results in phantom measurements, it is possible to estimate the errors occurring from counting statistics and instability of counting efficiency

Material and Methods

Detectors and electronic equipment Two cylindrical NaI detectors (crystal size, diameter 5 1 cm, length 5 1 cm), with one common high-potential supply, were each connected to a pulse-height discriminator and a scaler The timer was common to both spectrometers, and the measured values were punched on paper tape, thus permitting the use of an automatic measuring routine (Fig 2)

The collimators The two detectors were equally collimated The collimators were made of lead, cast in between an iron tube and a smaller square aluminium profile (wall thickness 2 mm) The collimators were inserted into larger lead shields, facing each other and arranged in such a way that the collimated detectors could be moved along their common axis to obtain a suitable distance between them (Fig 2) The collimator length was 30 cm and the aperture 3 cm × 3 cm The two detectors could also be moved congruently in an x − y plane, orthogonal to the central axis, in order to cover the skull in clinical examinations, with a fixed number of subregions

The isotope $^{99}Tc^m$ in the form of technetium pertechnetate was used in all determinations and all results were corrected for the activity decay

filled with pure water This performance simplifies the examination and the following eq is obtained

$$\bar{q} = \frac{\bar{z}}{\sigma_s} \approx \frac{\Delta \bar{N}_t}{\sqrt{\bar{N}_s}} \qquad (17)$$

Assume $\Delta\bar{N}_{t0}$ and $\bar{N}_{s0}$ to be the results obtained when the pulse-height discriminators are set to correspond to a reference energy acceptance interval ΔE_0 For any other energy acceptance interval ΔE, the corresponding results may be expressed as functions of ΔE

$$\Delta\bar{N}_t(\Delta E) = \Delta\bar{N}_{t0}\ f_t(\Delta E) \qquad (18)$$

and

$$\bar{N}_s(\Delta E) = \bar{N}_{s0}\ f_s(\Delta E) \qquad (19)$$

where $\Delta E = E_u - E_l$ is the interval between the upper and the lower discrimination levels Correspondingly, if E_u is set fixed, $\Delta\bar{N}_t(\Delta E)$ and $\bar{N}_s(\Delta E)$ can be expressed as functions of the lower discrimination level E_l

$$\Delta\bar{N}_t(E_l) = \Delta\bar{N}_{t0}\ f_t(E_l) \qquad (20\text{ a})$$

$$\bar{N}_s(E_l) = \bar{N}_{s0}\ f_s(E_l) \qquad (20\text{ b})$$

From eqs (17), (20 a) and (20 b), $\bar{q}$ as a function of E_l is expressed

$$\bar{q}(E_l) = \frac{\Delta\bar{N}_t(E_l)}{\sqrt{\bar{N}_s(E_l)}} \approx \frac{\Delta\bar{N}_{t0}}{\sqrt{\bar{N}_{s0}}}\ \frac{f_t(E_l)}{\sqrt{f_s(E_l)}} \qquad (21)$$

Spectral distributions of events from the isotope in a subregion of the skull phantom and of events from the isotope in a lesion phantom, located at three different depths within the water-filled skull phantom, were obtained by the use of a multichannel analyzer From the values thus obtained, the functions $f_t(E_l)$ and $f_s(E_l)$ were calculated giving $\bar{q}$ as a function of E_l with a reference interval $\Delta E_0 = 120$–170 keV (Fig 3)

The stability of the counting efficiency The counting efficiency of methods for detection of discrete ionizing particles may be defined as the ratio between the registered number of events/s and the number of ionizing particles/s incident on the detector The counting efficiency can be expanded into the product of the detector efficiency ε_d and the data transfer efficiency ε_{dt}, the definitions of which have been given by MacIntyre et coll (1969) in a report to the International Commission on Radiation and Units (ICRU)

Fluctuations of the counting efficiency, caused for instance by aging or termal effects or by instability of the power supply to the detectors and the discriminators, may be expected to influence on the detectability properties of the method

deviation, $\sigma_s = \sqrt{\eta_s}$ These values can be expected to be close to the calculated values $\overline{N}_s \approx \eta_s$ and $SD \approx \sigma_s$

Now, if a small volume of increased isotope content, represented by a lesion or a tumor phantom, is located within the subregion, the corresponding values obtained $\{N_t\}$, may be expected to differ from $\{N_s\}$ The difference z, between a value N_t and the mean value $\overline{N}_s$, can be calculated

$$z = N_t - \overline{N}_s$$

and for the mean value $\overline{N}_t$ of $\{N_t\}$

$$\bar{z} = \overline{N}_t - \overline{N}_s, \; \bar{z} > 0 \tag{13}$$

where the value of $\bar{z}$ may be expected to be mostly due to the activity of the lesion phantom

From the point of view of detectability, the most interesting problem arises when $\bar{z}$ is fairly small compared to N_s, and therefore, for the further calculation, $\bar{z} < N_s$ is assumed

A measure of the probability for a value N_t not to belong to the population $\{N_s\}$, may be expressed by the number of standard deviations, q

$$N_t - \overline{N}_s = z = qSD$$

For the most probable value $\overline{N}_t$ of $\{N_t\}$, is obtained

$$\overline{N}_t - \overline{N}_s = \bar{z} = \bar{q}SD \tag{14}$$

which is approximately equal to

$$\eta_t - \eta_s = \bar{q} \; \sigma_s \tag{15}$$

where η_t is the expectation value of the population $\{N_t\}$ The significance of the most probable deviation $\bar{z}$ can hence be expressed in number of standard deviations, $\bar{q}$

$$\bar{q} = \frac{\eta_t - \eta_s}{\sigma_s} \approx \frac{\bar{z}}{\sigma_s} \tag{16}$$

The size of the ratio $\bar{z}/\sigma_s$ was assumed to be dependent on the energy acceptance interval ΔE Such a dependence might be of practical importance since the significance of a deviation should be as large as possible in order to increase the possibility of detecting an accumulation of isotope within the subregion

σ_s could be estimated from the results of a measurement over a subregion of the skull phantom, filled with a homogeneously distributed isotope

As the difference $\bar{z}$ was assumed to be mostly due to the lesion phantom, the value of $\bar{z}$ could be set approximately equal to $\Delta\overline{N}_t$, *the value from a small lesion* phantom containing isotope, and located within a subregion of the skull phantom

filled with pure water This performance simplifies the examination and the following eq is obtained

$$\bar{q} = \frac{\bar{z}}{\sigma_z} \approx \frac{\Delta \overline{N}_t}{\sqrt{\overline{N}_s}} \tag{17}$$

Assume $\Delta\overline{N}_{t0}$ and $\overline{N}_{s0}$ to be the results obtained when the pulse height discriminators are set to correspond to a reference energy acceptance interval ΔE_0 For any other energy acceptance interval ΔE, the corresponding results may be expressed as functions of ΔE

$$\Delta\overline{N}_t(\Delta E) = \Delta\overline{N}_{t0}\ f_t(\Delta E) \tag{18}$$

and

$$\overline{N}_s(\Delta E) = \overline{N}_{s0}\ f_s(\Delta E) \tag{19}$$

where $\Delta E = E_u \quad E_l$ is the interval between the upper and the lower discrimination levels Correspondingly, if E_u is set fixed, $\Delta\overline{N}_t(\Delta E)$ and $\overline{N}_s(\Delta E)$ can be expressed as functions of the lower discrimination level E_l

$$\Delta\overline{N}_t(E_l) = \Delta\overline{N}_{t0}\ f_t(E_l) \tag{20 a}$$

$$\overline{N}_s(E_l) = \overline{N}_{s0}\ f_s(E_l) \tag{20 b}$$

From eqs (17), (20 a) and (20 b), $\bar{q}$ as a function of E_l is expressed

$$\bar{q}(E_l) = \frac{\Delta\overline{N}_t(E_l)}{\sqrt{\overline{N}_s(E_l)}} = \frac{\Delta\overline{N}_{t0}}{\sqrt{\overline{N}_{s0}}}\ \frac{f_t(E_l)}{\sqrt{f_s(E_l)}} \tag{21}$$

Spectral distributions of events from the isotope in a subregion of the skull phantom and of events from the isotope in a lesion phantom, located at three different depths within the water-filled skull phantom, were obtained by the use of a multichannel analyzer From the values thus obtained, the functions $f_t(E_l)$ and $f_s(E_l)$ were calculated giving $\bar{q}$ as a function of E_l with a reference interval $\Delta E_0 = 120$–170 keV (Fig. 3)

The stability of the counting efficiency The counting efficiency of methods for detection of discrete ionizing particles may be defined as the ratio between the registered number of events/s and the number of ionizing particles/s incident on the detector The counting efficiency can be expanded into the product of the detector efficiency ε_d and the data transfer efficiency ε_{dt}, the definitions of which have been given by MacIntyre et coll (1969) in a report to the International Commission on Radiation and Units (ICRU)

Fluctuations of the counting efficiency, caused for instance by aging or termal effects or by instability of the power supply to the detectors and the discriminators, may be expected to influence on the detectability properties of the method

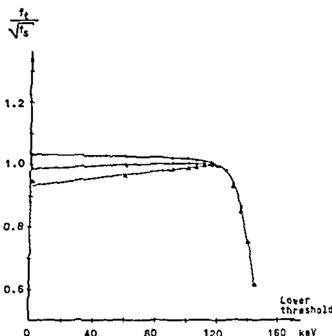


Fig 3 The function $f_t/\sqrt{f_s}$, obtained from measurements of a tumour phantom located at three different depths plotted against the lower threshold of pulse height discrimination E_l Estimated errors are approximately within the size of the symbols ▲ depth = 2 5 cm, ● depth = 6 5 cm, ○ depth = 10 5 cm

To investigate whether such effects were of importance, the count rate stability was tested on a phantom system The skull phantom was filled with a homogeneous $^{99}Tc^m$ solution with a concentration corresponding to an initial count rate of about 80 000 cpm from each detector In view of the results presented in Fig 3, the pulse height discriminators were set corresponding to the energy interval between 120 and 170 keV The count rate was registered automatically for one minute periods for several hours The registrations were also repeated at different times of three days The values obtained were arranged in 18 groups of 24 consecutive registrations, each group corresponding to a patient examination (LIND et coll) The mean value and standard deviation of each were calculated and related to the theoretical calculation of the count rate statistics

Collimation of the detectors The detector response was determined by measurement of the count rate from a $^{99}Tc^m$ point source at different locations in the water of the skull phantom The point source was made using an electrolytic procedure in which $^{99}Tc^m$ pertechnetate ions were attached to the tip of a thin needle The tip was then given a thin cover to prevent loss The detector response is illustrated by means of isoresponse curves (Fig 4), which were constructed from the measuring values obtained

The sensitivity of the method The sensitivity or the number of units of the evaluation parameter per unit of local accumulations of isotope in a subregion, may be derived experimentally from measurements on a phantom system

The skull phantom and the three different lesion phantoms were all filled with the

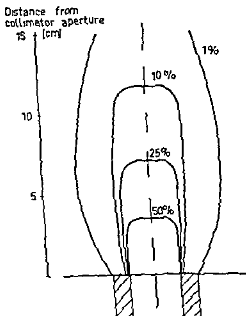


Fig 4 Isoresponse curves of the detectors

same solution $^{99}Tc^m$ pertechnetate in water The count rate from one subregion of the skull phantom only was registered by one of the detectors Thereafter the skull phantom was rinsed, refilled with pure water, and the count rates from the three different lesion phantoms at five different depths within the subregion were measured From these results I_R, I_L and D were calculated for the concentration ratios $c_0 = 2$ 1, 4 1, 8 1 and 12 1, assuming the two detectors to be equal in counting efficiency and assuming I_R, I_L and D to be proportional to $(c_0 - 1)$

Results obtained with two detectors, corrected for imbalance, were in good accordance with the results obtained with the method described above

Results

Pulse height discrimination The upper limit of pulse height discrimination was set to correspond to $E_u = 170$ keV, and the reference energy acceptance interval (ΔE_0) was between 120 and 170 keV The relation $f_t(E_l)/\sqrt{f_s(E_l)}$ was plotted in Fig 3 against E_l for three different depths, 2 5, 6 5 and 10 5 cm within the subregion of the skull phantom This relation, proportional to the significance $\bar{q}$, was almost independent of the location x of the lesion phantom in the subregion (Fig 3) Moreover the effect of reducing E_l below approximately 120 keV was only small

Since E_l should be chosen to discriminate against scattered radiation, it should be set as high as possible without decreasing the detectability Therefore, in view

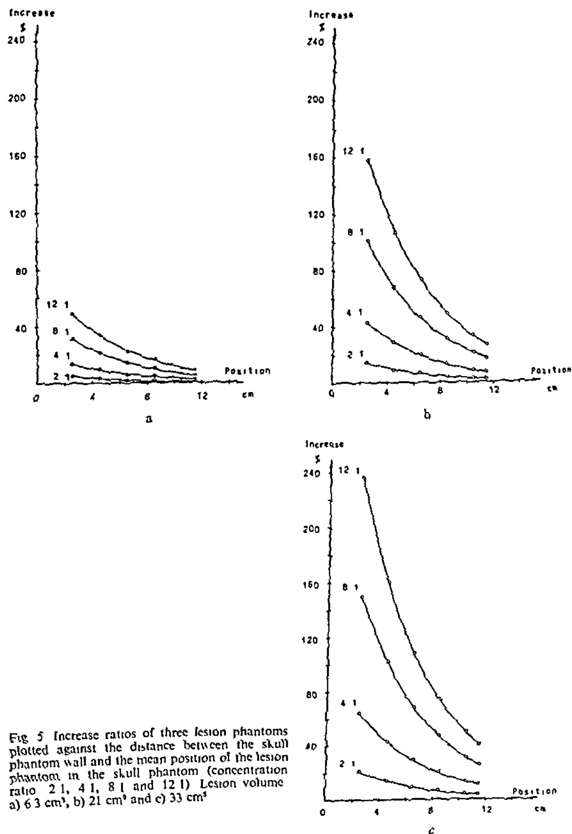
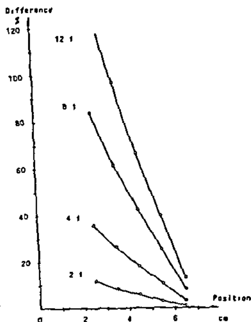


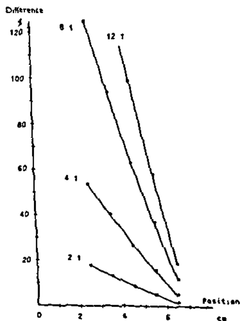
Fig 5 Increase ratios of three lesion phantoms plotted against the distance between the skull phantom wall and the mean position of the lesion phantom in the skull phantom (concentration ratio 2 1, 4 1, 8 1 and 12 1) Lesion volume a) 6 3 cm³, b) 21 cm³ and c) 33 cm³



a

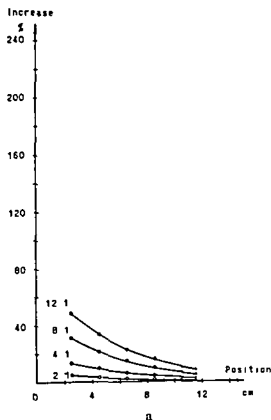


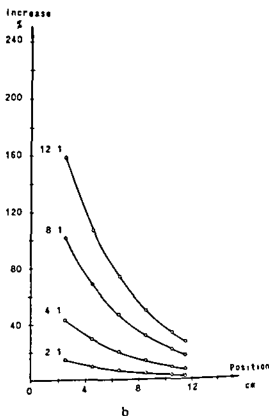
b



c

Fig 6 Difference ratios of three lesion phantoms plotted against the distance between the skull phantom wall and the mean position of the lesion phantom (concentration ratios 2 1, 4 1, 8 1, and 12 1) Lesion volume a) 6 3 cm³, b) 21 cm³ and c) 33 cm³





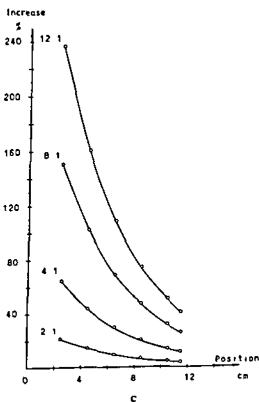


Fig 5 Increase ratios of three lesion phantoms plotted against the distance between the skull phantom wall and the mean position of the lesion phantom in the skull phantom (concentration ratio 2 1, 4 1, 8 1 and 12 1) Lesion volume a) 6 3 cm^3, b) 21 cm^3 and c) 33 cm^3

use of different lesion volumes, V_t, may be supposed to be due to a systematic error in positioning of the phantoms and also due to the approximation of assuming the volume source V_t to be equal to a point source

Discussion

Radiation hazards limit the amount of isotope administered to a single patient or population, and hence the amount of available information is limited because the distribution measurements obtained are disturbed by statistical noise Most methods for external measurement of the isotope distribution of the skull are based on image interpretation with high geometrical resolution (BURROWS 1972), and the presence and location of a possible lesion is decided subjectively, using an unknown number of parameters The choice of a small number of standardized subregions decreases the geometrical resolution, but has the advantage of giving a statistical error which may be estimated and a limited number of parameters which may be objectively compared with the corresponding values of a normal group

The chosen number of such subregions is important for the detectability properties of the method because it decides, within the given examination time, the relation between spatial resolution and precision from counting statistics

In the method described, the size and number of the subregions was determined by the collimation properties and the standardized movement of the detectors The area of the collimator apertues, 9 cm², was chosen to correspond approximately to the area of increased isotope concentration caused by a small brain lesion (BURROWS) The concentration ratios used were chosen to correspond to concentration ratios in brain tumour cases (SCHWARTZ & TATOR 1972) The length of the collimators was determined by compromising between counting statistical considerations, total investigation time, geometrical resolution at different depths and discrimination against high accumulation of pertechnetate in the skull base

Energy discrimination The choice of energy acceptance interval may be made with respect to different parameters, i e the discrimination levels can be set to compensate for drift effects in the photomultiplier and pulse electronics (Ross et coll 1968), or to obtain a high detector figure of merit, Q, in the discrimination between two different count rates (BECK & HARPER 1968) However, highly stabilized solid state devices were used for the pulse electronic equipment and the high voltage supply, and as the instability of the equipment used was shown to be unimportant, there was no need to use the settings of the pulse height discriminators to compensate for drift effects

To accord with the principles laid down for result evaluation by the method presented, the significance $\bar{q}$ was assumed to be a more suitable parameter than the figure of merit for investigating the effect of energy discrimination

$\bar{q}$ was shown from eq (21) to consist of a fixed ratio $\Delta\bar{N}_\omega/\sqrt{\bar{N}_s}$ and a function

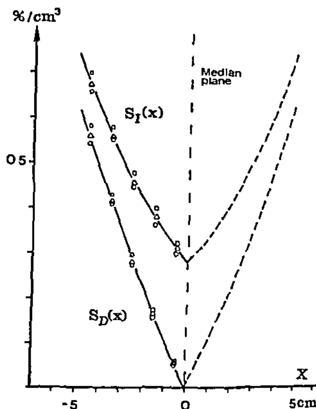


Fig 7 The sensitivity S_I of the evaluation parameter $\max(I_R, I_L)$ and the sensitivity S_D of the evaluation parameter D as derived from the phantom experiments with different lesion volumes, V_t, are plotted against the location x □ $V_t = 6.3$ cm³, △ V_t 21 cm³, ○ $V_t = 33$ cm³

of the results presented in Fig 3 the lower level was set to correspond to 120 keV In this interval, 120 to 170 keV, the background radiation was found to be around 100 to 150 cpm

Stability of counting efficiency The error due to instability effects in the counting efficiency for the two detectors with pulse height discrimination corresponding to 120 to 170 keV was negligible compared to the error due to counting statistics at the count rate level of interest (10 000 cpm)

The sensitivity of the method The relation between the ratios I, D and the location of a lesion is plotted in Figs 5 and 6 for the three different volumes V_t The concentration ratio c_0 has been used as a parameter and as an example a tumour phantom of 21 3 cm³ with a concentration ratio of 4 1 situated 2 cm from the median plane of the skull phantom increased the count rate almost 27 per cent with a difference of about 14 per cent

The sensitivity as a function of the location x was calculated from the results obtained for the two evaluation parameters max (I_R, I_L) and D, using eqs (12 a) and (12 b) This is illustrated in Fig 7 where the values of S_I and S_D are plotted against the location x of the lesion phantoms used The deviation of these results caused by the

The sensitivity of an evaluation parameter is possible to estimate from phantom experiments, but a rational choice of evaluation parameters for clinical use must be based on the detectability, which is estimated from the sensitivity of the parameter related to its normal range (LARSSON & LIND, LIND et coll.)

SUMMARY

A symmetry detector method for gammaencephalography is described. It is based on two detectors, collimated by square tubes with large apertures. Increase ratios and side difference ratios should be used as evaluation parameters in clinical applications and are therefore analysed theoretically and experimentally from measurements on a phantom system. The effect of energy discrimination is analyzed and found to be small over a wide range of the lower discrimination level setting. The chosen performance of the measuring routine used made errors caused by the electronic devices negligible in relation to the loss of precision occurring from counting statistics.

ZUSAMMENFASSUNG

Es wird eine Methode mit symmetrischen Detektoren [illegible]
schrieben. Diese [illegible]
toren mit grosser [illegible]
unterschied Verhältnis-werte sollten als Beurteilungsparameter bei der klinischen Anwendung verwendet werden, diese wurden deshalb theoretisch und experimentell von Messungen an einem Phantomsystem analysiert. Der Effekt der Energiediskrimination wurde analysiert, er erwies sich über einen weiten Bereich niedriger Diskrimitator Einstellungsniveaus als gering. Bei der gewählten Durchführung der verwendeten Messroutine können Fehler, hervorgerufen durch die elektronische Anordnungen, im Verhältnis zum Verlust der Genauigkeit, die mit der Messstatistik zusammenhängt, vernachlässigt werden.

RÉSUMÉ

Description d'une méthode à détecteur de symétrie pour la [illegible]
Elle est basée sur [illegible]
devrait [illegible]
comme [illegible] sont donc
analyses théoriquement et exérimentalement à partir de mesures faites sur un système de fantôme. Les auteurs examinent l'effet de la discrimination d'énergie et constatent que cet effet est petit sur un grand domaine de réglage du niveau inférieur de discrimination. Le fonctionnement choisi pour les mesures de routine utilisées rend négligeable les erreurs dues aux dispositifs électroniques par rapport a la diminution de la précision provenant des statistiques de comptage.

REFERENCES

BECK R. N. A theory of radioisotope scanning system. *In* Medical radioisotope scanning. Proc. IAEA Symp., Athens 1964, Vol. 1, p. 15. IAEA, Vienna 1964.

$f_t(E_l)/\sqrt{f_s(E_l)}$ and it was therefore only necessary to examine the latter in order to estimate the influence on $\bar{q}$ of E_l

The measurements were performed with an idealized measuring situation, in which the lesion phantom was located within the subregion and the skull phantom contained a homogeneous distribution of the isotope In clinical measurements the results will be affected by regions of accumulated isotope close to the measured subregion The choice of $E_l = 120$ keV can nevertheless be expected to be relevant for most of the subregions in a skull examination (Fig 3)

The results obtained are in agreement with the results obtained by BECK & HARPER, who used the figure of merit concept for an estimation of a suitable setting of the lower discrimination level

The stability of the counting efficiency To compensate against aging and long-term drift effects in clinical examinations an accurate check of the counting efficiency of the two detectors is made before each measuring procedure, and from these results, all values are corrected for imbalance The value for a subregion is also always related to a reference value, obtained from the actual measurement, thus giving a relative distribution pattern independent of long-term effects (LIND et coll)

The drift effects of interest are thus the short-term effects which could affect the values within the examination time of 30 minutes However, no such effects of any significance could be observed

The sensitivity of the method The sensitivity of measuring devices used in nuclear medicine, is usually defined as the ratio of the number of registered events/s to the total number of γ-photons/s emitted from a point-, line-, plane- or volume-source As the number of emitted γ-photons is proportional to the activity, the sensitivity will be expressed in absolute values as the count rate per unit of activity

However, this general definition is not well suited to demonstrate the properties and the differences of the relative evaluation parameters used in the clinical application of the present method Besides, reports on the accumulation of isotope in brain lesions are concerned with the lesion/brain ratio rather than with any absolute fraction of the total activity administered (BURROWS) The sensitivity was therefore derived from the relation between the relative evaluation parameters I_R, I_L and D, and the relative accumulation of isotope, $V_t(c_0$ 1)

The sensitivity could be calculated using eqs (7) to (11 b) but since scattering and penetration effects are not taken into account in these equations the results might not be sufficiently accurate and the relations between I, D and x, V_t and c_0 representing the sensitivity functions $S_I(x)$ and $S_D(x)$, have therefore been determined experimentally (Fig 7) If a phantom lesion is located between two or four fixed subregions the sensitivity is obviously less than the sensitivity for the same lesion located well within one of the subregions In patient measurements this effect is counteracted by overlapping subregions

FROM THE DEPARTMENT OF RADIOLOGY, UNIVERSITY OF COLORADO MEDICAL CENTER, DENVER, COLORADO 80220, USA

CROSS-SECTIONAL ANATOMIC IMAGES BY GAMMA RAY TRANSMISSION SCANNING

G A THIEME W R HENDEE, G S IBBOTT, P L CARSON and D L KIRCH

In the present practice of radiation therapy, a treatment regimen for a patient usually is selected by examining dose distributions computed for one or more treatment plans proposed for the patient Rarely are the dose distributions corrected for perturbations introduced by inhomogeneous structures such as lung and bone between the beam entrance surfaces and the treated region These perturbations are not accounted for, even though they may affect the tumor dose by as much as 20 to 30 percent primarily because the exact location and extent of the inhomogeneous regions within the patient are unknown

Various techniques have been proposed for delineation of the cross sectional anatomy of patients scheduled for radiation therapy Among the techniques are

(1) demonstration of cross sectional anatomic displays from orthogonal roentgenograms projected in a special viewing device This approach suffers from inaccuracy the need for a special viewing device, the time required to align the roentgenograms the corrections necessary for differences in magnification of the roentgenograms and most important, the inflexible positioning requirements for film exposure which are difficult to satisfy with seriously ill patients,

(2) display of cross sectional anatomy on roentgenograms obtained by transverse

Submitted for publication 5 March 1974

— and HARPER P V Criteria for evaluating radioisotope imaging systems *In* Fundamental problems in radioisotope scanning, chapter 30 Edited by A Gottschalk and R N Beck Charles C Thomas, Springfield, Illinois 1968

BROWNELL G L Theory of isotope scanning *In* Medical radioisotope scanning p 1 Proc IAEA and WHO seminar, Vienna 1959

BURROWS E H The clinical utility of brainscanning in nuclear medicine *In* Progress in nuclear medicine, Vol I, p 287 Edited by E J Potchen and V R McCready S Karger Basel 1972

GOTTSCHALK A Brain scanning—is it becoming unnecessarily complicated? Amer J Roentgenol 111 (1971), 851

LARSSON S and LIND M Symmetry detector method for gammaencephalography Objective diagnosis of abnormal $^{99}Tc^{m}O_4$ distribution in the skull To be published in Acta radiol Ther Phys Biol 14 (1975)

LIND M, LARSSON S and SÖDERBORG B Normal range of a symmetry detector method for gammaencephalography To be published in Acta radiol Diagnosis 16 (1975)

MACINTYRE W J, FEDORUK S O, HARRIS C C, KUHL D E and MALLARD J R Sensitivity and resolution in radioisotope scanning Nucl-Med (Stuttg) 8 (1969) 99

MAYNEORD W V Some applications of nuclear physics to medicine Brit J Radiol (1950) Suppl No 2

MOORE G E Use of radioactive diiodofluorescein in the diagnosis and localization of brain tumors Science 107 (1948) 569

MUNDINGER F und ASAI A Ergebnisse der digitalen Gammaencephalographie bei Hirntumoren Vergleich von Wismut^{206}, Quecksilber ^{203} — Neohydrin und Technetium^{99m} Arch Psychiat Nervenkr 210 (1967), 297

PLANIOL T Diagnostic des lésions intra craniennes par les radio isotopes (gammaencéphalographie) Masson et Cie, Paris 1959

— Gamma encephalography after ten years utilization in neurosurgery Progr Neurol Surg 1 (1966), 93

ROSS D A, HARRIS C C, KUHL D E, REBA R C, WAGNER H N JR and KARMEN A Measurement of radioactivity Physical principles of radionuclide scanning Whole body counting Liquid scintillation counting *In* Principles of nuclear medicine, chapter 5, p 129 Edited by H N Wagner Jr W B Saunders, Philadelphia 1968

SCHWARTZ M L and TATOR C H Shortcomings of ^{99m}Tc pertechnetate as a tracer for brain tumour detection as shown by well counting of human brain tumours and mouse ependymoblastoma J nucl Med 13 (1972) 321

FROM THE DEPARTMENT OF RADIOLOGY, UNIVERSITY OF COLORADO MEDICAL CENTER, DENVER, COLORADO 80220, USA

CROSS-SECTIONAL ANATOMIC IMAGES BY GAMMA RAY TRANSMISSION SCANNING

G A THIEME, W R HENDEE, G S IBBOTT, P L CARSON and D L KIRCH

In the present practice of radiation therapy, a treatment regimen for a patient usually is selected by examining dose distributions computed for one or more treatment plans proposed for the patient Rarely are the dose distributions corrected for perturbations introduced by inhomogeneous structures such as lung and bone between the beam entrance surfaces and the treated region These perturbations are not accounted for, even though they may affect the tumor dose by as much as 20 to 30 percent, primarily because the exact location and extent of the inhomogeneous regions within the patient are unknown

Various techniques have been proposed for delineation of the cross sectional anatomy of patients scheduled for radiation therapy Among the techniques are

(1) demonstration of cross sectional anatomic displays from orthogonal roentgenograms projected in a special viewing device This approach suffers from inaccuracy, the need for a special viewing device, the time required to align the roentgenograms, the corrections necessary for differences in magnification of the roentgenograms, and, most important, the inflexible positioning requirements for film exposure which are difficult to satisfy with seriously ill patients,

(2) display of cross-sectional anatomy on roentgenograms obtained by transverse

Submitted for publication 5 March 1974

tomography The cost of transverse tomographic equipment capable of flexible patient positioning, and the poor quality of transverse tomographic images, are the major limitations of this technique,

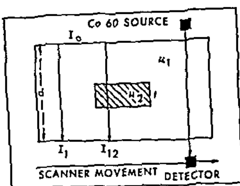
(3) representation of cross-sectional anatomy by obtaining individual patient contours and superimposing standard anatomic displays available in pictoral atlases This method is no more than a crude approximation, because it offers no compensation for anatomic variations among patients,

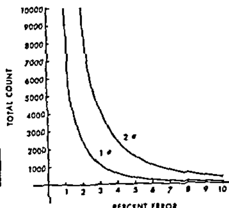
(4) development of cross-sectional anatomic displays by B-mode ultrasound scanning This approach is being utilized in a few institutions, including our own However, the usefulness of ultrasound scanning techniques in the thorax, the region where dose perturbations caused by inhomogeneities may be greatest, is limited severely by the poor transmission of ultrasound energy in lung Furthermore, current B-mode ultrasound techniques provide only limited information about the internal anatomy of patients, primarily because the information contained in the amplitude of returning ultrasound pulses is discarded Current work in ultrasound B-mode imaging, involving the development of constant depth scanning techniques, promises to improve the spatial resolution and amplitude information of ultrasound images As this work has progressed, it has become clear that ultrasound imaging of internal anatomy is complementary to, and not competitive with, the approach to delineation of cross-sectional anatomy outlined in this report Moreover, it has become apparent that ultrasound scanning at constant depth may be more amenable to tumor localization and, possibly, identification, than to display of cross-sectional anatomy across an entire plane containing a tumor,

(5) determination of cross sectional anatomy by measurement of roentgen or γ-ray transmission through the patient at a number of angular orientations, and reconstruction of cross-sectional images by data processing techniques, this approach is described here

Some attention already has been directed toward the demonstration of cross-sectional anatomy by roentgen or γ-ray scanning CORMACK (1964, 1973) has examined the problem mathematically and experimentally in an effort to identify a method for outlining the cross sectional anatomy of radiation therapy patients However, both the experimental apparatus and the mathematical reconstruction process used by CORMACK were intentionally simplistic, because they were developed primarily as a test of the feasibility of the approach Consequently, the question has remained unanswered of the practicality of roentgen or γ-ray transmission scanning for routine display of the cross sectional anatomy of radiation therapy patients

For many years, KUHL and his associates have been interested in the production of transverse tomographic images from data recorded by an isotope scanner which scans transversally across a patient containing an administered isotope (KUHL & EDWARDS 1970) Primarily, KUHL's work has been directed towards use of transverse tomographic scanning methods to improve the detectability of small concentrations of activity in the brain Application of the analytic techniques developed by KUHL





a

b

to the transmission data collected in the present work produced reassembled images with unacceptably poor resolution and considerable distortion

A few persons have attempted to use linear equations in the construction of three-dimensional images from two-dimensional projections (GORDON et coll 1970, GOITIEN 1971, GILBERT 1972, SMITH et coll 1973) This method appears impractical for the project described here, primarily because the number of linear equations is too formidable

A potentially more useful approach is that described by RADON (1917) This work offers an approach to computation of surface integrals analogous to certain physical processes such as transmission γ ray scanning at increments around a circle encompassing the patient Limitations in RADON's approach, including its suitability primarily for objects of spherical shape with constant attenuation coefficients, have led to selection of an alternate approach for the project described here

Recently, FARMER & COLLINS (1971) described an approach to delineation of anatomic cross sections which, in some ways, resembles the method described in this report These investigators used a Ge(Li) detector and pulse height analyzer to detect scattered photons as a ^{13} Cs source was scanned across a phantom Successive scans at different elevations were displayed on an oscilloscope screen to produce a two-dimensional image of the cross section of the phantom No data processing, other than background cut off, was employed For a patient thickness of 30 cm, the theoretical spatial resolution is quoted as 5 mm for the Farmer-Collins method Limitations of this method include considerable variations in intensity and spatial resolution over the displayed image, particulary for patients of thickness greater

Table I

Linear attenuation coefficients for muscle, compact bone, and lung, and fractional changes b in the transmission of 1 25 MeV γ-ray photon when lung or compact bone of thickness t is present in muscle

Material	Linear attenuation coefficient (cm^{-1}) 1 25 MeV photons	Thickness		
		t (cm)	b (bone)	b (lung)
Muscle	0 064*	0 25	+0 013	−0 011
Compact bone	0 114*	0 50	+0 025	−0 021
Lung	0 021**	1 00	+0 051	−0 042
		1 50	+0 078	−0 062
		2 00	+0 105	−0 082

* From JOHNS & CUNNINGHAM

** From IBBOTT & HENDEE

than 30 cm As an alternative to the Farmer-Collins method, the method discussed below provides increased sensitivity by measurement of transmitted rather than scattered photons and by employment of a higher photon yield ^{60}Co source in place of ^{137}Cs

Instrumentation design

Discussed in this section are physical considerations affecting the design and performance of a γ-ray transmission scanner In Fig 1 a, muscle of thickness d and linear attenuation coefficient μ_1 for photons of energy E surrounds an inhomogeneous structure such as lung or bone of thickness t and linear attenuation coefficient μ_2 for photons of the same energy A narrow beam of monoenergetic γ-ray photons passes through the medium and impinges upon a detector equipped with a pinhole collimator With proper collimation of the γ-ray beam and detector, the influence of scattered radiation can be minimized, and the fraction of γ-ray photons transmitted through the medium is an exponential function which varies only with the attenuation coefficients and the thicknesses of the materials traversed That is,

$$I_1 = I_0 \, EXP\,(-\mu_1 d) \tag{1}$$

where $EXP\,(-\mu_1 d)$ is the fractional transmission of the γ-ray beam passing only through muscle, and

$$I_{12} = I_0 \, EXP\,[-\mu_1(d-t)] \, EXP\,(-\mu_2 t) \tag{2}$$

where $EXP\,[-\mu_1(d-t)]\, EXP\,(-\mu_2 t)$ is the fractional transmission of the γ-ray beam passing through both muscle and lung or bone

If b is defined as the fractional change in beam intensity caused by the presence of an inhomogeneity of thickness t, then

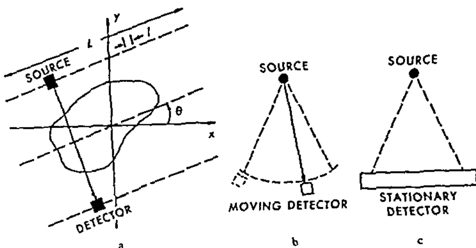


Fig 2 Different approaches to γ ray transmission scanning, including (a) moving source, moving detector technique, (b) stationary source, moving detector technique, and (c) stationary source, stationary detector technique

$$b = \frac{I_1 - I_{12}}{I_1} = 1 - \mathrm{EXP}\left[-(\mu_2 - \mu_1)t\right] \tag{3}$$

That is, the fractional change in beam intensity depends only upon the thickness of the inhomogeneity and the linear attenuation coefficients of the two materials Linear attenuation coefficients for muscle, compact bone and lung irradiated with photons of 1 25 MeV, the average energy of γ ray photons from ^{60}Co, are listed in Table 1 Included in the table are fractional changes in γ-ray transmission computed for different thicknesses of bone or lung embedded in muscle and irradiated with 1 25 MeV photons Positive values of b indicate an inhomogeneity with a linear attenuation coefficient greater than that for muscle, and negative values imply an inhomogeneity with a coefficient smaller than that for muscle

For a 0 25 cm thick inhomogeneity of either bone or lung in muscle, the change in beam intensity is slightly greater than 1 percent Whether a measured change of 1 percent in beam intensity is considered statistically reliable, and indicative of a change in physical density along the beam path, depends upon the total number N of photons collected for the measurement and upon the confidence and significance levels chosen as statistical criteria (Fig 1 b)

For gamma transmission measurements, ^{60}Co was chosen as the source of γ-ray photons Advantages of ^{60}Co include (1) high specific activity, (2) ready availability at reasonable cost, (3) decay to a stable product, (4) emission of two γ-ray photons, each with an emission probability >99 percent, (5) negligible error introduced by considering the emitted photons (1 17 and 1 33 MeV) as photons of a single average

energy of 1 25 MeV, (6) photon attenuation almost entirely by Compton interaction, and (7) high transmission of photons in biologic tissues

Two approaches to transmission scanning, a moving source technique and a stationary source technique, were considered (Fig 2) For the moving source approach, transmission data are obtained with a tightly collimated source and detector moving linearly and in synchrony on opposite sides of the patient at an angle θ with respect to a reference axis (Fig 2 a) For the stationary point source technique, either a pencil beam of radiation is swept across the patient in synchrony with a single moving detector (Fig 2 b), or a wedge of radiation is directed through the patient onto a long, stationary detector with adequate spatial resolution (Fig 2 c) Analysis of the image reconstruction process for both approaches favors the parallel beam approach to transmission scanning Consequently, this approach has been employed for the investigation described here

If a scan interval (the distance between successive transmission measurements) is represented by I, and the total linear scan distance for one angular orientation of source and detector is represented by L, then the number of transmission measurements M per orientation is $M = L/I$

With the fractional transmission through the maximum thickness of tissue encountered during the scan represented as P, and the total time required to scan a distance L designated as T, the measurement time at each of M points along L is T/M or TI/L For the maximum tissue thickness encountered during the scan, at least N photons must be detected, where N is the minimum number of photons required for the desired level of statistical significance This number of photons would increase to N/P in the absence of tissue The number N/P of photons must be detected in the interval TI/L, consequently, the photon detection system must be capable of detecting photons at a rate δ equal to

$$\delta = \frac{N/P}{TI/L} = \frac{NL}{TIP} \quad (4)$$

The parameter δ is an important consideration in the selection of a photon detection system for γ-ray transmission scanning

For detection of photons at the rate δ, the source must supply photons at a rate Φ equal to

$$\Phi = \frac{\delta}{\varepsilon A} = \frac{NL}{\varepsilon ATIP} \quad (5)$$

where Φ is the photon flux density at the detector, A is the cross-sectional area of the detector collimator, and ε is the detector efficiency The photon flux density is related to the exposure rate χ by

$$\frac{\Phi}{X} = \frac{1\,5 \times 10^{3}}{h\nu(\mu_{en})} \quad (6)$$

with Φ, χ, $h\nu$, and μ_{en} in units of photon/cm^2 − s, R/h, MeV, and m^2/kg in air, respectively For ^{60}Co, $h\nu = 1.25$ MeV and $(\mu_{en}) = 2.67 \times 10^{-3}$ m^2/kg for air, and the exposure rate χ necessary for a photon flux density Φ is

$$\chi(\mathrm{R/h}) = 2.23 \times 10^{-6}\,\Phi(\mathrm{photon/cm^2 - s}) \tag{7}$$

A lower limit (self absorption neglected) on the activity of a ^{60}Co source which will provide an exposure rate χ at a distance r in meters is

$$N_{Ci} = \frac{\chi(\mathrm{R/h})\,r^2}{\Gamma} \tag{8}$$

where N_{Ci} is the activity in curies, and Γ is the exposure rate constant ($\Gamma = 1.29$ R/h − Ci at 1 meter for ^{60}Co) By combining equations (5), (7), and (8), the minimum ^{60}Co source activity required for a least N detected photons per measurement point may be written

$$N_{Ci} = \frac{2.23 \times 10^{-6}\,NLr^2}{\varepsilon ATIP\Gamma} \tag{9}$$

Equation (9) illustrates the importance of detector efficiency in minimizing source size and patient exposure to radiation, and suggests that a high efficiency scintillation detector is preferable to an ionization chamber for γ-ray transmission measurements However, the choice of a detector also depends upon the ability of various detectors to respond to high photon flux densities To estimate the maximum photon flux density to which a detector must respond, a maximum patient thickness of 40 cm (fractional transmission P 0 077 for ^{60}Co photons in muscle) and a smallest scan interval I of 0 25 cm may be assumed For any patient, the scan time should not exceed, say 30 minutes In actual practice, a scan time of <5 minutes may be desired to reduce voluntary motion artefacts If no deconvolution and data smoothing techniques are used during image reconstruction, 120 separate transmission scans would be required to satisfy the image reconstruction criterion described later In a fully automated scanner, a time T of 10 seconds might be needed to scan a 40 cm length at a constant speed of 4 cm/s If rotation of the source-detector assembly by 1 5° requires 3 seconds, then each transmission scan at a separate angular orientation would require 13 seconds, and 26 minutes would be required to accumulate transmission data for 120 orientations For 1 percent, 1 σ counting statistics, at least 10 000 photons must be detected at each measurement point With these values, a maximum photon detection rate δ of 2.08×10^6 photons/s is required (Eq 4)

The computed photon detection rate is twice the maximum detection rate for a NaI detector operated in pulse mode (Table 2) Hence, use of a NaI detector in pulse mode appears marginal for transmission scanning

To take advantage of the high detection efficiency of NaI for ^{60}Co photons, the detector may be operated in current mode, where limitations on the photon detec-

Table 2

Characteristics of common scintillators (in part from KAISER)

Scintillator	Time constant τ (μs)	Density (g/cm^3)	Detection efficiency relative to anthracene	Maximum detection rate for pulse mode operation (photon/s)
NaI(Tl)	0 25	3 67	2 1	$8\ 7 \times 10^5$
CsI(Tl)	1 1	4 51	1 75	$2\ 0 \times 10^5$
CsI(Na)	0 65	4 51	1 10	$3\ 3 \times 10^5$
Anthracene	0 032	1 25	1 00	$6\ 8 \times 10^6$
Plastics	0 0025–0 005	1 06	0 28–0 48	$4\ 3–8\ 7 \times 10^7$
Liquid	0 0015–0 008	0 86	0 27–0 49	$2\ 7–14\ 5 \times 10^7$

tion rate are imposed by the characteristics of the photomultiplier tube rather than NaI Another advantage of current mode operation is an increase in detection efficiency for ^{60}Co photons For example, a 4 5 cm diameter, 4 cm long NaI detector operated in pulse mode under conditions of photopeak counting yields a detection efficiency of 22 percent, in current mode, the detection efficiency is close to 61 5 percent (BERGER & DOGGET 1956) For a maximum patient thickness of 30 cm and a total scan time of up to 30 min, the source activity could be 60 percent less than that required for a 40 cm thick patient, and operation of a NaI detector in pulse mode would be marginally acceptable With this source, however, more than 1 hour would be required to scan a 40 cm thick patient However, operation of a NaI detector in current mode has two drawbacks First, the signal is sensitive to slight changes in high voltage applied to the photomultiplier tube and signal amplification in the amplifier Second, pulse height discrimination is not available to differentiate primary from scattered photons

In our apparatus, signal drift is not noticeable provided that the amplifier and high voltage supply are turned on a few minutes before measurements are taken To examine the handicap of using a NaI detector without pulse height discrimination, a ^{60}Co pulse height spectrum was measured with a 1×1 inch NaI detector From the results, it was apparent that the lower discriminator of the pulse height analyzer must be set at about 1 05 MeV to include both photopeaks This setting would transmit to the scaler pulses representing 1 33 MeV photons scattered through angles up to 26°, and 1 17 MeV photons scattered through angles up to 18° That is, for a source-detector collimator arrangement with a scatter acceptance angle less than 18°, and negligible penetration of scattered photons through the collimator walls, pulse height analysis does not contribute to rejection of scattered photons when the lower level discriminator is set below both photopeaks Consequently, the loss of pulse height analysis accompanying use of a NaI detector in current mode

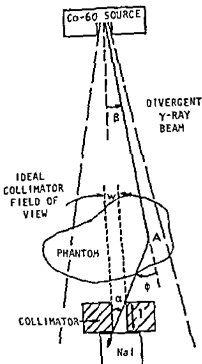


Fig. 3 Geometry for rejection of scattered photons by the detector collimator

poses no handicap if the collimation of source and detector is made sufficiently restrictive

The admission into a detector of photons scattered from outside the region of interest is illustrated in Fig 3 With a detector collimator of length l and diameter w, the acceptance angle α for scattered photons entering the detector is $\alpha = \tan^{-1} w/l$ For a photon traversing the patient at an angle β with respect to the central axis of the collimator bore, the scattering angle Φ which will just permit a scattered photon to reach the detector is $\Phi = \alpha + \beta$ The amount of scattered radiation reaching the detector can be minimized by (1) reducing α by decreasing the bore size w and increasing the length l of the detector collimator, and (2) reducing β by decreasing the diameter and increasing the length of the source collimator, at least to the limit of retaining a uniform photon flux density across the detector Both of these options have been exercised in this investigation the detector collimator slit has been reduced to dimensions comparable to the spatial resolution desired in the image, and the source collimator has been designed to provide a γ-ray beam which only slightly overlaps the detector collimator slit

For photons of 1 33 MeV, 15 cm of lead yields an attenuation of 99 995 percent and an energy absorption of 99 9 percent With a detector collimator of this length containing a 2 5 mm × 5 mm slit, the maximum acceptance angle α is 2 1° along a

Table 3

Upper limits for the ratio of scattered to primary photons accepted by the detector collimator for selected tissue thicknesses

Tissue thickness (cm)	N_s/N	$[(N_s/N)f]$ (%)	Upper limit per cent scatter 0 1 f N_s/N (%)	Scatter angle ϕ	Fraction f of all scattered photons (×10)
10	0 90	0 27	0 03	0-6°	1 4153
15	1 61	0 43	0 04	0-5°	0 9866
20	2 60	0 70	0 07	0-4°	0 6328
25	3 95	1 07	0 11	0-3°	0 3559
30	5 82	1 57	0 16	0-2°	0 1575
35	8 39	2 26	0 23	0-1°	0 0386
40	11 94	3 23	0 32		

diagonal in the collimator slit For a source collimator with a 2 mm × 4 mm slit positioned 50 cm from the source, the maximum divergence angle β is 0 51° along the slit diagonal With this combination of collimators, the maximum scattering angle Φ is 2 6° for photons reaching the detector From the Klein-Nishina equation, the fraction f of all ^{60}Co scattered photons confined to scattering angles from 0° to 2 6° is f = 0 0027 Under the good geometry conditions employed for transmission scanning, the ratio N_S/N of photons scattered in the patient to primary photons reaching the detector is

$N_S = N_0 - N$ N_0 = number of primary photons reaching detector with no
but $N_0 = N \, \mathrm{EXP}(\mu t)$ scattering medium present
$N_S = N[\mathrm{EXP}(\mu t) - 1]$
$N_S/N = \mathrm{EXP}(\mu t) - 1$ N = number of primary photons reaching detector with scattering medium present

The product of N_S/N and f is an overestimate of the ratio of scattered to primary photons reaching the detector, because photons are scattered at an angle ϕ isotropically about the direction of primary photons, and only a few ($<1/10$) of the scattered photons enter the solid angle subtended by the detector-collimator assembly As upper limits for the ratio of scattered to primary photons reaching the detector, values of 0 1 f N_S/N are listed in Table 3 for selected tissue thicknesses From these data, it is apparent that the collimator design described above will reduce scattered photons to a negligible level (0 3 %) This analysis has been confirmed experimentally by attenuation curves measured in water and lead for detector collimators with dimensions of 3 cm × 3 cm, 1 cm × 1 cm, 4 mm × 6 mm and 2 mm × 4 mm For the smallest collimator slit, measured attenuation curves correspond closely to curves computed for a narrow beam of ^{60}Co photons

With the source and detector arrangement described above, a minimum source

activity can be computed which will provide 10 000 detected photons (1 %, 1σ statistics) per measurement point with a maximum patient thickness of 40 cm between source and detector For ^{60}Co photons, a cylindrical NaI crystal 10 cm thick provides an estimated detector efficiency $\varepsilon = 0.85$ in current mode A detector collimator slit with dimensions of 2 5 mm × 5 mm has a cross sectional area $A = 0.125\ cm^2$ With these values and equation (5), the maximum photon flux density Φ at the detector is 19.6×10^6 photon/cm²/s for L = 40 cm, T = 10 s, I = 0 25 cm and P = 0 077 This value of Φ corresponds to an exposure rate of 43 3 R/h at the detector with the patient absent For a source detector distance 1 5 meters, a lower limit (self absorption in ^{60}Co source neglected) of 77 Ci may be estimated for the ^{60}Co source

A most important consideration is the absorbed dose to a patient examined with the transmission scanning assembly To estimate the patient dose, the absorbed dose distribution was computed for a single transmission scan of a patient with a 40 cm diameter circular cross section These data were summed over k_{max} angular orientations of source and detector to obtain the absorbed dose distribution delivered during the entire examination Data for the computation included a beam width of 0 5 cm, depth dose data for 0 cm × 0 cm field, a scanning time of 10 seconds at one angular orientation, and an exposure rate of 1 R/min at 80 cm from the ^{60}Co source For 60 angular orientations of source and detector, the maximum dose delivered to a 40 cm thick circular patient is 0 084 rad, for 120 orientations, this value would double to 0 169 rad The exposure rate computed above of 43 3 R/h at the detector corresponds to 2 54 R/min at the 80 cm distance from source to patient surface Hence, the absorbed dose of 0 169 rad for 120 angular orientations and 0 25 cm spatial resolution should be increased by a factor of 2 54 to a maximum dose of 0 43 rad For patients less than 40 cm thick, the maximum dose would be decreased significantly

Image reconstruction

In an object exposed to a narrow parallel beam of monoenergetic photons, the transmitted intensity I_x (e g the photon flux density) is related to the incident intensity I_0 by the expression

$$I_x = I_0 \, \mathrm{EXP}\left[-\int_{\infty}^{\infty} \mu(x, y)\varrho(x, y)\, dy\right] \tag{10}$$

where $\mu(x\ y)$ is the mass attenuation coefficient distribution function of the object for the photons employed, and $\varrho(x, y)$ is a function describing the physical density distribution of the object Equation 10 may be rewritten

$$\log I_0 - \log I_x = \int_{\infty}^{\infty} \mu(x, y)\varrho(x\ y)\, dy = \int_{\infty}^{\infty} f(x, y)\, dy = g(x) \tag{11}$$

where $f(x, y)$ is a general density function (specifically, $f(x, y)$ is the linear attenuation coefficient) incorporating the mass attenuation coefficient and the physical

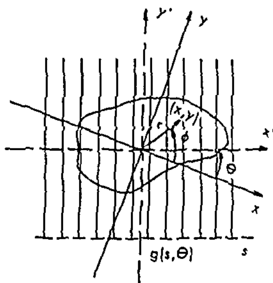


Fig 4 Set of functions $g(s, \theta)$ describing the transmitted photon intensity at any location along a line parallel to the x' axis

density functions, and $g(x)$ is a transmission function If the object is scanned at several angles θ by rotating the coordinate axes, then a set of functions $g(s, \theta)$ is obtained which describes the transmitted intensity at any location s along a line parallel to the x' axis below the object for any scan angle θ (Fig 4)

By application of Fourier transform properties, $f(x, y)$ may be reconstructed from transmission scan data $g(s, \theta)$ The Fourier transform of $f(x, y)$ in cartesian coordinates is

$$F(X, Y) = \int_{-\infty}^{\infty}\int_{-\infty}^{\infty} f(x, y)\, \mathrm{EXP}\,[+2\pi i(xX + yY)]\, dxdy$$

and the inverse transform is

$$f(x, y) = \int_{-\infty}^{\infty}\int_{-\infty}^{\infty} F(X, Y)\, \mathrm{EXP}\,[-2\pi i(xX + yY)]\, dXdY \tag{12}$$

In polar coordinates

$$f(r, \phi) = \int_{0}^{2\pi}\int_{0}^{\infty} F(R, \theta)\, \mathrm{EXP}\,[-2\pi iRr \cos(\phi - \theta)]\, RdRd\theta \tag{13}$$

Through a series of manipulations, this equation may be expressed in terms of the transmission function $g(s, \theta)$ according to the two equations

(a) The one-dimensional Fourier transform of $g(s, \theta)$ given by

$$F(R, \theta) = \int_{-\infty}^{\infty} g(s, \theta)\, \mathrm{EXP}\,(2\pi isR)\, ds$$

(b) The two-dimensional Fourier transform of the function $F(R, \theta)$ given by

$$f(r, \phi) = \int_0^{2\pi} \int_{\infty}^{\infty} F(R, \theta) \, EXP[-2\pi i Rr \cos(\phi - \theta)] \, R dR d\theta \tag{15}$$

By application of the convolution theorem (RAMACHANDRAN & LAKSHMINARAYANAN 1971), the Fourier transforms above may be reduced to two single discrete summations The first is

$$g'(na, \theta) = a \sum_{m=-\infty}^{\infty} g(ma, \theta) \, q[(m-n)a] \tag{16}$$

where $g(ma, \theta)$ describes the transmission data at a set of equally spaced points s ma, where m is a positive or negative integer and a is the spacing interval between points In equation 16, the function $g(ma, \theta)$ is convolved with the expression $q[(m-n)a]$ to yield $g(na, \theta)$, the convolved form of the transmission data Since $q[(m-n)a]$ equals $1/4a^2$ for $(m \; n)=0$,

$$\frac{-1}{\pi^2(m-n)^2 a^2} \text{ for } (m-n) \text{ odd, and zero for } (m-n) \text{ even,} \tag{17}$$

equation (16) may be rewritten

$$g(na \; \theta) = \frac{g(na \; \theta)}{4a} - \frac{1}{a\pi^2} \sum_{p\,odd} \frac{g[(n+p)a, \theta]}{p^2} \tag{18}$$

where p now equals $(m-n)$ The second summation calculates $f(r, \phi)$ in the discrete form $f(jr_0 \; k\phi_0)$ by summing $g'(na \; \theta)$ over θ as follows

$$f(r, \phi) = f(jr_0, k\phi_0) = \theta_0 \sum_{k=1}^{k_{max}} g'[jr_0 \cos(t\phi_0 - k\theta_0), k\theta_0] \tag{19}$$

where j, k, k_{max} and t are integers, and r_0 and ϕ_0 are spacing intervals for r and ϕ The spacing interval for θ is $\theta_0 - \pi/k_{max}$, where k_{max} is the number of transmission scans recorded at periodic intervals between $-\pi/2$ and $\pi/2$ Since the value of $jr_0 \cos(t_{\phi_0} - k_{\theta_0})$ is generally not a multiple of a, interpolation between computed values of $g(na \; \theta)$ is necessary The resolution of the final data $f(r, \phi)$ is dependent upon the accuracy of this interpolation, and, consequently, upon the size of the spacing interval a for the transmission data

Equations 18 and 19 are readily adaptable to computer analysis Furthermore, these equations permit the reconstruction to take place in real space only, and a transformation to reciprocal space is not required

The array $I(M, k)$ consists of data describing the transmitted beam intensity for a finite number M_{max} of points separated by an interval a for each angle $k = 1$ to k_{max} at which transmission data are obtained The positive integers M and k are suitable for use with a variety of programing languages From equation 11, for an incident intensity I_0 the transmission function $G(M, k)$ corresponding to $g(ma, \theta)$ may be expressed as

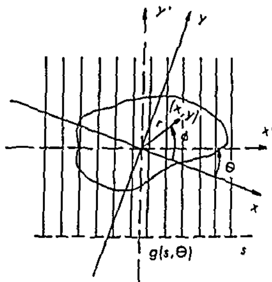


Fig 4 Set of functions $g(s, \theta)$ describing the transmitted photon intensity at any location along a line parallel to the x' axis

density functions, and $g(x)$ is a transmission function If the object is scanned at several angles θ by rotating the coordinate axes, then a set of functions $g(s, \theta)$ is obtained which describes the transmitted intensity at any location s along a line parallel to the x' axis below the object for any scan angle θ (Fig 4)

By application of Fourier transform properties, $f(x, y)$ may be reconstructed from transmission scan data $g(s, \theta)$ The Fourier transform of $f(x, y)$ in cartesian coordinates is

$$F(X, Y) = \int_{\infty}^{\infty} \int_{\infty}^{\infty} f(x, y) \, EXP \, [+2\pi i(xX + yY)] \, dxdy$$

and the inverse transform is

$$f(x, y) = \int_{-\infty}^{\infty} \int_{-\infty}^{\infty} F(X, Y) \, EXP \, [-2\pi i(xX + yY)] \, dXdY \qquad (12)$$

In polar coordinates

$$f(r, \phi) - \int_{0}^{\pi} \int_{0}^{\infty} F(R, \theta) \, EXP \, [-2\pi iRr \cos(\phi \quad \theta)] \, RdRd\theta \qquad (13)$$

Through a series of manipulations, this equation may be expressed in terms of the transmission function $g(s, \theta)$ according to the two equations

(a) The one-dimensional Fourier transform of $g(s, \theta)$ given by

$$F(R, \theta) = \int_{\infty}^{\infty} g(s, \theta) \, EXP \, (2\pi isR) \, ds$$

(b) The two-dimensional Fourier transform of the function $F(R, \theta)$ given by

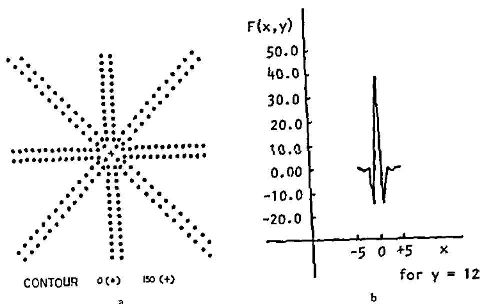


Fig 6 Image reconstruction for simulated transmission scan data generated by a delta function a) zero contour plot for the point spread function resulting from the image reconstruction program,

Point spread function for the image reconstruction process Transmission data generated with a delta function were submitted to the image reconstruction program The resultant point spread function (PSF) was a characteristic two-dimensional star image (Fig 6) not unlike those often encountered in data processing techniques for nuclear medicine images The number of rays intersecting at the image center equals the number of angles for which simulated scan data were entered The rays are symmetrical about the x–y axes and are spaced equally from each other, as were the transmission scans

The integration in equations 10 and 11 can be interpreted as 'looking through' the delta function at zero and summing the values of everything seen along the line of sight—in this case only the spike at (0, 0) Effectively then, GP(N, k) is not a one dimensional but a two-dimensional function whose extension into the second dimension is shown in Fig 7 a By superimposing GP(N, k) extended planes at appropriate angles θ, the data ensemble shown in Fig 7 b is obtained

The radial rippling effect exhibited in Figs 6 a and 7 b accompanies the convolution process and decreases markedly with an increase in the number of orientations at which transmission data are obtained That is, the radial rippling effect decreases with increasing k_{max} (decreasing θ_0), moreover, as $k_{max} \to \infty$, the ensemble of GP(N, k)

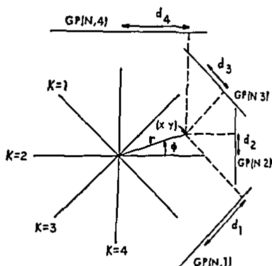


Fig 5 The parallel beam scanning technique of the summation process described by equations 20, 21 and 22

$$G(M, k) = \log I_0 - \log I(M, k) \tag{20}$$

The simplest form of the convolved transmission data GP(N, k) corresponding to $g'(na, \theta)$ is derived under conditions of a one-to-one correspondence for M and N (i e $M_{max} = N_{max}$) From equation 18,

$$GP(N, k) = \frac{G(N, k)}{4a} - \frac{1}{a\pi^2} \sum_{p\,odd} \frac{G[(N+P), k]}{p^2} \tag{21}$$

where p is limited to odd values, $-M_{max} < p \leq M_{max}$, for the finite case To determine the general density function f(x, y) in rectangular coordinates (Fig 5), values of r and ϕ are computed for each location (x, y), and f(x, y) is computed by an interpolative procedure for equation 22

$$f(x, y) = f(r, \phi) = \theta_0 \sum_{k=1}^{k_{max}} GP(d_k, k) \tag{22}$$

where $d_k = r \cos(\phi - k\theta_0) + N_0$

The point $M = N = N_0$ falls on a line passing through the origin and perpendicular to GP(M, k) and, therefore, I(M, k) and G(M, k) Since M and N are defined as sets of positive integers, the translation N_0 is necessary so that $d = N_0$ when $r = 0$ In general, integer values for d_k are not obtained (i e , usually $N < d_k < N+1$), and the projection of transmission scan data upon GP(N, k) for each point (x, y) must be determined by interpolation of $GP(d_k, k)$ between GP(N, k) and GP(N+1, k)

To determine the correctness of this approach to two-dimensional image reconstruction, equations 20, 21, and 22 were evaluated for several simulated experiments utilizing computer generated, moving source and detector transmission data These experiments are described below

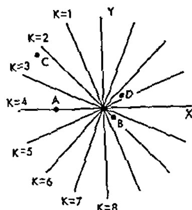


Fig 8 Four locations (*A B, C* and *D*) selected, in addition to the origin, for analysis of point spread functions for the moving source and detector scanning technique

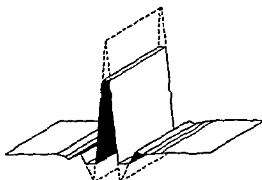


Fig 9 Graphical display of the function GP(N, k) where the interpolation procedure has reduced the peak value of the function

the function centered at B, since the perpendicular distance from the ray k = 6 through the origin to the point B is $\sqrt{2}$ rather than an integral multiple of a = 1, and the value of the function falls to 6 The result is a 'clipped' GP(N, k) function in the plane extended to two dimensions (compare Fig. 9 to Fig 7 a) The values of the PSF are constant along rays k = 4 and k = 8 for all (x, y), because the spike coordinates are all integral multiples of the spacing interval a = 1 For the spike location (0, 0), all values for the function equal 19 for k = 1 to 8, because every ray (i e , every value of k) intersects (0, 0), and no interpolation for the function is necessary

If the sampling intervals for transmission scan data were much smaller than the

Table 4

Point spread function values for selected values of k, illustrating the apparent nonisoplanicity in the PSF introduced by discrete sampling intervals and interpolation procedures

Spike value at (x, y)	Coordinates of spike (x, y)	Approximate average value of PSF along ray k for k = 1 to 8 at a radius > 8 units								Sum of average PSF values for k = 1 to 8	Average value of PSF for all k	Ratio of average PSF to spike value
		k = 1	2	3	4	5	6	7	8			
154	(0, 0)	19	19	19	19	19	19	19	19	152	19.0	0.123
96	A (−5, 0)	8	6	16	19	16	6	8	19	98	12.3	0.128
92	B (1, −1)	6	19	6	19	10	6	19	19	95	11.9	0.129
89	C (−7, 5)	7	6	16	19	9	5	7	19	88	11.0	0.124
105	D (3, 2)	6	6	17	19	10	8	17	19	102	12.8	0.122

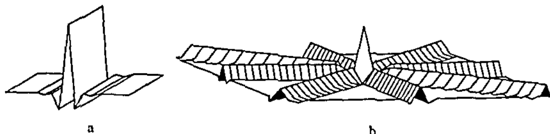


Fig 7 The two dimensional function GP(N, k) a) GP(N, k) along one angular orientation b) GP(N, k) summed at appropriate angular orientations

approaches a smoothly varying function with no periodicity and resembles a delta function surrounded by a zero plane of radius $r \to \infty$ Of course, to obtain a zero plane without variations, N must approach ∞ along with k_{max} In the practical case, a generally satisfactory criterion relating the mean radius $\langle r \rangle$ of the scanned region, the sampling distance a for transmission data, and the equiangular interval θ_0 in radians is $\langle r \rangle \theta_0 \approx a$ As will be seen later, this criterion places rather severe restrictions on the image quality obtainable for a given combination of a, r, and θ_0

Isoplanatic nature of the point spread function The discussion above indicates that the PSF for parallel beam transmission scanning should be isoplanatic (i e, the description of the function should be independent of the coordinates chosen for the center of the function) For an $x-y$ array of data describing the function for a selected value of k_{max} for central coordinates chosen at random, however, significant variations in the function are found when transmission data generation and image reconstruction programs are implemented A few locations, in addition to the origin, selected for study of PSF's are shown in Fig 8 These locations are A $(-5, 0)$ located on the x-axis at an integral multiple of the sampling interval $a=1$ from the y-axis, B $(1, -1)$, located on a ray at an angle θ to the coordinate axes with x and y coordinates which are integral multiples of the sampling interval $a=1$, and C $(-7, 5)$ and *D (3, 2)* not located on rays but with x and y coordinates which are integral multiples of the sampling interval $a=1$

From digital printouts of the PSF at each location, an average of the PSF values along each ray through the spike center for a radius eight units or greater is given in Table 4 Sampling intervals of finite size for γ-ray transmission scans cause a loss of information for objects approximately the same size as the sampling interval During the image reconstruction process, interpolation procedures cause additional information loss These losses are illustrated in Table 4, where all values of the PSF should be 19 along rays 1–8 for all spike coordinates

Specifically, the interpolation procedures affect the GP(d_k, k) value determined between GP(N, k) and GP(N+1, k) In Fig 8 and Table 4, for example, point B lies directly on the ray $k=2$, and a value of 19 is obtained for the function determined with this value for k For $k=6$, interpolative procedures are necessary for

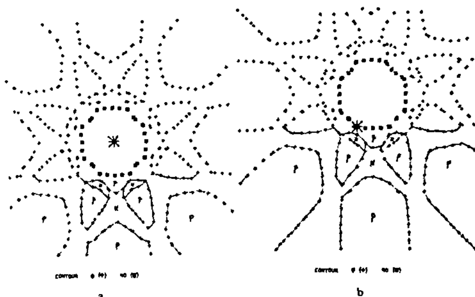


Fig 11 Contour plot for circle of 5 units radius centered at (a) [(0, 0)] and (b) [(2, 4)] for $k_{max} = 4$ and $\theta_0 = \pi/4$ N and P indicate regions of negative and positive overshoot Contours are 0(+) and 90 (■) the origin is denoted as (✳)

effect was symmetrical in Fig 7 b for multiples of θ_0 Within the limitations of interpolation and plotting, the displays in Fig 11 are identical, implying that the image reconstruction process does not introduce nonisoplanicity for data obtained by the moving source, moving detector scanning technique

By closer adherence to the criterion

$$\langle r \rangle \theta \simeq a$$

the degree of scalloping can be greatly reduced For the data in Figs 10 and 11, $r = 10$ and $a = 1$, and the ideal value for θ_0 is 0 1 radian However, in Fig 10, $\theta = \pi/8$ 0 392 radians, and in Fig 11, $\theta_0 = \pi/4 = 0$ 785 radians These values are too large to provide unscalloped reconstruction images with adequate spatial resolution

Image reconstruction process for three nonoverlapping circles each of uniform density Transmission data were computed for circular objects of relative densities 50, 75 and 100 aligned as in Fig 12 a Reconstructed images of the objects displayed in Figs 12 b–12 d demonstrate the influence of k_{max} upon the quality of the reconstructed image The image in Fig 12 d was obtained under conditions which satisfy the criterion $\langle r \rangle \theta \simeq a$, where $a = 1$ and $\langle r \rangle = 10$ The relative densities of the circles in the image 12D are estimated as 50, 75 and 100, corresponding to the densities of the original object Image degradation increases as the approximation of $\langle r \rangle \theta$ to $a = 1$ decreases

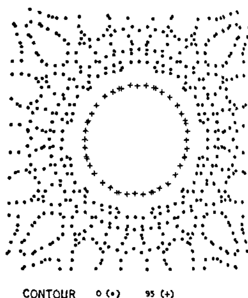


Fig 10 Contour plot for circle centered at (0, 0), with $k_{max}=8$ and $\theta=\pi/8$ Scalloping outside the edge of the circle reflects a summation of the radial rippling effects depicted in Fig 7 b

interval a used for image reconstruction, then the interpolated value would reflect more accurately the actual value at d_k Under these conditions, all PSF values in Table 4 would be much closer to 19, and the PSF would appear more isoplanatic

The summation process described in Fig 5 suggests that the sum of the average PSF values for each spike should be equal (within round-off error) to the maximum value of the spike Also, the ratio of the average of all PSF values for all k to the spike value at (x, y) should be constant for all values of (x, y) These relationships are confirmed rather well in Table 4

It may be concluded that the PSF is isoplanatic for the moving source, moving detector scanning technique, but that limitations accompanying use of discrete sampling intervals and interpolation procedures during image reconstruction furnish a PSF which appears nonisoplanatic However, for an object much larger than the *sampling interval, the PSF is isoplanatic even when discrete data sampling methods* are used (see next section)

For the stationary source scanning technique, an analysis similar to that above reveals that, except for the point (0, 0), the radial arms of the PSF do not intersect at equiangular intervals, and the PSF is nonisoplanatic

Image reconstruction process for a circle of uniform density A contour plot is shown in Fig 10 for a circle of uniform density and radius 7 5 (arbitrary units) centered at (0, 0) with $k_{max}=8$ and $\theta_0=\pi/8$ The scalloped configuration outside the circle boundary (identified by 95 isodensity contour) reflects a summation of the radial rippling effects depicted in Fig 7 b, except that in Fig 10 the summation is over the PSF for every point within the circle Similar scalloping effects are displayed in Fig 11 where $k_{max}=4$, $\theta=\pi/4$, and r = 5 0 for circles centered at (0, 0) and (2, 4) Scalloping effects are symmetrical about multiples of θ_0, just as the radial rippling

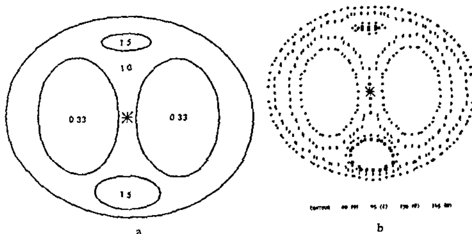


Fig 13 a) Simulated human thoracic phantom, b) reconstructed image with $k_{max}=30$ ($\theta_o=\pi/30$) Contours are 40(+), 95(|), 130('), and 145(■), the origin is denoted as (✶)

Image reconstruction process for objects simulating the human chest region The thoracic cross section of a patient was approximated as an ellipse of unit density containing two ellipses of density 0 33 to represent lung, and two smaller ellipses of density 1 5 to represent the vertebral column and sternum (Fig 13 a) Transmission data computed for the phantom with $k_{max}=30$ ($\theta=\pi/30$) were used to obtain the reconstructed image in Fig 13 b Slight distortions in the reconstructed image are a reflection primarily of interpolation inaccuracies Some smoothing of boundaries is caused by finite sampling intervals In the digital printout for the contour plot in Fig 13 b, the density values average 0 334 for lung, 1 501 for bone and 1 000 for muscle, indicating good preservation of input density values during the image reconstruction process

The reconstruction process as a clinical tool for determination of cross sectional anatomy Discussion of the image reconstruction process has been confined so far to convolution processes in the spatial domain For these processes, either approach to γ ray transmission scanning—moving source, moving detector, or stationary source, moving or stationary detector—may be used The moving source and detector technique may be slightly superior because transmission measurements are independent of source to-center-of-rotation and source-to-detector distances, and because the PSF is isoplanatic Certain modifications to the γ-ray transmission procedure might reduce the data storage requirements for the image reconstruction process Among these modifications are

(1) Use of a circular or elliptical, rather than square, matrix for digital display of density values

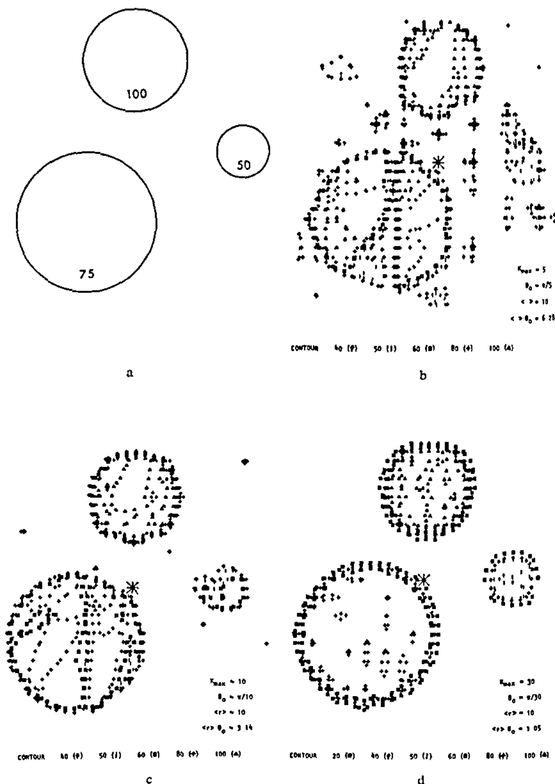


Fig 12 Reconstructed images (b, c and d) for data depicted in (a), with increasing correspondence to the criterion $\langle r\rangle\theta_0 \simeq a$ For (b), $k_{max}=5$ and $\langle r\rangle\theta_0 \simeq 6\ 28$ For (c), $k_{max}=10$ and $\langle r\rangle\theta_0 \simeq 3\ 14$ For (d), $k_{max}=30$ and $\langle r\rangle\theta_0 \simeq 1\ 05$

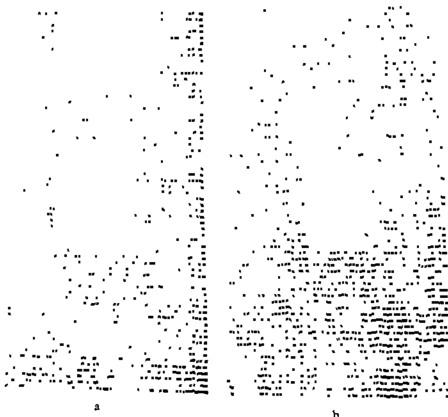


Fig 14 a) Image obtained with 8 comp...

effort to identify the potential advantages of performing the image reconstruction process in the spatial frequency domain, a reconstructed image I of a circular object was transformed with a fast Fourier transform algorithm to obtain I(ω) With a single function H(ω) derived from the isoplanatic PSF, the image I(ω) was deconvolved with equation (24) to obtain O(ω) With equation 25, the object O(ω) then was transformed to the original object O This process illustrates the importance of PSF isoplanicity if the PSF were not isoplanatic, a separate function H(ω) would be required for every point in the spatial frequency domain

Rather unsophisticated applications of this approach to image reconstruction indicate that unscalloped images with satisfactory resolution may be obtained with considerably fewer transmission scans The highly scalloped image in Fig 14 a was

(2) Use of a logarithmic amplifier to express g(x) in equation 11 directly from input transmission scan data

(3) Electronic convolution of the signal from a logarithmic amplifier to obtain GP(N, k) according to equation 21

(4) Use of an analog-to-digital converter on the electronically processed signal and storage of GP(N, k) directly on disc

(5) Transferral of a transmission scan from disc to core, calculation of its contribution to each point in a circular array, and repetition of the process k_{max} times until the image is complete

Although modifications such as those described above may improve the practicality of the image reconstruction process, a second problem may limit the clinical usefulness of cross-sectional anatomy reconstruction This problem is the difficulty of obtaining at least 120 transmission scans of a patient in a reasonable length of time Obviously, this time could be reduced by decreasing the number of transmission scans required for data accumulation and manipulation The degradation of image quality accompanying a decrease in the number of transmission scans has been discussed, however, and this approach should not be contemplated unless a method can be identified to maintain image quality at an acceptable level The approach discussed below—image deconvolution with a suitable PSF—appears capable of reducing the number of transmission scans with retention of acceptable image quality

In the process of obtaining an image, an object 0 is distorted by the imaging system to furnish an image I (METZ 1969) The distortion introduced by the imaging system may be described by the function H characteristic of the system The expressions O, H, and I in the spatial domain may be represented in the frequency domain by their respective Fourier transforms $0(\omega)$, $H(\omega)$ and $I(\omega)$

$$0(\omega) \rightarrow H(\omega) \rightarrow I(\omega) \quad \text{where} \quad I(\omega) = 0(\omega) H(\omega) \tag{23}$$

That is, the image transform is the product of the object transform and the processing function transform In transmission scanning, as in most imaging processes, the Fourier transform $I(\omega)$ can be computed from knowledge of the image I in the spatial domain, and the Fourier transform $H(\omega)$ of the processing system may be computed from physical measurements such as those yielding the point and line spread functions Thus, the transform of the object may be obtained by the deconvolution process

$$0(\omega) = \frac{I(\omega)}{H(\omega)} \tag{24}$$

The inverse transform of $0(\omega)$ then provides the original object 0

$$0 = \mathfrak{F}^{-1}[0(\omega)] \tag{25}$$

The function H characteristic of the imaging system can be the point spread function (PSF), and the function $H(\omega)$ can be the Fourier transform of the PSF In an

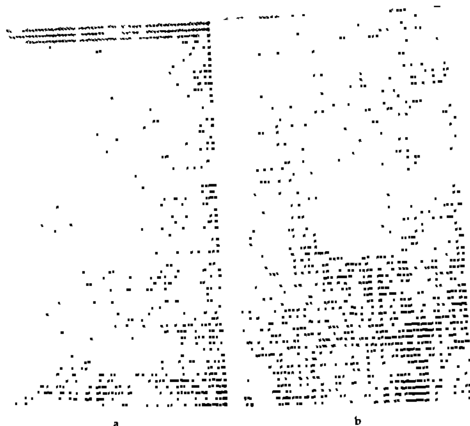
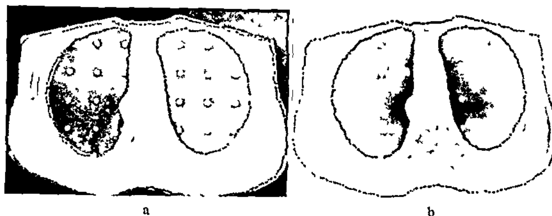


Fig 14 a) Image ... lustrating the se ... ellip ... ma ... tair ... cor ... val

effort to identify the potential advantages of performing the image reconstruction process in the spatial frequency domain, a reconstructed image I of a circular object was transformed with a fast *Fourier transform* algorithm to obtain $I(\omega)$ With a single function $H(\omega)$ derived from the isoplanatic PSF, the image $I(\omega)$ was deconvolved with equation (24) to obtain $O(\omega)$ With equation 25, the object $O(\omega)$ then was transformed to the original object O This process illustrates the importance of PSF isoplanicity if the PSF were not isoplanatic, a separate function $H(\omega)$ would be required for every point in the spatial frequency domain

Rather unsophisticated applications of this approach to image reconstruction indicate that unscalloped images with satisfactory resolution may be obtained with considerably fewer transmission scans The highly scalloped image in Fig 14 a was



a b

obtained with ^{60}Co γ rays The similar transmission of ^{60}Co photons through bone and muscle components of the section is apparent

reconstructed for $k_{max} = 8$ computer-generated transmission scans under conditions where 30 transmission scans would be required according to the criterion $\langle r \rangle \theta_0 \simeq a$ By processing the data in the spatial frequency domain, scalloping can be eliminated almost completely (Fig 14 b) However, some degree of image unsharpness has been introduced into Fig 14 b, and the large numbers in the far corners indicate spectral foldover. Nevertheless, these initial results have encouraged further investigation in our laboratory of this approach to image reconstruction with more sophisticated deconvolution techniques

Experimental verification

Initial efforts towards reconstruction of cross-sectional anatomical images by γ-ray transmission scanning utilized a 2 5 cm thick thoracic section of a Rando simulated human phantom (Alderson Research Laboratories, Stamford, Conn.) and an elementary scanning apparatus consisting of a 10 mCi ^{60}Co source and a 2 5 cm × 2 5 cm NaI(Tl) detector The detector was operated in pulse mode and was collimated by a lead cylinder 5 3 cm in length with a 5 mm × 15 mm slit Transmission measurements equivalent to those obtained with the moving source, moving detector technique were achieved by aligning the source and detector in a stationary configuration and moving the thoracic section between the two Angular orientations of the scanning assembly were simulated by manual rotation of the section

The thoracic section had a mean radius $\langle r \rangle = 10$ cm, and, for a scan interval of 0 5 cm, transmission measurements at 60 angular orientations ($\theta_0 = 3°$) were required to satisfy the image reconstruction criterion For each transmission measurement, at least 3 000 counts were accumulated to provide better than 2 percent counting statistics at the 1σ confidence level

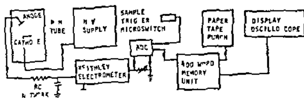


Fig 16 Electronic assembly for γ ray scanning

Radiographic images in Fig 15 a and 15 b were obtained by exposing the thoracic section to 50 kV roentgen and ^{60}Co γ rays, respectively In Fig 15 b, the similar transmission of ^{60}Co photons through muscle and bone in the phantom is apparent This observation suggests that transmission scanning with ^{60}Co photons will not clearly reveal bony structures in the phantom, because these structures have a density near that of muscle

Superimposed upon the radiographic images in Fig 15 are isodensity plots (relative density = 40) of reconstructed cross sectional images of the thoracic section The body contour and lung outlines in the isodensity plots conform closely to those depicted in the radiographic images, and the chest wall and mediastinum are exhibited rather well These results indicated the feasibility of the γ-ray transmission scanning approach to delineation of cross sectional anatomy The next step was development of an improved scanning assembly which incorporated a multicurie ^{60}Co source and a NaI(Tl) detector operated in current mode

The new transmission scanning apparatus was constructed to conform closely to criteria established for a clinical γ-ray transmission scanner A ^{60}Co teletherapy source was oriented with the beam directed horizontally at the detector collimator A 15 cm long lead cylinder with a 2 5 mm × 5 mm slit served as the detector collimator The source was collimated with four lead bricks (5 cm × 10 cm × 20 cm) forming a 2 mm × 4 mm slit at a distance of 50 cm from the source Dimensions of the source-collimator slit provided a slight overlap of the ^{60}Co beam with the detector-collimator slit To simplify mechanical construction, the source and detector remained stationary, and the phantom was mounted on a rotatable platform attached to the arm of a Picker Magnascanner The scanner arm provided the linear motion of the phantom through the beam The detector was a 2 5 cm × 2 5 cm NaI(Tl) crystal mounted permanently to a photomultiplier tube and surrounded by a lead housing for protection against scattered radiation A negative high voltage (490 V) was applied to the cathode of the P M tube, and the anode current, after passing through a signal averaging RC network, was measured with a Keithley 610B electrometer (Fig 16) A time constant of 0 047 seconds (~1/10 the sampling interval of 0 5 s) provided sufficient smoothing of the incoming signal and an adequate response to significant gradients in beam intensity An analog-digital converter, on command of a microswitch attached to the scanning apparatus, sampled the output of the Keithley electrometer and produced a pulse train proportional to the input signal A scaler in the 400 word memory unit counted the number of pulses in the train

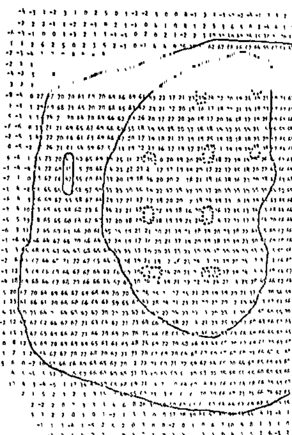


Fig. 17. Digital printout of relative densities in left part of thoracic section of simulated human phantom

These numbers were stored in memory and, later, punched onto paper tape for delivery to the computer As the phantom moved through the beam, the microswitch was activated by detents spaced at 0 5 or 0.25 cm intervals on a linear track.

Seven 2.5 cm thick slabs from the thoracic region of the Rando phantom were mounted on the scanner platform so that the photon beam traversed the center of the middle slab Transmission of ^{60}Co photons was measured at 0 5 cm increments for $k_{max} = 60$ angular orientations ($\theta_0 = 3°$). By submitting the transmission data to the image reconstruction program, a density distribution was obtained for a cross section through the middle thoracic slab. The left portion of the printout is reproduced in Fig. 17. Division of the relative density values in Fig 17 by 1 000 yields the linear attenuation coefficient (cm^{-1}) at each location. For ^{60}Co, this coefficient varies essentially only with the physical density (g/cm^3) and electron density (electrons/g) of the absorbing medium Since biologic tissues have similar electron densities, the linear attenuation coefficients in Fig 17 are a reasonable reflection of the physical density at each location. In Fig. 17, relative densities range from 60-68 for muscle and 16-24 for lung, divided by 1 000, these values agree well with the values of 0.064 cm^{-1} for muscle and 0.021 cm^{-1} for lung listed in Table 1.

When comparing structures in radiographic images to those outlined by isodensity



Fig. 18 Isodensity contours of 50 superimposed upon a radiographic image obtained with ^{60}Co γ rays

contours or identified by inspection of digital density printouts, it is important to recognize that the reconstructed density distributions describe only those structures lying within the center 5 mm thickness of the phantom cross section whereas the radiographic images depict the anatomy of the entire 2 5 cm thick slab For example, this distinction helps to explain the slight displacement of the reconstructed image in Fig 18 from the outer boundary of the slab depicted in the radiographic image The displacement is a reflection primarily of the beveled outer surface of the phantom

In Fig 18 a number of structures, including the body and lung contours, are well defined by the 50 isodensity contour plot In the upper left corner of the image, a rib contains a low density artefact (I) which extends into the 5 mm scanning section A low density area (II) appears also inside the rib in the lower right corner of Fig 18 Relative density values for these regions in the digital printout are reduced to just above 50 compared to muscle values of 60–68 The density value of 50 at (III) is caused probably by incomplete impregnation of the sternum with tissue equivalent plastic The indentation of the body contour at (IV) is caused by a low density artefact confirmed by numerical values in the digital printout

The Mix D plugs (approximately 5 mm diameter) used to fill dosimeter voids in the phantom are significantly more dense than surrounding lung tissue, and are identified easily in the radiographic image in Fig 18 Inspection of the digital print out (Fig 17) distinctly reveals all plug locations in the lungs because corresponding density values are significantly larger than density values for lung The digital printout for Fig 15 does not reveal the presence of the plugs confirming the greater spatial resolution achieved with improved scanning and collimation techniques

Seven sections of the head of the Rando phantom were mounted on the scanning platform so that the ^{60}Co beam scanned across a 0 5 cm thick cross section through the center slab of the phantom The center of the scanned region was 0 75 cm above the base of the slab and included as major structures the nose, ears, nasopharynx, teeth and upper extensions of the mandible In the radiographic images, the base of the skull is prominent in the 50 kV roentgenogram (Fig 19 a) but only vaguely

a b

Fig 19 Isodensity contours superimposed upon (a) 50 kV roentgenogram and (b) ^{60}Co γ ray radiographic images for $k_{max}=60$ transmission scans at 0 5 cm intervals The middle of the 5 mm thick scanned region lies 0 75 cm above the base of this slab of the Rando phantom

a b

Fig 20 Isodensity contours superimposed upon a ^{60}Co γ ray image for k_{max} 90 transmission scans at 0 25 cm intervals The middle of the 5 mm thick scanned region lies 1 25 cm above the base of this slab of the Rando phantom

distinguishable in the ^{60}Co image (Fig 19 b) Hence, an image of the phantom skull cannot be expected with ^{60}Co transmission scanning The ^{60}Co image suggests that structures which will be imaged most satisfactorily include the mandible teeth, and nasopharynx, together with the outer contour of the head Transmission data were accumulated for $k_{max}=60$ angular orientations (θ_0 3) at 0 5 cm scan increments The relative *density contour 40 outlines the facial contour, ears, back of the head,* and nasopharynx The beveled edge of the back of the head interferes with correlation of the reconstructed contour and the radiographic image in this region Inspec-



a



b



c

Fig. 21 Computer-aided logarithmic oscilloscope displays of the digital density distributions used for isodensity contours in (a) Fig 18 (b) Fig 19 and (c) Fig 20

tion of the phantom indicates that the reconstructed contour (I) should be inset approximately 0 75 cm from the blurred image of the back of the head Both ear lobes were intersected by the ^{60}Co beam and no indentation of the contour is apparent at the ears (II) The nasopharynx density values range from -2 to 6, corresponding to expected values near zero for an air cavity The cavity at (III) is enclosed by an isodensity contour of 40 The constriction at (IV) reflects the presence of a septum slightly above the 0 75 cm scanning height The mandible bones (V) exhibit density values of 84–96 and are fairly well defined by the 76 isodensity contour Muscle density values range from 60 to 68 The scanning plane traverses the most dense parts of the teeth (VI) with density values from 100 to 120 The front teeth (VII) are imaged incompletely probably because the phantom is asymmetrical in this region The scanning plane slices the roots of the teeth at (VIII) and the back molars at (IX) and provides density values of 80–86

To compare image resolution for transmission data obtained at scanning increments of 0 5 and 0 25 cm, transmission data for the phantom slab imaged in Fig 19 were accumulated at 0 25 cm scan intervals for 90 angular orientations An alignment discrepancy caused the center of the scanned region to be positioned at a height of 1 25 cm above the base of the slab (i e , 0 5 cm above the region scanned for Fig 19) A ^{60}Co image with superimposed relative density contours of 40 and 76

is shown in Fig 20 At a height of 1 25 cm, the scanning plane traverses an indentation in one ear (I), and the 40 isodensity contour reveals this indentation The mandible at (II) is better defined in the 0 25 cm scan image The nasopharynx (two cavities at this height) is well defined The protrusion of the cavity at (IV) has been confirmed in the phantom as a hole in the front of the palate The high density areas (V) superimposed upon the teeth are, at this height, regions where the image plane intersects the hard palate just above the teeth The palate is nonuniform, and the lower density areas (VI) above the teeth correspond to regions where the ^{60}Co beam passes through the roots of the teeth For the missing Mix-D plug at (VII), density values of 38, much lower than muscle values of approximately 60, indicate that the 4 mm airfilled hole is just resolved

With the aid of a small laboratory computer, the digital density distributions used for Figs 18 to 20 were displayed logarithmically on an oscilloscope screen These displays (Fig 21) provide considerably more information than plotted isodensity contours, and suggest that a display technique of this type may be preferred

Conclusion

The feasibility of the transmission scanning approach to delineation of patient cross-sectional anatomy has been confirmed Spatial resolution is limited primarily by scanner design considerations such as collimation, and by data handling and storage capabilities and the time available for data accumulation The data accumulation time can be reduced (e g , below the 30 minutes assumed for certain computations in the text) by using a source with higher photon flux density, replacing the single detector with a detector array, and employing selected data processing techniques By redesign of the source collimator and the employment of multiple detectors, cross-sectional images for different planes could be obtained simultaneously

The potential usefulness in radiation therapy treatment planning of the transmission scanning approach to delineation of cross-sectional anatomy is apparent Extensions of the technique to medical diagnosis, facilitated by substitution of lower-energy photons for the ^{60}Co γ rays employed here, appear potentially rewarding For control of resolution loss caused by patient motion, the collection of data in synchrony with predictable motion such as the respiratory cycle is being investigated With the technique described here, a constant diameter water path is not needed around the anatomic region to be imaged The technique is applicable to all regions of the body, and can be extended to higher resolution investigations of limited anatomic regions

SUMMARY

^{60}Co γ-ray transmission data were measured along linear scan paths at a number of angular orientations with respect to the patient and submitted to a computer software program Reconstructed images are displayed as digital density printouts and as isodensity

contours on an x – y plotter or oscilloscope screen Image resolution is limited primarily by factors such as collimation and the amount of transmission data collected, with the rather rudimentary apparatus at disposal, a spatial resolution better than 5 mm has been achieved

ZUSAMMENFASSUNG

Die ^{60}Co Gammastrahlen Transmissions Werte längs linearer Scan Wege wurden bei einer Anzahl von Winkelorientierungen gegenuber dem Patienten gemessen und mit Hilfe eines Komputerprogramms bearbeitet Die rekonstruierten Bilder wurden als digitale Dichteziffcrwerte und als Iso Dichte Konturen mit einem x y Schreiber oder auf einem Oscilloskopschirm dargestellt Die Bildauflosung ist primär durch Faktoren wie die Kollimation und die Menge der gesammelten Transmissionswerte begrenzt, mit der fur die vorliegende Untersuchung ziemlich rudimentaren Ausrustung wurde eine raumliche Auflosung von weniger als 5 mm erreicht

RÉSUMÉ

Les auteurs ont mesuré la transmission du rayonnement gamma du ^{60}Co le long de balayage lineaire fait suivant différentes orientations angulaires par rapport au malade et ils ont soumis ces résultats à un programme d ordinateur Les images reconstruites sont representées par des clichés indiquant la densite digitale et par des contours d isodensité sur un traceur x y ou sur un écran d oscilloscope La resolution de l image est limitee à la base par des facteurs tels que la collimation et la quantité des mesures de transmission enregistrées Cet appareil plutôt rudimentaire a donné une résolution spatiale superieure a 5 mm

REFERENCES

Berger M and Doggett J Response function of NaI(Tl) scintillation counters Rev Sci Inst 27 (1956) 269

Cormack A Reconstruction of densities from their projections with applications in radio-

—

with some radiological applications

Fa

Gilbert P Iterative methods for the three-dimensional reconstruction of an object from projections J theoret Biol 36 (1972) 105

... oscopy and x ray photography J theoret Biol 29 (1970) 471

Ibbott G and Hendee W Unpublished data

Johns H and Cunningham J The physics of radiology Third edition, p 746 Charles C Thomas Springfield Illinois 1970

Kaiser W Scintillation spectrometry The state of the art Anal Chem 38 (1966) 28

KUHL D and EDWARDS R The Mark III scanner A compact device for multiple view and section scanning of the brain Radiology 96 (1970), 563

METZ C A mathematical investigation of radioisotope scan image processing Ph D thesis University of Pennsylvania, 1969

RADON J Über die Bestimmung von Funktionen durch ihre Integralwerte langs gewisser Mannigfaltigkeiten Ber Verh Sachs Akad Wiss 69 (1917), 262

RAMACHANDRAN G and LAKSHMINARAYANAN A Three dimensional reconstruction from radiographs and electron micrographs application of convolutions instead of Fourier transforms Proceedings of the National Academy of Sciences, USA, Vol 68, No 9 September, 1971

SMITH P, PETERS T and BATES R Image reconstruction from finite numbers of projections J Phys A Math, Nucl Gen 6 (1973), 361

ACTA RADIOLOGICA

OFFICIAL ORGAN OF THE RADIOLOGICAL SOCIETIES OF
DENMARK, FINLAND, NORWAY AND SWEDEN

Vol 14 Fasc 2 THERAPY PHYSICS BIOLOGY 1975 April

^{11}C AND ^{15}O INDUCED IN THE MOUSE BY 175 MeV PROTONS

S GRAFFMAN and B JUNG

The primary yield of nuclides from high energy radiation passing through tissue may be estimated with fair accuracy from empirical formation cross sections and the elemental composition of the tissue The chemical behaviour of the nascent radiating products in the living body has, however, been almost completely neglected Some investigations of the chemical fate of nuclides induced in aqueous solutions have been reported (e g STENSTRÖM 1970), but it appears hazardous to extrapolate from such simple systems to the complexity of living tissue The behaviour of nuclides induced by high energy α particles in human beings was reported by SARGENT (1961), who found production of ^{11}CO and $^{11}CO_2$ LARSSON et coll (1964) irradiated blood in vitro with high energy protons and found a considerable attachment of ^{11}C to blood corpuscles Neutron activation of living material has been analysed by BIGGIN & MORGAN (1972) and others but has little bearing on the present work

From the estimated production yield it may be shown that for high energy protons the radiation dose given by the decay of the induced nuclides may be ignored, compared to the primary proton dose, provided a rather drastic accumulation of the nuclides to small, radiation sensitive organs does not occur That this is not the case has not been strictly proved, however

There are also other reasons for analysing the behaviour of induced nuclides One

From the Department of Physical Biology Gustaf Werner Institute, University of Uppsala, S 753 20 Uppsala, Sweden Submitted for publication 3 October 1974

is the possible use of induced activity for dosimetry in the therapy and following radiation accidents (GRAFFMAN & JUNG 1964, MILLER & PATTERSON 1972) another that the behaviour of induced activity reflects the physiologic state of irradiated tissue such as oxygen tension, vascularity, water content, membrane permeability, etc It is also conceivable that the chemical behaviour of the recoiling nuclides in nascent state elucidates the radical processes that precede the radiation injury (STENSTRÖM 1970) The aim of this communication is to present some basic information for an evaluation of these possibilities

The investigation was concentrated on the behaviour of 20 5 min ^{11}C, which is the dominating nuclide with respect to activity during the interval from 10 min to 4 h after high energy proton irradiation of tissue During earlier periods, ^{15}O dominates, but its short half-life, 2 0 min, prevents its analysis in greater detail The following factors were primarily considered (a) fractional amount of induced nuclides remaining close to the production site, (b) fractional amount excreted through the lungs and the kidneys, and (c) the chemical composition of mobile activities

Material White mice of the NMRI strain, weighing 18 ± 2 g, of both sexes were used Ascarite (NaOH *on asbestos, A H Thomas Co, Phil, USA*) was used to absorb CO_2, and Dehydrite ($MgClO_4$, A H Thomas Co, Phil, USA) to dehydrate respiration gases Hopcalite ($CuO_2 + MnO_2$, B Karlsson Co, Stockholm, Sweden) *is a catalyst which facilitates the oxidation of CO to* CO_2 *at room temperature* It was used to transfer CO to CO_2 before absorption on Ascarite Nembutal (Abbott Laboratories) was given intraperitoneally (0 04 mg/g body weight) for anaesthesia Sephadex G-25 (*Pharmacia, Uppsala, Sweden*) was used to separate urine ^{11}C *activity* according to molecular size Dowex 50W-X8 cation exchange resin on H_3O^+ form and Dowex I-X8 (Feinbiochemia, Heidelberg, BRD), 75 to 100 mesh, anion exchange resin on F^- form were used in the search for the chemical form of urine *activities*

Methods

The irradiation was performed in the external, 185 MeV proton beam from the synchrocyclotron of the Gustaf Werner Institute The beam was shaped with collimators and sweeping magnets to a laterally sharply defined field with a transverse homogeneity better than ± 5 per cent The dose was measured with a nitrogen flushed ionisation chamber of transmission type to an estimated accuracy better than 5 per cent The dose rate was normally 100 rad/min The stopping power in animal tissue for 185 MeV protons is about 5 MeV/cm The mean proton energy was thus about 175 when a mouse was irradiated The general layout of the irradiation facility was described by LARSSON (1961)

Activity was measured in lead shielded 7 5 cm × 7 5 cm and 4 5 cm × 5 cm NaI(Tl) crystals with wells measuring 3 8 cm × 6 4 cm and 2 5 cm × 3 8 cm, respectively Both crystals were equipped with conventional electronics, including single channel

analysers and printers The larger crystal was used for wholebody animal measurements In a special test it was found that the counting efficiency for positron annihilation quanta was constant (within ± 1 %), irrespective of the size of the source provided this did not extend outside two thirds of the height of the well Most measurements were made as activity ratios for samples of similar physical form which should reduce any remaining counting efficiency variations to a negligible level The absolute counting efficiency of the crystals was determined by ^{22}Na and ^{60}Co samples from the National Bureau of Standards, calibrated to an accuracy of ± 3 per cent (LARSSON & SARBY 1974) All nuclides under investigation are pure positron emitters

The total production of ^{11}C, ^{13}N and ^{15}O was determined by measuring the induced positron activity in a dead mouse irradiated for 27 s over the whole body The absorbed dose in animal tissue was 11 6 rad The initial disintegration rate of the three nuclides was determined by least squares techniques assuming three components of half lives 2 0 min (^{15}O), 10 min (^{13}N) and 20 5 min (^{11}C)

Expiration of ^{11}C activity was determined by measuring the remaining wholebody ^{11}C activity in mice killed after prescribed intervals after irradiation Animals killed before irradiation served as standards Five animals, placed on a turntable, were irradiated simultaneously The experiment was repeated several times Measurement of the ^{11}C activity was made when ^{13}N and ^{15}O had decayed to negligible levels The turntable arrangement secured that the groups of five animals received the same dose

The chemical composition of expired ^{11}C activity was analysed with a gas chromatograph (Aerograph 202 B, Varian) with a packing of the molecular sieve type (5A, Waters Ass USA) A mouse, placed in a sealed, 100 ml syringe, filled with pure oxygen, was exposed to the proton beam for 5 min After irradiation, half of the syringe volume was injected repeatedly at about 15 min intervals into the chromatographic column Following injection, the remaining gas volume was washed several times with pure oxygen for about half a minute and the syringe filled with O_2 and kept closed until the next sample was drawn The effluent gas from the chromatograph was led through a glass spiral with 2 ml volume placed in the small NaI(Tl) crystal The relative amounts of the various ^{11}C activities were obtained by adding the counts registered under the peaks In some experiments macro-amounts of CO and CO_2 were added for identification of expired gas ^{11}C activities The macro-amounts were detected with the thermal conductivity detector of the instrument and were registered in parallel with the well-crystal counting-rate on a two-pen strip-chart recorder

The elimination rate of $^{11}CO_2$ and the ratio between induced ^{11}CO and $^{11}CO_2$ as well as between these gases and total induced ^{11}C activity were determined in experiments in which a mouse was placed in a 60 ml glass chamber through which air was sucked by a membrane pump at a constant rate of 200 to 400 ml/min The air flow was controlled by a conventional flow meter Two alternating, identical absorber-

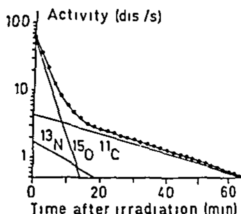


Fig 1 Disintegration rate of induced nuclides per g rad in a mouse after whole body irradiation with 175 MeV protons The composite decay curve was decomposed in three components, with half lives corresponding to ^{15}O, ^{13}N and ^{11}C, by the method of weighted least squares Points indicate experimental data, lines the result of analysis

catalyst chains were inserted in parallel between the chamber and the pump The chains consisted of eight exchangeable tubes, containing, in order from the chamber, Ascarite, Ascarite, Dehydrite, Hopcalite, Ascarite, Dehydrite, Hopcalite and Ascarite The animal was exposed to the proton beam for 2 to 6 min and the absorber system shifted repeatedly after intervals equal to the irradiation time The first interval was counted from the irradiation mean time New Ascarite tubes were replaced for old ones after each shift of absorber chain The activity of the tubes was measured in the large crystal when short-lived activities (^{15}O and ^{13}N) had decayed sufficiently to be negligible

The gas chromatograph was also used to obtain pure samples of ^{11}CO from proton-irradiated tap water The gas was given to several mice either through venous injection of blood shaken with the gas or through inhalation by keeping the animals for 10 min in a 100 ml syringe containing the gas The elimination rate of ^{11}C from the animal was followed with measurements of the whole-body activity in the large crystal The small plastic bottle containing the mouse in counting position was ventilated at a rate of about 2 l/min by normal air from a pump or by a mixture of O_2 95 % and CO_2 5 % from an anaesthetic stand

Table 1

Production of ^{11}C, ^{13}N, ^{15}O in mice irradiated with 175 MeV protons

	Initial disintegration rate (dis/s g rad)			Production (nuclei /g rad)		
	^{11}C	^{13}N	^{15}O	^{11}C	^{13}N	^{15}O
Experiment	4 9	1 7	78	8 200	1 500	14 000
Theory*	4 4	1 7	59	7 800	1 500	10 000

* Assumed composition (ICRP 1959) 18 % C, 3 % N and 65 % O by weight
Assumed production cross section (JUNG 1964) ^{16}O (p 3p3n) ^{11}C 11 mb ^{12}C (p pn) ^{11}C 45 mb, ^{14}N (p, 2p2n) ^{11}C 7 mb, ^{16}O (p, 2p2n) ^{13}N 4 5 mb ^{14}N (p, pn) ^{13}N 14 mb ^{16}O (p pn) ^{15}O 45 mb

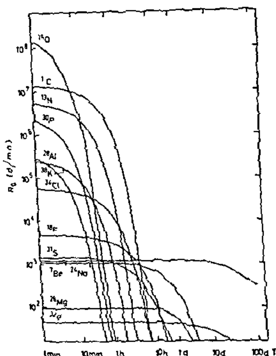


Fig 2 The disintegration rates R_a of the most important nuclides as a function of time after irradiation of 1 g/cm² with the elemental composition of the human body (ICRP 1959) with 6×10^{11} protons during 1 min (from HALLER & JUNG 1963)

^{11}C activity in urine was measured in animals irradiated over the upper part of the body Before irradiation the animals were anaesthetized and the urethra ligated The animals were killed after different intervals after irradiation and the total amount of urine in the bladder was collected The urine was measured in the large well crystal and the activity related to the total remaining activity in the carcass plus urine Correction for expired ^{11}C activity was performed

Attempts to characterize the chemical composition of ^{11}C activity in urine were made on some 30 min urine samples The urine was boiled for five minutes in neutral and strong acid and alkaline solution Neutral urine was separated on a Sephadex G 25 column Urease was added to some samples in a search for active urea Boiling with concentrated sulphuric acid was performed in order to test for active formic acid Ion exchange with cation exchange and anion exchange resins was also tried

The activity remaining at the irradiation site in muscle and bone was measured in several mice irradiated over their right hind leg The irradiated volume did not exceed 5 per cent of the total body volume Some mice were killed before, others at various times after irradiation Samples of muscle and bone ...

... mice At preselected intervals following

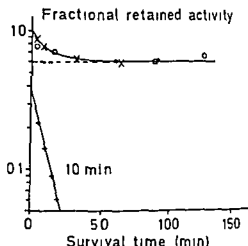


Fig 3 Fractional retained ^{11}C activity in mice irradiated over the whole body as a function of survival period after mean time of irradiation The elimination rate through respiration corresponds to a half life of 10 *min Corrections for* physical decay performed

irradiation the heparinized mice were partially exsanguinized through decapitation The blood samples, including that irradiated in vitro were weighed and measured for activity The activity concentrations in the samples were related to the ^{11}C activity of the mice

The loss of ^{15}O from irradiated animals during the first minutes after irradiation was determined by measuring the whole-body activity of mice killed at preselected intervals after irradiation Irradiated dead mice served as controls

The redistribution of ^{15}O activity during and after irradiation was determined following irradiation of the upper or lower halves of mice At 1, 3 and 5 min after irradiation the animals were submerged in liquid nitrogen The frozen bodies were cut into one non-irradiated part and one which had been partially irradiated The ^{15}O activity per gram body weight of the two halves was determined

The behaviour of ^{15}O activity *induced in irradiated* human whole blood was analysed in one model experiment Blood samples were irradiated for 10 s and two aliquots of 1 ml taken One of these served as standard, the other was boiled under reduced pressure for 1, 2 or 3 min Both samples were measured repeatedly for activity and the 2-min ^{15}O component extracted

Results and Discussion

Results regarding total induced ^{11}C, ^{13}N and ^{15}O activity in the mouse appear in Fig 1 and Table 1 In the latter, theoretical data on estimated production rate of the three nuclides are included The data were obtained by assuming the mice to contain (by weight) O 65 %, C 18 % and N 3 % (ICRP 1969) The three nuclides are the dominant ones as is *evident from Fig 2, taken from a report by* HALLER & JUNG *(1963)* The close agreement between the empirical and theoretical values is surprising in view of the uncertainties in the elemental composition and in the formation cross sections introduced in the theoretical estimates

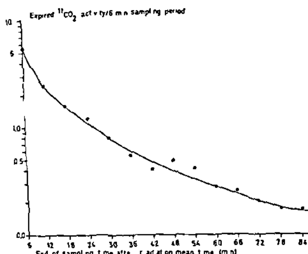


Fig 4 Elimination curve of $^{11}CO_2$ from a mouse irradiated over the whole body Corrections for physical decay performed

The expiration loss of ^{11}C activity was characterized by a rapid initial fall in retained activity followed by a more gradual decrease to an asymptotic value of about 0 60 (Fig 3) The loss of ^{11}C through expiration followed a time course which is compatible with a single half-life of about 10 min

Only two, well separated, active peaks were obtained by gas chromatography of expiration gas These could be ascribed unambiguously to ^{11}CO and $^{11}CO_2$ in the experiments with added macro-amounts of these gases Also metabolic CO_2, which was always present, followed the $^{11}CO_2$ peak Other active gases were not found in amounts larger than 1 per cent of ^{11}CO Due to inevitable gas recirculation in the syringe in which the mouse was kept, elimination rates could not be determined in this experiment

The elimination of $^{11}CO_2$ from irradiated mice, as found in the experiments with the absorber—catalyst chains, appears in Fig 4 The collection efficiency of Ascarite for $^{11}CO_2$ was excellent and the second Ascarite tube contained only about 1 per cent of the activity of the first tube

Table 2

Expiration of ^{11}C activity from mice irradiated over the whole body

Irradiation period (min)	Total collection period (min)	Total expired fraction of total induced ^{11}C activity (corrected for physical decay)		Ratio between expired ^{11}CO and $^{11}CO_2+^{11}CO$
		^{11}CO	$^{11}CO_2$	
2	30	0 210	0 135	0 61
4	52	0 237	0 121	0 66
6	84	0 320	0 145	0 69

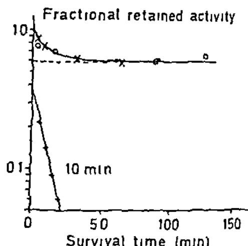


Fig 3 Fractional retained ^{11}C activity in mice irradiated over the whole body as a function of survival period *after mean time of irradiation* The elimination rate through respiration corresponds to a half life of 10 min Corrections for physical decay performed

irradiation the heparinized mice were partially exsanguinized through decapitation The blood samples, including that irradiated in vitro were weighed and measured for activity. The activity concentrations in the samples were related to the ^{11}C activity of the mice

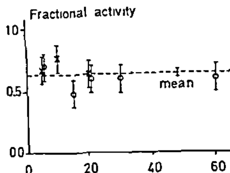
The loss of ^{15}O from irradiated animals during the first minutes after irradiation was *determined by measuring the whole-body activity of mice killed at preselected* intervals after irradiation Irradiated dead mice served as controls

The redistribution of ^{15}O activity during and after irradiation was determined following irradiation of the upper or lower halves of mice At 1, 3 and 5 min after irradiation the animals were submerged in liquid nitrogen The frozen bodies were cut into one non-irradiated part and one which had been partially irradiated The ^{15}O activity per gram body weight of the two halves was determined

The behaviour of ^{15}O activity induced in irradiated human whole blood was analysed in one model experiment Blood samples were irradiated for 10 s and two aliquots of 1 ml taken One of these served as standard, the other was boiled under reduced pressure for 1, 2 or 3 min Both samples were measured repeatedly for activity and the 2-min ^{15}O component extracted

Results and Discussion

Results regarding total induced ^{11}C, ^{13}N and ^{15}O activity in the mouse appear in Fig 1 and Table 1 In the latter, theoretical data on estimated production rate of the three nuclides are included The data were obtained by assuming the mice to contain (by weight) O 65 %, C 18 % and N 3 % (ICRP 1969) The three nuclides are the dominant ones as is evident from Fig 2, taken from a report by HÄLLER & JUNG (1963) The close agreement between the empirical and theoretical values is surprising in view of the uncertainties in the elemental composition and in the formation cross sections introduced in the theoretical estimates



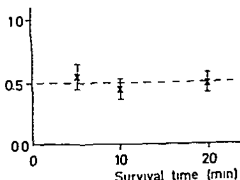


Fig 7 Fig 8

Fig. 7 Remaining ^{11}C activity in muscle after localized irradiation. The fractional activity (corrected for physical decay) is given as the ratio between activity concentrations in muscle extirpated from mice living or dead during irradiation. Crosses and open circles refer to two different experiments.

Fig. 8 Fractional ^{11}C activity remaining in bone after localized irradiation.

From the attempts to characterize the chemical composition of ^{11}C activity in urine it may be reported that the activity could not be made volatile by adding acids or alkalines and that most activity was bound to compounds of molecular weights less than 1 000 Tests for active urea and formic acid gave negative results No activity was absorbed from neutral urine on cation exchanger, while about 60 per cent was retained by anion exchange resin when the eluent was distilled water In view of the apparent variety of the chemical forms of ^{11}C activity in urine no further tests were made

Muscle, representating about 40 per cent of total body weight, and bone, in which blood circulation is comparatively low, were taken as representatives of the whole body in measurements of stationary activity The results are given in Figs 7 and 8 The observed stationary activity represents the relative amount of nuclides which remained at the production site, i e nuclides which were bound to chemical compounds which did not migrate rapidly in the body and which were not transformed to such compounds at a high rate It may be noted that JOHANSON et coll (1974) have found ^{11}C bound to nucleic acids and protein isolated from proton irradiated mouse liver Non-stationary ^{11}C activity disappeared from the irradiated site at such a high rate as to prevent its time-course being determined with available techniques From the measurements it cannot be excluded, however, that a small fraction, 5 per cent at most, of the stationary induced ^{11}C activity disappeared at a slow rate, possibly secondary to metabolic processes

The course for ^{11}C activity in blood appears in Fig 9 Initially, the relative activity concentration in the blood increased rapidly to a value six times the one found for blood irradiated in vitro Subsequently, there was a gradual decrease to about 0 7

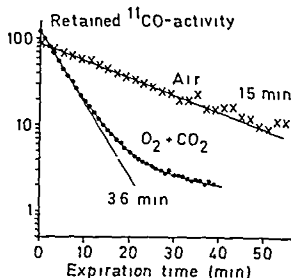


Fig 5

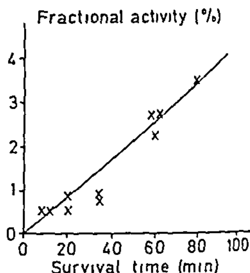


Fig 6

Fig 5 Retained activity in a mouse given ^{11}CO by intravenous injection as a function of time The labels air and O_2 95 % + CO_2 5 % indicate the respiration gas used in the two experiments Corrections for physical decay performed

Fig 6 The fraction of the total induced ^{11}C activity in whole body irradiated mice collected in urine at different times after irradiation Corrections for physical decay performed

The ^{11}CO elimination rate was difficult to determine by the chain, however, since it was found that ^{11}CO to a non-negligible degree was absorbed by Hopcalite, possibly after conversion to $^{11}CO_2$ This did not influence the estimate of the total ^{11}CO activity eliminated during the experimental periods, which is given in Table 2

From the experiments with ^{11}CO administered in breathing gas or in blood by venous injection it was found that essentially all ^{11}CO was eliminated at a rate corresponding to a single half-life of 15 min when the animal was breathing ordinary air (Fig 5) A half-life of about 3 6 min was found when the animal was breathing the O_2-CO_2 mixture A similar increase in elimination rate has been found in human beings treated for carbon monoxide poisoning (ROOT 1965) A small component eliminated at a lower rate was found in the O_2-CO_2 experiment It may be due to ^{11}CO absorption on myoglobin or a conversion of ^{11}CO to $^{11}CO_2$ (TOBIAS et coll 1945, ALLEN & ROOT 1957) The two types of administration gave similar results *It is presumable that expiration of ^{11}CO from an irradiated animal follows a time course that closely simulates that for injected or inhaled ^{11}CO A rapid accumulation in blood of ^{11}CO induced in the irradiated mouse is indicated by the results appearing in Fig 9*

The ^{11}C *activity in urine increased linearly with time during the first hour after* irradiation (Fig 6) *About 2 5 per cent of the totally induced* ^{11}C *activity* was collected in urine after 1 h *The relative amount of* ^{13}N *was found to be higher in urine* than in whole body and correction *for* ^{13}N *activity had to be carried out* although the measurements were made after a considerable decay period

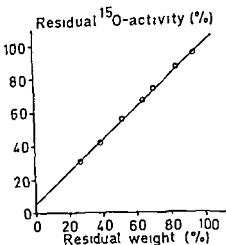


Fig 10

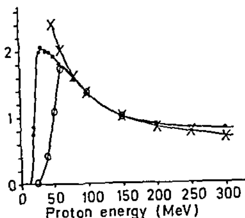


Fig 11

Fig 10 Residual ^{15}O activity as a function of residual weight after irradiation of human whole blood in vitro and boiling under reduced pressure Correction for physical decay performed

Fig. 11 Production cross section of ^{11}C from carbon ( ) and oxygen (o) and the mass stopping power of proton in tissue (x) as functions of proton energy The data are normalized to 1 0 at 150 MeV (from GRAFFMAN & JUNG 1964)

The observations do not allow conclusions regarding the potential use of induced activity for an analysis of physiologic parameters The formation cross sections for ^{11}C from ^{12}C and ^{16}O are such, however, that the total amount of ^{11}C per g rad will depend on the water content of the irradiated tissue Observations on mice with varying amounts of intraperitoneal fluid irradiated with high energy protons support this hypothesis

In experiments with mice the ratio between ^{11}CO and total production of ^{11}C was found not to be changed substantially when the animals were kept in low oxygen atmosphere or in hyperbaric (3 atm) pure O_2 during irradiation

Conclusions

The distribution throughout the body of the additional dose due to the decay of induced ^{15}O is complex Assuming total absorption of positrons and annihilation photons within the body it may be calculated from the production values in Table 1, that the additional integral dose from ^{15}O is 3×10^{-4} g rad per g rad proton dose Under the same assumptions and neglecting the elimination from the body the corresponding figure for ^{11}C is 2×10^{-4} g rad per g rad The CO fraction of this activity is rapidly accumulated in the blood which, together with the vessels, will receive some extra dose especially from the positrons The annihilation photons are

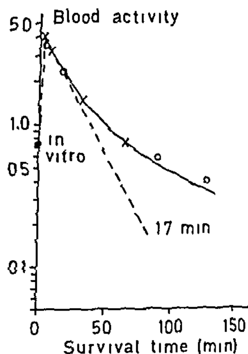


Fig 9 ^{11}C concentration in blood related to total ^{11}C concentration in a mouse irradiated over the whole body as a function of sampling time after mean time of irradiation Crosses and open circles refer to two separate experiments Correction for physical decay performed The in vitro point gives the ^{11}C concentration in a blood sample irradiated simultaneously with the mice

times the in vitro value These findings may suggest a nearly momentary accumulation in the blood of almost all induced ^{11}CO, followed by expiration of ^{11}CO Under this assumption, and correcting for 60 per cent stationary activity in the blood, the elimination constant for ^{11}CO was found to correspond to a half-life of about 17 min, in fair agreement with other measurements of this rate, reported here (The change in blood content of $^{11}CO_2$ can be neglected in this determination) Also the initial increase to a relative activity concentration in the blood of 4 5 corroborates this suggestion, provided the relative blood content of the mouse and the fraction of induced ^{11}C activity present as ^{11}CO, were 6 and 26 per cent, respectively Further, it is confirmed by the finding that in blood samples, taken one minute after irradiation, 80 to 90 per cent of the ^{11}C activity was attached to the blood corpuscles whereas for blood irradiated in vitro this figure was about 40 per cent

The comparison of the ^{15}O activity in irradiated living and dead mice indicated that less than 5 per cent of the ^{15}O activity was lost per minute through expiration and perspiration The transport of ^{15}O activity from the irradiation site was found to be very fast in the experiments with partially irradiated mice More than 60 per cent of the induced ^{15}O activity was distributed from the irradiation site throughout the body within 5 min The results of the model experiment with irradiated whole blood indicate clearly that most of the ^{15}O activity behaved as water (Fig 10), further supported by the finding that the ^{11}C and ^{13}N activities did not behave in this manner In preliminary experiments, $H_2{}^{15}O$, administered intravenously, was found not to be homogeneously distributed throughout the body within the first 15 min after injection

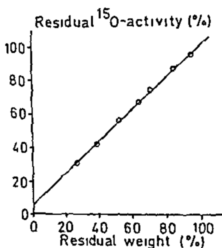


Fig 10

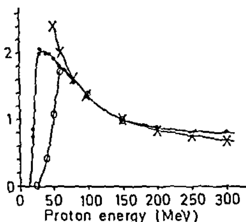


Fig. 11

Fig 10 Residual ^{15}O activity as a function of residual weight after irradiation of human whole blood in vitro and boiling under reduced pressure Correction for physical decay performed

Fig 11 Production cross section of ^{11}C from carbon ( ) and oxygen (o) and the mass stopping power of proton in tissue (x) as functions of proton energy The data are normalized to 1 0 at 150 MeV (from GRAFFMAN & JUNG 1964)

The observations do not allow conclusions regarding the potential use of induced activity for an analysis of physiologic parameters The formation cross sections for ^{11}C from ^{12}C and ^{16}O are such, however, that the total amount of ^{11}C per g rad will depend on the water content of the irradiated tissue Observations on mice with varying amounts of intraperitoneal fluid irradiated with high energy protons support this hypothesis

In experiments with mice the ratio between ^{11}CO and total production of ^{11}C was found not to be changed substantially when the animals were kept in low oxygen atmosphere or in hyperbaric (3 atm) pure O_2 during irradiation

Conclusions

The distribution throughout the body of the additional dose due to the decay of induced ^{15}O is complex Assuming total absorption of positrons and annihilation photons within the body, it may be calculated from the production values in Table 1, that the additional integral dose from ^{15}O is 3×10^{-4} g rad per g rad proton dose Under the same assumptions and neglecting the elimination from the body the corresponding figure for ^{11}C is 2×10^{-4} g rad per g rad The CO fraction of this activity is rapidly accumulated in the blood which, together with the vessels, will receive some extra dose especially from the positrons The annihilation photons are

of long range and their contribution to the dose will not be concentrated to blood and vessels The 2 5 per cent fraction collected in urine in 1 h will not give much dose to bladder tissue and gonads because of the slow rate of accumulation

Assuming that all nuclides induced by high energy protons in tissue (cf Fig 2) decay within the body and that all secondary radiation is absorbed within the body the additional, fractional, integral dose is found to be less than 0 001

For estimating integral, high energy proton dose from induced activity ^{11}CO and $^{11}CO_2$ probably offer the best means except for, possibly, whole body counting In *tissue, the ratio between* ^{11}C production and linear energy transfer is *fairly constant* for protons above 50 MeV (Fig 11) There are no reasons to believe that the chemical fate of ^{11}C is strongly dependent on proton energy Both ^{11}CO and $^{11}CO_2$ are easily sampled from the expired air by absorbers ^{11}CO is concentrated in red blood corpuscles and blood samples offer an attractive alternative for measuring this activity It appears that CO is most suitable due to its simple rate of elimination, which can be accelerated by using O_2–CO_2 as breathing gas

Acknowledgements

This work has been financially supported by grants from the Swedish Cancer Society and the Swedish Atomic Research Council

SUMMARY

The total production of ^{11}C, ^{13}N and ^{15}O in the mouse by protons with a mean energy of about 175 MeV was found to be 8 200, 1 500 and 14 000 nuclei per g rad, respectively About 40 per cent of the total induced ^{11}C activity was eliminated through expiration and about 2 5 per cent with the urine during the first hour after irradiation The expired gas contained ^{11}CO and $^{11}CO_2$ in the ratio 2/1 The urinary ^{11}C activity was bound to several compounds, the chemical nature of which was not established The ^{15}O activity behaved as H_2O and was found not to be eliminated from the body during the short observation time available The additional, fractional, integral radiation dose due to decay of induced nuclides is less than 0 1 per cent, and can be neglected since no accumulation to any small organ was seen Sensitive means for an estimate of integral dose based on the induced nuclides would be the detection of ^{11}CO activity in expired gas or in blood

ZUSAMMENFASSUNG

Die gesamte Produktion von ^{11}C, ^{13}N und ^{15}O *in* der Maus durch Protonen mit einer mittler Energie von etwa 175 MeV wurde mit 8 200, 1 500 bzw 14 000 Nuclei per g rad gefunden Etwa 40 % der gesamten induzierten ^{11}C Aktivitat wurde nach Bestrahlung durch die Atmung und etwa 2,5 % durch den Harn wahrend der ersten Stunde eliminiert Das Ausatmungsgas enthielt ^{11}CO und $^{11}CO_2$ im Verhaltnis 2/1 Die ^{11}C Aktivitat des Harns war an verschiedene Verbindungen gebunden deren *chemische Natur nicht festgestellt* wurde Die ^{15}O Aktivitat trat als H_2O auf und wurde wahrend der kurzen zur Verfugung

stehenden Beobachtungszeit nicht vom Korper abgegeben Die zusätzliche, unbedeutende Integraldosis infolge des Zerfalls der induzierten Nukleide beträgt weniger als 0,1 % und kann vernachlässigt werden, da keine Akkumulation in irgende einem der kleinen Organe gesehen wurde Eine empfindliche Weise zur Bestimmung der Integraldosis, die sich auf die induzierten Nukleide stutzt, wäre die Messung der ^{11}CO-Aktivität im ausgeatmeten Gas oder im Blut

RÉSUMÉ

La production totale de ^{11}C, ^{13}N et ^{15}O chez la souris par les protons ayant une énergie moyenne d'environ 175 MeV est [illegible]

du ^{11}CO et du $^{11}CO_2$ dans le rapport 2/1 L'activité ^{11}C urinaire était liée à differents composes dont la nature chimique n'a pas été établie L'activité ^{15}O se comportait comme H_2O; il semble qu'elle n'ait pas éte eliminee du corps pendant la courte période d'observation La dose de radiation supplementaire, fractionnaire, intégrale due à la desintegration des nuclides induits est inferieure a 0,1 pour cent et peut être negligée étant donné qu'on n'a pas observé d'accumulation dans aucun petit organe Les moyens sensibles pour estimer la dose integrale basée sur les nuclides induits devrait être la détection de l'activité ^{11}CO dans le gaz expire ou dans le sang

REFERENCES

Allen T H and Root W S Partition of carbon monoxide and oxygen between air and whole blood of rats, dogs and men as affected by plasma pH J appl Physiol 10 (1957), 186

Biggin H C and Morgan W D Fast neutron activation analysis of the major body elements J nucl Med 12 (1972), 808

Graffman S and Jung B Radioactivity of human blood as a measure of integral dose from high energy protons SR 4, AF EOAR Contract No, AF 61 (052)–740, 1964

Haller I B and Jung B Radionuclides produced in man by high energy protons SR I, AF EOAR Contract No AT 61 (052)–740, 1963

ICRP Report of Committee II on permissible dose for international radioactivity Pergamon Press New York 1959

Johansson K J, Johansson U and Larsson B Personal communication (1974)

Jung B Radionuclide production and effects on nuclear reactions on dose from 193 MeV protons stopped in tissue, SR 2, AF EOAR Contract No AF 61 (052)–740, 1964

Larsson B Pre therapeutic physical experiments with high energy protons Brit J Radiol 34 (1961), 143

Larsson B and Sarby B Equipment for radiation surgery using narrow 185 MeV proton beams To be published as a Suppl to Acta radiol

— Graffman S and Jung B Fixation of carbon-11 in the cells of proton-irradiated blood Nature 207 (1964), 543

Miller A [illegible] to estimate personnel [illegible] 23 (1972), 671

[illegible] ogy Edited by W O [illegible] American Physiological Society, Washington D C 1965

SARGENT T. W Metabolic studies with Fe^{59} Ca^{47} and C^{11} in various diseases *In* Whole-body counting Proc IAEA Symp Vienna (1961), 447

STENSTRÖM T On the chemical fate of nascent ^{11}C atoms induced by irradiation of water and aqueous solutions with 185 MeV protons Thesis, University of Uppsala 1970

TOBIAS C A, LAWRENCE I H, ROUGHTON F J W, ROOT W S and GREGERSEN M I The elimination of carbon monoxide from the human body with the reference to the possible conversion of CO to CO_2 Amer J Physiol 145 (1945), 253

FROM RADIUMHEMMET, KAROLINSKA SJUKHUSET, S-104 01 STOCKHOLM, AND THE CENTRAL MICROBIOLOGICAL LABORATORY, STOCKHOLM COUNTY COUNCIL, S-101 22 STOCKHOLM, SWEDEN

CAPACITY OF SERA FROM PATIENTS WITH MAMMARY CARCINOMA TO PROMOTE PHA-STIMULATION OF HUMAN LYMPHOCYTES

HENRIC BLOMGREN, JERZY WASSERMAN and ULLA GLAS

There is considerable evidence that a patient may develop an immune response against his own, autochtonous tumor, including both cellular and humoral immunity (KLEIN *et coll* 1967, MORTON et coll 1968, HELLSTRÖM et coll 1968, EILBER & MORTON 1970, HELLSTRÖM *et coll* 1971) This immune response must be considered to be comparatively weak since it only occasionally causes clinical rejection of a patient's own tumor (for a review see EVERSON & COLE 1966) However, the immune system may have a more critical role in immunesurveillance, destroying and inhibiting proliferation of new clones of neoplastic cells Patients receiving immunosuppressive therapy (MCKHAN 1969, PENN & STARZL 1970) and those with an inherent immune deficiency (KERSEY et coll 1973) have a highly increased incidence of malignant tumors. A number of authors have reported that patients with neoplasms have impaired immunological reactivity as reflected by their capacity to reject allogeneic grafts (SOUTHAM 1960) and to develop delayed skin reactions to antigens like dinitrofluorobenzene and PPD (SOUTHAM 1960, BROOKS et coll 1972, STEWARD 1973) Moreover, the peripheral blood lymphocytes from cancer patients may exhibit an impaired responsiveness in vitro to stimulants such as phytohaemagglutinin (PHA)

Submitted for publication 3 July 1974

and purified protein derivate of tuberculin (PPD) (RICCI et coll 1966, GARRIOCH et coll 1970, BROOKS et coll 1972, GATTI et coll 1972, WATKINS 1973) indicating an impaired function of the thymus-dependent line of lymphocytes

Reports have appeared showing that the poor immunologic reactivity of patients with malignancies may be due to an immunosuppressive factor present in their sera (TRUBOWITZ et coll 1966, SILK 1967, NELSON 1969, WHITTAKER et coll 1971, BROOKS et coll 1972, GATTI et coll 1972, STEWARD 1973) Fractionation of the components in sera indicate that immunosuppressive activity resides in a polypeptide fraction in patients with malignancy and Hodgkin's disease (SCHLURLEN et coll 1971) and in the IgG fraction in patients with brain tumors (BROOKS et coll 1972) Others have not been able to confirm the finding that the low PHA response of lymphocytes in patients with malignancy is due to an inhibitory serum factor (GOLUB et coll 1969, THOMAS et coll 1971)

Whether sera of patients with mammary carcinoma promote a lesser degree of stimulation of lymphocytes from healthy donors with PHA than do sera from women with non-malignant breast lesions forms the subject of the present investigation

Materials and Methods

The sera from 171 women attending the Radiumhemmet for breast lesions were examined Palpable tumors were subjected to fine needle aspiration biopsy (FRANZEN & ZAJICEK 1968) and the diagnosis established by cytology Sera were obtained from 86 women with cytologically verified mammary carcinoma and from a group of 85 patients of similar age without any clinical or cytologic evidence of malignancy Patients with operable primary breast carcinoma and less than 70 years old were randomized into the following three treatment groups A) Local irradiation followed by radical mastectomy, B) radical mastectomy followed by local irradiation, C) radical mastectomy only Details of the irradiation and surgery of the patients have been given before (GLAS & WASSERMAN 1974 a) Sera were also obtained from a group of 31 patients with mammary carcinoma and metastatic spread Patients who had been treated with cytostatic drugs were omitted Most of the patients with metastatic spread were treated with anabolic steroids, cortisone or estrogens

Sera Venous blood was drawn into 10 ml glass tubes The blood was allowed to clot over night at 5°C and the serum was then collected after centrifugation and stored at −20°C for a period not exceeding 2 years Sera were collected at three occasions from patients with primary malignancy Group A The first sample was taken within two weeks before radiation therapy was started, the second sample 3 weeks after completion of therapy and the third 3 weeks after surgery Group B The first sample was obtained within three weeks before surgery, the second 3 weeks after surgery and the third 3 weeks after completion of radiation therapy Group C The first sample was obtained within 1 week before surgery, the second 3 weeks after surgery and the third 3 months later

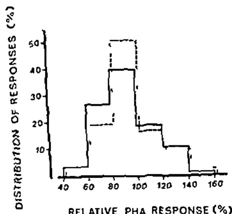


Fig 1 Stimulation of lymphocytes from healthy subjects by PHA in the presence of serum obtained from patients with primary breast carcinoma before therapy was started (86 sera) or in the presence of serum from control patients without evidence of malignancy (85 sera) The PHA responses are expressed as per cent of the values obtained in cultures containing a reference serum The distribution of the responses in the two groups of patients is shown Sera from patients with malignancy ——, sera from control patients

Cell preparations Venous blood from healthy subjects was drawn in heparinized syringes The leukocytes were separated from the erythrocytes by centrifugation on a Ficoll Isopaque gradient (JONDAL et coll 1972) The leukocytes were washed once by centrifugation in a balanced salt solution (BSS) and resuspended in Eagle's Minimal Essential Medium supplemented with Earle's salts (MEM) The number of lymphoid cells was determined in a Burker chamber after crystal violet staining

Phytohaemagglutinin PHA (Bacto phytohaemagglutinin M, Difco Lab Detroit, Mich USA) was employed as stimulant for lymphocytes

Culture conditions $2\,5\times10^5$ lymphoid cells were cultured in 15 ml screw cap glass tubes containing 1 0 ml of MEM with 10 % of human serum (HS), 150 μg of streptomycin and 100 units of penicillin per ml The HS was either obtained from a pool of normal donors with blood group AB or patients with malignant or benign lesions of the breasts All sera were decomplemented by heating at 56°C for 30 min and stored at −20°C Some cultures received PHA, unless otherwise stated, at a final concentration of 3 % and other cultures containing HS from the same serum batch,

Table 1

Stimulation of lymphocytes from healthy subjects by PHA in the presence of serum obtained from 86 patients with primary mammary carcinoma before any specific therapy or serum from 85 control patients Isotope incorporations in the presence of patients sera were related to values obtained in cultures containing a reference serum and expressed as per cent

Serum donors	Age of serum donors (years) M±SE	Relative PHA response (%) M±SE
Carcinoma patients	54 8±0 9	91.2±2 5 (p<0 9)
Control patients	52 4±1 6	93 0±2 2

and purified protein derivate of tuberculin (PPD) (RICCI et coll 1966, GARRIOCH et coll 1970, BROOKS et coll 1972, GATTI et coll 1972, WATKINS 1973) indicating an impaired function of the thymus dependent line of lymphocytes

Reports have appeared showing that the poor immunologic reactivity of patients with malignancies may be due to an immunosuppressive factor present in their sera (TRUBOWITZ et coll 1966, SILK 1967, NELSON 1969, WHITTAKER et coll 1971, BROOKS et coll 1972, GATTI et coll 1972, STEWARD 1973) Fractionation of the components in sera indicate that immunosuppressive activity resides in a polypeptide fraction in patients with malignancy and Hodgkin's disease (SCHEURLEN et coll 1971) and in the IgG fraction in patients with brain tumors (BROOKS et coll 1972) Others have not been able to confirm the finding that the low PHA response of lymphocytes in patients with malignancy is due to an inhibitory serum factor (GOLUB et coll 1969, THOMAS et coll 1971)

Whether sera of patients with mammary carcinoma promote a lesser degree of stimulation of lymphocytes from healthy donors with PHA than do sera from women with non-malignant breast lesions forms the subject of the present investigation

Materials and Methods

The sera from 171 women attending the Radiumhemmet for breast lesions were examined Palpable tumors were subjected to fine needle aspiration biopsy (FRANZÉN & ZAJICEK 1968) and the diagnosis established by cytology Sera were obtained from 86 women with cytologically verified mammary carcinoma and from a group of 85 patients of similar age without any clinical or cytologic evidence of malignancy Patients with operable primary breast carcinoma and less than 70 years old were randomized into the following three treatment groups A) Local irradiation followed by radical mastectomy, B) radical mastectomy followed by local irradiation, C) radical mastectomy only Details of the irradiation and surgery of the patients have been given before (GLAS & WASSERMAN 1974 a) Sera were also obtained from a group of 31 patients with mammary carcinoma and metastatic spread Patients who had been treated with cytostatic drugs were omitted Most of the patients with metastatic spread were treated with anabolic steroids, cortisone or estrogens

Sera Venous blood was drawn into 10 ml glass tubes The blood was allowed to clot over night at 5°C and the serum was then collected after centrifugation and stored at −20°C for a period not exceeding 2 years Sera were collected at three occasions from patients with primary malignancy Group A The first sample was taken within two weeks before radiation therapy was started the second sample 3 weeks after completion of therapy and the third 3 weeks after surgery Group B The first sample was obtained within three weeks before surgery, the second 3 weeks after surgery and the third 3 weeks after completion of radiation therapy Group C The first sample was obtained within 1 week before surgery, the second 3 weeks after surgery and the third 3 months later

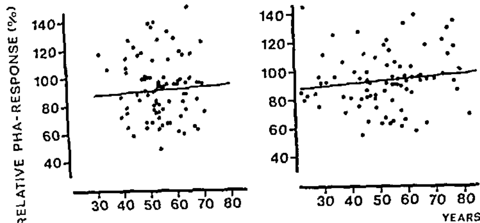


Fig 3 Scatter diagrams Relation between the capacity of sera from patients with carcinoma (left) and from control patients (right) to promote PHA stimulation of lymphocytes and the age of the serum donors y 0 12 × 84 51 and r = 0 04 for carcinoma patients and y = 0 16 × 84 92 and r = 0 11 for control patients

Since other authors have suggested a correlation between clinical state of tumor and capacity of the patients' sera to stimulate lymphocytes with PHA (GATTI et coll 1972), an attempt was made to correlate our serum results with the size of the tumor at the time the serum sample was taken A weak negative correlation was found (Fig 2), but statistically non significant, between tumor size and capacity of the patient's serum to promote PHA-stimulation of lymphocytes A correlation between age of the patients and the serum activity was also performed Scattergrams and linear regression equation (Fig 3) show a weak, non-significant positive correlation between age of the patients and the serum activity in both groups It has recently been emphasized that women may develop a factor in their serum during pregnancy which inhibits the response of lymphocytes to PHA in vitro and stimulation by allogeneic lymphocytes (GATTI 1971) Thus, the variation of the present sera in promoting stimulation of lymphocytes by PHA may be due to whether the serum donors have been pregnant or not and the time interval between the serum sample and last pregnancy Fig 4 reveals that there was neither a correlation between number of pregnancies nor the time which had elapsed between pregnancy and the activity of the serum

Serum activity of patients during and after specific therapy Patients with newly diagnosed carcinoma were randomized into three treatment groups at the time the first serum sample was taken Serum was then collected at two different occasions during and after treatment No difference between the first and the second serum samples was found, indicating that neither surgical removal of the tumor nor local irradiation change the activity of a patient's serum (Table 2) However, the third

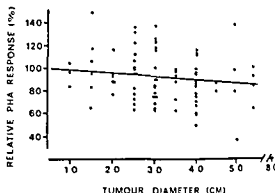


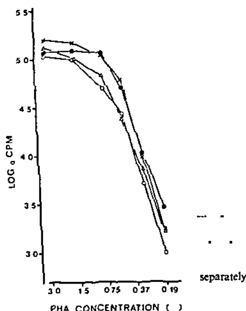
Fig 2 Scatter diagram Relation between the capacity of sera from carcinoma patients to promote PHA stimulation of lymphocytes and the size of the primary tumour of the patients The calculated regression line corresponding to the equation $y = mx + b$ is shown $y = -2.66 \times + 100.48$ $r = 0.15$

without PHA served as controls The cells were incubated for five days at 37 C in a humidified 5% CO_2-air atmosphere Twentyfour hours before completion of the cultures each tube received 0 1 ml of MEM containing 0 4 μCi of ^{14}C-thymidine (specific activity 54 mCi/mM, the Radiochemical Center Amersham, England) The cultures were terminated by centrifugation in the cold, washed twice in ice-cold BSS, the cells precipitated twice in trichloroacetic acid and then dissolved in Soluene The contents of the tubes were then transferred to vials containing scintillation fluid Activity, expressed as counts per min (cpm), was measured by a Packard Scintillation Counter Model 3380

Design of the tests The lymphocytes from one healthy subject were cultured in medium containing HS from patients with malignancy or control patients Six cultures were set up for each serum, 4 cultures with PHA and 2 without Cultures were also set up in parallel containing serum from a pool of healthy AB positive donors Six cultures were set up with PHA and 4 without This AB serum served as a reference for the patients' sera throughout the investigation Thymidine uptakes in control cultures without PHA were deduced from the isotope incorporations obtained in mitogen stimulated cultures The mean ^{14}C-thymidine incorporation by lymphocytes stimulated by PHA in the presence of a patient's serum was then related to isotope uptakes in the control cultures containing the reference serum Statistical significance between mean values was evaluated using the Student's t-test

Results

Serum activity of patients at the time of diagnosis Initially, 86 sera from patients with newly diagnosed mammary carcinoma not yet treated were examined as well as 85 sera from women of similar age with benign breast lesions Sera from patients with malignancy promoted PHA-stimulation of normal lymphocytes to the same extent as did sera from control patients (Table 1) Fig 1 illustrates the distribution of the values obtained in the two groups of patients It can be seen that there exist 'low responsive' sera in both groups although there was a slightly increased frequency of 'low responsive' sera in the malignant group



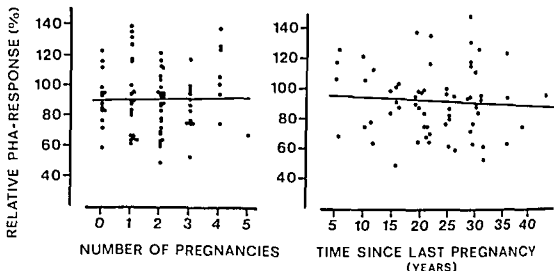
as cpm It is obvious that the response of the lymphocytes decreased as the mitogen concentration was diminished

The relative PHA responses in the presence of sera from patients with malignancy and control patients appear in Table 3 The stimulations obtained at the lower concentrations of PHA varied extensively between the different serum samples There was no statistically significant difference between the cancer group and the control group at any mitogen concentration employed

Table 3

Stimulation of lymphocytes from healthy subjects by PHA in the presence of serum from patients with mammary carcinoma and distant spread 31 sera were tested The cells were stimulated with various concentrations of PHA Statistical significance between values obtained for malignant patients and control patients (31 sera) are presented

PHA concentration (%)	Relative PHA response (%) M ± SE		
	Carcinoma patients	t test	Control patients
3 0	89 5 ± 4 6	p < 0 9	90 4 ± 3 6
1.5	96 5 ± 4 5	p < 0 4	101 8 ± 3 6
0 75	113 5 ± 7 9	p < 0 8	116 5 ± 7 1
0.38	148 7 ± 17 8	p < 0 3	181 4 ± 21 6
0 19	190 3 ± 57 4	p < 0 8	208 0 ± 32 2



and r = 0 02, and y = −0 19 × +96 03 and r = 0 07, respectively

serum samples of all three groups exhibited an increased capacity to promote PHA-stimulation of lymphocytes

Serum activity of patients with distant metastases The sera of patients with clinical signs of distant spread of their disease were also examined In the tests described, the lymphocytes were exposed to PHA at a final concentration of 3 per cent As PHA at this concentration is extremely stimulatory it is possible that the addition of a relatively weak inhibitor does not result in any detectable change of the response of the cells For this reason lymphocytes were stimulated with decreasing concentrations of PHA in the presence of patients' sera Fig 5 illustrates the stimulatory capacity of varying concentrations of PHA in the presence of reference serum expressed

Table 2

Stimulation of lymphocytes from healthy subjects by PHA in the presence of serum obtained from patients with primary mammary carcinoma before, during and after specific therapy The patients were randomized into three different treatment groups designated A, B and C 29, 27 and 30 serum samples were tested from each group respectively Three different serum samples were taken from each patient (I, II and III) Statistical significance between values obtained between the first and the second serum samples and between the second and third are presented

Treatment	Relative PHA response (%), M ± SE				
	I	t test	II	t test	III
A	86 6 ± 3 4	p 0 6	90 1 ± 4 6	p < 0 01	118 9 ± 3 2
B	95 6 ± 4 4	p < 0 2	87 3 ± 4 6	p < 0 01	117 4 ± 4 1
C	94 0 ± 4 2	p < 0 4	89 0 ± 2 7	p < 0 01	111 9 ± 4 1

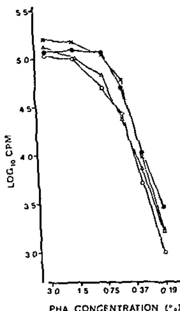


Fig 5 Stimulation of lymphocytes from four healthy subjects by varying concentrations of PHA in the presence of the reference serum (AB Rh neg donor) The background isotope uptakes in cultures without PHA are deducted The result of each lymphocyte preparation is presented separately

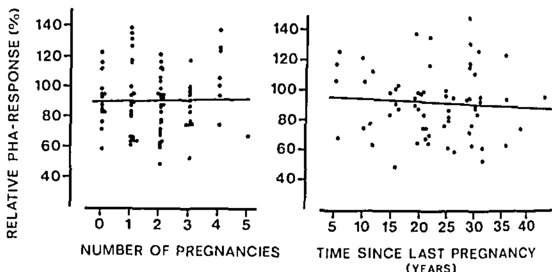
as cpm It is obvious that the response of the lymphocytes decreased as the mitogen concentration was diminished

The relative PHA responses in the presence of sera from patients with malignancy and control patients appear in Table 3 The stimulations obtained at the lower concentrations of PHA varied extensively between the different serum samples There was no statistically significant difference between the cancer group and the control group at any mitogen concentration employed

Table 3

Stimulation of lymphocytes from healthy subjects by PHA in the presence of serum from patients with mammary carcinoma and distant spread 31 sera were tested The cells were stimulated with various concentrations of PHA Statistical significance between values obtained for malignant patients and control patients (31 sera) are presented

PHA concentration (%)	Relative PHA response (%), M ± SE		
	Carcinoma patients	t test	Control patients
3 0	89.5±4 6	p<0 9	90 4±3 6
1 5	96 5±4 5	p<0 4	101 8±3 6
0 75	113 5±7 9	p<0 8	116 5±7 1
0 38	148 7±17 8	p<0 3	181 4±21 6
0 19	190 3±57 4	p<0 8	208 0±32 2



and r = 0 02, and y = − 0 19 × + 96 03 and r = 0 07, respectively

serum samples of all three groups exhibited an increased capacity to promote PHA-stimulation of lymphocytes

Serum activity of patients with distant metastases The sera of patients with clinical signs of distant spread of their disease were also examined In the tests described, the lymphocytes were exposed to PHA at a final concentration of 3 per cent As PHA at this concentration is extremely stimulatory it is possible that the addition of a relatively weak inhibitor does not result in any detectable change of the response of the cells For this reason lymphocytes were stimulated with decreasing concentrations of PHA in the presence of patients' sera Fig 5 illustrates the stimulatory capacity of varying concentrations of PHA in the presence of reference serum expressed

Table 2

Stimulation of lymphocytes from healthy subjects by PHA in the presence of serum obtained from patients with primary mammary carcinoma before during and after specific therapy The patients were randomized into three different treatment groups designated A B and C 29, 27 and 30 serum samples were tested from each group respectively Three different serum samples were taken from each patient (I, II and III) Statistical significance between values obtained between the first and the second serum samples and between the second and third are presented

Treatment	Relative PHA response (%) M ± SE				
	I	t test	II	t test	III
A	86 6±3 4	p < 0 6	90 1±4 6	p<0 01	118 9±3 2
B	95 6±4 4	p < 0 2	87 3±4 6	p<0 01	117 4±4 1
C	94 0±4 2	p<0 4	89 0±2 7	p<0 01	111 9±4 1

PHA promoting capacity of sera from women with primary breast malignancy was not significantly changed after radical mastectomy or local radiation therapy A close analysis demonstrated that the serum activities exhibited only random variation after irradiation or surgery Thus, some patients' sera exhibited increased activity whereas others decreased However, an unexplained increase was observed 6 weeks after primary diagnosis At this time all specific therapy was completed

The present results do not reveal whether the poor PHA stimulatory capacity of some sera from patients with malignancy and controls is due to the presence of inhibitory factors or whether other substances, such as certain macromolecules known to enhance PHA-stimulation, are present in suboptimal concentrations (FORSDYKE 1973) In any case, this stimulation depressing activity of serum is not characteristic for patients with breast carcinoma Consequently it seems likely that the poor PHA-responsiveness of lymphocytes from patients with breast carcinoma is due to other factors than coating of PHA-receptors on the lymphocytes by serum inhibitory factors Changes in the composition of the peripheral lymphocyte population could be one possibility Thus it has been reported that the frequency of lymphocytes in malignancy patients binding sheep erythrocytes is lower than in healthy controls (WYBRAN & FUDENBERG 1973) Human lymphocytes adhering sheep erythrocytes to their cell membranes are generally considered being thymus-dependent (T-cells) (JONDAL et coll 1972) The results of WYBRAN & FUDENBERG do not show, however, whether there is a changed proportion of T-cells in the blood of patients with carcinoma, since they used a method which only detects lymphocytes with a very strong tendency to bind sheep erythrocytes Previously (BLOMGREN et coll 1974), on the other hand, it has been demonstrated that the proportion of lymphocytes binding sheep erythrocytes (T-cells) and those having receptors for activated complement (thymus independent cells) were similar to that of healthy controls It is possible, however, that the composition of the T-cell population, which is probably composed of several subpopulations (RAFF & CANTOR 1971) is changed in patients with malignancy Another explanation of the poor mitogen responsiveness of lymphocytes from such patients may be that there is an intrinsic cellular abnormality without any changed cellular composition of the lymphocyte pool

In conclusion, sera from some patients with mammary carcinoma promote a poor PHA response of lymphocytes from normal subjects However, such sera are almost as frequent in control patients without evidence of malignancy The results are not contradictory to other reports describing PHA-inhibitory activity in the sera of patients with other types of malignancy than mammary carcinoma Nor do they exclude the possibility that in patients with mammary carcinoma serum factors develop which can suppress the in vitro response of normal lymphocytes to other stimuli such as PPD These questions are currently being investigated in our laboratory

Discussion

It is well known that patients with malignancy may display varying degrees of impaired immunologic reactivity. In particular, patients with metastases of non lymphoid malignancies may exhibit impaired cellular immune reactivity (GROSS 1965), and also patients with Hodgkin's disease and reticulum cell sarcoma (AISENBERG 1962, HERSH & OPPENHEIM 1965). Lymphocytes from patients with mammary carcinoma exhibit a lower response to PHA and PPD in vitro than do lymphocytes from healthy controls and it is further reduced in patients with metastases (BLOMGREN et coll. 1974, STEWARD 1973, GLAS & WASSERMAN 1974 b). In general, the degree of immunologic depression is positively linked to the extension of the disease. There is evidence that the PHA response of lymphocytes in patients with malignancy is increased after successful surgery (WATKINS 1973) and the depressed tuberculin response is reversed (STEWARD 1973). These observations indicate that malignant patients may develop immunologic impairment because of the malignant lesion.

Several reports indicate that the poor response of lymphocytes of patients with malignancy to PHA and PPD in vitro is caused by a factor present in the patients' plasma (TRUBOWITZ et coll. 1966, SILK 1967, NELSON 1969, GOLUB et coll. 1969, WHITTAKER et coll. 1971, BROOKS et coll. 1972, GATTI et coll. 1972, STEWARD 1973). Such plasma inhibitory activity has also been observed in patients with multiple sclerosis (HUGHES et coll. 1968), tuberculosis (HEILMAN & MACFARLAND 1966) and syphilis (LEVENE et coll. 1969). Alpha$_2$-globulin present in human plasma has been shown to inhibit immunologic responses (COOPERBAND et coll. 1968, MCFARLAND & OPPENHEIM 1969), but elevated alpha$_2$-globulin levels have not been observed in a higher incidence in malignant patients' sera than in healthy controls (GATTI et coll. 1972). Others observed an inhibitory activity on stimulation by PPD in a polypeptide fraction in the plasma of patients with Hodgkin's disease (SCHEURLEN et coll. 1971). On the other hand the depressed immunologic reactivity of lymphocytes from patients with primary intracranial tumors seems to be caused by inhibitory IgG molecules. Interestingly, their inhibitory activity disappears after removal of the tumor (BROOKS et coll. 1972). Moreover, a serum factor is produced in pregnant women which may inhibit the response of lymphocytes to PHA and to allogeneic cells in vitro. This inhibitor has been identified as a γ globulin (GATTI et coll. 1973).

A large number of sera from patients with mammary carcinoma and from women without evidence of malignancy were examined and it was observed that there do exist patients with primary breast carcinoma whose sera promote a very poor stimulation of normal lymphocytes with PHA. However, such inhibitory sera also occurred at almost the same frequency in control patients without evidence of malignancy. The same results were obtained when sera from malignant patients with distant spread were examined. It has not been possible to demonstrate any significant correlation between serum activity on the one hand and tumor size, age of the patients, number of pregnancies and time after last pregnancy on the other. The mean

PHA promoting capacity of sera from women with primary breast malignancy was not significantly changed after radical mastectomy or local radiation therapy A close analysis demonstrated that the serum activities exhibited only random variation after irradiation or surgery Thus, some patients' sera exhibited increased activity whereas others decreased However, an unexplained increase was observed 6 weeks after primary diagnosis At this time all specific therapy was completed

The present results do not reveal whether the poor PHA-stimulatory capacity of some sera from patients with malignancy and controls is due to the presence of inhibitory factors or whether other substances, such as certain macromolecules known to enhance PHA-stimulation, are present in suboptimal concentrations (FORSDYKE 1973) In any case, this stimulation depressing activity of serum is not characteristic for patients with breast carcinoma Consequently it seems likely that the poor PHA-responsiveness of lymphocytes from patients with breast carcinoma is due to other factors than coating of PHA receptors on the lymphocytes by serum inhibitory factors Changes in the composition of the peripheral lymphocyte population could be one possibility Thus it has been reported that the frequency of lymphocytes in malignancy patients binding sheep erythrocytes is lower than in healthy controls (WYBRAN & FUDENBERG 1973) Human lymphocytes adhering sheep erythrocytes to their cell membranes are generally considered being thymus-dependent (T-cells) (JONDAL et coll 1972) The results of WYBRAN & FUDENBERG do not show, however, whether there is a changed proportion of T-cells in the blood of patients with carcinoma, since they used a method which only detects lymphocytes with a very strong tendency to bind sheep erythrocytes Previously (BLOMGREN et coll 1974), on the other hand, it has been demonstrated that the proportion of lymphocytes binding sheep erythrocytes (T-cells) and those having receptors for activated complement (thymus independent cells) were similar to that of healthy controls It is possible, however, that the composition of the T-cell population, which is probably composed of several subpopulations (RAFF & CANTOR 1971) is changed in patients with malignancy Another explanation of the poor mitogen responsiveness of lymphocytes from such patients may be that there is an intrinsic cellular abnormality without any changed cellular composition of the lymphocyte pool

In conclusion, sera from some patients with mammary carcinoma promote a poor PHA response [illegible]
as frequent in c[illegible]
contradictory tc[illegible] reports describing PHA-inhibitory activity in the sera of patients with other types of malignancy than mammary carcinoma Nor do they exclude the possibility that in patients with mammary carcinoma serum factors develop which can suppress the in vitro response of normal lymphocytes to other stimuli such as PPD These questions are currently being investigated in our laboratory

Acknowledgements

The authors wish to thank Mrs Cecilia de Laval for her excellent technical assistance This work was supported by grants from King Gustaf the Vth Jubilee Fund

SUMMARY

Lymphocytes from patients with carcinoma have been reported to exhibit impaired immunologic reactivity and responsiveness to non specific stimuli both in vivo and in vitro due to inhibitory serum factors In the present investigation it is tested whether sera from patients with mammary carcinoma may inhibit the response of lymphocytes from normal donors to phytohaemagglutinin (PHA) in vitro Neither sera from patients with newly diagnosed breast malignancy nor patients with wide spread disease differed from control patients with benign breast lesions Serum activity did not change within 3 weeks after radical mastectomy or local irradiation but increased slightly after 6 weeks It is suggested that the impaired PHA-responsiveness of lymphocytes in patients with mammary carcinoma is not due to blocking serum factors but to intrinsic cellular abnormality

ZUSAMMENFASSUNG

Es ist berichtet worden, dass die Lymphozyten von Patienten mit einem Karzinom eine herabgesetze immunologische Reaktivitat gegenuber nicht spezifischen Stimuli sowohl in vivo als auch in vitro durch inhibierende Serumfaktoren aufweisen In der vorliegenden Untersuchung wird getestet, ob Sera von Patienten mit einem Mammakarzinom die Antwort der Lymphozyten von normalen Donatoren auf Phythamagglutinin (PHA) verhindern konnen Es unterscheiden sich die Sera weder von Patienten mit neu diagnostizierter Malignitat der Brust noch der von Patienten mit einer weit fortgeschrittenen Erkrankung von Kontrollpatienten mit einer benignen Brustveranderung Die Serumaktivität veranderte sich innerhalb von drei Wochen nach radikaler Mastektomie oder lokaler Bestrahlung nicht stieg jedoch leicht nach 6 Wochen Es wird angenommen, dass die herabgesetzte PHA Reaktivitat von Lymphozyten bei Patienten mit einem Mammakarzinom nicht auf einem Block durch Serumfaktoren sondern auf einer wirklichen zellularen Veranderung beruht

RÉSUMÉ

D'après certains travaux, les lymphocytes de malades atteints de cancer auraient une réactivité immunologique et une capacité de réponse aux stimuli non spécifiques diminuées aussi bien in vivo que in vitro sous l effet de facteurs inhibiteurs sériques Dans le présent travail on a cherché si les sérums de malades atteintes de cancer du sein peuvent inhiber la réponse de lymphocytes de donneurs normaux à la phytohémaglutinine (PHA) in vitro Ni les sérums de malades ayant une tumeur maligne du sein diagnostiquée depuis peu, ni ceux de malades ayant un cancer largement disséminés n'ont été différents de ceux des malades témoins ayant des lésions bénignes du sein L'activité sérique ne change pas dans les 3 semaines qui suivent la mammectomie radicale ou l irradiation locale mais elle augmente légèrement après 6 semaines Les auteurs pensent que la diminution de la capacité de réponse à la PHA des lymphocytes de malades atteintes de cancer du sein n est pas due à un blocage de facteurs sériques mais à une anomalie cellulaire intrinsèque

REFERENCES

AISENBERG A C Studies on delayed hypersensitivity in Hodgkin's disease J Clin Invest 41 (1962) 1964

BLOMGREN H, GLAS H, MELÉN B and WASSERMAN J Blood lymphocytes after radiation therapy of mammary carcinoma Acta radiol Ther Phys Biol 13 (1974), 185

BROOKS W H, NETSKY M G, NORMANSELL D E and HORWITZ D A Depressed cell-mediated immunity in patients with primary intracranial tumors J exp Med 136 (1972), 1631

COOPERBAND S R., BONDEVIK H, SCHMIDT K and MANNICK J A Transformation of human lymphocytes Inhibition by homologous alpha globulin Science 159 (1968), 1243

EILBER F R and MORTON D L Sarcoma specific antigens Detection by complement fixation with serum from sarcoma patients J nat Cancer Inst 44 (1970), 651

EVERSON T C and COLE W H Spontaneous regression of cancer Saunders, Philadelphia 1966

FORSDYKE D R Serum and lymphocyte activation by phytohaemagglutinin (PHA) Exp Cell Res 77 (1973), 216

FRANZÉN S and ZAJICEK J Aspiration biopsy in diagnosis of palpable lesions of the breast Acta radiol Ther Phys Biol 7 (1968), 241

GARRIOCH D B GOOD R A and [illegible]

C [illegible]

— [illegible] lymphoid malignancies *In* Fifth leukocyte culture conference Edited by J J Harris Academic Press, New York, London 1972

— YUNIS E J and GOOD R A Characterization of a serum inhibitor of MLC reactions Clin exp Immunol 13 (1973) 427

GLAS U and WASSERMAN J (a) Effect of radiation treatment on the cell mediated immune response in carcinoma of the breast Acta radiol Ther Phys Biol 13 (1974) 83

— — (b) (unpublished results)

GOLUB E K, ISRASENA T, QUATRALE A C and BECKER K L Effect of serum from cancer patients on homologous lymphocyte cultures Cancer 23 (1969), 306

GROSS L Immunological defect in aged populations and its relation to cancer Cancer 18 (1965) 201

HEILMAN D H and MACFARLAND W Inhibition of tuberculininduced mitogenesis in cultures of lymphocytes from tuberculous donors Int Arch Allergy 30 (1966), 58

HELLSTRÖM I HELLSTRÖM K E, PIERCE G E and YANG J P S Demonstration of cell-bound and humoral immunity to different types of neoplasms Nature (London) 220 (1968) 1352

— — and SJÖGREN H Demonstration of cell mediated immunity to human neoplasms of various histological types Int J Cancer 7 (1971), 1

HERSH E M and OPPENHEIM J J Impaired in vitro lymphocyte transformation [illegible] kin s disease [illegible]

HUGHES D, [illegible] cephalito [illegible] (1968), 1

JONDAL M, HOLM G and WIGZELL H Surface markers on human T- and B-lymphocytes J exp Med 136 (1972) 207

KERSEY J H, SPECTOR B D and GOOD R A Primary immunodeficiency diseases and cancer The immuno deficiency-cancer registry Int J Cancer 12 (1973), 333

KLEIN G, CLIFFORD P, KLEIN E, SMITH R T, MINOWADA J, KOURILSKY F M and BURCHENAL J. H Membrane immunofluorescence reactions of Burkitt lymphoma cells from biopsy specimens and tissue culture J nat Cancer Inst 39 (1967), 1027

LEVENE G M, TURK J L, WRIGHT D J M and GRIMBLE A G S Reduced lymphocyte transformation due to a plasma factor in patients with syphilis Lancet 2 (1969) 246

MCFARLAND D E and OPPENHEIM J J Impaired lymphocyte transformation in ataxia telangiectasia in part due to a plasma inhibitory factor J Immunol 103 (1969), 1212

MCKHAN C F Primary malignancy in patients undergoing immunosuppression for renal transplantation Transplant Bull 8 (1969), 209

MORTON D L, MALMGREN R. A, HOLMES E C and KETCHAM A S Demonstration of antibodies *against human malignant melanoma by immunofluorescence* Surgery 64 (1968), 233

NELSON H S Delayed hypersensitivity in cancer patients Cutaneous and in vitro lymphocyte response to specific antigens J nat Cancer Inst 42 (1969), 765

PENN I and STARZL T E Malignant lymphomas in transplantation patients A review of the world experience Int J clin Pharmacol Ther Toxicol 3 (1970), 49

*RAFF M C and CANTOR H Subpopulations of thymus cells and thymus derived lympho-*cytes *In* Progress in immunology First International Congress of Immunology Academic Press, New York, London 1971

RICCI M, PASSALEVA A and RICCA M Mixed lymphocyte reaction in cancer Lancet 2 (1966), 503

SCHEURLEN P G, SCHNEIDER W and PAPPAS A Inhibition of transformation of normal lymphocytes by plasma factor from patients with Hodgkin's disease and cancer Lancet 2 (1971), 1265

SILK M Effect of plasma from patients with carcinoma on in vitro lymphocyte transformation Cancer 20 (1967), 2088

SOUTHAM C M Relationships of immunology to cancer A review Cancer Res 20 (1960), 271

STEWARD A M Tuberculin reaction in cancer patients, 'Mantoux release' and lymphosuppressive stimulatory factors J nat Cancer Inst 50 (1973), 3

THOMAS J W, COY P, LEWIS H S and YUEN A Effect of therapeutic irradiation on lymphocyte transformation in lung cancer Cancer 27 (1971), 1046

TRUBOWITZ S, MASEK B and DEL ROSARIO A Lymphocyte response to phytohemagglutinin in Hodgkin's disease, lymphocytic leukemia and lymphosarcoma Cancer 19 (1966), 2019

WATKINS S M The effects of surgery on lymphocyte transformation in patients with cancer Clin exp Immunol 14 (1973), 69

WHITTAKER M G, REES K and CLARK C G Reduced lymphocyte transformation in breast cancer Brit J Surg 1 (1971), 892

WYBRAN J and FUDENBERG H H Thymus derived rosette forming cells in various human disease states cancer, lymphoma, bacterial and viral infections, and other diseases J clin Invest 52 (1973), 1026

FROM THE DEPARTMENT OF PHYSICAL BIOLOGY, THE GUSTAF WERNER INSTITUTE, UPPSALA UNIVERSITY, S-751 21 UPPSALA, SWEDEN AND THE DEPARTMENT OF NEUROSURGERY, KAROLINSKA SJUKHUSET, S-104 01 STOCKHOLM, SWEDEN

INFLUENCE OF ABSORBED DOSE AND FIELD SIZE ON THE GEOMETRY OF THE RADIATION-SURGICAL BRAIN LESION

H DAHLIN, B LARSSON, L LEKSELL, KERSTIN ROSANDER, B SARBY and L STEINER

A ^{60}Co irradiation equipment for clinical use specially constructed for irradiation of small restricted volumes in the brain has been described by LARSSON et coll (1970) A number of specimens from cases irradiated for intractable pain where this method has been used for thalamotomy by radiation are now available for examination The aim of this report is to evaluate the effects of absorbed dose, beam geometry and period of survival on the size and shape of the lesions Clinical aspects have been reported elsewhere (LEKSELL et coll 1973)

Methods

Irradiation technique All the lesions were produced in the thalamus, in some cases bilaterally, by a stereotactic method (LEKSELL 1971) A total number of 21 lesions were available for investigation (Table) The apparatus consisted of 179 ^{60}Co sources symmetrically situated on a sector of a sphere, 76 cm in diameter, the centre of which coincided with the centre of the target volume Two field sizes were used 3 mm × 5

Submitted for publication 9 April 1974

Table

Data of lesions

Field size (mm)	Sex, age	Absorbed dose (krad)	Survival time (days)	Axes (mm) A × B × C	Calculated lesion volume (mm³)	Comments
3 × 5	M 68	12	39			No lesion
	F 35	15	129	9 × 7 5 × 4	141 4	
	M 68	16	39			No lesion
	F 35	20	129	7 × 6 × 4	88 0	
	M 61	20	211	7 × 6 × 3	66 0	
	M 61	20	211	7 × 6 × 3	66 0	
	F 54	22	210	6 × 6 × 4	75 4	
	M 72	25	78	7 × 6 × 3 5	77 0	
	M 61	25	79	7 × 6 × 3	66 0	
	F 73	25	133	9 × 7 × 5	164 9	
	F 54	25	169	5 5 × 5 5		Not calculated
Mean			144	7 4 × 6 3 × 3 7	93 1	
3 × 7	M 62	14	400	5 × 4 5 × 2	23 6	
	F 64	16	220	8 5 × 7 5 × 3 5	116 8	
	F 64	16	42	6 × 4 × 2 5	31 4	
	F 84	16	63	8 × 7 × 3	88 0	
	F 84	16	93	7 × 5 × 3	55 0	
	M 68	18	55	7 × 7 5 × 3	82 5	
	M 68	18	55	7 × 7 5 × 3	82 5	
	F 34	18	73	7 × 6 × 3	66 0	
	F 50	20	25	6 × 6 × 3	56 5	
	M 59	20	25	8 × 6 × 3	75 4	
	M 74	20	58	10 × 7 × 5	183 3	
	F 34	20	73	6 5 × 6 5 × 3 5	77 4	
	M 54	20	198	5 × 4 × 3 5	36 7	
Mean			123	7 × 6 × 3 2	75 0	

mm (8 patients) and 3 mm × 7 mm (13 patients) The dose rate was about 150 rad/min and the absorbed doses at the centre of the lesions ('beam focus') are given in the Table By a method of calculation described by DAHLIN (1970) it was possible to obtain the three-dimensional distribution of absorbed dose expressed as isodoses in the horizontal, frontal and sagittal planes

Histologic method Specimens fixed in 40 % formaldehyde were frozen and sectioned at 15 μm Consecutive sections from equidistant levels were stained with Htx-eosin and by the method of Palmgren & Weigert, respectively Each lesion was measured along three axes (A, B and C) in a sagittal (AC) and a frontal (AB) plane of symmetry

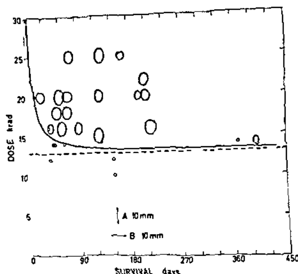


Fig. 1 Size and shape of the lesions in the AB (frontal) plane together with absorbed dose and survival time The dashed line indicates a threshold dose 13 krad and the curve indicates the expected latency time for necrosis Field size ● 3 mm × 5 mm ○ 3 mm × 7 mm ○ no lesion.

Results

As the lesions were found in various phases of the necrotic or resorptive stages, a strict definition of their border line characteristics could not easily be given The width of the border zone between the area of complete necrosis and the area of apparently normal tissue was, however, very narrow (1 mm or less) The lesions were more or less ellipsoidal in shape and the volumes were calculated as $\frac{1}{6}\pi$ ABC (Table)

The size and shape of the lesions in the AB plane together with absorbed dose and survival time appear in Fig 1 A threshold dose of 13 krad is indicated The relation between absorbed dose and time of latency estimated from previously published animal experiments (LARSSON 1960) is also illustrated

Fig 2 gives the relation between A and B Fitting a straight line to the experimental values of A and B gives the slope 0 85

In Fig 3 a plot of lesion volume versus absorbed dose is shown In order to determine whether differences in average lesion volume obtained by the two field sizes existed a Student s t test was performed No difference at the 5 % level of significance was found Furthermore, the analysis of variance revealed no significant difference between lesions grouped for doses of 12 to 16 krad, 18 krad, 20 krad and 25 krad (F 0 2, $df = 3$ 17, $p > 0$ 05) Thus it seems probable that there is no relation between absorbed dose and lesion volume

When the mean lesion volume is superposed on the isodose distributions (Fig 4) it is evident that for the field size 3 mm × 5 mm the lesion is extended to about the 55 to 60 per cent level in the AB plane where the dose gradient is small In the C-direction where the dose gradient is steeper it extends to the 45 per cent level For the field size 3 mm × 7 mm the corresponding isodoses are 80 to 85 per cent and 60 per cent, respectively

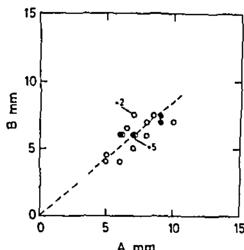


Fig 2

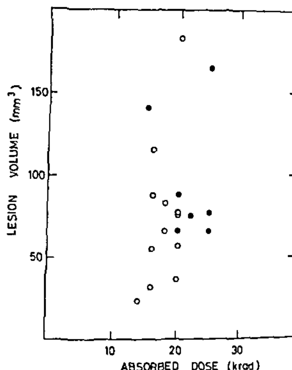


Fig 3

Fig 2 Relation between the widths of the lesion in the postero anterior (A) and lateral (B) directions respectively Field size ○ 3 mm × 7 mm, ● 3 mm × 5 mm
Fig 3 Calculated lesion volume versus absorbed dose Field size ○ 3 mm × 7 mm, ● 3 mm × 5 mm

Discussion

It is well-known from previous experiences with local irradiation of the central nervous system that the field size is inversely related to the absorbed dose at threshold conditions (LARSSON 1960, ZEMAN et coll 1961 BERG & LINDGREN 1963, HAYMARKER 1969) In the present investigation no relation could be verified between field size, absorbed dose or lesion volume Evidently, the difference between the two field sizes is too small to give any effects Such a difference in lesion volume should be demonstrable in either a larger or a more homogeneous material

The data (Fig 1), especially at short survival and small dose, indicate a dose time relationship very similar to that found by LARSSON, in experiment on rats irradiated laterally through the thalamus with a 185 MeV circular proton beam of 3 mm diameter When a comparison is made between the present results and those of LARSSON it is important to consider differences in the size of the brain and in the relative size of the irradiated volume It is believed that for relatively large irradiated volumes the variation in the appearance of the lesion is more marked (ZEMAN et coll) Probably this is contributing to the variability in lesion geometry illustrated in Fig 1

Although satisfying from the physical point of view, the present method of irradiation did not permit the lesion volume to be predetermined at the expected degree of accuracy From the radiation biologic point of view, therefore, the results clearly demonstrate our lack of knowledge of the processes leading to local tissue damage and of the possible causes of the observed variation in the size of the local radiation

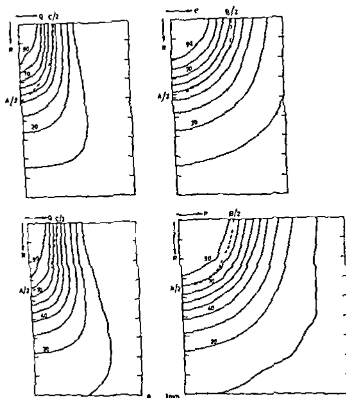


Fig 4 The mean lesion volume (dashed curves) for field sizes 3 mm × 5 mm and 3 mm × 7 mm, respectively, superposed on the isodose distribution in the frontal (−PR) plane and the sagittal (−QR) plane The isodoses are normalized versus the absorbed dose at beam focus

lesions as well as in the period of delay between irradiation and the occurrence of tissue necrosis In the use of the ^{60}Co equipment on patients in which late effects are not expected to be important, clinical experience rather than biologic considerations should determine the choice of dose and field size (Table)

Acknowledgements

This work was supported by grants from the Swedish Atomic Research Council and the Swedish Medical Research Council

SUMMARY

Specimens from a number of patients locally irradiated in the thalamus for intractable pain with a multiple gamma beam technique have been examined The geometry of well circumscribed necrotic lesions was ascertained No correlation was seen between the dimensions of the lesions and the size of the field, 3 mm × 5 mm or 3 mm × 7 mm, within the clinically useful dose range, 16 to 25 krad

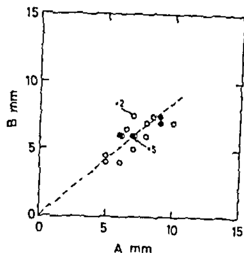


Fig 2

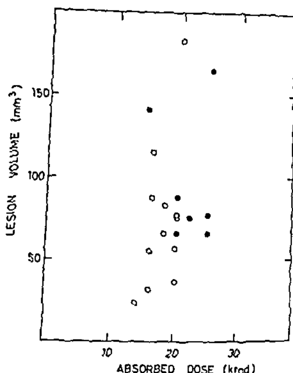


Fig 3

Fig 2 Relation between the widths of the lesion in the postero anterior (A) and lateral (B) directions respectively Field size ○ 3 mm × 7 mm, ● 3 mm × 5 mm
Fig 3 Calculated lesion volume versus absorbed dose Field size ○ 3 mm × 7 mm, ● 3 mm × 5 mm

Discussion

It is well-known from previous experiences with local irradiation of the central nervous system that the field size is inversely related to the absorbed dose at threshold conditions (LARSSON 1960, ZEMAN et coll 1961 BERG & LINDGREN 1963, HAYMARKER 1969) In the present investigation no relation could be verified between field size, absorbed dose or lesion volume Evidently, the difference between the two field sizes is too small to give any effects Such a difference in lesion volume should be demonstrable in either a larger or a more homogeneous material

The data (Fig 1), especially at short survival and small dose, indicate a dose-time relationship very similar to that found by LARSSON, in experiment on rats irradiated laterally through the thalamus with a 185 MeV circular proton beam of 3 mm diameter When a comparison is made between the present results and those of LARSSON it is important to consider differences in the size of the brain and in the relative size of the irradiated volume It is believed that for relatively large irradiated volumes the variation in the appearance of the lesion is more marked (ZEMAN et coll) Probably this is contributing to the variability in lesion geometry illustrated in Fig 1

Although satisfying from the physical point of view, the present method of irradiation did not permit the lesion volume to be predetermined at the expected degree of accuracy From the radiation biologic point of view, therefore, the results clearly demonstrate our lack of knowledge of the processes leading to local tissue damage and of the possible causes of the observed variation in the size of the local radiation

FROM THE DEPARTMENT OF OTOLARYNGOLOGY, KAROLINSKA SJUKHUSET, THE DEPARTMENT OF RADIATION PHYSICS, KAROLINSKA INSTITUTET, S-104 01 STOCKHOLM, AND THE DEPARTMENT OF RADIATION PHYSICS, SÖDERSJUKHUSET, S-100 64 STOCKHOLM, SWEDEN

OBJECTIVE SYMMETRY DETECTOR METHOD FOR GAMMAENCEPHALOGRAPHY

II. Normal range

MAGNUS LIND, STIG LARSSON and BERNDT SÖDERBORG

Encephalography or cerebral angiography are not well suited for screening purposes, because they involve a certain risk, are inconvenient to the patient and also demand great economic, technical and personnel resources There is a need for safer, simpler and more convenient methods and therefore nuclides have become important aids in the diagnosis of brain lesions, especially tumours Radiation hazards from amounts and types of short lived nuclides, commonly used, are small (SMITH 1965, PLANIOL 1966, Swedish National Institute of Radiation Protection 1969, PAOLETTI et coll 1969, MUNDINGER & OSTERTAG 1971, YOUNG & ROCKETT 1972)

Scanners and gamma cameras have been technically improved offering increased spatial resolution Digital handling of data by integrated computers has become more common Despite the development of complicated and expensive instruments, skilful subjective evaluation of results is still necessary (CHARLESTON et coll 1964, MALLARD 1966, PAOLETTI et coll , BURROWS 1972)

Originally, one detector methods were used in gammaencephalography and with experience a high level of diagnostic accuracy could be obtained with these methods, taking advantage of the symmetry of the skull However, positioning of the detectors over the head created a source of variation, including different levels of body-background, difficult to control The digital results were difficult to evaluate as they

Submitted for publication 15 January 1974

ZUSAMMENFASSUNG

Es wurden Teile des Thalamus bei einer Anzahl von Patienten, die wegen intrakranial *hervorgerufener Schmerzzustände mit der multiplen Gammabestrahlungs Technik* lokal bestrahlt worden waren, untersucht Die Geometrie der wohl umschriebenen nekrotischen Läsionen wurde festgestellt Es fand sich keine Korrelation zwischen den Dimensionen der Schädigung und der Grosse des Feldes, 3 mm × 5 mm oder 3 mm × 7 mm, innerhalb des *klinisch anwendbaren Dosisbereichs von 16 bis 25 krad*

RÉSUMÉ

Les auteurs ont examiné des pièces d'autopsie prélevées sur un certain nombre de malades irradiés localement dans le thalamus pour des douleurs insupportables par une technique de faisceaux gamma multiples Ils ont établi la géométrie de lésions nécrotiques bien circonscrites *Ils* n'ont pas trouvé de corrélation entre les dimensions des lésions et *les dimensions* du champ, 3 mm × 5 mm ou 3 mm × 7 mm, dans le domaine de doses utiles cliniquement qui est de 16 à 25 krad

REFERENCES

BERG N O and LINDGREN N Relation between field size and tolerance of rabbits brain to roentgen irradiation (220 keV) via a slit-shaped field Acta radiol Ther Phys Biol 1 *(1963)*, *147*

DAHLIN H Internal report Gustaf Werner Institute (1970)

HAYMARKER W Effects of ionizing radiation on nervous tissue *In* The structure and function of nervous tissue, Vol III Edited by G H Bourne Academic Press, London 1969

ARSSON B *Blood vessel changes following local irradiation of the brain with high energy* protons Acta Soc Med upsalien 65 (1960), 61

— LIDÉN K and SARBY B Irradiation of small structures through the intact skull Acta radiol Ther Phys Biol 13 (1974), 525

LEKSELL L *Stereotaxis and radiosurgery An operative system Charles* C Thomas Publisher, Springfield, Illinois 1971

— LARSSON B, ANDERSSON B, REXED B, SOURANDER P and MAIR W Lesions in the depth *of the brain produced by a beam of high energy protons* Acta radiol Ther Phys Biol 54 *(1969)*, 251

— STEINER L, FORSTER D, LARSSON B, BOETHIUS J and MEYERSSON B Gammathalamotomy for intractable pain Paper presented at the V Int Congr of Neurol Surgery, Tokyo 1973

ZEMAN W, CURTIS H J and BAKER C P Histopathologic effect of high energy particle microbeams on the visual cortex of the mouse brain Radiat Res 15 (1961), 496

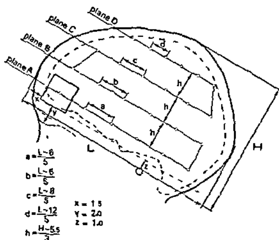


Fig. 1 The positions of the 24 measuring areas of each side of the skull are defined by circles, marking the central axis common for both collimators Each position is identified by plane (A–D) and number (1–6) Number 1 is the most frontal and 6 the most occipital position of each plane The aperture is indicated at position A1 The principles of the positioning diagram are given by the formulas Position C1 is located 1 1/3 cm behind B1 and D1 is located 2 2/3 cm behind C1

tions (30 mm × 30 mm) located in relation to the size and shape of the skull, were measured from both sides simultaneously by the movable detectors The measuring positions were orientated in 4 parallel planes, each with 6 positions (Fig 1)

To achieve standardized positioning, independent of the size of the skull, different diagrams were constructed, using the lateral projection outlines of skulls with various [illegible] was chosen A pointer indicated the actual position of the collimators and their movements on the [illegible] ying each position are demonstrated in Fig 1

Measurement I started about 30 min after the injection and lasted 30 min The instrument was programmed for recording periods of 60 s with 15-s intervals The intervals were used to move the detector system to the next measuring position

Measurement II started after one hour and consisted of a second identical measuring sequence including a balance test, about 120 min after the injection of activity

Calculation of evaluation parameters The number of counts, N_R and N_L, obtained from each subregion in the right and left detector, respectively, was recorded on paper tape for an off-line calculation by a PDP-8 computer All results were corrected for imbalance between the detectors from mean values of the balance test and also for the radiation decay Each measuring value was related to two different reference values the central mean value, C_{mv}, and the plane mean value, P_{mv} The C_{mv} was the calculated mean number of counts registered per measuring position of the central area of the skull (B2–B5, C2–C5, right and left) The P_{mv} was the calculated mean number of counts of all measuring positions of the corresponding measuring planes

depend upon the subjective estimation of several different criteria (MOORE 1948 MOORE et coll 1948, PEYTON et coll 1952, PLANIOL 1959, 1966, WENDE 1963, VAN DER WERFF et coll 1964, CONRAD & HORST 1966, MUNDINGER & ASAI 1967)

To avoid subjective influence, objective statistical analysis of isotope distribution measurements should be made This demands knowledge of the normal ranges of digital parameters The normal appearance of nuclide distribution in the skull after intravenous administration has been described by several authors (WEBBER 1965 SCHNEIDER & PRÉVOT 1966, PENNING & FRONT 1970) MUNDINGER has reported the normal distribution obtained at gammaencephalography in digital terms (MUNDINGER & ASAI), normal ranges of digitalized brain scanning data has also been published (DOWSETT & PERRY 1970, POPHAM et coll 1970, DOWSETT 1972) However, it has been difficult to achieve reproduceable positions for measuring in relation to the size and shape of the head and to restrict the error of counting statistics to a level where it is unimportant compared to the total variance of the results

The general purpose of this work was to develop the original gammaencephalographic methods into an objective and simple method, suitable for neurologic screening work

This has been achieved by assessing the performance in clinical routine work of a symmetry detector method for gammaencephalography as well as the normal ranges of the $^{99}Tc^mO_4$ activity distribution of the skull, permitting the statistical analysis of results from clinical cases by a routine procedure The physical characteristics of the instrument and the method have been described previously (LARSSON et coll 1975)

Method

The use of few, clearly defined stationary measuring positions was combined with large collimator apertures For the whole skull the number of measuring parameters was small as a result of the large apertures, thus facilitating a simple statistical analysis and an objective classification of results in clinical routine, using defined criteria

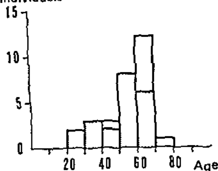
Each examination was performed as follows

(1) 0 4 g potassium perchlorate was administered orally (WITCOFSKI et coll 1967, SILBERSTEIN & LEVY 1970, HARPER et coll 1972)

(2) Between 20 and 70 min later 10 mCi technetium pertechnetate ($^{99}Tc^mO_4$) was injected intravenously

(3) A 'balance test' was performed by measuring a carefully mixed solution of $^{99}Tc^mO_4$ in a plastic vessel (15 cm × 20 cm × 20 cm) placed between the detectors The number of counts per minute (between 50 000 and 100 000) was recorded for 3 min before and after each examination

(4) The patient was placed supine with the head slightly bent forward A plastic bar fitting the root of the nose and the supraorbital arches prohibited movements of the head, using the supraorbital arches and external auditory canals as reference points Twenty-four overlapping subregions of the skull, with square lateral projec-



Results

The $^{99}Tc^{m}O_4$ distribution in the skull was measured in a total of 48 positions, 24 on each side of the skull The value of each position was related to a central mean value, C_{mv}, and a plane mean value, P_{mv}, in order to obtain an idea of the relative distribution, allowing comparison between individuals The position ratios r_{Rp}, and r_{Lp}, obtained from the same region, were compared with each other by the evaluation parameter *D*, describing the side difference of the skull The sum and adjacent ratios (S, A) of each region, also comparable between individuals, were calculated, and altogether 208 parameters were obtained, dependent on each other to a varying extent Hence each region was analysed by 9 parameters The mean values and standard deviations (SD) of the reference group were calculated for each parameter, giving the interindividual variation (between individuals) The intra individual variation (within individuals) of each parameter was approximated from the values of the first and second measurement and expressed in SD, thus including variation caused by the method and variation caused by different time intervals between the $^{99}Tc^{m}O_4$ injection and measurement (Fig 3) Generally between 6 000 and 12 000 counts were recorded in each position

The results of measurement II were in agreement with the results of measurement I and therefore only the latter are presented in detail

Position ratio parameters (1) *Per cent* of the central mean value C_{mv} The calculated r_{Rc} and r_{Lc} values from measurement I of the reference group are displayed in Table 1 and Fig 3, where the obtained mean values and their inter-individual SD values are plotted, corresponding to a vertex projection of the skull, giving profile diagrams for each measuring plane

The inter individual SD of the r_c parameters varied between different positions and were higher in marginal positions, i e in plane A, D and the positions B1, B6, C1 and C6 than in centrally located positions (Fig 3, Table 1)

(2) *Per cent of the plane mean value* P_{mv} Position ratios, r_{Lp} and r_{Rp}, calculated from the results of measurement I of the reference group are presented in Table 2

(A, B, C or D, Fig 1) A relative conception of the distribution was thus obtained and the calculated ratios, (r) for each subregion were expressed by

$$r_{Rp} = \frac{N_R}{P_{mv}} \cdot 100\,\% \quad r_{Lp} = \frac{N_L}{P_{mv}} \cdot 100\,\% \qquad (1\text{a b})$$

which were position ratios with the plane mean value as reference, and

$$r_{Rc} = \frac{N_R}{C_{mv}} \cdot 100\,\% \quad r_{Lc} = \frac{N_L}{C_{mv}} \cdot 100\,\% \qquad (2\text{a b})$$

position ratios with the central mean value as the reference, as indicated by the index c in the position ratios The index p refers to the plane mean value and R and L to the right and left detector, respectively

The percentage position ratios and their combinations, difference D and sum S were used as evaluation parameters

$$D = (r_{Rp} - r_{Lp})\,\% \qquad (3)$$

$$S_p = \frac{r_{Rp} + r_{Lp}}{2}\,\% \text{ and } S_c = \frac{r_{Rc} + r_{Lc}}{2}\,\% \qquad (4\text{a,b})$$

Further, the difference between two adjacent values in the same measuring plane $(N(j) - N(j-1))$, related to the most occipital of the paired values $(N(j))$, was used as evaluation parameter (adjacent ratio, A_R and A_L) (Fig 1)

$$A_R = \frac{N_R(j) - N_R(j-1)}{N_R(j)}\ 100\,\%$$

$$A_L = \frac{N_L(j) - N_L(j-1)}{N_L(j)}\ 100\,\% \qquad (5\text{a b})$$

Material For ethical reasons nuclide was not administered to healthy volunteers Instead patients without history or signs of neurologic disease, but subjected to radiation therapy because of carcinoma of the uterus, bladder or vulva, were used as a reference group Hence the selection of cases was not randomized There were no history nor signs of brain lesions (an infrequent complication of these types of cancer, RUSSELL & RUBINSTEIN 1971) However, the incidence of brain lesions could be somewhat higher in a patient group selected in this way, as compared to a group of truly normal individuals It might thus be reasonable to presume that the normal ranges obtained in this group were wider than corresponding normal ranges of a true normal group (SCHIEFER 1972) Cytotoxic agents had not been administered About one third of the patients originally selected refused to participate Three patients were measured but later excluded 2 women aged 72 and 46 years with previous mammary carcinoma and ovarian carcinoma, respectively, and one male with prostatic carcinoma The second measurement was excluded in another three cases in 2 of these due to failure of tape punch, the third patient refused to participate It was for practical reasons not possible to make a careful neurologic examination of the patients in the reference group, which finally comprised 29 individuals (Fig 2)

Table 1

Mean values inter individual and intra individual SD values of r_c from measurement I

Position	r_{Rc}			r_{Lc}		
	Mean	Inter individual SD	Intra individual SD	Mean	Inter individual SD	Intra individual SD
A1	102 0	9 4	3 9	103 8	9 5	3 3
A2	122 4	10 4	4 3	124 8	10 7	4 6
A3	130 1	8 4	4 8	133 8	9 2	4 3
A4	140 4	11 7	4 6	143 0	11 8	3 8
A5	154 1	14 2	4 1	155 5	14 9	3 1
A6	154 5	15 5	6 2	153 2	16 2	6 4
B1	93 1	4 4	2 2	93 0	4 2	1 9
B2	89 9	2 8	1 6	91 8	3 3	1 4
B3	94 7	3 9	1 9	96 7	3 2	1 6
B4	101 6	3 9	2 4	103 0	3 7	1 7
B5	121 8	6 9	3 1	123 1	7 3	3 0
B6	136 3	10 6	4 5	133 2	10 9	3 7
C1	103 0	6 7	2 2	102 0	5 9	2 1
C2	93 2	4 5	2 2	92 8	4 7	1 7
C3	89 8	3 4	1 6	90 2	3 4	1 6
C4	94 4	3 0	1 8	95 1	3 4	1 9
C5	110 9	4 8	1 8	111 1	4 4	2 0
C6	118 4	9 2	3 6	115 6	9 1	3 2
D1	110 1	9 4	4 1	109 1	9 2	4 0
D2	113 0	9 2	4 1	111 5	9 4	3 8
D3	115 1	9 2	4 3	113 1	10 0	4 6
D4	119 8	9 3	4 1	118 2	9 2	3 4
D5	122 7	8 8	3 6	120 3	7 9	3 3
D6	113 5	10 2	7 0	110 8	9 2	6 7

The obtained inter individual SD values of the r_p varied between 2 7 and 8 4 per cent and were especially in plane A and D less than the corresponding SD values of the r_c parameters, 2 8 to 16 2 per cent (Tables 1, 2) The lower standard deviations were to a certain extent but not completely, explained by the difference in magnitude between C_{mv} and the different P_{mv}

Difference parameter The calculated mean values, inter individual and intra-individual standard deviations of parameter D, calculated from the results of measurement I of the reference group are tabulated in Table 4 The calculated mean value of D varied between −2 7 and +2 9 per cent in all subregions (Fig 3)

The inter individual SD values of D were always of the same order as or less (SD = 2 0 % to 4 8 %) than the standard deviations of the corresponding r_c and r_p

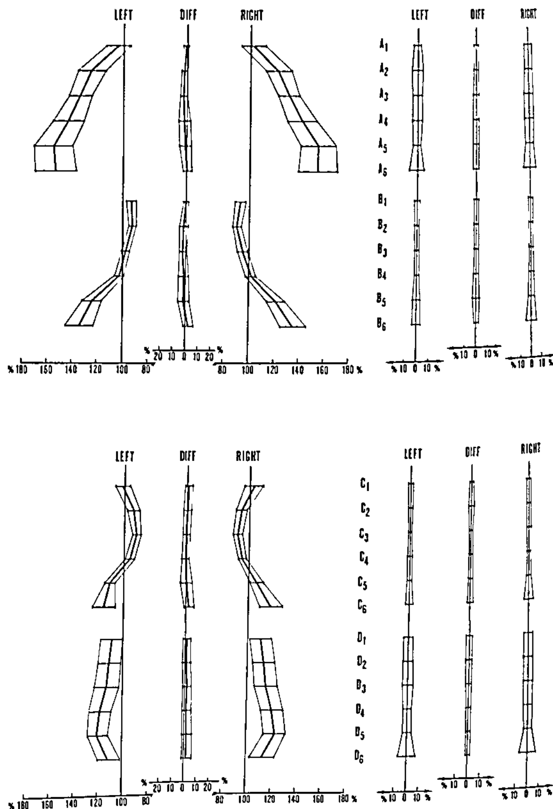


Fig 3 Mean values ± SD of r_0 and D of measurement I are calculated for each position and indicated to the left, corresponding intra individual SD values are indicated to the right

Table 1

Mean values inter individual and intra individual SD values of r_c from measurement I

Position	r_{Rc}			r_{Lc}		
	Mean	Inter individual SD	Intra individual SD	Mean	Inter-individual SD	Intra individual SD
A1	102.0	9.4	3.9	103.8	9.5	3.3
A2	122.4	10.4	4.3	124.8	10.7	4.6
A3	130.1	8.4	4.8	133.8	9.2	4.3
A4	140.4	11.7	4.6	143.0	11.8	3.8
A5	154.1	14.2	4.1	155.5	14.9	3.1
A6	154.5	15.5	6.2	153.2	16.2	6.4
B1	93.1	4.4	2.2	93.0	4.2	1.9
B2	89.9	2.8	1.6	91.8	3.3	1.4
B3	94.7	3.9	1.9	96.7	3.2	1.6
B4	101.6	3.9	2.4	103.0	3.7	1.7
B5	121.8	6.9	3.1	123.1	7.3	3.0
B6	136.3	10.6	4.5	133.2	10.9	3.7
C1	103.0	6.7	2.2	102.0	5.9	2.1
C2	93.2	4.5	2.2	92.8	4.7	1.7
C3	89.8	3.4	1.6	90.2	3.4	1.6
C4	94.4	3.0	1.8	95.1	3.4	1.9
C5	110.9	4.8	1.8	111.1	4.4	2.0
C6	118.4	9.2	3.6	115.6	9.1	3.2
D1	110.1	9.4	4.1	109.1	9.2	4.0
D2	113.0	9.2	4.1	111.5	9.4	3.8
D3	115.1	9.2	4.3	113.1	10.0	4.6
D4	119.8	9.3	4.1	118.2	9.2	3.4
D5	122.7	8.8	5.6	120.3	7.9	3.3
D6	113.5	10.2	7.0	110.8	9.2	6.7

The obtained inter-individual SD values of the r_p varied between 2.7 and 8.4 per cent and were especially in plane A and D less than the corresponding SD values of the r_c parameters, 2.8 to 16.2 per cent (Tables 1, 2) The lower standard deviations were to a certain extent, but not completely, explained by the difference in magnitude between C_{mv} and the different P_{mv}

Difference parameter The calculated mean values, inter individual and intra-individual standard deviations of parameter D, calculated from the results of measurement I of the reference group, are tabulated in Table 4 The calculated mean value of D varied between −2.7 and +2.9 per cent in all subregions (Fig 3)

The inter individual SD values of D were always of the same order as or less (SD = 2.0% to 4.8%) than the standard deviations of the corresponding r_c and r_p

Table 2

Mean values, inter-individual and intra-individual SD values of r_p from measurement I

Position	r_{Rp}			r_{Lp}		
	Mean	Inter individual SD	Intra-individual SD	Mean	Inter individual SD	Intra individual SD
A1	75 8	6 3	2 0	77 1	5 9	1 5
A2	90 8	5 3	1 7	92 6	5 0	2.1
A3	96 6	3 1	2 1	99 3	3 0	1 9
A4	104 2	5 8	3 6	106 1	5 0	3 5
A5	114 2	5 7	2 6	115 3	5 9	2 4
A6	114 5	7 1	3 4	113 5	7 5	3 8
B1	87 5	4 6	2 1	87 4	4 5	1 5
B2	84 5	3 4	1 4	86 2	3 9	1 6
B3	88 9	3 8	1 6	90 9	2 9	1 3
B4	95 4	3 2	1 8	96 7	3 0	1 6
B5	114 3	5 0	2 7	115 5	5 4	2.8
B6	127 8	7 1	3 0	124 9	7 6	2 5
C1	101 6	5 3	1 6	100 6	4 4	1 6
C2	92 0	3 6	1 5	91 5	3 8	1 4
C3	88 6	3 4	1 2	89 0	3 3	1 3
C4	93 1	2 7	1 9	93 8	3 2	1 7
C5	109 4	4 0	2 2	109 6	3 4	2 1
C6	116 8	8 2	3 0	114 1	8 4	2 5
D1	95 9	5 5	2 8	95 0	4 8	2 6
D2	98 4	3 6	1 9	97 0	4 0	2 1
D3	100 2	3 4	2 7	98 5	4 9	3 0
D4	104 3	2 7	2 6	103 0	4 4	2 4
D5	107 0	3 9	1 7	104 9	3 1	1 5
D6	99 0	8 4	5 4	96 8	7 8	5 3

parameters (SD = 2 8 % to 16 2 %) This decrease was largest in the marginal positions of the skull base plane A and top plane D and in the marginal positions B1, B6, C1, and C6 (Fig 3, Tables 1, 2, 4)

Sum parameter The parameters S_c and S_p calculated from results of measurement I of the reference group, are tabulated in Table 5 The inter-individual SD of these sums were generally smaller than the corresponding SD values of r_c and r_p (Tables 1, 2, 5)

Adjacent ratio parameters The results of measurement I of the reference group, calculated according to eq 5 a, b are presented in Table 3 Each value obtained in this way gave information about the difference between two adjacent values The

Table 3

Mean values, inter-individual and intra individual SD values of A from measurement I

Position	A_R			A_L		
	Mean	Inter-individual SD	Intra-individual SD	Mean	Inter-individual SD	Intra-individual SD
A1	—	—	—	—	—	—
A2	+20 1	5 4	2 5	+20 4	5 2	2.7
A3	+ 6 6	6 1	2 2	+ 7 4	5 8	1 8
A4	+ 7 9	5 1	4 5	+ 6 9	4 9	4 9
A5	+ 9 8	6 1	3 0	+ 8 7	5 3	2.8
A6	+ 0 4	6 7	4 4	− 1 4	6 4	4 2
B1	—	—	—	—	—	—
B2	− 3 2	5 1	2 4	− 1.2	5 0	2.0
B3	+ 5 3	3 8	2 6	+ 5 5	3 9	2 7
B4	+ 7 4	3 7	2 7	+ 6 6	4 2	2.2
B5	+19 9	5 6	2.3	+19 5	5 6	2.9
B6	+12 0	7 7	4 3	+ 8 4	8 6	3 8
C1	—	—	—	—	—	—
C2	9 3	4 2	1 7	− 9 0	3 8	1 7
C3	3 6	3 3	1 7	− 2.7	3 3	1 9
C4	+ 5 2	3 2	2 4	+ 5 5	2 8	1 8
C5	+17 6	5 2	2 5	+16 9	4 8	2.5
C6	+ 6 8	7 6	4 1	+ 4 2	7 8	3 6
D1	—	—	—	—	—	—
D2	+ 2.8	5 4	1 8	+ 2 4	6 1	3 4
D3	− 1 9	2 8	1 9	+ 1.5	2.8	1 7
D4	+ 4 1	2 6	2 0	+ 4 7	3 1	2.5
D5	+ 2 6	4 3	2 8	+ 1 9	4 3	3.0
D6	7 4	6 7	4 9	− 7 7	6 9	4 7

inter-individual SD values were of about the same sizes as the standard deviations of the r_s parameters and consequently *less than SD* of the r_e parameters (Tables 1, 2, 3)

The intra individual standard deviations of all parameters were in all subregions less than the corresponding inter-individual standard deviations, and generally about 50 per cent less (exception *SD of D* in subregion A1) The

Discussion

The necessary limitations of the measuring time and the amount of nuclide administered, restricted the amount of information available The purpose of avoiding

Table 4

Mean values, inter-individual and intra individual SD values of D from measurement I

Position	D		
	Mean	Inter-individual SD	Intra-individual SD
A1	−1 3	2 0	2 2
A2	−1 8	2 2	1 6
A3	−2 7	3 0	2 4
A4	−1 9	4 8	2 4
A5	−1 0	4 6	2.5
A6	+1 0	3 5	2 2
B1	+0 1	2 0	1 6
B2	−1 7	3 8	1 7
B3	−1 9	3 2	1 6
B4	−1 3	3 9	2 6
B5	−1 2	4 6	3 1
B6	+2 9	4 3	2 2
C1	+1 0	3 3	1 6
C2	+0 5	3 0	1 9
C3	−0 4	3 3	1 7
C4	−0 7	3 2	1 4
C5	−0 1	4 6	2 0
C6	+2 7	4 3	2 3
D1	+0 9	3 6	2 5
D2	+1 4	3 5	2 2
D3	+1 8	3 5	2 3
D4	+1 3	4 0	2 1
D5	+2 1	4 0	1 8
D6	+2 3	4 1	2 1

both complicated equipment and subjective evaluation of results made the use of gamma cameras or brain scanners impossible Counting statistic errors and variation of counting efficiency and positioning of measuring areas, as well as the error caused by a varying body-background were difficult to restrict They tend to decrease the significance of a pathologic deviation outside the biologic normal range of the nuclide distribution in the skull

Statistical analysis of brain scans and gamma camera images includes an error caused by difficulties in getting reproduceable measuring areas in relation to the skull, and the performance demands complicated computation (POPHAM et coll

1970) Besides, the gamma camera has an inhomogeneous sensitivity over the viewing field at best of about ± 10 per cent that can be compensated for only by computer correction to obtain reliable results (MALLARD 1972, SPECTOR et coll 1972, BROOKEMAN 1973)

The results obtained by the gammaencephalographic technique of PLANIOL includes an error caused by varying body background in the measurement perpendicular to the surface of the skull Variation in positioning as well as in direction of the detector was involved and therefore a reproduceable measuring procedure was difficult to obtain Side differences were also difficult to reproduce because only one detector was used In each position only about 300 to 500 counts were registered which have a considerable counting statistic error of about 6 to 8 per cent of the position value in difference parameters, which should be compared to the values in Tables 1 to 5 (PLANIOL 1959, 1966)

MUNDINGER did not relate the measuring position to the size of the head and side differences were not calculated from simultaneous measurements by two symmetrically located detectors of each subregion The total skull was not completely covered and the different sources of variation and the physical characteristics of the method were not discussed in detail (MUNDINGER & ASAI)

Generally adopted principles for premedication with 0 4 g postassium perchlorate were applied before the brain scanning with 10 mCi $^{99}Tc^{m}O_4$ was performed (HARPER et coll 1964, 1972, MCAFFEE et coll 1964, WITCOFSKI et coll 1967, SILBERSTEIN & LEVY 1970) This amount of pertechnetate is reported to give a whole body dose of about 0 1 rad and after premedication with 0 4 g $KClO_4$ a critical organ dose of about 1 rad (colon, kidney, salivary glands) (SMITH, Swedish National Institute of Radiation Protection)

Several sources of variation (1—counting statistics, 2—electronic device, 3—positioning of detectors 4—movements of the head, 5—change of $^{99}Tc^{m}O_4$ distribution with time, 6—individual size and shape of the head, 7—individual distribution of $^{99}Tc^{m}O_4$ in the skull) will be considered in detail The intra-individual variations calculated from results obtained in measurements I and II were composed of variations according to points 1 to 5, but the inter individual variation included all sources of variation (points 1 to 7) To exemplify the relative importance of these different sources of variation, the calculated SD values of the reference group are given in Table 6 for positions A3, A6, B3 and B6 B3 was a central position and the other marginal ones

Clinical measurement procedure

Counting statistics The error caused by estimation of the balance factor could be neglected, because about 150 000 to 300 000 counts were registered in each detector The large collimator apertures permitted registration of about 6 000 to 12 000 counts in each stationary position, within a total measuring time of 30 min The loss of precision by counting statistics in side differences was unimportant compared to

Table 5

Mean values, inter individual and intra individual SD values of S_c and S_p from measurement I

Position	S_c			S_p		
	Mean	Inter-individual SD	Intra individual SD	Mean	Inter individual SD	Intra individual SD
A1	102 9	9 4	3 3	76 4	6 0	1 4
A2	123 6	10 5	4 3	91 7	5 0	1 8
A3	131 9	8 6	4 3	97 9	2 6	1 6
A4	141 7	11 3	3 9	105 2	4 9	3 3
A5	154 8	14 2	3 2	114 7	5 3	2 2
A6	153 9	15 6	6 1	114 0	7 1	3 4
B1	93 1	4 2	1 8	87 4	4 4	1 6
B2	90 9	2 3	1 2	85 4	3 1	1 2
B3	95 7	3 2	1 5	89 9	3 0	1 2
B4	102 3	3 1	1 6	96 1	2 4	1 1
B5	122 4	6 7	2 6	114 9	4 7	2 3
B6	134 7	10 5	3 9	126 3	7 0	2 5
C1	102 5	6 1	2 0	101 1	4 6	1 4
C2	93 0	4 4	1 7	91 7	3 4	1 1
C3	90 0	3 0	1 4	88 8	2 9	0 9
C4	94 7	2 8	1 7	93 5	2 5	1 6
C5	111 0	4 0	1 6	109 5	2 9	1 9
C6	117 0	8 9	3 2	115 4	8 1	2 5
D1	109 6	9 1	3 8	95 5	4 8	2 4
D2	112 2	9 1	3 7	97 7	3 4	1 7
D3	114 1	9 4	4 2	99 3	3 8	2 6
D4	119 0	8 9	3 6	103 7	3 1	2 3
D5	121 5	8 1	3 3	105 9	2 9	1 3
D6	112 2	9 4	6 8	97 9	7 9	5 2

the decrease in total standard deviation (Table 6) However, the diminished relative counting statistic error in sums might be of importance in central positions A3 and B3 (Table 6) It may be concluded that the error of counting statistics should not exceed about 2 per cent and that a deviation of less than 1 per cent was not relevant for most parameters compared to other sources of variation (Table 6) *Regarding* side differences this corresponded to between 5 000 and 20 000 registered counts in each position PLANIOL (1966) and POPHAM et coll (1970) have used only 300 to 1 000 recorded counts in each measuring area, thus accepting an error of counting statistics of about 8 to 4 5 per cent in side difference parameters which is *high enough* to influence the total variation of a normal group (PLANIOL 1966, POPHAM et coll) The large number of counts in each position was thus essential to get the low total normal variation (BENDER & BLAU 1964)

Table 6

Four different types of estimated SD-values are compared in this table for 16 different parameters of four positions

Parameter	Error caused by the electronic device SD %	Error caused by counting statistics SD %	Intra-individual variation SD %	Inter individual variation SD %
r_{Rc} (A3)	Negligible	1.0	4.8	8.4
r_{Rp} (A3)	Negligible	1.0	2.1	3.1
D (A3)	Negligible	1.4	2.4	3.0
S_p (A3)	Negligible	0.7	1.6	2.6
r_{Rc} (A6)	Negligible	1.0	6.2	15.5
r_{Rp} (A6)	Negligible	1.0	3.4	7.1
D (A6)	Negligible	1.4	2.2	3.5
S_p (A6)	Negligible	0.7	3.4	7.1
r_{Rc} (B3)	Negligible	1.0	1.9	3.9
r_{Rp} (B3)	Negligible	1.4	1.6	3.2
D (B3)	Negligible	1.4	1.6	3.2
S_p (B3)	Negligible	0.7	1.2	3.0
r_{Rc} (B6)	Negligible	1.0	4.5	10.6
r_{Rp} (B6)	Negligible	1.0	3.0	7.1
D (B6)	Negligible	1.4	2.2	4.3
S_p (B6)	Negligible	0.7	2.5	7.0

Equipment The mechanical construction offered stable positions of the movement and the error caused by instability of counting efficiency was negligible compared to the total standard deviation of results obtained (LARSSON et coll) The use of a correction factor for imbalance between the detectors was important in order to compensate for errors in the evaluation parameters caused by variation in the counting efficiencies of the detectors from day to day (Table 6)

Positioning of detectors The variation caused by positioning was restricted by several means The collimators being unfocused with large apertures made a small variation in positioning less important Influence of varying levels of body background including stomach, thorax, thyroid and skull base activity was avoided by pulse height discrimination and by always keeping the axis of the collimators orthogonal to the median plane of the skull (PLANIOL 1966)

Involuntary movements of the head during the measuring procedure constituted an important source of variation which could be expected to be particularly relevant in neurologically diseased patients It was thus mandatory to get a simple and convenient as well as effective fixation of the head A plastic bar fitting the root of the nose and the supraorbital arches, was found to be a satisfactory solution in the ref-

erence cases, as demonstrated by the small intra-individual variation compared to corresponding inter-individual variation (Tables 1 to 5)

Unavoidable positioning variation was most important in marginal positions near the borders of the skull area, i e positions A1 to A6, D1 to D6 and B1, B6, C1 and C6 This probably explained why the obtained SD values of these positions were considerably larger than the SD values of more central positions (Fig 3, Tables 1 to 5)

The use of the plane mean value, P_{mv}, instead of the central mean value, C_{mv}, as a reference, reduced the variation of the evaluation parameter caused by a varying distance between the measuring planes (A–C) and the skull base Only about one third of this obtained reduction of SD values was explained by the different bases for calculation of the ratios r_p and r_c (Tables 1, 2, 6) Hence, the much lower inter individual and intra-individual standard deviations of the r_p parameters in the skull base plane A, compared to the standard deviations of corresponding r_c values, demonstrated the advantage of using r_p as evaluation parameter (Tables 1, 2, 6) However, positions B3 and B6 were not close to the skull base and hence they did not have the corresponding reduction of SD between the r_c and r_p ratios (Table 6)

The penumbra zones of the collimators were narrow (LARSSON et coll) and therefore the precisely opposed detectors measured almost the same region from right and left, respectively Thus some biologic and positioning variation could be avoided in parameters based on side difference, taking advantage of the symmetry of the head which was demonstrated to be high with mean values of side differences obtained between 2 7 and +2 9 per cent The inter-individual standard deviations of difference parameters were smaller than the SD values of corresponding r_c and r_p parameters, especially in marginal positions of the skull area as skull base plane A, top plane D and the positions B1, B6, C1 and C6 (Fig 3) Again, this decrease of the percentage SD values of differences D was to a certain extent, but not completely, explained by the difference in magnitude between the reference values, P_{mv} and C_{mv} Side difference in positions A6 and B6 offered a considerable reduction of SD, probably because a variation in position in relation to the border of the skull area here involved a large change of count rate, not compensated for otherwise The effect was less important in centrally located measuring area, for instance position B3 (Tables 1, 2, 4, 6)

Side differences, measured simultaneously by carefully opposed detectors thus constituted measuring parameters with a comparatively small error caused by positioning, and they might therefore be important for the overall diagnostic accuracy of the method Side differences cannot easily be obtained from measurements with gamma cameras or any single detector system (MOORE 1948, MOORE et coll 1948, WENDE, PLANIOL 1966, MUNDINGER & ASAI, DOWSETT & PERRY 1970 MÜKE & SAEGER 1970)

Change of $^{99}Tc^{m}O_4$ distribution with time was included in the intra-individual variation and from the results obtained it was seen that this source of variation was of little importance between 30 and 150 min after the administration of activity Stu-

dent s t test was applied to the difference between the mean values of the r_c, D and S_c parameters of measurements I and II There were no significant ($p > 0\ 01$) changes of the mean values of D parameters between the first and second measurements Significant ($p < 0\ 01$) increases of the mean values of the r_c and S_c parameters were obtained only in position A4 and C4 (A4+3 5 %, and C4+1 5 %) Significant ($p < 0\ 01$) decreases of the mean values of r_c or S_c parameters were obtained only in position A2, A3, B6 and D5 (A2−3 0 %, A3−3 0 %, A6−6 0 %, B6−2 5 % and D5−2 0 %) However, 96 parameters were regarded together and therefore about one of them should be expected to have a t value outside the levels given by $p = 0\ 01$ (TAUXE & THORSEN 1969)

Individual size and shape of the head Differences in head size was an important source of variation and was limited by the use of individualized positioning diagrams and the use of plane mean values as the bases for reference and the differences as parameters (Tables 1, 2, 4) Variation in head size and shape was compensated for in the design of the measuring procedure and not only afterwards in the calculation of the obtained results, as in statistically analysed brain scans (DOWSETT & PERRY 1970 POPHAM et coll, DOWSETT 1972) In particular, the large inter individual variation of marginally located parameters compared to the smaller inter individual variation of centrally located ones, indicated that a varying head shape was an important source of variation (Tables 1, 2)

The low spatial resolution of the method did not permit conclusive comparison between anatomic structures and the distribution pattern and its variation Further improvements could probably be made by an even more carefully chosen measuring position related to the individual head size and shape and with the aid of roentgen monitoring However, this would defeat the purpose of simplicity (CHEVALIER & METHLIN 1964 PLANIOL 1966, MUNDINGER & ASAI)

Individual distribution of $^{99}Tc^mO_4$ in the skull constituted a fundamental source of variation that limited the theoretical possibilities of detecting a pathologic distribution of activity The importance of varying accumulation of $^{99}Tc^mO_4$ in the choroid plexus was diminished by premedication with potassium perchlorate (WITCOFSKI et coll 1967 [illegible]

[illegible] large collimator aperture gave a smoothing of the normal biologic variation of the $^{99}Tc^mO_4$ distribution in the skull The sizes of the aperture were chosen to correspond approximately to the projection of areas with increased amount of $^{99}Tc^mO_4$ caused by small brain tumours (BECK 1964, BROWNELL 1964, PLANIOL 1966, MUNDINGER & ASAI, ZEIDLER et coll 1970, BURROWS 1972)

Inter and intra individual variation From Tables 1 to 5 it is evident that the intra-individual SD was almost always about 50 per cent of corresponding inter-indi-

erence cases, as demonstrated by the small intra-individual variation compared to corresponding inter-individual variation (Tables 1 to 5)

Unavoidable positioning variation was most important in marginal positions near the borders of the skull area, i e positions A1 to A6, D1 to D6 and B1, B6 C1 and C6 This probably explained why the obtained SD values of these positions were considerably larger than the SD values of more central positions (Fig 3, Tables 1 to 5)

The use of the plane mean value, P_{mv}, instead of the central mean value, C_{mr} as a reference, reduced the variation of the evaluation parameter caused by a varying distance between the measuring planes (A–C) and the skull base Only about one third of this obtained reduction of SD values was explained by the different bases for calculation of the ratios r_p and r_c (Tables 1, 2, 6) Hence, the much lower inter individual and intra-individual standard deviations of the r_p parameters in the skull base plane A, compared to the standard deviations of corresponding r_c values, demonstrated *the advantage of using r_p as evaluation parameter* (Tables 1, 2, 6) However, positions B3 and B6 were not close to the skull base and hence they did not have the corresponding reduction of SD between the r_c and r_p ratios (Table 6)

The penumbra zones of the collimators were narrow (LARSSON et coll) and therefore the precisely opposed detectors measured almost the same region from right and left, respectively Thus some biologic and positioning variation could be avoided in parameters based on side difference, taking advantage of the symmetry of the head which was demonstrated to be high with mean values of side differences obtained between 2 7 and +2 9 per cent The inter-individual standard deviations of difference parameters were smaller than the SD values of corresponding r_c and r_p parameters, especially in marginal positions of the skull area as skull base plane A, top plane D and the positions B1, B6, C1 and C6 (Fig 3) Again, this decrease of the percentage SD values of differences D was to a certain extent, but not completely, explained by the difference in magnitude between the reference values, P_{mv} and C_{mr} Side difference in positions A6 and B6 offered a considerable reduction of SD, probably because a variation in position in relation to the border of the skull area here involved a large change of count rate, not compensated for otherwise The effect was less important in centrally located measuring area, for instance position B3 (Tables 1, 2, 4, 6)

Side differences, measured simultaneously by carefully opposed detectors thus constituted measuring parameters with a comparatively small error caused by positioning, and they might therefore be important for the overall diagnostic accuracy of the method Side differences cannot easily be obtained from measurements with gamma cameras or any single detector system (MOORE 1948, MOORE et coll 1948, WENDE, PLANIOL 1966, MUNDINGER & ASAI, DOWSETT & PERRY 1970, MÜKE & SAEGER 1970)

Change of $^{99}Tc^mO_4$ distribution with time was included in the intra-individual variation and from the results obtained it was seen that this source of variation was of little importance between 30 and 150 min after the administration of activity Stu-

en Positionen erhalten worden waren, untersucht Durchschnittswerte und zugehorige inter- und intra individuelle Standard-Abweichungen werden gegeben Unterschiedliche Ursachen fur die Abweichung werden im Verhältnis zu den erhaltenen Ergebnissen diskutiert Es war das Ziel, die $^{99}Tc^{m}O_4$ Verteilung im Schadel objektiv als normal oder nicht normal zu klassifizieren

RESUME

Presentation d'une technique d examen standardisé basée sur une methode de detecteur de symetrie decrite prealablement Les auteurs presentent les resultats obtenus à partir d un groupe temoin de malades sans troubles neurologiques connus La distribution du $^{99}Tc^{m}O_4$ dans le crâne a éte etudiee par 208 paramètres d'evaluation obtenus a partir des mesures de 24 sous régions due crâne a partir de 48 positions symétriques Les auteurs indiquent les valeurs moyennes et les déviations standard interindividuelle et intraindividuelle Ils examinent differentes sources de variation en rapport avec les resultats obtenus Le but etait de permettre de classer objectivement comme normale ou comme anormale la distribution dans le crâne du $^{99}Tc^{m}O_4$

REFERENCES

BECK R N A theory of radioisotope scanning systems *In* Medical radioisotope scanning Proc IAEA Symp Athens, 1964 Vol I, p 35, Vienna 1964

BENDER M A and BLAU M Collimator evaluation with the IAEA scanning phantom *In* Medical radioisotope scanning Proc IAEA Symp Athens, 1964 Vol I, p 175, Vienna 1964

BROOKEMAN V A Analysis and correction of spatial dissortions produced by the gamma camera J nucl Med 14 (1973) 125

BROWNELL G L Theory of radioisotope scanning *In* Medical radioisotope scanning *Proc IAEA Symp Athens*, 1964 Vol I, p 3, Vienna 1964

BURROWS E H The clinical utility of brain scanning in nuclear medicine *In* Progress in nuclear medicine Vol I, p 287 Edited by E J Potchen and V R McCready S Karger, Basel 1972

CHARLESTON D B, *BECK* R N, EIDELBERG P and SCHUH M W Techniques which aid in quantitative interpretation of scan data *In Medical* radioisotope scanning Proc IAEA Symp Athens, 1964 Vol I, p 509, Vienna 1964

CHEVALIER A *et METHLIN G* Considérations sur l utilisation d'une technique de gamma-encéphalographie a deux compteurs opposes Ann Radiol 7 (1964), 797

CONRAD B and *HORST W* Present state and possibilities of future development of radioisotope scanning with particular reference to the diagnosis of brain tumors Progr neurol Surg 1 (1966) 150

DOWSETT D J A quantitative analytical display programme (QUAD) designed for radioisotope brain scans Comput Biol Med *2 (1972), 27*

— and PERRY B J A comparative statistical *analysis of* brain scans using a digital computer Brit J Radiol 43 (1970), 617

HARPER A G, FRIEDMAN *B I*, AVIS K *E* and WENNEMARK J Perchlorate blocking of $^{99m}TcO_4$-uptake by simultaneous intravenous injection in dogs J nucl Med 13 (1972), 363

HARPER P V., *LATHROP U A*, MCCARDLE R J and ANDROS G The use of technetium-99m as a clinical scanning agent for thyroid, *liver* and brain *In* Medical radioisotope scanning Proc. IAEA Symp Athens, 1964 Vol II, p 33, Vienna 1964

vidual SD values or less It could thus be concluded that the methodologic error was small enough compared to the total variation, and further limitation of methodologic sources of variation was unnecessary, with the important exception of the shape and size of the head On the other hand the decrease of the total normal standard deviation obtained by the use of precision equipment, large number of registered counts, individualized positioning diagrams, plane mean values as reference as well as the difference parameters was of great importance

Adjacent ratio A pathologic increase of activity in one position might be within the normal range of the r, D or S parameters but the difference between two adjacent positions might be significantly abnormal if the boundary between them approximately corresponds to the boundary between a pathologic and a normal area Therefore all values were related to an adjacent value as previously described, thus offering a further type of parameter The inter-individual SD of these parameters varied between 2 6 and 7 7 per cent and the intra-individual variation was considerably smaller (Table 3) Their influence upon the diagnostic accuracy of the method is impossible to evaluate as yet

Clinical utility The examination was convenient for the patient, lasted 30 min and was easily carried out by a technician Results from patients can be correlated to the normal range presented and can automatically be evaluated statistically, thus avoiding subjective evaluation (LIND & LARSSON) The method might thus be valuable in clinical routine work even outside large medical centres, where fewer specialists are available The diagnostic accuracy in a patient material will be the subject of a forthcoming publication (LIND)

SUMMARY

A standardized clinical examination procedure of a previously described symmetry detector method for gammaencephalography is presented and the results obtained from a reference group of subjects without known neurologic disorders are reported The $^{99}Tc^{m}O_4$ distribution in the skull was investigated by 208 evaluation parameters obtained from measurements of 24 subregions of the skull from 48 symmetrical positions Mean values and associated inter-individual and intra-individual standard deviations are given Different sources of variation are discussed in relation to the results obtained The method enables the $^{99}Tc^{m}O_4$ distribution in the skull to be objectively classified as normal or abnormal

ZUSAMMENFASSUNG

Ein standardisiertes klinisches Untersuchungsverfahren einer zuvor beschriebenen symmetrischen Detektor-Methode zur Gammaencephalographie wird vorgestellt und über die an einer Referenzgruppe von Personen ohne bekannte neurologische Veränderungen erhaltenen Ergebnisse berichtet Die $^{99}Tc^{m}O_4$ Verteilung im Schädel wurde durch 208 bestimmte Parameter, die von Messungen von 24 Subregionen des Schädels von 48 symmetrisch

SPECTOR S S, BROOKEMAN V A, KYLSTRA C D and DIAZ N J Analysis and correction of spatial distortions produced by the gamma camera J nucl Med 13 (1972) 307

TAUXE W N and THORSEN H C Cerebrovascular permeability studies in cerebral neoplasms and vascular lesions optimal dose to-scan interval for pertechnetate brain scanning J nucl Med 10 (1969) 34

WEBBER M M Technetium 99m normal brain scans and their anatomic features Amer J Roentgenol 94 (1965) 815

WENDE S Technik und Wert der Gamma Enzephalographie Fortschr Rontgenstr 98 (1963) 466

VAN DER WERFF J TH, PRICK, J J, WALDER H A D and TAN WEN HIAN Gammaencephalografie (In Dutch) Ned T Geneesk 108 (1964) 646

WITCOFSKI R L., JANEWAY R, MAYNARD C D, BEARDEN E K and SCHULTZ J L Visualization of the choroid plexus on the technetium 99m brain scan Arch Neurol 16 (1967), 286

YOUNG R L and ROCKETT J F The brain scan as a routine screening procedure Sth med J 65 (1972), 65

ZEIDLER U SUMMER K, BRUNNGRABER C V, KOTTKE S und HUNDESHAGEN H Untersuchungen zur pathophysiologischen Grundlage der Hirnszintigraphie mit ^{99m}Tc-Pertechnetat Arch Psychiat Nervenkr 213 (1970) 200

LARSSON S and LIND M Symmetry detector method for gammaencephalography Objective diagnosis of abnormal $^{99}TcO_4$ distribution in the skull To be published in Acta radiol Ther Phys Biol

— — and SÖDERBORG B A symmetry detector method for gammaencephalography Physical characteristics of the method Acta radiol Ther Phys Biol 14 (1975) 63

LIND M Symmetry detector method for gammaencephalography of brain tumours To be published in Acta radiol Diagnosis

MALLARD J R Medical radioisotope visualization (A review of 'scanning') Int J appl Radiat 17 (1966), 205

— The radionuclide imaging process and factors influencing the choice of an instrument for brain scanning *In* Progress in nuclear medicine Vol I, p 1 Edited by E J Potchen and V R McCready S Karger, Basel 1972

MCAFFEE J G, FUEGER C F, STERN H S, WAGNER H N JR and MIGITA T Tc^{99m} Pertechnetate for brainscanning J nucl Med 5 (1964), 811

MOORE G E Use of radioactive diiodofluorescein in the diagnosis and localization of brain tumors Science 107 (1948) 569

— PEYTON W T, HUNTER S W and FRENCH L The clinical use of sodium fluorescein and radioactive diiodofluorescein in the localization of tumors of the central nervous system Minn Med 31 (1948) 1073

MUNDINGER F und ASAI A Ergebnisse der digitalen Gammaencephalographie bei Hirntumoren Vergleich von $Wismut^{206}$, $Quecksilber^{203}$-Neohydrin und $Technetium^{99m}$ Arch Psych Z ges Neurol 210 (1967), 297

— und OSTERTAG CH Radio Isotope in der neurologisch neurochirurgischen Diagnostik Hippokrates 42 (1971), 135

MÜKE R und SAEGER W *Zur Radioisotopendiagnose von langsam wachsenden Gliomen* Zbl Neurochir 31 (1970) 51

National Institute of Radiation Protection, Stockholm, Sweden Stråldoser från radioaktiva ämnen i medicinskt bruk (In Swedish) 1969

PAOLETTI P, VIALLANI R, FRIGENI G and MASSAROTTI M Four years of experience in *scanning brain lesions Minerva neurochir 13 (1969) 212*

PENNING L and FRONT D Technetium scinti anatomy of the head Neuroradiology 1 (1970), 210

PEYTON W T, MOORE G E, FRENCH L A and CHOU S N Localization of intracranial *lesions by radioactive isotopes J Neurosurg 9 (1952) 432*

PLANIOL T Diagnostic des lésions intra-craniennes par les radio isotopes (gammaencéphalographie) Masson et Cie Paris 1959

— Gamma encephalography after ten years of utilization in neurosurgery Progr neurol Surg *1 (1966), 93*

POPHAM M G, BULL J W D and EMERY E W Interpretation of brain scans by computer analysis Brit J Radiol 43 (1970) 835

RUSSELL D S and RUBINSTEIN L J Pathology of tumours of the nervous system 3rd edition Edward Arnold, London 1971

SCHIEFER W Fruhdiagnose raumfordernder Prozesse im Schädelinneren Dtsch med Wschr 23 (1972), 551

SCHNEIDER D und PRÉVÔT H JR Das normale Hirnszintigramm mit ^{203}Hg Chlormerodrin und *^{99m}Tc Pertechnat Fortschr Rontgenstr 105 (1966), 98*

SILBERSTEIN A B and LEVY L M ^{99m}Tc localization in the choroid plexus Radiology 95 (1970), 529

SMITH E M Internal dose calculation *for ^{99m}Tc J nucl Med 6 (1965) 231*

SPECTOR S S, BROOKEMAN V A, KYLSTRA C D and DIAZ N J Analysis and correction of spatial distortions produced by the gamma camera J nucl Med 13 (1972), 307

TAUXE W N and THORSEN H C Cerebrovascular permeability studies in cerebral neoplasms and vascular lesions optimal dose to-scan interval for pertechnetate brain scanning J nucl Med 10 (1969), 34

WEBBER M M Technetium 99m normal brain scans and their anatomic features Amer J Roentgenol 94 (1965) 815

WENDE S Technik und Wert der Gamma Enzephalographie Fortschr Rontgenstr 98 (1963) 466

VAN DER WERFF J TH, PRICK, J J, WALDER H A D and TAN WEN HIAN Gammaencephalografie (In Dutch) Ned T Geneesk 108 (1964), 646

WITCOFSKI R L, JANEWAY R, MAYNARD C D, BEARDEN E K and SCHULTZ J L Visualization of the choroid plexus on the technetium 99m brain scan Arch Neurol 16 (1967), 286

YOUNG R L and ROCKETT J F The brain scan as a routine screening procedure Sth med J 65 (1972), 65

ZEIDLER U, SUMMER K, BRUNNGRABER C V, KOTTKE S und HUNDESHAGEN H Untersuchungen zur pathophysiologischen Grundlage der Hirnszintigraphie mit ^{99m}Tc-Pertechnetat Arch Psychiat Nervenkr 213 (1970), 200

FROM THE INSTITUTE OF CANCER RESEARCH, RADIUMSTATIONEN, DK-8000 AARHUS, DENMARK

HISTOLOGIC AND HISTOCHEMICAL REACTIONS IN A MOUSE MAMMARY CARCINOMA FOLLOWING EXPOSURE TO COMBINED HEAT-ROENTGEN IRRADIATION

K. OVERGAARD and J. OVERGAARD

Heating of experimental tumours in situ might in many cases effect an elective and total destruction of all the tumour cells. The necessary values of temperature and time of application (curative heat dose = cHD) in the temperature range of 41 to 42.5°C were determined revealing a regular mutual relation (OVERGAARD & OVERGAARD 1972 a). The compilation of all the mutually combined temperature and time values formed a contingent regular line in a logarithmic system. It was designed "standard heat dose" (StHD) and could be used as working unit for the heat effect independent of the actual temperature range.

Similar experimental tumours were exposed successively to a local heat dose in the size of 1-1/8 StHD in the temperature range of 40.5 to 42.5°C and to local roentgen irradiation, 400 to 1 600 R (OVERGAARD & OVERGAARD 1974). Though most of the used partial doses separately were without any curative effect, cures were obtained in a reproducible number of cases depending on the size of doses of both of the components. The sequence of the components and the interposition of an interval of 24 hours between the applications did not influence the results.

The existence of a synergistic curative effect between heat and roentgen irradiation on tumour tissue was supposed. As this synergism has not been seriously considered,

Submitted for publication 17 June 1974

no information on the microscopic appearances of tumours treated that way is available and no suggestions as to the nature of this reaction have been advanced Therefore a series of histologic and histochemical examinations was performed concurrently with the afore mentioned curative experiments

Method

More than 600 C_3H mice inoculated with a highly malignant anaplastic mammary carcinoma (HB) were exposed to successive heat and roentgen irradiation (cHR) covering all combinations of doses and variations of sequence and intervals put in use in the curative experiments Moreover, many intermediate dose combinations and a number of higher and lower doses were used Animals were killed at short intervals for microscopy following a part of the treatment or at its end to obtain a conception of the development of the tissue reaction from the end of treatment to the final scar formation Microscopy of the site of tumour and adjacent tissues was performed in all cured cases

The animals were killed by suboccipital luxation, the tumour and its surroundings were excised and fixed in Helly's fluid embedded in paraffin, routinely stained in Heidenhain s iron haematoxylin, Mayers' haematoxylin-eosin and Harris haematoxylin sirius dye for connective tissue Histochemical examinations of the acid phosphatase activity were performed on quickly frozen, unfixed tumour tissue Seven μ cryostate sections were incubated at 37°C for 30 min in Gomori s medium for acid phosphatase and treated by the method of BARKA & ANDERSON (1963)

The technique employed permits of a reliable estimation only of the oecologic reactions in the tissues, only the main features of the internal reaction in the individual cell can be assessed, however

Basic Investigations

Mostly, the untreated tumour forms a central bulk of densely packed, uniformly resting tumour cells (B cells) displaying a small number of mitoses The cells are large and bright with indistinct cell membranes The nuclei are large and vacuolated with a sparse granular and partly reticular chromatin structure and mostly include one large nucleolus (Fig 1) The stroma and the vascularity are sparse Commonly, spots of spontaneous necrosis are present, even in small tumours

Surrounding this bulk a narrow rim of active A cells appears, placed singly or in small clusters inside or outside some streaks of loose connective tissue encircling the tumour Moderate irregular outgrowths of tumour cells may invade adjacent tissue The mitotic activity in this area is higher

Microscopically, tumours treated with a curative heat dose revealed intense shrinkage of the cytoplasm and nuclei in all tumour cells within a few hours (OVERGAARD & OVERGAARD 1972 a) These alterations progressed by pyknosis and karyolysis, and all the cells disintegrated completely within a few days No mitotic activity occurred



Fig 1



Fig 2

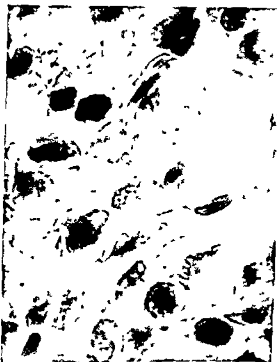
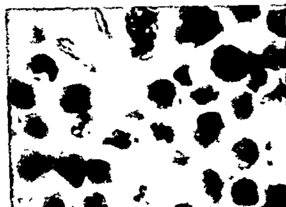


Fig 3

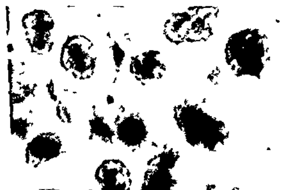


Fig 4

(For legends see opposite page.)



a



b

Fig. 5 Rapid shift of cellular appearance by roentgen irradiation to preheat treated tumour tissue a) Central tissue 24 h after heat treatment 42 5°C/30 min (1 600×) Tumour cells isolated Nucleus moderately shrunken, chromatin condensed in large clumps b) 1 h after cHR treatment 42 5°C/30 min, 24 h 800 R (1 600×) Nuclei somewhat larger Nuclear membrane clearly marked Chromatin splitting up in minor granules

The non-malignant stromal cells remained uninjured and grew rapidly, isolating the disintegrating tumour cells and forming a scar tissue

After exposure to smaller heat doses, some tumour cells may be destroyed completely, but many displayed disturbances of various types The number of injured

Fig 1 Untreated tumour Densely packed large cells, poorly demarcated Nucleus large, bright with scattered chromatin spots and more intensely stained central nucleolus, abundant mitoses in the more peripheral regions few mitoses in the more central parts 525×

F[illegible] 2 Ce[illegible]

Fig. 3 Central tumour tissue 4 h after the same treatment as in Fig 2 (1 350×) Tumour cells isolated, sparse cytoplasm Nucleus with irregular granular concretions, some more diffusely condensed Stroma cells shrunken with condensed nuclei some demarcation of fibrils

Fig 4 Central tissue 6 days after cHR treatment 42.5 C/30 min 1 600 R [illegible]
tumour tissue Cell stru[illegible]
placed in the central regi[illegible]
necrosis scattered remn[illegible]

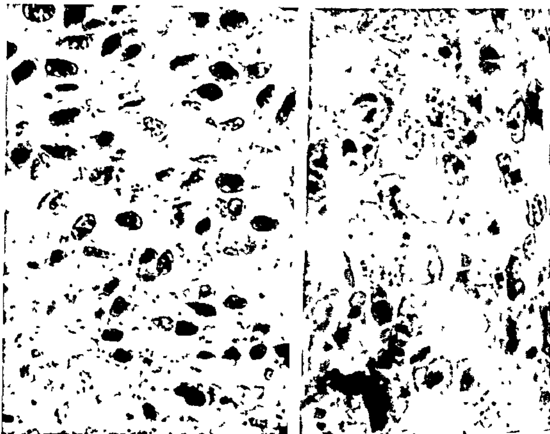


Fig 6 Tumour tissue in the border zone 4 h after cHR treatment 800 R 41 5°C/30 min (620 ×) Tumour cells loosely placed in connective tissue Different forms of chromatin alterations, cells with 'large dark nuclei', some cells with one single chromatin clot, other cells with a few medium-sized clumps and clear karrhyoplasm

[illegible] HR treatment [illegible] our [illegible] rge [illegible] of different size, some cells with [illegible] ytic decay Connective tissue unhurt (adjoining central tissue downward left)

cells and the prominent types of injuries depended on the size of the heat dose Following relatively low heat doses, a number of mitotic irregularities—especially arrested metaphases—were visible Some tumour cells apparently remained uninjured, and pluricentric newgrowth of tumour always occurred within a few days (OVERGAARD & OVERGAARD 1972 a)

Microscopically, following roentgen irradiation with doses within the experimental range, tumour cells mostly displayed cellular enlargement with a large, somewhat 'empty' nucleus, the chromatin being usually condensed in one or a few lumps The nucleolus was large Within one or a few days a number of irregular mitoses were present. Later, many cells disintegrated—some of them with great cytoplasmic growth, but invariably some cells remained uninjured, and new tumour growth could occur.

Usually, rapid growth of the connective tissue was encountered

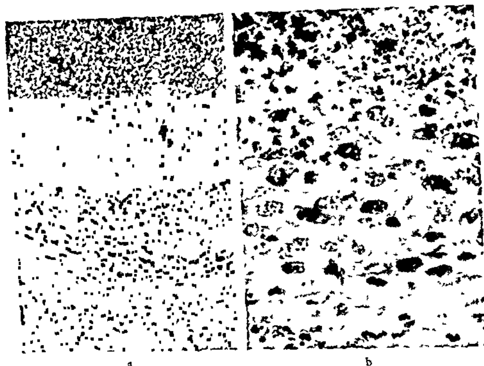


Fig 8 a) 4 days after cHR treatment 42 5 C/30 min 800 R (87 ×) Marginal part of tumour Mass of highly decaying central tumour tissue, sharply delineated by a narrow border zone containing necrobiotic tumour cells in different stages of decay, placed in the loose ring like streaks of connective tissue b) Detail of (a) (570 ×)

Special Findings

Just after the end of combined heat-roentgen (cHR) treatment, moderate hyperaemia might occasionally but not constantly be present Almost at the same time, initial signs of a very special reaction could also be revealed The alterations were widely different in the central (hypoxic) part of the tumour and in the peripheral (euoxic) rim of tumour cells

A fine granulation of the nuclear chromatin occurred a few hours after cHR treatment in the central tumour cells The nucleolus was not visible, the nuclear border was distinct, often somewhat angulated The cell borders were marked, and the cells isolated, cytoplasmic staining more intense No clear shrinkage of cells or nuclei was visible (*Figs 2, 3*) At intervals of a few hours the reaction was uniform, quite independent of sequence of the components At intervals of 24 hours the tissue could immediately after the completed cHR treatment display some similarity to the alterations produced by the factor first applied (*Fig 5 a*), but in a very short time (½ to 2 hours) the type of reaction changed to the type just described (Fig 5 b)

During the next few days the nuclear granules became finer and more indistinct;



Fig 9 13 days after cHR treatment 800 R 42 5 C/30 min (545 ×) Progressing necrobiotic decay of tumour cells Growth of connective tissue

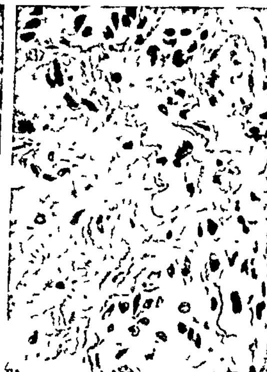


Fig 10 21 days after cHR treatment 42 5 C 60 min 800 R (545 ×) Unclear remnants of tumour cells in more mature fibrotic connective tissue

the cellular and nuclear borders disappeared Existing mitoses and the stromal tissue were somewhat resistant, but in the following days the decay progressed, and the central part of tumour was totally transformed to an amorphic necrosis (Figs 4, 8 a) If no newgrowth of tumour occurred in the peripheral part, this necrosis could remain unchanged for 2 to 3 weeks before it was invaded by connective tissue

In the peripheral zone of the tumour the reaction was quite different Within hours heterogeneous chromatin alterations appeared in many cells Cells with 'diffuse dark nuclei', cells with lumps of chromatin in an 'empty' nucleus or fine chromatin granules were intermingled with cells without any definite alterations (Fig 6) In a couple of days, mostly cells with a clear empty' nucleus containing a small number of chromatin fragments were present (Figs 7, 8 b) No tendency to shrinkage of the nucleus or cytoplasm appeared, on the contrary, a number of cells had a large amount of cytoplasm combined with a sparse irregular chromatin No fresh mitoses were seen, existent mitoses were arrested

In the following weeks, the tumour cells gradually disappeared with progressive karyolysis, reduction of the cytoplasm and blurring of the cellular borders (Fig 9) The loose connective tissue augment isolated the tumour cells in the network (Fig 10), and finally—in about a month—all tumour cells disappeared and a scar was formed

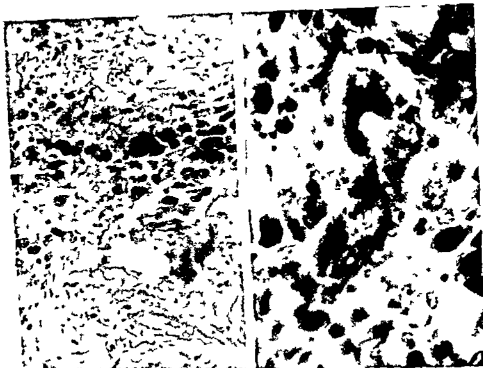


Fig. 11 6 days after cHR treatment 42 5 C/30 min 800 R (570) New growth of tumour along the border of central necros s A few new necrobiotic tumour cells in the peripheral parts of tumour

Fig 12. 11 days after cHR treatment 42.5 C/60 min 1 600 R (570) Undamaged glandular tissue (hostess) from the normal mamma included in decaying tumour tissue

During the first week it was impossible to point out any viable tumour cell About this time it could be possible in cases of unsuccessful treatment to recognize a fresh normal mitosis and soon some newgrowth tumour cells could be demonstrated commonly as a halo around the central necrosis (Fig. 11) Apart from a moderate number of macrophages no cellular reaction occurred in the tissue The surrounding normal tissue was quite unaltered The final scar consisted of irregular streaks of connective tissue in highly varying amounts In some cases normal mammary gland tissue remained (from the hostess) enclosed in the scar (Fig 12) In deep-seated tumours normal visceral organs (liver spleen pancreas, adrenals, kidney or lung) could be intimately continuous with or partly enclosed in the scar

Microscopically it was impossible to distinguish between cases treated with high and with low subcurative doses In all cases total destruction of the central part of tumour occurred and the real difference could be only small variations in the number of viable cells in the border zone Heat doses of curative size or higher displayed a similar appearance Possibly the peripheral reaction was somewhat 'speeded up

Histochemical examinations of untreated tumour tissue revealed evidence of a

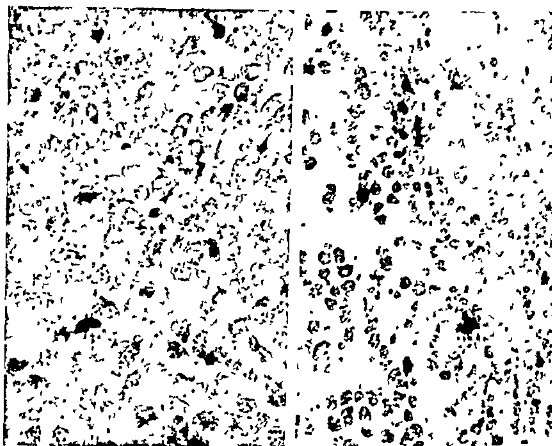


Fig 13 Acid phosphatase reaction in untreated tumour tissue Few small and uniform positive granules indicate a very slight lysosomal activity (365 ×)

[illegible] 14 48 h [illegible] (1 000 R)

very slight activity of lysosomal enzymes in all parts of tumour except in scattered areas of spontaneous necrosis (Fig 13) After roentgen irradiation with doses within the range used no definite alterations in activity were observed during the first two days (Fig 14) Just after isolated heat doses in the range used an increase in active granules was observed all over the tumour, in particular, in the more central parts The activity reached a maximum at about 24 hours (Fig 15) After a completed cHR treatment in all the used ranges intensification of the activity occurred Even in the isolated and invasive cells at the tumour periphery some activity was seen (Fig 16) In about 48 hours, the reaction had decreased in most of the tumour, signs of total necrosis appeared in the tissue, only in a narrow peripheral rim (the border zone) some signs of activity persisted

Discussion

In previous literature it has been supposed that heat might enhance the curative radiation effect by setting up a state of hyperaemia (Schmidt 1909, Theilhaber 1914)



Fig 15 Heat therapy 42.5 C/30 min 24 h after treatment Closely packed small tumour cells with increased number and size of granules demonstrate an active lysosomal reaction (365 ×)

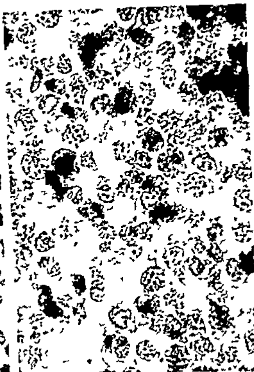


Fig 16 Large peripheral cells 24 h after combined therapy 42 5 C 30 min 800 R Increased acid phosphatase and distribution with large dense granules in the tumour cells (570 ×)

or some synchronization of the mitotic activity (BERKMAN & DESSAUER 1937, MARTIN & SCHLOERB 1964 RAO & ENGLEBURG 1965, SAPOZINK et coll 1973 SISKEN et coll 1965 WESTRA & DEWEY 1971) but no supportive evidence has been published

The present results may give some hints on the nature of the reaction In the central tissue reaction a very intense lysosomal activity is common for heat and cHR reaction However the appearance of the cellular decay is quite different After exposure to heat the heavy shrinkage of the cytoplasm nuclei and chromatin in the tumour cells, and the undamaged stroma with rapid formation of connective tissue are in sharp contrast to the cHR reaction in which there is no shrinkage of cells but fine granulation (Fig 5) of the disintegrating chromatin and secondary destruction of the stroma are characteristic features Here the terminal phase is very similar to the spontaneous necrosis the inclusion of some decaying mitoses being the principal difference (Fig 4)

As no significant difference in the content of acid phosphatase and catepsin D seems to exist (OVERGAARD & OVERGAARD 1972 b) some alterations in the cellular

pH might perhaps explain this finding The existence of such a mechanism has not been demonstrated, however

Some features in the later part of the cellular decay in the border zone may bear resemblance to the roentgen reaction Presumably, some metabolic potential may be left in cells whose reproductive functions have been severely injured as well by *cHR* as by roentgen irradiation However, after separate exposure to roentgen irradiation with doses in the ranges used a large number of irregular mitoses occur within a few days, while the total absence of mitotic activity in cHR-treated tumour cells is a striking feature

As also mitotic irregularities may be demonstrated (MARTIN & SCHLOERB RAO & ENGLEBURG, SAPOZINK et coll, SISKEN et coll) after separate exposure to heat in low doses, it seems possible that two different injuries in the mitotic apparatus (separately, reparable or below a vital threshold) may work together to effect a blockade of the mitotic activity Only the experimental evidence exists, but previous results (KEMP & JUUL 1931, JUUL & KEMP 1933) suggest the existence of some differences in the way heat and roentgen radiation hamper mitogenesis, and these authors also mentioned the possibility of some synergism between the factors

Possibly a confirmation of the suggestions concerning the missing mitogenesis may be provided by recent findings Some frequent and mostly reparable radiation lesions in malignant cells (single-strand breaks) were distinctly aggravated and might even lead to death after heat application (ORMEROD & STEVENS 1971, BEN-HUR et coll 1972)

In addition, the high lysosomal activity may presumably play a role in the rapid and severe cellular destruction As this activity is confined to the tumour cells—just as in the heat reaction—the special metabolic relations in tumour cells are presumably of importance

Acknowledgements

This work was supported by grants from the Krista and Viggo Petersen Foundation and the Danish Cancer Society

SUMMARY

In mouse experiments a high curative effect on implanted tumours was obtained by successive application of low local heat and roentgen doses Histologic and histochemical examinations of tumours so treated revealed a special reaction in the tissues A total and rapid destruction of all hypoxic tumour tissue was observed and (in successful cases) a total blockade of all mitotic activity in euoxic tumour tissue was followed by a long drawn necrobiotic decay of the existent tumour cells The disturbances are electively bound to the tumour cells, only some normal tissues may secondarily be injured A rapid and intensive lysosomal activity in all the tumour cells may probably be of importance in the reaction

ZUSAMMENFASSUNG

In Mäuseexperimenten wurde durch aufeinanderfolgende Anwendung lokaler Erwärmung und Röntgenbestrahlung ein hoher kurativer Effekt bei implantierten Tumoren erhalten. Histologische und histochemische Untersuchungen derartig behandelter Tumoren wiesen spezielle Reaktionen der Gewebe auf. Es wurde eine totale und rasche Destruktion aller hypoxischen Tumorgewebe beobachtet und (bei erfolgreichen Fällen) eine vollständige Blockierung jeglicher mitotischen Aktivität im gut Sauerstoff versorgten Tumorgeweben, der ein langanhaltender nekrobiotischer Zerfall der vorhandenen Tumorzellen folgte. Diese Störungen betrafen ausschliesslich die Tumorzellen, lediglich etwas Normalgewebe mag sekundär geschädigt werden. Eine rasche und intensive lysosomale Aktivität in allen Tumorzellen ist wahrscheinlich für diese Reaktionen von Bedeutung.

RÉSUMÉ

L'application locale successive de petites quantités de chaleur et de petites doses de rayon roentgen sur des tumeurs greffées à des souris a donné un effet curatif très important. Les examens histologiques et histochimiques des tumeurs ainsi traitées ont montré une réaction spéciale des tissus. On a observé une destruction totale et rapide de tout le tissu tumoral hypoxique et (dans les bons cas) un blocage total de toute l'activité mitotique dans le tissu [illegible]

[illegible]

[illegible] ...ique rapide et intense dans toutes les cellules tumorales a une importance dans cette réaction.

REFERENCES

BARKA T and ANDERSON P J Histochemistry, theory, practice and bibliography Hoeber, New York 1963

BEN HUR E, BRONK B V and ELKIND M M Thermally enhanced radiosensitivity of cultured Chinese hamster cells Nature (Lond) 238 (1972), 209

BERKMAN T und DESSAUER F Versuch, die fraktionierte Bestrahlung durch Provokation sensibler Zellphasen zu unterstützen (Provokationsbestrahlung) Strahlentherapie 58 (1937) 551

JUUL J und KEMP T Über den Einfluss von Radium und Röntgenstrahlen, ultraviolettem Licht und Hitze auf die Zellteilung bei warmblütigen Tieren, Studien an Gewebekulturen Strahlentherapie 48 (1933) 457

KEMP T und JUUL J Der Einfluss der Wärme auf die Zellteilung Arch exp Zellforsch 9 (1931) 602

MARTIN R J and SCHLOERB P R Induction of mitotic synchrony by intermittent hyperthermia in the Walker 256 rat carcinoma Cancer Res 24 (1964) 1997

ORMEROD M G and STEVENS U The rejoining of x ray induced strand breaks in the DNA of a murine lymphoma cell (L5178Y) Biochim biophys Acta (Amst) 232 (1971), 72

OVERGAARD K and OVERGAARD J (a) Investigations on the possibility of a thermic tumour therapy I Short wave treatment of a transplanted isologous mouse mammary carcinoma Europ J Cancer 8 (1972) 65

— — (b) Investigations on the possibility of a thermic tumour therapy II Action of combined heat roentgen treatment on a transplanted mouse mammary carcinoma Europ J Cancer 8 (1972) 573

— — Radiation sensitizing effect of heat Acta radiol Ther Phys Biol 13 (1974) 501

RAO P N and ENGLEBURG J HeLa cells Effects of temperature on the life cycle Science 148 (1965) 1092

SAPOZINK M D, DESCHNER E E and HAHN E W Induction of mitotic synchrony by intermittent hyperthermia in Ehrlich carcinoma in vivo Nature (Lond) 244 (1973) 299

SCHMIDT H E Zur Rontgenbehandlung tieferliegender Tumoren Fortschr Rontgenstr 14 (1909), 134

SISKEN J E, MORASCA L and KIBBY S Effects of temperature on the kinetics of the mitotic cycle of mammalian cells in culture Exp Cell Res 39 (1965) 103

THEILHABER A Die Entstehung und Behandlung der Karzinome, p 146 Karger Berlin 1914

WESTRA A and DEWEY W C Variation in the sensitivity to heat shock during the cell-cycle of Chinese hamster cells in vitro Int J Radiat Biol 19 (1971) 467

FROM THE RADIUM CENTRE, THE E N T DEPARTMENT AND THE INSTITUTE OF PATHOLOGY, ÅRHUS MUNICIPAL HOSPITAL, UNIVERSITY OF ÅRHUS, DK-8 000 ÅRHUS, DENMARK

MALIGNANT TUMOURS OF THE NASOPHARYNX

K BERTELSEN, A P ANDERSEN, O ELBROND and C LUND

The frequency of malignant tumours in the nasopharynx varies with race, geographic locality, sex, and age In white populations these tumours are rare, in Scandinavia about 0 3 per cent of all malignant tumours (GODTFREDSEN 1944), in other white populations around 0 25 per cent (BAILAR 1967) On the other hand, the frequency among the Chinese of South-East Asia, especially in the Kwangtung province, is about 25 times higher than in Scandinavia (HO 1967) The explanation is not purely genetic, since among Chinese born outside of China and living in Australia, Hawaii or California, the rate is significantly lower, but yet higher than among the white populations (CLIFFORD 1970)

Accordingly, environmental factors may be supposed to exert an influence upon the frequency of malignant tumours of the nasopharynx Fungi and virosis are possibly of importance in some areas, whereas physical and chemical factors or combinations thereof may play a role in others Chronic infections of the nasal cavity and nasal sinuses may precede a malignant process in the nasopharynx Thus, HENLE et coll (1970) found a higher antibody titre to the Epstein Barr virus in Chinese and East-African patients with malignant tumours of the nasopharynx than in patients with other neoplasms of the head and neck Infections with adeno-virus 7 and 12 were apparently more common among Chinese patients with nasopharyngeal tumours than in a control group (LAING 1969)

In all published series a preponderance of men, ranging from 2 5 to 4 4 1 was

Submitted for publication 8 August 1974

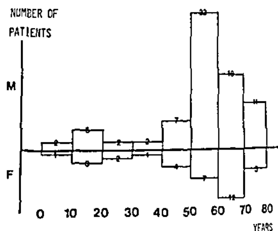


Fig 1 Age and sex incidence

encountered, and this ratio appears to be most marked in Chinese populations Among the Chinese the disease is most common in the age group 40 to 45, in the white race 55 to 65 years

Material During the period Jan 1958 to April 1969 a total of 115 patients with malignant tumours of the nasopharynx were treated in close collaboration between the Radium Centre and the Departments of E N T and of Pathology The material comprises all patients referred during this period for primary treatment One patient referred for treatment of distant metastases after having received the primary treatment elsewhere was not included All cases except 3 were followed for at least 5 years

The age and sex distribution appears in Fig 1, 80 were males, 35 females (male-female ratio 2 3 1) with a peak for the males in the age group 50 to 60, for the females 60 to 70 years

The symptoms and signs of malignant nasopharyngeal tumours are uncharacteristic, often identical with those of benign diseases in this region In addition, a detailed and thorough examination of the nasopharynx is often difficult and requires special routine The most common primary symptoms were nasal or otologic (Table 1) A lump on the neck was the first sign in 37 per cent On the other hand, pain occurred in only 19 per cent and cranial nerve paresis in 4 per cent as the first sign About half of the patients had only one symptom or sign, the remainder two or more

On admission 20 per cent (23/115) had cranial nerve pareses, 17 affecting only one cranial nerve, 6 several The nerves III, IV, VI were involved in 18 cases, V in 2 VII in 1, IX and X in 10 XI in 1 and XII in 3 cases

Due to the varying and uncharacteristic symptomatology several patients had had symptoms and signs for some time before final diagnosis Thus 41 per cent had had symptoms for more than 6 months 23 per cent (27/115) 6–11 months, 18 per cent (21/115) for more than one year About half of these patients had been treated for a

Table 1

Main symptoms

	No of cases	Per cent
Nasal bleeding with or without obstruction	56	48 7
Ear blocking, decreased hearing	52	45 2
Lump on the neck	42	36 5
Cranial nerve paresis	5	4 3
Headache, pains	22	19 1
Other symptoms	5	4 3

varying length of time under a wrong diagnosis before the correct nature of the lesion could be established 57 per cent (65/115) had had symptoms for less than 5 months and in 2 cases the length of the history was uncertain

The histologic classification was performed by a blind review and revision of all specimens in accordance with the present internationally accepted principles for classifying malignant pharyngeal tumours established by WHO (1971) The distribution of the 115 patients by type of tumour is given in Table 2 Two main groups may be distinguished, viz squamous-cell carcinomas, 71 % and malignant lymphomas, 22 % The re classification led to the fact that 20 cases originally classified as malignant lymphomas, were now classified as squamous-cell carcinomas of a lympho-epithelial type, reducing the original group of lymphomas by nearly half, whereas only one case was revised from carcinoma to lymphoma This indicates that the present material can be compared with other series only if they have been re-classified according to the current principles of WHO (1971)

All 83 cases of carcinoma were TNM classified in retrospect, partly on the basis of meticulous descriptions in the case records and partly, in almost all cases, detailed radiography The UICC criteria of TNM classification of nasopharyngeal carcinomas were used The N classification was performed by the ordinary UICC criteria In cases of doubt about the classification, the lower N value was chosen A retrospective TNM classification must carry some inaccuracy, however, due to the difficulty of distinguishing between T1 and T2 cases in retrospect It is easier to distinguish between T1–T2 cases on the one hand and T3–T4 on the other

Table 3 illustrates the distribution of the carcinomas by the TN classification At the time of diagnosis 40 % (33/83) were in an advanced stage T4, and 72 % (60/83) had possible lymph node metastases in the neck

Treatment Radiation was the primary treatment except in one case Before 1963 conventional roentgen, irradiation, 160 to 250 kV, 3 500 to 4 500 rad tumour dose, was used except in 6 cases After 1963 ^{60}Co only was used, tumour dose to the carcinomas

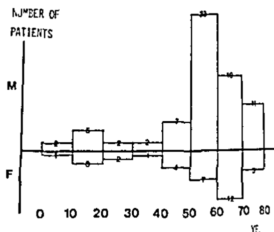


Fig 1 Age and sex incidence

encountered, and this ratio appears to be most marked in Chinese populations Among the Chinese the disease is most common in the age group 40 to 45, in the white race 55 to 65 years

Material During the period Jan 1958 to April 1969 a total of 115 patients with malignant tumours of the nasopharynx were treated in close collaboration between the Radium Centre and the Departments of E N T and of Pathology The material comprises all patients referred during this period for primary treatment One patient referred for treatment of distant metastases after having received the primary treatment elsewhere was not included All cases except 3 were followed for at least 5 years

The age and sex distribution appears in Fig 1, 80 were males, 35 females (male-female ratio 2 3 1) with a peak for the males in the age group 50 to 60, for the females 60 to 70 years

The symptoms and signs of malignant nasopharyngeal tumours are uncharacteristic, often identical with those of benign diseases in this region In addition, a detailed and thorough examination of the nasopharynx is often difficult and requires special routine The most common primary symptoms were nasal or otologic (Table 1) A lump on the neck was the first sign in 37 per cent On the other hand, pain occurred in only 19 per cent and cranial nerve paresis in 4 per cent as the first sign About half of the patients had only one symptom or sign, the remainder two or more

On admission 20 per cent (23/115) had cranial nerve pareses, 17 affecting only one cranial nerve, 6 several The nerves III, IV, VI were involved in 18 cases, V in 2, VII in 1, IX and X in 10, XI in 1 and XII in 3 cases

Due to the varying and uncharacteristic symptomatology several patients had had symptoms and signs for some time before final diagnosis Thus 41 per cent had had symptoms for more than 6 months 23 per cent (27/115) 6–11 months 18 per cent (21/115) for more than one year About half of these patients had been treated for a

Table 1

Main symptoms

	No of cases	Per cent
Nasal bleeding with or without obstruction	56	48 7
Ear blocking, decreased hearing	52	45 2
Lump on the neck	42	36 5
Cranial nerve paresis	5	4 3
Headache pains	22	19 1
Other symptoms	5	4 3

varying length of time under a wrong diagnosis before the correct nature of the lesion could be established 57 per cent (65/115) had had symptoms for less than 5 months and in 2 cases the length of the history was uncertain

The histologic classification was performed by a blind review and revision of all specimens in accordance with the present internationally accepted principles for classifying malignant pharyngeal tumours established by WHO (1971) The distribution of the 115 patients by type of tumour is given in Table 2 Two main groups may be distinguished, viz squamous cell carcinomas, 71 % and malignant lymphomas, 22 % The re-classification led to the fact that 20 cases originally classified as malignant lymphomas, were now classified as squamous-cell carcinomas of a lympho-epithelial type, reducing the original group of lymphomas by nearly half, whereas only one case was revised from carcinoma to lymphoma This indicates that the present material can be compared with other series only if they have been re-classified according to the current principles of WHO (1971)

All 83 cases of carcinoma were TNM classified in retrospect, partly on the basis of meticulous descriptions in the case records and partly, in almost all cases, detailed radiography The UICC criteria of TNM classification of nasopharyngeal carcinomas were used The N classification was performed by the ordinary UICC criteria In cases of doubt about the classification, the lower N value was chosen A retrospective TNM classification must carry some inaccuracy, however, due to the difficulty of distinguishing between T1 and T2 cases in retrospect It is easier to distinguish between T1–T2 cases on the one hand and T3–T4 on the other

Table 3 illustrates the distribution of the carcinomas by the TN classification At the time of diagnosis 40 % (33/83) were in an advanced stage T4, and 72 % (60/83) had possible lymph node metastases in the neck

Treatment Radiation was the primary treatment except in one case Before 1963 conventional roentgen irradiation, 160 to 250 kV, 3 500 to 4 500 rad tumour dose, was used except in 6 cases After 1963 ^{60}Co only was used, tumour dose to the carcinomas

Table 2

Distribution by histology

	No. of cases	Per cent
Squamous cell carcinoma (high diff.)	8	(7.0)
Squamous cell carcinoma (low diff.)	42	(36.5)
Lymphoepithelioma	32	(27.8)
Adenocarcinoma	1	(0.9)
Lymphoma	25	(21.7)
Sarcoma	1	(0.9)
Plasma cell myeloma	2	(1.7)
Unclassified malignant tumour	4	(3.5)
Total	115	(100.0)

about 6 000 rad in 6 weeks, to the lymphomas 4 500 rad in 4 to 5 weeks. The conventional irradiation was administered to relatively small fields; if the tumour was believed to be restricted to the nasopharynx, the regional lymph nodes were not irradiated; if enlarged regional lymph nodes existed, these were irradiated as a rule through separate fields. The ^{60}Co irradiation was administered to large, parallel opposed lateral fields comprising the nasopharynx as well as all enlarged lymph nodes on the neck in one field.

Results

The follow up period ranges from 4 to 15 years, being less than 5 years in only 3 cases.

The 3 year crude survival rate for patients with carcinoma was 36.1 per cent, for patients with lymphoma 60.0 per cent (Fig. 2). The corresponding 5 year and 10 year rates were 23.8 per cent and 5.0 per cent respectively for carcinomas, 40.0 per cent and 25.0 per cent respectively for lymphomas. Thus malignant lymphomas had

Table 3

Distribution by TN classification

	TX	T0	T1	T2	T3	T4	Total
NX	1	0	0	0	0	2	3 (3.6%)
N0	0	1	3	3	3	10	20 (24.1%)
N1	0	3	10	4	4	11	32 (38.5%)
N2	0	0	5	2	2	7	16 (19.3%)
N3	0	1	0	8	0	3	12 (14.5%)
Total	1 (1.2%)	5 (6.0%)	18 (21.7%)	17 (20.5%)	9 (10.8%)	33 (39.8%)	83 (100.0%)

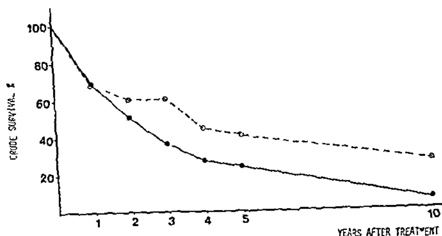


Fig. 2 Carcinomas (—●—) compared with lymphomas (--○--)

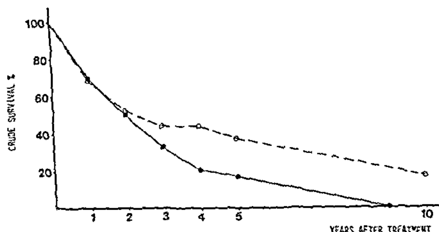


Fig. 3 Females (--○--) compared with males (—●—)

a better prognosis than carcinomas and during the period from 5 to 10 years a *marked decrease in the survival rate occurred*

It is generally assumed that the prognosis of head neck carcinoma is better for women than for men In Fig 3 the carcinomas of the present material are compared The 3-year crude survival rate for men proved to be 32 8 per cent, for women 44 0 per cent This difference was even more evident after 5 and 10 years The TN classification was about the same for males and females

Previously has been suggested that the lymphoepithelial carcinomas had a better prognosis than other *poorly differentiated* squamous-cell nasopharyngeal carcinomas

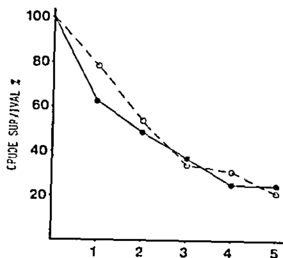


Fig 4

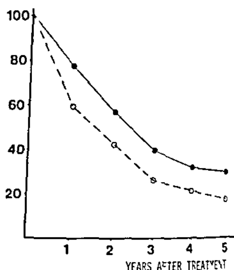


Fig 5

Fig 4 Lymphoepithelioma (--o--) compared with other carcinoma (—•—)

Fig 5 Results according to T-classification (—•—) T0, T1, T2, (--o--) T3, T4

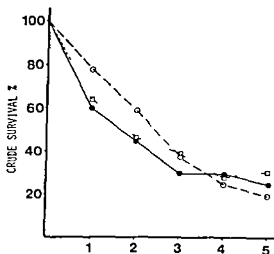


Fig 6

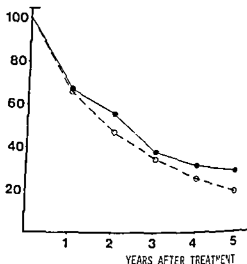


Fig 7

Fig 6 Results according to N-classification (—•—) N0, (--o--) N1 (--□--) N2 N3

Fig 7 Results according to type of irradiation (—•—)^{60}Co (--o--) conventional roentgen

The survival rate for these two groups is compared in Fig 4, no difference exists between the groups

As it was difficult to differentiate between T1 and T2 cases, the T0, T1 and T2 cases were considered together and compared with T3 and T4 cases (Fig 5) As might be expected the prognosis was poorer for the T3–T4 cases Surprisingly, the prognosis did not seem to be definitely dependent on the N value (Fig 6)

The results following conventional and ^{60}Co irradiation appear in Fig 7 There seems to be a tendency for a more favourable prognosis after cobolt irradiation, but the numbers of cases are small and the series probably not entirely comparable

The primary tumour was irradiated successfully in almost all the cases of malignant lymphoma, but 35 per cent of the patients with carcinoma developed recurrence within the area of the primary tumour and 11 developed recurrence of regional lymph node metastases without simultaneous local recurrence These patients were treated by radical dissection of the cervical nodes Nine died soon after recurrence, one of an intercurrent disease after 3 years, one only is alive and free of recurrence after 9 years

Complications It is difficult to assess late complications, as many patient survived for only a short time The most evident late sequela to the radiation therapy was annoying and persisting dryness of the mucous membranes, this appeared in the majority of the patients The spinal cord was included in the radiation beam without any resulting neurologic deficits

Discussion

The therapeutic results in malignant tumours of the nasopharynx are not satisfactory, as is also apparent from the present analysis Many factors contribute to the disappointing outcome and have to be taken into consideration when assessing the results and in prospective planning

As malignant tumours of the nasopharynx are difficult to diagnose, the tumour has often reached an advanced stage when treatment begins, reducing the possibilities of curative treatment The most common initial symptoms and signs in the present material were nasal and otologic, as well as enlargement of cervical lymph nodes The material of GODTFREDSEN (1944) comprising patients from the Radium Centres in Sweden and Denmark, also included several patients with ophthalmoneurologic initial symptoms (16 %) He stated that these symptoms, and particularly combinated, should invariably suggest a malignant lesion in the nasopharynx

Pain affecting especially the trigeminal area, but also the vertex, temporal and occipital regions, is stated to have been the main symptom in 11 5 per cent of LEDERMAN's (1961) cases Examination of the nasopharynx is important in patients with unexplained headache or facial pain LEDERMAN states that the prognosis usually is poor if the patient is not relieved of pain in the course of treatment

Microscopic difficulties exist as well as divergent classifications (SCANLON 1967) The often poor differentiation, as well as the growth of the squamous-cell [illegible] in [illegible]

and [illegible]

have [illegible] as special types Conventional microscopy (SHU YEH 1962) as well as electron microscopy (BAUER & MCGAVRAN 1968) have indicated

that these poorly differentiated malignant tumours are squamous cell carcinomas from which they do not differ in clinical course, regardless of their differentiation and appearance (WHO 1971) This is in complete conformity with the reclassification of the present material Thus, lympho epithelial carcinoma should not be maintained as a special group of tumours

TNM classification of carcinomas in the nasopharynx gives rise to considerable uncertainty In particular, it is difficult to distinguish between T1 and T2 cases This applies primarily to retrospective classification which must, therefore, be considered with some reserve A TNM classification seems to be mainly of prognostic value, playing less role in planning the radiation therapy

It seems to be generally accepted that high-voltage irradiation of the primary tumour area and the groups of lymph nodes on the neck affords the best results This is also indicated by the analysis of the results in the present material There is apparently seldom any indication for surgical procedures (CHEN & FLETCHER 1971, PEREZ et coll 1969) Whether combined treatment, including administration of cytostatics, improves the prognosis, is still uncertain

The therapeutic results were less satisfactory, but still better than those in a material of 124 patients reported by LEDERMAN (1961) He found a 5-year crude survival rate of 17 per cent almost independently of whether or not lymph-node metastases were present The present analysis seems to confirm this statement He also found the prognosis to be better for women than for men (30 per cent and 12 per cent respectively) The most recent reports on 5 year survival give 28 per cent (ATKINSON & SCOTT 1967), 34 per cent (PEREZ et coll 1969), and 38 per cent (MEYER & WANG 1971) However, it is uncertain whether these series are comparable with the present one

SUMMARY

A series of 115 patients with malignant tumours of the nasopharynx were primarily irradiated All the cases of carcinoma were TNM classified in retrospect ^{60}Co irradiation appeared to afford a somewhat better prognosis than conventional irradiation previously used The 5 year crude survival rate for the patients with lymphoma and with carcinoma was 40 0 per cent and 23 8 per cent respectively A distinctly better prognosis was found for women than for men and the prognosis was independent of whether or not lymph node metastases were present There seems to be no indication for maintaining lympho-epithelial carcinoma as a special group of tumour Surgical procedures are rarely indicated in the treatment of malignant nasopharyngeal tumours

ZUSAMMENFASSUNG

40 0 bzw 23,8 % Es wurde eine klar bessere Prognose fur Frauen als fur Manner gefunden, und die Prognose war unabhangig davon ob Lymphknoten Metastasen vorhanden waren oder nicht Es scheint kein Anlass dafur vorzuliegen, lympho-epitheliale Karzinome als eine besondere Gruppe von Tumoren beizubehalten Chirurgische Eingriffe sind selten bei der Behandlung maligner Tumoren des Naso-Pharynx indiziert

RESUMÉ

Une série de 115 malades atteints de tumeurs malignes du nasopharynx ont ete irradiés d emblée Tous les cas de carcinome ont été classes rétrospectivement suivant la classification TNM L'irradiation par le ^{60}Co paraît donner un pronostic un peu meilleur que l ir radiation ordinaire utilisée auparavant Le taux brut de survie à 5 ans a été de 40 % pour les malades atteints de lymphone et de 23 8 % pour les malades atteints de carcinome Les auteurs ont constanté que le pronostic est nettement meilleur chez les femmes que chez les hommes et qu il est indépendant de la présence ou de l absence de metastases ganglionnaires lymphatiques Il semble ne plus y avoir de raison de continuer à considérer le car cinome lympho-épithélial comme un groupe special de tumeur Les techniques chirurgicales sont rarement indiquees dans le traitement des tumeurs malignes du nasopharynx

REFERENCES

ATKINSON L and SCOTT G C Cancer of nasopharynx in Australia 1953–1963 Some clinical features and results *In* Cancer of nasopharynx Edited by C S Muir and K Shanmugaratnam UIIC monograph series 1, p 222. Munksgaard, Copenhagen 1967

BAILAR J C Nasopharyngeal cancer in white populations A world wide survey *In* Cancer of the nasopharynx Edited by C. S Muir and K. Shanmugaratnam UICC monograph series 1, p 18 Munksgaard, Copenhagen 1967

BAUER W C and MCGAVRAN M H Ultrastructure and surgical pathology *In* Surgical pathology p 6 Edited by L V Ackerman and H R Butcher The C V Mosby Company, Saint Louis 1968

CHEN K Y and FLETCHER G H Malignant tumors of the nasopharynx Radiology 99 (1971) 165

CLIFFORD P On the epidemiology of nasopharyngeal carcinoma J Cancer 5 (1970), 287

GODTFREDSEN E Ophthalmologic and neurologic symptoms at malignant nasopharyngeal tumours Acta oto-laryng. (1944) Suppl No 59

HENLE W, HENLE G, HUNG-CHIU HO, BURTIN P, CACHIN Y, CLIFFORD P, DE SCHRYVER A, DE THE G, DIEHL V and KLEIN G Antibodies to Epstein Barr virus in nasopharyngeal carcinoma, other head and neck neoplasms and control groups J nat Cancer Inst 44 (1970) 225

HO H C Nasopharyngeal carcinoma in Hong Kong *In* Cancer of the nasopharynx Edited by C S Muir and K Shanmugaratnam UIIC monograph series 1, p 58 Munksgaard Copenhagen 1967

LAING D Virus as the cause of rhinopharyngeal carcinoma Acta oto-laryng 67 (1969), 190

LEDERMAN M Cancer of the nasopharynx. Its natural history and treatment Charles C Thomas, Springfield, Illinois 1961

MEYER J E. and WANG C C. Carcinoma of the nasopharynx Factors influencing results of therapy Radiology 100 (1971), 385

PEREZ C A, ACKERMAN L V MILL W B, OGURA J H and POWERS W E. Cancer of the nasopharynx Factors influencing prognosis Cancer 24 (1969) 1
SCANLON P W, RHODES R E Jr, WOOLNER L N, DEVINE K D and McLEAN J B Cancer of the nasopharynx 142 patients treated in the 11 year period 1950–1960 Amer J Roentgenol 99 (1967) 313
UICC Union Internationale Contre le Cancer Geneva 1968
YEH SHU A histological classification of carcinoma of the nasopharynx with a critical review as to the existence of lymphoepitheliomas Cancer 15 (1962) 895

FROM THE STATE INSTITUTE OF RADIATION HYGIENE (DIRECTOR K KOREN), MONTEBELLO, OSLO, NORWAY

RADIATION HYGIENE IN PHOTOFLUOROGRAPHY

F WELDE

This paper presents the results of a comprehensive survey of all the photofluorographic units used in Norway Patient doses in photofluorographic examinations of the chest are given and protection of the personnel in mass chest roentgen examinations will also be discussed

The complex problem whether mass roentgen examinations should be continued or not, is not discussed The data given may, however, serve as a necessary and valuable background material for such a discussion

The total number of photofluorographic examinations in Norway in 1971 was approximately 700 000, civil mass chest surveys 570 000, and military ones 130 000 This number is based on information from the institutions involved The population is about 3 890 000 and 534 new cases of tuberculosis were detected in 1970 according to the official statistics

Benefit and radiation risks in mass chest photofluorography was discussed by KITABATAKE et coll (1973) They found that for each expected case of radiation induced malignancy, resulting from the examinations considered, about 1 000 cases of open tuberculosis and curable pulmonary carcinoma were detected This number is of the order of 100 in Norway

Military personnel are examined annually, recruits being examined three times during their obligatory military service An increasing part of the civil mass chest surveys are selective, which means that population groups that are especially exposed

Submitted for publication 3 April 1974

PEREZ C A, ACKERMAN L V, MILL W B, OGURA J H and POWERS W E Cancer of the nasopharynx Factors influencing prognosis Cancer 24 (1969), 1

SCANLON P W, RHODES R E Jr, WOOLNER L N, DEVINE K D and MCLEAN J B Cancer of the nasopharynx 142 patients treated in the 11 year period 1950–1960 Amer J Roentgenol 99 (1967), 313

UICC Union Internationale Contre le Cancer Geneva 1968

YEH SHU A histological classification of carcinoma of the nasopharynx with a critical review as to the existence of lymphoepithelomas Cancer 15 (1962), 895

FROM THE STATE INSTITUTE OF RADIATION HYGIENE (DIRECTOR K. KOREN), MONTEBELLO, OSLO, NORWAY

RADIATION HYGIENE IN PHOTOFLUOROGRAPHY

F. WELDE

This paper presents the results of a comprehensive survey of all the photofluorographic units used in Norway. Patient doses in photofluorographic examinations of the chest are given and protection of the personnel in mass chest roentgen examinations will also be discussed.

The complex problem whether mass roentgen examinations should be continued or not is not discussed. The data given may, however, serve as a necessary and valuable background material for such a discussion.

The total number of photofluorographic examinations in Norway in 1971 was approximately 700 000, civil mass chest surveys 570 000, and military ones 130 000. This number is based on information from the institutions involved. The population is about 3 890 000, and 534 new cases of tuberculosis were detected in 1970 according to the official statistics.

Benefit and radiation risks in mass chest photofluorography was discussed by KITABATAKE et coll. (1973). They found that for each expected case of radiation induced malignancy, resulting from the examinations considered, about 1 000 cases of open tuberculosis and curable pulmonary carcinoma were detected. This number is of the order of 100 in Norway.

Military personnel are examined annually, recruits being examined three times during their obligatory military service. An increasing part of the civil mass chest surveys are selective, which means that population groups that are especially exposed

Submitted for publication 3 April 1974.

PEREZ C A, ACKERMAN L V, MILL W B, OGURA J H and POWERS W E Cancer of the nasopharynx Factors influencing prognosis Cancer 24 (1969), 1
SCANLON P W, RHODES R E Jr, WOOLNER L N, DEVINE K D and McLEAN J B Cancer of the nasopharynx 142 patients treated in the 11 year period 1950–1960 Amer J Roentgenol 99 (1967), 313
UICC Union Internationale Contre le Cancer Geneva 1968
YEH SHU A histological classification of carcinoma of the nasopharynx with a critical review as to the existence of lymphoepithelomas Cancer 15 (1962), 895

FROM THE STATE INSTITUTE OF RADIATION HYGIENE (DIRECTOR K KOREN), MONTEBELLO, OSLO, NORWAY

RADIATION HYGIENE IN PHOTOFLUOROGRAPHY

F WELDE

This paper presents the results of a comprehensive survey of all the photofluorographic units used in Norway Patient doses in photofluorographic examinations of the chest are given and protection of the personnel in mass chest roentgen examinations will also be discussed

The complex problem whether mass roentgen examinations should be continued or not is not discussed The data given may, however, serve as a necessary and valuable background material for such a discussion

The total number of photofluorographic examinations in Norway in 1971 was approximately 700 000, civil mass chest surveys 570 000, and military ones 130 000 This number is based on information from the institutions involved The population is about 3 890 000, and 534 new cases of tuberculosis were detected in 1970 according to the official statistics

Benefit and radiation risks in mass chest photofluorography was discussed by KITABATAKE et coll (1973) They found that for each expected case of radiation induced malignancy, resulting from the examinations considered, about 1 000 cases of open tuberculosis and curable pulmonary carcinoma were detected This number is of the order of 100 in Norway

Military personnel are examined annually, recruits being examined three times during their obligatory military service An increasing part of the civil mass chest surveys are selective, which means that population groups that are especially exposed

Submitted for publication 3 April 1974

Table 1

Skin exposure and bone marrow doses

Tube potential kV	Size mm	Filtering	No of units	Mean skin exposure (mR)	Range skin exposure (mR)	Mean bone marrow dose (mrad)
125	70	2 mm Al total	17	255	151–462	36
125	100	2 mm Al total	2	246	212–280	35
125	100	2 mm Al total, rapid processing	1	580		82
115	100	3 mm Al total	1	110		15
93	100	3 mm Al total	1	450		60
85	100	2 mm Al total, rapid processing	2	905	709–1 020	130
85	70	1 mm Al added	4	895	470–1 780	128
85	70	no added filter, improper processing	2	1 650	1 035–2 260	220
85	35	1 mm Al added	6	430	192– 685	62

to tuberculosis are examined more often than other groups Usually only persons above the age of 13 to 16 years are included in mass chest surveys

Dose measurements The doses to the patients in photofluorographic examinations were measured using 25 mg LiF Tl dosimeters For measuring skin exposures a dosimeter was taped to the back of the patient in the middle of the radiation beam Bone marrow doses were calculated from skin exposure and transmitted exposure using data from WEBER (1964) and the Adrian Committee (1960)

Male gonad doses were measured by taping a dosimeter outside the trousers close to testes The same dosimeter was used for 20 to 40 men Female gonad doses and approximately mean foetal doses were measured by a method combining phantom measurements and measurements on women Phantom (Alderson Rando phantom)

Table 2

Gonad doses

Tube potential kV	Size mm	Filtering	Skin exposure (mR)	No of patients	Male (mrad)	Female (mrad)	Foetal (mrad)
125	70	2 mm Al total	210	M 295 F 57	0 17	0 43	0 60
85	70	1 mm Al added	540	M 40	0 09	—	—

Table 3

Measurements with different filtration of the radiation beam

Tube potential kV	Total filtration	Half value layer (mm Al)	Mean exposure time (s)	Ratio of skin exposure to exit exposure. Patient measurements
125	2 mm Al	4 0	0.26	29 1
125	3 mm Al	4 6	0 29	25 8
125	4 mm Al	5 5	0 32	21 2
125	4 mm Al +0 1 mm Cu	8 0	0 38	17 7

measurements were carried out with dosimeters in the ovarial and foetal positions and on the back in the middle of the radiation beam The gonad doses were normalized to the same skin exposure as the mean value measured for 57 women

Results

Measured skin exposure and calculated bone marrow doses are given in Table 1 The bone marrow doses found for a tube potential of 100 to 125 kV agreed well with those found by HASHIZUME et coll (1972), and for tube potentials below 100 kV with the bone marrow doses reported by the Adrian Committee (1960, 1966)

High tube potential and heavy filtration lowered skin exposures and bone marrow doses (Table 1) Films and processing procedures also influenced patient doses considerably Automatic rapid processing in photofluorography resulted in about 2 times higher patient doses than proper ordinary processing The effect of film size on patient doses could not be evaluated with certainty

Measured gonad doses appear in Table 2 and agree well with those found by LARSSON (1958), KOREN et coll (1967) and HASHIZUME et coll The male gonad doses increased with increasing tube potential

From measured doses and statistical data the following mean doses to the whole population are calculated

Mean bone marrow dose 11 2 mrad/person/year

Genetically significant dose 0 045 mrad/person/year

Photofluorography contributes considerably to the total mean bone marrow dose from radiography The genetically significant dose from photofluorography is of the order of promilles of the total genetically significant dose from diagnostic radiology (KOREN et coll 1967)

The contributions to population doses are calculated for each photofluorographic unit separately

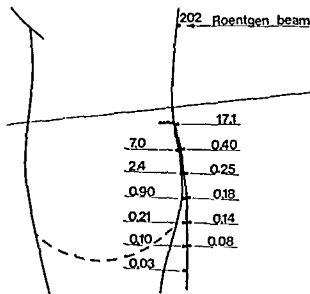


Fig 1

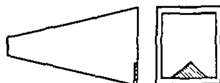


Fig 2

Fig 1 Exposure inside and outside a lead rubber apron (0 5 mm Pb) Dosimeters were taped inside and outside a lead rubber apron with intervals of 5 cm in the vertical central axis The lead rubber apron was worn by 57 women

Fig 2 Diaphragm and lead insert used

Protection of patient Measurements were carried out to evaluate the importance in patient protection of the filtration and the size of the roentgen beam and the use of a lead insert in the diaphragm or a lead rubber skirt worn by the patient (Tables 3 to 5, Figs 1, 2)

Increased filtration resulted in a considerably reduced ratio of skin exposure to exit exposure (Table 3) For a constant exposure to the recording system, the data in Table 3 illustrate how the incident skin exposure decreases with increasing filtration The effect on the bone marrow dose is less evident Increased filtration results in increased exposure times For some photofluorographic units it may be difficult to obtain a reasonably short exposure time when a heavy filtration is used

Table 4 indicates a slight decrease of the male gonad dose with body height From the low values of the doses it can be concluded that the testes very rarely are located in the primary beam

The doses inside and outside a lead rubber skirt worn by women during photofluorographic examinations were measured Due to the predominance of the radia-

Table 4

Variation in male gonad doses with body height

Group	Number of men	Gonad dose (mrad)	Mean height (cm)
≥ 175 cm	152	0 16	179 9
< 175 cm	108	0 18	167 8
Age 13–16	35	0 18	166 0

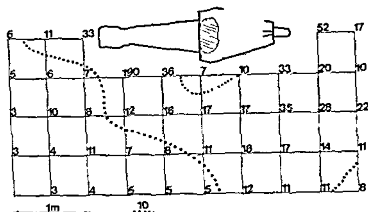


Fig. 3 Scattered radiation around a photofluorographic unit Door closed *mR/1000 exposures Height 1 m*

tion scattered inside the patient (Fig 1) the lead rubber skirt only affords a moderate protection On the other hand, a small lead insert in the diaphragm (Fig 2) provides a better protection than a lead rubber skirt worn by the patient (Table 5) but the skirt is considered more practical The use of the smallest practicable radiation beam and its accurate positioning is of course of the utmost importance

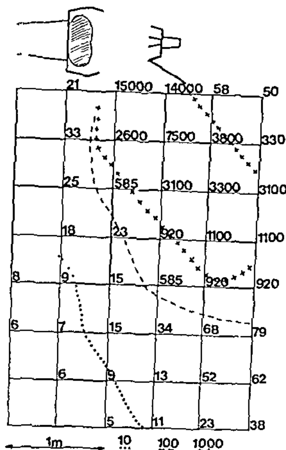
Patients awaiting examination close to a cabin with one open side receive gonad doses of the same order of magnitude as the gonad doses received during the examination itself Thus, men waiting at a distance of 1 m from the screen on the open side of the cabin received a gonad dose of about 0 5 mrad/exposure

Doses to the personnel The radiation level around a photofluorographic unit was measured using a Victoreen 444 dosimeter Scattered radiation was generated by a Temex-phantom The results are given in mR per 1 000 exposures for a tube potential of 125 kV, a total filter of 2 mm Al and a tube current of 40 mA The measurements

Table 5

Gonad doses using a lead insert in the diaphragm and a lead rubber apron Phantom measurements (Temex phantom) with the ovaries 10 cm below the edge of the primary beam and the top of the lead rubber apron 1 cm below the edge of the primary beam

Specifications	Foetal (mrad)	Female (mrad)	Male (mrad)
Fixed rectangular diaphragm	0 86	0 50	0 21
Lead insert in the diaphragm (3 mm Pb)	0 32	0 26	0 15
Lead rubber apron (0 5 mm Pb)	0 60	0 35	0 15



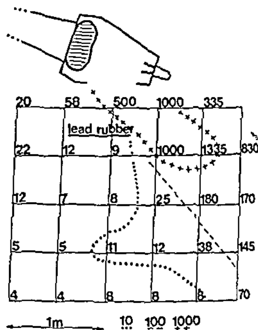


Fig 5

Fig 4 Scattered radiation around a photofluorographic unit Door open mR/1000 exposures Height 1 m

Fig 5 Scattered radiation around a photofluorographic unit Effect of a lead rubber curtain mR/1000 exposures Height 1 6 m

refer to photofluorographic units with open top The distance from the floor to the ceiling (concrete) was approximately 3 m

Under normal conditions (the door closed) the radiation level was considered safe at the position of the operator and elsewhere in the room on that side of the cabin (Fig 3)

Measurements with the door open (Fig 4) indicated that the practice of supporting persons during the exposure gave doses of the order of 1 000 times the normal when a lead rubber coat is not worn

The lead rubber curtain on the other side of the cabin affords limited shielding (Fig 5) There may be more than one working place in the laboratory during photofluorography The unit should be positioned in such a way that none of these is located in front of the cabin opening

Conclusion

The results and experiences gained have led to the following instructions for the radiation protection surveys of photofluorographic units (besides the general recommendations of the ICRP)

(1) The tube potential should be at least 125 kV Units with low tube potential will gradually be replaced The following minimum filtration will be required 85 kV–2 mm Al total, 125 kV–3 mm Al total

(2) Units occasionally used for children must have an adjustable diaphragm Ambulatory units used only for adults may have a proper fixed diaphragm When examining children and pregnant women a lead insert in the diaphragm or a lead rubber skirt should be used

(3) Fast films and proper processing must be used The fluorescent screen has to be replaced if its sensitivity deteriorates or is considerably less than for newer photofluorographic screens

(4) Photofluorographic units should not be used for examinations where it is necessary to support the patient

(5) Cabins with one open side shall be so oriented that no working place is located in front of the opening where patients should not wait either

SUMMARY

This paper comprises measurements and experiences from the surveillance of 36 photofluorographic units in Norway Measured patient doses are given Practical means for reducing the doses are emphasized The radiation hygiene for the personnel in mass chest surveys is discussed

ZUSAMMENFASSUNG

Diese Arbeit umfasst Messungen und Erfahrungen von der Überwachung von 36 photo-

RÉSUMÉ

Ce travail présente des mesures et une expérimentation concernant la surveillance de 36 appareils de radio-photographie en Norvège Les doses reçues par le patient sont indiquées, l'auteur insiste sur les moyens pratiques pour réduire ces doses Il examine les moyens de protection contre les radiations concernant le personnel dans les examens thoraciques de dépistage systématique

REFERENCES

HASHIZUME T KATO Y MARUYAMA T, KUMAMOTO Y, SHIRAGAI A and NISHIMURA A Population mean bone marrow dose and leukemia significant dose from diagnostic medical x ray examinations in Japan 1969 Hlth Phys 23 (1972), 845

JOHNS H E and WILSON J C Gonadal dose from mass miniature chest x rays Canad med Ass J 8 (1958) 571

KITABATAKE T, YOKOYAMA M, SAKKA M and KOGA S Estimation of benefit and radiation risk from mass chest radiography Radiology 109 (1973), 37

KOREN K, MAUDAL S, FLATBY J and BERTEIG L Radiation to the gonads in diagnostic and therapeutic procedures Acta radiol Ther Phys Biol 5 (1967) 385

LARSSON L-E Radiation doses to the gonads of patients in Swedish roentgen diagnostics Acta radiol (1958) Suppl No 157

Radiological hazards to patients Second report of the Committee Her Majesty's Stationary Office, London 1960

— Final Report of the Committee Her Majesty's Stationary Office, London 1966

WEBER J Beenmergdosis tengevolge van de Rontgendiagnostiek (In Dutch) Leiden 1964

FROM THE DEPARTMENT OF RADIATION PHYSICS (DIRECTOR ASSOC PROF HOLGER SKÖLDBORN), UNIVERSITY OF GOTHENBURG, S-413 45 GOTHENBURG, SWEDEN

AUTOMATED THERMOLUMINESCENCE READER

I Technical construction and function

B LINDSKOUG and B -E BENGTSSON

Thermoluminescence means the ability of certain substances to absorb and store energy of ionizing radiation, which upon heating is re-emitted in the form of electromagnetic radiation, mainly within the visible wavelength range Since the radiation energy stored can be related to the dose absorbed by the material, thermoluminescent materials may be used for the determination of ionizing radiation Thermoluminescent dosimeters are commercially available in many different forms and varying chemical composition For example, LiF, $CaSO_4$ and $Li_2B_4O_7$ are available in the form of powder, crystals, extruded rods or plates and also enclosed in teflon in the form of thin discs, cut rods, continuous rods and tape

Several types of TLD readers are commercially available For heating the thermoluminescent material so-called planchettes are normally used, the material being placed on these by means of forceps or a dispenser When reading, the planchette and thus indirectly the dosimeter material, is heated by an electric current The light emitted by the dosimeter is detected by means of a photomultiplier tube (PM tube), the signal of which is integrated Reader designs and measurement errors in thermo luminescent dosimetry (TLD) have been discussed by KARZMARK et coll (1966) In order to obtain reproducible results with thermoluminescence dosimetry the dosimeter material must be subjected to various types of thermal treatment The expres

Submitted for publication 12 March 1974

KITABATAKE T., YOKOYAMA M., SAKKA M. and KOGA S.: Estimation of benefit and radiation risk from mass chest radiography. Radiology 109 (1973), 37.
KOREN K., MAUDAL S., FLATBY J. and BERTEIG L.: Radiation to the gonads in diagnostic and therapeutic procedures. Acta radiol. Ther. Phys. Biol. 5 (1967), 385.
LARSSON L.-E.: Radiation doses to the gonads of patients in Swedish roentgen diagnostics. Acta radiol. (1958) Suppl. No. 157.
Radiological hazards to patients. Second report of the Committee. Her Majesty's Stationary Office, London 1960.
— Final Report of the Committee. Her Majesty's Stationary Office, London 1966.
WEBER J.: Beenmergdosis tengevolge van de Röntgendiagnostiek. (In Dutch.) Leiden 1964.

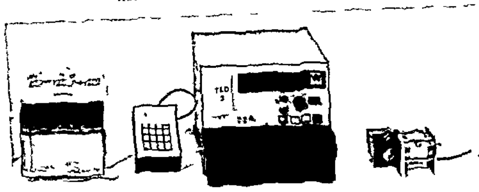


Fig 2 Instrumentation. From left to right tape punch with keyboard, reader- and calibration radiation source

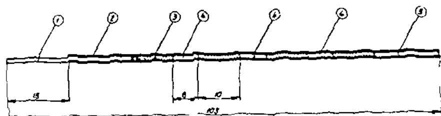


Fig 3 A measuring probe with three dosimeters (1) Rod joint (2) Outer teflon tube (3) Spacer with number (4) Dosimeters (5) Empty tube for coupling

stability when filled with teflon spacers and dosimeters Teflon tubes of this dimension are commercially available Teflon resists temperatures up to approximately 325°C without notable weight loss According to the manufacturer, six months exposure at 260 C will not result in any loss of weight At 350°C the weight loss is less than 0 5 per cent after five days

A teflon tube containing dosimeters will here be denominated a 'measuring probe' A typical measuring probe and its various components is illustrated in Fig 3 For identification of measuring probes they are allotted individual numbers placed on one of the outer teflon spacers The figures consist of lettra set and are visible through the wall of the teflon tube At one end of the measuring probe a 15 mm space is left and at the other end there is a teflon rod joint, which protrudes 15 mm By means of the rod joints, several measuring probes can be joined together forming a long series which can be read and calibrated consecutively No complete investigation of the life of measuring probes has been performed, but as long as no mechanical damage occurs a measuring probe may be used for at least 50 measurements, with a total dose of approximately 30 krad, without loss of precision However, measuring probes successfully used in daily routines for a considerably greater number of times have

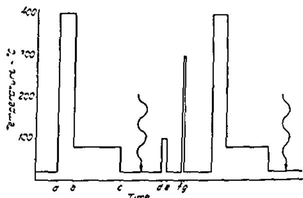


Fig 1 Schematic description of the thermal history of TLD material Thermal treatment according to ZIMMERMAN et coll (1966) Waved arrow indicates irradiation Interval a–c, pre-annealing a–b 1 5 h, b–c 24 h Interval d–e, post-annealing 10 min Interval f–g, reading, 30 s

sions 'pre-annealing' and 'post-annealing' (Fig 1) are used, depending on whether thermal treatment takes place before or after irradiation of the dosimeter Storage at room temperature must also be considered to be thermal treatment In modern instrumentation the thermal treatment is usually performed in connection with reading, by programming the heating process

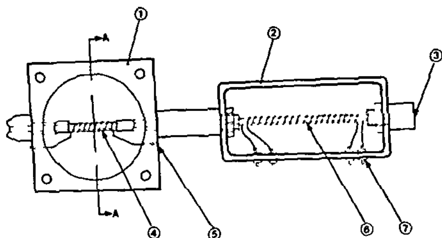
TLD has a natural place in clinical dosimetry as a substitute for, or alternative to, the condenser chambers which have previously been used (SKÖLDBORN 1959) The latter have a relatively large volume, are more or less energy-dependent, and sensitive to humidity and mechanical shock They are constructed for certain definite dose ranges, for example 300 or 500 rad The TLD dosimeter represents a major advance as regards small dimensions, energy independence, dose range and mechanical tolerance

An automated TLD system mainly intended for the dose range 1 to 500 rad has been developed to meet the needs of the radiation therapy clinic with regard to detailed dosimetry in phantoms and in vivo, primarily as a substitute for the condenser chamber The system permits simple and reliable operation and has a large measuring capacity The system consists of four main components dosimeters, reader, tape punch and a calibration radiation source (Fig 2)

Technical Description

Dosimeter material The dosimeter material consists of LiF, which occurs naturally as LiF (TLD 100), enriched on isotope ^{6}Li (TLD 600) or enriched on isotope ^{7}Li (TLD 700) These forms of LiF are delivered extruded or embedded in teflon (PTFE) in the form of cylindrical rods The usual dimensions are 1 mm × 6 mm but the length of the dosimeter can be selected arbitrarily in this system

The dosimeters are permanently enclosed in thin-walled transparent teflon tubes and separated by spacers made of teflon The lengths of the spacers can be varied within wide limits, 10 mm has proved to be suitable Teflon tubes with an internal diameter of 1 mm and an external diameter of 1 5 mm have proved to give good



ment Emitted light is detected by the photomultiplier tube which is coupled to an integrator consisting of an operational amplifier The output of the integrator is coupled to a digital voltmeter and two differentiators The signals from the differentiators are proportional to the current from the PM tube and thus proportional to the light emission from a dosimeter The signal from one of the differentiators is used to trigger punching of the integrated signal value This is done by comparing the signal from the differentiator in a comparator with a pre set reference level When the diminishing signal is beneath the reference level, the comparator gives a trigger signal which after a certain delay causes the value of the digital voltmeter to be recorded and the integrator is then zeroed After the value has been punched out, the arrival of the next dosimeter in the read out oven is awaited, which occurs within five seconds This means that the irradiated dosimeters are read and the recorded values punched out on tape while the measuring probes are transported through the instrument at a constant rate A pre set counter gives a signal when all dosimeters have been read, whereupon the motor stops and heating is interrupted

The feeder device (Fig 8) is powered by a stepper motor with electronic controls The driving gear consists of a grinding wheel against which a springloaded, plastic-coated brass wheel rests

Calibration radiation source Changes in the reflective properties of the mirror and of the light transmission in the glass tube and the teflon tube which surrounds the dosimeters necessitate frequent calibration The principle of transporting the dosimeters enclosed in measuring probes enables very simple and rapid calibration of

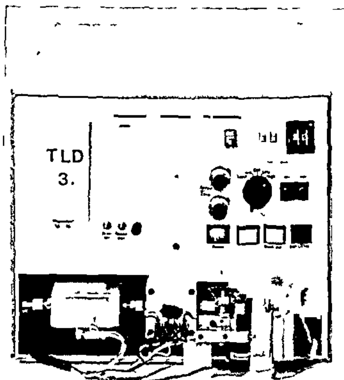


Fig 4 The reader with protective hood removed From left to right pre heater oven, read out oven and transport device

been encountered Their usability is normally limited by wear to the rod joint and the joint end of the tube, which leads to interruption of the probe chain Discolouration of the teflon tube may lead to difficulties in interpreting the number of the tube In both these situations, the probe is dismantled and the dosimeters placed in a new teflon tube marked with the same number

The reader The reader consists of the following main components transport device for measuring probes, pre-heater oven and read-out oven, optical system with PM tube, integrator and remaining electronic equipment All parts are mounted in a common instrument case (Fig 4)

The design of the preheater and read-out ovens appear in Figs 5 and 6 Heating is achieved by means of conducting coils wound round the glass tubes through which the dosimeters are transported at constant speed The temperatures in the glass tubes are maintained at pre-set values by means of an automatic regulator system coupled to a temperature sensor of resistance type, situated within the glass tubes and along their walls The glass tube in the read-out oven is mounted in a spherical chamber made of aluminium (Fig 6) The wall of the sphere is coated with silver, which has good reflective properties in the spectral range of interest The read-out chamber opens onto a light guide leading to a heat filter in front of the PM tube

The block diagram (Fig 7) illustrates the principle of the electronics of the instru-

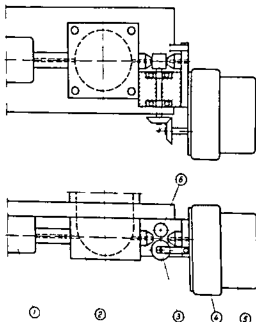


Fig. 8 Feeder mechanism for transport of measuring probes (1) Pre heater oven, (2) Read-out oven. (3) Springloaded, plastic-coated brass wheel (4) Gear box (5) Stepper motor (6) Driving gear

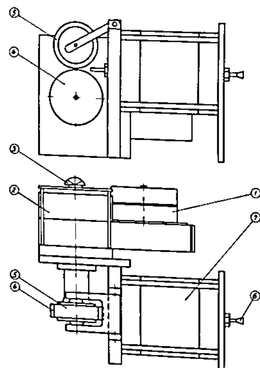


Fig. 9 [illegible] shield [illegible]

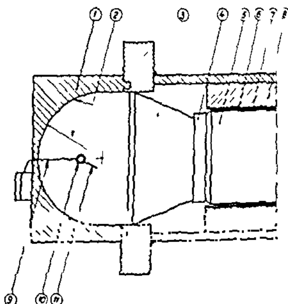


Fig 6 Cross section of the optical system The radius (r) of the spherical part of the mirror is indicated by an arrow (1) Aluminium block. (2) Silvered spherical surface (3) Perspex light guide (4) Heat filter (5) Photomultiplier tube. (6) Electrostatic shield (7) Magnetic shield (8) Thermal isolation (9) Connection for heating current (10) Glass tube. (11) Connection for temperature sensor

each individual dosimeter For this purpose, a special radiation source with a feeding mechanism has been designed (Fig. 9)

The radiation source is shielded (Fig 10) The source consists of a radioactive cylinder through which the measuring probes are passed during calibration irradia-

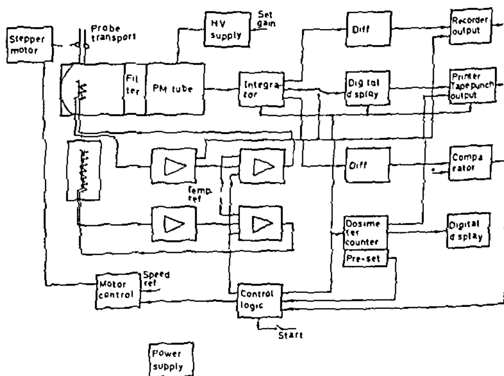


Fig 7. Electronics of the instrument, block diagram

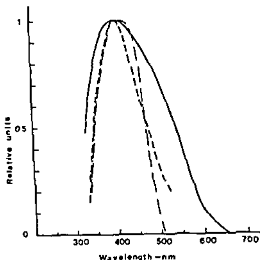


Fig 12 ——— Relative sensitivity of PM tube's photocathode - - - Relative transmission of heat absorbing filter - - - - Relative emission of LiF (TLD-100)

that absorption and reflection together caused a 2 per cent reduction in light yield Secondly, the practically dot-shaped light source was continuously moved through the glass tube by means of the feeder device Fig 14 illustrates the variation in light sensitivity along the glass tube The two lateral peaks are edge effects caused by scattered light, which penetrates into the cavity before the light source has passed the entry aperture The difference is evident between the constantly shining light source and a dosimeter which only emits light in the hot region centrally in the glass tube

Temperature distribution in the pre-heater and read out ovens The temperature distribution along the transport path through the pre-heater and read-out ovens was measured by means of a thermocouple (Copper-Constantan) enclosed in a teflon tube and surrounded by teflon bolts in the same way as a dosimeter A thermocouple used in this way cannot be said to record exactly the same temperature as a dosimeter since the thin afferent wires and the metal in the element itself cause some disturbance The thermal process recorded as a function of the position of the thermocouple along the path of transport appears in Fig 13 Measurement commences shortly before the pre-heater oven and ceases when the thermocouple leaves the read-out oven The maximum values were 130°C in the pre-heater oven and 270°C in the read-out oven

Emission of light from a dosimeter element The emission of light from the TLD material was determined in an 0 7 mm long part of a dosimeter This length-element was enclosed in a teflon tube and surrounded by teflon bolts in the same way as a whole dosimeter This test probe was irradiated and measured, the signal being recorded on a recorder at the same time as the position of the dosimeter element was marked out In Fig 15 the signal curve proportional to the light emission is

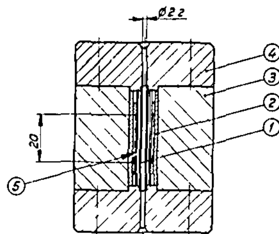


Fig. 10

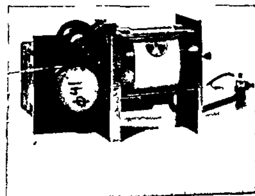


Fig. 11

Fig. 10. Calibration radiation source enclosed in radiation shield. (1) Steel tube. (2) Aluminium. (3) Lead. (4) Steel. (5) Cylindrical radiation source (^{90}Sr–^{90}Y). (By courtesy of AB Atomenergi Studsvik, Sweden.)

Fig. 11. Calibration radiation source with transport device in action.

tion at a constant and adjustable rate. The active cylinder consists of a 20 mm long aluminium tube with an internal diameter of 5.8 mm and an external diameter of 6.2 mm, coated on the outside with a layer of ^{90}Sr–^{90}Y. The coating thickness of the Sr is 2.0 mg cm^{-2} (HOLMÉR et coll. 1973). Inside the aluminium tube a thin-walled steel tube acts as an absorber. The steel tube, the dimensions of which are selected according to the dose rate required, also constitutes a mechanical shield. The feeder mechanism consists of a synchronous motor with a gearbox, a driving gear and a rubberized wheel, which due to its weight presses against the driving gear. As the gear ratio is variable, 10 different rates can be obtained. The absorbed dose which the dosimeters receive during passage is inversely proportional to the rate of transport and may be varied within a dose range of 22 rad to 22 400 rad (Fig. 11).

Function

Function of the optical system. The optical system, in combination with the heating device, has provided the greatest constructional problems. The light has to be emitted when the dosimeter is situated centrally in the glass tube. Reflection and transmission must be made optimal for the blue wavelength range concerned and thermal noise must be filtered out as far as possible. The transmission spectrum of the thermal filter together with the emission spectrum of LiF and the spectral sensitivity of the PM tube appear in Fig. 12.

For investigation of the optical system, a small quantity of a light-emitting powder was introduced into a teflon tube, surrounded by teflon bolts and compressed to a thin layer (<1 mm thick). Firstly, measurements with and without glass tube showed

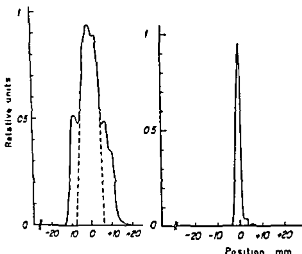


Fig 14

Fig 15

Fig 14 Sensitivity to light of the system when a dot-shaped light source was transported along the glass tube at constant speed The abscissa indicates the position of the light source in the glass tube Origo represents the centre of the glass tube

Fig 15 Emission of light from a 0 7 mm long element of a dosimeter The abscissa indicates the position of the element in the glass tube Origo represents the centre of the glass tube

MAN et coll 1966), is eliminated in the pre-heater oven The light emission as a function of position during reading of a measuring probe containing 10 dosimeters is illustrated in Fig 17 Each individual peak represents the emission of light from a dosimeter and after each peak the integrated value is punched out on tape

Dirt and dust cause great problems in all luminescence dosimetry In the procedure described here, the dosimeters are well protected since they are enclosed in a teflon tube throughout The measuring probes should be protected from dirt and cleaned routinely with 96 per cent alcohol before being placed in the apparatus The entry of small amounts of dirt into the glass tube cannot be prevented, however Cleaning is performed by passing a pipe-cleaner dipped in 96 per cent alcohol through the glass tube The read out oven should occasionally be dismantled and the glass tube cleaned with polish Since the method of measurement includes calibration irradiation and subsequent reading of the dosimeters on each occasion of measurement, any changes of sensitivity occurring will not effect the reproducibility of dose determination to any great extent Changes in sensitivity may of course occur for reasons other than soiling The dosimeters themselves alter in sensitivity due to the radiation and thermal treatments to which they are subjected All these disturbances are compensated for by the fact that each individual dosimeter is calibrated after measurement

Calibration The coupled chain of recently read measuring probes is passed through the calibration device described above The rate is selected to give the desired dose level Irradiation of a 100 cm long chain of measuring probes with 100 rad takes about half a minute After irradiation the chain of measuring probes, still intact, is reintroduced into the measuring instrument and subjected to a new reading procedure This has the advantage that the calibration values will be punched out in

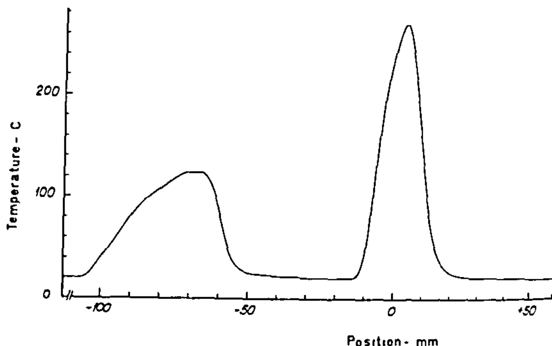


Fig 13 Temperature course recorded with a dot shaped thermocouple (Copper–Constantan) enclosed in a teflon tube Measurement commences at left, shortly before pre heater oven, and continues until the thermocouple leaves the read out oven Maximum in the pre heat oven is 130° C and in the read out oven 270° C The abscissa indicates the position of the thermocouple in the glass tube Origo represents the centre of the glass tube

demonstrated The light was emitted during a short passage in the glass tube, approximately 5 mm In Fig 16 the thermal course (from Fig 13) and the position dependence of light sensitivity (from Fig 14) are plotted, as well as the light emission from a dosimeter element (from Fig 15) with the corresponding specification of position The emission of light from a dosimeter occurs during an interval (with regard to time and position) which should give optimal conditions for measurement

Method of Measurement

Reading Before reading, the irradiated measuring probes are coupled together by means of the rod joints, forming a chain which is pushed into a 3 mm long black plastic tube which lies in coils on the bottom of the instrument case In the anterior end of the chain is inserted a leader probe which is introduced through the pre-heater and read-out ovens to the feeder mechanism Reading is commenced by pressing a button, whereupon the temperature in the pre-heater and read-out ovens rises to 130°C and 270°C respectively (measured as described above) Simultaneously, the stepper motor starts and the feeder mechanism pulls the probes at a constant rate through the system

Thermoluminescence noise, i e that part of light emission which comes from shallow traps and tends to be affected even by storage at room temperature (ZIMMER-

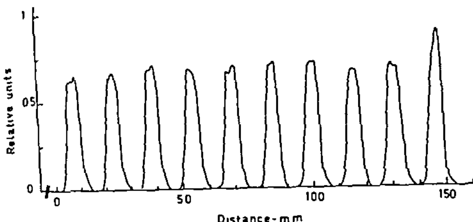


Fig 17 Emission of light on reading a measuring probe containing 10 dosimeters The abscissa indicates the distance along the probe

Advantages

The dosimeter system described has many advantages, mainly regarding practical and rational handling The measuring probes are robust and stand up to handling, and they are easy to find even if dropped on the floor The dosimeters cannot be confused or mislaid If the dosimeters are clean when the measuring probes are produced they will remain clean The surface of the probes is easy to keep clean Each measuring probe has a number and each dosimeter within a measuring probe is allotted its own number Consequently, each individual dosimeter can be referred to by a number, which enables individual calibration The individual calibration values are stored in a file in the memory of the computer and used for calculation of the absorbed dose for the dosimeter in question The main advantage of this system, however, is the high degree of automation This enables 100 dosimeters to be read in sequence without direct supervision The subsequent calibration may be considered a disadvantage since each measurement requires two reading procedures However, it does not take more than a few minutes to irradiate the probes for calibration and recommence the measurement procedure Thereafter, the instrument continues automatically until it stops after reading the last dosimeter

Acknowledgement

This work has been financed by funds made available by the Swedish Cancer Society and by the Swedish Board for Technical Development

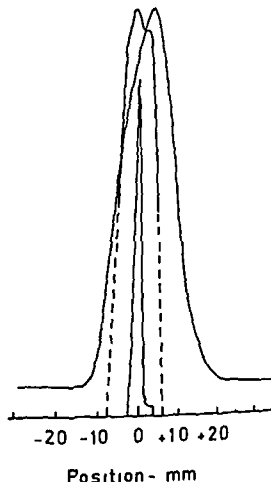


Fig 16 Variation in light sensitivity (from Fig 14) and temperature course in the read-out oven (from Fig 13) depicted together with the emission of light from a dosimeter element (from Fig 15) with equivalent specification of position

exactly the same order as the preceding measurement values, which facilitates data processing

Production of measuring probes For production of measuring probes a number of teflon tubes are placed between two perspex slabs, one of which is covered with soft rubber and the other has milled slots Firmly fixed in the slots, the teflon tubes can with ease be filled with dosimeters and teflon spacers When introduced in the teflon tubes, the dosimeter material must be clean, which it usually is when delivered If the dosimeters or spacers have been used before, they are cleaned by ultrasonic washing, rinsing in alcohol and dust-free drying in an oven

It is essential that the whole of the measuring probe be homogeneously filled with plastic material, thus maintaining constant thermal radiation, which may easily be counterbalanced when zeroing If thermal noise is perfectly counterbalanced the signal-to-noise ratio will be high If air cavities are formed at the joint between two measuring probes there is a certain risk, due to expansion, that they may separate during the reading procedure

A C T A R A D I O L O G I C A

OFFICIAL ORGAN OF THE RADIOLOGICAL SOCIETIES OF
DENMARK, FINLAND, NORWAY AND SWEDEN

Vol 14 | THERAPY PHYSICS BIOLOGY | 1975
Fasc 3 | | June

DESTRUCTION OF SMALL INTRACRANIAL TUMOURS WITH ^{60}Co GAMMA RADIATION

Physical and technical considerations

HANS DAHLIN and BERT SARBY

Benign tumours situated in the central parts of the brain, e g craniopharyngiomas, pinealomas, acoustic neurinomas and certain pituitary tumours may cause serious disturbances of the function of vital structures, either directly or through perturbation of the intracranial pressure Considerable risk is involved in the conventional surgical treatment of these tumours, both regarding postoperative deficits and mortality (OLIVECRONA 1967, BINGAS & WOLTER 1968, SUZUKI & HORI 1969, STEIN 1971) It is also difficult to ascertain whether all tumour tissue has been completely removed The possibility of destroying such tumours by means of stereotactic irradiation through the intact skull was first discussed and tested by LEKSELL (1951) Accelerated ions, such as protons or alpha particles, have also been used successfully for various targets in the head (TOBIAS et coll 1952, 1964, LARSSON et coll 1963, LAWRENCE

From the Department of [illegible]

SUMMARY

An automated TLD reader has been developed and constructed The dosimeter material consisting of LiF is permanently enclosed in thin walled teflon tubes Dosimeters are identified by numbers, which simplifies individual calibration A calibration radiation source consisting of a cylinder (^{90}Sr–^{90}Y) is used for the calibrations The function of the reader and the calibration radiation source is described, and the method of measurement briefly reported

ZUSAMMENFASSUNG

Es wurde eine automatischer TLD Leser entwickelt und konstruiert Das aus LiF bestehende Dosimetermaterial ist permanent in dunn wandigen Tefflon Behaltern verschlossen Die Dosimeter sind mit Nummern identifiziert, welche eine individuelle Kalibrierung erleichtern Eine aus einem Cylinder (^{90}Sr–^{90}Y) bestehende Strahlenquelle wird beschrieben und uber die Methode der Messung kurz berichtet

RESUMÉ

Les auteurs ont mis au point et construit un lecteur automatique de dosimétrie par thermo luminescence Le matériau dosimétrique est fait de LiF enfermé de façon permanente dans des tubes de téflon à parois minces Les dosimètres sont identifiés par des numéros, ce qui simplifie l étalonnage de chaque dosimètre Une source de radiations pour l étalonnage, faite d un cylindre de (^{90}Sr–^{90}Y) est utilisée pour les étalonnages Les auteurs décrivent le fonctionnement du lecteur et la source d étalonnage et décrivent brièvement la méthode mesure

REFERENCES

HOLMÉR A, ERICSON M, SVENSSON H and WESTLING P A ^{90}Sr–^{90}Y applicator for extra corporeal blood irradiation Acta radiol Ther Phys Biol 12 (1973) 107

KARZMARK C J, FOWLER J F and WHITE J T Problems of reader design and measurement error in Lithium Fluoride thermoluminescent dosimetry Int J appl Radiat 17 (1966), 161

SKÖLDBORN H On the design, physical properties and practical application of small condenser ionization chambers Acta radiol (1959) Suppl No 187

ZIMMERMAN D W, RHYNER C R and CAMERON J R Thermal annealing effects on the thermoluminescence of LiF Hlth Phys 12 (1966), 525

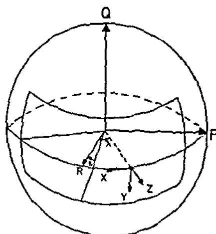


Fig 2 Spherical coordinate system for definition the beam channels in space

Proposed irradiation geometry Based on discussions with the manufacturer (AB Motala Verkstad, Motala, Sweden), a ^{60}Co construction of a similar type as the original gamma unit (LARSSON et coll 1974), was proposed The technical data were as follows (Fig 1)

(1) The 179 sources were located as close to one another as possible on a spherical surface with a radius of 38 cm between latitudes of $\pm 51°$ and longitudes of $\pm 85°$ (Fig 2) It was kept in mind that even when the largest collimator aperture is being used, no untoward radiation should hit the patient The individual sources were cylinders 1 mm in diameter, 20 mm long and of 20 Ci initial activity, identical to those used previously (SARBY 1974) The distance between adjacent sources on the spherical surface was between 59 and 92 mm

(2) The distance between the intersection point of the beam axes, the 'beam focus', and the inner edge of the collimating systems was 145 mm, in order to allow adequate space for the head and its fixture

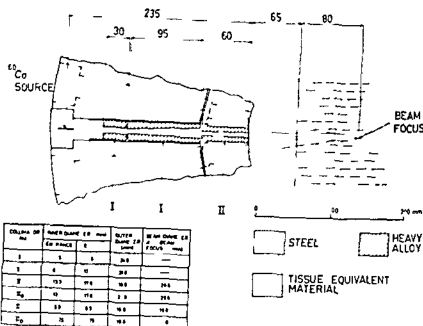
(3) The collimating system of the single beam channel consisted of three parts one non-exchangeable primary collimator made in two parts, and one beam defining exchangeable collimator It should permit definition of circular conical beams with diameters between 4 mm and 28 mm

(4) The accuracy of alignment towards an ideal beam focus must imply that all beam axes pass through a sphere with a radius of 0 3 mm

(5) The radiation protection of the patient and the staff should comply with the current recommendations for a sealed source beam therapy apparatus (ICRP 1970)

Experimental methods

Irradiation arrangements The principal outlines of model experiments arranged so as to simulate irradiations of structures in the centre of the brain are presented in Fig



et coll 1962, KJELLBERG et coll 1964, 1972, LINFOOT et coll 1971, LARSSON & SARBY 1975) The clinical advantages of such 'closed' techniques as compared with open surgical methods are reduced risks of injury to adjacent structures, bleeding, infection and operative shocks, and shorter postoperative care (LEKSELL 1966, 1971)

The aim of the present investigation was to evaluate the physical aspects of a closed multiple gamma beam technique intended for routine clinical application in patients with the above mentioned types of malformations The work is closely related to the use of small circumscribed disc shaped lesions in functional neuro surgery with the use of narrow beams of 185 MeV protons or ^{60}Co radiation (LEKSELL 1968, 1971, WENNERSTRAND & UNGERSTEDT 1970, LARSSON et coll 1974, SARBY 1974)

Technical considerations

Photon radiation in the energy range 0 5 to 10 MeV has suitable properties for precise irradiation of small intracranial structures LARSSON et coll (1974) considered both ^{60}Co gamma radiation and roentgen radiation from electron sources and recommended a multiple beam ^{60}Co gamma unit for the production of disc shaped lesions 5 to 12 mm in diameter

An irradiation technique for destruction of benign intracranial tumours should permit irradiation of spherical target volumes from 5 to 30 mm in diameter in the central parts of the brain (LEKSELL 1970)

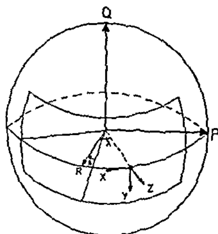


Fig 2. Spherical coordinate system for definition the beam channels in space

Proposed irradiation geometry Based on discussions with the manufacturer (AB Motala Verkstad, Motala, Sweden), a ^{60}Co construction of a similar type as the original gamma unit (LARSSON et coll 1974), was proposed The technical data were as follows (Fig 1)

(1) The 179 sources were located as close to one another as possible on a spherical surface with a radius of 38 cm between latitudes of $\pm 51°$ and longitudes of $\pm 85°$ (Fig 2) It was kept in mind that even when the largest collimator aperture is being used no untoward radiation should hit the patient The individual sources were cylinders 1 mm in diameter, 20 mm long and of 20 Ci initial activity, identical to those used previously (SARBY 1974) The distance between adjacent sources on the spherical surface was between 59 and 92 mm

(2) The distance between the intersection point of the beam axes, the 'beam focus', and the inner edge of the collimating systems was 145 mm, in order to allow adequate space for the head and its fixture

(3) The collimating system of the single beam channel consisted of three parts one non-exchangeable primary collimator made in two parts, and one beam-defining exchangeable collimator It should permit definition of circular conical beams with diameters between 4 mm and 28 mm

(4) The accuracy of alignment towards an ideal beam focus must imply that all beam axes pass through a sphere with a radius of 0 3 mm

(5) The radiation protection of the patient and the staff should comply with the current recommendations for a sealed source beam therapy apparatus (ICRP 1970)

Experimental methods

Irradiation arrangements The principal outlines of model experiments arranged so as to simulate irradiations of structures in the centre of the brain are presented in Fig

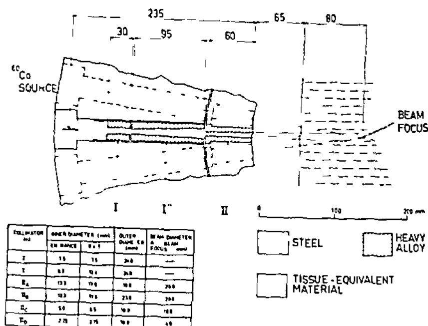


Fig 1 Experimental arrangement for determinat
of the openings (inner
The positions of adjac
contours

et coll. 1962, KJELLBERG et coll 1964, 1972, LINFOOT et coll 1971, LARSSON & SARBY 1975) The clinical advantages of such 'closed' techniques as compared with open surgical methods are reduced risks of injury to adjacent structures, bleeding, infection and operative shocks, and shorter postoperative care (LEKSELL 1966, 1971)

The aim of the present investigation was to evaluate the physical aspects of a closed multiple gamma beam technique intended for routine clinical application in patients with the above-mentioned types of malformations The work is closely related to the use of small circumscribed disc-shaped lesions in functional neurosurgery with the use of narrow beams of 185 MeV protons or ^{60}Co radiation (LEKSELL 1968, 1971, WENNERSTRAND & UNGERSTEDT 1970, LARSSON et coll 1974, SARBY 1974)

Technical considerations

Photon radiation in the energy range 0 5 to 10 MeV has suitable properties for precise irradiation of small intracranial structures LARSSON et coll (1974) considered both ^{60}Co gamma radiation and roentgen radiation from electron sources and recommended a multiple beam ^{60}Co gamma unit for the production of disc-shaped lesions 5 to 12 mm in diameter

An irradiation technique for destruction of benign intracranial tumours should permit irradiation of spherical target volumes from 5 to 30 mm in diameter in the central parts of the brain (LEKSELL 1970)

DUDLEY 1966) For the outcome of the subsequent calculation (vide infra) of the total dose distribution for all the beams in the planned clinical apparatus the dose range 0 5 to 100 per cent in the single beam was found relevant The overall uncertainty in the photographic dosimetry for points within this range, including errors in the density calibration and the densitometer reading of 3 per cent each (SARBY), was ±5 per cent, corresponding to a confidence level of 95 per cent

Outside the primary beam the spectral and directional distributions of the photons are degenerated as compared with the energy distribution at the point of calibration, and there is a risk of overestimation of the dose, which may amount to 30 per cent (SARBY) No correction was considered necessary, since the results in this region only formed the basis for qualitative comparisons of the properties of the collimator systems and a relatively rough calculation of the integral dose to the brain (Table 2)

With the 1 mm measuring spot of the densitometer a minor distortion occurred in the reproduction of the dose gradient in the penumbra region No correction of the obtained dose values was found necessary when calculating the total dose distribution (GREENE 1962)

Calculations

Superposed dose distributions The calculations were performed with a modification of a previously developed computer program (DAHLIN 1970) for superpositioning of dose distributions from arbitrarily distributed cylindrical beams in a spherical coodinate system (Fig 2) The target volume was assumed to be spherical and centrally situated in a tissue equivalent sphere with a radius of 8 cm The symmetrical space quadrants permitted reduction of the computation volume to 1/4

Idealized and proposed beam geometries Calculations were made for a number of different situations, in order to provide a basis for the clinical dosimetry

(1) Optimum multiple beam technique, sector $\beta = \pm 85°$, $\lambda = \pm 81°$ A multiple beam irradiation is thought to be optimal when the average dose gradient in the entire boundary region of the planned lesion is as large as possible In order to achieve such a situation a number of idealized beam geometries were tested The sources were positioned over the whole hemisphere as densely as possible with respect to the technical and practical requirements Each beam was assumed to give a dose of 1 inside and 0 outside the geometrical edges of the beam The most favourable situation was achieved for 223 sources distributed within $\beta = \pm 85°$ and $\lambda = \pm 81°$ (Fig 2) The result, smoothed to a spherical symmetry, is referred to below as the optimum technique (Fig 8)

(2) Idealized multiple beam technique, sector $\beta = \pm 51°$, $\lambda = \pm 85°$ Within the sector available in the suggested clinical apparatus 179 sources could be positioned Each beam was assumed, as in (1), to give a dose of 1 within and 0 outside the geometrical edges of the beam The object was to analyse the principal limitations of the technique

1 The centre of the target volume, i e the point of aim in the stereotactic localization procedure, which is to be positioned at the beam focus, was assumed in all measurements and calculations to lie at a depth of 8 cm in a polystyrene (density 1 04 g/cm³) phantom simulating an adult skull The spherical coordinate system used to define the spatial distribution of the beam channels appears in Fig 2

Four collimator combinations were constructed according to the requirements outlined above (Fig 1) The experiments were performed with the test channel used previously by SARBY, containing a cylindrical 6 Ci ^{60}Co source 1 mm in diameter and 20 mm long The collimators were made of 17 2 g/cm³ heavy alloy (90% Wo, 7% Ni, 3% Cu) with a half value layer of 7 mm for 1 25 MeV photons The beam defining collimators (II) were cone-shaped so as to define beams 28 mm (A and B) 10 mm (C) and 4 mm (D) in diameter at a depth of 8 cm The apertures of collimators II defined cones whose mantle surfaces had a radius of 0 71 mm at the centre of the source, corresponding to its cylinder of inertia

Dosimetry

Photographic dosimetry In the experimental evaluation of the dose distributions the phantom (Fig 1) was loaded with dosimetry films (Microtex) between polished polystyrene slabs perpendicular to the beam axis For each collimating system two exposures were made, one for convenient measuring of relative doses in the range 1 to 100 per cent and one, 20 times longer, for convenient measuring in the range 0 1 to 5 per cent The measurements could thus be based on the linear part of the characteristic film curve The films were developed automatically (Kodak Versamat) accompanied by separate calibration films irradiated for various periods at a phantom depth of 1 cm in a ^{60}Co beam defined by collimator A All phases of the experiments, including the film developing procedures, were performed under constant conditions

The dose distributions were determined from density distributions on the films, measured along a line through the centre of symmetry with a Quantalog densitometer, at a spot size of 1 mm

The relative depth dose distributions on the beam axis were calculated and normalized to 100 per cent at a phantom depth of 1 cm, assuming narrow beam attenuation according to SARBY The correctness of the assumption was tested experimentally The doses at a depth of 8 cm in relation to the dose at 1 cm were determined to be for collimator A 43 per cent, B 41 per cent, C 43 per cent and for collimator D 45 per cent, which is to be compared with the theoretical value 42 8 per cent

Uncertainty The photographic dosimetry was based on the assumption that the film had the same sensitivity at every point in the irradiated volume as that given by the calibration curve This situation applied within the geometrical edges of the beam and the immediately adjacent region where the film density can be attributed largely to the effect of undegraded photons (EHRLICH 1954, MAUDERLI et coll 1960,

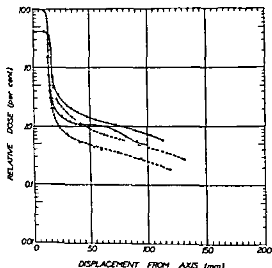


Fig. 3 Transverse dose distributions at phantom depths of 1 cm and 8 cm for single beams defined by collimators A and B Collimator A ●—● 1 cm depth, ×—× 8 cm depth Collimator B o—o 1 cm depth, Δ—Δ 8 cm depth

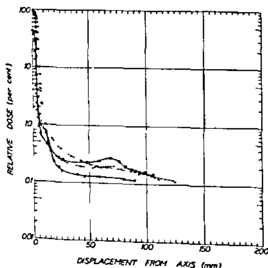


Fig 4 Transverse dose distributions at depths of 1 cm and 8 cm for a single beam defined by collimator C and a single beam defined by collimator D Collimator C o—o 1 cm depth, Δ—Δ 8 cm depth Collimator D ●—● 1 cm depth ▼—▼ 8 cm depth

The radial dose distributions obtained for all the beam alternatives are presented for depths of 1 cm and 8 cm in the phantom (Figs 3, 4) For the clinically most interesting alternatives, isodose curves are also given in a principal plane (Figs 5, 6) The doses in the diagrams are presented relative to the depth dose distribution along the beam axis as calculated by SARBY, with the reference point at a depth of 1 cm

The distribution found for the various collimators at a phantom depth of 8 cm appears in Fig 7, together with a transverse distribution for an optimized 2 5 mm wide ^{60}Co beam (LARSSON et coll 1974)

Table 1

Estimated uncertainties at various parts of the superimposed dose distributions in per cent of the central dose to the target volume for collimators B, C and D

	Central part of target volume (%)	Gradient region (%)	Outside the target volume (%)
Collimator B	±1	±19	±5
Collimator C	±1	±18	±5
Collimator D	±1	±13	±3

and the way in which the cross section of the beams influenced the distribution of the total dose for the proposed beam geometry.

(3) Proposed ^{60}Co beam geometry, sector $\beta = \pm 51°$, $\lambda = \pm 85°$ For the proposed ^{60}Co beam geometry with 179 sources, the individual conical beam approximated a circular-symmetrical, cylindrical beam for which the relative depth dose distribution on any line parallel to the beam axis was determined by the depth dose relation for narrow beam attenuation (SARBY 1974) The transverse dose profiles were determined from measurements at a depth of 8 cm in the phantom (Figs 1, 3, 4) The relative dose range of the transverse distribution at a depth of 8 cm ranged from 0 5 to 43 per cent of the maximum dose at a depth of 1 cm The effect of the geometrical simplifications was determined for collimator B by means of the transverse distribution in the single beam at phantom depths of 6 cm and 10 cm (Fig 5, Table 1) The errors due to the mathematical approximation of the measured transverse distributions by step functions were negligible

Integral doses Integral dose calculations were performed for the proposed beam geometry (3) and for the idealized multiple beam technique (2) The original skull phantom was replaced in these calculations by an approximately equivalent 13 cm cube The unit of the space matrix was 1 cm and the mean dose in each sub cube, obtained from the experimental results, was assumed to be equal to the dose value at the centre of the cube concerned The uncertainty in the integral dose (Table 2) was estimated to be ±20 per cent or less The values were overestimated as judged from the results of Monte-Carlo calculations For the latter calculations scattering and transmission in the material between adjacent beam channels in the proposed three-dimensional geometry were also taken into account (LEIMDÖRFER 1973)

Results

Dose distribution in the single beams Doses measured in the phantom on the beam axis at a depth of 8 cm for the various collimators are given on page 212 The values obtained were not significantly related to the beam size or to the design of the collimators

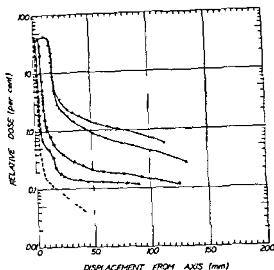


Fig 7 Comparison between the transverse dose distributions at a depth of 8 cm for single beams defined by collimators A (■), B (▲) C (●) and D (×) and the corresponding dose distribution for a 2.5 (---) mm wide ^{60}Co beam optimized for the original gamma unit (LARSSON et coll 1974) The curves have been normalized to same value (100 %) at the beam axis

Discussion

General considerations The present report concerns the planning of destruction of tumours of diameters between 5 and 30 mm with minimum risk of side effects The possibilities are dependent on the following factors, aside from diagnostic premises

(1) Accuracy in localizing and positioning of the target volume in relation to the beam focus

(2) The dose to be administered to the target volume

(3) The adaptation of the geometrical irradiation parameters and the beam channel to the target volume, which in turn determines (a) The distribution of dose absorbed by the target volume, (b) the gradient of the dose distribution at the boundary of the planned lesion, (c) the dose absorbed by tissues outside this boundary and (d) the integral dose absorbed by the brain

(4) Radiation protection of other organs

However, various individual biologic factors affect the relation between dose and local effect in the target structures and surrounding tissues (Table 3) Great demands must therefore be placed on the above mentioned factors in order to reduce as far as possible the uncertainty of the anatomic agreement between the predetermined target volume and the resulting lesion Risks of inadvertent injury to healthy structures in the brain are hereby also minimized The accuracy of positioning (1) is ± 1 mm with the present stereotactic procedure (LEKSELL 1971)

Since the tumours concerned generally approximate spheres (LEKSELL 1970) the flexibility of the technique should allow spherical dose distributions with effective

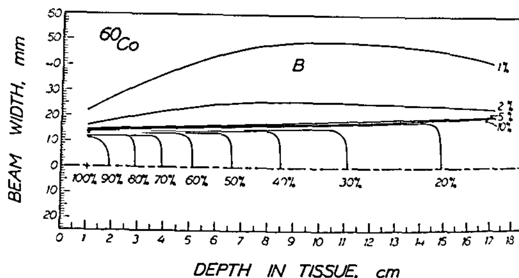


Fig. 5. Isodose diagram of a principal plane for a single beam defined by collimator B.

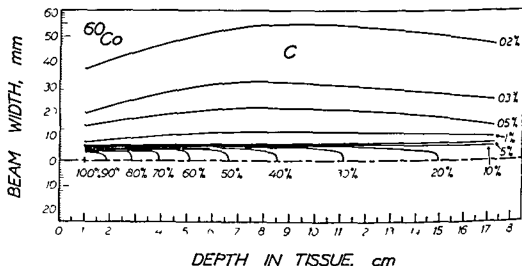


Fig. 6. Isodose diagram of a principal plane for a single beam defined by collimator C.

Superposed dose distribution. The dose on the axes P, Q and R (Fig. 2) for the optimum technique with 223 beams, the idealized multiple beam technique and the proposed beam geometry appear in Fig. 8. In one case, for collimator C, isodose diagrams are also given for the proposed beam geometry (Fig. 9).

The errors due to neglect of the divergence of the beams are summarized in Table 1. These correspond to a deviation of the positions of calculated isodose curves within ±1.5 mm for collimator B, ±0.5 mm for collimator C and ±0.15 mm for collimator D.

The integral dose to the brain for the idealized multiple beam technique with 179 beams and the proposed beam geometry for a given dose of 1 000 rad at the centre of the target volume are presented in Table 2.

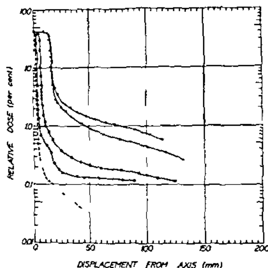


Fig 7 Comparison between the transverse dose distributions at a depth of 8 cm for single beams defined by collimators A (■), B (▲), C (●) and D (×) and the corresponding dose distribution for a 2.5 (---) mm wide ^{60}Co beam optimized for the original gamma unit (LARSSON et coll 1974) The curves have been normalized to same value (100 %) at the beam axis

Discussion

General considerations The present report concerns the planning of destruction of tumours of diameters between 5 and 30 mm with minimum risk of side effects The possibilities are dependent on the following factors, aside from diagnostic premises

(1) Accuracy in localizing and positioning of the target volume in relation to the beam focus

(2) The dose to be administered to the target volume

(3) The adaptation of the geometrical irradiation parameters and the beam channel to the target volume, which in turn determines (a) The distribution of dose absorbed by the target volume, (b) the gradient of the dose distribution at the boundary of the planned lesion, (c) the dose absorbed by tissues outside this boundary and (d) the integral dose absorbed by the brain

(4) Radiation protection of other organs

However, various individual biologic factors affect the relation between dose and local effect in the target structures and surrounding tissues (Table 3) Great demands must therefore be placed on the above mentioned factors in order to reduce as far as possible the uncertainty of the anatomic agreement between the predetermined target volume and the resulting lesion Risks of inadvertent injury to healthy structures in the brain are hereby also minimized The accuracy of positioning (1) is ±1 mm with the present stereotactic procedure (LEKSELL 1971)

Since the tumours concerned generally approximate spheres (LEKSELL 1970) the flexibility of the technique should allow spherical dose distributions with effective

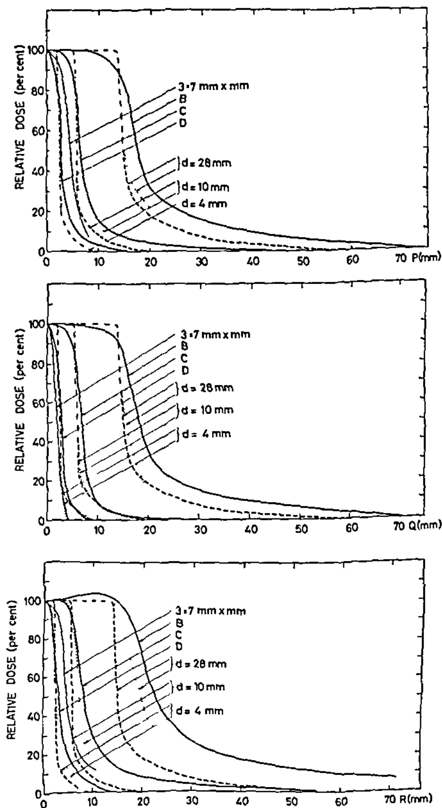


Fig 8 (For legend see opposite page)

Table 2

Integral doses absorbed in the brain phantom for the idealized multiple beam technique with 179 beams and the proposed ^{60}Co beam geometry at a given dose of 1 000 rad to the centre of the target volume

Idealized multiple beam technique		Proposed ^{60}Co beam geometry	
Beam diameter	Integral dose (kg rad)	Collimator	Integral dose (kg rad)
4 mm	2	D	14
10 mm	13	C	38
28 mm	98	B	190

diameters in the range 5 to 30 mm. A certain margin of healthy tissue should be included in the target volume to reduce the risk of recurrence. Such a technique would offer an improvement of the treatment as compared with the mechanical removal of tumour tissue (LEKSELL 1970).

Collimation of the beams. The size and mounting of the source, which cause geometrical penumbra effects, were determined by practical and technical reasons, considering self absorption. One requirement for acceptable collimation is that the geometrical penumbra should not be permitted to cause more influence on the dose distribution than the secondary electron diffusion. This condition was approximately met for the selected distance (145 mm) between the edge of the final collimator and the beam focus (SARBY 1974 and Fig. 1). Thus, for the relevant source diameter the geometrical penumbra width was 0.6 mm, at a depth of 8 cm, while the effective extension of the diffusion region outside the geometrical edges of the beam was approximately 0.5 mm.

Important factors affecting the radiation outside the geometrical edges of the beam and influencing the collimator design are (SARBY): (1) Transmission penumbra, (2) wall effects and (3) leakage radiation (i.e. transmission).

Because of the limited space for the collimators in the proposed construction the primary intention to their construction was to get the effects of leakage and scattering in the walls tolerable. The chosen condition that there should be a fixed primary collimator and an interchangeable final collimator meant that the final beam-defining collimator had to be made at a thickness of 60 mm, a maximum value, settled by technical reasons. The aim was to reduce the leakage through this colli-

Fig. 8. Superimposed dose
in the spherical
posed beam geo
β-
β
wi
et

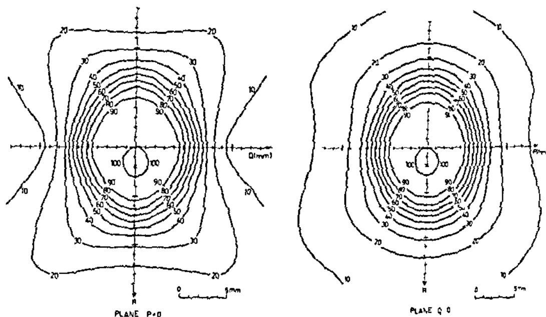


Fig 9 Calculated isodoses for the proposed beam geometry with 179 beams defined by collimator C in two perpendicular planes P 0 and Q 0 (cf Fig 2)

mator as far as possible This applied particularly for the smaller beam cross sections with limited *primary collimator* screening The contributions from leakage radiation and *transmission penumbra* for the final collimators C and D appear in the dose *range 0 2 to 1* per cent in comparison with the distribution for the 2 5 mm wide ^{60}Co beam (*Figs 4, 7*)

The primary collimator was made as thick as the practical conditions allowed *The role of the cylindrical section I' of the primary collimator is evident from Fig 3 The background dose to the brain was twice as large for collimator A as for collimator B, a fact which cannot be ignored in any clinical application An important function of the primary collimator I is also to reduce leakage to the adjacent channels (Fig 1)*

The properties of the collimator system are *illustrated in Fig 7, where the measured transverse dose distributions for a depth of 8 cm are compared with the corresponding distribution* for a *2 5* mm wide ^{60}Co beam optimized for the original gamma *unit* (LARSSON et *coll* 1974) For all the collimator alternatives in Fig 1 the gradients of the dose distributions in the penumbra region were comparable in magnitude to the gradient of the narrow ^{60}Co beams used earlier for producing lesions for functional neurosurgery However, for wider beams (represented *in the figure by alternative B*), *the straight steep section* of the dose curve in the penumbra region was shorter The relative dose outside the geometrical edges of the beam was also considerably greater than in previous clinical applications which may limit the usefulness of the technique For collimator D, 80 per cent of the dose outside the region of the steep gradient may be ascribed to leakage radiation and wall effects (SARBY) However,

Table 3

Estimated single doses for destruction of small brain tumours with the proposed ⁶⁰Co beam geometry (collimator C) Comparison between expected and tolerable doses to adjacent tissues All the tumours have been assumed to have the same size and to be enclosed by the 50 per cent isodose surface in the dose distribution

Type of tumour	Required dose at the boundary of the target volume (rad)	Dose at the centre of the target volume (rad)	Adjacent sensitive structures			Integral dose to the brain	
			Structure	Calculated maximum dose (rad)	Tolerable dose (rad)	Calculated dose (kg rad)	Tolerable dose (kg rad)
Craniopharyngioma	1 000[a]	2 000	Brain stem	1 000	1 000[e]	76	100[k]
			Optic nerves	1 000	1 500[f, g]		
			Hypothalamus	1 000	1 000[e]		
Pituitary adenoma	1 500[b]	3 000	Brain stem	500	1 000	114	100
			Optic nerves	500	1 500		
			Cranial nerves	600	4 000[f]		
Pinealoma[i]	1 250[c]	2 500	Brain stem	1 250	1 000	76	100
			Great vein of Galen	1 250	5 000[h]		
Acoustic neurinoma	2 000[d]	4 000	Brain stem	2 000	1 000	152	100
			Facial nerve	2 000	4 000[f]		
Acromegaly	2 000[b]	4 000	Optic nerves	2 000	1 500	152	100
			Cranial nerves	800	4 000		
			Sellar floor	3 000	4 000[i]–14 000[f]		
Cushing's disease	3 000[b]	6 000	Optic nerves	3 000	1 500	190	100
			Cranial nerves	1 200	4 000		
			Sellar floor	4 400	4 000–14 000		

[a] Estimated from WEISS & RASKIND (1969) BACKLUND (1973)
[b] Estimated from LINFOOT et coll (1971) KJELLBERG et coll (1972) BACKLUND (1974)
[c] Estimated from SUZUKI & HORI (1969) BACKLUND et coll (1974)
[d] Estimated value corresponding to a dose which according to LINDGREN (1958) and BERG & LINDGREN (1963) involves a considerable risk of cerebral necrosis (LEKSELL 1971 b)
[e] [illegible]
[f] [illegible] (1971)
[g] [illegible]
[h] Estimated from ARNOLD et coll (1954 b)
[i] [illegible]

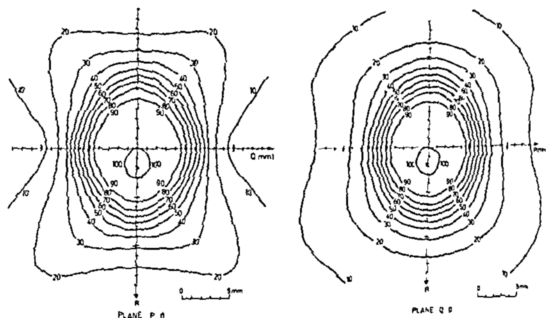


Fig 9 Calculated isodoses for the proposed beam geometry with 179 beams defined by collimator C in two perpendicular planes P = 0 and Q 0 (cf Fig 2)

mator as far as possible This applied particularly for the smaller beam cross sections with limited primary collimator screening The contributions from leakage radiation and transmission penumbra for the final collimators C and D appear in the dose range 0 2 to 1 per cent in comparison with the distribution for the 2 5 mm wide ^{60}Co beam (Figs 4, 7)

The primary collimator was made as thick as the practical conditions allowed The role of the cylindrical section I' of the primary collimator is evident from Fig 3 The background dose to the brain was twice as large for collimator A as for collimator B, a fact which cannot be ignored in any clinical application An important function of the primary collimator I is also to reduce leakage to the adjacent channels (Fig 1)

The properties of the collimator system are illustrated in Fig 7, where the measured transverse dose distributions for a depth of 8 cm are compared with the corresponding distribution for a 2 5 mm wide ^{60}Co beam optimized for the original gamma unit (LARSSON et coll 1974) For all the collimator alternatives in Fig 1 the gradients of the dose distributions in the penumbra region were comparable in magnitude to the gradient of the narrow ^{60}Co beams used earlier for producing lesions for functional neurosurgery However, for wider beams (represented in the figure by alternative B), the straight steep section of the dose curve in the penumbra region was shorter The relative dose outside the geometrical edges of the beam was also considerably greater than in previous clinical applications which may limit the usefulness of the technique For collimator D, 80 per cent of the dose outside the region of the steep gradient may be ascribed to leakage radiation and wall effects (SARBY) However,

distribution, which affects the predictability of the edge of the radiation lesion With regard to the dose gradients in the calculated dose distributions (Fig 8), the mean deviation in the alignment of the beam axes should not exceed 0 1 mm This is evident from a hypothetic extreme case with all deviations being in the same direction relative to the beam focus For this situation, the doses at the edge of the target volume at two diametrically opposite points would differ by 10 per cent (for collimator C) As a consequence, it was established that the maximum deviation for the proposed apparatus, assuming three-dimensional statistical scattering of the errors was 0 3 mm

Dose planning Estimation of the minimum dose required to destroy tumours of various types in some relevant cases is presented in Table 3 All values are recalculated to be valid for ^{60}Co radiation with the aid of RBE relationship

The conversion to single from fractionated doses was made using the data given by STRANDQVIST (1944), which data were verified for nerve tissue by LINDGREN (1958) They were also used for the pituitary irradiation with heavy charged particles (TOBIAS et coll 1964) However, the data given in Table 3 are only to be regarded as an approximate indication of applicable doses in view of the uncertainties introduced by extrapolation of single doses from fractionated doses The relationship between dose, irradiated volume and necrosis (BERG & LINDGREN 1963) was not considered and neither were individual variations in the radiation sensitivity of different structures due to age, oxygenation, possible anaesthesia etc

The doses to adjacent vital critical structures (Table 3) were calculated for relevant types of tumours in a simulated application of the dose distribution obtained for the proposed beam geometry with collimator C (Fig 9) The positions of the tumours were represented by clinical cases of normal anatomy (BACKLUND 1973) In a few cases the doses absorbed by the critical structures, often located close (tangential) to the target volumes, exceeded the estimated tolerance doses However, local overdosage near the target volume might be tolerable since the risk of injuries decreases rapidly with the dimensions of the irradiated tissue at diameters under 6 mm (BERG & LINDGREN)

The integral dose absorbed by the brain, which is directly proportional to the cross section of the beams and the dose applied to the centre of the target volume, should be acceptable for the cases of Table 3 For larger tumours, however, the integral dose may exceed the tolerable level of 100 kg rad by a factor of 2 or more (Table 2) For these situations fractionated treatment should be considered

The importance of carefully shaped dose distributions as well as an accurate localization technique cannot be overemphasized

Radiation protection External shielding, if designed in conformity with the original gamma unit, should not present any difficulties (LARSSON et coll 1974)

The radiation protection of the patient is more complicated, however, since

additional improvement of the collimation does not seem possible with the given prerequisites for the design of the beam channel

Electron irradiation from the collimator system In order to reduce the skin dose resulting from secondary electrons produced in the beam channel it may be desirable to place an electron absorber with a thickness of 0 5 g/cm² between the inner edge of the collimator and the patients head (SARBY)

Comparison of the different beam geometries A dose distribution with a steep gradient in the border region of the planned lesion is necessary for a selective destruction of a well defined tissue volume (LEKSELL et coll 1960) In the following discussion it has been assumed that the dose at the centre of the target volume should be chosen so that the edge of the lesion will coincide with the 50 per cent isodose surface

The effect of the beam collimation on the gradient of the dose distribution is evident from Fig 8 In spite of the efforts to optimize the transverse dose distribution of the single beams, a significant difference exists between the curves calculated for the proposed beam geometry and the curves representing the idealized multiple beam technique This is true both for the dose gradient in the boundary zone of the target volume and for the untoward irradiation of the surrounding tissue (Table 2) However, further improvements in the gradient could be achieved if practical considerations did not limit the spatial distribution of the beam channels, as is evident from comparison with the optimum technique (Fig 8)

In general, it may be concluded that with increasing beam diameter the gradient in the dose distribution decreases, while the integral dose increases rapidly (Fig 8, Table 2) It is also evident that the radius of the dose distribution as measured at the 50 per cent dose level is 20 to 30 per cent greater along the R axis than along the P and Q axes for the proposed geometry This eccentricity in the dose distribution, as well as the displacement of the centre of gravity obtained for wider beam cross sections represent minor deviations from the desired spherical shape

The dose distributions for collimators C and D should, however, be satisfactory for clinical applications The shapes of these distributions appear to be fully comparable with the shape of the dose distributions used clinically for functional neuro surgery with the original gamma unit (LARSSON et coll 1974) and for pituitary irradiation with light ions (TOBIAS et coll 1964, KJELLBERG et coll 1972) Whether the dose gradient is clinically acceptable in a dose distribution formed by the widest beam (28 mm) is not quite clear However, this distribution covers a larger target volume (35 mm) than those for which the technique is intended

Accuracy in the mechanical alignment of the beams Minor deviations in the mechanical alignment of the beam axes in relation to the ideal beam focus occur in a practical situation (point 4, p 211) This results in a decrease of the dose gradient at the edge of the target volume as compared with the theoretically calculated dose

Acknowledgement

This work was supported by the King Gustaf V Jubilee Foundation and the Swedish Association of Medical Radiology The collimator systems were manufactured by AB Motala Verkstad, Motala, Sweden The authors wish to thank Hans Sundqvist, Motala Verkstad, for technical co-operation

SUMMARY

The clinical and physical conditions for the destruction of small intracranial tumours by means of multiple gamma beam irradiation are evaluated The effects of the collimation of the single beam and the spatial distribution of 179 beams on the superimposed three-dimensional dose distribution are investigated experimentally and theoretically Techniques for selective irradiation of tumours of various types and sizes are discussed

ZUSAMMENFASSUNG

Die klinischen und physikalischen Bedingungen fur die Destruktion kleiner intrakranialer Tumoren mit Hilfe der multiplen Gammabestrahlungs-Technik werden festgestellt Der Effekt der Kollimation des einzelnen Strahls und die räumliche Verteilung der 179 Strahlen auf die übereinandergelagerte dreidimensionale Dosisverteilung werden experimentell und theoretisch untersucht Die Technik zur selektiven Bestrahlung von Tumoren verschiedener Typen und verschiedener Grossen werden diskutiert

RÉSUMÉ

Les auteurs étudient les conditions cliniques et physiques pour la destruction de petites tumeurs intracrâniennes au moyen de l'irradiation par des faisceaux gamma multiples Ils ont fait une [illegible]
faisceau unique [illegible]
tridimensionnelle [illegible]
de différents types [illegible] dimensions

REFERENCES

ARNOLD A, BAILEY P and HARVEY R A (a) *Intolerance* of the primate brain stem and hypothalamus to conventional and high energy radiations Neurology 4 (1954) 575

— — and LAUGHLIN J S (b) *Effects of betatron* radiations on the brain of primates Neurology 4 (1954) 165

BACKLUND E O Studies on craniopharyngiomas IV Stereotaxic treatment with radiosurgery Acta chir scand 139 (1973), 344

— Personal comm[illegible]

— [illegible]

— [illegible]

radio[illegible]

photons multiple scattered in the head and collimators may hit the body An approximate estimation of the dose to various organs is possible by comparing an irradiation situation formed by collimator C (Table 3) with the conditions around the original gamma unit, on the assumption that the number of scattered photons passing out into the body is proportional to the irradiated volume of the brain For a central dose of 2 krad, such an extrapolation gives a dose of 15 rad and 5 rad for the blood forming organs and gonads, respectively These results are probably overestimations, as may be concluded from comparison with Monte Carlo calculations later performed by LEIMDÖRFER (1973) In any case the secondary radiation doses to various organs must be carefully considered at every clinical application of the final apparatus

Conclusions

(1) Physical and technical considerations indicate that external multiple ^{60}Co beam irradiation of small intracranial tumours may be recommended for clinical trial In comparison with conventional surgery it should be possible to achieve safer treatment both in regard to the required selective tumour destruction and to possible complications

(2) In view of the biologic uncertainties and possible individual and local variations in the dose-effect relationship, the following requirements must be placed on the irradiation technique (a) The accuracy in the stereotactic procedure for positioning a particular anatomic point at the beam focus should be sufficiently high (at least $\pm$ 1 mm) (b) The dose absorbed at the centre of the tumour should be carefully selected (Table 3) (c) The applied dose distribution should present a steep gradient in the border zone of the planned radiation lesion (Fig 8) (d) The mechanical accuracy in the definition of the beam focus should be within a sphere of 0 3 mm radius

These requirements are also fundamental for the avoidance of radiation injuries to vital structures in the vicinity of the tumours (Table 3)

(3) The gradient in the superimposed dose distribution (cf 2c) is greatly dependent on the collimation and the spatial distribution of the beams The suggested apparatus limits the diameter of the accessible target volumes to a maximum of about 30 mm due to the fact that even with ideal collimation and spatial distribution the gradient in the dose distribution decreases with increasing beam diameter (Fig 8) In addition the integral dose to the brain is dependent on collimation and increases considerably with increasing beam diameter (Table 2)

(4) The following precautions should be taken at clinical application of the technique (a) Individual determination of the dose distribution for each patient, including an estimation of the risk of injury to sensitive structures The divergence of the beams as well as the anatomy of the patient must be considered in the computer routines (b) Continuous follow-up of both the biologic factors which influence the predictability of the lesions and the tolerance doses for various structures

LINDGREN M On tolerance of brain tissue and sensitivity of brain tumours to irradiation Acta radiol (1958) Suppl No 170

— Personal communications 1963 and 1973

LINFOOT J A, CHONG C Y, GARCIA J F, CLEVELAND A S, CONNELL G M, MANOUGIAN E, OKERLUND M D, BORN J L and LAWRENCE J H Heavy-particle therapy for acromegaly, Cushing's disease, Nelson's syndrome, and nonfunctioning pituitary adenomas *In* Progress in atomic medicine Recent advances in nuclear medicine Vol 3, p 219 Edited by J H Lawrence Grune & Stratton, New York 1971

MAUDERLI W, GOULD D and LANE J Film dosimetry of cobalt 60 radiation Amer J Roentgenol 83 (1960), 520

OLIVECRONE H The surgical treatment of intracranial tumours *In* Handbuch der Neurochirurgie, Vol 4, p 4 Springer, Berlin 1967

SARBY B Cerebral radiation surgery with narrow gamma beams Physical experiments Acta radiol Ther Phys Biol 13 (1974), 425

DE SCHRYVER A, WACHTMEISTER L and BÅRYD I Opthalmologic observations on long term survivors after radiotherapy for nasopharyngeal tumours Acta radiol Ther Phys Biol 10 (1971), 193

STEIN B M The infratentorial supracerebellar approach to pineal lesions J Neurosurg (1971), 197

STRANDQVIST M *Studien uber die kumulative Wirkung der Röntgenstrahlen bei Fraktionierung* Acta radiol (1944) Suppl No 55

SUZUKI J and HORI S Evaluation of radiotherapy of tumours in the pineal region by ventriculographic studies with iodized oil J Neurosurg 30 (1969), 595

TOBIAS C A, ANGER H O and LAWRENCE J H Radiological use of high energy deuterons and alpha particles Amer J Roentgenol 67 (1952), 1

— LAWRENCE J H, LYMAN J BORN J L, GOTTSCHALK A, LINFOOT J A and McDONALD J Progress report on pituitary irradiation *In* Response of the nervous system to ionizing radiation, p 19 Edited by T J Haley and R S Snider Little, Brown & Co, Boston 1964

WEISS S R and RASKIND R Non neoplastic intra sellar cysts Int Surg 51 (1969), 282

WENNERSTRAND J and UNGERSTEDT U Cerebral radiosurgery II An anatomical study of gamma radiolesions Acta chir scand 136 (1970), 133

WOODWARD H Q Some effects of X rays on bone Clin Orthop 9 (1957), 118

BERG N O and LINDGREN M Relation between field size and tolerance of rabbit's brain to roentgen irradiation (200 kV) via a slit-shaped field Acta radiol Ther Phys Biol 1 (1963), 147
BINGAS B und WOLTER M Das Kraniopharyngiom Fortschr Neurol Psychiat 36 (1968) 117
DAHLIN H Om optimering av stråldosfordelningar vid cerebral strålkirurgi (In Swedish) Internal report (GWI-R 1/70) Gustaf Werner Institute, Uppsala, Sweden 1970
DUDLEY R A Dosimetry with photographic emulsions *In* Radiation dosimetry, Vol II, p 325 Edited by F H Attix and W C Roesch Academic Press, New York and London 1966
EHRLICH M Photographic dosimetry of x- and gamma rays NBS Handbook 57 (1954)
GREENE D Observations on the effect of chamber size on measurements at the edge of an x-ray beam Brit J Radiol 35 (1962), 420
HOLDORFF B und SCHIFFTER R Strahlenspatnekrosen des Hirnstammes, einschliesslich Hypothalamus nach Bestrahlung mit ultraharten Rontgenstrahlen und schnellen Elektronen Acta neurochir 25 (1971), 37
ICRP, International Commission on Radiological Protection Protection against ionizing radiation from external sources Publication 15 Pergamon Press, Oxford 1970
KJELLBERG R N Proton beam irradiation of the pituitary *In* Clinical endocrinology, Vol 2, p 103 Edited by E B Astwood and C E Cassidy Grune & Stratton, New York 1968
— NGUYEN N C et KLIMAN B Le Bragg peak protonique en neuro-chirurgie stéreotaxique Neuro-chirurgie 18 (1972), 235
— KOEHLER A M, PRESTON W M and SWEET W H Intracranial lesions made by Bragg peak of a proton beam *In* Response of the nervous system to ionizing radiation p 36 Edited by T J Haley and R S Snider Little, Brown & Co, Boston 1964
LARSSON B and SARBY B Equipment for radiation surgery using narrow 185 MeV proton beams To be published in a Suppl to Acta radiol
— LEKSELL L and REXED B The use of high energy protons for cerebral surgery in man Acta chir scand 125 (1963), 1
— LIDÉN K and SARBY B Techniques for irradiation of small intracranial structures through the intact skull Acta radiol Ther Phys Biol 13 (1974), 512
LAWRENCE J H, TOBIAS C A, BORN J L, WANG C and LINFOOT J A Heavy-particle irradiation in neoplastic and neurologic disease J Neurosurg 19 (1962) 717
LEIMDÖRFER M Personal communication 1973
LEKSELL L The stereotaxic method and radiosurgery of the brain, Acta chir scand 102 (1951), 316
— Some principles and technical aspects of stereotaxic surgery *In* Pain, p 493 Edited by R S Knighton and P R Dumke Little, Brown and Company Inc, Boston 1966
— Cerebral radiosurgery I Gammathalamotomy in two cases of intractable pain Acta chir scand 134 (1968), 585
— Personal communication 1970
— (a) Stereotaxis and radiosurgery An operative system Charles C Thomas, Springfield, Ill 1971
— (b) A note on the treatment of acoustic tumours Acta chir scand 137 (1971), 763
— LARSSON B, ANDERSSON B, REXED B, SOURANDER P and MAIR W Lesions in the depth of the brain produced by a beam of high energy protons Acta radiol 54 (1960), 251
LIDÉN K Physikalische Grundlagen fur die Verwendung ionisierender Strahlung bei gezielter Hirnchirurgie *In* Handbuch der Neurochirurgie, Vol 6 p 199 Edited by H Olivecrona and W Tonnis Springer, Berlin 1957

LINDGREN M On tolerance of brain tissue and sensitivity of brain tumours to irradiation Acta radiol (1958) Suppl No 170
— Personal communications 1963 and 1973
LINFOOT J A, CHONG C Y, GARCIA J F, CLEVELAND A S, CONNELL G M, MANOUGIAN E, OKERLUND M D, BORN J L and LAWRENCE J H Heavy particle therapy for acromegaly, Cushing's disease, Nelson's syndrome, and nonfunctioning pituitary adenomas *In* Progress in atomic medicine Recent advances in nuclear medicine Vol 3, p 219 Edited by J H Lawrence Grune & Stratton, New York 1971
MAUDERLI W, GOULD D and LANE J Film dosimetry of cobalt 60 radiation Amer J Roentgenol 83 (1960), 520
OLIVECRONE H The surgical treatment of intracranial tumours *In* Handbuch der Neurochirurgie, Vol 4, p 4 Springer, Berlin 1967
SARBY B Cerebral radiation surgery with narrow gamma beams Physical experiments Acta radiol Ther Phys Biol 13 (1974), 425
DE SCHRYVER A, WACHTMEISTER L and BÅRYD I Opthalmologic observations on long term survivors after radiotherapy for nasopharyngeal tumours Acta radiol Ther Phys Biol 10 (1971), 193
STEIN B M The infratentorial supracerebellar approach to pineal lesions J Neurosurg (1971), 197
STRANDQVIST M Studien uber die kumulative Wirkung der Rontgenstrahlen bei Fraktionierung Acta radiol (1944) Suppl No 55
SUZUKI J and HORI S Evaluation of radiotherapy of tumours in the pineal region by ventriculographic studies with iodized oil J Neurosurg 30 (1969), 595
TOBIAS C A, ANGER H O and LAWRENCE J H Radiological use of high energy deuterons and alpha particles Amer J Roentgenol 67 (1952), 1
— LAWRENCE J H, LYMAN J, BORN J L, GOTTSCHALK A, LINFOOT J A and MCDONALD J Progress report on pituitary irradiation *In* Response of the nervous system to ionizing radiation, p 19 Edited by T J Haley and R S Snider Little, Brown & Co, Boston 1964
WEISS [illegible]
WEN[illegible]
WOODWARD H Q Some effects of X rays on bone Clin Orthop 9 (1957), 118

FROM THE DEPARTMENTS OF RADIATION PHYSICS (DIRECTOR PROF G HETTINGER) AND RADIATION THERAPY (DIRECTOR PROF L-G LARSSON), UNIVERSITY OF UMEÅ, S 901 85 UMEÅ, SWEDEN

RADIATION-INDUCED LESIONS OF THE BRACHIAL PLEXUS CORRELATED TO THE DOSE-TIME-FRACTION SCHEDULE

H SVENSSON, P WESTLING and L G LARSSON

Lesions of the brachial plexus have been reported by several authors (STOLL & ANDREWS 1966, WESTLING et coll 1967, 1972, NOTTER et coll 1970) to be a possible complication following post operative radiation therapy of mammary carcinoma WESTLING et coll (1972) found a correlation between the frequency of these lesions and the cumulative absorbed dose according to the formula of STRANDQVIST (*1944*) Further analysis of this series is now presented, also considering the number of treat ments and the dose per fraction This analysis was based on Ellis' formula (ELLIS 1968) and the mathematical treatment made according to KIRK et coll (1971) The radiation tolerance levels of the patients were expressed in a frequency distribu tion curve of the plexus lesions Observations made by STOLL & ANDREWS and NOTTER et coll also fitted well into this curve

Material and Methods

The aim of the radiation treatment was to deliver a cancerocidal absorbed dose to the regional lymph node areas through one parasternal, one supraclavicular and one

Submitted for publication 7 January 1975

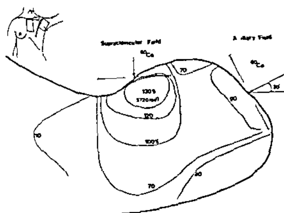


Fig 1 A typical dose distribution through the centres of the axillary and supraclavicular fields. The treatment regime for this patient is given in Fig. 2.

axillary field The treatment technique was standardized Details of the technique were given by WESTLING et coll (1972) All patients treated with this technique and at risk for radiation induced lesions during a period of 5 years or more following treatment were included, 130 patients in all

The development of the lesions and their severity have been described in the previous report (WESTLING et coll) In the present analysis no attempt was made to differentiate between different degrees of neurologic lesions Thus, in addition to motor lesions, all types of sensory disturbances were regarded as lesions, i e symptoms varying from slight numbness of the fingers to total paresthesia of the arm

The absorbed dose to the brachial plexus region was received from the axillary and supraclavicular irradiations An isodose distribution for a typical treatment appears in Fig 1 It was assumed that the affected part of the plexus was located at an average depth of 3 cm below the surface of the supraclavicular field The plexus dose was for most cases approximately equal to the maximum absorbed dose Injury to the connective tissue cells in the plexus region was thought to be the cause of the lesions (STOLL & ANDREWS 1966 WESTLING et coll 1972) The Ellis formula is probably within certain limits valid for this tissue The formula was rewritten according to KIRK et coll and the Cumulative Radiation Effect, CRE, computed

$$\mathrm{CRE} = d\ \varrho\ N^{0.65} (= D\ N^{-0.24}\ T^{-0.11}, \text{Ellis' formula})$$

where d is the daily dose to plexus in rad, $\varrho = (T/N)^{-0.11}$ is the repetition parameter, T is the total time for the treatment in days, and D is the total absorbed dose to plexus for the whole course in rad

The formula was assumed to be valid also for irregular treatment regimes Fig 2 illustrates the build up of the CRE for a typical treatment course in which a total of 5 720 rad was given in 17 fractions over a period of 23 days

The frequency of plexus lesions in patients grouped according to the CRE values

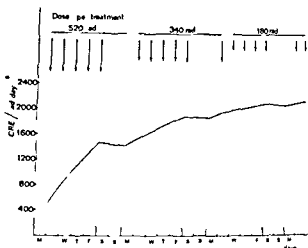


Fig. 2. The build up of the CRE-value during the treatment course.

is given in Table 1. Group No. 1 was composed of patients irradiated with ^{60}Co through two fields with a treatment schedule similar to that in Fig. 2. The total dose for these patients varied only a few per cent. The overall time, T, varied somewhat between different patients which was the major reason for the spread of the CRE-values within this group.

Three patients received CRE-values lower than those mentioned above because a larger number of fractions were given. The treatment of the supraclavicular field in these cases was completed before the irradiation of the axillary field was started. These three patients together with one who received a somewhat lower total dose, D, were included in Group 2.

Groups 3, 4 and 5 were composed of patients who received 13 to 16 MeV electron radiation through the supraclavicular field and ^{60}Co radiation on the axillary field. Both the electron and the ^{60}Co fields were irradiated on each treatment day. As a rule, the two irradiations were made within 5 to 15 minutes and may thus be regarded as one dose fraction.

CRE-values were also calculated for data on the treatment schedules for series of patients from STOLL & ANDREWS, and NOTTER et coll. The frequencies of plexus lesions reported for these patients were related to the CRE-values (Table 2).

The patients in groups 6 and 7 were irradiated with 4 MV roentgen-rays through one supraclavicular-axillary field. The irradiated volume was approximately the same as in groups 1 and 2. Group 8 was also treated with 4 MV radiation but with a large, single, supraclavicular field, as large as 22 cm by 13 cm. The patients in group 9 received 200 kV roentgen treatment against one small field 4 cm by 6 cm, to the apical axillary region. The patients in these groups were followed for at least 30 months after the end of the irradiation period.

The patients in group 10 were irradiated through one supraclavicular-parasternal and one axillary field. The irradiated volume was approximately the same as in groups 1 and 2. Some patients were also treated through an electron field to the chest

Table 1

The frequency of plexus lesions as a function of the CRE-values from the authors' material Patients irradiated on the supraclavicular field with electrons and with ^{60}Co are assigned to different groups The confidence intervals have been calculated according to CLOPPER & PEARSON (1934)

Group No	Irradiation fields		CRE-interval	Mean CRE in the interval	No of lesions/ No of patients	95 % confidence interval
	Axillary	Supra clavicular				
1	^{60}Co	^{60}Co	2 048–2 230	2 147	31/48 = 0 65	0 48–0 78
2	^{60}Co	^{60}Co	1 967–1 984	1 972	0 4 = 0	
3	^{60}Co	e^-	2 064–2 239	2 192	7/18 = 0 39	0 17–0 64
4	^{60}Co	e^-	1 851–2 037	1 921	5/30 = 0 17	0 05–0 22
5	^{60}Co	e^-	1 707–1 841	1 777	2/30 = 0 07	0 01–0 22

wall which, however, did not influence the brachial plexus dose The patients were followed for at least two years

Results

Radiation quality and volume effects The frequency of plexus lesions of 0 65 (31/48) at CRE 2 147 (rad day$^{-0\ 11}$) of the pure ^{60}Co technique should be compared with 0 39 (= 7/18) for CRE 2192 (rad day$^{-0\ 11}$) of the combined ^{60}Co and electron technique (Table 1) χ^2-test of this difference gave a p value of 0 08

A somewhat higher effect from the pure ^{60}Co treatments could be expected as the irradiated volume was larger than that of the combined technique This difference was due to the sharp dose fall-off at about 4 to 5 cm depth for the electron radiation which resulted in a high dose level within a relatively limited volume It is well established that the tolerance dose level increases as the irradiation volume is decreased The effect has been found empirically to be proportional to $(V/V_{ref})^{0\ 16}$ (RAGNHULT et coll 1973) where V_{ref} was the reference volume, in this investigation defined as the volume irradiated through the two ^{60}Co fields (groups 1 and 2), and V was the volume irradiated with the combined electron and ^{60}Co fields (groups 3, 4 and 5) From the isodose distributions, V/V_{ref} was estimated to be 0 75 The correction for volume differences resulted in a decrease of the CRE-value for group 3 from 2 192 (Table 1) to 2 093 (CRE_{corr}) rad day$^{-0\ 11}$ The expected difference in the frequency of lesions corresponded to the difference actually found between group 1 (0 65) and group 3 (0 39)

Another possible reason for the difference between groups 1 and 3 may be a difference between the RBE-values for ^{60}Co and electron radiation Some authors suggest a lower RBE [illegible]

however, was

et coll 1965)

Table 2

The CRE values for groups 6, 7, 8 and 9 determined from information given by Stoll & Andrews *(1966). Group 6 was irradiated with a peak dose of 6 300 rad in 12 increments in 25 to 25 days, group 7 with a peak dose of 5 775 rad in 11 to 12 increments in 25 to 28 days, group 8 with a peak dose between 4 650 and 5 500 rad three times weekly with increments of 400–500 rad, and group 9 with a plexus dose of 4 300–5 300 rad three times weekly during 25 to 28 days. The relative depth dose values at 3 cm depth for 4 MV roentgen-rays were taken from HPA (the Hospital Physicists' Association) 1972. The data in group 10 were taken from* Notter *et coll. (1970) and were determined from a graph given by the authors. They have estimated the dose level for low frequency lesions (≈ 15 %) as a function of the over-all time for the treatment series. This curve passes 4 800 rad over 21 days. Each week 3 to 5 treatments were given which is the reason for the CRE-interval*

Reference	Group No	Technique	CRE at plexus	Mean CRE in the interval	No. of lesions/ No. of patients	95 %-confidence level
Stoll & Andrews (1966)	6	4 MV, supraclavicular field, moderate volume	2 350	2 350	24/33 = 0.73	0.55–0.87
	7	4 MV, supraclavicular field, moderate volume	2 170	2 170	13/84 = 0.15	0.08–0.25
	8	4 MV, supraclavicular field, large volume	1 870–2 130	1 900	4/25 = 0.16	0.04–0.37
	9	200 kV, field to apical axilla, small volume	1 767–2 030	1 898	14/139 = 0.10	0.05–0.16
Notter et coll. (1970)	10	^{60}Co supraclavicular and axillary fields, moderate to large volume	1 800–2 030	1 915	≈0.15	

Uncertainty in dosimetry may also be of importance in comparing groups 1 and 3. The difference in the frequencies for the two groups corresponded to a change of approximately 5 per cent in the absorbed dose calibration. For both electron and photon radiation, the absorbed dose measurements were made with $FeSO_4$ dosimeters which were assumed to have equal sensitivity (G-value) for the two qualities. This assumption may be incorrect but the difference in sensitivity should certainly not be as great as 5 per cent. The largest error was probably due to variation in the anatomic

Table 3

The frequency for the same patient material as in Table 1 The groups of patients treated with electron- and ^{60}Co radiation on the supraclavicular fields have been combined in new groups according to CRE-values

CRE interval	Mean CRE in the interval	No of lesions/ No of patients	95 %-confidence interval
1 707–1 800	1 770	2/26 = 0 08	0 02–0 27
1 800–1 900	1 857	2/20 = 0 10	0 02–0 33
1 900–2 000	1 950	2/11 = 0 18	0 02–0 55
2 000–2 100	2 048	4/12 = 0 33	0 09–0 67
2 100–2 230	2 166	35/61 = 0 57	0 43–0 70

position of the brachial plexus The difference between groups 1 and 3 due to this variation cannot probably have exceeded a few percent

A volume dependence was probably of importance also in groups 7 and 8 These groups had approximately the same frequency of lesions while the CRE-values were considerably lower for group 8 for which a large volume was irradiated

It was more difficult to compare group 9 with the other groups as both the RBE and the technique differed from those of the remaining groups However, the frequency would appear to be in agreement with the remainder of the results from STOLL & ANDREWS if corrections were made for both the RBE and the small volume

Complications The data in Table 1 were used in order to analyse the frequency distribution as a function of CRE-value (Table 3) No classification of patients in this analysis was made with regard to the irradiation technique A possible volume or quality effect, discussed above, was thus not taken into consideration The data from Table 3 and from groups 6 and 7 in Table 2 were plotted in Fig 3 The two points in Fig 3 from STOLL & ANDREWS have been displaced along the CRE-axis in order to make them coincide with the data from Table 3, a displacement which was equivalent to multiplying the CRE-values for the two groups by a factor of 0 93 This correction was thought to be justified by the fact that dosimetric differences of this order of magnitude between hospitals are not uncommon The remaining groups in Table 2 were not included in the figure as they did not provide any further information on the shape of the curve, because groups 8 and 9 were irradiated using very different techniques compared with groups 6 and 7, and group 10 represented only a single data point from the patient material of NOTTER et coll

The fitting of the curve to the observed points was made on the assumption that the tolerance level, or more exactly, the threshold for neurologic symptoms or signs expressed as a function of CRE followed a normal distribution curve The statistical uncertainties of the different points were taken into account The solid line represented the best fitting normal distribution The curve revealed that the lesion

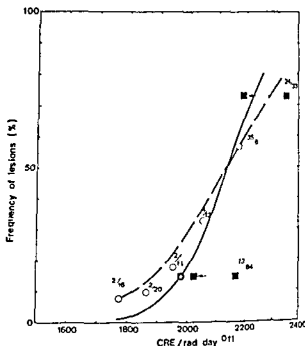


Fig 3 The frequency of neurologic lesions as a function of the CRE The open circles represent the authors' values from Table 3 The filled squares represent the data from STOLL & ANDREWS The solid line represents the best fit taking the statistical uncertainties of the different points into consideration and assuming a normal distribution of the tolerance level The solid curve is tied to a mean value from four groups of patients, indicated with a star The broken line has been constructed to analyse the uncertainty, cf text

frequency increased very rapidly above a given CRE-value An increase of 7 per cent for the CRE from 1 980 rad day$^{-0\ 11}$ in Fig 3 thus caused an increase in the lesion frequency from 15 to 50 per cent

Not only the relative but also the absolute relation between frequency of lesions and CRE could be estimated from the curve The lesion frequencies for group 4, 7, 8 and 10 lay all between 15 and 17 % The CRE-values in these groups, the means given in Tables 1 and 2, lay within the interval 1 900-2 170 with a mean value of 1 976 rad day$^{-0\ 11}$ The solid curve thus passed through CRE ≈ 1 976 rad day$^{-0\ 11}$ for a frequency of 15 %, i e the mean CRE for this frequency level for the four groups The curve was therefore tied to a fairly well established point

In comparing the three sets of data, no uniform definition of neurologic symptoms or signs was possible and the follow-up time varied considerably Both these factors may have influenced the relation between the CRE-value and the frequency The frequency of lesions for group 1 was 0 65 after 5 years and only 0 44 after 3 years The lesions which appeared late were often mild which may explain why STOLL & ANDREWS did not observe initial symptoms later than 30 months after the irradiation Differences between the series may also be due to dosimetrical, technical (e g irradiation volume and dose uniformity), biologic (RBE for group 9) and statistic factors The width of the interval, 1 976 (−5, +9 %) rad day$^{-0\ 11}$ for groups 4, 7, 8 and 10, may seem small considering the number of factors which influenced the CRE-lesion frequency relation One explanation of the narrow width might be the very rapid change of lesion frequency with the CRE-values Different definitions of lesions and different lengths of observation time (time at risk) cause only a small

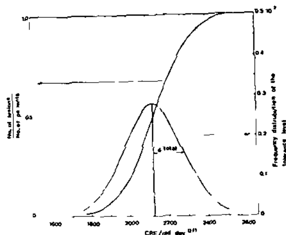


Fig. 4 The s-shaped curve is identical with the solid curve in Fig 3 (The corresponding abscissa is given to the left in the figure) This curve corresponds to a normal distribution of the dose tolerance level with $\sigma_{total}=150$ rad days$^{-0.11}$ The area under this curve from a low CRE-value to some arbitrary CRE-value is equal to the numerical value found on the s-shaped curve The area under the complete curve is unity

displacement of the frequency curve along the CRE-scale It was also significant that the maximum and minimum CRE-values came from the same hospital (groups 7 and 8) and that the difference between the frequencies for these two groups might be explained by the volume factor

Discussion

The uncertainty of the shape of the frequency—CRE-curve is dependent on dosimetric, anatomic and statistic factors The solid curve in Fig 3 was redrawn in Fig 4 to illustrate the influence of these factors It was assumed in the fitting of the curve to the observed points that the tolerance level for neurologic lesions was normally distributed The standard deviation of this best fitting normal distribution, σ_{total}, was 150 rad day$^{-0.11}$ (Fig 4) The uncertainty of this value was evaluated A standard deviation, σ_{total}, of 250 rad day$^{-0.11}$ meant that the corresponding curve (broken line, Fig 3) passed just outside the 95 per cent confidence interval of two of the observed values (filled squares, Fig 3) σ_{total} ought therefore to be less than this value

The value of σ_{total} depended on the differing sensitivity to irradiation among the patients, and also on the relative dosimetric uncertainty This may be realized from the fact that a presumed equal biologic sensitivity of all the patients, $\sigma_{biol}=0$, also meant a standard deviation, that is $\sigma_{total}=\sigma_{dos}$ The pure biologic variation of the tolerance level for the patients can be evaluated if the precision of the dosimetry can be estimated It is reasonable to assume that $\sigma_{dos}>5\%$ The uncertainty due to anatomic, dosimetric and technical factors is included in this error An error of 1 cm in the estimate of the site of the brachial plexus would alone cause an error of approximately 5 per cent In addition there are uncertainties due to technical (e g placing the patient) and pure dosimetric factors Furthermore, the numerical method

used above to determine the curves in Fig 3 probably implies an overestimate of σ_{total} and therefore also of σ_{biol} as no separation was made between the pure ^{60}Co- and the combined electron and ^{60}Co-method An upper limit for σ_{biol} can be estimated from the relation

$$\sigma^2_{total} = \sigma^2_{biol} + \sigma^2_{dos}$$

For a σ_{total} of CRE 150 rad days$^{-0\ 11}$ $\sigma_{biol} < 5\%$ The extreme curve (broken line, Fig 3) implies $\sigma_{biol} < 12\%$ Thus even with the larger of the two estimates of the biologic variation, which is not a very realistic estimate, the frequency of lesions increases very rapidly for small increases in the CRE above a threshold level

It may be suggested that the special type of analysis, i e the use of Ellis' formula which includes an exponential expression, may have caused the small standard deviation However, this fact should be of minor importance, as the repetition number, ρ, and the number of treatments, N, are nearly the same for the two sets of groups in Fig 3 The main reason for the variation in the CRE-values in Table 3 was the variation in the daily dose, d, (cf the equation page 3) among the patients (from 400 to 300 rad) A different treatment strategy for some of the patients had surely been chosen if the present knowledge of complication—dose level had been available Difficulties in the transfer of experiences from one facility to another may however arise even with this knowledge, due to uncertainties in the dosimetry HERRING & COMPTON (1970) concluded from the literature that, "since changes in the radiation dose of either plus or minus 10 per cent can give marked changes in the probability of necrosis or of local control, respectively, it is apparent that the therapist needs a system which will permit him to deliver the desired dose distribution to within ±5 per cent or possibly even more accurately" One part of their conclusions is based on the correlation between dose and symptoms for such diverse complications as severe cases of laryngeal oedema and severe sigmoiditis These observations are in agreement with the present results for brachial plexus lesions In order to obtain a reasonably low risk for such lesions it is obvious that the CRE value should not exceed about 1 900 rad day$^{-0\ 11}$

The need of this high accuracy for some situations in radiation therapy may to some extent be overcome if tables of numerical values for CRE at the tolerance level or NSD could be available (the NSD and CRE concepts have the same meaning at the tolerance level) New treatment techniques might thus be adopted more safely if the local NSD levels for some well established techniques and the technique to be adopted could be compared Some tables of this type have already been published (ELLIS 1971, RUBIN & CASARETT 1972) but more data are desirable

SUMMARY

Radiation induced brachial plexus lesions were correlated to the dose-time-fraction schedule Ellis' formula was used and the mathematical treatments were made according to

KIRK et coll (1971) It was found that the frequency of lesions increases very rapidly for small increases of CRE over a certain level

ZUSAMMENFASSUNG

Strahlenverursachte Lasionen des Plexus brachialis wurden zu dem Dosis–Zeit Fraktionierungs Schema korreliert Es wurden die Ellis'sche Formel verwendet und die mathematische Bearbeitungen entsprechend KIRK et coll (1971) vorgenommen Es zeigte sich, dass die Frequenz von Schädigungen sehr rasch mit einem kleinen Anstieg der CRE über ein gewisses Niveau hinaus anstieg

RÉSUME

Les auteurs ont établi une relation entre les lésions du plexus brachial causées par l irradiation et le schema de fractionnement de la dose en fonction du temps Ils ont utilise la formule d Ellis et le traitement mathématique a eté fait suivant la méthode de KIRK et collaborateurs (1971) Ils ont constaté que la fréquence des lésions augmente très rapidement pour de petites augmentations de l effet cumulatif des radiations au dessus d un certain niveau

REFERENCES

CLOPPER C J and PEARSON E S The use of confidence and field limits illustrated in the case of binomial Biometrika 26 (1934) 404

ELLIS F Time fractionation and dose rate in radiotherapy Front Radiat Ther Onc 3 (1968) 131

— Nominal standard dose and the ret Brit J Radiol 44 (1971), 101

HERRING D F and COMPTON D M J The degree of precision required in the radiation dose delivered in cancer radiotherapy *In* Computors in radiotherapy, p 51 Edited by A S Glicksman M Cohen and J R Cunningham The British Institute of Radiology, London 1971

HETTINGER G BERGMAN S and ÖSTERBERG S The relative biological efficiency (RBE) of 30 MeV electrons on haploid yeast Biophysik 2 (1965), 276

KIRK J GRAY W M and WATSON E R Cumulative radiation effect Part I Fractionated treatment regimes Clin Radiol 22 (1971) 145

LINDEN W A [illegible]

No[illegible]

Ra[illegible] Nordic Meeting on Clinical Physics, p 115 Edited by R Jahren Department of Medical Physics the Norwegian Radium Hospital, Montebello Oslo 3

RUBIN P and CASARETT G A direction for clinical radiation pathology The tolerance dose Front Radiat Ther Onc 6 (1972), 1

STOLL B A and ANDREWS J T Radiation induced peripheral neuropathy Brit med J 1 (1966) 834

STRANDQVIST M Studien uber die kumulative Wirkung der Rontgenstrahlen bei Fraktionierung Acta radiol (1944) Suppl No 55

SVENSSON H Dosimetri measurements at the nordic medical accelerators II Absorbed dose measurements Acta radiol Ther Phys Biol 10 (1971) 632

WESTLING P and NORDIN G Cervical plexus lesions following postoperative telecobalt therapy for carcinoma of the breast (In Swedish) 28th Congress of Scandinavian Society of Radiology 1967

— and HELE P Cervikalplexuslasioner efter postoperativ strålbehandling vid cancer mammae (In Swedish) Nord Med 80 (1968), 1636

— SVENSSON H and HELE P Cervical plexus lesions following post operative radiation therapy of mammary carcinoma Acta radiol Ther Phys Biol 11 (1972) 209

FROM THE DEPARTMENTS OF RADIATION THERAPY AND RADIATION PHYSICS, AKADEMISKA SJUKHUSET, THE UPPSALA UNIVERSITY DATA CENTER, AND THE DEPARTMENT OF COMPUTER SCIENCE, UNIVERSITY OF UPPSALA, S-750 14 UPPSALA, AND SIEMENS-ELEMA, S-171 95 SOLNA, SWEDEN.

ERRORS AND UNCERTAINTIES IN EXTERNAL RADIATION THERAPY

A system analysis with a cell kinetic model

S GRAFFMAN, T GROTH, B JUNG, G SKÖLLERMO and J-E SNELL

Various sources of inaccuracy and uncertainty in external radiation therapy may be established by error analysis but their relevance for the final outcome of the treatment is difficult to estimate from clinical data and may best be evaluated in terms of a treatment response model Such a model, based on tumour cell kinetics and a dose volume relationship for normal tissue tolerance was recently introduced and applied in treatment field optimisation (GRAFFMAN et coll 1975) Although the validity of the model is uncertain it was considered appropriate to demonstrate its use also in a preliminary analysis aiming at a gross ranking of the importance of some of the sources of inaccuracy met with in external radiation therapy Similar cell kinetic models have been proposed by FISCHER (1969, 1971 a, b), CURTIS et coll (1973), COHEN (1968, 1971), COHEN & SCOTT (1968), DIENES (1966, 1971), HEATHCOTE & WALTMAN (1973) and PREWITT (1972)

A simulated clinical situation was considered The variation in the fraction of surviving tumour cells and in the probability of zero surviving cells was estimated

Submitted for publication 11 July 1974

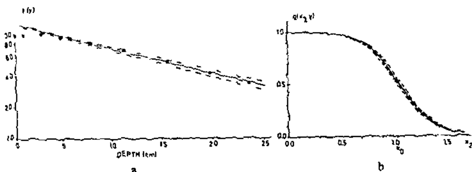
STRANDQVIST M Studien über die kumulative Wirkung der Rontgenstrahlen bei Fraktionierung Acta radiol (1944) Suppl No 55

SVENSSON H Dosimetri measurements at the nordic medical accelerators II Absorbed dose measurements Acta radiol Ther Phys Biol 10 (1971), 632

WESTLING P and NORDIN G Cervical plexus lesions following postoperative telecobalt therapy for carcinoma of the breast (In Swedish) 28th Congress of Scandinavian Society of Radiology 1967

— and HELE P Cervikalplexusläsioner efter postoperativ strålbehandling vid cancer mammae (In Swedish) Nord Med 80 (1968), 1636

— SVENSSON H and HELE P Cervical plexus lesions following post-operative radiation therapy of mammary carcinoma Acta radiol Ther Phys Biol 11 (1972) 209



was considered to consist of an inner region of constant surface cell density (10^9 cells/cm^2, equivalent to a tumour height of 10 cm and a volume density of 10^8 cells/cm^3) and a marginal zone with a radially diminishing tumour cell density (the density in this zone was described with the error function with a standard deviation equal to one sixth of the distance between the borders of the inner and outer regions) Two tumour cell populations, simulating euoxic and hypoxic cells, were considered in both regions Radiation therapy was assumed to be given in 30 fractions with two open ^{60}Co fields, one anterior and one angled posterior The tumour and treatment data for the reference case are given in the Table as well as the range of parameter values The values for the reference case are within the range of published data (TROTT 1972, MONRO & GILBERT 1961) and were selected by trial and error so that about one clonogenic cell remained after the full course of simulated irradiation

Dose calculations The dose distributions for the various cases were calculated by a computer program, incorporated in a software package (UASDOS) used routinely for dose delivery simulation at Akademiska Sjukhuset, Uppsala, and were analysed with a cell kinetic treatment response program All programs were written in FORTRAN IV and run on an IBM 370/155 computer

Body and organ outline of the patient were represented by strings of coordinates and a density factor related to the photon absorption properties within the contour

The radiation fields were calculated with a technique applying curved decrement lines. The dose, $D(x, y)$, in a point (x, y) (x = orthogonal distance from central ray of the radiation field and y = depth from patient surface) was approximated by the product of three functions

$$D(x, y) = f(y)\, g(x, y)\, ((SSD + y)/SSD)^2 \qquad (1)$$

where the first function is the central depth dose distribution, the second the trans-

Table

Parameters

Symbol	Description	Range of variation	Reference value
DMAX	Maximum dose/fraction	209–255 rad	232 rad
D_0EUOX	Mean lethal dose for euoxic cells	84–92 rad	88 rad
D_0HYPOX	Mean lethal dose for hypoxic cells	251–277 rad	264 rad
Hypox outer	Percentage of hypoxic cells in the outer tumour region	0–10 %	5 %
Hypox inner	Percentage of hypoxic cells in the inner tumour region	5–15 %	10 %
Lung	Correction factor for lung tissue	1 020–1 050	1 035
Body	The minor half-axis of the ellipse which described the body outline	8 5–10 0 cm	10 0 cm
Tumour	Extension of the outer tumour region relative to the reference case	−0 5–+0 5 cm	
Depth, b	Depth dose parameter	0 437–0 529 cm^{-1}	0 483 cm^{-1}
Weight	Weight of the posterior field	0 8–1 2	1 0
Angle	Angle of the posterior field	223°–229°	226°
Width	Field width of the posterior field	8–10 5 cm	9 5 cm

under reasonable assumptions regarding the uncertainty in some of the parameters related to (a) the clinical situation, e g patient outline and lung density, (b) the dose calculation and delivery, e g depth dose approximation, and gantry angle and (c) the cell kinetic model, e g mean lethal doses for euoxic and hypoxic tumour cells In total 15 parameters were analysed

Methods

Simulated therapeutic situation The system analysis was performed on the therapeutic situation (cf Fig 1, GRAFFMAN et coll) In the neighbourhood of the cross section the shape of the patient was approximated with right cylinders The computations were therefore limited to two dimensions only The tumour-infiltrated volume

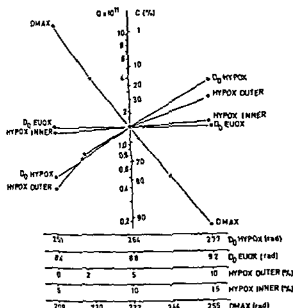


Fig 2 Surviving cell fraction, Q, and curability, C, for variation of DMAX, depth dose parameter b, correction factor for lung absorption and body and tumour out lines

Changes in dosage prescription, errors in absolute dosimetry and timing errors were simulated by ascribing different dose values to the grid point receiving the highest relative dose in the dose distribution Uncertainties in the parameters of the cell kinetic model were analysed by variation of D_0 and of the initial distribution between euoxic and hypoxic tumour cells in the inner and outer regions Variation in patient size, related to errors in the representation of the patient outline, was simulated by variation of the length of the minor half-axis of the ellipse describing the outer patient outline The importance of lung corrections was illustrated by a variation of the factor 1 035 used in the heterogeneity correction formula The parameter b in the approximation of the central depth dose distribution and the parameters p and x_0 in the transversal dose distribution were also varied at reasonable intervals (Fig 1) in order to illustrate the importance of numerical uncertainties in the field representation The remaining three parameters considered were gantry angle, weight and field width of the posterior field The latter parameters are related to errors in the delivery of treatment to the patient

Results

The results of the calculations are summarized in Figs 2 to 5

The predicted effect of the treatment, in terms of curability, C, and surviving cell fraction, Q, was sensitive to changes in the total administered dose A 220 to 244 rad increase in DMAX, the dose per fraction to the point receiving the highest

versal dose distribution and the third the beam divergency factor (SSD = source skin distance)

The central depth dose distribution was approximated by

$$f(y) = a \exp(-by) - c/(d+y) \tag{2}$$

in which the last term corrects for dose build-up. The parameters a, b, c and d were determined for each pertinent field width from empirical data (Fig 1a)

The transversal dose distribution was approximated by

$$g(x, y) = \begin{cases} (1+\exp(p(x_2 - X_0)))^{-1} & x_2 < x_0 \\ (1+\exp(p(x_2 - x_0)))^{-1} + h(x_2 - x_0) & x_2 > x_0 \end{cases} \tag{3}$$

where $x_2 = 2 \times SSD/(W(SSD+y))$ and W = field width at the body contour (Fig 1b). The parameters p, h and x_0 were determined for the appropriate field widths from measurements at y = 5, 10 and 15 cm. Polynomials were used for interpolation between these values of y

Oblique incidence was taken into account by the inverse square law. Decreased absorption in lung tissue was corrected for by multiplication of the dose in points behind the heterogeneity with, normally, 1.035^l, where l = distance (in cm) traversed in lung tissue by the ray from the source. A similar correction could be applied for osseous tissue, the correction factor then being 0.965 (BATHO 1964, JOHNS & CUNNINGHAM 1969)

The dose calculations were carried out in a net with a grid size of, normally, 1 cm

Cell kinetic model The tumour cells were considered to be concentrated in the grid points used in the dose calculations and were assumed to respond to radiation according to a single hit-multi target model (FISCHER 1969)

After 30 fractions the remaining number of surviving, clonogenic tumour cells in the grid point (i, j) was thus assumed to be

$$N_s(i,j) = N_O(i,j)(1 - (1 - \exp(-D(i,j)/D_O))^n)^{30} \tag{4}$$

where $N_O(i,j)$ is the initial number of tumour cells, D_O the mean lethal dose and n the extrapolation number

Summation over all grid points yielded the total number of initial and surviving tumour cells, N_O and N_S, respectively from which the quotient $Q = N_S/N_O$ was calculated. Assuming the total number of surviving cells to obey Poisson statistics the chance for zero surviving cells could be estimated as $C = \exp(-N_S)$. Two tumour populations were considered and the formulae above were generalized by setting $N = N' + N''$ for both subscripts

Sensitivity analysis One parameter was varied at a time, the others were kept constant and equal to their reference values (Table)

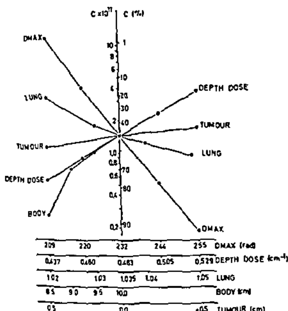


Fig 4 Surviving cell fraction, Q, and curability, C, for variation in mean lethal dose for hypoxic and euoxic tumour cells and in the fraction of hypoxic tumour cells in the inner and outer regions The variation with DMAX is included for reference purposes

Due to the pointwise representation of tumour cell density, tumour cell sensitivity and absorbed dose, the calculations might have been influenced by the choice of grid size, especially in regions where the dose or the distribution of tumour cells changed rapidly This circumstance was tested in a few cases by decreasing the grid size from 1 cm × 1 cm to 0 5 cm × 0.5 cm The absolute value of C differed by typically 3 to 4 per cent On the other hand the difference in C between two cases, in which the fraction of hypoxic cells in the outer region was 10 and 5 per cent, respectively, was found to be the same within 0 5 per cent for the two grid sizes

Discussion

The results reported here are strongly related to the model situation chosen It is believed that the dose distribution, the absolute dose and the fractionation scheme may be representative for a clinical case but there might be considerable variation in the relative distribution of tumour cells, the absolute number of tumour cells, the fraction of hypoxic tumour cells and the sensitivity of euoxic and hypoxic tumour cells to radiation

The cell kinetic formalism, as applied here, has been questioned from clinical grounds (FLETCHER 1973) and it does not take into account effects such as cell loss, cell repopulation and reoxygenation during therapy (CURTIS et coll 1973) It also neglects changes in the sensitivity of euoxic and hypoxic tumour cells during the course of irradiation as well as a more gradual dependence of mean lethal dose and extrapolation number on local oxygen concentration (LITTBRAND & RÉVÉSZ 1969)

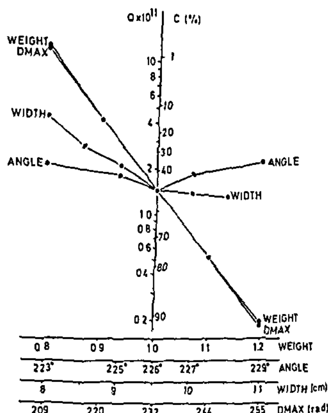


Fig 3 Surviving cell fraction, Q, and curability, C, for variation in weight, angle and width of the posterior field The variation with DMAX is included for reference purposes

relative dose in the reference case, decreased Q with a factor 8 and increased C from 0 14 to 0 75 This relation is given in all three figures for reference purposes

As illustrated in Fig 2, also reasonable changes in the lung correction factor, the body half-axis, the tumour extent and the depth-dose parameter b (Fig 1 a) induced quite sizable changes in Q and C On the other hand, the effects on Q and C from changes in the approximation of the transversal dose distribution (*Fig* 1 b) were negligible and are not illustrated It is believed that the ranges of the parameters displayed in Fig 2 reflect uncertainty and common measuring errors in the pertinent parameters rather realistically

It may be seen that reasonable errors in the angle of incidence of the posterior field and in its width induced rather small changes in Q and C (Fig 3) Only when the width of the field was so narrow that it did not cover the tumour region adequately did Q increase and C drop correspondingly Even small changes in the weight of the posterior field induced drastic changes in Q and C since the weight directly influenced the absolute dose in the tumour region (Fig 5)

The predicted treatment response was significantly influenced by the fraction of hypoxic cells in the outer region and by their mean lethal dose, whereas accurate knowledge about the mean lethal dose of euoxic cells and the fraction of hypoxic cells in the inner region was not critical for the particular case (Fig 4)

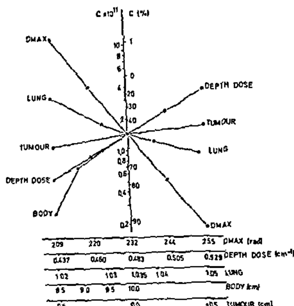


Fig 4 Surviving cell fraction, Q, and curability, C, for variation in mean lethal dose for hypoxic and euoxic tumour cells and in the fraction of hypoxic tumour cells in the inner and outer regions The variation with DMAX is included for reference purposes.

Due to the pointwise representation of tumour cell density, tumour cell sensitivity and absorbed dose, the calculations might have been influenced by the choice of grid size, especially in regions where the dose or the distribution of tumour cells changed rapidly This circumstance was tested in a few cases by decreasing the grid size from 1 cm × 1 cm to 0 5 cm × 0 5 cm The absolute value of C differed by typically 3 to 4 per cent On the other hand the difference in C between two cases, in which the fraction of hypoxic cells in the outer region was 10 and 5 per cent, respectively, was found to be the same within 0 5 per cent for the two grid sizes

Discussion

The results reported here are strongly related to the model situation chosen It is believed that the dose distribution, the absolute dose and the fractionation scheme may be representative for a clinical case but there might be considerable variation in the relative distribution of tumour cells, the absolute number of tumour cells, the fraction of hypoxic tumour cells and the sensitivity of euoxic and hypoxic tumour cells to radiation

The cell kinetic formalism, as applied here, has been questioned from clinical grounds (Fletcher 1973) and it does not take into account effects such as cell loss, cell repopulation and reoxygenation during therapy (Curtis et coll 1973) It also neglects changes in the sensitivity of euoxic and hypoxic tumour cells during the course of irradiation as well as a more gradual dependence of mean lethal dose and extrapolation number on local oxygen concentration (Littbrand & Révész 1969)

conclusions can be drawn from such models, i e conclusions that are valid for all the models and parameter values which are not directly excluded by empirical facts Work along both these lines seems to be worthwhile and advanced model building necessary for a fuller understanding of what happens when a tumour is eradicated by ionising radiation Only with a synthesis of facts from a vast experience from pertinent fields, inserted in a quantitative formalism may the existing information best be exploited and the importance of various known and unknown factors be indicated

Conclusions

A sensitivity analysis of external radiation therapy with regard to various sources of error and uncertainty was performed by means of a simple single hit multi target cell kinetic model, applied to a simulated clinical situation Factors directly influencing the dose to the tumour cells were found to dramatically influence the number of remaining clonogenic tumour cells One such factor is the target dose per fraction, but also corrections for diminished photon absorption in lung tissue and changes in body outline, within ranges of clinical uncertainty, appeared to be of considerable importance The same seemed to be true also of depth dose approximations used in automatic dose calculations Of less importance are errors in gantry angle and field width, provided the composite radiation field covers the tumour region adequately An accurate knowledge of the extension and cellular composition of the tumour bearing volume seems to be necessary for predictive purposes

SUMMARY

The relative importance of accurate knowledge and control of various biologic and physical factors in external radiation therapy was estimated with a simple cell kinetic treatment response model for a simulated tumour therapy situation A set of parameter values was chosen for a reference case so that the calculated probability of zero surviving tumour cells was about 0 5 The parameters were varied one at a time over a range that was considered representative with respect to uncertainty in dose calculation dose delivery and the description of the pertinent patient data Also parameters in the cell kinetic model were varied

The calculations demonstrated a strong influence on the number of surviving cells from even moderate changes in the parameters which affect the tumour dose Predictions with regard to curability are heavily dependent on the reliability of the biologic parameters in the model

ZUSAMMENFASSUNG

Die relative Bedeutung der genauen Kenntnis und Kontrolle der verschiedenen biologischen und physikalischen Faktoren bei der externen Strahlentherapie wurde an einem einfachen zellkinetischen Behandlungs Respons Modell um die Therapie Situation zu simulieren bestimmt Fur den Referenzfall wurde eine Reihe von Parameterwerten so gewählt dass die berechnete Wahrscheinlichkeit fur das Null Überleben der Tumorzellen etwa 0 5 betrug

Die Parameter wurden einzelnd uber einen Bereich, der als repräsentativ im Hinblick auf die Unsicherkeit bei der Dosisberechnung, der verabfolgten Dosis und der Beschreibung der entsprechenden Patienten-daten angesehen wurde, verändert Es wurden ebenfalls die Parameter des zellkinetischen Modells verändert Die Berechnungen zeigten einen starken Einfluss auf die Zahl der uberlebenden Zellen auch bei mässigen Änderungen derjenigen Parameter, die die Tumordosis beeinflussen Voraussagen hinsichtlich der Kurabilität sind weitgehend von der Gultigkeit der biologischen Parameter des Modells abhängig.

RÉSUMÉ

L'importance relative d'une connaissance précise et de l action sur différents facteurs biologiques et physiques dans le traitement par l irradiation externe a été estimée grâce à un modèle simple de réponse au traitement de la cinétique cellulaire pour une simulation de traitement de tumeur Un ensemble de valeurs de paramètres a éte choisi pour un cas de référence de façon que la probabilité calculée de survie nulle de cellules tumorales soit d environ 0,5 Les paramètres ont eté modifiés l un après l'autre dans un domaine qui a été considere comme representatif, compte tenu de l'imprécision du calcul de dose, de la dose délivree et de la description des donnees du malade concerne On a fait varier aussi les parametres du modèle de cinetique cellulaire Les calculs ont montre que meme des

REFERENCES

BATHO H F Lung corrections in Cobalt 60 beam therapy J Canad Ass Radiol 15 (1964) 79

BLOEDORN F G Rationale and benefit of preoperative irradiation of lung cancer J Amer med Ass 9 (1966) 340

COHEN L Theoretical 'iso-survival' formulae for fractionated radiation therapy Brit J Radiol 41 (1968), 522.

— A cell population kinetic model for fractionated radiation therapy I Normal tissues Radiology 101 (1971), 419

— and SCOTT M J Fractionation procedures in radiation therapy A computerized approach to evaluation Brit J Radiol 41 (1968), 529

CURTIS S B BARENDSEN G W and HERMENS A F Cell kinetic model of tumour growth and regression for a rhabdomyosarcoma in the rat Undisturbed growth and radiation response to large single dosis Europ J Cancer 9 (1973), 81

DIENES G J A kinetic model of biological radiation response Radiat Res 28 (1966), 183

— Survival curves and dose fractionation Some general characteristics Radiat Res 48 (1971), 551

FISCHER J J Theoretical considerations in the optimisation of dose distribution in radiation therapy Brit J Radiol 42 (1969), 925

— (a) Mathematical simulation of radiation therapy of solid tumours I Calculations Acta radiol Ther Phys Biol 10 (1971), 73

— (b) Mathematical simulation of radiation therapy of solid tumours II Fractionation Acta radiol Ther Phys Biol 10 (1971), 267

FLETCHER G H Clinical dose response curves of human malignant epithelial tumours Brit J Radiol 46 (1973), 1
FOWLER J F The rationale of dose fractionation *In* Frontiers of radiation therapy and oncology Vol 3, p 6 Edited by J M Vaeth S Karger, Basel New York 1968
GRAFFMAN S and JUNG B Clinical trials in radiotherapy and the merits of high energy protons Acta radiol Ther Phys Biol 9 (1970), 1
— GROTH T, JUNG B, SKÖLLERMO G and SNELL J E Cell kinetic approach to optimizing dose distribution in radiation therapy Acta radiol Ther Phys Biol 14 (1975) 54
HEATHCOTE H W and WALTMAN P Theoretical determination of optimal treatment schedules for radiation therapy Radiat Res 56 (1973), 150
JOHNS H E and CUNNINGHAM J R The physics of radiology, p 457 Charles C Thomas Springfield Ill, 1969
LITTBRAND B and RÉVÉSZ L The effect of oxygen on cellular survival and recovery after radiation Brit J Radiol 42 (1969), 914
MUNRO T. R and GILBERT C H The relation between tumour lethal doses and the radiosensibility of tumour cells Brit J Radiol 34 (1961), 246
PREWITT J M S A radiobiological model for optimizing radiation treatment *In* Proceedings from 4th International Conference on Computers in Radiotherapy 1972
TROTT K R Strahlenwirkungen auf die Vermehrung von Saugetierzellen *In* Encyclopedia of Medical Radiology Vol II/3 g p 43 Edited by O Hug and A Zuppiger Springer Verlag, Berlin 1972
VAN PUTTEN L M and KALLMAN R F Oxygenation status of a transplantable tumour during fractionated radiation therapy J nat Cancer Inst 40 (1968), 441

FROM THE GYNECOLOGIC SECTION (DIRECTOR J E JOHNSSON), DEPARTMENT OF RADIATION THERAPY, AND THE DEPARTMENT OF RADIATION PHYSICS (DIRECTOR PROF K LIDÉN), UNIVERSITY HOSPITAL, S 221 85 LUND, SWEDEN

DOSIMETRY OF COMBINED INTRACAVITARY AND EXTERNAL IRRADIATION OF CARCINOMA OF THE UTERINE CERVIX

J E JOHNSSON and ULLA BRITA NORDBERG

Intracavitary irradiation plays an important role in treatment of carcinoma of the uterine cervix The rather high gradient of dose distribution around the intracavitary applicators prevents giving an adequate dose to more than a limited volume of tissue, and thus necessitates complementary external irradiation to the peripheral parts of the parametrium and to the regional lymph nodes, in order to obtain a satisfactory absorbed dose in these regions This complementary treatment is given with various methods at different centres and the dose distribution between the intracavitary and the external treatment also varies (FLETCHER et coll 1962 [illegible]

[illegible] treatment is often given first and then supplemented with external irradiation

The purpose of the present report is to demonstrate the difficulties which are met in obtaining an adequately summarized distribution of dose in the entire treatment volume when external treatment is given after intracavitary treatment with a full tumour dose to the primary tumour

Submitted for publication 19 September 1974

Table 1

Differences in angle at two radium treatments between the intrauterine applicators projected in the frontal plane

No of cases	Angle°
1	0
4	5
7	10
1	15
1	30
Mean value	10^{+20}_{-10}

Material and Methods

Fifteen patients with carcinoma of the uterine cervix in Stages I and II were investigated

Intracavitary treatment was given with a rod shaped intrauterine applicator (Ø7 mm × 68 mm, 90 mCi ^{226}Ra) fixed by a special locking device to a flat vaginal applicator (5 mm × 44 mm × 44 mm, 110 mCi ^{226}Ra) (JOHNSSON & NORDBERG 1973) This locking device holds the applicators in a fixed relation to one another during the course of treatment, and thus enables getting a well-defined distribution of dose around the applicators Two equal treatments were given with an interval of three weeks The total dose in Point A, which lies 2 cm laterally and 2 cm cranially from the intrauterine applicator's point of contact with the vaginal applicator (approximately external os) was 6 500 rad (Fig 1)

The angle of the longitudinal axis of the uterus and the position of the portio in the true pelvis during the two intracavitary treatments and during external irradiation have proved to be of significance

Changes in the position of the combined applicators in the true pelvis between the two treatments have been expressed as the difference in the angle of the intrauterine applicator and the difference in the position of the portio in the true pelvis on the two treatment occasions Only measurements of projections in the frontal plane were performed

Films were exposed immediately after application of the combined intracavitary applicators at 29 treatment occasions in 14 patients at two successive treatments Establishment of the position of the portio without intracavitary applicators inserted was done in all of the patients One or two days after intracavitary treatment, a light metal sound with a cross-piece in one end was inserted in the uterus The cross-piece was attached to the portio with a clip, and films were then taken The enlargement factor was kept constant

Results

The differences in angle and in the positions of the applicator and the portio in the frontal projection at the two treatments appear in Tables 1 and 2

Table 2

Distances between the position of the portio projected in the frontal plane at two radium treatments

Left right		Cranial–caudal	
No of cases	cm	No of cases	cm
2	0	6	0
9	0 5	2	0 5
3	1	4	1 0
		1	1 5
		1	2.5
Mean value	0 5±0 5	Mean value	$0\ 6^{+1\ 9}_{\ \ 0\ 6}$

In no case was the position of the uterus the same on both treatment occasions nor was the position of the portio the same with the intracavitary applicators inserted as without them Only variations detectable in the frontal plane were investigated Changes of the uterus during the actual intracavitary treatment were not considered

The differences in the position of the portio with and without the radium applicators inserted appear in Table 3

Discussion

External treatment is often given following intracavitary irradiation in order to increase the dose in the middle and lateral parts of the parametrium and in the regional lymph nodes on the pelvic walls either with central shielding with lead blocks (KOTTMEIER 1964, CAMPBELL & DOUGLAS 1966, COWELL & LAURIE 1967) or with the multiple fields technique, alternatively with arc therapy (FRIESCHBIER & SEIFERT 1965 OBERHEUSER & SCHUBERT 1965, KAHR & SCHREYER 1968), so that only small additional doses are given to the central parts of the true pelvis

The dose decreases so rapidly with increasing distance from the intracavitary applicators that it is difficult to obtain a satisfactory distribution of dose in the transitional zone between the intracavitary and external treatment areas The dose around the combined applicators used in this material during the entire course of treatment fell from 6 500 to 3 600 rad within 1 cm in a region where no considerable dose reduction was desired The complementary dose from the external irradiation ought thus to increase rapidly in this region The precision required in setting up such a treatment would, however, be practically impossible to attain in routine clinical practice, irrespective of whether central shielding with lead blocks is used, or if multiple fields technique is employed

The reduction of dose from 6 500 to 3 600 rad is dependent on the position of the applicators being exactly the same on the two occasions of treatment It was not possible to verify this circumstance in any of the present cases The different positions

Table 1

Differences in angle at two radium treatments between the intrauterine applicators projected in the frontal plane

No of cases	Angle°
1	0
4	5
7	10
1	15
1	30
Mean value	10^{+20}_{-10}

Material and Methods

Fifteen patients with carcinoma of the uterine cervix in Stages I and II were investigated

Intracavitary treatment was given with a rod shaped intrauterine applicator (Ø7 mm × 68 mm, 90 mCi ^{226}Ra) fixed by a special locking device to a flat vaginal applicator (5 mm × 44 mm × 44 mm, 110 mCi ^{226}Ra) (JOHNSSON & NORDBERG 1973) This locking device holds the applicators in a fixed relation to one another during the course of treatment, and thus enables getting a well defined distribution of dose around the applicators Two equal treatments were given with an interval of three weeks The total dose in Point A, which lies 2 cm laterally and 2 cm cranially from the intrauterine applicator s point of contact with the vaginal applicator (approximately external os) was 6 500 rad (Fig 1)

The angle of the longitudinal axis of the uterus and the position of the portio in the true pelvis during the two intracavitary treatments and during external irradiation have proved to be of significance

Changes in the position of the combined applicators in the true pelvis between the two treatments have been expressed as the difference in the angle of the intrauterine applicator and the difference in the position of the portio in the true pelvis on the two treatment occasions Only measurements of projections in the frontal plane were performed

Films were exposed immediately after application of the combined intracavitary applicators at 29 treatment occasions in 14 patients at two successive treatments Establishment of the position of the portio without intracavitary applicators inserted was done in all of the patients One or two days after intracavitary treatment, a light metal sound with a cross piece in one end was inserted in the uterus The cross piece was attached to the portio with a clip, and films were then taken The enlargement factor was kept constant

Results

The differences in angle and in the positions of the applicator and the portio in the frontal projection at the two treatments appear in Tables I and 2

Table 2

Distances between the position of the portio projected in the frontal plane at two radium treatments

Left–right		Cranial–caudal	
No of cases	cm	No of cases	cm
2	0	6	0
9	0.5	2	0.5
3	1	4	1.0
		1	1.5
		1	2.5
Mean value	0.5±0.5	Mean value	$0.6^{+1.9}_{-0.6}$

In no case was the position of the uterus the same on both treatment occasions nor was the position of the portio the same with the intracavitary applicators inserted as without them Only variations detectable in the frontal plane were investigated. Changes of the uterus during the actual intracavitary treatment were not considered

The differences in the position of the portio with and without the radium applicators inserted appear in Table 3

Discussion

External treatment is often given following intracavitary irradiation in order to increase the dose in the middle and lateral parts of the parametrium and in the regional lymph nodes on the pelvic walls either with central shielding with lead blocks (KOTTMEIER 1964, CAMPBELL & DOUGLAS 1966, COWELL & LAURIE 1967) or with the multiple fields technique, alternatively with arc therapy (FRIESCHBIER & SEIFERT 1965, OBERHEUSER & SCHUBERT 1965, KAHR & SCHREYER 1968), so that only small additional doses are given to the central parts of the true pelvis

The dose decreases so rapidly with increasing distance from the intracavitary applicators that it is difficult to obtain a satisfactory distribution of dose in the transitional zone between the intracavitary and external treatment areas The dose around the combined applicators used in this material during the entire course of treatment fell from 6 500 to 3 600 rad within 1 cm in a region where no considerable dose reduction was desired The complementary dose from the external irradiation ought thus to increase rapidly in this region The precision required in setting up such a treatment would, however, be practically impossible to attain in routine clinical practice, irrespective of whether central shielding with lead blocks is used, or if multiple fields technique is employed

The reduction of dose from 6 500 to 3 600 rad is dependent on the position of the applicators being exactly the same on the two occasions of treatment It was not possible to verify this circumstance in any of the present cases The different positions

Table 3

Differences in the position of the portio with and without the radium applicators projected in the frontal plane

Left–right		Cranial–caudal	
No of cases	cm	No of cases	cm
6	0	3	0
12	0 5	4	0 5
8	1 0	2	1 0
2	1 5	3	1 5
1	2 0	7	2 0
		8	2 5
		1	3 0
		1	4 5
Mean value	$0\,7^{+1\,3}_{\;\;0\,7}$	Mean value	$1\,7^{+2\,8}_{\;\;1\,7}$

of the applicators during the two treatments, and uncontrolled movements during the actual treatment time reduce the steepness of the dose gradient, which is an advantage when setting up the treatment with central shielding When shielding with lead blocks is used, however, it must be individually designed, at least for thin or stout patients (WALTZ et coll 1973) The variations in the position of the applicators ought also to be advantageous when using the multiple fields technique Due to the differences in size of the cross-section of the patient and the position of the applicators, multiple fields technique cannot be standardized Size, form and position of the fields, and the direction of the central beam must all be individually planned

The resultant position of the intracavitary applicators in relation to easily ascertainable skeletal structures in the true pelvis must also be defined for each individual case, regardless of whether central shielding or multiple fields technique is used, in order to obtain adequate complementary external irradiation

Roentgen examination of a few patients during the treatment period showed that uncontrolled movements projected into the frontal plane were insignificant

Variation in the position of the portio also occurred both when the combined applicators were inserted and when they were not inserted—in some cases considerably The portio sank caudally when the applicators were taken out, sometimes also laterally No corrections for varying contents in the bladder and intestines or for

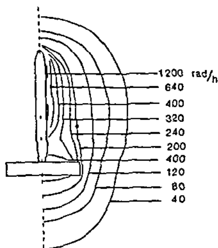


Fig 1 Isodose distribution around the uterine and vaginal applicators in ideal position The numbers represent the absorbed dose in rad/h Point A, marked by a dot, lies 2 cm laterally and 2 cm cranially from the point of contact between the intrauterine and vaginal applicators

prone and supine position of the patient were carried out However, the variations of the position of the uterus under normal conditions seem to be slightly projected into the frontal plane

The distribution of absorbed dose in the cervix and its surroundings was calculated in four hypothetical cases in order to get an idea of the importance of the positional variations of the uterus In all four cases, 6 500 rad were given to Point A (Fig 1), primarily from the intracavitary radium

The distribution of absorbed dose laterally from the axis of the uterus was calculated 3 cm cranially from the portio No dose contribution from the external irradiation was assumed to be added to Point A The total dose to the pelvic wall which was desired was about 4 000 rad

For reducing the dose contribution from external irradiation to already heavily irradiated tissues, an ideal central shielding block was used with the shielding effect of the central part hypothetically assumed to be total The dose from external and intracavitary treatment was simply summarized, and no attempt was made to equalize their different biologic effects (ELLIS & SORENSEN 1974)

The postulated transverse diameter of the uterine cervix was 3 cm The longitudinal axis of the uterus was assumed to be *parallel to the axis of symmetry of the true pelvis*, and the position of the combined intracavitary applicators at two successive treatments to be the same The position of the sigmoid in the true pelvis is not thought to be affected by the different positions of the uterus (with and without applicators inserted) but parts of the bladder are attached to the isthmus, so that its position is dependent on the uterus

Case I The pos[illegible]

as without the [illegible]

Table 3

Differences in the position of the portio with and without the radium applicators projected in the frontal plane

Left–right		Cranial–caudal	
No of cases	cm	No of cases	cm
6	0	3	0
12	0.5	4	0.5
8	1.0	2	1.0
2	1.5	3	1.5
1	2.0	7	2.0
		8	2.5
		1	3.0
		1	4.5
Mean value	$0.7^{+1.3}_{0.7}$	Mean value	$1.7^{+2.8}_{1.7}$

of the applicators during the two treatments, and uncontrolled movements during the actual treatment time reduce the steepness of the dose gradient, which is an advantage when setting up the treatment with central shielding When shielding with lead blocks is used, however, it must be individually designed, at least for thin or stout patients (WALTZ et coll 1973) The variations in the position of the applicators ought also to be advantageous when using the multiple fields technique Due to the differences in size of the cross-section of the patient and the position of the applicators, multiple fields technique cannot be standardized Size, form and position of the fields, and the direction of the central beam must all be individually planned

The resultant position of the intracavitary applicators in relation to easily ascertainable skeletal structures in the true pelvis must also be defined for each individual case, regardless of whether central shielding or multiple fields technique is used, in order to obtain adequate complementary external irradiation

Roentgen examination of a few patients during the treatment period showed that uncontrolled movements projected into the frontal plane were insignificant

Variation in the position of the portio also occurred both when the combined applicators were inserted and when they were not inserted—in some cases considerably The portio sank caudally when the applicators were taken out, sometimes also laterally No corrections for varying contents in the bladder and intestines or for

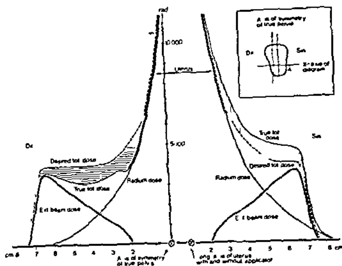


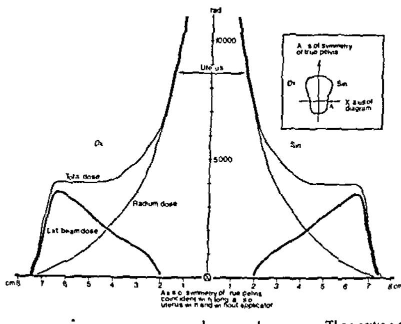
Fig 3 Distribution of dose in the

It was assumed that in cases 3 and 4 the uterus had moved 1 cm laterally to the right when the applicators had been removed The caudal movement of the uterus has not been taken into account in the calculations, but will aggravate the difficulties described here The longitudinal axis without the radium applicators inserted was assumed to be identical with the axis of symmetry of the true pelvis The variation in position of the uterus is close to the mean value achieved in the present material (Table 3)

The distribution of dose laterally from the axis of symmetry of the uterus to the extent of 1 cm from the uterus has been drawn in with the uterus in the position it assumes when the radium applicators are not inserted and represents the absorbed dose received by the uterus and the proximal part of the parametrium which follows the movements of the uterus

The distribution of dose laterally from the uterus (1 5 cm from the axis of symmetry of the uterus) towards the walls of the pelvis has been drawn in with the uterus in the position it assumes when the radium applicators are inserted and represents the absorbed dose received by tissues lying outside the uterus and inflexible in the true pelvis

Case 3 The external irradiation was administered with the shielding block placed with its longitudinal axis identical with the axis of symmetry of the true pelvis (routine shielding procedure) *In this* case the uterus and the proximal part of the parametrium



position of the uterus is
nal axis of the shielding
lvis

symmetry of the true pelvis The external irradiation was given with the shielding block placed in the usual manner, with the longitudinal axis identical with the axis of symmetry of the true pelvis The total dose from intracavitary and external ir radiation in this case must be the one aimed at, as shown in Fig 2 by the curves representing the distribution of dose laterally from the uterus along an axis 3 cm cranially from the portio Regions outside the uterus along this axis received a dose of 8 600, 6 500, 5 500 rad within a distance of 0, 0 5, 1 0 cm from the uterine cervix, respectively

Case 2 The position of the uterus with applicators inserted and without them was unchanged, but its longitudinal axis was placed 1 cm to the left from the axis of symmetry of the true pelvis (Fig 3)

The shielding block was also in this case placed with its longitudinal axis identical with the axis of symmetry of the true pelvis during the external treatment This means that the total dose from the intracavitary and external irradiation (solid line in the figure) to the left of the uterus will be higher than the desired dose (broken line in the figure) and regions lying 0, 0 5, 1 0 cm outside the uterus receive a dose of 9 300, 7 700 6 500 rad, respectively, which is an overdosage of 700 to 1 200 rad (the vertical dashed area in the figure) Regions at the same distance to the right of the uterus receive no dose contribution from the external irradiation (the horizontal dashed area in the figure represents this underdosage)

If the shielding is placed properly in relation to the actual position of the uterus, this over- and underdosage in the vicinity of the uterus may be avoided

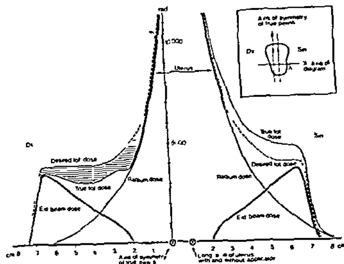


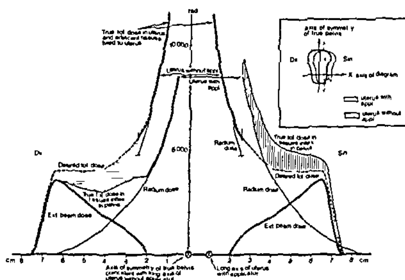
Fig 1 D

It was assumed that in cases 3 and 4 the uterus had moved 1 cm laterally to the right when the applicators had been removed The caudal movement of the uterus has not been taken into account in the calculations, but will aggravate the difficulties described here The longitudinal axis without the radium applicators inserted was assumed to be identical with the axis of symmetry of the true pelvis The variation in position of the uterus is close to the mean value achieved in the present material (Table 3)

The distribution of dose laterally from the axis of symmetry of the uterus to the extent of 1 cm from the uterus has been drawn in with the uterus in the position it assumes when the radium applicators are not inserted, and represents the absorbed dose received by the uterus and the proximal part of the parametrium which follows the movements of the uterus

The distribution of dose laterally from the uterus (1 5 cm from the axis of symmetry of the uterus) towards the walls of the pelvis has been drawn in with the uterus in the position it assumes when the radium applicators are inserted, and represents the absorbed dose received by tissues lying outside the uterus and inflexible in the true pelvis

Case 3 The external irradiation was administered with the shielding block placed with its longitudinal axis identical with the axis of symmetry of the true pelvis (routine shielding procedure) In this case the uterus and the proximal part of the parametrium



... laterally

of overdosage The area marked with horizontal dashes to the right of the uterus represents the area of underdosage

(1 cm) received a total dose from intracavitary and external irradiation (the solid line in the upper left part of Fig 4) corresponding exactly to the dose which had been aimed at, i e 8 600, 6 500, 5 500 rad at 0, 0 5, 1.0 cm laterally from the uterus, respectively Tissues lying outside the uterus and which do not follow its movements, but lie inflexible in the true pelvis, receive at the left of the uterus a total dose of 9 300, 7 700, 6 500 rad at 0, 0 5, 1 0 cm outside the uterus, respectively, in its position with radium applicators inserted, the solid line to the left of the uterus in the lower part of the figure The overdosage is represented by the vertical dashed area Parts of the sigmoid lie in that area The absorbed dose of irradiation to the right of the uterus in regions outside the uterus and inflexible in the true pelvis is lower than desired This is also the case for the distal parts of the parametrium which either do not at all follow the movements of the uterus, or only to an unimportant extent This underdosage is represented by the horizontal dashed area

Case 4 The external treatment was given with the shielding block placed with its longitudinal axis exactly corresponding to the axis of the uterus when radium applicators are inserted 1 cm to the left of the axis of symmetry of the true pelvis This shielding technique based on the position of the intracavitary applicators is used in an attempt to avoid overdosage of tissues lying outside the uterus and inflexible in the true pelvis (sigmoid) The calculated (and desired) dose (dotted, broken line) for regions outside the uterus and inflexible in the true pelvis correspond exactly to the given dose (solid line).

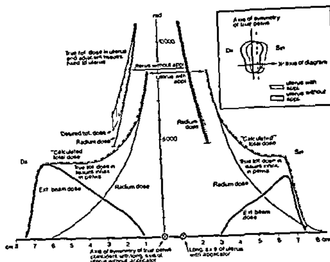


Fig 5 Distribution of dose in the uterus and surrounding tissues The uterus moved 1 cm laterally to the right when the applicators had been removed The long

area of under
area of overd

The proximal part of the left parametrium (1 cm) and tissues fixed to the uterus receive a lower dose than desired, however, represented in the figure by the horizontal dashed area The proximal part of the right parametrium (1 cm) and tissues which are attached to the uterus (parts of the vesical trigone) receive higher doses than desired 9 300, 7 700, 6 500 rad at 0, 0 5, 1 0 cm outside the uterus, respectively (vertical dashed area)

The practical importance of this overdosage and underdosage to the areas in the immediate vicinity of the uterus for the frequency of compl
difficult to estimate The dose leve
even before the complementary ex
assume that even relatively small unpredictable dose contributions to these areas may give undesired reactions to irradiation It is probable that some unexpected and quite troublesome complications in the intestines and bladder in patients given external irradiation following intracavitary treatment are due to the varying position of the uterus It is evident from the figures that a cervix thicker than normal, and less sensitive tissues outside the cervix, for example fatty tissue, will decrease the dose to the sigmoid, and this agrees with clinical experience of radiation induced complications

Conclusion

Adequate dose distribution is not possible to achieve by complementary external irradiation after the primary tumour has received a full tumour dose with intra cavitary radium treatment due to the steep dose gradient around the radium applicators and the varying position of the uterus

The unpredictable dose will be reduced if the external irradiation dose in the central parts of the parametrium and in the uterus is increased at the expense of the intra cavitary dose External irradiation without shielding before the intracavitary treatment will prevent this risk

SUMMARY

Dose distribution around intracavitary applicators (Stockholm technique) has been investigated The gradient of dose around the combination of intrauterine and vaginal applicators used is steep The position of the uterus with and without the radium applicators inserted varies Together with the steep dose gradient this implies that external irradiation following intracavitary treatment involves a risk for overdosage to tissues in the vicinity of the uterus and underdosage to the parametrium

ZUSAMMENFASSUNG

Es wurde die Dosisverteilung um die intrakavitaren Applikatoren (Stockholm Technik) untersucht Der Dosisgradient um die verwendete Kombination von intrauterinen und vaginalen Applikatoren ist steil Die Lage des Uterus mit und ohne eingelegte Radiumapplikatoren variert Zusammen mit dem steilen Dosisgradienten bedeutet das, dass externe Bestrahlung nach einer intracavitaren Behandlung des Risiko einer Überdosierung der Gewebe in der Nahe des Uterus und einer Unterdosierung des Parametriums in sich birgt

RÉSUMÉ

Les auteurs ont étudié la distribution de doses autour d'applicateurs intracavitaires (*technique de Stockholm*) *Le gradient de dose autour de l'association* d applicateurs intra-utérin et vaginal utilisés est raide La position de l'utérus avec et sans applicateurs de radium en place est différente Cette variation de positions associee au gradient de dose raide implique que l'irradiation externe qui suit le traitement intracavitaire comporte un risque de surdosage aux tissus dans le voisinage de l utérus et de sous dosage au paramètre

REFERENCES

CAMPBELL E M and DOUGLAS M The treatment of carcinoma of the uterine cervix using a linear vaginal source and 4 MeV X-rays Brit J Radiol 39 (1966), 537

COWELL M A C and LAURIE J The treatment of carcinoma of the cervix uteri stage I and II, with radium and 4 MeV supplementary X-rays Brit J Radiol 40 (1967), 43

ELLIS F and SORENSEN A S A method of estimating biological effect of combined intracavitary low dose rate radiation with external radiation in carcinoma of the cervix uteri Radiat Biol 110 (1974) 681

FLETCHER G H, RUTLEDGE F N and CHAN P M Policies of treatment in cancer of the cervix uteri Amer J Roentgenol 87 (1962) 6

FRIESCHBIER H J und SEIFERT A Zur Dosisverteilung bei der kombinierten Radium- und Telekobalttherapie des Kollumkarzinoms Strahlentherapie 127 (1965), 357

— und WURTHNER K Dosisverteilung bei der Telekobalt bestrahlung des Kollumkarzinoms

Acta radiol Ther Phys Biol 11 (1972) 289

JOHNSSON J E and NORDBERG U B Dosimetric problems with radium in the intracavitary treatment of carcinoma of the uterine cervix Acta radiol Ther Phys Biol 12 (1973) 257

des Kollum

the uterine

kombinierten Radium-Supervolt-Therapie gynaekologischer Karzinome nach der Hamburger Methode Strahlentherapie (Sonderb) 61 (1965), 158

WALTZ B J, PEREZ C A FELDMAN A, DEMIDECKI A J and POWERS W E Individualized compensating filter and dose optimization in pelvic irradiation Radiology 107 (1973), 611

ZARGHAMI O H and KUROHARA S S A simple modification of the Stockholm applicator for the treatment of early cancer of the uterine cervix Amer J Roentgenol 105 (1969) 115

FROM THE STATE INSTITUTE OF RADIATION HYGIENE (DIRECTOR: P. GRANDE), BRONSHOJ, DK-2700 COPENHAGEN AND THE RADIOPHYSICAL LABORATORY (DIRECTOR: C. B MADSEN), RADIUM CENTRE, DK-8000 ÅRHUS, DENMARK

SPECTRAL MEASUREMENTS AND MONTE CARLO CALCULATIONS OF SCATTERED RADIATION FROM THERAPEUTIC RADIATION SOURCES

K ENNOW and K A JESSEN

Generally, it has been assumed that the variation of the radiation quality due to scattering with increasing depth in a medium is small for photon radiation Investigations (BRUCE et coll 1963) based upon ^{60}Co have proved this assumption For other radiation sources of interest, especially roentgen rays from linear accelerators, such investigations have been scarce It is the purpose of the present report to give the results both of experiments and of calculations of the photon spectral distribution at various depths for 6 MeV roentgen rays and ^{60}Co gamma rays both used as therapeutic radiation sources

The spectral measurements have been made on scattered radiation in a perspex phantom placed in a beam of gamma radiation from a T E M Stabilatron kilocurie ^{60}Co therapy unit, and in a beam of roentgen radiation from a Varian Clinac 6 MeV linear accelerator The measurements are performed with a NaI spectrometer It was possible to change both the depth and the angle for analysis of the scattered radiation in the phantom

For each depth the spectral distributions of the scattered radiation at the different angles are integrated to give the spectral distribution of the total fluence of scattered

Submitted for publication 13 December 1974

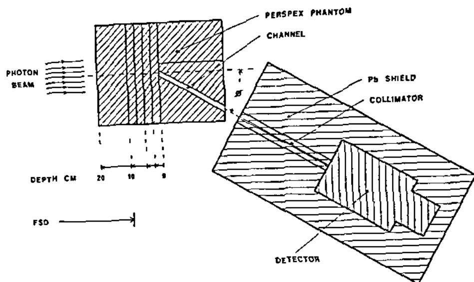


Fig. 1 Experimental arrangement.

photons The integrated distributions are compared with Monte Carlo calculations The computer program uses the measured primary spectra (JESSEN 1973) as input data and calculates the spectrum of scattered photons in the point of interest together with scaling factors for the angular distribution Although the number of photons in the calculated spectra is much lower than in the resulting measured spectra, the calculations are an essential confirmation of the integration of the contributions from the various scattering angles

The integrated spectral distributions together with the distributions of the primary radiation for the same depths are used to calculate the spectra of the initial electrons released by the photon interaction processes, photoelectric effect, Compton effect and pair production These electron spectra are applied for a calculation of the distributions of absorbed dose, of track length and of their average values, with respect to LET Variations in the radiation qualities for the different depths in the phantom are examined in this way for the two different radiation sources

Experimental procedure and data handling

The experimental arrangement is illustrated in Fig 1 The phantom was a 30 cm × 30 cm × (20 + d) cm cubic block of commercial, attainable perspex (mass density 1 19 g/cm³ and electron density 3 833 10^{23} el/cm³) d is the depth varying from 2 5 cm to 20 cm The scattering angle is defined by an air channel 1 5 cm in diameter It is possible to change the scattering angle between seven values ranging from 7 5°

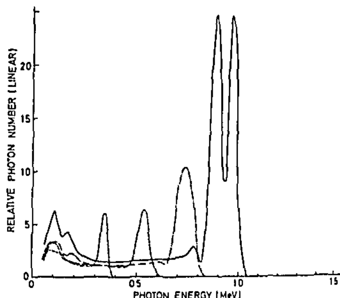


Fig 2 Iterated spectral distributions from the ^{60}Co unit Field size 4 cm × 4 cm Depth 10 cm Scattering angles 30 deg (——), 45 deg (– –), 60 deg (— —) and 90 deg (- - -)

to 135° by replacing a perspex plate containing the channel The phantom was placed in front of the spectrometer with facilities for fine alignement

The spectrometer has a NaI(Tl) detector (diameter 12 7 cm) as described previously (JESSEN 1973) The cylindrical collimator, 30 cm in length, has a diameter of 3 or 5 mm depending on the fluence rate of scattered photons The phantom was placed in the same measuring geometry as the scattering foil when measuring primary spectra The SSD for the ^{60}Co source was 80 cm and the FSD for the measurements on the linear accelerator 685 cm In order to reduce the background, measurements with the linear accelerator were performed with the phantom and the spectrometer placed behind a 1 6 m thick concrete wall supplied with a cylindric channel (6 cm in diameter), resulting in a field diameter on the phantom surface of 7 cm

The pulse height distributions were measured by passing the output from the detector directly through a double delay-line amplifier into a multichannel analyser A response-matrix for the detector was used to correct the pulse height distributions for effects from the crystal and the following electronics, after subtraction of the spectrum of background radiation measured with the phantom removed from the radiation beam Mathematically, it may be expressed by the matrix equation P = R N, where P is measured pulse height distribution, R the response-matrix and N the scattered photon spectrum An iterative procedure was applied for solving this complicated equation (SKARSGÅRD et coll 1961)

The iterated spectral distributions at four different measuring angles on the ^{60}Co unit for a field size of 4 cm × 4 cm and in a phantom depth of 10 cm are given in Fig 2 The distributions are normalized to the same absorbed dose The figure illustrates the preferred forward scattering and the good resolution of the two peaks up to 30 degrees scattering angle

The spectral distributions of the scattered radiation in the different measuring

Table 1

The ratio between the total measured and calculated photon numbers for various scattering angles and collimator diameters (relative to the ratio at 45°)

Φ deg	Stabilatron coll 3 or 5 mm	Accelerator	
		coll 5 mm	coll 3 mm
7.5	1.09	—	—
15	1.07	—	0.98
30	1.00	0.67	1.07
45	1	1	1
60	0.94	1.02	—
90	1.04	1.00	—

angles for the same field and depth were integrated over all angles Φ. This was carried out after inter- and extrapolation between the measured values to Φ intervals of 15 degrees for the roentgen rays and 3 degrees for the ^{60}Co gamma rays, respectively. The system is radially symmetrical about the central axis of the primary beam and integration over the azimuthal angle may therefore be performed by multiplying by $2\pi \sin \Phi$. Integration of all scattering angles was then done by numerical integration after Simpson's rule of the function $2\pi f(\varepsilon, \Phi) \sin \Phi$ for the center value ε of each energy interval. $f(\varepsilon, \Phi)$ is the photon number at the scattering angle Φ and with energy ε.

Monte Carlo calculations

The solution of transport problems for photon radiation by means of Monte Carlo calculations is a wellknown method (BRUCE & JOHNS 1960, ZERBY 1963) which may be applied successfully if a large computer is available. The main problem is the sampling from the Klein-Nishina formula and in the present calculations the method given by Kahn was applied (ZERBY 1963).

The program has been written to simulate the experimental setup as much as possible: the starting energy and number of photons were defined by the measured primary spectra and each photon was followed individually through a 30 cm × 30 cm × 30 cm perspex phantom, from when it entered through a 4 cm × 4 cm rectangular field for the ^{60}Co source or a 7 cm in diameter circular field for the linear accelerator until it escaped from the phantom or was absorbed within it.

Photons which cross a small sphere around the centerpoints in the depths 3.5, 10 and 20 cm (only 10 cm for the Co source) are recorded by energy and angle and the result of the calculation is presented as the spectrum of scattered photons in the different depths and the total number of photons scattered into the measuring angles specified above.

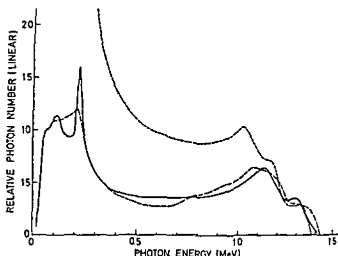


Fig 3 Integrated distributions of the scattered photons from the ^{60}Co unit Depth 10 cm Field size 4 × 4 cm Monte Carlo calculations (——) and measured (— —) Field size 15 cm × 15 cm measured (- - -)

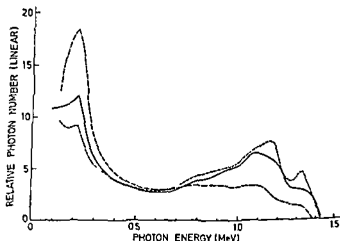


Fig 4 Integrated distributions of the scattered photons from the ^{60}Co unit Field size 4 cm × 4 cm Depths 2 5 cm (— —) 10 cm (——) and 20 cm (- - -)

The values of the interacting coefficients for perspex are taken from NBS 29 (HUBBELL 1969) and the following simplifications have been made below 10 keV or 25 keV for the Co source and the linear accelerator respectively all photons are absorbed immediately, between 150 and 1 500 keV only compton scattering is effective, and above 1 500 keV a small fraction of the photons undergoes pair production If a photon is absorbed by pair production one 511 keV photon is sent out in an arbitrary direction from the point of interaction For the linear accelerator 0 3 per cent of all the interactions were pair productions In this calculation it is computer-time saving to express the energy in keV as an integer variable which may be used to call attenuation coefficients etc from numerical arrays

The calculations have been carried out in several steps, and it is therefore possible to estimate the coefficient of variation of the number of photons given by the calculations to be below 5 per cent in most cases

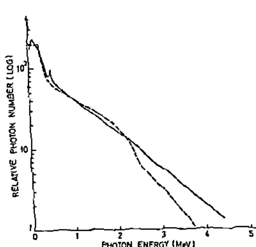


Fig 5

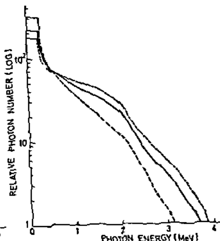


Fig 6

Fig 5 Integrated distributions of the scattered photons from the 6 MeV roentgen rays Depth 10 cm Monte Carlo calculations (——) and measured (– – –)

Fig 6 Integrated distributions of the scattered photons from the 6 MeV roentgen rays Depths 3 5 cm (— —) 10 cm (——) and 20 cm (– – –)

Results and Comparisons

The ratio r between the total measured and calculated photon numbers for the scattering angle 45 degrees is about 10^6 The ratio relative to this number for the various scattering angles appears in Table 1 The distributions for the different angles were normalized to the same absorbed dose for the incoming radiation For the ^{60}Co source no dependence on collimator size was observed and all measurements can be carried out with both the 3 mm and the 5 mm collimators at all angles For the linear accelerator the fluence rate is too high at 15 and 30 degrees for the 5 mm collimator to be used, and only the 3 mm collimator was applied at these angles This probably means a saturation of the analyser system caused by the great number of forward scattered photons sent towards the solid angle of the detector at high energies The analyser cannot analyse more than one photon per radiation pulse from the accelerator

In Fig 3 the Monte Carlo calculations are compared with the measured distribution of scattered photons for the 4 cm × 4 cm field in a phantom depth of 10 cm for ^{60}Co gamma radiation The two curves are normalized to the same total photon number Although there are some differences in the resolutions around the backscatter peak about 215 keV, there seems to be a good agreement between the calculated and measured spectra, which verified the method used for integration of the measured distributions From this agreement for the 4 cm × 4 cm field it is concluded that the measured distributions for other fields and depths are valuable representations In

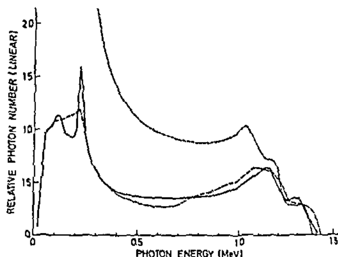


Fig 3 Integrated distributions of the scattered photons from the ^{60}Co unit Depth 10 cm Field size 4 × 4 cm Monte Carlo calculations (——) and measured (— —) Field size 15 cm × 15 cm measured (- - -)

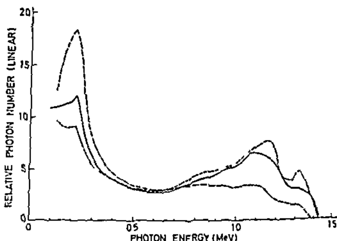


Fig 4 Integrated distributions of the scattered photons from the ^{60}Co unit Field size 4 cm × 4 cm Depths 2 5 cm (— —), 10 cm (——) and 20 cm (- - -)

The values of the interacting coefficients for perspex are taken from NBS 29 (HUBBELL 1969) and the following simplifications have been made below 10 keV or 25 keV for the Co source and the linear accelerator respectively all photons are absorbed immediately, between 150 and 1 500 keV only compton scattering is effective, and above 1 500 keV a small fraction of the photons undergoes pair production If a photon is absorbed by pair production one 511 keV photon is sent out in an arbitrary direction from the point of interaction For the linear accelerator 0 3 per cent of all the interactions were pair productions In this calculation it is computer-time saving to express the energy in keV as an integer variable which may be used to call attenuation coefficients etc from numerical arrays

The calculations have been carried out in several steps, and it is therefore possible to estimate the coefficient of variation of the number of photons given by the calculations to be below 5 per cent in most cases

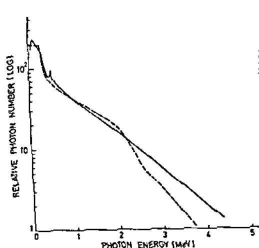


Fig 5

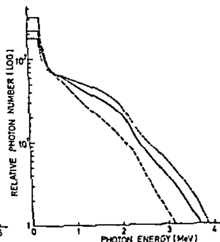


Fig 6

Fig 5 Integrated distributions of the scattered photons from the 6 MeV roentgen rays Depth 10 cm Monte Carlo calculations (——) and measured (---)

Fig 6 Integrated distributions of the scattered photons from the 6 MeV roentgen rays Depths 3 5 cm (— —) 10 cm (——) and 20 cm (---)

Results and Comparisons

The ratio r between the total measured and calculated photon numbers for the scattering angle 45 degrees is about 10^6 The ratio relative to this number for the various scattering angles appears in Table I The distributions for the different angles were normalized to the same absorbed dose for the incoming radiation For the ^{60}Co source no dependence on collimator size was observed and all measurements can be carried out with both the 3 mm and the 5 mm collimators at all angles For the linear accelerator the fluence rate is too high at 15 and 30 degrees for the 5 mm collimator to be used, and only the 3 mm collimator was applied at these angles This probably means a saturation of the analyser system caused by the great number of forward scattered photons sent towards the solid angle of the detector at high energies The analyser cannot analyse more than one photon per radiation pulse from the accelerator

In Fig 3 the Monte Carlo calculations are compared with the measured distribution of scattered photons for the 4 cm × 4 cm field in a phantom depth of 10 cm for ^{60}Co gamma radiation The two curves are normalized to the same total photon number Although there are some differences in the resolutions around the backscatter peak about 215 keV, there seems to be a good agreement between the calculated and measured spectra, which verified the method used for integration of the measured distributions From this agreement for the 4 cm × 4 cm field it is concluded that the measured distributions for other fields and depths are valuable representations In

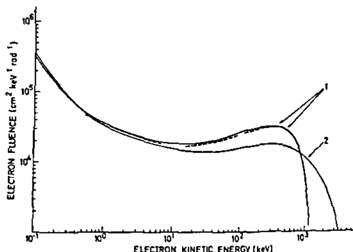


Fig 7 Electron fluence distributions of secondary and slowing down electrons for (1) ^{60}Co gamma radiation and (2) 6 MeV roentgen rays Depth 10 cm ---- from ICRU 16

Fig 3 is also plotted a curve for the 15 cm × 15 cm field at the same depth and normalized to the same absorbed dose as for the 4 cm × 4 cm field

The integrated distributions of the measured scattered photons in three depths of the phantom are drawn in Fig 4 for the 4 cm × 4 cm fields again normalized to the same total photon number The figure illustrates a filtration with depth, i e the relative content of the high energy photons in the scattered spectrum is increased for increasing depth in the phantom material

For the pulsed 6 MeV roentgen rays from the accelerator the analogous comparisons were performed and the distributions for the calculated and measured scattered photons at a depth of 10 cm appear in Fig 5 Only a circular radiation field of 7 cm in diameter was used for the accelerator experiments The 511 keV annihilation peak in the Monte Carlo calculations, which could be caused by the model used, is not seen in the measured distribution Probably also the response matrix cleans the pulse height distributions too strongly at this energy The deviation for the higher energies could be expected in this semilog plot, as the lowest measuring angle used for the integration is 15 degrees

In Fig 6 the integrated distributions of the measured scattered photons for three depths are plotted The distributions are also here normalized to the same total photon number, and illustrate, as for the distributions for ^{60}Co, a filtration with depth

LET calculations The primary photon distributions measured previously (Jessen 1973) are added to the scattered distributions to obtain the total photon fluence for LET calculations The primary spectra were corrected to the measuring depth for filtration in the phantom material and were normalized to the same absorbed dose as represented by the scattered distributions

These total photon distributions were used to calculate the spectra of the initial electrons set in motion per gram of the perspex material at an absorbed dose of 1

Table 2

The absorbed dose average LET, $\bar{L}_{100\text{-}D}$, and the track average LET, $\bar{L}_{100\text{-}T}$, for the ^{60}Co gamma rays for different field sizes and depths in the perspex phantom. The average values are in keV/μm

Depth cm	4 cm × 4 cm		15 cm × 15 cm	
	$\bar{L}_{100\text{-}D}$	$\bar{L}_{100\text{-}T}$	$\bar{L}_{100\text{-}D}$	$\bar{L}_{100\text{-}T}$
2.5	6.72	0.289	6.68	0.295
5	6.72	0.288	6.68	0.294
10	6.72	0.287	6.67	0.293
20	6.73	0.285	6.65	0.293

rad. The lower energy cut off value for the photon spectra was 100 keV set by the analyser system. Cross sections for the photoelectric effect were calculated after NBS 29 (HUBBELL 1969), and the mean excitation-ionization potential ($I = 65.7$ eV) for defining the energy distributions of the photoelectrons is given by Bragg's rule (ICRU 16, 1970). Cross sections and energy distributions of the electrons formed by Compton and pair production processes were calculated after formulas given by BETHE & ASHKIN (1953).

From the normalized initial electron spectra the electron slowing down spectra were calculated by means of McGinnies' tables (NBS 597, 1959) for water. The values are extrapolated graphically from 451.7 eV down to 100 eV, the cut-off energy for the LET calculations, although the limit is exceeded for the Born approximation, as the binding energies for the K electrons of the oxygen and the carbon are 532 eV and 284 eV respectively. But the binding energies for the rest (74 per cent) of the electrons in the molecules are below 100 eV and therefore it was assumed that the Born approximation still was valid. The extrapolation of the slowed-down and secondary electrons for a certain initial electron energy is in agreement with the results from BRUCE et coll. (1963), where a similar assumption was made. The small differences in Z/A and I between water and perspex are neglected.

Fig. 7 illustrates the calculated energy spectrum resulting from slowing down and secondary electrons produced by (1) ^{60}Co gamma radiation and (2) 6 MeV roentgen rays at a depth of 10 cm. There seems to be a good agreement with the spectrum for ^{60}Co taken from ICRU 16.

The slowing down spectra were used for calculations, for all depths and field sizes measured, of the track length distributions, the absorbed dose distributions and their averages with respect to LET. The energy cut-off in these calculations were 100 eV. The restricted electron stopping power for 0.1 to 10 keV electrons was taken from table A1 in ICRU 16 and for the kinetic energies above 10 keV, the restricted stopping power was calculated after ROHRLICH & CARLSON (1964). The density correction was performed after STERNHEIMER (1956). Fig. 8 illustrates the cumulative absorbed dose

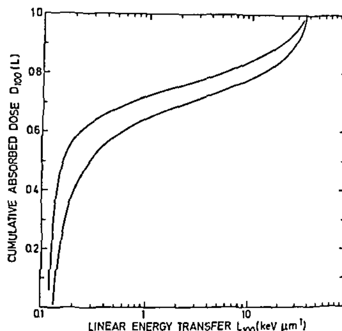


Fig 8 Cumulative absorbed dose distributions in LET for ^{60}Co gamma radiation (lower curve) and for 6 MeV roentgen rays (upper curve) Depth 10 cm

distributions in LET for the 4 cm × 4 cm field of ^{60}Co gamma rays and for the 6 MeV roentgen rays at a depth of 10 cm Sixty per cent of the absorbed dose are deposited *with LET values below 0 58 keV/μm for* ^{60}Co *and below 0 23 keV/μm for the 6* MeV roentgen rays

In Table 2 the average values in LET for the ^{60}Co source are given for different fields and depths There seems to be only a little spread in these data which supports the assumption that there should be a very small variation in the radiation quality with increasing depth There is a good agreement with the dose average with respect to LET given by ICRU 16 (6 9 keV/μm) for cut-off energy at 100 eV, but the track average is given a little lower by ICRU (0 229 keV/μm) Otherwise the agreement is

Table 3

The absorbed dose average LET, $L_{100\ D}$ and the track average LET, $L_{100\ T}$, for the 6 MeV roentgen rays different depths in the phantom The average values are in keV/μm

Depth cm	Diam 7 cm	
	$L_{100\ D}$	$L_{100\ T}$
3 5	6 97	0 243
10	6 96	0 239
20	6 97	0 235

reversed with the data given by BRUCE et coll ($\bar{L}_D = 8.3$ keV/μm and $\bar{L}_T = 0.32$ keV/μm). Table 3 gives the average values in LET for the 6 MeV roentgen rays. The results indicate small variations with depth similar to the results for the ^{60}Co source, but suggest a deviation in average values for the two radiation sources. The calculated averages in LET are very sensitive to the stopping power for the low energy electrons, but the calculations are based upon the same stopping power for these energies indicating that there should only be a small difference in biologic effect for the two radiation sources.

Acknowledgement

The data handling and the LET calculations were performed on the CDC 6400 computer at the University of Aarhus and for the Monte Carlo calculations the IBM 370/165 computer at NEUCC, Copenhagen was used. The computer programs are written in Fortran IV.

SUMMARY

Spectral measurements have been made on scattered radiation in a perspex phantom in various depths from a kilocurie ^{60}Co unit and a 6 MeV linear accelerator using a NaI crystal spectrometer. The measurements are compared to Monte Carlo calculations and a good agreement is obtained. The measured total photon distributions make the basis for calculations of absorbed dose and track length distributions in LET and their average values for the different depths and fields.

ZUSAMMENFASSUNG

Es wurden spektrale Messungen der Streustrahlung unter Verwendung eines NaJ Kristall Spektrometers an einem Perspex Phantom in verschiedenen Abständen von einer Kilokuri ^{60}Co-Einheit und einem 6 MeV Lin[illegible]
mit Monte Carlo Be[illegible]
Die gemessene Ges[illegible]
bierten Dosis und [illegible] ...echnungen der LET und deren Durchschnittswerte für verschiedene Tiefen und Felder.

RÉSUMÉ

Des mesures spectrales ont été faites au moyen d'un spectromètre à cristal de NaI sur le rayonnement diffusé dans un fantome de perspex à différentes profondeurs recevant le rayonnement d'une source d'un kilocurie de ^{60}Co et d'un accélérateur linéaire de 6 MeV. Ces mesures ont été comparées aux calculs de Monte Carlo et les auteurs ont constaté une bonne concordance. Les distributions totales de photons mesurées ont servi de base pour les calculs de dose absorbée et pour les distributions de longueur de trajectoire en LET et pour leur valeur moyenne pour les différentes profondeurs et les différents champs.

REFERENCES

BETHE H A and ASHKIN J Passage of radiations through matter *In* Experimental nuclear physics Vol 1, p 166 Edited by E Segre Wiley, New York 1953

BRUCE W R and JOHNS H E The spectra of X-rays scattered in low atomic number materials Brit J Radiol (1960) Suppl No 9

— PEARSON M L and FREEDHOFF H S The linear energy transfer distributions resulting from primary and scattered X rays and gamma rays with primary HVL's from 1 25 mm Cu to 11 mm Pb Radiat Res 19 (1963), 606

HUBBELL J H Photon cross sections, attenuation coefficients, and energy absorption coefficients from 10 keV to 100 GeV NSRDS-NBS 29 (1969)

ICRU report 16 Linear energy transfer (1970)

JESSEN K A Measurements of primary spectra from a kilocurie Cobalt 60 unit and a 6 MeV linear accelerator Acta radiol Ther Phys Biol 12 (1973) 561

McGINNIES R T Energy spectrum resulting from electron slowing down Natl Bur Std (U S) Circ 597 (1959)

ROHRLICH F and CARLSON B C Positron electron differences in energy loss and multiple scattering Phys Rev 93 (1954) 38

SKARSGÅRD L D, JOHNS H E and GREEN L E S Iterative response correction for a scintillation spectrometer Radiat Res 14 (1961) 261

STERNHEIMER R M Density effect for a ionization loss in various materials Phys Rev 103 (1956) 511

ZERBY C D A Monte Carlo calculation of the response of gamma ray scintillation counters *In* Methods in computational physics Vol 1, p 89 Edited by B Alder and S Fernbach Academic Press New York 1963

FROM THE DEPARTMENTS OF OTOLARYNGOLOGY AND NEURORADIOLOGY, KAROLINSKA SJUKHUSET, AND THE DEPARTMENT OF RADIATION PHYSICS, KAROLINSKA INSTITUTET, S-104 01 STOCKHOLM, SWEDEN

OBJECTIVE SYMMETRY DETECTOR METHOD FOR GAMMAENCEPHALOGRAPHY

III. Diagnosis of abnormal $^{99}Tc^mO_4$ distribution in the skull

M LIND and S LARSSON

The equipment and the physical characteristics of the symmetry detector method have been described previously (LARSSON et coll 1975) as well as the normally obtained range of the $^{99}Tc^mO_4$ distribution in the skull following intravenous injection (LIND et coll 1975) Alterations of the normal distribution of nuclides in the skull caused for instance [illegible]
placed [illegible]
Moor[illegible] [illegible] Later moving scanners and stationary gamma cameras were used These methods demand great technical, economical and personnel resources, available only in large medical centres and even so the interpretation of results is mainly subjective (BURROWS 1972)

Scintigraphic information has been digitalized and by computation related to the normal ranges of several evaluation parameters, in order to enhance the diagnostic accuracy of brain scanning (DOWSETT & PERRY 1970, POPHAM et coll 1970, DOWSETT

Submitted for publication 15 January 1974

1972) However, since the normal ranges obtained were not related to *the sensitivity* of the evaluation parameters as *described by* LARSSON *et coll*, *the detectability of an increased* isotope content in different subregions of the head is not possible to estimate The reported diagnostic accuracy, defined as successful *separation of pathologic* from normal cases, is *thus difficult* to evaluate in relation to other results reported (BURROWS)

Gamma encephalography, *described* inter alia by PLANIOL and MUNDIGER means *estimation* of the isotope distribution in the skull by determination of count rates over several stationary positions on the skull (PLANIOL 1966, MUNDIGER & ASAI 1967) The evaluation parameters *of* these methods included considerable errors caused mainly by poor counting statistics from small numbers of counts recorded *in each position*, *variation in* positioning of the *detectors*, *varying levels of recorded* body background, and varying reference values used for the calculation of the relative isotope distribution These sources of variation were not very carefully analysed, nor were attempts to reduce their influence *reported*, *furthermore*, *the separation of* pathologic cases from normal ones was based on the subjective evaluation of several criteria, together with additional clinical information (PLANIOL, MUNDIGER & ASAI)

The *purpose* of *the* present work is to describe the choice of parameters of the symmetry detector method and a criterion with different fixed classification boundaries that makes a simple and objective separation of abnormal cases from normal ones possible in routine clinical work

Material and Methods

Measurements of the distribution of 99m Technetium pertechnetate ($^{99}Tc^{m}O_4$) in the skull was performed using the symmetry detector *method previously described* (LIND et coll) A premedication of 400 mg $KClO_4$ was given orally 30 to 60 minutes before the intravenous administration of 10 mCi $^{99}Tc^{m}O_4$ The measuring procedure started about 30 minutes after the injection of the isotope *Two NaI-detectors face to face on* the same axis and shielded by collimators 30 cm in length with 3 cm × 3 cm square apertures were used and the isotope distribution was determined from measurements over 24 measuring positions, in a constant *pattern*, *given by* a positioning diagram designed to approximately suit the individual size and shape of the skull (cf Fig 2, LIND et coll 1975) Values obtained were recorded on punched tape and 9 parameters per subregion were calculated, altogether 208 (LIND *et coll*)

The mean values and standard deviations (SD) of all evaluation parameters of subregions of the skull obtained from a reference group of 29 patients without known brain lesions have been described previously and were used as the basis for interpretation (LIND *et coll*)

Values representing the depth dependent sensitivity of the increase-(I) and difference-(D) ratio parameters have been obtained from measurements of a skull lesion-phantom system (LARSSON et coll)

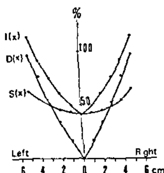


Fig 1

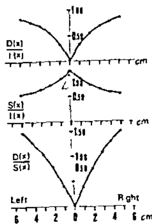


Fig 2

Fig. 1 Percentage alterations of count rate I(x) differences D(x) and sums S(x) of right and left detector values are plotted against the distance x from the median plane of the skull phantom Tumour phantom volume 21.3 ml Conc ratio 8 1 (LARSSON et coll)

Fig. 2. The ratios D(x)/I(x), S(x) I(x) and D(x)/S(x) are plotted against the distance x from the median plane of skull phantom (LARSSON et coll)

Five patients, one patient with a vascular malformation and four with brain tumours, later histologically verified, were examined by the symmetry detector method The histologic examination was made as proposed by RINGERTZ (1950)

Evaluation parameters The normal ranges of the evaluation parameters are given by LIND et coll The number of counts N_R and N_L obtained from the right and left detector of each subregion respectively were related to two different reference values, P_{mv} and C_{mv} P_{mv}, the plane mean value, is the calculated mean value of all 12 measuring values from the six subregions of one plane (A, B, C or D) C_{mv}, the central mean value, is the calculated mean of the 16 measuring values, obtained from the central subregions (B2 B5, C2–C5) (cf Fig 2, LIND et coll 1975)

The relations r_p, obtained for each subregion j, were defined as position ratios according to

$$r_{Rp}(j) = \frac{N_R(j)}{P_{mv}} 100\%, \; r_{Lp}(j) = \frac{N_L(j)}{P_{mv}} 100\% \qquad (1\,a, b)$$

with the plane mean value, P_{mv}, as the reference, as indicated by index p The indices R and L refer to the right and left position of the subregion

The corresponding position ratios, r_c (j), with the central mean value, C_{mv}, as the reference (indicated by index c) were expressed

$$r_{Rc}(j) = \frac{N_R(j)}{C_{mv}} 100\%, \; r_{Lc}(j) = \frac{N_L(j)}{C_{mv}} 100\% \qquad (2\,a, b)$$

The difference between the two position ratios r_{Rp} and r_{Lp}, (with the P_{mv} as the reference), was calculated for each subregion and defined as the difference parameter D

$$D(j) = (r_{Rp}(j) - r_{Lp}(j))\,\% \qquad (3)$$

The sum parameters S_p and S_c were defined as the mean of r_{Lp} and r_{Rp} (reference value = P_{mv}), and the mean of r_{Lc} and r_{Rc} (reference value = C_{mv}), respectively

$$S_p(j) = 1/2(r_{Rp}(j) + r_{Lp}(j)) \% \quad (4a)$$

$$S_c(j) - 1/2(r_{Rc}(j)) + r_{Lc}(j) \% \quad (4b)$$

Finally, the adjacent parameters A were defined as the relative difference between one subregion ($N_R(j)$) and the adjacent frontal subregion ($N_R(j-1)$) of the same plane

$$A_R = \frac{N_R(j) - N_R(j-1)}{N_R(j)} 100\% \quad (5a)$$

$$A_L = \frac{N_L(j) - N_L(j-1)}{N_L(j)} 100\% \quad (5b)$$

Detectability properties of the position ratio, sum and difference parameters The need of the three different evaluation parameters (position ratio r_p, sum S_p and difference D) could be demonstrated by a comparison of the detectability properties of the parameters at different depths in a subregion

The detectability, δ, defined as the smallest effect of interest (for instance the increase of isotope content in a subregion) which can be detected with a significance, corresponding to q standard deviations

$$\delta = \frac{q\sigma}{S} \quad (6)$$

where S is the sensitivity (true mean number of parameter units obtained per unit of the defined effect of interest) and σ the normal standard deviation (SD) of the parameter (LARSSON et coll)

The depth dependent sensitivity functions S_I, S_D and S_S of the increase ratio I, difference ratio D and sum ratio S, were defined from measurements on a phantom system (LARSSON et coll), and assumed to be valid also for the evaluation parameters defined for clinical measurements (position ratio r_p, difference D and sum S_p) The normal standard deviations σ_p, σ_D and σ_S of the latter parameters were calculated from results of the reference group (LIND et coll) Hence, the detectability of an abnormal accumulation of $^{99}Tc^mO_4$ could be expressed for each evaluation parameter as a function of the location x in the subregion j according to eq (6)

$$\delta_p(j, x) = \frac{q \; \sigma_p(j)}{S_I(x)} \quad (7a)$$

$$\delta_D(j, x) = \frac{q \; \sigma_D(j)}{S_D(x)} \quad (7b)$$

$$\delta_S(j \; x) = \frac{q \; \sigma_S(j)}{S_S(x)} \quad (7c)$$

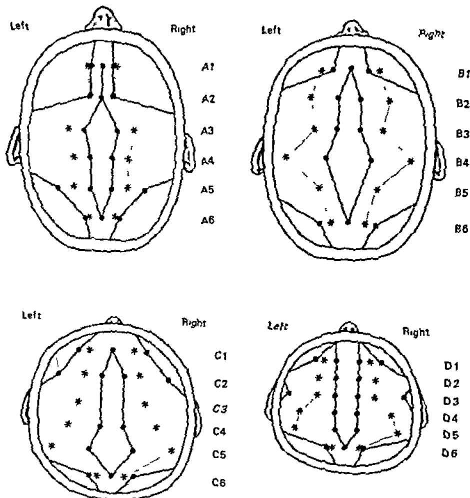


Fig 3 Pathologic accumulation of ... give the most s... the *central* arc... meters and the... logic accumula... Planes A to D

By ... solut... where ... the same detectability

$$\delta_P(j, x) = \delta_D(j, x) = \frac{q\ \sigma_P(j)}{S_1(x)} = \frac{q\ \sigma_D(j)}{S_D(x)} \quad \frac{S_D(x)}{S_1(x)} = \frac{\sigma_D(j)}{\sigma_P(j)} \tag{8a}$$

Position	r_{Le}	r_{Re}	S_e
A1	6 89	2.97	5.19
B1	26.38	9.84	18.87
B2	7.31	5.89	1.73
C1	3.04	0.97	2 01
C4	- 2.23	- 2.28	- 2.62
D5	- 2.04	- 1.82	- 2 00

Position	r_{Lp}	D	r_{Rp}	S_p
A1	5.21	- 8.36	1.52	3.43
A4	- 2.76	1.13	- 1.12	- 2 03
B1	17.81	-15.88	5 79	12.70
B2	2.82	- 1.76	1.28	2.40
B3	- 2.89	0.32	- 1.78	- 2.80
B4	- 5.21	0.89	- 4.59	- 5 74
B5	- 3.19	- 0.32	- 4.25	- 4.70
B6	- 2.16	0.09	- 2.44	- 2.38
C1	4.91	- 4.08	3.73	3.36
C4	- 2.00	- 0.12	- 1.71	- 2.13

Position	A_L	A_R
A2	- 5.34	- 1.72
A4	- 2.64	- 2.21
B2	- 8.43	- 4.61
B3	- 6.45	- 3.14
B4	- 2.84	- 2.79
C2	- 1.95	- 0.28
C3	- 3.19	- 2.54
D6	- 1.30	- 0.48

Fig 4 Printout of results from Case 4 by the PDP-8 computer

$$\delta_p(j, x) = \delta_S(j, x) = \frac{q\ \sigma_p(j)}{S_I(x)} = \frac{q \cdot \sigma_S(j)}{S_S(x)} \quad \frac{S_S(x)}{S_I(x)} = \frac{\sigma_S(j)}{\sigma_p(j)} \tag{8b}$$

$$\delta_D(j, x) = \delta_S(j, x) = \frac{q\ \sigma_D(j)}{S_D(x)} = \frac{q \cdot \sigma_S(j)}{S_S(j)} \quad \frac{S_D(x)}{S_S(x)} = \frac{\sigma_D(j)}{\sigma_S(j)} \tag{8c}$$

$S_I(x)$, $S_D(x)$ and $S_S(x)$ can be represented by the corresponding (I(x), D(x) and S(x), ratio-functions obtained from phantom measurements (Fig. 1) To solve eq (8 a, b, c) the ratios between these functions, independent of tumour volume (V_t) and concentration ratio (c_0), were calculated and plotted as functions of x (Fig 2) The corresponding constant ratios between the standard deviations of the evaluation parameters were also calculated for each subregion j The values of x_0 were obtained from comparison between these constant ratios and the ratios given in Fig 2

As only one of the right and left parts of each subregion was considered in each equation (8 a, b, c), the values of x_0 obtained, are between 0 and d, where d is the distance from the median plane to the right or left side of the skull ($0 \leq x_0 \leq d$) Hence, considering only one of the right or left halves of the skull, the monotonously increasing functions and the monotonously decreasing function in Fig 2 offer only one or none solution of each equation (8 a, b, c) If a solution exists, one of the two evaluation parameters in the ratios (Fig 2) has a higher degree of detectability for accumulations of $^{99}Tc^{m}O_4$ located at depths $x < x_0$, and the other for accumulations located at depths $x > x_0$ As an example the difference parameter has a higher detectability of accumulations of $^{99}Tc^{m}O_4$ located lateral to the relevant x_0 and the corresponding sum-parameter has a higher detectability of accumulations located medial to x_0 (Figs 2, 3).

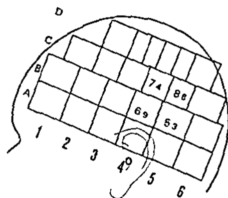


Fig 5

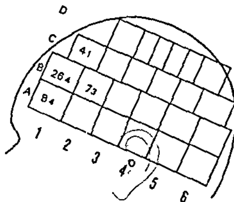


Fig 6

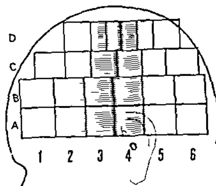


Fig 7

Fig 5 Case 5 Areas with evaluation parameters deviating more than 3 SD

Fig 6 Case 4 Areas with evaluation parameters deviating more than 3 SD

Fig 7 The border between the anterior and posterior groups of measuring areas is marked by the heavy line An intermediate group is marked by the hatched area, which overlaps the border

The advantage of using adjacent values and different reference values is illustrated by exemplification

[illegible] e compared [illegible] Deviations [illegible] values of each evaluation parameter were given in number of SD and the separation of abnormal from normal $^{99}Tc^{m}O_4$ distributions in the skull was determined from the parameter giving the maximum deviation (SD_{max})

All negative deviations from the normal were excluded, except in difference parameters, in which negative values arbitrarily indicated increased count rates on the left side, and in adjacent parameters (AV) in which negative deviations indicated a higher value in the more frontal of two regions (LIND et coll)

To save time in routine clinical work, only parameters deviating more than 2 SD were printed out by the computer (Fig 4) To make clinical interpretation easier, positions which had a deviation of the evaluation parameters larger than 3 SD

Table 1

The parameters used in measuring the whole skull are marked by + [1] A1, A2, A6, B1, B6 C1 C6 D1 and D6 were excluded [2] A3, A4, A5, B2, B3, B4, B5, C3, C4, C5, D2, D4 and D5 were excluded

	r_c	r_p	A	S_c	S_p	D
208 parameters						
A1–A6	+	+	+	+	+	+
B1–B6	+	+	+	+	+	+
C1–C6	+	+	+	+	+	+
D1–D6	+	+	+	+	+	+
123 parameters						
A1–A6	–	+	+	–	+[1]	+[2]
B1–B6	–	+	+	–	+[1]	+[2]
C1–C6	–	+	+	–	+[1]	+[2]
D1–D6	–	+	+	–	+[1]	+[2]
75 parameters						
A1–A6	–	+	–	–	+[1]	+[2]
B1–B6	–	+	–	–	+[1]	+[2]
C1–C6	–	+	–	–	+[1]	+[2]
D1–D6	–	+	–		+[1]	+[2]

from the normal mean were indicated on a lateral projection of the head by the actual maximal deviation in number of SD (Figs 5, 6)

The value of SD_{max} was calculated for each individual included in the reference group, using 208 parameters (Table 1)

The same procedure was repeated using 123 and 75 parameters, respectively (Table 1)

In order to take a smaller number of parameters into consideration the skull was also divided into six areas (Fig 7) The different areas were supposed to correspond approximately to the frontal, temporal + parietal and occipital + posterior fossa regions, respectively The maximal deviation, expressed in the number of SD in any of the parameters of each area, was calculated for each individual of the reference group

Results

Each subregion was divided into several parts in regard to the type of parameter expected to offer the highest significance in the detection of a small tumour activity (Fig 3) (1) Central part, where sum parameters on average will give the highest significance in measuring a tumour activity, (2) lateral parts, where the difference parameters on average will give the highest significance, (3) intermediate parts, where the position ratio parameters on average will give the highest significance

The boundaries between the three parts were determined by the values of x_0 and varied between the subregions Despite the inaccuracy of the estimation of the

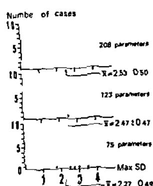


Fig 8

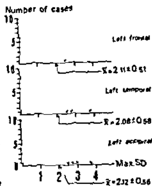


Fig 9

Fig 8 Normal ranges of SD_{max} of the 208, 123 and 75-groups of parameters, which cover the whole measured skull area obtained from the reference group

Fig 9 Normal ranges of SD_{max} of the left frontal, temporal and occipital groups of parameters obtained from the reference group

values of detectability, it was concluded that all the parameters were important in clinical examinations

Separation of laterally from centrally located accumulations of $^{99}Tc^mO_4$ The high depth dependence of the ratio D(x)/S(x) (Fig 2), indicates a possibility to estimate the depth location of a $^{99}Tc^mO_4$ accumulation From the solution of eq (8 c) $(\delta_D(j\ x) = (\delta_S(j\ x))$ the skull volume could be divided into a central part where the sum parameters on average will give larger significance of an accumulated amount of isotope than the difference parameters and lateral parts with the opposite conditions (Fig 3)

Normal and abnormal isotope distribution in the whole skull The maximal deviation in number of SD in any of the used parameters (SD_{max}) was used as a criterion for separating pathologic cases from normal ones The normal mean value of SD_{max}, calculated from the reference group (208 parameters) was large (2 53 ± 0 50 SD) which was explained by the large number of parameters, increasing the probability of getting a large deviation from the mean value in any of them The distribution of SD_{max} among the 29 reference cases is presented in Fig 8 From this diagram it was decided to use the following classification for the clinical examinations

Criterion = Maximal deviation in number of SD (SD_{max}) in any of the 208 parameters used

I 0–3 0 Definitely normal $^{99}Tc^mO_4$ distribution
II 3 0–3 5 Probably normal $^{99}Tc^mO_4$ distribution
III 3 5–4 0 Probably abnormal $^{99}Tc^mO_4$ distribution
IV 4 0–∞ Definitely abnormal $^{99}Tc^mO_4$ distribution

The number of parameters could be reduced thus offering a smaller normal mean value of SD_{max} 123 and 75 parameters were selected to find out if relevant advantage could be made of such reduction Sum and difference parameters of the subregions,

Position	r_{La}	r_{Ra}	S_a
A2	0 48	0 12	0 19
A6	2 16	- 2 69	- 2 44
B1	- 4 78	- 4 95	3 01
B2	0 47	5 85	- 2 02
B4	3.05	2 28	3.20
B6	- 1 99	2 65	- 2 37
C1	- 3 04	- 3 20	- 3 24
C2	- 1 45	2 85	2 26
C3	- 1 80	2 93	2 71
C6	- 3 52	- 3 80	3 77
D1	- 1 80	2 06	- 1 98
D2	- 1 45	- 2 23	1 88
D5	- 2 78	- 2 94	2 97
D6	- 4 55	4 39	- 4 60

Position	r_{Lp}	D	r_{Rp}	S_p
A2	2 69	- 2 41	1 51	2 15
A6	- 2 27	- 1 55	3 17	- 2 79
B1	3 42	- 1 02	3 77	3 69
B2	1 49	- 3 27	- 1 93	0 11
B4	5.29	- 0 60	4 21	6.08
B5	2 97	0 54	3 69	3 71
B6	- 1 96	- 1 41	- 2 96	- 2 55
C1	1 64	1 13	- 2 09	- 2 00
C2	1 05	2 24	- 0 73	0 20
C4	4.90	0 42	5 23	6.00
C5	4.4	- 0 51	3 22	4.11
C6	2 52	0 70	2 94	2 82
D2	2 02	1 99	0 51	1 36
D3	2 25	- 1 78	1 36	2 03
D4	2 85	1 45	2 45	3 10
D6	2 91	0 60	- 2 98	- 3 04

Position	A_L	A_R
A2	2 70	1 04
A3	2 16	1 08
A6	- 2 68	- 2 90
B2	5 81	2 84
B3	0 70	2 78
B4	2 96	3 49
B6	2 89	4.10
C2	2 95	1 93
C4	4.12	5 00
C6	3 81	4.10
D5	2 40	2 04
D6	3 24	3 20

Fig 10 Printout of results from Case 1

where they were not expected to offer higher detectability of lesions than corresponding position ratios were excluded (Fig 3) The remaining parameters are tabulated in Table 1 The mean value of the criterion used in the reference group was in this way decreased from 2 53±0 50 SD to 2 47±0 47 and 2 27±0 49, respectively (Fig 8)

Normal and abnormal distribution in one defined subdivision of the skull The number of parameters used could also be reduced by regarding only a small part of the head It is common in clinical work that symptoms and signs as well as the results of preliminary investigations indicate pathology in a limited part of the brain To investigate this approach the head was divided into six overlapping areas (Fig 7)

The 208 group of parameters was reduced corresponding to these subdivisions and SD_{max} in any of the reduced number of parameters of each subdivision was used as a criterion The mean values of SD_{max} of each subdivision were calculated from the results of the reference group (Fig 9) It was found that these mean values were

Position	r_{cc}	t_p	S_c
5	-2 16	-1 04	-2 23
6	2 27	4 15	3.15
C4	0 62	4.22	1.46
C?	-0 68	0 44	-0 22
P5	0 85	2 08	1 52
S4	0 [illegible]	1 93	1 14

Position	r_r	B	t_{pd}	S_p
1	-2	1 95	-0 95	-1 65
[illegible]	1 52	2 07	2 97	2.50
C6	-0 83	2 80	0 11	-0 40
P5	0 77	2 56	2 22	1 64
P4	-0 12	2 94	2 28	1 78
P5	2 04	1 34	-0 22	-1 32

Position	a_I	L_R
[illegible]	1 [illegible]	1 74
C3	3 33	3 09
C4	-1 77	-4 03

Fig. 11 Printout of results from Case 2

reduced by about 0 5 for all subdivisions compared to the mean value of SD_{max} of the whole head There were no relevant differences between right and left sides The variance of SD_{max} was found to be of about the same size in all subdivisions and also of the same size when the whole head was regarded It was therefore concluded that the boundaries of the criterion used to classify an individual $^{99}Tc^mO_4$ distribution as normal or abnormal could be decreased by 0 5 SD if, for clinical reasons, only one subdivision was regarded (Fig 9) The classification will then be as follows

Criterion = Maximal deviation in number of SD (SD_{max}) in any of the *parameters used*

I 0–2 5 Definitely normal $^{99}Tc^mO_4$ distribution
II 2 5–3 0 Probably normal $^{99}Tc^mO_4$ distribution
III 3 0–3 5 Probably abnormal $^{99}Tc^mO_4$ *distribution*
IV 3 5–∞ Definitely abnormal $^{99}Tc^mO_4$ *distribution*

Use of plane mean value P_{mv} as the reference Case 1 had an arteriovenous malformation in the central parts of the brain The deviations from the normal mean of the C_{mv} group of parameters in number of SD *were classified* as probably normal, but the deviations of the P_{mv} *group of parameters* were large enough to classify the patient as definitely abnormal (*Fig 10*) The region of increased activity was almost completely equivalent to that *constituting the* C_{mv} but not equivalent to the region of the P_{mv} Hence, the *detectability of the* accumulation of $^{99}Tc^mO_4$ evaluated by the r_c and S_c parameters should be *less than the detectability* of the accumulation evaluated by the r_p or S_p parameters as *demonstrated* by the case

The use of C_{mv} as the reference Case 2 had a cystic tumour within the right parietal region, histologically an *astrocytoma* grade II The deviations from the normal *mean* values of the r_p *and* S_p *parameters* in number of SD were classified as definitely

Position	r_{Lo}	r_{Ro}	S_o
A2	0 48	- 0 12	0 19
A6	- 2 26	- 2 69	- 2 44
B1	- 4 78	- 4 95	- 5 01
B2	0 47	- 3 85	- 2 02
B4	3,05	2 8	3, 0
B6	- 1 99	- 2 65	- 2 37
C1	- 3 04	- 3 70	- 3 24
C2	- 1 45	- 2 85	2 6
C3	- 1 80	- 2 93	2 71
C6	- 3 52	- 3 80	3 77
D1	- 1 80	- 2 06	1 98
D?	- 2 45	- 2 23	1 89
D5	- 2 78	- 2 94	- 2 97
D6	- 4 55	- 4 39	- 4 60

Position	r_{Lr}	D	r_{Rr}	S_p
A2	69	- 2 41	1 51	2 33
A6	- 2 27	- 1 55	- 3 37	2 79
B1	- 3 42	- 1 02	- 3 77	- 3 69
B.	1 49	- 3 27	- 1 93	0 31
B4	5,29	- 0 60	4 21	6,09
B5	2 93	0 54	3 03	3 71
B6	- 1 96	- 1 41	- 2 96	- 2 35
C1	- 1 64	- 1 15	- 2 09	2 ?3
C?	1 05	- 2 ?4	- 0 73	0 20
C4	4,90	- 0 42	5 ?3	6,00
C5	4,42	- 0 51	3 22	4,77
C6	- 52	- 0 70	- 94	- 2 82
D2	2 02	- 1 99	0 51	1 36
D3	2 23	- 1 78	1 36	2 03
D4	2 83	1 45	2 45	3 10
D6	- 2 91	- 0 60	- 2 98	- 3 04

Position	A_L	A_R
A?	2 70	1 04
A5	2 16	- 1 08
A6	- 2 68	- 2 90
B2	5,81	2 84
B3	0 70	2 78
B4	2 96	3 49
B6	- 2 89	4,10
C2	2 95	1 93
C4	4,12	5 00
C6	3 81	4,10
D5	2 40	2 04
D6	- 3 24	3 20

Fig 10 Printout of results from Case 1

where they were not expected to offer higher detectability of lesions than corresponding position ratios, were excluded (Fig 3) The remaining parameters are tabulated in Table 1 The mean value of the criterion used in the reference group was in this way decreased from 2 53±0 50 SD to 2 47±0 47 and 2 27±0 49, respectively (Fig 8)

Normal and abnormal distribution in one defined subdivision of the skull The number of parameters used could also be reduced by regarding only a small part of the head It is common in clinical work that symptoms and signs as well as the results of preliminary investigations indicate pathology in a limited part of the brain To investigate this approach the head was divided into six overlapping areas (Fig 7)

The 208 group of parameters was reduced corresponding to these subdivisions and SD_{max} in any of the reduced number of parameters of each subdivision was used as a criterion The mean values of SD_{max} of each subdivision were calculated from the results of the reference group (Fig 9) It was found that these mean values were

Position	r_{Lc}	$r_{\Delta c}$	S_c
2	2 16	- 1 64	2 23
5	27	4 15	3 73
C4	0 62	1 22	1 66
C6	0 64	0 24	- 0 22
D5	0 85	2 08	2 52
D4	0 77	1 95	1 14

Position	r_p	D	$r_{\Delta p}$	S_p
C1	- 2 23	1 95	- 0 73	- 1 47
C3	1 52	2 07	2 97	2 50
C6	- 0 83	2 08	0 33	- 0 43
D5	0 77	2 56	2 22	1 64
D4	- 0 32	2 34	2 24	1 20
D6	2 04	1 74	- 0 22	- 1 30

Position	A_L	S_a
[illegible]	1 5	1 4
C3	5 20	4 09
C4	1 73	1 65

Fig. 11 Printout of results from Case 2

reduced by about 0 5 for all subdivisions compared to the mean value of SD_{max} of the whole head There were no relevant differences between right and left sides The variance of SD_{max} was found to be of about the same size in all subdivisions and also of the same size when the whole head was regarded It was therefore concluded that the boundaries of the criterion used to classify an individual $^{99}Tc^mO_4$ distribution as normal or abnormal could be decreased by 0 5 SD if, for clinical reasons, only one subdivision was regarded (Fig 9) The classification will then be as follows

Criterion = Maximal deviation in number of SD (SD_{max}) in any of the parameters used

I	0–2 5	Definitely normal $^{99}Tc^mO_4$ distribution
II	2 5–3 0	Probably normal $^{99}Tc^mO_4$ distribution
III	3 0–3 5	Probably abnormal $^{99}Tc^mO_4$ distribution
IV	3 5–∞	Definitely abnormal $^{99}Tc^mO_4$ distribution

Use of plane mean value P_{mv} as the reference Case 1 had an arteriovenous malformation in the central parts of the brain The deviations from the normal mean of the C_{mv} group of parameters in number of SD were classified as probably normal, but the deviations of the P_{mv} group of parameters were large enough to classify the patient as definitely abnormal (Fig 10) The region of increased activity was almost completely equivalent to that constituting the C_{mv} but not equivalent to the region of the P_{mv} Hence, the detectability of the accumulation of $^{99}Tc^mO_4$ evaluated by the r_c and S_c parameters should be less than the detectability of the accumulation evaluated by the r_p or S_p parameters as demonstrated by the case

The use of C_{mv} as the reference Case 2 had a cystic tumour within the right parietal region, histologically an astrocytoma grade II The deviations from the normal mean values of the r_p and S_p parameters in number of SD were classified as definitely

Position	r_{Lo}	r_{Ro}	S_o
A2	0.48	-0.12	0.29
A6	-2.26	-2.69	-2.44
B1	-4.78	-4.95	-5.01
B2	0.47	-3.85	-2.02
B4	3.05	2.28	3.20
B6	-3.99	-2.65	-2.37
C1	-3.04	-3.20	-3.28
C2	-2.45	-2.85	-2.26
C3	-2.80	-2.93	-2.71
C6	-3.57	-3.80	-3.77
D1	-1.80	-2.06	-1.98
D2	-2.45	-2.23	-1.88
D5	-2.79	-2.94	-2.97
D6	-4.55	-4.39	-4.60

Position	r_{Lr}	D	r_{Rr}	S_r
A2	2.67	-2.41	3.51	2.13
A6	-2.27	-1.55	-3.17	-2.78
B1	-5.42	-1.02	-3.77	-3.69
B2	2.49	-3.27	-1.93	-0.44
B4	5.74	-0.60	4.21	6.09
B5	2.93	0.54	3.69	3.74
B6	-4.96	-1.41	-2.96	-2.55
C1	-2.64	-1.13	-2.09	-3.00
C2	1.05	-2.24	-0.73	0.70
C4	4.90	-0.42	5.25	6.00
C5	4.47	-0.51	3.22	4.11
C6	-2.52	-0.70	-2.94	-2.82
D2	2.02	-1.99	0.53	3.36
D3	2.25	-1.78	1.36	2.03
D4	2.83	-1.45	2.45	3.20
D6	-2.91	-0.60	-2.98	-3.04

Position	A_L	A_R
A2	2.70	1.04
A3	-2.15	-1.08
A6	-2.68	-2.90
B2	5.87	2.84
B3	-0.70	2.78
B4	2.96	3.49
B6	-2.89	-4.10
C2	2.99	1.93
C4	4.12	5.00
C6	-3.81	-4.23
D5	-2.40	-2.04
D6	-3.24	-3.20

Fig 10 Printout of results from Case 1

where they were not expected to offer higher detectability of lesions than corresponding position ratios, were excluded (Fig 3) The remaining parameters are tabulated in Table 1 The mean value of the criterion used in the reference group was in this way decreased from 2 53 ± 0 50 SD to 2 47 ± 0 47 and 2 27 ± 0 49, respectively (Fig 8)

Normal and abnormal distribution in one defined subdivision of the skull The number of parameters used could also be reduced by regarding only a small part of the head It is common in clinical work that symptoms and signs as well as the results of preliminary investigations indicate pathology in a limited part of the brain To investigate this approach the head was divided into six overlapping areas (Fig 7)

The 208-group of parameters was reduced corresponding to these subdivisions and SD_{max} in any of the reduced number of parameters of each subdivision was used as a criterion The mean values of SD_{max} of each subdivision were calculated from the results of the reference group (Fig 9) It was found that these mean values were

Discussion

Investigation of the isotope distribution in the skull by conventional methods involves the use of several basic parameters and their combinations The evaluation based on image interpretation is subjective and complicated, and demands great experience (MALLARD 1966, BURROWS 1972)

Long experience of a subjective method adds information to the diagnostic process, thus enhancing the diagnostic accuracy, especially if a large number of parameters with large normal variations is used, as for instance in gamma encephalography according to PLANIOL and MUNDIGER or in the interpretation of brain scans and gamma camera images (PLANIOL, MUNDIGER & ASAI, DOWSETT & PERRY, POPHAM et coll, MUNDIGER & OSTERTAG 1971, DOWSETT) An evaluation of diagnostic accuracy is therefore difficult, and a strictly objective and automatic interpretation of the results should be of great value

To obtain a strictly objective diagnosis, one defined criterion of abnormal isotope distribution with fixed classification boundaries must be chosen It might include several parameters and also their combinations The maximum deviation in any of the 208 defined parameters was chosen as criterion in this work

The significance of a pathologic deviation corresponding to q standard deviations outside the normal range of a parameter could be expressed

$$q = \frac{X_p - \bar{X}}{\sigma_x}$$

X_p = actual parameter value
$\bar{X}$ = normal mean of the parameter value
σ_x = standard deviation of X

A criterion of abnormality could be defined as the maximum q value (SD_{max}) of any of several parameters A large number of parameters will increase the normal mean value of SD_{max} above 0 and thus decrease the significance of a pathologically high value of SD_{max} Thus, ideally (1) the parameters chosen should have a high sensitivity to the diagnostic problem of interest, giving large values of $(X_p - \bar{X})$ (2) their standard deviations in a normal group should be small, and (3) the number of the parameters should be small

Variance of parameters Each evaluation parameter was obtained by dividing a measuring value with a reference value The variance of a parameter (σ_x^2) was thus dependent on two sources of variation and both should be restricted in order to increase the diagnostic accuracy (DUGGAN et coll 1964, PLANIOL, MUNDIGER & ASAI, DOWSETT & PERRY, POPHAM et coll, DOWSETT) The important problem of restricting the normal variation has been discussed elsewhere (LIND et coll)

Detectability properties of the position ratio, sum and difference parameters Theoretical calculation and phantom experiments demonstrated that the increase ratio is

Position	r_{Lc}	r_{Rc}	S_c
B1	2.62	1 69	2 20

Position	r_{Lp}	D	r_{Rp}	S_p
A6	- 1.89	- 0.57	- 2.29	- 2 14
C4	- 0.72	- 1.16	- 2 21	- 1 67
D3	- 0.99	- 1.19	- 2.64	- 1 81
D4	- 1.38	- 0.79	- 3.38	- 2 49

Position	A_L	A_R
A2	- 3.20	- 1.74
A6	- 2.54	- 2.62
D2	- 1.83	- 2.07
D6	2.05	1.62

Fig 12 Printout of results from Case 3

normal (Fig 11) However, the deviations of r_c parameter were classified as definitely abnormal (This measurement was made 2 hours after the injection of $^{99}Tc^mO_4$ and related to the corresponding normal ranges, LIND et coll) Probably, the region of accumulated $^{99}Tc^mO_4$ corresponded more to a P_{mv} region than to the C_{mv} region In that case the detectability of the accumulation, evaluated by the r_p and S_p parameters can be expected to be less than the detectability of the accumulation evaluated by the r_c and S_c parameters, as demonstrated by this case

Use of adjacent values as the reference Case 3 had a small meningeoma close to the skull base and to the median plane, above the olfactory region Characteristic calcifications were found at roentgen examination of the skull The deviations from the mean of all parameters but one A parameter were classified as definitely normal This parameter displayed a deviation that was classified as probably normal, when regarding the whole skull, but probably abnormal, when regarding the frontal region (Fig 12) The SD values of the r_c, r_p, S_c and S_p parameters of the reference group were high in the A1 to A2 region (LIND et coll) However, the A parameters had comparatively small normal SD values (5 2 %–5 4 %) in these positions (LIND et coll) Hence, the detectability of an accumulation of $^{99}Tc^mO_4$ in this position, close to the median plane of the skull, might be higher in A parameters compared to the detectability of the r_c, r_p, S_c, S_p or D parameters, as demonstrated by this case

It was hence concluded that the use of the reference values P_{mv} and C_{mv} as well as the A parameters, was important in clinical investigation, to avoid some risks of diagnostic failure

Examples of diagnostic results Case 4 had a low differentiated metastasis in the left frontal lobe, possibly originating from the kidney or the thyroid gland SD_{max} was at a level far above the borders chosen (26 4 SD) (Figs 4, 6)

In case 5 a tumour, histologically an astrocytoma grade III, was present with a $SD_{max} = 8$ 6, thus far above the borders chosen (Fig 5)

Table 2

The maximum deviation in the C_{mv}, P_{mv} and A groups of parameters are given in number of SD for the five pathologic cases The maximum deviation in any of all 208 parameters is marked in boldface This maximum deviation can occur in any of the three groups of parameters (Case 2 was measured 2 hours after injection of $^{99}Tc^mO_4$ values obtained were related to a corresponding norm alrange, (LIND et coll)

Case No	Maximal deviation of any of the parameters in the		
	r_c, S_c	r_p, S_p, D	A
1	3 2	6 1	5 8
2	**4.2**	3 0	4 0
3	2 6	1 2	**3.2**
4	**26.4**	17 8	8 4
5	7 9	11 3	**12.1**

Reference values C_{mv}, P_{mv} and A Ideally, a reference value should be unaffected by the pathologic accumulations analysed and have a negligible variation, otherwise the relation between the measuring value and the reference value may remain constant and the parameter value lie within the normal range in spite of the pathologically increased amount of isotope

C_{mv} was assumed to be more stable than a mean value of all measuring areas which would include marginal areas with high variation P_{mv} was for the same reason assumed to be less constant, but provided a possibility of compensating for unavoidable differences in the positioning height above the skull base plane The adjacent parameter was used because the relation between the isotope contents in two adjacent subregions might be abnormal, even if both are within the normal range when evaluated by the r_p or r_c parameters (PLANIOL, MUNDIGER & ASAI, DOWSETT & PERRY, POPHAM et coll)

Cases 1 and 2 demonstrated areas with pathologic amounts of isotope almost covering the C_{mv} or P_{mv} regions, thus giving false negative C_{mv} or P_{mv} parameter values, respectively (Figs 10, 11)

The maximum deviation might occur in any of the C_{mv}, P_{mv} or a A groups of parameter (Table 2) This clearly demonstrates the advantage of using several reference values and therefore the C_{mv}, P_{mv} and A were used as references in this work It is possible to use a large number of differently constructed parameters, but for reasons given previously, the use of the 208 parameters investigated was considered to be adequate

Criteria A theoretical calculation of the boundaries between normal and abnormal criteria values was impossible, even if the normal SD values of the parameters included were known the degree of dependence between the parameters was un-

always more sensitive to added tumour phantom activities than the sum or difference parameters (LARSSON et coll) (Fig 1) However, according to eq (6) the normal standard deviation of the chosen parameter in clinical measurements exert influence on detectability, and hence position ratio parameters do not always imply a higher degree of detectability than the sum and difference parameters, in spite of being more sensitive Calculation of results from the phantom experiments correlated to results obtained from the reference group are presented in Fig 3, which demonstrates that the sum parameters (S_p) should give the highest significance (q) for pathologic accumulations of $^{99}Tc^{m}O_4$ in the central regions of the skull and difference parameters (D) for accumulations in the lateral parts of the skull Position ratios (r_p) should give the highest significance in between these central and lateral regions Position ratios, sums and side differences were therefore all regarded as important for the diagnostic accuracy (MOORE, BASCHIERI et coll 1965, MCALISTER 1965 POPOVIC 1965, CONRAD & HORST 1966, PLANIOL, MUNDIGER & ASAI, POPHAM et coll)

The number of measuring parameters used and hence the spatial resolution of the symmetry detector method had to be limited in order to obtain a simply applicable diagnostic criterion, SD_{max}, with a small normal mean value, which was dependent on the size of each measuring area and on the number of reference values used A large number of measuring parameters should increase the probability of obtaining one optimal measurement from one subregion with abnormally high isotope content (high sensitivity of the effect of interest, high value of $(X_p - \bar{X})$), but the probability of a large value among normals of SD_{max} will also increase and thus decrease the relevance of high values of SD_{max} The 208 parameters were reduced to 123 and 75, respectively, to find out if such reductions changed the criteria boundaries between normal and abnormal favourably The normal mean value of SD_{max} was only reduced by 0 06 and 0 27 SD, respectively, in spite of the loss of several important parameters (Fig 8) It was therefore concluded that a reduction of parameters below 208 could not be expected to increase the diagnostic accuracy

On the other hand, a larger number of parameters might increase the diagnostic accuracy This, however, would interfere with the purpose of designing an uncomplicated method

The measuring areas were generally overlapping and square, 3 cm × 3 cm, in order to obtain a good coverage of the skull Consequently, there were 24 measuring areas of each side of the skull offering 48 measuring values The size 3 cm × 3 cm was chosen to correspond approximately to the size of a lateral projection of a region with the effect of interest, i e increased amount of isotope, caused by a small brain tumour (PLANIOL, MUNDIGER & ASAI, DOWSETT & PERRY, ZEIDLER et coll 1970, BURROWS, DOWSETT)

sponding standard deviation in a normal group makes it possible to use the conception of detectability in order to choose those parameters, that are most relevant for the detection of the effect of interest

Hence, the choice of evaluation parameters of a diagnostic method can be made on these rational bases and objective comparison between the diagnostic accuracy obtained by different methods facilitated by use of this conception of detectability

The uncomplicated symmetry detector method was developed on these bases Objective and semiautomatic classification of $^{99}Tc^{m}O_4$ distributions in the skull as normal or abnormal were obtained without the need for experienced evaluation of individual results

Acknowledgement

The histologic examination was made at the Department of Tumour Pathology, Karolinska Sjukhuset by Prof G Moberger according to the principles given by N Ringertz

SUMMARY

The objective classification of results of the previously described symmetry detector method for gamma encephalography is reported The different evaluation parameters were chosen after comparing their detectability in different subregions of the head or as a result of findings in certain patients The detectability was estimated from the results of phantom measurements related to the normal ranges of evaluation parameters The borders of the classification criterion are discussed in relation to the number of evaluation parameters used

ZUSAMMENFASSUNG

Die objektive Klassifizierung der Ergebnisse der zuvor beschriebenen symmetrischen Detektor Methode zur Gammaencephalographie wird beschrieben Die verschiedenen Untersuchungsparameter wurden nach dem Vergleich ihrer Nachweisbarkeit in verschiedenen Subregionen des Kopfes oder als Ergebnis von Befunden bei bestimmten Patienten gewahlt Die Grenzen der Nachweisbarkeit wurde aus Phantommessungen die auf den normalen Bereich der Untersuchungsparameter bezogen waren bestimmt Die Grenzen der Klassifikations Kriteria werden im Verhältnis zur Zahl der verwendeten Messparameter diskutiert

RÉSUMÉ

Présentation de la ...
symetrie précedémment ...
d evaluation ont et ...

known It was thus necessary to apply the chosen criterion on the reference group of cases without brain lesions, in order to obtain a basis for a rational choice of boundaries between normal and abnormal It was also necessary to know the relative number of false positive cases, obtained with the chosen boundaries, otherwise the usefulness of the method for diagnostic screening purposes could not be evaluated (DUGGAN et coll , PLANIOL, MUNDIGER & ASAI, DOWSETT & PERRY, POPHAM et coll , DOWSETT)

The distribution of the SD_{max} obtained from the reference group is presented in Fig 8 It is seen that the classification boundaries chosen should restrict the false positive cases to a very small number However, the parameters used were chosen after estimation of their SD values in this reference group, and thus application of the criterion to the same (selected) group will not give correct information about the normal range of the SD_{max} (PLANIOL, MUNDIGER & ASAI, POPHAM et coll)

Often, in clinical work, only one defined subdivision of the whole brain is the possible location of a lesion This clinical information can be combined with the measuring results, in order to increase the diagnostic accuracy by reducing the number of parameters analysed, thus decreasing the criterion boundaries between normal and abnormal A division of the skull area into six subdivisions (Fig 7) made a reduction of the criterion boundaries by about 0 5 SD possible (Fig 9) This might be of special interest in attempts to exclude the existence of a pathologically increased amount of isotope in a defined brain area

Separation of laterally located lesions from centrally located ones Comparison between sum and difference parameters (Fig 3) offers a possibility of estimating the depth of an abnormal source of activity Fig 2 clearly demonstrates the depth sensitivity of D/S

Case examples Cases 1 to 3 are presented to illustrate the necessity of using several types of parameters to avoid false negative classification (Figs 10–12) (PLANIOL, MUNDIGER & ASAI, DOWSETT & PERRY, POPHAM et coll)

Case 4 demonstrates the evident, semiautomatically obtained objective diagnosis of an accumulation of $^{99}Tc^{m}O_4$ caused by a brain metastasis (Figs 4, 6)

The results in case 5 were also evident and easily interpretated diagnosis astrocytoma grade III (Fig 5)

Conclusion

Knowledge of the normal ranges of parameters of the distribution of $^{99}Tc^{m}O_4$ in the skull is necessary for the separation of abnormal from normal

Knowledge of the relative importance of different sources of variance in the evaluation parameters facilitates the limitation of the most important contributions to variance and the choice of evaluation parameters

Knowledge of the sensitivity of each evaluation parameter related to the corre-

FROM THE RADIATION PHYSICS DEPARTMENT (DIRECTOR ASSOC PROF H SKÖLDBORN)
SAHLGRENSKA SJUKHUSET, UNIVERSITY OF GOTHENBURG, S-413 45 GOTHENBURG, SWEDEN

DUAL PHOTON ABSORPTIOMETRY IN LUMBAR VERTEBRAE

II Precision and reproducibility

B O Roos

Details of the experimental technique for the determination of the bone mineral content in a lumbar vertebra have been described previously (Roos et coll 1970, Roos & Sköldborn 1974) The method involves the use of two isotopes which emit gamma radiation with different energies (^{241}Am with 59 6 keV and ^{137}Cs with 662 keV) The radiation sources are so arranged that their gamma radiation passes the object to be measured in a common collimated radiation beam (Fig 1) The trans mitted gamma radiation is registered digitally with a scintillation detector—both photon energies simultaneously The measurement is performed during a pre set period of time at a number of points along a path transversally (x-direction) over the patient The measuring path is projected over the centre of a selected vertebra (usually L3) Application of the law of exponential attenuation enables calculation of the amount of bone mineral (g cm $^{-2}$) at each point along the measuring path irrespective of the amount of soft tissue The bone mineral values are plotted as a function of position thus giving a bone profile curve which may be integrated over a base line between end points on either side of the vertebra The resulting area is termed A and is proportional to the bone mineral content in the unit g cm $^{-1}$

Submitted for publication 2 August 1974

REFERENCES

BASCHIERI I, PAVONI P, SEMPREBENE L and BENEDETTI G A Improvements in tumour detection by scanning Nuclearmedizin 2 (1965) 181

BURROWS E H The clinical utility of brainscanning in nuclear medicine *In* Progress in nuclear medicine Vol 1, p 287 Edited by E J Potchen and V R McCready S Karger Basel 1972

CONRAD B and HORST W Present state and possibilities of future development of radioisotope scanning with particular reference to the diagnosis of brain tumors Progr neurol Surg 1 (1966) 150

DOWSETT D J A quantitative analytical display programme (QUAD) designed for radio isotope brain scans Comput Biol Med 2 (1972) 27

— and PERRY B J A comparative statistical analysis of brain scans using a digital computer Brit J Radiol 43 (1970) 617

DUGGAN M J BRICE J JONES E MALLARD J R and MYERS M I Scanning techniques for brain tumour localization *In* Medical radioisotope scanning Proc IAEA Symp Athens 1964 Vol II p 121 Vienna 1964

LARSSON S LIND M and SÖDERBORG B Objective symmetry detector method for gamma encephalography I Physical characteristics Acta radiol Ther Phys Biol 14 (1975) 63

LIND M, LARSSON S and SÖDERBORG B Objective symmetry detector method for gamma encephalography II Normal range Acta radiol Ther Phys Biol 14 (1975) 145

MCALISTER J A brief report on work carried out on the prototype of the E D L whole body scanner Brit J Radiol 38 (1965) 317

MALLARD J R Medical radioisotope visualization (A review of scanning) Int J appl Radiat Isotopes 17 (1966) 205

MOORE G E Use of radioactive diiodofluorescein in the diagnosis and localization of brain tumors Science 107 (1948) 569

— PEYTON W T HUNTER S W and FRENCH L The clinical use of sodium fluorescein and radioactive diiodofluorescein in the localization of tumors of the central nervous system Minn Med 31 (1948) 1073

MUNDINGER F und ASAI A Ergebnisse der digitalen Gammaencephalographie bei Hirntumoren Vergleich von Wismut ^{206} Quecksilber ^{203} Neohydrin und Technetium ^{99m} Arch Psych Z Ges Neurol 210 (1967) 297

— und OSTERTAG CH Radio Isotope in der neurologisch neurochirurgischen Diagnostik Hippokrates 42 (1971) 135

PLANIOL T Gamma-encephalography after ten years of utilization in neurosurgery Progr neurol Surg 1 (1966) 93

POPHAM M G BULL J W D and EMERY E W Interpretation of brain scans by computer analysis Brit J Radiol 43 (1970) 835

POPOVIC S Survey of properties and parameters of focusing collimators Brit J Radiol 38 (1965) 316

RINGERTZ N Grading of gliomas Acta path microbiol scand 27 (1950) 51

ZEIDLER U SUMMER K BRUNNGRABER C V KOTTKE S und HUNDESHAGEN H Untersuchungen zur pathophysiologischen Grundlage der Hirnszintigraphie mit ^{99m}Tc Pertechnetat Arch Psychiat Nervenkr 213 (1970) 200

Repeated measurements in the same individual give varying values of A The scatter of these values is called the total precision, which consists of variations caused by the decay and subject variations "Subject variations" include all factors which cannot be reproduced exactly from one measurement to another, for example adjustment variations, movements of the subject during the measurement or variations in the position of the subject

Theory for the influence of the poisson scatter on A

Fundamental statistical concepts The standard deviation of a variable x, which is assumed to be normally distributed, is estimated using the following formula

$$s = \sqrt{\frac{\sum(x-\bar{x})^2}{n-1}} \tag{1}$$

where

x = the individual measurement values,
$\bar{x}$ = the mean value of the measurement values,
n = number of determinations of x

The coefficient of variation V represents the standard deviation in per cent of the mean value

$$V = 100\frac{s}{\bar{x}} \tag{2}$$

For the Poisson distribution, the standard deviation of the distribution is equal to the root of the true mean value For a value y, included in a Poisson distribution, the standard deviation σ is thus estimated according to the following

$$\sigma = \sqrt{y} \tag{3}$$

If z is a function of the variables $y_1, y_2, \quad y_n$, the standard deviation of z is estimated as follows

$$\sigma = \sqrt{\sum_{i=1}^{n}\left(\frac{\partial z}{\partial y_i}\right)^2 \sigma_{y_i}^2} \tag{4}$$

When comparing two independent series of measurements with the mean values $\bar{x}_1$ and $\bar{x}_2$ Student's t test is used for testing the significance of difference between the mean values If each measurement series comprises n measurements, the standard deviation for the difference is

$$s_{diff} = \sqrt{\frac{s_1^2 + s_2^2}{n}} \tag{5}$$

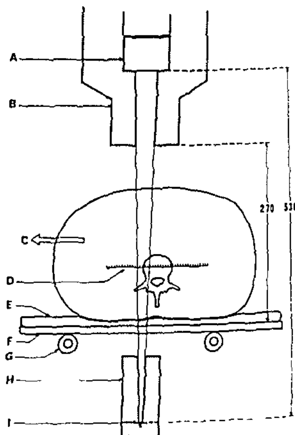


Fig 1 Diagram showing measuring procedure A = scintillation crystal, B = lead collimator for the detector, C = patient's direction of movement, D = scale for demonstrating the successive measuring positions, E = polythene mattress, F = couch, G = ball bearing, H = source container with collimation of emitted radiation beam, I radiation sources Distances stated in mm

The photon flux which meets the scintillation crystal depends upon radiation geometry, thickness and structure of the object being measured, and the activity of the radiation sources The distance between the radiation sources and the scintillation crystal is 530 mm The beam is collimated so that the cross-sectional area is rectangular At a height of 90 mm above the couch (Fig 1) it has an effective size of 14 mm × 25 mm with the long side parallel to the couch In measurements in patients the radiation beam passes the trunk in the p a direction at the level of the third lumbar vertebra A large individual variation exists, which has a considerable influence on the attenuation of the radiation especially the low energy part from ^{241}Am

The ^{137}Cs source has an activity of 5 mCi and an effective diameter of 3 mm The ^{241}Am source is flat and circular with an activity of 100 mCi and an active diameter of 7 2 mm Due to self-absorption, the source must be relatively thin (0 7 mm) and if higher activity is required the diameter must also be increased, which was not desirable with the measuring geometry chosen The flux of low energy photons to the scintillation crystal is thus also limited by the physical properties of the radiation source

The random nature of the radiation decay means that the number of counts obtained will vary according to the Poisson distribution This results in a mathematically well-defined precision in the final result—the area A



Fig 2. Bone profile showing N as a function of measuring position x for normal subject ML, measurement No 4

$$\frac{\partial N}{\partial R} = -\frac{\mu_s'}{R-kR'}$$

$$\frac{\partial N}{\partial R'} = -\frac{\mu_s}{R'} + \frac{k\mu_s'}{R-kR'}$$

$$\sigma_R = \sqrt{R}$$

$$\sigma_{R'} = \sqrt{R'}$$

Insertion in equation (4) gives the standard deviation for N

$$\sigma_N = \sqrt{\left(\frac{\mu_s'}{R-kR'}\right)^2 R + \left(\frac{\mu_s}{R'} + \frac{k\mu_s'}{R-kR'}\right)^2 R'} \tag{10}$$

Equation (10) thus gives the standard deviation for the individual variables N_1, N_2 , N_n By applying equation (4) the standard deviation of the area A may be calculated as follows

$$\sigma_A = \sqrt{\left[\sum_{i=2}^{n-1} \sigma_{N_i}^2 + \left(\frac{n-2}{2}\right)^2 (\sigma_{N_1}^2 + \sigma_{N_n}^2)\right] (\Delta x)^2} \tag{11}$$

Numerical example As an example, measurement no 4 in the normal subject ML is taken from the measurement series presented below Fig 2 presents the resulting polygon (N) as a function of the measurement position x for this example The

and the confidence interval is

$$(\bar{x}_2 - \bar{x}_1) - t\ s_{diff},\ (\bar{x}_2 - \bar{x}_1) + t\ s_{diff} \tag{6}$$

For example, if $n = 10$ and the confidence level is 95 %, $t = 2\ 262$

Formalism of the method Theoretical deductions (ROOS & SKÖLDBORN 1974) have shown that the result of a stationary measurement may be expressed as

$$m_B = \frac{N - D_{SF}\, m_F}{D_{SB}} \tag{7}$$

where

m_B = the bone mineral mass in the path of the radiation beam (g cm^{-2})
m_F = adipose tissue mass in the path of the beam (g cm^{-2})
D_{SF} and D_{SB} = terms comprising mass attenuation coefficients only

Further,

$$N = \mu'_S \ln (R - kR\ ) + \mu_S \ln R' + C \tag{8}$$

where

μ'_S = the mass attenuation coefficient (cm^2 g^{-1}) for 662 keV (^{137}Cs) in lean soft tissue
μ_S = *the mass attenuation coefficient* (cm^2 g^{-1}) *for 59 6 keV* (^{241}*Am*) *in lean soft* tissue
R = number of counts in the ^{137}Cs channel
R = number of counts in the ^{241}Am channel
k = the fraction of R registered in the ^{241}Am channel due to Compton scattering
C = a constant

N is calculated according to equation (8) for each measurement point and plotted as a function of the position x (Fig 2) Integration between the points x_1 and x_n gives the area A, which in practice is summed according to the following

$$A = \left[\sum_{i=2}^{n-1} N_i - \frac{n-2}{2}(N_1 + N_n) \right] \Delta x \tag{9}$$

If the summation limits x_1 *and* x_n *are chosen so that the radiation beam passes* outside the vertebra, the values N_1 and N_n will represent the soft tissue on either side of the vertebra The summation includes values which exceeds the straight base line, connecting N_1 and N_n The area A divided by the constant D_{SB} gives the bone mineral content (g cm^{-1}) in a transverse section through the vertebra From here on the results of the measurements will be presented as the relative quantity A

The standard deviation of N and A In the expression for N, equation (8), the two variables, the number of counts R and R′, are Poisson distributed Differentiation and application of equation (3) gives

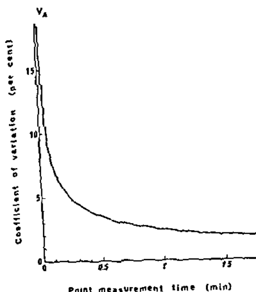


Fig. 3 Coefficient of variation V_A as a function of measuring time t for normal person ML, measurement No 4

(x_1 and x_{19}) are weighted with the factor $((n-2)/2^2)$, which in this case will be 72 25 Differentiation of equation (11) and insertion of the numerical values from Table 1 (x_{10}) shows that in the differential of σ_A in this case the end points contribute 89 per cent and intermediate points 11 per cent The positioning of the base line thus has a great influence on the precision This problem is discussed further below

σ_N is dependent upon the mass attenuation coefficients and the number of counts Partial differentiation of equation (10) with respect to R and R′ and insertion of the numerical values for a measurement point (x_{10} in Table 1) gives the following result

$$\frac{\partial \sigma_N}{\partial R} \approx -2\ 15 \times 10^{\ 10}$$

$$\frac{\partial \sigma_N}{\partial R'} \approx -11\ 17 \times 10^{\ 10}$$

σ_N thus shows 5 times greater dependence on R′, which represents the higher photon energy In order to improve the precision with the given photon energies the activity of ^{137}Cs may therefore be increased The influence of the mass attenuation coefficients has been analysed by WOOTEN (1971) His results show that in dichromatic measurements through a tissue thickness of 1 2 cm bone plus 20 cm soft tissue the lower photon energy should be in the range 35 to 40 keV and the higher should exceed 200 keV in order to give maximum precision of the bone mineral measurement However, WOOTEN used different and optimal measuring times for the two photon energies, while the method using simultaneous measurement requires the same measuring times The results of WOOTEN are thus not applicable in detail in the present investigation

Table 1

Measurement results and standard deviation for the normal person ML, measurement no 4 Measurement time 0 5 min per point, $\Delta x = 0\ 4$ cm

Position	R	R′	N	σ_N
x_1	230 844	172 265	$10\ 7 \times 10^{-4}$	$4\ 9 \times 10^{-4}$
x_2	240 097	176 650	$25\ 2 \times 10^{-4}$	$4\ 8 \times 10^{-4}$
x_3	233 592	174 776	$28\ 2 \times 10^{-4}$	$4\ 9 \times 10^{-4}$
x_4	212 866	171 070	$65\ 9 \times 10^{-4}$	$4\ 9 \times 10^{-4}$
x_5	191 121	168 283	$125\ 9 \times 10^{-4}$	$5\ 0 \times 10^{-4}$
x_6	177 982	167 069	$172\ 6 \times 10^{-4}$	$5\ 1 \times 10^{-4}$
x_7	179 683	168 709	$183\ 1 \times 10^{-4}$	$5\ 0 \times 10^{-4}$
x_8	188 505	170 838	$166\ 2 \times 10^{-4}$	$5\ 0 \times 10^{-4}$
x_9	*194 905*	*171 924*	*$149\ 9 \times 10^{-4}$*	*$5\ 0 \times 10^{-4}$*
x_{10}	200 838	173 807	$145\ 2 \times 10^{-4}$	$4\ 9 \times 10^{-4}$
x_{11}	200 719	172 434	$130\ 7 \times 10^{-4}$	$5\ 0 \times 10^{-4}$
x_{12}	195 537	171 431	$141\ 7 \times 10^{-4}$	$5\ 0 \times 10^{-4}$
x_{13}	186 919	169 732	$161\ 0 \times 10^{-4}$	$5\ 0 \times 10^{-4}$
x_{14}	191 254	170 477	$149\ 9 \times 10^{-4}$	$5\ 0 \times 10^{-4}$
x_{15}	219 873	176 698	$100\ 0 \times 10^{-4}$	$4\ 9 \times 10^{-4}$
x_{16}	254 799	184 871	$61\ 4 \times 10^{-4}$	$4\ 7 \times 10^{-4}$
x_{17}	273 260	186 755	$21\ 8 \times 10^{-4}$	$4\ 7 \times 10^{-4}$
x_{18}	275 272	186 170	$9\ 7 \times 10^{-4}$	$4\ 7 \times 10^{-4}$
x_{19}	300 693	192 806	$1\ 8 \times 10^{-4}$	$4\ 6 \times 10^{-4}$

end-points chosen as the summation limits are designated x_1 and x_{19} (Fig 2) The number of counts recorded and the corresponding values for N and σ_N obtained from equations (8) and (10) are given in Table 1 For the calculations the following experimentally determined values of the mass attenuation coefficients and the factor of Compton contribution, k, have been used (Roos 1970)

$$\mu_S = 0\ 1867 \quad cm^2\,g^{-1}$$

$$\mu'_S = 0\ 0814 \quad cm^2\,g^{-1}$$

$$k = 0\ 045$$

By means of equations (9) and (11)

$$A = 692\ 7 \times 10^{-4}$$

$$\sigma_A = 24\ 2 \times 10^{-4}$$

$$V_A = 100\frac{\sigma_A}{A} = 3\ 5\,\%$$

is calculated

According to equation (11) the measurement points x_2 x_{18} contribute equally to the coefficient of variation (3 5 %) while the contributions of the end points

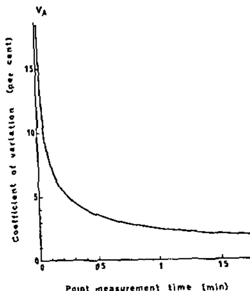


Fig. 3 Coefficient of variation V_A as a function of measuring time t for normal person ML, measurement No 4

(x_1 and x_{19}) are weighted with the factor $((n-2)/2^2)$, which in this case will be 72 25 Differentiation of equation (11) and insertion of the numerical values from Table 1 (x_{10}) shows that in the differential of σ_A in this case the end points contribute 89 per cent and intermediate points 11 per cent The positioning of the base-line thus has a great influence on the precision This problem is discussed further below.

σ_N is dependent upon the mass attenuation coefficients and the number of counts Partial differentiation of equation (10) with respect to R and R′ and insertion of the numerical values for a measurement point (x_{10} in Table 1) gives the following result

$$\frac{\partial \sigma_N}{\partial R} = -2\ 15 \times 10^{-10}$$

$$\frac{\partial \sigma_N}{\partial R'} = -11\ 17 \times 10^{-10}$$

σ_N thus shows 5 times greater dependence on R′, which represents the higher photon energy In order to improve the precision with the given photon energies the activity of ^{137}Cs may therefore be increased The influence of the mass attenuation coefficients has been analysed by WOOTEN (1971) His results show that in dichromatic measurements through a tissue thickness of 1 2 cm bone plus 20 cm soft tissue the lower photon energy should be in the range 35 to 40 keV and the higher should exceed 200 keV in order to give maximum precision of the bone mineral measurement However, WOOTEN used different and optimal measuring times for the two photon energies, while the method using simultaneous measurement requires the same measuring times The results of WOOTEN are thus not applicable in detail in the present investigation

Table 2

Sex, age, height and weight of four normal subjects

Case	Sex	Age	Height (cm)	Weight (kg)
1	m	22	187	84
2	m	35	180	78
3	f	48	157	54
4	f	24	160	57

The influence of the measuring time The precision of N, σ_N, is inversely proportional to the root of the measuring time t This is deducted from equation (10) Let R_1 R_1' and $\sigma_{N\,1}$ represent measured number of counts and the standard deviation at the measuring time 1 min per point With another measuring time, t min per point the number of counts will be t R_1 and t R_1', respectively Insertion of these number of counts in equation (10) gives $\sigma_N = \sigma_{N\,1}/\sqrt{t}$ and insertion of these σ_N in equation (11) gives $\sigma_A = \sigma_{A\,1}/\sqrt{t}$ Fig 3 illustrates the coefficient of variation V_A as a function of the measuring time t for the example shown in Table 1 The coefficient of variation increases rapidly with decreasing time of measuring With the present source activities we have chosen to measure each point 0 5 min

Reproducibility

The reproducibility of the method including both decay and subject variation has been investigated by repeated measurements in 4 normal subjects The standard deviation of the results was compared with the theoretical standard deviation according to counting statistics

The sex, age, height and weight of the four normal subjects are given in Table 2 The measurements in the normal subjects were performed during a period of 12 days A maximum of one measurement per day was performed except for subject SS who was once measured in the morning and in the afternoon on the same day

Measuring conditions The electrical equipment was powered throughout the period of measurement Adjustment of the spectrum was performed routinely both in the morning and in the afternoon The stability was good and only small changes of the positions and widths of the channels were necessary No permanent drifting in the electronics could be demonstrated Each measurement was performed using the following routine

Measurement with the subjects lying on their backs with cushions under their knees in order to achieve stability with the lumbar region horizontal,

Fluoroscopy and focusing the central beam through the centre of L3

Distance between measurement points, $\Delta x = 0\ 4$ cm,

Measuring time $t = 0\ 5$ min at each point

Table 3

Results of measurements in four normal subjects. A_{mean} = mean value of 10 measurements, s_A = standard deviation of these measurements and $\sigma_{A\ mean}$ = mean value of σ_A for each subject ($\times 10^{-4}$). Figures within brackets after each standard deviation represent the corresponding coefficient of variation

	Case			
	1	2	3	4
A_{mean}	822.7	631.3	660.2	672.2
s_A	41.2 (5.0%)	35.9 (5.7%)	22.3 (3.4%)	24.1 (3.6%)
$\sigma_{A\ mean}$	29.2 (3.6%)	30.5 (4.8%)	23.7 (3.6%)	23.2 (3.5%)

Data Processing. The primary data consisted of the number of counts R and R' for each measurement point. After completion of the measurement these data were processed as follows:

Calculation of N and σ_N according to equations (8) and (10),
Plotting of N as a function of the position x (Fig. 2),
Measurement of the width at half maximum of the curve and, knowing the width of the radiation beam (14 mm), localization of the end points (x_1 and x_n) which are definitely located outside the vertebra,
Calculation of A and σ_A according to equations (9) and (11),
Calculation of the mean value of A and the standard deviation s_A according to equation (1),
Calculation of the mean value of σ_A for each normal person.
The results for the four normal persons appear in Table 3.

Long-term precision

The stability of the apparatus during a prolonged period of time was checked with 5 cm wide aluminium discs measured in a water phantom. Discs of two different thicknesses were used, Al 1 and Al 2. The results of the measurement series, each comprising 10 measurements appear in Table 4.

For the aluminium disc Al 1 the change in A_{mean} was -17.4×10^{-4} (2.2%). The standard deviation of this change, s_{diff}, was 10.8×10^{-4} and the corresponding confidence interval at the 95% level was (-41.9×10^{-4}, $+7.1 \times 10^{-4}$). Theoretically the standard deviation of the change, σ_{diff}, was 8.5×10^{-4} with a 95% confidence interval of (-34.1×10^{-4}, -0.7×10^{-4}). The three measurement series of Al 2 gave a mean value of 560.1×10^{-4}.

Discussion

The standard deviation of N, σ_N, is partly due to the relationship between the registered number of counts R and R'. It has previously been demonstrated that the

Table 4

Results of five series of measurements of aluminium discs, each series comprising 10 measurements A_{mean} = mean value of measurements in each series, s_A = standard deviation for each series and $\sigma_{A\ mean}$ = mean value of σ_A for each series, (× 10^{-4}) Figures within brackets after each standard deviation represent the corresponding coefficient of variation

	Al 1		Al 2		
	June 1972	Jan 1974	Jan 1974	April 1974	June 1974
A_{mean}	803 5	786 1	561 9	556 9	561 4
s_A	32 0 (4 0 %)	12 3 (1 6 %)	6 8 (1 2 %)	8 6 (1 6 %)	12 5 (2 2 %)
$\sigma_{A\ mean}$	17 8 (2 2 %)	20 3 (2 6 %)	15 5 (2 8 %)	14 9 (2 7 %)	14 9 (2 7 %)

precision is improved if the number of counts of the higher photon energy is increased at the expense of the lower energy Fig 4 shows σ_N as a function of R providing $R + R' = 374645$ (measuring point x_{10} in Table 1) The curve is limited by the asymptotes A, where $R = k\ R'$, and D, where $R - 0$ C represents the number of counts for the particular measuring point and B the minimum of the curve where $\sigma_N = 4\ 6 \times 10^{-4}$ This minimum would have been reached if the activity of the ^{241}Am source had been reduced from 100 to 70 mCi and the activity of the ^{137}Cs source had been increased from 5 to 7 mCi It should be observed that the result is valid for this example only A somewhat fatter patient would permit a relatively lesser transmission of the lower photon energy and thus a value of σ_N closer to the optimum If the thickness of the subject is increased further there is a risk of arriving on the ascending leg of the curve between A and B, with rapid increase of σ_N

The question of the optimal lower photon energy and the optimal activity ratio has not been analysed further It seems clear, however, that an evaluation of this should be related to the expected variation of subject thickness

Base line errors When calculating σ_A, the contribution of the end points will be weighted according to equation (11) by the factor $((n-2)/2)^2$ The position of the base line is thus critical for the precision of the method In the four normal subjects the manual positioning of the base line was partly governed by the widths of the vertebra and radiation beam The points situated outside the end points were also taken into consideration, however, so that the end points should be in agreement with a reasonable extrapolation of these The practical precision of the end points is therefore probably sometimes better than the theoretical precision, which may explain why the normal subject ML has a total precision s_A which is less than $\sigma_{A\ mean}$ (Table 3) This phenomenon is even more marked in Table 4 concerning the series of measurements of aluminium, in which four out of five demonstrate lower s_A In phantom measurements, however, the measuring conditions are so idealized that all points outside the object can often be approximated by a straight line, which will then

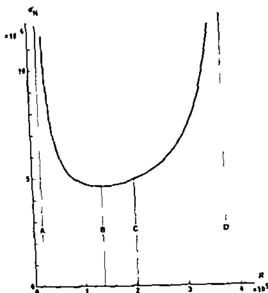


Fig. 4 σ_N as a function of number of

coincide with the base line The reliability of the base line is in this case considerably greater than is suggested by equation (11)

There are possibilities, without changing the total investigation time, of reducing the errors due to the end points by (1) eliminating unnecessary measuring points at the beginning and end of the measuring path, (2) increasing the measuring time or density of points in the end point region itself, and (3) possibly reducing the measuring time at the intermediate points $(x_2 - x_{n-1})$

These measures, however, necessitate considerable modifications of the present procedure and probably also require a minicomputer for direct read-out of the N diagram

Normal cases With regard to the four normal cases (Table 3), it should be observed that s_A is the estimation of the standard deviation in an individual measurement s_A varies within the range of 3 4 to 5 7 per cent (expressed as the coefficient of variation) The difference between s_A and $\sigma_{A\ mean}$ may be regarded as a (probably low) estimate of the previously mentioned subject variations For the normal subjects ML and SS the subject variations were small while the other two normal subjects showed greater differences between s_A and $\sigma_{A\ mean}$ One reason for this may be movement of the subject during the measurement, which can be counteracted by a suitable fixation device The four normal subjects were measured without any arrangements for fixation It may be concluded from this limited test material that the short term reproducibility is in the range of 3 4 to 5 7 per cent and with improved technique these values may probably be improved to 3 to 4 per cent

DALÉN (1973) reports a precision with an X-ray spectrophotometric method of 1 9 per cent theoretically and 10 per cent experimentally in measuring of the third lumbar vertebra The latter value was, however, improved to 2 7 per cent when the base line was adjusted manually JUDY et coll (1972) used a similar scanning method with ^{153}Gd (44 keV and 100 keV) as a dichromatic radiation source They state the total precision to be 5 to 7 per cent for in vivo measurements of L3. The greatest source of error is considered to be the variation in determining the position of the base line

Long-term control with aluminium The results in Table 4 reveal that the total precision, s_A, is better than the theoretical precision, $\sigma_{A\ mean}$ (except for Al 1 in June 1972) This fact may be explained on the basis of the discussion above concerning the influence of end points

The change in A_{mean} for disc Al 1 from June 1972 to January 1974 is not significant at the 95 per cent level, calculated on the total precision, while, theoretically the change is significant at this level During 1973 exchange of the detector took place and extensive service was performed on the electronic equipment Bearing this in mind, the change of A_{mean} (2 2 %) must be considered small, suggesting a good working precision Concerning the measurements of Al 2 there is no significant change from January to June 1974

Acknowledgement

This investigation has received financial support from the Swedish Medical Research Council

SUMMARY

Bone mineral content in lumbar vertebrae is determined by the attenuation of 59 6 keV (^{241}Am) and 662 keV (^{137}Cs) photons using the intermittent scanning technique The precision, mainly influenced by decay variations, is analyzed mathematically The reproducibility in patient measurements is also affected by variations in positioning, movements during measurement and base line errors In four normal subjects the reproducibility ranged from 3 4 to 5 7 % The long term stability was better than 1 % during a five-month period as tested by phantom measurements

ZUSAMMENFASSUNG

Der knocherne Mineralgehalt der lumbalen Wirbel wurde durch die Dampfung von 59,6 keV (^{241}Am) und 662 keV (^{137}Cs) Photonen under Verwendung der intermittenten Skanning Technik bestimmt Die Genauigkeit, hauptsachlich durch Schwankungen des Zerfalls beeinflusst, wurde mathematisch analysiert Die Reproduzierbarkeit bei Patienten wird auch durch Veranderungen der Lage, Bewegungen wahrend der Messung und Fehler in der Grundlinie beeinflusst Bei vier normalen Personen schwankte die Reproduzierbarkeit zwischen 3,4 und 5,7 % Die Langzeit Stabilitat war wahrend einer funf monatigen Testperiode mit Phantommessungen besser als 1 %

RÉSUMÉ

Le contenu minéral osseux des vertèbres lombaires est mesuré par l'atténuation de photons de 59,6 keV (^{241}Am) et de 662 keV (^{137}Cs) en utilisant la technique de balayage intermittent. L'auteur analyse mathématiquement la précision de cette méthode qui dépend principalement des variations de décroissance La reproductibilité des mesures sur les malades depend aussi des différences de mise en place des malades, des mouvements au cours des mesures et des erreurs sur la ligne de base Chez 4 malades normaux, la reproductibilité a varié de 3,4 à 5,7 % La stabilité à long terme est meilleure que 1 % au cours d'une période de 5 mois d'après des tests de mesure faits sur fantôme

REFERENCES

DALÉN N Bone mineral assay Measuring sites, clinical applications Thesis Department of Medical Engineering Karolinska Institutet, Stockholm 1973

JUDY P F, CAMERON J R, JONES K M and ORT M G Determination of vertebral bone mineral mass by transmission measurements USAEC Progress Report COO-1442-126 (1972)

ROOS B Bestämning av [illegible]

[illegible]

— [illegible] method Acta radiol Ther Phys B [illegible]

— [illegible], p 243

WOOTEN W W Bone densitometry The two photon technique and fat content of the bone Thesis University of California, Los Angeles 1971

Books received

We acknowledge with thanks under this heading books received for review, we trust this will be regarded as a sufficient mark of appreciation of the courtesy of the sender Reviews of selected items will appear as soon as an opportunity affords

BÉCLÈRE ANTOINETTE Première partie L'œuvre et la vie du docteur Antoinette Béclère J B Baillière, Paris 1973

BUCKTON K E and EVANS H J World Health Organization, Geneva 1973

DELAND F H and WAGNER H N Atlas of nuclear medicine Vol III Reticuloendothelial system, liver, spleen and thyroid W B Saunders Company Ltd, London 1972

FRONTIERS OF RADIATION THERAPY AND ONCOLOGY Radiation therapy and the cancer center Vol 8 Edited by J M Vaeth S Karger AG, Basel 1973

HALL E J Radiobiology for the radiologist Harper & Row Medical Department, Hagerstown 1973

HOFFMANN M J A Medizinische Informations-Verarbeitung Planung und Organisation Walter de Gruyter & Co, Berlin 1973

LEE Y-T N and SPRATT JR J S Malignant lymphoma Nodal and extranodal diseases. Grune & Stratton, Inc, New York 1974

MALLET L La rançon de prométhee et le danger atomique Maloine S A Editeur, Paris 1973

MOLECULAR STUDIES IN VIRAL NEOPLASIA A collection of papers presented at the Twenty Fifth Annual Symposium on Fundamental Cancer Research 1972 The William Wilkins Company, Baltimore 1974

MONOGRAPHS IN CLINICAL CYTOLOGY Aspiration biopsy cytology Vol 4 Part I Cytology of supradiaphragmatic organs Edited by Josef Zajicek S Karger AG, Basel 1974

PRASAD K N Human radiation biology Harper & Row, Publishers, Inc, Hagerstown 1974

RADIATION PROTECTION Implications of Commission Recommendations that Doses Be Kept as Low as Readily Achieveable ICRP Publication 22 Pergamon Press Ltd, Oxford 1973

WOOD R G Computer in radiotherapy—Physical aspects The Butterworth Group, London 1974

REYNIER J Monographie du collège de médecine Face au cancer du Sein Expansion Scientifique Française, Paris 1974

RODIER J et CHASSANY J P Manuel de radioprotection pratique Maloine S A éditeur, Paris 1974

SMITHERS D Hodgkin's disease Churchill Livingstone Publishers Edinburgh 1973

SYMPOSIUM INTERNATIONAL, STRASBOURG JUNE 1972 Thérapeutiques non mutilantes des cancéreuses du sein Conservative treatment of breast cancer Masson & Cie Paris 1974

THE UNIVERSITY OF TEXAS M D ANDERSON HOSPITAL & TUMOR INSTITUTE AT HOUSTON Environment and cancer A collection of Papers Presented at the Twenty Fourth Annual Symposium on Fundamental Cancer Research 1971 The Williams & Wilkins Company, Baltimore 1972

THE YEAR BOOK OF RADIOLOGY 1974 Radiologic diagnosis Edited by W M Whitehouse Radiation therapy Edited by H B Latourette Lloyd Luke (Medical Books) Ltd, London 1974

ACTA RADIOLOGICA

OFFICIAL ORGAN OF THE RADIOLOGICAL SOCIETIES OF
DENMARK FINLAND NORWAY AND SWEDEN

Vol 14 THERAPY PHYSICS BIOLOGY 1975
Fasc 4 August

CARCINOMA OF THE LARYNX

V Relationship between biologic effect and failure of irradiation

M HJELM HANSEN K JORGENSEN and A SELL

During the period 1963–1968 a total of 152 patients were treated for carcinoma of the larynx 147 primarily by irradiation and 5 primarily by surgery The results have been published previously (JORGENSEN 1974) Within a 5 year follow up period 58 cases of residual tumour or recurrence of the local tumour were observed The series was analysed when the follow up period for all patients was 5 to 10 years (1st Aug 1973) Three had developed local recurrence after the 5th year Thus among the 152 patients 61 cases of residual tumour or local recurrence occurred

It was endeavoured to elucidate the possible causes of residual tumour or local recurrence following irradiation two factors in particular, seemed to be of special interest the site of the field and the biologic effect of irradiation Only the response of the primary tumour to irradiation was taken into account The groups 'no local recurrence include patients who died of intercurrent diseases or of regional or distant metastases within the first 5 years In the glottic group this applies to 7 patients 5 died of other causes than laryngeal carcinoma during the 3rd 4th and 5th year of the follow up i e at times when there was little probability of developing local recurrence One died of lymph node metastases during the 1st year and one of distant metastases in the 3rd year

From the Department of Radiation Physics the E N T Department and the Radium Centre Municipal Hospital University of Århus DK 8000 Århus Denmark Submitted for publication 7 January 1975

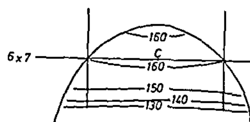


Fig 1

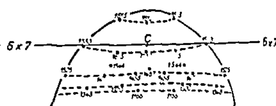


Fig 2

Fig 1 Typical dosage distribution for treatment using 2 opposed fields (6 cm × 7 cm) The figures indicate the dose in rad for 100 rad in the dosage maximum from each field SSD = 80 cm, ^{60}Co

[illegible] one field per [illegible]

Within the supraglottic group, the corresponding figures were 2 died of intercurrent diseases during the 1st and 5th year, 3 of lymph node metastases during the 2nd year.

Method

Irradiation was administered by a kilocurie ^{60}Co unit, the intention generally being to administer a central tumour dose of 5 700 rad in 30 fractions, 5 fractions a week The irradiation was delivered to two opposing fields (one field per session), measuring at least 6 cm × 6 cm (during the early part of the period the fields might have been smaller) A typical dose distribution is presented in Fig 1 The placement of the fields was determined by a simulator technique, and the marked fields were

Table 1

Survey of treatment groups, stating local response Only group C, in which the planned treatment was carried out with correct field placement, is included in the analysis of biologic effect

	No of cases		Local failure		No local recurrence	
Group A	9		4 + (1)		4	
Primary surgery		5		1		4
Palliative irradiation		3		3		0
Died after 2 sessions		1		(1)		0
Group B	9		9		0	
Unassessable field placement		4		4		0
Possible field error		4		4		0
Definite field error		1		1		0
Group C						
Analysis of biologic effect	134		48		86	
Total	152		61 + (1)		90	

Table 2

Distribution by region, stage, and sex of 134 patients, stating response by primary tumour

		Sub-glottic	Glottic	Supra-glottic	Total
Female		0	11	4	15
Male		3	84	32	119
Total		3	95	36	134
st I	local failure	0	10	4	14
st I	no local recurrence	0	41	6	47
st II	local failure	0	11	2	13
st II	no local recurrence	0	13	6	19
st III	local failure	2	8	10	20
st III	no local recurrence	1	11	7	19
st IV	local failure	0	0	1	1
st IV	no local recurrence	0	1	0	1
st I-IV	local failure	2	29	17	48
st I-IV	no local recurrence	1	66	19	86

controlled by exposure of a film (For further details of the technique cf. JORGENSEN & SELL 1971.)

The films of the treatment fields as well as the case notes were reviewed, and all primary tumours as well as any residual tumours or local recurrences were plotted on the films and dosage plans to determine that the so-called dosimetric field had been correctly placed. This meant that the shortest distance from the outline of the tumour to the border of the field was 1 cm or more, and that each part of the tumour received a dose which was at least 95 per cent of the calculated central tumour dose.

Calculation of the biologic effect was performed by the procedure proposed by ELLIS (1968, 1969). If a standard treatment consists of N fractions of d rad, administered in f fractions/week, within a total of T days, and NSD value may be calculated by using the formula

$$\mathrm{NSD} = \frac{N \cdot d}{N^{0.24} \cdot T^{0.11}} \text{ ret} \tag{1}$$

This value is considered constant in the following and the value was chosen as 1 800 ret, i.e.

$$\mathrm{NSD} = \frac{N_{1\,800} \cdot d}{N_{1\,800}^{0.24} \, T_{1\,800}^{0.11}} = 1\,800 \text{ ret} \tag{2}$$

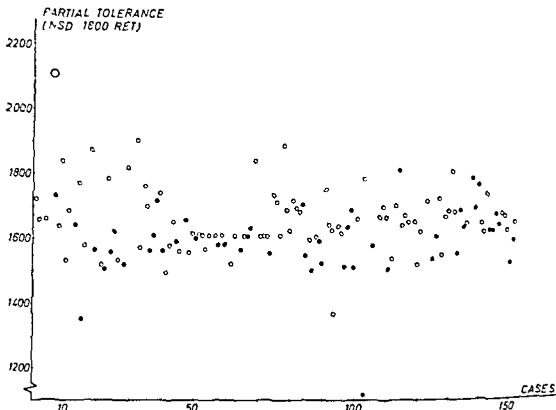


Fig 3 Distribution of $PT_{1\,800}$ for the analysed 134 of the original material of 152 patients ∘ local recurrence free, • local failure, ○ necrosis

(Suffix 1 800 refers to the number needed to attain 1 800 ret)

Each treatment or part of treatment is compared with the above treatment by the quantity $PT_{1\,800}$ (Partial Tolerance, when NSD = 1 800 ret)

Thus, if N fractions of d rad are administered, the Partial Tolerance of these fractions is

$$PT_{1\,800} = \frac{N}{N_{1\,800}} \times 1\,800 \text{ ret} \tag{3}$$

If the actual treatment consists of a number of fractional treatments, the $PT_{1\,800}$ is calculated for each fractional treatment and summarized to afford the final value for the entire treatment

If, after a fractional treatment (T days), resulting in $PT^{I}_{1\,800}$ ret, a gap in the treatment is interposed (G days), the $PT^{I}_{1\,800}$ value is corrected by the factor

$$F = \left(\frac{T}{T+G}\right)^{0\,11} \tag{4}$$

After the fractional treatment and the gap, is obtained a Partial Tolerance of

$$PT_{1\,800} = F\ PT^{I}_{1\,800} \tag{5}$$

Table 3

Result in 95 cases of glottic carcinoma, divided by PT_{1800} level (above and below 1 650 ret)

	st I	st II	st III	st IV	Total
PT_{1800} < 1 650 ret	31	12	12	0	55
Local failure	9	7	7	0	23 (41 8 %)
No local recurrence	22	5	5	0	32 (58 2 %)
PT_{1800} 1 650 ret	20	12	7	1	40
Local failure	1	4	1	0	6 (15 0 %)
No local recurrence	19	8	6	1	34 (85 0 %)

Table 4

Result in 36 cases of supraglottic carcinoma divided by PT_{1800} level (above and below 1 650 ret)

	st I	st II	st III	st IV	Total
PT_{1800} < 1 650 ret	5	4	10	1	20
Local failure	1	1	9	1	12 (60 %)
No local recurrence	4	3	1	0	8 (40 %)
PT_{1800} 1 650 ret	5	4	7	0	16
Local failure	3	1	1	0	5 (31 3 %)
No local recurrence	2	3	6	0	11 (68 7 %)

The central tumour dose (d) included in the calculations is the dose at c (cf Fig 1) A typical distribution of PT_{1800} appears in Fig 2

Before the analysis, 9 of the 152 cases were excluded 5 patients who had primary laryngectomy, 3 patients who received palliative irradiation, and 1 patient who died after 2 sessions (Table 1)

Results

In reviewing the field placement for the remaining 143 cases, 9 were found, all with recurrence of residual tumour, in whom the failure might be due to an incorrect dosimetric field In 4 cases, all of stage III, an evaluation was impossible because of unsatisfactory films, in 4 cases part of the tumour was outside the dosimetric field, and in 1 case outside the marked field This left 134 patients with correctly placed dosimetric fields (Table 1) The distribution of these 134 patients by sex, site and stage appears in Table 2 (AJC and UICC 1972) Of these 134 patients, 48 developed local recurrence or had residual tumour

The calculated Partial Tolerance (item c in Fig 1) for the 134 cases appears in Fig 3 Although generally the intention was to administer 5 700 rad in 30 fractions, delivering 5 fractions a week, which would result in $PT_{1800} = 1\,612$ ret, there was a

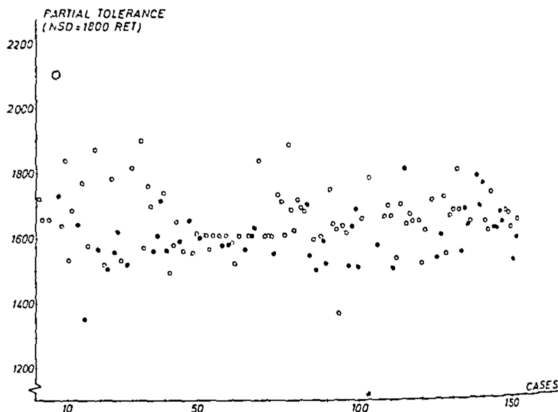


Fig 3 Distribution of $PT_{1\,800}$ for the analysed 134 of the original material of 152 patients ∘ local recurrence free, • local failure, O necrosis

(Suffix 1 800 refers to the number needed to attain 1 800 ret)

Each treatment or part of treatment is compared with the above treatment by the quantity $PT_{1\,800}$ (Partial Tolerance, when NSD = 1 800 ret)

Thus, if N fractions of d rad are administered, the Partial Tolerance of these fractions is

$$PT_{1\,800} = \frac{N}{N_{1\,800}} \times 1\,800 \text{ ret} \tag{3}$$

If the actual treatment consists of a number of fractional treatments, the $PT_{1\,800}$ is calculated for each fractional treatment and summarized to afford the final value for the entire treatment

If, after a fractional treatment (T days), resulting in $PT^{1}_{1\,800}$ ret, a gap in the treatment is interposed (G days), the $PT^{1}_{1\,800}$ value is corrected by the factor

$$F = \left(\frac{T}{T+G}\right)^{0\,11} \tag{4}$$

After the fractional treatment and the gap, is obtained a Partial Tolerance of

$$PT_{1\,800} = F\ PT^{1}_{1\,800} \tag{5}$$

Table 3

Result in 95 cases of glottic carcinoma, divided by PT_{1800} level (above and below 1 650 ret)

	st I	st. II	st III	st IV	Total
PT_{1800} < 1 650 ret	31	12	12	0	55
Local failure	9	7	7	0	23 (41 8 %)
No local recurrence	22	5	5	0	32 (58 2 %)
PT_{1800} 1 650 ret	20	12	7	1	40
Local failure	1	4	1	0	6 (15 0 %)
No local recurrence	19	8	6	1	34 (85 0 %)

Table 4

Result in 36 cases of supraglottic carcinoma divided by PT_{1800} level (above and below 1 650 ret)

	st I	st II	st III	st IV	Total
PT_{1800} < 1 650 ret	5	4	10	1	20
Local failure	1	1	9	1	12 (60 %)
No local recurrence	4	3	1	0	8 (40 %)
PT_{1800} > 1 650 ret	5	4	7	0	16
Local failure	3	1	1	0	5 (31 3 %)
No local recurrence	2	3	6	0	11 (68 7 %)

The central tumour dose (d) included in the calculations is the dose at c (cf Fig 1) A typical distribution of PT_{1800} appears in Fig 2

Before the analysis, 9 of the 152 cases were excluded 5 patients who had primary laryngectomy, 3 patients who received palliative irradiation, and 1 patient who died after 2 sessions (Table 1)

Results

In reviewing the field placement for the remaining 143 cases, 9 were found, all with recurrence of residual tumour, in whom the failure might be due to an incorrect dosimetric field In 4 cases, all of stage III, an evaluation was impossible because of unsatisfactory films, in 4 cases part of the tumour was outside the dosimetric field, and in 1 case outside the marked field This left 134 patients with correctly placed dosimetric fields (Table 1) The distribution of these 134 patients by sex, site and stage appears in Table 2 (AJC and UICC 1972) Of these 134 patients, 48 developed local recurrence or had residual tumour

The calculated Partial Tolerance (item c in Fig 1) for the 134 cases appears in Fig 3 Although generally the intention was to administer 5 700 rad in 30 fractions, delivering 5 fractions a week, which would result in PT_{1800} = 1 612 ret, there was a

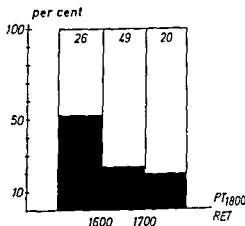


Fig 4 95 cases of glottic carcinoma, divided by PT_{1800} level □ local recurrence free, ■ local failure

marked dispersion of the calculated values, which raised the question whether a relationship existed between Partial Tolerance and recurrence rate

An analysis was performed for the glottic and the supraglottic groups separately, but, because of the small number of cases (3), not for the subglottic group

The glottic cases were 95 and divided into 3 groups by PT_{1800} level (Fig 4) A declining frequency of recurrence or residual tumour with increasing PT_{1800} value is evident The difference observed (31 4 and 33 8 per cent respectively) between group 1 and the other two groups is clearly significant ($0\ 005 < p < 0\ 01$ and $0\ 01 < p\ 0\ 025$)

All glottic cases were divided into 2 groups to obtain comparability with respect to sex, age and stage of disease one group of 55 patients with PT_{1800} below 1 650 ret and one group of 40 patients with PT_{1800} over 1 650 ret (Fig 5) The figure demonstrates reasonable comparability The difference observed in the recurrence rate between the 2 groups is 26 8 per cent, which is statistically significant (Table 3, $0\ 005 < p < 0\ 01$)

The supraglottic cases are divided into 3 groups in Fig 6 The differences observed in the recurrence rate between group 1 and groups 2 and 3, viz 26 1 and 40 3 per cent, respectively, are not statistically significant, but nevertheless indicate a certain decrease in the recurrence rate with increasing PT_{1800}

In Fig 7 and Table 4 the supraglottic cases are divided into 2 groups according to the same principle that was applied in the glottic group The difference of 28 7 per cent observed in the recurrence rate between the two groups is not statistically significant ($0\ 05 < p < 0\ 1$), but the same difference observed in an approx 50 per cent larger group would have been statistically significant

Complications Among the 134 cases one case of radiation necrosis occurred, $PT_{1800} = 2\ 105$ ret More uncertain complications, such as perichondritis or pharyngeal complaints more than 2 years after the completion of the irradiation, occurred in only 4 patients (PT_{1800} – 1 730, 1 694, 1 700 and 1 610 ret)

Field placement In 5 cases the fields were incorrectly placed, in 1 case only the carcinoma extended outside the treatment field The definition of the dosimetric

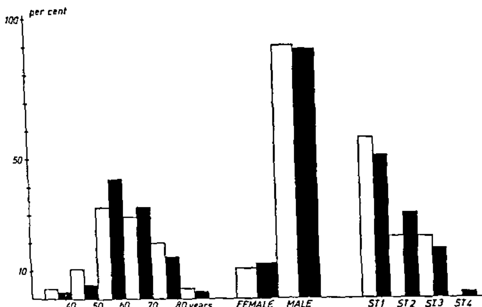


Fig 5 95 cases of glottic carcinoma, divided by PT_{1800} level (above and below 1 650 ret) in relation to age, sex, and stage □ $PT_{1800} < 1\ 650$ ret, ■ $PT_{1800} > 1\ 650$ ret

field used in the present material, was an applicable parameter. A somewhat different definition of the dosimetric field (90 per cent isodose curve) has been used by FEDER et coll (1973)

By a similar analysis, MARKS et coll (1971) found, in a series of 110 cases, 5 in which an incorrect field placement had presumably led to a recurrence. HORIOT et coll (1972) found 16 presumed field errors in a series of 67 supraglottic cases

A correct field placement is of decisive importance, both in the primary simulation and in the individual treatments An accurate reproducibility is secured by using an individually moulded shell of plaster in which the patient rests during the irradiation On its anterior aspect is mounted a plastic shield fenestrated at the site of the fields

Table 5

PT_{1800} obtained by $N = 30$ fractions of d rad, administered by $f = 5$ fractions/week

d rad	PT_{1800} ret
180	1 483
190	1 612
200	1 746
210	1 883
220	2 025
230	2 170
240	2 318

Table 6

Present values of $k(f)$ and $\alpha(f)$ in the approximation $T = kN^{\alpha}$

f	k(f)	α(f)
1	4 747	1 121
2	2 508	1 095
3	1 779	1 070
5	1 113	1 057

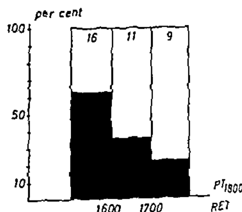


Fig 6 36 cases of supraglottic carcinoma, divided by PT_{1800} level □ local recurrence free, ■ local failure

Biologic effect The analysis reveals that a dosage having a biologic effect corresponding to PT_{1800} – 1 650 ret or more is needed in the irradiation of glottic carcinomas if a satisfactorily high curative effect is to be obtained The material does not permit a determination of a higher limit, as an intersection e g at 1 700 ret did not result in a significant difference Whether better results are obtainable at a PT_{1800} higher than 1 650 ret was not possible to estimate due to the small number of cases, but 1 700, 1 750 or 1 800 ret in the present series did not alter the frequency of residual tumour or recurrence 4/20 (20 per cent) at PT_{1800} higher than 1 700 ret, 2/10 (20 per cent) at PT_{1800} higher than 1 750 ret, and 1/5 (20 per cent) at PT_{1800} higher than 1 800 ret

Analysis of the supraglottic cases affords no possibility of setting a definitely lower limit of the PT_{1800} The following frequencies of residual tumour or local recurrence were obtained 12/20 (60 per cent) at a PT_{1800} lower than 1 650 ret, 5/16 (31 25 per cent) at PT_{1800} higher than 1 650 ret, 3/10 (30 per cent) at a PT_{1800} higher than 1 700 ret, 1/5 (20 per cent) at a PT_{1800} higher than 1 750 ret, and 0/3 (0 per cent) at a PT_{1800} higher than 1 800 ret Even though the figures are small, they indicate that the dosage should be higher than in the glottic cases

For both groups it may be stated that residual tumour or local recurrence did not occur at a PT_{1800} higher than 1 820 ret The only measure of the upper limit of the dosage is the one case of necrosis which occurred at a PT_{1800} 2 105 ret The analysis thus indicates that in the irradiation of laryngeal carcinoma the dosage should be in the interval 1 650 to 2 105 ret

Since 1970 all carcinomas of the larynx have been irradiated with a central tumour dose of 6 000 rad, delivered in 30 fractions, 5 fractions a week, corresponding to PT_{1800} = 1 746 ret (Table 5)

Conversion from NSD to PT_{1800} It is of considerable interest to compare the present results with those of other authors in order to narrow the mentioned interval (1 650 < PT_{1800} < 2 105), if at all possible As only a few authors use the concept Partial Tolerance, but calculate the biologic effect by direct insertion of parameters

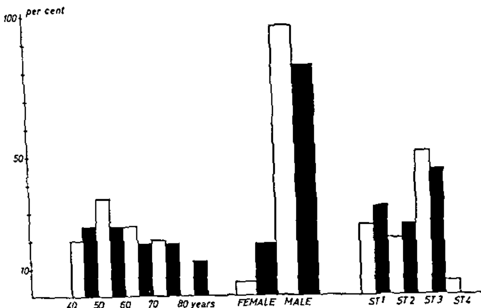


Fig 7 36 cases of supraglottic carcinoma, divided by PT_{1800} level (above and below 1 650 ret) in relation to age, sex, and stage □ $PT_{1800} < 1\,650$ ret, ■ PT_{1800} 1 650 ret

in eq 1 (i e NSD being a variable rather than a constant magnitude), the values thus calculated had to be converted into Partial Tolerance (PT_{1800}) at NSD = 1 800 ret.

If eq 1 is solved with respect to N and eq 2 with respect to N_{1800}, is found

$$N = \left(\frac{NSD}{d}\right)^{1/0.76} T^{0.11/0.76} \qquad (6)$$

$$N_{1800} = \left(\frac{1\,800}{d}\right)^{1/0.76} \cdot T_{1800}^{0.11/0.76} \qquad (7)$$

If the fractionation is fixed (f = 1, 2, 3 or 5 fractions/week), a certain relationship between N and T exists, but depending on the day of the week on which the treatment is started (WINSTON et coll 1969) However, the variation is not greater than allowing, with satisfactory accuracy, an approximation of the type

$$T = kN^{\alpha} \qquad (8)$$

WINSTON et coll suggested $k = k(f)$ and α = const = 1 13, but a better approximation may be attained by also letting α be a function of f (Table 6)

If $T = kN^{\alpha}$ is inserted in eq 6 and $T_{1800} = kN^{\alpha}_{1800}$ in eq 7, N/N_{1800} is evaluated and if inserted into eq 3, this gives

$$PT_{1800} = 1\,800\left(\frac{NSD}{1\,800}\right)^{1/(0.76-0.11\alpha)} \qquad (9)$$

Thus, PT_{1800} will depend somewhat upon the fractionation when it is to be calculated from NSD As $f = 5$ fractions/week is most often used $\alpha = 1\ 057$ In the interval concerned, NSD = 1 500 to 2 400 ret, the maximum error on PT_{1800} will thus be 14 ret, which is negligible

Example HORIOT et coll (1972) used the following treatment

D (total dose of N fractions in rad) = 5 500 rad
N − 20 fractions, f = 5 fractions/week
NSD = 1 872 ret

The NSD value is found by using eq 1, as T − 26 3 days (WINSTON et coll) (exactly T = 25 days when starting Monday, otherwise T = 27 days)

According to eq 9 it is found that

$$PT_{1\ 800} = 1\ 800\left(\frac{1\ 872}{1\ 800}\right)^{1\ (0\ 76 - 0\ 11 \times 1\ 057)} = 1\ 913 \text{ ret}$$

This value may also be calculated directly from HORIOT's information in this case

$$d - D/N = 5\ 500/20 = 275 \text{ rad/fract}$$

From eq 8 with f = 5 fract /week (Table 6) it is found that

$$T_{1800} = 1\ 113\ N_{1\ 800}^{1\ 057}$$

If this is inserted into eq 7, which is solved with respect to N_{1800} it is found that

$$N_{1800} = 18\ 86 \text{ fractions}$$

To attain 1 800 ret, then, 18 86 fractions of 275 rad would be required

Therefore, the Partial Tolerance of the 20 fractions given is (eq 3)

$$PT_{1800} = (20/18\ 86)\ 1\ 800 \text{ ret} - 1\ 909 \text{ ret}$$

The slight difference is due to the approximation $T = kN^{\alpha}$, *which in the approximation* entails NSD − 1 869 6 ret If this value is inserted, instead of 1 872, into eq 9, the conversion also gives PT_{1800} − 1 909 ret

DISCUSSION

MARKS et coll (1973), in an analysis of 58 T1 and T2 N0M0 glottic cases found 80 per cent cure at PT exceeding 1 650 ret Cases of their material having PT_{1800} ~ 1 800 ret or PT_{1800} 1 960 ret again gave approx 80 per cent cured Although MARKS et coll are dealing only with T1 and T2 cases, their figures, like the present ones, show that the results are not evidently better at dosage levels even considerably higher than 1 650 ret VAETH et coll (1972) found a cure rate of 81 per cent at a PT_{1800} of 1 815 ret in a series of 23 T1 and T2 cases, and HORIOT et coll (1972) a

cure rate of 82 per cent at a PT_{1800} of 1 835 to 2 200 ret in a material of 304 glottic T1 and T2 cases Accordingly, these 3 reports give results with an approx 80 per cent cure rate despite considerable differences in PT_{1800} Against this background it is surprising that MARKS et coll, as well as VAETH et coll, recommend a PT_{1800} of 1 960 ret and HORIOT et coll a PT_{1800} of 1 835 to 2 100 ret Very large series would be required to assess whether a definite gain by using these higher levels would be obtained

In the supraglottic group a distinct correlation was found between the frequency of residual tumour or recurrences and PT_{1800} Contrary to the glottic group, the frequency seemed to fall gradually with increasing PT_{1800}, and above 1 800 ret, no residual tumours or recurrences occurred The number of cases is small, but indicates that the frequency of residual tumours and recurrences might be reduced by increasing the dose DEFFEBACH & PHILLIPS (1972), in a series of 54 supraglottic cases (T1–4, N0M0) found that 32 per cent (10/31) had been cured at a PT_{1800} below 1 650 ret (follow up period a minimum of 2 years) and 74 per cent (17/23) at a PT_{1800} higher than 1 650 ret, i e figures very similar to the present ones SHUKOVSKY (1970) in a material of 97 cases found a distinct reduction in the frequency of residual tumour or recurrence at high PT_{1800} values at PT_{1800} – 1 650 to 1 800 ret 50 per cent (10/20) free of recurrence at PT_{1800} = 1 800 to 1 960 ret 68 per cent (19/28) at PT_{1800} = 1 960 to 2 130 ret 76 per cent (28/37), and at PT_{1800} = 2 100 to 2 800 ret 83 per cent free of recurrence (10/12) Thus SHUKOVSKY found a total of 30 per cent (30/97) recurrences at a PT_{1800} exceeding 1 650 ret In the present material the frequency was 31 per cent (5/16) These figures indicate that the number of recurrences may be reduced by increasing the PT_{1800}

The question how much the dose may be increased without causing complications must then be evaluated In the present material there was only one instance of radia [illegible]

[illegible] necroses have been reported, e g SHUKOVSKY 2 000 ret, MARKS et coll 2 130 ret and ARISTIZABAL [illegible]
ever, other authors have reported [illegible]
in a series of 68 patients (9 per cer[illegible]
with necroses had received PT_{1800} 2 065 to 2 200 ret After lowering the dose, only 3 necroses occurred at PT_{1800} = 1 835 to 2 100 ret in a series of 236 patients (1 3 per cent) The 3 cases of necrosis had received PT_{1800} = 2 040 to 2 100 ret Thus the risk of necrosis would seem to become impending at PT_{1800} = 2 050 ret

However, the upper limit of the therapeutic dose level may also be influenced by complications other than actual necrosis, i e in connection with supplementary surgery and it is quite conceivable that such complications may occur at a lower dose level than the actual radiation induced necroses The present material is too small to allow a definite statement but it should be mentioned that in cases of residual tumour or recurrence, 26 total laryngectomies were performed without the

Thus, $PT_{1\,800}$ will depend somewhat upon the fractionation when it is to be calculated from NSD As f = 5 fractions/week is most often used $\alpha = 1\,057$ In the interval concerned, NSD = 1 500 to 2 400 ret, the maximum error on $PT_{1\,800}$ will thus be 14 ret, which is negligible

Example HORIOT et coll (1972) used the following treatment

D (total dose of N fractions in rad) = 5 500 rad
N = 20 fractions, f = 5 fractions/week
NSD = 1 872 ret

The NSD value is found by using eq 1, as T = 26 3 days (WINSTON et coll) (exactly T = 25 days when starting Monday, otherwise T = 27 days)
According to eq 9 it is found that

$$PT_{1\,800} = 1\,800\left(\frac{1\,872}{1\,800}\right)^{1\,(0\,76-0\,11\;\;1\,05^{*})} = 1\,913 \text{ ret}$$

This value may also be calculated directly from HORIOT's information in this case

$$d = D/N = 5\,500/20 = 275 \text{ rad/fract}$$

From eq 8 with f = 5 fract /week (Table 6) it is found that

$$T_{1\,800} = 1\,113\,N_{1\,800}^{1\,057}$$

If this is inserted into eq 7, which is solved with respect to $N_{1\,800}$ it is found that

$$N_{1\,800} = 18\,86 \text{ fractions}$$

To attain 1 800 ret, then, 18 86 fractions of 275 rad would be required
Therefore, the Partial Tolerance of the 20 fractions given is (eq 3)

$$PT_{1\,800} - (20/18\,86)\,1\,800 \text{ ret} - 1\,909 \text{ ret}$$

The slight difference is due to the approximation $T - kN^{\alpha}$, which in the approximation entails NSD = 1 869 6 ret If this value is inserted, instead of 1 872, into eq 9, the conversion also gives $PT_{1\,800} - 1\,909$ ret

Discussion

MARKS et coll (1973), *in an analysis of 58 T1 and T2 N0M0 glottic cases,* found 80 per cent cure at PT exceeding 1 650 ret Cases of their material having $PT_{1\,800} \sim 1\,800$ ret or $PT_{1\,800} \sim 1\,960$ ret again gave approx 80 per cent cured Although MARKS et coll *are dealing only with T1 and T2 cases, their figures, like the present ones,* show that the results are not evidently better at dosage levels even considerably higher than 1 650 ret VAETH et coll (1972) found a cure rate of 81 per cent at a $PT_{1\,800}$ of *1 815 ret in* a series of 23 T1 and T2 cases, and HORIOT et coll (1972) a

REFERENCES

AJC American Joint Committee on Cancer Staging and end results reporting Clinical staging system for carcinoma of the larynx Chicago 1972

ARISTIZABAL S A and CALDWELL W L Radiation tolerance of the normal tissues of the larynx Radiology 103 (1972), 419

DEFFEBACH R and PHILLIPS T L Role of radiation therapy in the treatment of supraglottic carcinoma Cancer 30 (1972) 1159

ELLIS F The relationship of biological effect to dose-time fractionation factors in radiotherapy *In* Current topics in radiation research 4 (1968), 357

— Dose, time and fraction A clinical hypothesis Clin Radiol 120 (1969), 1

FEDER B H, SCHAEFLEIN J W and STEIN J J Early carcinoma of the vocal cords Amer J Roentgenol 108 (1970), 269

HORIOT J C, FLETCHER G H, BALLANTYNE A J and LINDBERG R D Analysis of failures in early vocal-cord cancer Radiology 103 (1972) 663

JORGENSEN K Carcinoma of the larynx III Therapeutic results Acta radiol Ther Phys Biol 13 (1974), 446

— and SELL A Carcinoma of the larynx II Treatment by ^{60}Co supervoltage irradiation Acta radiol Ther Phys Biol 10 (1971), 161

MARKS J E, LOWRY L D, LERCH I and GRIEM M L Glottic cancer An analysis of recurrence as related to dose, time, and fractionation Amer J Roentgenol 117 (1973), 540

MARKS R D, FITZ HUGH G S and CONSTABLE W C Fourteen years experience with ^{60}Co radiation therapy in the treatment of early cancer of the true vocal cords Cancer 28 (1971) 571

SHUKOVSKY L J Dose, time and volume relationships in squamous cell carcinoma of the supraglottic larynx Amer J Roentgenol 108 (1970), 27

UICC Union Internationale Contre le Cancer Geneva 1972

VAETH J M, GREEN J P and SCHROEDER A F Radiation therapy of cancer of the vocal cord and NCD implications Amer J Roentgenol 114 (1972), 63

WINSTON B M ELLIS F and HALL E J The Oxford NSD calculator for clinical use Clin Radiol 20 (1969), 8

occurrence of any fistula (mean PT_{1800} = 1 635 ret) However, in 8 cases with mean PT_{1800} = 1 619 ret, fistulas were encountered

Conclusion

Irradiation through correctly placed fields should be performed with a minimum dosage of PT_{1800} = 1 650 ret Without a major risk of necrosis this dosage may be raised to PT_{1800} = 2 050 ret There is no definite evidence that the failure rate in the treatment of glottic carcinomas decreases if the dosage is increased above 1 650 ret, as this frequency is fairly constant at about 20 per cent The cause of these failures is probably related to the biology of the tumour

On the other hand, in supraglottic tumours the failure rate seems to decrease with increasing PT_{1800} Therefore, it must be considered reasonable to aim at a dosage level closer to 2 050 ret

SUMMARY

Among 147 patients with laryngeal carcinoma, treated with ^{60}*Co irradiation* and followed for 5 to 10 years, there were 5 cases of recurrence due to incorrectly placed fields The glottic cases consisted of one group below and one above a Partial Tolerance of 1 650 ret In the *latter group the recurrence rate was significantly lower than in the former* Higher ret levels did not lower the residual tumour or recurrence rate in the glottic group but seemed to lower the rate in the supraglottic group

ZUSAMMENFASSUNG

Unter 147 Patienten mit einem Karzinom des Larynx, die mit ^{60}Co Bestrahlung behandelt *und 5 bis 10 Jahre lang verfolgt worden waren, fanden sich 5* Fälle mit Rezidiv infolge ungenau eingestellter Felder Die Glottis Fälle bestanden aus einer Gruppe unter und einer über einer Teil Toleranz von 1 650 ret In der letzteren Gruppe war die Rezidivfrequenz *signifikant niedriger als in der ersteren* Höhere ret Niveaus verminderten nicht die Rest tumoren oder die Rezidivfrequenz in der Glottis Gruppe, schien jedoch deren Frequenz in der Supraglottis Gruppe zu verringern

RESUMÉ

Sur 147 malades atteints de cancer du larynx et traités par l irradiation du ^{60}Co et suivis pendant 5 à 10 ans il y a eu 5 cas de récidive dus à des champs incorrectement placés Les cas de cancer glottique comprennent un groupe *au dessous et un au dessus d une tolérance* partielle de 1 650 ret Dans ce dernier groupe le taux de récidive a été significativement inférieur à celui du premier groupe Des niveaux de ret plus éleves n abaissent pas le taux de tumeur résiduelle ou *de récidive dans le groupe glottique mais semblent* abaisser le taux dans le groupe de cancer supraglottique

Table 1

Age and sex distribution of T1N0 glottic carcinoma (1959–1970)

Age	Male	Female
30–34	1	—
35–39	1	—
40–44	2	—
45–49	8	—
50–54	8	2
55–59	18	2
60–64	15	—
65–69	19	—
70–74	7	—
75 79	7	—
80–84	1	—

This report is based on a retrospective analysis of 91 early carcinomas of the vocal cords, as to the survival and cure rates, survival rates with preserved larynx, recurrences, treatment of recurrences, cause of death, and other primary malignancies

Material and Methods

From 1959 through 1970 91 early cases of histologically proven squamous cell carcinomas of the vocal cord (T1N0M0) were treated by radical radiation therapy The patients were classified according to the TNM system proposed by the UICC (1968) Excluding one patient who was lost after 5 years observation, the other 90 patients could be followed up until the end of 1973 Therefore, all patients were observed for at least 3 years

The age and sex distribution appears in Table 1 The youngest patient was a male 34 years old, the oldest, a male 80 years old The ages of the majority of the patients (86 per cent) varied between 50 and 70 years, with a mean age of 62 years for males and 53 years for females

Four patients were treated with 190 kV using a pendulum irradiation (3 cm × 4 cm, 180 arc) before August 1961, 63 patients were treated with a ^{137}Cs gamma ray unit using parallel opposing fields (size 4 cm × 5 cm or 5 cm × 5 cm, 40 cm SSD) until the end of 1968 Thereafter, 24 patients were treated with ^{60}Co through parallel opposing fields (size 5 cm × 5 cm, 60 cm SSD) In 1966, the fractionation was changed from 6 times per week to 5 times per week In general, the total tumor dose at a depth of 3 cm was 5 500 rad (22 fractions in 4½ weeks) or 7 000 rad (35 fractions in 7 weeks)

Results

Crude and determinate survival rates appear in Table 2 Some of the patients, who developed local recurrence after primary irradiation, were operated upon and

FROM THE DEPARTMENTS OF RADIOLOGY AND OTO-RHINO-LARYNGOLOGY, OSAKA UNIVERSITY MEDICAL SCHOOL, OSAKA, JAPAN

RESULTS OF RADIATION THERAPY OF EARLY CARCINOMA OF THE VOCAL CORDS

T INOUE, Y SHIGEMATSU and T SATO

Carcinoma of the larynx is common among males in some parts of Latin America France, North Africa, the Eastern Mediterranean and India The age standardized mortality rates per 100 000 males of laryngeal carcinoma are 19 6 in Brazil, 11 4 in Argentina and 11 1 in France, but in Japan the rate is 1 8 only (DUNHAM & BAILOR 1968) It is one of the characteristics in Japan that the incidence of supraglottic tumors is higher than glottic ones (IWAMOTO 1971) The districts with high ratios of carcinoma of the larynx are located in West Japan, particularly in Kinki District (SEGI et coll 1965) Approximately 700 patients with laryngeal carcinoma have been annually registered by Head and Neck Society of Japan (IWAMOTO 1971) At Osaka University Hospital, located in Kinki District, about 100 patients are annually registered glottic tumors have increased steadily in number, now being 50 per cent of all laryngeal carcinomas At the same time the average age of the patients has become higher SMITH et coll (1973) reported that patients with glottic tumors were slightly older than those with supraglottic ones

In early vocal cord carcinoma, radiation therapy is considered the best treatment with 90 per cent 5 year cure rate Treatment failures have been analysed by many authors In the previous report (INOUE et coll 1969), one of the failures was due to incorrect apprehension of tumor extension, and the other was a well differentiated lesion with poor response to ordinary irradiation

Submitted for publication 16 December 1974

Table 4

91 patients with T1N0 glottic carcinoma (1959–1970) NED No evidence of disease DT Death from primary tumor DID Death from intercurrent disease D other Ca. Death from other primary carcinoma

	Cured (70)	Recurrences (21)*				
		Total laryng	Partial laryng.	Partial, later total laryng	Irradiation	Irradiation, later total laryng.
NED	56	8	1	1		2
DID	8	1				
D other Ca	4	1				
DT		2		1	1	1
Lost	1					
Death from traffic accident	1					

* Two refused treatment 1 died of primary tumour and 1 of suicide

Four patients developed metastatic cervical lymph nodes after the completion of the primary irradiation Two of them underwent radical neck dissection with total laryngectomy, and one neck dissection following total laryngectomy The other one developed lymph node metastases after total laryngectomy and was irradiated Of the 21 patients with local recurrence, the 5-year survival rate was 68 per cent Survival rate with preserved larynx appears in Table 5 Eighteen patients underwent total laryngectomy, of these 17 for local recurrence and 1 for other primary carcinoma of the trachea

The majority of the local recurrences appeared in the anterior commissure and in the subglottic region (Table 6) and behaved as advanced glottic tumors However, in 2 cases the recurrence extended posteriorly upwards, appearing as an advanced supraglottic tumor

Table 5

Survival rate with retaining larynx in T1N0 glottic carcinoma (1959–1970)

Year	Crude per cent	Determinate per cent
1	95 (86/91)	96 (86 90)
3	75 (68/91)	81 (68 84)
5	71 (49 69)	79 (49 62)
8	64 (28 44)	78 (28/36)
10	71 (15/21)	94 (15/16)

Table 2

Survival rates of T1N0 glottic carcinoma treated by radical radiation therapy (1959–1970)

Year	Crude per cent	Determinate per cent
1	99 (90/91)	100 (90/90)
3	89 (81/91)	96 (81/84)
5	86 (59/69)	95 (59/62)
8	75 (33/44)	92 (33/36)
10	76 (16/21)	100 (16/16)

permanent cure was obtained Thus, it seems unsatisfactory to assess the treatment results of early carcinoma of the vocal cords by survival figures alone In the present analysis, the cure rate with primary irradiation was evaluated by a slightly modified life table method (Table 3) Of 21 patients who developed local recurrences, 17 recurred within 2 years It seemed that the subglottic extension was erroneously estimated in the majority of these cases, as previously reported (INOUE et coll) However, 2 patients recurred at 4 and 9 years, respectively, after completion of radiation therapy A long term follow-up is thus necessary

With irradiation only, 70 of 91 patients (77 per cent) were locally cured Of 21 patients with local recurrence, 12 underwent total laryngectomy, and 8 of them were controlled at the end of 1973 Partial laryngectomy was performed in 3 patients with local recurrence, 1 patient only was cured This latter case had a highly differentiated squamous cell carcinoma, the other 2 patients subsequently underwent total laryngectomy Four patients were treated with repeat irradiation without satisfactory result, two were finally operated upon with total laryngectomy (Table 4)

Table 3

Actuarial cure rate of T1N0 glottic carcinoma (1959–1970) DID Died of intercurrent disease

Year of observ	No of cases at risk	Recurrence dur interval	Lost and DID dur interval	Withdrawn alive dur interval	Proportion recurring	Proportion without recurrence	Cumulative recurrence free rate
0–1	91	6	1	—	6 6	93 4	93 4
1–2	84	11	2	—	13 3	86 7	81 0
2–3	71	2	3	—	2 9	97 1	78 7
3–4	66	—	—	10	0	100	78 7
4–5	56	1	1	7	1 9	98 1	77 2
5–6	47	—	2	2	0	100	77 2
6–7	43	—	3	3	0	100	77 2
7–8	37	—	1	9	0	100	77 2
8–9	27	1	—	6	4 2	95 8	73 9
9–10	20	—	—	7	0	100	73 9

that the primary examination of the tumor had been unsatisfactory in the cases of subglottic extension He also reported that total laryngectomy was to be preferred for recurrent cases, primarily irradiated, resulting in a 5-year survival of 69 per cent in his series Also in the present material, total laryngectomy in cases with radiation failure resulted in 68 per cent survival at 5 years Partial laryngectomy has also been suggested in cases with small recurrences and good results have been obtained However, in old patients, partial laryngectomy for recurrent lesion involves much more difficulties than total laryngectomy As with glottic carcinoma, patients are often very old total laryngectomy is thus to be preferred in recurrences after radiation therapy A repeat irradiation of a recurrence following primary radiation therapy is hazardous and rarely indicated (VERMUND 1970) In the present material, 4 patients were treated with re-irradiation without success, 2 were finally cured by total laryngectomy, 2 refused laryngectomy and died from advanced local disease

Six patients died from laryngeal carcinoma, but none from distant metastases or lymph node metastases in the neck Other primary malignant tumors developed in 9 per cent of the cases SATO et coll (1971) reported that 35 out of 692 patients with laryngeal carcinoma developed other primary tumors until the end of 1970 at our hospital The incidence of other primary malignancies is thus very high among patients with early carcinoma of the vocal cords In the material of Tl glottic carcinoma reported by GOFFINET et coll (1973), 10 of 78 patients developed other primary tumors It seems likely that the advanced age of the patients and the high curability of the glottic carcinoma resulted in this high incidence of other primary malignancies

SUMMARY

A material of 91 early carcinomas of the vocal cord treated by radiation therapy were reviewed The 5 year crude and determinate survival rates were 86 and 95 per cent, respectively Primary irradiation only, resulted in a 5 year cure rate of 77 per cent Of the 21 patients who developed local recurrences, 11 were cured by total, and one by partial laryngectomy Eight patients developed other primary carcinomas

ZUSAMMENFASSUNG

Die Verfasser behandeln zusammanfassend ein Material von 91 fruhen Karzinomen des Stimmbands die mit Bestrahlung behandelt worden waren Die grobe und die schliessliche 5 Jahres Überlebensraten betrugen 86 bzw 95 % Eine ausschliessliche primäre Bestrahlung fuhrte zu einer groben 5 Jahres Heilungsrate von 77 % Von den 21 Patienten bei denen sich lokale Rezidive entwickelt hatten, wurden 11 durch totale und einer durch partielle Laryngektomie geheilt Acht Patienten entwickelten andere primare Karzinome

RÉSUMÉ

Les auteurs ont passe en revue une série de 91 carcinomes de la corde vocale au début traités par les radiations Les taux brut et definitif de survie à 5 ans ont ete respectivement

Table 6

Type of recurrence in T1N0 glottic carcinoma treated by irradiation

Type	No patients
Localized	2
Anterior commissure	6
Subglottic	10
Supraglottic	2
Unclassified	1

Cause of death and other primary tumors Of 91 patients treated, 22 had died of various causes by the end of 1973 6 from recurrent primary lesions, 9 from intercurrent diseases, 1 from suicide, 1 from traffic accident, and 5 from other malignancies (Table 4)

Other primary tumors were found in 8 patients, 2 at the time of the laryngeal carcinoma, the other 6 occurred later The longest interval between the primary and the second carcinoma was 8 years Considering the site of the lesion, 2 were found in the stomach, 2 in the colon, 1 in the maxillary sinus, 1 in the floor of mouth, 1 in the oropharynx and 1 in the trachea One patient with gastric tumor and the 2 with carcinoma of the colon were cured by radical surgery, but one patient died from gastric carcinoma and all the 4 patients with head and neck carcinoma died

Discussion

T1N0M0 lesions of glottic tumors have a good prognosis In the survey by VERMUND (1970), there were 751 5-year survivals among 967 patients treated by primary irradiation (78 per cent) as compared with 378 of 458 patients treated by primary surgery (83 per cent) He stated that irradiation was to be preferred in stage I, because of high cure rate with a normal voice practically preserved MORRISON (1971) reported that the overall 5-year cure rate of 65 per cent was the same among patients treated by laryngofissure and those treated by orthovoltage radiation, but the functional results after radiation therapy were better than after surgery However, HARRIS (1961) suggested that partial laryngectomy should be performed for well differentiated lesions

In the present report 2 kinds of survival rates appear, as VERMUND (1970) emphasized the importance of a comparison between the crude and the determinate survival data, because there was a considerable death rate from intercurrent diseases

If a recurrence develops, this occurs within 2 years in the majority of cases, as reported by many authors, in a few cases late recurrences may be encountered, however Also in this material, two late recurrences appeared Thus, a long term follow-up is necessary for these patients The majority of recurrences extended to the anterior commissure or to the subglottic regions MÅRTENSSON et coll (1967) reported

FROM THE SECTION OF DIAGNOSTIC RADIOLOGY, RADIUMHEMMET, AND THE DEPARTMENT OF CLINICAL RADIATION PHYSICS (DIRECTOR PROF R WALSTAM), NATIONAL INSTITUTE OF RADIATION PROTECTION, S 104 01 STOCKHOLM, SWEDEN

RADIATION THERAPY FOR CARCINOMA OF THE URINARY BLADDER

Radiologic planning and treatment techniques

C Lagergren and B Sarby

Modern equipment for therapy with high energy roentgen radiation enables large doses to be administered accurately with uniform distribution to deeply located structures without injury to adjacent tissues A detailed and accurate knowledge of the anatomy in the particular case is then a prerequisite as well as of the physiologic variations that may occur Such variations may introduce discrepancy between the real dose distribution absorbed in the body and a predetermined dose plan It is also essential that all positionings of the patient during treatment should be performed with a high degree of precision

The intention of this report is to obtain as great accuracy as possible in planning and irradiation of carcinoma of the urinary bladder

Anatomy The shape and position of the normal bladder varies according to the extent to which it is filled and to whether the patient is in prone or supine position The caudal and dorsal parts of the bladder are fixed and only insignificantly affected by physiologic variations of the bladder The main points of anchorage are (1) the ventral part of the urogenital diaphragm, which is reinforced by the preurethral

Submitted for publication 6 June 1974

de 86 et 95% L'irradiation primaire isolée donne un taux de survie à 5 ans de 77% Parmi les 21 malades qui ont présenté des récidives locales, 11 ont été soignés par laryngectomie totale et 1 par laryngectomie partielle Huit malades ont présenté d autres carcinomes primitifs

REFERENCES

DUNHAM L J and BAILOR III J C World maps of cancer mortality rate and frequency ratios J nat Cancer Inst 41 (1968), 155

GOFFINET D R, ELTRINGHAM J R, GLATSTEIN E and BAGSHAW M A Carcinoma of the larynx Results of radiation therapy in 213 patients Amer J Roentgenol 117 (1973) 553

HARRIS H H Deficits in irradiation therapy for carcinoma of the larynx followed by surgery Ann Otol (St Louis) 70 (1961), 463

INOUE T, KANEMITSU M and SHIGEMATSU Y Radiotherapy of laryngeal carcinoma with special reference to the treatment policy of cordal cancer Nippon Acta radiol 29 (1969) 322

IWAMOTO H Cancer of the larynx in Japan Laryngoscope 81 (1971), 387

MÅRTENSSON B, FLUUR E and JACOBSSON F Aspects on treatment of cancer of the larynx Ann Otol (St Louis) 76 (1967), 313

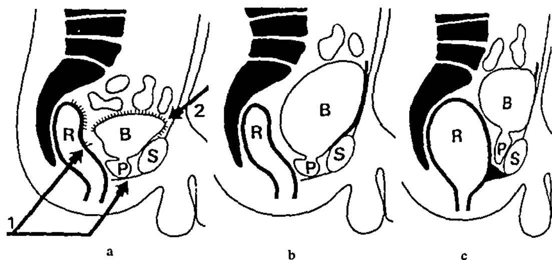
MORRISON R Review article Radiation therapy in diseases of the larynx Brit J Radiol 44 (1971), 489

SATO T, SAKAI S and IKEDA H Multiple primary cancers in patients of laryngeal, hypopharyngeal and maxillary cancers Otologica Fukuoka 17 (1971), 51

SEGI M, KURIHARA M and MATSUYAMA T Cancer mortality in Japan (1899 1962) Dept of Public Health Tohoku University School of Medicine, Sendai, Japan 1965

SMITH R R, CAULK R, FRAZELL E, HOLINGER P H, MACCOMB W S, RUSSELL W D SCHULZ M D and TUCKER G F Revision of the clinical staging system for cancer of the larynx Cancer 31 (1973) 72

VERMUND H Role of radiotherapy in cancer of the larynx as related to the TNM system of staging A review Cancer 25 (1970) 485



ler, S symphysis a) Empty
of the internal fascia of the
diaphragm Arrow 2 The
c) Rectal ampulla filled
The prostate and bladder are displaced cranioventrally even on moderate distention of rectum

ligament, and (2) the fold of the internal fascia of the pelvic diaphragm where it passes on to the the bladder When the bladder fills, the urachus which is attached to its ventro cranial part pulls the bladder up and anterior to the symphysis In the female the bladder is located slightly further caudally than on the male and the fascia of the pelvic diaphragm passes from the posterior surface of the symphysis directly over to the bladder to form the two pubovesical ligaments The position of the bladder is also dependent on the size, shape and location of the uterus In both sexes the extent to which the rectal ampulla is filled also influences the shape and position of the bladder (Fig 1)

Abnormalities of the bladder and its surrounding tissues may radically alter the normal position of the bladder A tumour of the bladder and inflammatory reaction of the adjacent tissues may also modify the normal physiologic mobility of the bladder at different phases of filling (Fig 2) As tumours of the bladder usually occur in elderly patients, age changes in the surrounding structures are also to be considered In the male, enlargement of the prostate may elevate the floor of the bladder and interfere with emptying, thereby altering the anatomy (Fig 3) In the female the appearance is affected by the uterus (Fig 4) and by the pelvic floor if insufficient

Planning and performance of irradiation

Anatomic planning The planning starts with urography of the patient in position for irradiation which is routinely performed in supine position Films of the bladder are exposed in a p and lateral projections The target volume, which covers the empty bladder with a reliable margin, is entered on the dose plan, as are the rectum

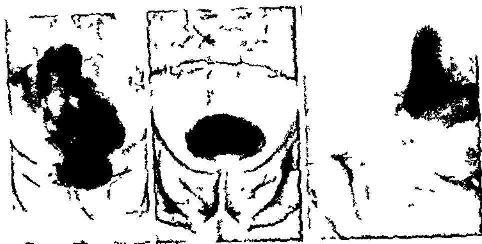


Fig 2 Fig 3a Fig 3b

Fig. 2. Deformity and cranial displacement of the ventral part of the bladder due to extensive carcinoma

Fig. 3 a) Hypertrophy of the prostate with elevation of the floor of the bladder b) With the patient *supine the bladder is displaced* ventrocranially to the symphysis

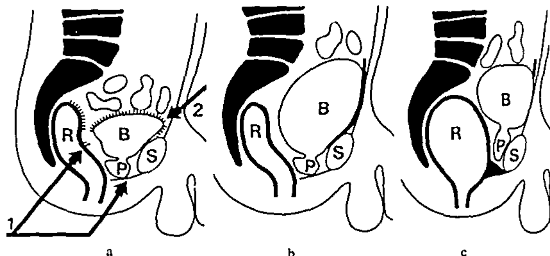


a b

Fig. 4 Carcinoma of the uterus deforming the bladder and displacing its cranial port on ventrally to the symphysis.

and the femoral heads irradiation of which should be avoided as much as possible It has proved important to plan and administer the treatment with empty bladder As it fills *with urine the position* is changed and part of it may lie outside the irradiated volume (*Fig 5) as well as for a short* time after emptying The extent of any anatomic variations that affect *the location of the bladder* has to be determined from previous films with contrast *medium in the bladder* if necessary supplemented with transverse tomography of the bladder and rectum after filling with contrast medium

Physical planning A homogeneous *dose distribution* within ± 5 per cent in the target volume is aimed at The irradiation techniques used appear *in Fig 6 (c*



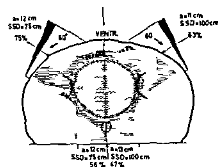
The prostate and bladder are displaced cranioventrally even on moderate distention of rectum

ligament, and (2) the fold of the internal fascia of the pelvic diaphragm where it passes on to the the bladder When the bladder fills, the urachus which is attached to its ventro cranial part pulls the bladder up and anterior to the symphysis In the female the bladder is located slightly further caudally than on the male and the fascia of the pelvic diaphragm passes from the posterior surface of the symphysis directly over to the bladder to form the two pubovesical ligaments The position of the bladder is also dependent on the size, shape and location of the uterus In both sexes the extent to which the rectal ampulla is filled also influences the shape and position of the bladder (Fig 1)

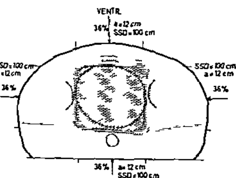
Abnormalities of the bladder and its surrounding tissues may radically alter the normal position of the bladder A tumour of the bladder and inflammatory reaction of the adjacent tissues may also modify the normal physiologic mobility of the bladder at different phases of filling (Fig 2) As tumours of the bladder usually occur in elderly patients age changes in the surrounding structures are also to be considered In the male enlargement of the prostate may elevate the floor of the bladder and interfere with emptying thereby altering the anatomy (Fig 3) In the female the appearance is affected by the uterus (Fig 4) and by the pelvic floor if insufficient

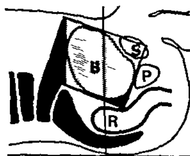
Planning and performance of irradiation

Anatomic planning The planning starts with urography of the patient in position for irradiation which is routinely performed in supine position Films of the bladder are exposed in a p and lateral projections The target volume, which covers the empty bladder with a reliable margin is entered on the dose plan as are the rectum



two dose plans have been cut along their line of symmetry and then jointed The anatomic cross section is 1 cm above the superior border of the symphysis





a

b

dose planning.

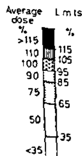
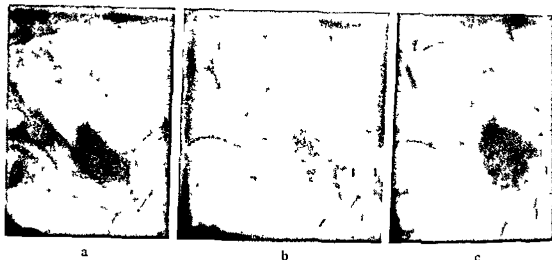


Fig. 8 Code for dose distribution of the plans in Figs 6 and 7



a b c

EDSMYR et coll 1964, 1967, LARSSON & SARBY 1972) Between 1961 and 1968 ^{60}Co was used but was then replaced by a similar technique using 6 MV radiation from a linear accelerator A third alternative using 42 MV radiation which has become available in recent years has been tested in only a few patients (Fig 7) The quantitative description of the dose plans in Figs 6 and 7 is given by the code in Fig 8

A comparison between the three beam technique used at present (Fig 6) and the four beam technique (Fig 7) demonstrates that the latter gives a lower subcutaneous dose, a lower dose in the rectum, but a slightly higher dose in the femoral heads The integral dose of the four beam technique is about 10 per cent higher than that of the linear accelerator technique assuming that the same anatomic conditions apply One advantage of the four beam technique that is not evident from the dose plan is that the cross section of the lateral beams can be shaped so as to provide optimal adaptation to the projection of the target volume, by rotating the diaphragm housing or inserting lead absorbers At the same time protection of the entire length of the rectum is obtained (Fig 7 b)

Patient positioning and beam controls The patient is oriented in the coordinate system of the irradiation apparatus with the cranial border of the symphysis having been chosen as the reference point This enables satisfactory reproducibility of the alignment of the beams relative to the pelvis without additional fixation of the patient on the treatment table However, in view of the anatomic and physiologic variations, it is of the outmost importance for the accuracy of the whole treatment series that the position of the radiation beam in the target volume be repeatedly controlled and recorded This is conveniently done photographically by usage of the irradiation beam during treatment (Fig 9) (JEVBRATT et coll 1971) or by means of a simulator

Thus, in planning radiation therapy for carcinoma of the bladder it is necessary to perform an accurate radiographic examination of the patient to detect any individual anatomic and physiologic variation present and to modify the geometric irradiation parameters in order to minimize the effects of these variations. The irradiation method of choice would appear to be a four beam technique with supervoltage irradiation. It permits a favourable three-dimensional dose distribution with protection of the whole rectum. This is accomplished by shaping the cross section of the lateral beams to fit that of the lateral projection of the target volume and by considering the deviations which may be caused by expansion of the bladder during filling (Fig. 8). The accuracy of the irradiation should therefore be greater with this technique than with a three beam technique or a pendulum irradiation. The beam controls may also be performed with more ease and accuracy.

SUMMARY

In radiation therapy for carcinoma of the bladder, various anatomic and physiologic factors affect the position of the target volume and introduce errors in the treatment technique. The radiologic procedures for planning and follow up of the patients must consider these factors. The beam geometry is also of decisive importance for minimizing the effect of these factors and for avoiding injury to surrounding structures. The irradiation procedure of choice should be a four beam technique with supervoltage roentgen radiation.

ZUSAMMENFASSUNG

Bei der Strahlentherapie des Karzinoms der Blase verändern verschiedene anatomische und physiologische Faktoren die Lage des zu bestrahlenden Volumens und bilden Fehler bei der Behandlungstechnik. Die radiologischen Verfahren zur Planung und Follow up der Patienten müssen diese Faktoren berücksichtigen. Die Strahlengeometrie ist auch von entscheidender Bedeutung, um den Effekt dieser Faktoren auf ein Minimum herabzusetzen und eine Schädigung der umgebenden Strukturen zu vermeiden. Das Bestrahlungsverfahren der Wahl dürfte eine Vier Strahl-Technik mit Supervolt Röntgenstrahlung sein.

RÉSUME

Dans le traitement par les radiations du cancer de la vessie divers facteurs anatomiques et physiologiques affectent la position du volume cible et introduisent des erreurs dans la technique de traitement. Les techniques radiologiques pour l'établissement du traitement et la surveillance de ces malades doivent tenir compte de ces facteurs. La géométrie du faisceau a aussi une importance décisive pour minimiser l'effet de ces facteurs et pour éviter les lésions des structures voisines. La technique d'irradiation de choix devrait être une technique à quatre faisceaux par un rayonnement Roentgen de supervoltage.



Fig 9 Direct beam control with 6MV roentgen irradiation of bladder carcinoma in the treatment position on the linear accelerator, with insufflation of about 30 ml of carbon dioxide a) Posterior field b) Angled anterior beam, given according to the dose plan in Fig 6

A continuous adjustment is thus possible in the alignment of the beams towards the actual position of the target volume The routine includes a control of each portal at the beginning of the treatment and after applied tumour doses of 2 000, 4 000 and 6 000 rad However, because the radiation at the initial part of the treatment may cause rapid alterations of the anatomic conditions more frequent beam controls may be necessary

Follow-up The routine examination of the patient when the irradiation is finished includes urography After 6 months the renal function is determined by means of a *limited* or 'functional' urography to establish whether the ureters have been affected by the irradiation or whether there is any recurrence Twenty minutes after the intravenous injection of contrast medium, two films of the entire urinary tract are exposed, one in the prone and the other in the supine position If the function is found to be normal, the examination is terminated, otherwise further films are exposed The renal function may also be examined by means of isotope nephrography The methods are equivalent in practice and the choice of method will depend on the available resources

Discussion

A prerequisite for full advantage of high energy radiation equipment is an accurate and individual planning with attention paid to factors which may cause uncertain tumour doses, displacement of organs, degree of filling of the bladder and anatomic changes that may appear during the course of treatment In the three beam technique (Fig 6) where two of the beams are given with wedge filter and a 60° angle of incidence such factors may give rise to a discrepancy between the dose plan and the distribution of the dose administered Accurate controls of beams of oblique incidence on simulators may be difficult to perform because of the displacement of the bladder on filling it with contrast medium This difficulty can be eliminated by direct beam control at the treatment apparatus with a small volume of gas injected into the bladder (JEVBRATT et coll)

Thus, in planning radiation therapy for carcinoma of the bladder it is necessary to perform an accurate radiographic examination of the patient to detect any individual anatomic and physiologic variation present and to modify the geometric irradiation parameters in order to minimize the effects of these variations The irradiation method of choice would appear to be a four beam technique with supervoltage irradiation It permits a favourable three dimensional dose distribution with protection of the whole rectum This is accomplished by shaping the cross section of the lateral beams to fit that of the lateral projection of the target volume and by considering the deviations which may be caused by expansion of the bladder during filling (Fig 8) The accuracy of the irradiation should therefore be greater with this technique than with a three beam technique or a pendulum irradiation The beam controls may also be performed with more ease and accuracy

SUMMARY

In radiation therapy for carcinoma of the bladder, various anatomic and physiologic factors affect the position of the target volume and introduce errors in the treatment technique The radiologic procedures for planning and follow up of the patients must consider these factors The beam geometry is also of decisive importance for minimizing the effect of these factors and for avoiding injury to surrounding structures The irradiation procedure of choice should be a four beam technique with supervoltage roentgen radiation

ZUSAMMENFASSUNG

Bei der Strahlentherapie des Karzinoms der Blase verändern verschiedene anatomische und physiologische Faktoren die Lage des zu bestrahlenden Volumens und bilden Fehler bei der Behandlungstechnik Die radiologischen Verfahren zur Planung und Follow up der Patienten müssen diese Faktoren berücksichtigen Die Strahlengeometrie ist auch von entscheidender Bedeutung, um den Effekt dieser Faktoren auf ein Minimum herabzusetzen und eine Schädigung der umgebenden Strukturen zu vermeiden Das Bestrahlungsverfahren der Wahl dürfte eine Vier Strahl Technik mit Supervolt Röntgenstrahlung sein

RESUME

Dans le traitement par les radiations du cancer de la vessie divers facteurs anatomiques et physiologiques affectent la position du volume cible et introduisent des erreurs dans la technique de traitement Les techniques radiologiques pour l établissement du traitement et la surveillance de ces malades doivent tenir compte de ces facteurs La géometrie du faisceau a aussi une importance décisive pour minimiser l effet de ces facteurs et pour éviter les lésions des structures voisines La technique d irradiation de choix devrait etre une technique a quatre faisceaux par un rayonnement Roentgen de supervoltage

REFERENCES

EDSMYR F, JACOBSSON F, DAHL O and WALSTAM R Cobalt 60 teletherapy in treatment of carcinoma of the bladder Radiobiol Radiother 5 (1964), 641

— — — Cobalt 60 teletherapy of carcinoma of the bladder Acta radiol Ther Phys Biol 6 (1967), 81

JEVBRATT L, LAGERGREN C and SARBY B Direct beam control in radiotherapy with high energy photons Acta radiol Ther Phys Biol 10 (1971), 434

LARSSON L E and SARBY B Radiophysical means for adequate radiation therapy with supervoltage apparatus at Radiumhemmet Acta radiol (1972) Suppl No 313, p 84

FROM RADIUMHEMMET (DIRECTOR PROF J EINHORN) AND THE NATIONAL INSTITUTE OF RADIATION PROTECTION DEPARTMENT OF CLINICAL RADIATION PHYSICS (DIRECTOR PROF R WALSTAM), S 104 01 STOCKHOLM, SWEDEN

BONE SCANNING WITH $^{99}Tc^m$ COMPOUNDS IN METASTASIZING MAMMARY CARCINOMA

G LUNDELL, E MARELL A BACKSTRÖM S CASSEBORN and B I RUDEN

Since the introduction of short lived isotopes (^{18}F, $^{87}Sr^m$) for bone scanning this method has been generally accepted and its value recognized for the detection of bone metastases as it seems to be more sensitive than radiography (GREENBERG et coll 1966 GALASKO & DOYLE 1972) Other lesions of the skeleton may also cause an increased uptake of the bone seeking isotope however, and it is thus important that the results of scanning and of radiography be compared (GALASKO & DOYLE)

The use of this method in the routine clinical work has further increased after application of the $^{99}Tc^m$ polyphosphate compounds (SUBRAMANIAN et coll 1972) which have an energy more suitable for the gamma camera $^{99}Tc^m$ also gives a lower radiation dose to the patient than do ^{18}F and $^{87}Sr^m$ (PENDERGRASS et coll 1973, QUINN et coll 1973)

$^{99}Tc^m$ polyphosphate has been used routinely at our department since 1972 for the detection of bone metastases mainly in patients with mammary and prostatic carcinoma However more stable compounds with a higher and more regular uptake in the metastatic lesions and with as low an uptake as possible in the soft tissues would seem desirable $^{99}Tc^m$ labelled diphosphonate polyphosphate and pyrophosphate were compared by DUNSON et coll (1973) for bone scanning in animal experi

Submitted for publication 22 August 1974

ments They reached the conclusion that the diphosphonate compound was to be preferred

HOSAIN et coll (1973) compared the same three $^{99}Tc^m$ compounds, and ^{18}F and $^{87}Sr^m$, in animal experiments as well as in a number of patients They concluded that ^{18}F was the best agent for the rectilinear scanner, but that pyrophosphate appeared to be better from the aspect of ease of preparation, reproducibility and quality of scan

Bone scanning with the gamma camera, using $^{99}Tc^m$ polyphosphate, diphosphonate and pyrophosphate, was performed in patients with metastasizing mammary carcinoma, and the results are presented in the present report

Material and Methods The material consisted of 9 patients with mammary carcinoma and with several roentgenologically demonstrated and cytologically verified metastases in the skeleton All had been subjected to either pre- or postoperative radiation therapy to the mammary region and to the axillary glands, in some cases also to local radiation therapy of some of the metastases All patients were treated with cortisone or anabolic steroids Cytostatic or radiation therapy was however not delivered during the period of or immediately before the bone scanning procedures

Seven patients had a low-differentiated and two a moderately well-differentiated mammary carcinoma In each patient all three types of bone-imaging compounds were tested with an interval of at least two days between each examination in order to exclude any remaining activity from the previous compound The order of the different compounds was chosen at random $^{99}Tc^m$ polyphosphate and $^{99}Tc^m$ diphosphonate were obtained from Diagnostic Isotopes Inc (New Jersey, USA) and $^{99}Tc^m$ pyrophosphate from Nyegaard & Co (Oslo, Norway) and were prepared in strict accordance with the instructions supplied from the manufacturers

Each $^{99}Tc^m$ kit used was checked with respect to chemical purity through the use of descending paper chromatography with methanol 85 %, as solvent Polyphosphate, diphosphonate and pyrophosphate remained at the application point while the R_f value of free pertechnetate was 0 40 to 0 60 The amount of unbound pertechnetate present in the different preparations was in all cases below 5 per cent The chromatograms of pyrophosphate showed 0 to 20 per cent of the activity in the R_f 0 70 to 0 85 region This part we have not been able to identify chemically

The equipment used for the recordings was either the HP Gamma Camera or the Pho/Gamma III from Nuclear Chicago In both cases, the 140 keV diverging collimator was used For every patient, the same type of gamma camera was used throughout and the time between the injection of the active compound and the beginning of the scanning was three hours In each examination 5 recordings were made, posterior scans were obtained of the head and neck region, the thoracic region, the lower thoracic and lumbar region, and finally the pelvic region For the pelvic region, an anterior scan was also regularly obtained Each recording was evaluated independently by the two physicians in the team without knowledge of the type of

Table

Comparison of gamma camera images using ^{99}Tc^{m} polyphosphate, ^{99}Tc^{m} diphosphonate and ^{99}Tc^{m} pyrophosphate Mean numbers from 9 patients The uptake was estimated blindly by two independent examiners and scored 1 3 where 1 is low and 3 is high

	Pyrophosphate	p	Diphosphonate	p	Polyphosphate
Number of separate lesions observed + SE	11 0±2 2	—	18 1±3 1	—	13 4±3 1
Gradient skeleton/background ± SE	2 0±0 1	<0 05	2.6±0 2	—	2.1±0 2
Gradient separate lesions/skeleton + SE	2 1+0 1	<0 01	2.7±0 1	<0 05	2.1±0 2

compound used for the recordings The gradient of uptake in normal skeleton to background activity, the gradient of uptake in metastatic lesions to the normal skeleton and the number of lesions observed were evaluated from the Polaroid views

In the last three patients examined, the number of counts within a specified area was recorded for soft tissue activity, uptake in normal vertebrae and a vertebra with a metastatic deposit using the image data processing system Med II from Nuclear Data

Results

In all patients the best results for each of the criteria evaluated were obtained with ^{99}Tc^{m} diphosphonate (Table) For ^{99}Tc^{m} polyphosphate and ^{99}Tc^{m} pyrophosphate the results varied The disphosphonate was significantly better than the pyrophosphate ($p<0\,01$) and polyphosphate ($p<0\,05$) in regard to the gradient separate lesions/skeleton The diphosphonate was also significantly ($p<0\,05$) better than the pyrophosphate in regard to the gradient skeleton/background More metastatic lesions were identified by the gamma camera than by radiology in all cases, and the lesions were more evident and better outlined using diphosphonate When reviewing the computer data from the three patients, it was also found that diphosphonate exhibited the best results for the gradient skeleton/background and for the gradient separate lesions/skeleton

One patient with a metastasizing follicular thyroid carcinoma was also examined in the same way as the patients with mammary carcinoma This patient is not included in the table but also in this type of tumour the same results were obtained

Discussion In patients with mammary carcinoma the most suitable of the three tested compounds was the ^{99}Tc^{m} diphosphonate, as in the animal experiments of DUNSON et coll

All patients were undergoing therapy with cortisone or anabolic steroids The uptake of ^{18}F in metastatic lesions of the skeleton during the first four months after beginning of chemotherapy or hormonal therapy remains unchanged (KAMPFFMEYER et coll 1967) Thus, it is probable that the anti-tumour therapy in the present material did not influence the results obtained

SUMMARY

A comparison of three compounds for bone scanning has been carried out in 9 patients with metastatic mammary carcinoma for evaluating their effectiveness The best results were obtained with $^{99}Tc^{m}$ diphosphonate For the other two compounds tested, $^{99}Tc^{m}$ polyphosphate and $^{99}Tc^{m}$ pyrophosphate, no difference could be demonstrated

ZUSAMMENFASSUNG

Fur einen Vergleich von drei Substanzen wurden Knochenszintigraphie bei 9 Patienten mit metastatischen Mammakarzinom vorgenommen, um deren Effektivität festzustellen Die besten Ergebnisse wurden mit $^{99}Tc^{m}$ Diphosphat erhalten Fur die anderen beiden untersuchten Substanzen, $^{99}Tc^{m}$ Polyphosphat und $^{99}Tc^{m}$ Pyrophosphat, konnte kein Unterschied nachgewiesen werden

RÉSUMÉ

Pour apprécier l'efficacité de trois composés destinés a la scintigraphie osseuse les auteurs ont effectue une étude comparative sur 9 malades atteintes de metastase de cancer du sein Les meilleurs résultats ont été obtenus avec le diphosphate de $^{99}Tc^{m}$ Ils n'ont pas constaté de difference entre les deux autres composés expérimentes, le polyphosphate de $^{99}Tc^{m}$ et le pyrophosphate de $^{99}Tc^{m}$

REFERENCES

Dunson G L, Stevenson J S, Cole C M, Meilor M K and Hosain F Preparation and comparison of Technetium-99m diphosphonate, polyphosphate and pyrophosphate nuclear bone imaging radiopharmaceuticals Drug Intelligence and Clinical Pharmacy 7 (1973), 471

Galasko C S B and Doyle F H The detection of skeletal metastases from mammary cancer A regional comparison between radiology and scintigraphy Clin Radiol 23 (1972), 295

Greenberg E J, Rotschild E O, DePalo A and Laughlin J S Bone scanning for metastatic cancer with radioactive isotopes Med Clin N Amer 50 (1966), 701

Hosain F, Hosain P, Wagner Jr H N Dunson G L and Stevenson J S Comparison of ^{18}F, ^{87m}Sr and ^{99m}Tc-labelled polyphosphate diphosphonate and pyrophosphate for bone scanning J Nucl Med 13 (1973), 410

Kampffmeyer H G Dvorkin H, Carr E A and Bull F E The effect of drug therapy on the uptake of radioactive fluorine by osseous metastases Clin Pharmacol Ther 8 (1967), 647

Pendergrass H P Potsaid M J and Castronovo Jr F P Clinical use of diphosphonate ^{99m}Tc (HEDSPA) New agent for skeletal imaging Radiology 107 (1973), 557

Subramanian G, McAfee J H and Bell E G ^{99m}Tc labelled polyphosphate as a skeletal imaging agent Radiology 102 (1972), 701

Quinn III J L, Crews M C and Westerman B R Radiopharmaceuticals and labelled compounds Proceedings Symposium International Atomic Energy Agency, Copenhagen 1973

FROM THE DEPARTMENT OF RADIATION PHYSICS, BOSTON UNIVERSITY MEDICAL CENTER, BOSTON, MASSACHUSETTS 02118, U S A

VARIATION OF PERCENTAGE DEPTH DOSE WITH BEAM AREA OF 43 MV ROENTGEN RAY BEAM FROM A BETATRON

J P BHATNAGAR and J SPIRA

It is generally believed that the percentage depth doses at a given depth in phantom increase with beam area even for high energy roentgen ray beams from a betatron Brit J Radiol Suppl No 11 (1972) points out that for roentgen ray beams in the energy range 31 MV to 35 MV from betatrons 'small fields give reduced depth dose values Our measurements of the central axis percentage depth dose as a function of beam area of a 43 MV roentgen ray beam from a betatron have shown contradictory results In this report are presented our measurements and an investigation into the reasons of the observed variation in central axis percentage depth dose with beam area

Apparatus All measurements were performed on a 43 MeV Siemens betatron Percentage depth doses were measured for the roentgen ray beams generated at 43 MeV electron energy and for target to surface distance (TSD) of 120 cm with the larger field flattening filter (compensator No 2) in the roentgen ray beam With this compensator, roentgen ray beams of areas from 4 cm × 4 cm to 20 cm × 20 cm of uniform dose rate across the field (within ±2%) are obtained Compensator No 2

A part of this communication was presented to the XIII International Congress of Radiology Madrid October 1973 Submitted for publication 26 February 1974

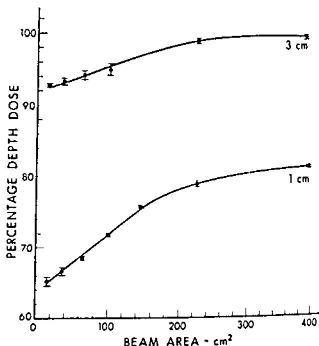


Fig 1 Central axis percentage depth dose versus roentgen ray beam area for depths of 1 and 3 cm These depths are less than the depth of maximum dose build-up which is about 5 cm Central axis percentage depth dose increases with beam area at these depths

is made of lead and is conical in shape, the height of the cone being 2 5 cm and the base diameter 7 cm The compensator is mounted between the accelerating donut and the collimator The collimator is also made of lead and is of 'block' type, i e, two pairs of lead blocks in the same plane, adjust the field size by moving in and out across the roentgen ray field

Acquisition of the central axis depth dose data Preliminary data which showed the variation of central axis percentage depth dose with beam area were obtained using a Baldwin–Farmer Secondary Standard Dosemeter in a water phantom A detailed measurement of the central axis percentage depth doses was then carried out using an Artronix automatic isodose plotter interfaced with the Artronix PC-12 computer In the automatic isodose plotter, two Shonka type ionization probes (each of 0 05 cm³ volume) were used (one scanning probe and one reference probe) In the routine measurements of isodose curves, the ratios of the ionization currents from the scanning probe and the reference probe, measured at a number of points in a plane parallel to the roentgen ray beam are stored on a magnetic tape For the measurements of central axis percentage depth doses, the reference probe was placed at a depth of 5 cm in the water phantom and the computer routine program was so modified that the scanning probe moved only along the central axis The ratios of the ionization currents from the scanning and the reference probes were measured at 15 different depth points along the central axis, each separated by 2 cm distance The top point was 1 cm from the surface of the water phantom The scanning probe was made to move 13 times along the central axis, thus collecting 13 independent samples of the

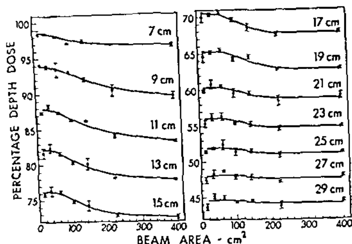


Fig 2 Central axis percentage depth dose versus roentgen ray beam area for depths ranging from 7 to 29 cm These depths are more than the depth of maximum dose build up which is about 5 cm Central axis percentage depth dose decreases with beam area at these depths

central axis percentage depth doses for each depth point This procedure was repeated for various square field sizes (4 × 4, 6 × 6, 8 × 8, 10 × 10, 12 × 12, 15 × 15, and 20 × 20 cm²)

Results

In Figs 1 and 2 the average values of central axis percentage depth doses with their standard deviations are plotted as a function of beam area for different depths in the phantom In these figures, the following characteristics appear

(1) At depths of 1 cm and 3 cm (Fig 1) which are less than the depth of maximum dose build up for the 43 MV roentgen ray beam (which is about 5 cm), the central axis percentage depth dose increases with beam area although quite rapidly at smaller areas

(2) At depths more than 5 cm (Fig 2), the central axis percentage depth dose first decreases with beam area, and then levels off

(3) A maximum decrease in percentage depth dose of about 4 5 per cent is seen for depths of 11 cm

(4) At very large depths (more than about 25 cm), the percentage depth dose becomes almost independent of beam area A decrease in percentage depth dose of less than 1 per cent occurs at these depths

The dose to any point in phantom is made of two parts The primary dose and the scattered dose The scattered dose depends on the contribution of the scatter arising in the collimator and the compensator of the betatron and on the phantom scatter arising within the phantom itself The variation of central axis percentage depth dose

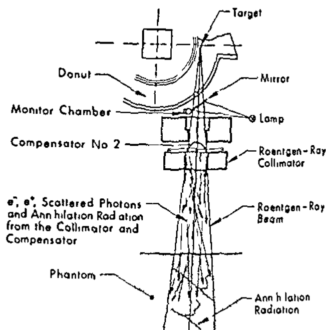


Fig 3 Origin and nature of collimator (and compensator) scatter

with beam area at a given depth must then be a function of collimator, compensator, and phantom scatter

Collimator scatter The term collimator scatter will be used hereafter to refer to the scatter from both the collimator and the compensator The collimator scatter mainly arises due to the pair-production as this process becomes predominant at photon energy of 5 MeV for lead (Fig 3 illustrates the origin and the nature of collimator scatter) The electrons and positrons of the pairs formed may have energy anywhere between 0 and (about) 42 MeV with an energy spectrum dependent on the spectrum of the primary roentgen ray photons and the interaction with the different thicknesses of lead in the compensator and the collimator The collimator and compensator scatter would also include some Compton scattered photons and recoil electrons In addition, the 0 51 MeV gamma photons produced by annihilation of the positrons will also contribute to the collimator scatter within the phantom But for a given collimator opening, the contribution of collimator scatter to dose with depth in phantom would decrease due to attenuation However, the contribution of collimator scatter to dose at a certain depth would increase when the phantom is brought closer to the collimator

Phantom scatter mainly arises due to Compton scatter as it is predominant for water up to 25 MeV Because at high energies, Compton scatter is mainly in the forward direction, the dose at the depth of maximum dose build-up due to Compton scatter alone should depend only very little on the size of the irradiating field How-

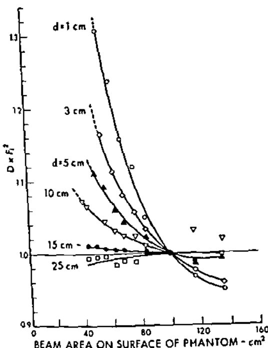


Fig. 4 Results of inverse square law experiment for a constant opening of the collimator which projects an area of 10 cm × 10 cm at 120 cm TSD Inverse square law experiment was repeated by placing the ionization chamber (Baldwin–Farmer) at different depths in the phantom. The product of the dose and the square of the distance of ion chamber from target, D F_1^2, after normalization at 100 cm² and at 120 cm TSD is plotted against the area of the roentgen ray beam on the surface of the phantom at other distances. For inverse square law to strictly follow, the product D F_1^2, should remain constant An increase in this product when the phantom is brought closer to the collimator demonstrates the presence of collimator scatter The collimator scatter attenuates with depth

ever, at greater depths, phantom scatter will build up (as it does for conventional lower energies) with its associated effect of increased dependence on field size

Presence of collimator scatter Results of inverse square law experiments Fig 4 shows the presence of collimator scatter at different depths in the phantom A set of inverse square law experiment was performed with the Baldwin–Farmer Secondary Standard Dosemeter placed at different depths in the phantom The product of the dose and the square of the distance of ion chamber from target, D F_1^2, after normalization at 100 cm² area at 120 cm TSD is plotted against the area projected on the surface of the phantom at other distances The collimator opening which projected an area of 100 cm² at 120 cm TSD was always kept constant For inverse square law to strictly follow, the product, D F_1^2, should remain constant An increase in this product when the phantom is brought closer to the collimator demonstrates the presence of collimator scatter, which attenuates with depth It should be pointed out here that the curves of Fig 4 represent the net increase in dose, i e , the difference in doses due to the increased collimator scatter and the reduced phantom scatter

The results of the inverse square law experiment are also plotted in a somewhat different manner in Fig 5 Here the readings of the ionization chamber are plotted against the distance of the chamber from the target on a log-log scale (solid lines) The values of the slope of these lines are also given in this figure For a set of experi-

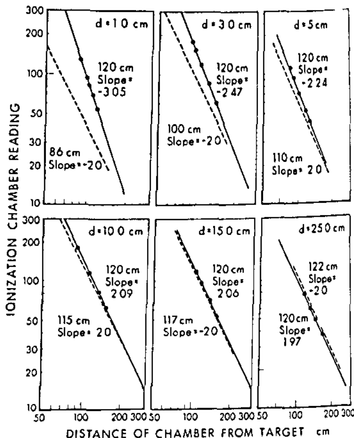


Fig 5 Results of inverse square law experiment of Fig 4 plotted differently The ionization chamber reading is plotted against the distance of chamber from target on log-log scale (solid curves) Virtual TSD refers to the virtual target (imaginary origin of roentgen radiation) to surface distance for which inverse square law holds true Dashed curves (slope −2 0) are drawn for virtual TSD

mental points through which a solid line is drawn, an 'imaginary source of roentgen radiation to surface distance' (virtual TSD) could be found out for which the experimental data follows the inverse square law This is done by shifting the experimental points laterally on the graph paper corresponding to an assumed value of the virtual TSD That value of virtual TSD is then selected for which the experimental points lie on a straight line having a slope of −2 0 Such lines (dotted lines) are drawn by the side of each solid line in Fig 6 and the value of virtual TSD for which the experimental data fits the inverse square law is also given The values of virtual TSD are seen to increase with the increased depth of ion chamber in phantom This suggests that there is some strong source of radiation located much closer to the surface than the roentgen ray target and that this radiation is attenuated by phantom at a rapid rate From a plot of virtual TSD against depth of chamber in phantom (Fig 6) it is obvious that at a depth of about 20 cm, the virtual TSD becomes equal to the actual TSD It should not be implied that at this depth, there is no contribution of collimator scatter but rather that the increase in the contribution of collimator scatter due to proximity of chamber to collimator is exactly balanced out by the decrease in the phantom scatter due to decrease in beam area now incident on the surface of the phantom At still larger depths mainly the phantom scatter will remain Also observe Fig 6 that the extrapolated value of virtual TSD for zero depth

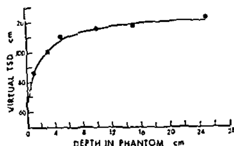


Fig 6 Virtual TSD versus depth of ion chamber in phantom.

in phantom is about 60 cm In betatron, the compensator-to surface distance for 120 cm TSD is 59 5 cm and the base of collimator to-surface distance is 49 cm. It would appear that the compensator is the main source of scattered radiation

In Fig 7 are given the results of inverse square law experiment for three different field sizes (5 cm × 5 cm, 10 cm × 10 cm, and 20 cm × 20 cm) projected at 120 cm TSD and obtained by adjustment of collimator opening Ionization chamber was placed in phantom at a depth of 5 cm For the respective field sizes, slopes of the curves are −2 41, 2 24, and −2 1, respectively These results indicate the reduced collimator scatter with the reduced collimator opening

Output variation with beam area Fig 8 shows a plot of the measured dose rates at the depth of maximum dose build up (5 cm) as a function of the beam area for 120 cm TSD The curve is also extrapolated back to zero area The zero area dose indicates the primary dose It should be noted in this figure that there is a 42 per cent increase in dose output above primary dose when the beam area is increased to 400 cm² This is relatively a large increase for the 43 MV roentgen ray beam In view of the results of the inverse square law experiments, and in view of the fact that the phantom scatter is mainly in the forward direction, it is estimated that most of the 42 per cent increase in dose output comes from the collimator scatter

The phantom scatter and the collimator scatter, however, cannot be easily separated The method of separating collimator and phantom scatter as suggested by HOLT et coll (1970) cannot be used in the present case because the contribution of collimator scatter to dose at a certain depth in phantom cannot be considered constant for the constant opening of the collimator when the phantom is brought closer to the collimator (Fig 4)

Discussion

From the results presented above, reasons of the observed variation of central axis percentage depth dose with beam area can be given as follows

(1) *Up to the depth of maximum dose build up*, the increase in dose with beam area is mainly due to the collimator scatter The contribution of collimator scatter to dose becomes smaller with depth due to attenuation The phantom scatter on the

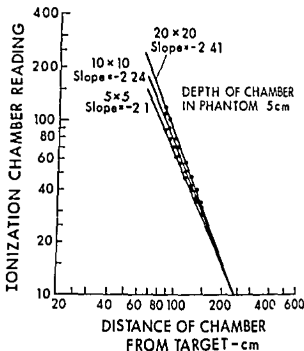


Fig 7 Results of inverse square law experiment repeated for three different field sizes (5 cm × 5 cm, 10 cm × 10 cm, and 20 cm × 20 cm) projected at 120 cm TSD and obtained by adjustment of collimator opening Ion chamber was always placed at 5 cm depth

other hand, being mainly in the forward direction, starts building up only at very large depths (well beyond 5 cm depth) Thus at depths less than 5 cm, increase in dose with beam area is more than that at 5 cm depth This results in an increase of central axis percentage depth dose with beam area at these depths

(2) The region of depths more than the depth of maximum dose build-up may be divided into two sub-regions (a) The subregion where the phantom scatter has not built up to such amounts which could compensate for a drop in the collimator scatter due to attenuation In this sub-region the percentage depth dose will decrease with beam area (b) The sub-region where the phantom scatter has built up to such amounts which could compensate for the drop in the collimator scatter due to attenuation In this sub-region, the percentage depth dose will either start becoming independent of beam area (at depths of more than 25 cm in Fig 2) or at still larger depths the percentage depth dose may even start increasing with beam area (as it conventionally does) depending upon the total amount of increase in phantom scatter with beam area The latter situation could not be observed in the present experiments because the measurements were carried out only up to a depth of 29 cm However, at still larger depths an increase in percentage depth dose with the beam area could be expected

Conclusions

(1) The central axis percentage depth dose of a 43 MV roentgen ray beam from a Siemens 43 MeV Betatron is found to decrease with beam area at depths more than the depth of maximum dose build-up and is found to increase with beam area at depths less than the depth of maximum dose build-up

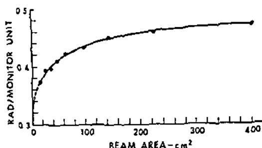


Fig. 8 Measured dose rates (rad/monitor unit) at 5 cm *depth versus roentgen ray* beam area The curve is extrapolated back to *zero area* The zero area dose rate indicates the primary beam dose rate

(2) This type of variation of the central axis percentage depth dose with beam area is mainly due to the presence of extraneous radiation originating in the compensator and the collimator of the betatron (collimator scatter)

Collimator scatter may be reduced by constructing the compensator of a low atomic number material and also by lining the collimator with such a material Alternatively, use of some magnetic field which removes the pair electrons contaminating the useful roentgen ray beam may also be considered

SUMMARY

The central axis percentage depth dose of a 43 MV roentgen ray beam from a betatron, is found to decrease with increasing beam area at depths more than the depth of maximum dose build up At depths less than the depth of maximum dose build-up, a reverse trend is seen This type of variation of central axis percentage depth dose with beam area is found due to the presence of extraneous radiation originating in the field flattening filter (compensator) and the collimator of the betatron

ZUSAMMENFASSUNG

Die prozentuelle Tiefendosis des Zentralstrahls einer 43 MV Rontgenstrahlung von einem Betatron fiel mit steigendem Strahlenfeld in den Tiefen starker als die Tiefe des maximalen Dosis *Build up Bei geringeren Tiefen als die Tiefe* des maximalen Dosis-Build-up wurde ein gegensätzlicher Trend gesehen Diese Form der Veränderung der prozentuellen Tiefendosis des Zentralstrahls mit dem Strahlenfeld beruht auf dem Vorkommen von fremder Strahlung, die vom Feld-Abschwachungsfilter (Kompensator) und dem Kollimator des Betatrons ausgeht

RÉSUME

Le pourcentage de doses en profondeur sur l axe central du rayonnement roentgen de 44 MV d'un bétatron decroit quand la surface du faisceau augmente, à des profondeurs supérieures à la profondeur du build-up maximum de doses A des profondeurs inferieures à la profondeur du build up maximum de doses on observe une tendance inverse Ce type de

variations du pourcentage de doses en profondeur sur l'axe central en fonction de la surface du faisceau est dû à la présence de rayonnements extérieurs provenant du filtre d'aplatissement du champ et du collimateur du bétatron

REFERENCES

Central axis depth dose data for use in radiotherapy Brit J Radiol Suppl No 11 (1972)

HOLT J G, LAUGHLIN J S and MORONEY J P The extension of the concept of tissue air-ratios (TAR) to high-energy X-ray beams Radiology 96 (1970), 437

FROM THE DEPARTMENT OF RADIATION PHYSICS (DIRECTOR ASSOC PROFESSOR HOLGER SKÖLDBORN), UNIVERSITY OF GOTHENBURG, S-413 45 GOTHENBURG, SWEDEN

AUTOMATED THERMOLUMINESCENCE READER

II Experiments and theory

B LINDSKOUG

Solid state dosimeters have rapidly achieved acceptance in the medical and biologic fields (IAEA 1967) In clinical dosimetry, thermoluminescence dosimeters have proved to be particularly valuable (D A E C 1971), partly for practical reasons The clinical environment necessitates easily handled and chemically and mechanically robust dosimeters Thermoluminescence dosimeters of LiF-teflon (BJÄRNGARD et coll 1967) have particularly good properties in these respects They are mechanically flexible but nevertheless strong and they can be cleaned with various solvents and sterilized without being damaged

Inconveniences in connection with the clinical use of TLD are the annealing procedures required to return the dosimeter material to its original sensitivity (CAMERON et coll 1964, ZIMMERMAN et coll 1966) and the manual work with forceps or a dispenser Simplification of the annealing procedure and automation of the method of reading is highly desirable in connection with the clinical application of TLD particularly in laboratories with a high patient load

In the first part of this work (LINDSKOUG & BENGTSSON 1975) a technical description of an automated TLD reader intended for radiation therapy dosimetry was given The present second part presents an experimental investigation performed with the TLD reader and discussion of the results

Submitted for publication 10 May 1974

variations du pourcentage de doses en profondeur sur l axe central en fonction de la surface du faisceau est dû à la presence de rayonnements extérieurs provenant du filtre d aplatissement du champ et du collimateur du bétatron

REFERENCES

Central axis depth dose data for use in radiotherapy Brit J Radiol Suppl No 11 (1972)

HOLT J G, LAUGHLIN J S and MORONEY J P The extension of the concept of tissue air ratios (TAR) to high energy X ray beams Radiology 96 (1970), 437

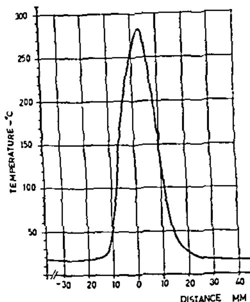


Fig. 3 Thermal course in the read-out oven

Light absorption in teflon tubes A 150 mm long rod of LiF teflon was used to determine the absorption and reflection of light in the teflon tube surrounding the dosimeters The long dosimeter could be read without the tube by inserting 4 mm of its end into a leader probe The irradiated dosimeter was read with and without the teflon tube The result for two different wall thicknesses relative to the uncovered dosimeter is illustrated in Fig 1 The emitted light is reduced by approximately 8 per cent with the wall thickness 0 055 g cm^{-2}, which is the dimension normally used in a measuring probe

Initial response The heating of the dosimeter material during reading causes an increase in sensitivity of the dosimeter material The initial responses of two previously untreated dosimeters are plotted in Fig 2 Curve A represents an increase in sensitivity with a factor of 1 8 between the first and second irradiation and read out In case B where the dosimeter was heated by read out three times before the first irradiation the high sensitivity is reached already at the first irradiation After the initial increase there is only a slight change in sensitivity when irradiations are repeated with a constant dose

Dependence on the temperature in the read out oven The temperature course in the read out oven is plotted as a function of the position of the thermocouple along the transport path in Fig 3 During the following measurements the temperature in the pre heater oven was held at a constant level After each irradiation the dosimeters were read twice the first reading for different temperature levels in the read out oven while the second reading was always performed at a temperature of 265°C At the second reading the residual TL light was recorded The response at the first and

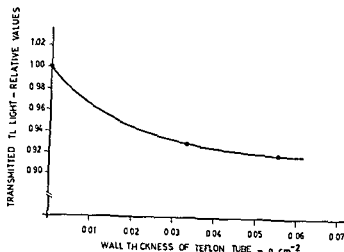


Fig 1

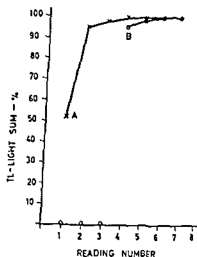


Fig 2

Fig 1 Fraction of thermoluminescent light transmitted through tubes of teflon with varying wall thicknesses

Fig 2 Initial response of TL light sum normalized to last reading A Irradiation and reading B Reading three times before irradiation

Experimental investigation

The special design and use of the measuring probes in this dosimetry system necessitates extensive experiments under varying conditions A detailed description of the instrument and dosimeters is given in part I, which also includes a brief description of the technical function and use of the instrument It should be mentioned that a reading means that the dosimeter material passes through first a pre-heater oven and then a read-out oven with a constant rate Peaks in the glow curve cannot be resolved in this system and therefore the TL-light sum emitted in the read-out oven was always recorded

The dosimeters used consist of cylindrical rods of LiF-teflon (MR-LiF-7, Teledyne, 1 mm × 6 mm) in teflon tubes of wall thickness 0 25 mm Unless otherwise stated the following experiments were performed with 18 mm long dosimeters (three dosimeters of the length 6 mm close together) and the integrated signal was recorded Integrating the signals from three dosimeters ensures good precision The short measuring probes are more easy to keep clean than long chains of probes

The temperatures were determined with a thermocouple of alumel-chromel enclosed in a teflon tube, external diameter 1 5 mm, internal diameter 0 5 mm This thermocouple was transported through the pre-heater and read-out ovens in the same way as the dosimeter material The peak temperature was recorded The dosimeters were usually irradiated with a cylindrical ^{90}Sr-^{90}Y β-source (see part I) In this case absorbed dose stated refer to absorbed dose of ^{60}Co γ-ray in polystyrene, calculated as described in the section 'Calculation of absorbed dose' below Where other radiation sources were used, this is stated specifically

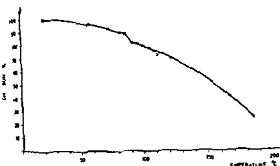


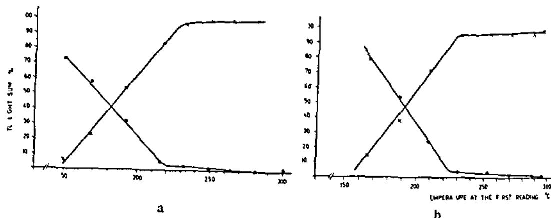
Fig. 5 Normalized TL light sum plotted as a function of the temperature in the pre heater oven

Dependence on rate of transport The transport rate of the measuring probes can be continuously varied between 0 5 and 1 2 mm per second The response of a dosimeter repeatedly irradiated with 110 rad appears in Fig 6 as a function of the rate, the reading temperature being 270°C Two readings were performed The second reading revealing the residual signal was always made at a rate of 0 9 mm per second, with rates between 0 6 and 1 1 mm per second a constant response was obtained The rate of 1 mm $^{-1}$ was used in the following, ensuring independence of small fluctuations in rate The lowest curve in Fig 6 illustrates the residual signal The curve is rising with increasing rate but is still below 1 per cent at the rate of 1 mm s^{-1}

Dependence on direction The dosimeters exhibit dependence on the angle of incidence of the radiation in relation to the axial direction of the dosimeter This effect was investigated by means of a perspex cylinder (5 cm diameter) in which three holes were bored at angles 0°, 45° and 90° to one another (Fig 7) Measuring probes each containing one dosimeter (length 6 mm) surrounded by teflon spacers were inserted into the holes with the centre of the dosimeter in the centre of the cylinder The cylinder was irradiated with 5 MV roentgen rays The dependence of the response on the angle of incidence is given in Fig 7 With axial irradiation of the dosimeter the reduction in response amounts to 7 per cent Normally, the dosimeters are used with their axes approximately at right angles to the direction of the radiation beam

Dependence on storage temperature The temperature at which the dosimeters are stored will influence their sensitivity This influence was determined for three different temperature levels 4°, 22 and 100 C Storage for up to 8 days at 4° and 22 C, respectively, did not cause any significant difference in sensitivity upon test irradiation Storage at 100 C gave a reduction in sensitivity after 1 and 4 days of 50 and 75 per cent respectively

Dependence of time lag between irradiation and read out A number of dosimeters were stored at room temperature for varying times after irradiation with 110 rad Read-outs were performed after 0 to 116 hours Immediately after read-out, the irradiation and read-out was repeated The relative response defined as S/S_0, where S and S_0 are the sensitivities (rad^{-1}) in the first and second read-outs respectively, is given in the Table There was no significant reduction after 116 hours, i e 5 days



a

b

: out oven The response is normalized
• at 265 C b) Irradiation with 450 rad
— — — — — C × first reading ● second reading

second reading is plotted in Fig 4 a against the temperature in the read out oven during the first reading The dosimeter was irradiated with 110 rad The TL-light sum is normalized to the last read-out With the lowest temperatures the greatest emission of light was recorded during the second read-out but as the temperature increased a greater part of the signal was emitted during the first read-out The residual value declines to less than 1 per cent, which is reached at 300°C Corresponding curves for a reference temperature of 290°C and a dose level of 450 rad are illustrated in Fig 4 b The last value, which is read at 300°C, amounts to 1 5 per cent

Dependence on the temperature in the pre-heater oven The function of the pre-heater oven is to eliminate light emission from shallow traps in the dosimeters before they enter the read-out oven The glow curve of LiF has five characteristic peaks, of which the three peaks emitted at the lowest temperatures have approximately the following half-lives at room temperature 5 min, 10 hours and 1/2 year (ZIMMERMAN et coll) The light emitted in these three peaks is unsuitable for clinical dosimetry as the fading causes a dependence on the time between irradiation and reading It should be expected that the response depicted as a function of the temperature in the pre-heater oven will appear as a plateau at the level where these three light peaks are eliminated since the two remaining peaks have considerably longer half-lives (approximatively 7 years and 80 years respectively at room temperature)

In order to obtain an idea of this temperature influence a dosimeter was irradiated and read repeatedly with successive increase of the temperature in the pre-heater oven The time between irradiation and read-out was kept constant The response normalized to the first reading is plotted in Fig 5 as a function of temperature As expected a tendency to a plateau appears between 90°C and 100°C Further increase of the temperature in the pre-heater oven causes successive emptying of the stored energy which brings useful information on the absorbed dose received by the dosimeter material The temperature of the pre-heater oven was set to 95°C during subsequent measurements

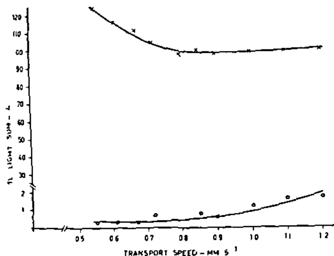


Fig 6

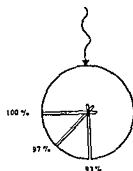


Fig 7

Fig. 6. TL light sum, normalized to last reading plotted as a function of the transport rate Residual values were read at a rate of 0 9 mm s^{-1}

Fig. 7 Determination of the dependence on the angle of incidence of radiation in relation to the axial direction of the dosimeter Relative response is given in percentage of the value at the angle of 90

after read-out at 300°C, storage at temperatures below 20°C for up to 10 days caused only slight reduction of sensitivity Storage at temperatures above 50°C reduced the sensitivity, and more rapidly the higher the temperature was On renewed read-out the thermal equilibrium in the dosimeter material was restored If the dosimeter material was stored at the read-out temperature the thermal equilibrium was maintained and the sensitivity was kept constant MÅRTENSSON (1969) found that high annealing temperatures decreased the precision of measurements

The results mentioned above have been utilized by ALM-CARLSSON (1973) for precision measurements in connection with dosimetry at interfaces In order to achieve the high level of precision of 0 3 per cent relative standard deviation the following precautions had to be taken individual calibration of the dosimeters before every measurement, the cumulated dose had to be the same for all dosimeters irradiated in one group, correction had to be made for inadequate transparency of the teflon material, and heating other than in connection with read-out had to be avoided

In clinical dosimetry a considerably lower level of precision can be accepted if the procedures can thereby be simplified With the rapid and reproducible cooling after each read out in the presented instrument it is possible to retain the high level of sensitivity which the dosimeters get in the high read-out temperature and utilize it for dosimetry A high temperature gradient is obtained during exit from the read-out oven (Fig. 3) With a rate of transport of 1 mm per second the cooling rate will be approximatively 20°C s^{-1} and equally reproducible as the rate of rotation of the

Table

Varying storage time between irradiation and reading

Storage time hours	Relative sensitivity S/S_0
0	1 00
1 5	0 99
3 5	0 99
6 5	0 99
16 5	1 03
20	1 00
46	1 02
49	1 01
64	1 04
116	1 00

Repeated irradiation with constant dose Upon repeated irradiation with constant dose the dosimeters demonstrate an increasing sensitivity The results of a number of irradiations with the absorbed dose of 450 rad appear in Fig 8 The residual value was read after a varying number of measurements The read-out temperature was 270°C The gradual increase in sensitivity is due partly to the effects of irradiation and partly to the thermal treatment during read-out

Repeated irradiation with varying doses One dosimeter was irradiated repeatedly First, with 10 × 110 rad, second, with 10 × 450 rad, and third, with 10 × 20 rad The read-out temperature was 290°C The sensitivity, normalized to the maximum sensitivity found, appears in Fig 9 The response increases more rapidly for the high doses but tends to decline when changing over from high doses to series of low doses The residual values, which were read between every tenth read-out, amount to less than 1 per cent

Results of irradiations with doses of alternatively 20, 110 and 450 rad are plotted in Fig 10 for two different dosimeters The two dosimeters, which were read immediately after one another but were enclosed in different measuring probes, gave almost exactly the same results until the cycle was interrupted at read out number 12, when one of the dosimeters was read without previous irradiation

Discussion

The sensitivity of the LiF-teflon dosimeters was found to increase by a factor 1 8 after the first irradiation and read-out (Fig 2) This change is due to thermally induced crystal defects which occur at high temperatures (ZIMMERMAN et coll) Rapid cooling to room temperature or lower makes this condition permanent, the high sensitivity persisting for a period of time depending on the storage temperature CARLSSON (1969) investigated the influence of the thermal history on the thermoluminescence of LiF-teflon material He pointed out that an appropriate heating process during read-out may satisfy the demands of both pre annealing and cooling He also found that

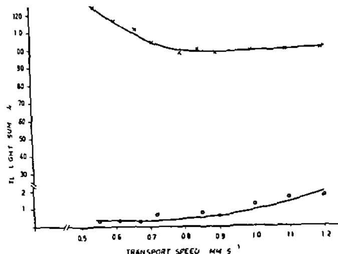


Fig 6

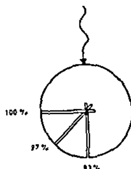


Fig. 7

Fig. 6 TL light sum normalized to last reading, plotted as a function of the transport rate Residual values were read at a rate of 0 9 mm s⁻¹

Fig. 7 Determination of the dependence on the angle of incidence of radiation in relation to the axial direction of the dosimeter Relative response is given in percentage of the value at the angle of 90

after read out at 300 C, storage at temperatures below 20 C for up to 10 days caused only slight reduction of sensitivity Storage at temperatures above 50°C reduced the sensitivity, and more rapidly the higher the temperature was On renewed read-out the thermal equilibrium in the dosimeter material was restored If the dosimeter material was stored at the read-out temperature the thermal equilibrium was maintained and the sensitivity was kept constant MÅRTENSSON (1969) found that high annealing temperatures decreased the precision of measurements

The results mentioned above have been utilized b ALM CARLSSON (1973) for *precision measurements in connection with dosimetry at interfaces In order to* achieve the high level of precision of 0 3 per cent relative standard deviation the following precautions had to be taken individual calibration of the dosimeters before every measurement, the cumulated dose had to be the same for all dosimeters irradiated in one group correction had to be made for inadequate transparency of the teflon material, and heating other than in connection with read out had to be avoided

In clinical dosimetry a considerably lower level of precision can be accepted if the procedures can thereby be simplified With the rapid and reproducible cooling after each read-out in the presented instrument it is possible to retain the high level of sensitivity which the dosimeters get in the high read out temperature and utilize it for dosimetry A high temperature gradient is obtained during exit from the read out oven (Fig 3) With a rate of transport of 1 mm per second the cooling rate will be approximatively 20 C s^{-1} and equally reproducible as the rate of rotation of the

Table

Varying storage time between irradiation and reading

Storage time hours	Relative sensitivity S/S_0
0	1 00
1 5	0 99
3 5	0 99
6 5	0 99
16 5	1 03
20	1 00
46	1 02
49	1 01
64	1 04
116	1 00

Repeated irradiation with constant dose Upon repeated irradiation with constant dose the dosimeters demonstrate an increasing sensitivity The results of a number of irradiations with the absorbed dose of 450 rad appear in Fig 8 The residual value was read after a varying number of measurements The read-out temperature was 270°C The gradual increase in sensitivity is due partly to the effects of irradiation and partly to the thermal treatment during read-out

Repeated irradiation with varying doses One dosimeter was irradiated repeatedly First, with 10×110 rad, second, with 10×450 rad, and third, with 10×20 rad The read-out temperature was 290°C The sensitivity, normalized to the maximum sensitivity found, appears in Fig 9 The response increases more rapidly for the high doses but tends to decline when changing over from high doses to series of low doses The residual values, which were read between every tenth read-out, amount to less than 1 per cent

Results of irradiations with doses of alternatively 20, 110 and 450 rad are plotted in Fig 10 for two different dosimeters The two dosimeters, which were read immediately after one another but were enclosed in different measuring probes, gave almost exactly the same results until the cycle was interrupted at read-out number 12, when one of the dosimeters was read without previous irradiation

Discussion

The sensitivity of the LiF-teflon dosimeters was found to increase by a factor 1 8 after the first irradiation and read-out (Fig 2) This change is due to thermally induced crystal defects which occur at high temperatures (ZIMMERMAN et coll) Rapid cooling to room temperature or lower makes this condition permanent, the high sensitivity persisting for a period of time depending on the storage temperature CARLSSON (1969) investigated the influence of the thermal history on the thermoluminescence of LiF-teflon material He pointed out that an appropriate heating process during read-out may satisfy the demands of both pre-annealing and cooling He also found that

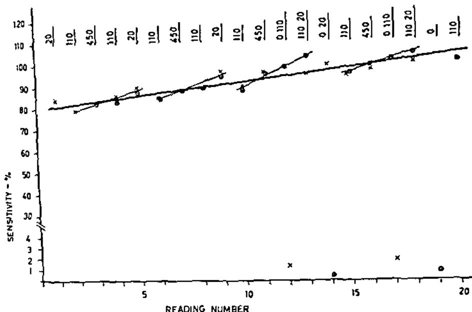


Fig 10 Variation of sensitivity for repeated irradiation and read-out of varying doses The two dosimeters are normalized to reading number 18 and 20 respectively Reading temperature 290 C

damage has occurred There is, however, no threshold for radiation damage to LiF (CAMERON et coll 1967) and this effect seems to be very difficult to repair

During multiple irradiation and thermal treatment sessions the effect of radiation damage will be more marked than in one single irradiation and thermal treatment (CAMERON et coll 1967) Combined effects of sensitization and damage was investigated by SPANNE & CARLSSON (1971) They concluded that both radiation sensitization and radiation damage seem to increase with increasing fractionation of irradiation and thermal treatment

In the present dosimetry system the situation is further complicated by the rather great residual signal, which will depend strongly on the absorbed dose given in previous irradiations Some of the luminescent traps will not be emptied during read-out but may partly be included in succeeding read outs This case is demonstrated in Fig 9 where the sensitivity decreases by about 1 *per cent at each read-out in the 20 rad* irradiations, while it is increasing for doses of 110 rad and higher Evidently it may be possible to choose the calibration dose so that an equilibrium of filled traps could be retained Fig 9 indicates that this calibration dose would be about 80 rad

Method for the dosimeter measurements Concluding the discussion above, the following method for using LiF teflon dosimeters may be suggested

the read out should include a reproducible heating process with rapid cooling to room temperature,

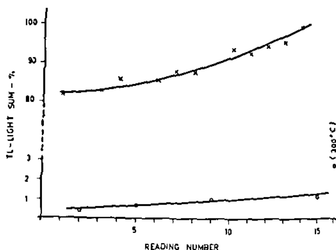


Fig 8 TL-light sum for repeated irradiation and read-out of 450 rad The response is normalized to reading number 14 Reading temperature 270 C Residual values are illustrated by the lowest curve

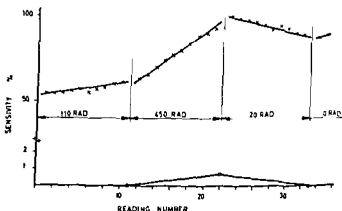


Fig 9 Variation of sensitivity for repeated irradiation and read-out of 10 × 110 rad, 10 × 450 rad and 10 20 rad Residual values are illustrated by the lowest curve Reading temperature 290 C

stepper motor The cooling from 290°C to room temperature will take place within about 20 seconds

The results presented in Figs 4, 6, 9 and 10 show that the sensitivity will increase with the number of read-outs and that complete release of trapped electrons in connection with read-out is not possible To release all electrons a temperature of more than 300°C would be necessary inside the dosimeter, which would mean such high temperatures at the surface of the measuring probe as to damage it It is therefore necessary to limit the temperature level to a maximum of 290°C determined as described above

In repeated use including various radiation and thermal treatments the efficiency of thermoluminescent LiF will vary considerably (Figs 8–11) The efficiency variations are a result of the combined effects of radiation sensitization, radiation damage and thermal history. The sensitization is caused by non-luminescent deep traps with higher capture cross-section for electrons, than the luminescent traps (SUNTHARALINGAM 1968). As the non-luminescent traps are filled, more electrons will be captured by the luminescent traps resulting in an increased TL response. Suitable annealing procedures will restore the increased sensitivity to its initial level unless no radiation

calibration will be performed subsequently for calculation of absorbed dose and it is essential that the procedures are identical

The following symbols are used

R_{Co} response to irradiation with 100 rad ^{60}Co gamma radiation
R_{β} response to succeeding irradiation with the β source
R_x *response to irradiation with radiation quality* X
D_{Co} calibration dose received at transport through the β source, according to the ^{60}Co measurement
D_x *calibration dose received at transport through the* β source, according to measurement with radiation quality X

The calibration dose for ^{60}Co γ radiation during transport through the β-source is obtained by means of the expression

$$D_{Co} = \frac{1}{n} \sum_{i=1}^{n} \frac{R_{\beta}}{R_{Co}} 100$$

where n is the number of times comparative measurements were performed

A series of comparative measurements are then performed between each type of radiation and the β source With a dose of 100 rad given the calibration dose is calculated from the expression

$$D_x = \frac{1}{n} \sum_{i=1}^{n} \frac{R_{\beta}}{R_x} 100$$

Calculation of the absorbed dose is simplified in routine application if correction factors (C_x) are formed related to the ^{60}Co calibration according to

$$C_x = \frac{D_x}{D_{Co}}$$

Calculation of absorbed dose

During arbitrary measurements with radiation quality X the absorbed dose is calculated from the expression

$$D = \frac{R}{R_{\beta}} D_{Co} C_x$$

where R is the response to read out of the measurement value

During read out the measurement values are automatically punched out on paper tape The results are calculated and written out by means of a PDP 8/E minicomputer Communication with the computer occurs via a Teletype Data input to the computer is made by a paper tape reader, the values are stored in sequence in an input area The calibration values are included on the same punched tape and in exactly the

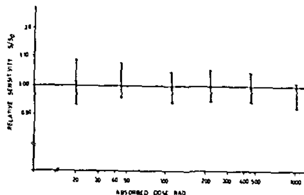


Fig 11

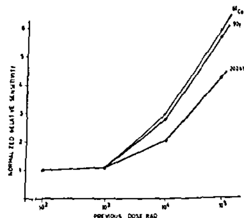


Fig 12

Fig 11 Relative sensitivity S/S_0, where S is the sensitivity (rad $^{-1}$) at an arbitrary reading and S_0 the sensitivity at the succeeding calibration with a dose of 110 rad The dispersion is stated as two standard deviations

Fig 12 Relative sensitivity for a test dose of 100 rad of different radiation qualities as a function of pre irradiation dose

pre-annealing procedures at high temperature levels should be avoided,
post-annealing should be made to reduce fading at room temperature,
dosimeters should be stored in or below room temperature, and
dosimeters should be individually calibrated between measurements

Obviously this schedule can be used with advantage only if the equipment and procedures are automated In an automated measurement system, calibration of the dosimeters can be performed after each measurement without entailing excessive work The calibration factor would reveal changes in the sensitivity of the dosimeter material The output data must be obtained in a form suitable for computer handling with identification of individual dosimeters

Calibration The energy stored by the dosimeters when passing through the calibration radiation source with a certain speed will give a light-emission that reveals the sensitivity of the dosimeter material to the particles generated in or passing through the sensitive regions The sensitivity to other radiation qualities or types of radiation may be different The dosimeters should thus be calibrated for all qualities of radiation to be determined The method presently used will be described as an example

In general, calibration is based on one of the ^{60}Co therapy sources which is consistently used for continuous control of constancy for all dosimetric equipment in the laboratory The measuring probes are irradiated with 100 rad ^{60}Co γ-radiation at the reference plane in a polystyrene phantom and read Immediately thereafter, they are irradiated in the calibration radiation source (β-source) and read again The rate of transport through the β-source is selected so that the response is of the same order of magnitude as the previous response to 100 rad from ^{60}Co The whole procedure is repeated a number of times When calculating the calibration dose the response for the succeeding irradiation with the β-source must always be used The succeeding

Test of the method

Limits of error Four measuring probes each containing 9 dosimeters with the length of 6 mm were submitted to different series of irradiations and read outs with doses varying between 20 and 500 rad and on one occasion 1 000 rad Twenty two irradiations were given the cumulated dose being about 5 000 rad Every other irradiation was a calibration irradiation with 110 rad The relative sensitivity is defined as S/S_0 where S is the sensitivity (rad^{-1}) in a measurement and S_0 the sensitivity in the succeeding calibration The relative sensitivity is plotted as a function of the absorbed dose (Fig 11) The dispersion is stated with two standard deviations The relationship between the sensitivity of an arbitrary dosimeter at the time of measurement and the sensitivity during the subsequent calibration irradiation will lie within the stated limits with 95 per cent probability Between 100 and 500 rad the deviation from the value 1 0 ($S = S_0$) amounts to 6 per cent For a dose of 20 rad the deviation increases to 9 per cent

In situations in which repeated measurements can be performed or in which several measuring probes can be placed adjacent to one another the precision will be considerably increased The automated read out instrument and the availability of a computer for calculating and processing the results makes it possible to use a high number of dosimeters

Dependence on LET Induced LET dependence in LiF has been reported and discussed by SUNTHARALINGAM and CARLSSON & ALM CARLSSON (1968) When dosimeters are irradiated with more than 10^3 rad this effect will be noticeable as the sensitivity will not increase as much for high LET particles as for low LET particles The effect exerts a maximum influence at 10^5 rad It is essential for the present method that the types of radiation measured have secondary charged particles of which the mean LET is equal to that of the beta particle spectrum in the calibration radiation source The phenomenon itself can be utilized for comparing the LET of different types of radiation (CARLSSON & ALM CARLSSON) The change in sensitivity of five measuring probes pre treated with various absorbed doses from 10^2 to 10^5 rad is illustrated in Fig 12 The deviation between ^{60}Co γ and ^{90}Sr ^{90}Y β irradiation lies within the errors of measurement which indicates that the β source can be used for calibration of high energy roentgen rays γ rays and electron radiation radiation qualities for which LET differs very little The situation will be different for low energy photons 200 kV radiation gives for example 30 per cent lower relative sensitivity (Fig 12) than ^{60}Co γ-radiation when dosimeters are pre treated with 10^5 rad When measurements are performed for this and other types of radiation with deviating LET fresh dosimeters or dosimeters which have been calibrated recently for the type of radiation concerned must be used

Acknowledgements

This work has been supported by the Swedish Cancer Society

same order as the measurement values The calibration values are fed in and simultaneously the absorbed dose is calculated and the result written out

In routine use the procedure is that the computer first writes out the identification number of the measuring probe to be calculated and then asks for the correction factor C_x by writing, for example

5-21
C=

the computer then continues by
[illegible] (RD) by writing

TD=   RD=

When these parameters have been allocated their values the result is written out for the whole measuring probe in the following table

5-21
C=1
TD−235   RD=200

NR	Dose	%TD	%RD
1	200	85	100
2	205	87	103
3	190	81	95
4	170	72	85
5	140	60	70

The number (NR) is the number which identifies the individual dosimeter within the measuring probe

The precision of the method of measurement is determined by the reproducibility of the sensitivity of the measuring instrument during read-out and succeeding calibration If soiling of the optical system or other disturbances occur between the first and the second reading the results may be more or less erroneous In order to check the sensitivity of the instrument during the two measurements, leader-probes containing a dosimeter of 18 mm length are used The leader-probe is always irradiated with the calibration dose of 110 rad and placed first in the row of measuring probes to be read The deviation between two consecutive readings with such a dosimeter and dose level is 1 per cent The leader-probe may then be used as a monitor of the state of the instrument

The methods used in the present dosimetry system diverge strongly from conventional systems The effects included in repeated use of TLD will have an essential influence on the results The reasons why radiation sensitization and damage increase with increasing fractionation of irradiation and thermal treatment are not satisfactorily understood The phenomenon of sensitization and radiation damage should be investigated further

application as LET meter Proc of the 2nd international conf on luminescence dosimetry CONF 680920 US Atomic Energy Commission, Springfield 1968

of a symposium, International Atomic Energy Agency Vienna 1967

LINDSKOUG B and BENGTSSON B E Automated thermoluminescence reader I Technical construction and function Acta radiol Ther Phys Biol 14 (1975), 195

LINSLEY G S and MASON E W Sensitization in LiF Teflon Dosemeters Phys Med Biol 16 (1971), 695

MÅRTENSSON B K A Thermoluminescence of LiF A statistical analysis of the influence of pre annealing on the precision of measurement Phys Med Biol 14 (1969), 119

SPANNE P and CARLSSON C A Efficiency variations of thermoluminescent LiF caused by radiation and thermal treatments *In.* Proceedings of the third international conference on luminescence dosimetry, p 48 Danish Atomic Energy Commission, Gjellerup 1971

SUNTHARALINGAM N Thermoluminescent response of LiF to radiations with widely different LET Ph D Thesis University of Wisconsin Madison (1968)

ZIMMERMAN D W, RHYNER C R and CAMERON J R Thermal annealing effects on the thermoluminescence of LiF Hlth Phys 12 (1966), 525

SUMMARY

A radiothermoluminescence dosimetry system based on an automated reader has been developed The system utilizes the high sensitivity of the dosimeter material after heating Thermal treatment is limited to the temperature process in connection with read-out The measurement values are punched out automatically on paper tape and calculations performed by means of a minicomputer PDP 8/E The dosimetric system meets the needs of routine use in clinical environment Recommendations for the practical use of the system are given

ZUSAMMENFASSUNG

Es wurde ein Strahlenthermolumiñiszens Dosimeter System das auf einem automatischen Leser aufbaut entwickelt Das System macht von der hohen Empfindlichkeit des Dosimetermaterials nach Erwarmung Gebrauch Die Warmebehandlung ist auf die Temperaturprozesse im Zusammenhang mit der Ablesung beschrankt Die Messwerte werden automatisch auf einem Papierstreifen gestanzt und die Berechnungen mit dem Minikomputer PDP 8/E ausgefuhrt Das dosimetrische System fullt die Forderungen der routinemassigen Verwendung unter klinischen Bedingungen Ratschlage fur den praktischen Gebrauch des Systems werden gegeben

RÉSUMÉ

L auteur a mis au point un système de dosimétrie par radiothermoluminescence basé sur un lecteur automatique Ce système utilise la haute sensibilité du matériel dosimétrique après chauffage Le traitement thermique est limité au chauffage au cours de la lecture Les résultats de mesure sont transcrits automatiquement en perforations sur une bande de papier et les calculs sont faits au moyen d un miniordinateur PDP 8/E Ce système dosimétrique répond aux besoins ordinaires dans l usage clinique L auteur fait des recommandations pour l utilisation pratique de ce systeme

REFERENCES

ALM CARLSSON G Dosimetry at interfaces Acta radiol (1973) Suppl No 332

BJARNGARD B McCALL R C and BERSTEIN I A Lithium fluoride teflon thermoluminescence dosimeters *In* Proceedings of international conference on luminescence dosimetry p 308 Report CONF 650637 United States Atomic Energy Commission Springfield 1967

CAMERON J R ZIMMERMAN D KENNY G BUCH R BLAND R and GRANT R Thermoluminescent radiation dosimetry utilizing LiF Hlth Phys 10 (1964) 25

— DE WERD L WAGNER J WILSON C DOPPKE K ZIMMERMAN D Non linearity of thermoluminescence as a function of dose for LiF (TLD 100) *In* Solid state and chemical radiation dosimetry in medicine and biology p 77 International Atomic Energy Agency Vienna 1967

CARLSSON C A Thermoluminescence of LiF Dependence of thermal history Phys Med Biol 14 (1969) 107

— and ALM CARLSSON G Induced LET dependence in thermoluminescent LiF and its

Table

Dose rate with distance from ^{137}Cs source

Transverse distance (cm)	Dose rate (rad mg h)	KRISHNASWAMY dose rate (rad/mg h)
1	7 086	7 010
2	1 786	1 878
3	0 774	0 838
4	0 426	0 468
5	0 267	0 296
6	0 182	—
7	0 132	—

Source specifications Source length 2 0 cm active length 1 2 cm equivalent thickness platinum filtration 0 5 mm 2 6 mCi ^{137}Cs = 1 mg Ra (HORSLER et coll 1964)

A simple system is now described which demonstrates good correlation between computer calculated dose rates based on simulation in a pelvic phantom, and with dose rates measured in the patient after the sources were loaded

Materials and Methods

Pelvic phantom simulator A single NBS calibrated source, containing 14 7 mg Ra eq of ^{137}Cs (cf Table), was carefully positioned in the center of the tissue equivalent section of a Rando-Alderson pelvic phantom, at the approximate level of the external os of the cervix Lithium Fluoride (LiF) detectors, calibrated with a standard ^{60}Co source, were placed at varying distances parallel to this source in the same plane Detectors consisted of cylindrical Teflon capsules measuring 2 0 cm (ID 3 mm) and filled with Harshaw LiF powder TLD 700 Teflon plugs were in each end of the capsule so that the LiF powder occupied only the central 1 2 cm of the linear axis Annealing of the powder was done by the method of CAMERON (1964)

Irradiations were performed over 17 to 18 5 h time intervals, and the LiF was read out immediately using a Harshaw TLD system The reading was recorded as a function of position of each capsule and the peak reading, after constructing a smooth curve was converted to absorbed dose and taken to correspond to the radiation dose at the perpendicular bisector of the source

Siemens probe calibration and clinical use A cadmium sulphide (CdS) Siemens gammameter was used to measure dose rates along the transverse axis of the same ^{137}Cs source in a water phantom 50 cm × 50 cm × 50 cm (see e g JOELSSON & BÄCKSTRÖM 1969) The sensitive volume of the probe was positioned parallel to the long axis of the source, which was encased in a narrow polyethylene tube to prevent movement The probe was then positioned remotely and the readings were recorded

DEPARTMENT OF RADIATION MEDICINE (DIRECTOR Y MARUYAMA), A B CHANDLER MEDICAL CENTER, UNIVERSITY OF KENTUCKY, LEXINGTON, KENTUCKY 40506, U S A

COMPUTER DOSIMETRY BASED ON PELVIC SIMULATION

B HOSKINS, D E WREDE, G H SOWELL and Y MARUYAMA

Many institutions today utilize computer output in order to obtain the dose distribution in the pelvis for gynecologic implants Through the use of computers, it is possible to calculate the dose distribution in various anatomic planes and display them in a three dimensional array Presently there is no published report which shows good correlation of computer-calculated dose rates with those measured in patients Corroboration of computerized dose rates by direct measurement would assure the accuracy of the implant dose distribution and allow the clinician confidence in the proper patient dosage at reference points

Measurements of dose rates immediately after application of the sources inform the physician of the immediate situation, such as necessity of reloading or repositioning in order to obtain a suitable arrangement of radiation sources for the implant, and to identify possible areas where complications may occur Through the combined efforts of direct monitor measurement and computerized output it is possible to evaluate whether modification of sources e g strength, size, etc is needed or whether the afterloading instruments need to be relocated or altered Optimization of the dose to the tumor is thus obtained, while minimizing the dose to the healthy tissues Many methods of dose measurements are too rigorous (e g JOELSSON et coll 1972) to be applied routinely in the clinic, and do not lend themselves easily to correlation with computer output

Submitted for publication 19 April 1974

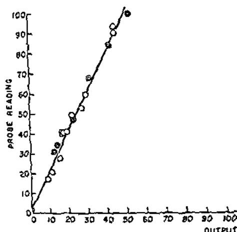


Fig. 2. Output in rad/h in relation to probe reading for rectal reading made in patients. Data points were from measurements made in the patient. Double circles are noted where multiple data points coincided. Equation of least square line and correlation coefficient are noted $y = 2.88 + 2.08x$, $r = 0.988$

formed in a tissue equivalent pelvic phantom. The results of measurements taken in the simulated situation appear in the Table. These data are plotted in Fig. 1 where dose rate is plotted with transverse distance along the perpendicular bisector distance. The present data determined in the phantom are shown relative to the infinite medium calculations by KRISHNASWAMY (1972). The dose measured was less at all distances.

Computer correlation with clinical measurement. The Table and Fig. 1 show the data of direct TLD measurement compared with KRISHNASWAMY's data (1972) drawn from the MIRD report (BERGER 1968). There was a systematic reduction in the measured, as compared to the expected dose (see discussion). For the purpose of this investigation, constants of the computer program were adjusted to correspond with the measured data.

Parameters in the computer program were fitted to the experimental results obtained by the TLD method. A point was designated on the orthogonal films for the Siemens gammameter probe and the coordinates used to calculate a computer determined dose rate (MARUYAMA et coll. 1974). The result of this calculation was then compared with the measurement taken with the calibrated probe after the sources were loaded into position in the patients.

The calibration of the Siemens gammameter yields a linear relationship in the clinically significant dose range, and varied from the curve shown by the manufacturer by only 3% (probable error in use of probe is 10%). There is a strong correlation between computed dose rates (based on parameters determined from simulation in a pelvic phantom) and those measured in the pelvis of a patient ($r = 0.988$) (Fig. 2).

Discussion

Computer calculated dose rates are used extensively in many radiation therapy departments today to determine the dose distribution in the pelvis (ADAMS & MEURK

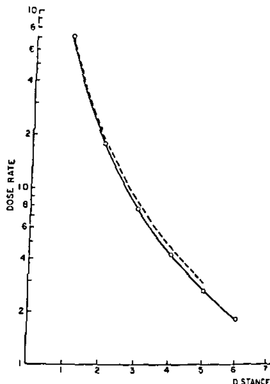


Fig 1 Dose rate in rad/mg-h at various transverse distances (in cm) along perpendicular bisector Interrupted curve is plotted from KRISHNASWAMY (1972), data points and full drawn curve were measured in a pelvic phantom using LiF

A calibration of the Siemens gammameter was performed using the dose rates obtained in the LiF experiment as standards By comparing the Siemens gammameter readings (temperature corrected) obtained in the water phantom at a particular transverse distance from the source with the dose measured in the pelvic phantom at the corresponding distance, a linear relationship was obtained by least squares fitting

Dose rate measurements taken during implants were correlated with the computer calculated dose rate after noting the probe position along the rectal mucosa from the orthogonal roentgenograms as described by MARUYAMA et coll (1974)

Computer calculations The computer program was originally based upon the data given in the MIRD report (BERGER 1968) in which dose buildup, absorbed fraction and infinite medium of density 1 g/cm^3 are considered Numerical integration was performed along the length of the source and oblique filtration was ignored After manipulation of the original program, this was altered to fit the experimental results from the pelvic phantom Computation was performed using an IBM 360/65 computer

Results

Dose measured by simulation Doses were measured as a function of transverse distance along the perpendicular bisector of a ^{137}Cs source The source used contained 14 7 mg Ra-equivalent on the date of calibration (NBS) and the simulation was per-

SUMMARY

A technique is described which shows a good correlation between computer dose rates based on a simulated pelvic irradiation system and dose rates measured in patients using a probe monitor With radiation sources in position, the system described permits a rapid check of computer dosimetry output in a clinical situation As a dual dose monitor system greater confidence in the accuracy of implant dose distribution is possible

ZUSAMMENFASSUNG

Es wird eine Technik beschrieben, die einen guten Zusammenhang zwischen Komputer-Dosis Raten, bei einem simulierten Becken Bestrahlungs System und Dosis Raten, die bei Patienten unter Verwendung eines Sondendosimeters gemessen wurden, ergeben Mit Strahlenquellen in Position ermoglicht das beschriebene System eine rasche Prufung der Komputer Dosimetrie in einer klinischen Situation Als zweifaches Dosis-Anzeige System ist eine grossere Zuverlassigkeit in der Genauigkeit der Dosis-Verteilung moglich

RESUME

Les auteurs décrivent une technique qui donne une bonne correlation entre les taux de dose détermines par ordinateur sur un système de simulation d irradiation pelvienne et les taux de dose mesures sur des malades en utilisant un dosimetre a sonde Quand les sources de radiation sont en place le système décrit permet un controle rapide en situation clinique du débit de doses détermine par ordinateur Ce système double de dosimetrie permet d accorder une plus grande confiance a la précision de la distribution de doses

REFERENCES

ADAMS G D and MEURK M L The use of a computer to calculate isodose information surrounding distributed gynecological radium sources Phys in Med Biol 9 (1964), 533

BERGER M J Energy deposition in water by photons from point isotopic sources J nucl Med Suppl 1 (1968) 15

CAMERON J R ZIMMERMAN D KENNEY G, BUCH R, BLAND R and GRANT R Thermoluminescent radiation dosimetry utilizing LiF Hlth Phys 10 (1964), 25

GREENFIELD M A FICHMAN M and NORMAN A Dosage tables for linear radium sources filtered by 0 5 mm and 1 0 mm of platinum Radiology 73 (1959), 418

HORSLER A F C JONES J C and STACEY A J Caesium 137 sources for use in intracavitary and interstitial radiotherapy Brit J Radiol 34 (1964) 385

JOELSSON I and BACKSTROM A Dose rate measurements in bladder and rectum Intracavitary radiation of carcinoma of the uterine cervix Acta radiol Ther Phys Biol 7 (1969) 343

— RUDÉN B I A DUTREIX A and ROSENWALD J C Determination of dose distribution in the pelvis by measurement and by computer in gynecological radiation therapy Acta radiol Ther Phys Biol 11 (1972) 289

JOHANSSON J M LINDSKOUG B A A and NYSTRÖM C E Pelvic dosimetry during radiotherapy of carcinoma of the cervix uteri Acta radiol Ther Phys Biol 8 (1969), 360

1964, POWERS et coll 1966) Theoretically derived computer programs have been implemented in treatment planning, but efforts to test their validity has not met with much success Problematic conditions posed by patient movement and source relocation has drastically hampered most attempts to demonstrate an uncomplicated method of surveillance which would serve as a monitor on the accuracy of the computer Localization of a calibrated dosimeter on roentgenograms, recording of the dose rate at that point, the subsequent comparison with the dose rate calculated by the computer at that same reference point should serve as a suitable criterion for the accuracy of the computer output

A calibrated Siemens gammameter was used in all dose rate measurements in patients, and the values obtained were compared to the computer-calculated rates The computer dosimetry used had its foundation in experimental measurements taken in a pelvic phantom under simulated conditions of radiation therapy for this anatomic area By a reiterative technique the computer dose rates about a specified source were brought into agreement with experimental data

Dose rates calculated by this method were compared to the published values of others (QUIMBY 1944, GREENFIELD et coll 1959, KRISHNASWAMY 1972) and found to be in agreement at very close distances, but low about 10 per cent at distances greater than 5 cm along the transverse axis (Fig 1) This may be attributed to the finite rather than infinite medium (MEISBERGER et coll 1968, KARTHA et coll 1966), presence of bony inhomogeneities, and reduced equivalence of the tissue density of the phantom Because primary, as well as secondary photons, may escape the medium, a dose reduction is quite likely Oblique angle filtration is inherently accounted for in this technique when small, but not at large angles of oblique filtration

The present investigation shows that the probe check system described here serves as an excellent monitor for implantation therapy Rather than a large number of readings made in the rectum and bladder at unknown distances from the radiation sources, the probe can be localized by orthogonal roentgenograms at an accurately known distance from the sources For an afterloading system, a single reading provides a rapid check on the accuracy of loading If contrast medium is placed in the rectum and bladder, one may also obtain information on doses in those structures A good correlation was found between computer dose rates, those based on simulated pelvic radiation system in phantom, and in patients under clinical conditions However, to provide absolute data, the different set of conditions under which data were measured must be taken into account

Acknowledgements

We thank Dr J A Sayeg for valuable criticisms The investigation was supported in part by National Cancer Institute grants CA 17-786, CA 05-528 and OVRMP grant RM 48 04-A[1]

FROM THE DEPARTMENT OF RADIOTHERAPY AND NUCLEAR MEDICINE, ST RADBOUD ZIEKENHUIS, NIJMEGEN, THE NETHERLANDS

$CaSO_4$ (Dy) THERMOLUMINESCENT DOSIMETERS FOR THE DETERMINATION OF GONADAL DOSES

A HASMAN and R T GROOTHEDDE

Thermoluminescent dosimeters can be regarded as almost ideal point detectors Accurate measurements of the absorbed dose can be performed The dosimeters are easily introduced into a patient and dose distributions in or near organs of interest are obtained

At the moment several thermoluminescent dosimetry systems are available on the market Some of these systems were reviewed previously (HASMAN & GROOTHEDDE) In our hospital a Teledyne 7300 reader is available and both LiF and $CaSO_4$ (Dy) discs embedded in a teflon matrix are used The LiF phosphors have the advantage of being almost tissue equivalent, whereas $CaSO_4$ (Dy) suffers from the fact that it is highly energy dependent (Fig 1) However, its sensitivity is about thirty times larger than that of LiF at cobalt energy An investigation was started on the female gonadal dose as compared to the delivered skin dose Since in most surveys the gonadal dose is rather low due to shielding of parts of the body, a very sensitive dosimeter was wanted enabling a read out of 1 mR with reasonable accuracy The high sensitivity LiF dosimeters from Harshaw are known to be able to measure an exposure of 5 mR with some accuracy, whereas $CaSO_4$ (Dy) dosimeters are able to measure 1 mR with at least the same accuracy The investigation was started on the actual energy dependence of $CaSO_4$ (Dy) in radiation beams with peak potentials varying from 50 to 150 kV

Submitted for publication 21 February 1974

KARTHA PONNUNNI K I, KENNEY G N and CAMERON J R An experimental determination of the absorption and buildup factor in water for radium, cobalt 60 and cesium 137 gamma rays Amer J Roentgenol 96 (1966), 66

KRISHNASWAMY V Dose distribution about cesium 137 in tissue Radiology 105 (1972) 181

MARUYAMA Y, HOSKINS B, WREDE D E, SOWELL G and VAN NAGELL J R Jr Probe check of computer dosimetry for gynecologic implant therapy Acta radiol Ther Phys Biol 13 (1974), 49

MEISBERGER L L, KELLER R and SHALEK R J The effective attenuation in water of the gamma rays of gold 198, iridium 192, radium 226 and Cobalt 60 Radiology 90 (1968), 953

POWERS W E, SCHNEIDER A K, SHUMATE K, FOTENOS H and GALLAGHER T Evaluation of methods of computer estimation of interstitial and intracavitary dosimetry Amer J Roentgenol 96 (1966), 59

QUIMBY E H Dosage table for linear radium sources Radiology 43 (1944), 572

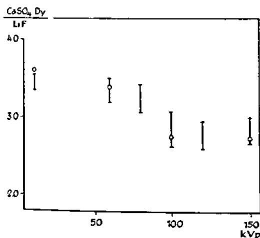


Fig. 3 The ratio in response of $CaSO_4$ (Dy) relative to LiF for the direct and scattered beam as a function of peak potential Filter 0.5 mm Al, ○ scattered beam, I direct beam

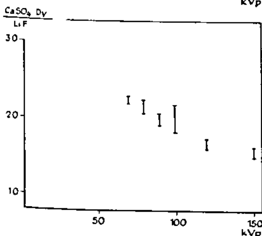


Fig. 4 The ratio in response of $CaSO_4$ (Dy) relative to LiF for a heavy filtered beam Filter 1.0 mm Cu + 1.0 mm Al

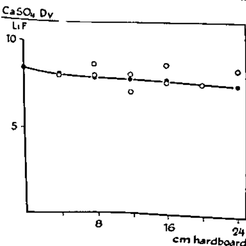


Fig. 5 Comparison of $CaSO_4$ (Dy) output with LiF output for different thickness of the hard board phantom ○ measured (100 kV, 0.5 mm Al), ● calculated (90 kV)

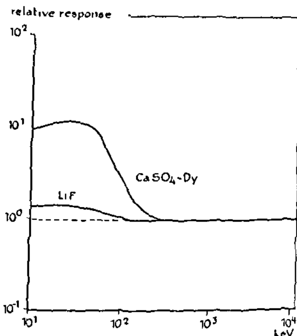


Fig 1 The energy dependence of $CaSO_4$ (Dy) and LiF dosimeters relative to water

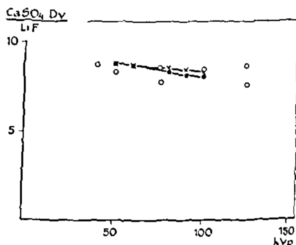


Fig 2 Comparison of $CaSO_4$ (Dy) output with LiF output as a function of peak potential The direct beam data have been calculated and measured ○ measured, × direct beam calculated, ● scattered beam calculated

Measurements have been performed with $CaSO_4$ (Dy) and LiF, and the ratio between the outputs was determined as a function of peak potentials

Some results obtained with the $CaSO_4$ (Dy) discs at urography are also reported In the last section a conclusion on the usefulness of $CaSO_4$ (Dy) discs is given

TLD measurements The energy dependence of $CaSO_4$ (Dy) has been determined with two roentgen machines Results have been obtained using a Philips Standard DLX with a Rotalix 0-75/125 diagnostic tube (total inherent filtration 1 mm Al) Additional measurements were performed with the Philips RT 250 deep therapy unit, having a higher filtration.

In the first place the energy response of $CaSO_4$ (Dy) and LiF dosimeters has been

Table 2

Gonadal exposure in mR delivered during urography

Case	kV	mAs	No of photos	Size	Gonadal dose in mR
1	70	97	5	35 × 43	24
			6	24 × 30	
2	80	214	5	35 × 43	34
			10	24 × 30	
3	72	146	1	35 × 43	9
4	70	146	4	35 × 43	23
			3	24 × 30	
5	70	97	4	35 × 43	7
			3	24 × 30	
6	70	146	3	35 × 43	25
			2	24 × 30	
7	70	91	4	35 × 43	72
			3	24 × 30	
			3	18 × 24	
8	70	65	4	35 × 43	36
			3	24 × 30	
9	74	146	3	35 × 43	21
			2	24 × 30	
			1	18 × 24	
10	80	86	3	35 × 43	8
			2	24 × 30	
			1	18 × 24	
11	70	146	2	35 × 43	36
			3	24 × 30	
			3	13 × 18	
12	75	146	3	35 × 43	17
			2	24 × 30	
13	72	146	2	35 × 43	36
			2	24 × 30	
			2	18 × 24	
14	68	146	5	35 × 43	49
			2	24 × 30	
			2	18 × 24	
15	70	146	5	35 × 43	61
16	75	146	3	35 × 43	26
			2	24 × 30	
17	80	344	5	35 × 43	80
			5	24 × 30	
18	85	312	5	35 × 43	83
			5	24 × 30	
19	72	91	3	35 × 43	34
			4	24 × 30	
20	72	103	3	35 × 43	37
			1	24 × 30	
			1	18 × 24	

Table 1

Dependence of LiF output from peak potential

0 5 mm Al, RT 250		1 mm Cu + 1 mm Al, RT 250	
kV	LiF output/mR	kV	LiF output/mR
60	1 4	60	1 2
80	1 4	80	1 3
100	1 4	100	1 3
120	1 4	120	1 2
150	1 2	150	1 2

measured The dosimeters were placed in the direct beam produced by the Rotalix tube Since the spectral distribution of the direct beam and a scattered beam (90°) was known the measured results could be compared with calculated values As could be expected the energy dependences are the same (Fig 2) Two important results are clear from measurement and calculations (a) the energy dependence of the $CaSO_4$ (Dy) dosimeters is rather small in this case, (b) measurements in the direct beam will give a similar energy dependence as measurements in scattered beams

These results may be explained by the fact that the contribution of low energy photons to the total spectrum is rather high due to the low filtration

Therefore, since the energy response of $CaSO_4$ (Dy) for energies less than 60 keV is rather uniform, only a small energy dependence can be expected for beams with low filtration and not too high peak potential The similarity in primary and scattered spectra was shown by WAGGENER et coll (1973) also for higher filtrations Since the inherent filtration of the diagnostic unit is rather low and cannot be considered as representative for most diagnostic units, additional experiments have been performed on a RT 250 deep therapy unit The inherent filtration of this unit varies from 1 5 mm Al at 50 kV to 2 5 mm Al at 250 kV In most of the experiments 0 5 mm Al was added In Fig 3 the ratio of the response of $CaSO_4$ (Dy) relative to LiF is shown as a function of energy for a moderately filtered beam Again the ratio varies over the energy range but the output from the $CaSO_4$ (Dy) discs does not vary more than ±10% over the potential range when compared with LiF Using a heavier filtration of 1 mm Al and 1 mm Cu the decrease in the ratio is more significant but the effective energy dependence of $CaSO_4$ (Dy) is still within ±15% as compared to LiF for the potentials considered (Fig 4) The ratio between the $CaSO_4$ (Dy) and LiF responses is also measured for scattered radiation and compared with the corresponding ratio for the primary beam Also in this case (Fig 4) both values lie close together over the whole potential range considered

As a last experiment the response of the $CaSO_4$ (Dy) and LiF discs behind a variable thickness of hard board has been measured (RT 250, 0 5 mm Al additional filtration, 100 kV), and compared with results calculated from the known spectra Calculation and measurement agree within the experimental error (Fig 5)

RÉSUMÉ

Les mesures des doses aux gonades necessitent des dosimetres sensibles Etant donne que les dosimetres thermoluminescents au $CaSO_4$ (Dy) sont tres sensibles, on a mesure leur dependance à l egard de l energie par comparaison au LiF dans l intervalle de differences de potentiel du tube entre 50 et 150 kV De plus le debit des dosimetres LiF a ete compare avec le resultat des mesures faites avec des chambres d ionisation Bien que la dependance à l egard de l energie du $CaSO_4$ (Dy) soit bien connue, la dependance reelle a l egard du potentiel parait etre dans un intervalle de ±10% pour des faisceaux moderement filtres dans le domaine de 50 a 150 kV

REFERENCES

BEENTJES L B An estimate of the genetically significant diagnostic roentgen-ray dose in the Netherlands (1967) Thesis, University of Utrecht 1969

HASMAN A and GROOTHEDDE R T Comparison of some TLD dosimetry systems. *Brit. J. Radiol* 46 (1973), 637

WAGGENER R. G., LEVY L B and ZANACA P Spectra of scattered diagnostic X-rays from an Alderson phantom. *Hlth Phys* 24 (1973), 59

In Table 1 the LiF output is compared with the output of an ionization chamber (ionisation chamber type 37480 of the Philips universal dosimetry system) to see whether the LiF dosimeters would still have some energy dependence Values of the LiF output per mR are given for two filtrations as a function of peak potential The sensitivity of the LiF dosimeters is somewhat less for the heavier filtration (Table 1) Nevertheless, the energy dependence is hardly noticeable for a given filtration and therefore it could be concluded that the LiF dosimeters could be used as a reference dosimeter instead of the ionization chamber for the comparison with the $CaSO_4$ (Dy) dosimeters

The gonadal dose has been determined in 20 male patients undergoing urography The gonads were shielded by lead to reduce the gonadal dose That this is effective can be seen by comparing the mean gonadal dose published here with other values quoted in the literature (on the average 900 mR per examination, BEENTJES, as compared to 36 mR in our case)

Since the energy response varies maximally $\pm 10\%$, no attempt has been made to determine the ratio of the responses of LiF and $CaSO_4$ (Dy) in the primary beam each time The output of $CaSO_4$ (Dy) has thus been directly converted to mR using a once measured conversion factor In Table 2 the results are tabulated together with information on the tube potential, mAs values and field dimensions An average gonadal dose of 36 mR was obtained

Conclusions Although the energy dependence of $CaSO_4$ (Dy) dosimeters is well-known these dosimeters can be used with a fair accuracy over a tube potential range varying from 50 to 150 kV, when the beam is not too heavily filtered It appears that the response of the $CaSO_4$ (Dy) dosimeters varies only $\pm 10\%$ as compared with the LiF response, whereas the sensitivity of the $CaSO_4$ (Dy) dosimeters is much higher

SUMMARY

For the measurement of gonadal doses sensitive dosimeters are necessary Since $CaSO_4$ (Dy) thermoluminescent dosimeters are very sensitive the energy dependence has been measured as compared to LiF in the tube potential region between 50 and 150 kV Moreover the output of the LiF dosimeters was compared with the results of ionization chamber measurements Although the energy dependence of $CaSO_4$ (Dy) is well known the actual dependence on the potential appears to be within $\pm 10\%$ for moderately filtered beams in the region from 50 to 150 kV

ZUSAMMENFASSUNG

Zur Messung von Gonaden Dosen sind empfindliche Dosimeter notwendig Da $CaSO_4$ (Dy) Thermolumineszens-Dosimeter sehr empfindlich sind, wurde die Energieabhangigkeit, verglichen mit LiF, bei Rohrenspannungen im Bereich von 50 und 150 kV gemessen Darüberhinaus wurden die Ausschlage der LiF Dosimeter mit den Ergebnissen von Ionisations-Kammermessungen verglichen Obwohl die Energieabhangigkeit von $CaSO_4$ (Dy) gut bekannt ist, scheint die aktuelle Abhangigkeit von der Spannung fur massig filtrierte Strahlen im Bereich von 50 bis 150 kV innerhalb von $+10\%$ zu liegen

Table 1

Case 1 6 mg Colcemid orally The 95 % confidence limits in brackets

Time (hours)	Mitotic cells/10^3 cells	Metaphase figures/10^3 cells
0	18 (11 28)	11 (6–19)
2	24 (16– 35)	15 (9–24)
4	16 (9– 25)	10 (5–18)
6	99 (82–119)	70 (55–87)
8	55 (42– 71)	40 (29–54)

Table 2

Case 2 6 mg Colcemid orally

Time (hours)	Mitotic cells/10^3 cells	Metaphase figures/10^3 cells
0	33 (23– 46)	25 (17–36)
2	44 (33– 58)	23 (15–34)
4	87 (71 106)	46 (34–60)
6	71 (56– 88)	37 (27–50)
8	55 (42– 71)	28 (19–40)

An increase in sensitivity to radiation after prior treatment with massive doses of Colchicine was found in animal tumours by GUYER & CLAUS (1939), but this was not confirmed by BRUES et coll (1940) with more moderate doses Similar results have been obtained by HIRSHFIELD et coll (1940) and TARNOWSKI et coll (1957)

It therefore seemed appropriate to undertake controlled investigations in order to try to determine if there was increased sensitivity to radiation under clinical conditions at an individually appropriate time after administration of the drug Accordingly five patients, three with squamous carcinomas (of lip, anus and skin) and two with adenocarcinoma (of the stomach) were investigated It was felt that by using the tumour as its own control, only a few cases needed to be investigated

Case reports

Case 1 A Cape coloured woman 55 years old presented with a history of ulcer on the lower lip for four months Examination showed a [illegible] of the right lower lip, [illegible]er below the right jaw [illegible]mous carcinoma [illegible]om the lip at two-hourly [illegible]

FROM THE DEPARTMENTS OF RADIATION THERAPY AND *BIO-ENGINEERING AND MEDICAL* PHYSICS, GROOTE SCHUUR HOSPITAL AND UNIVERSITY OF CAPE TOWN, SOUTH AFRICA

STATHMOKINETIC FAILURE TO ENHANCE RADIATION RESPONSE IN HUMAN TUMOURS

R. SEALY, ANITA GREENSTEIN and B. SHEPSTONE

Several reports have appeared in the literature suggesting that metaphase inducing agents improve the response to radiation in human tumours. SUTTON (1965) has demonstrated that Demecolcine may improve the clinical results of roentgen treatment of squamous carcinoma. GRIEM & MALKINSSON suggested in 1966 that there is an optimal time for the administration of radiation after Colchicine, and in 1962 that there is a possible increase in sensitivity to radiation in human tumours after the use of Colchicine. They have also (1961) used mouse hair root systems and human tumours (mycosis fungoides) to elucidate the optimal timing of the radiation and consider that metaphase inducing agents may produce a synchronous cell population. BONOMINI & FIORENTINO (1965) have treated a large series of patients with advanced squamous carcinoma and adenocarcinoma with various spindle agents and radiation, and they conclude that the combination is of value. However, they had no controls in their series. A similar comment may be made in respect of some earlier reports of considerable series of patients (CONSTANTIN 1946, GIRGIS et coll. 1946, HUANT 1944 a, b, HUGUENIN et coll. 1955, KEIBL & LOETSCH 1950, REVIGLIO 1948).

Submitted for publication 7 October 1974.

Table 8

Case 5 Serial biopsies during course of treatment with cobalt therapy and Vincristine

Treatment		Mitotic cells/10^3 cells	Metaphase figures/10^3 cells
1	T = 0	12	8
	T = 6	70	50
2	T = 0	6	3
	T = 6	39	4
3	T = 0	12	6
	T = 6	5	3
4	T = 0	6	[illegible]2
	T = 6	3	[illegible]0
5	T 0	0	0
	T = 6	0	0
6	T - 0		
	T 6		

of the masses was observed in the seven days before the patient's death At autopsy, the two treated areas had the same histologic appearance Abnormal mitotic figures and pyknotic degenerating cells were found in both areas in equal numbers

Comment Although treatment was not completed in this case, it might be expected that some histologic difference would be seen at this dose level if a significant effect was to be produced

Case 4 A Caucasian male, aged 77, had a radical gastrectomy and presented 5 months later with a painful mass, 3 5 cm in diameter, in the right flank A biopsy of the mass confirmed the presence of a mucous secreting adenocarcinoma and a course of 5-Fluoro Uracil was instituted The patient, however, found this treatment to be unpleasant, and failed to reattend hospital for 8 months The pain then became persistent and the patient sought further help Examination then revealed the mass to be fungating and to measure 8 cm × 7 cm in size

Serial biopsies after 6 mg of Colcemid were taken on two successive days *On the first* day a peak of mitotic and metaphase figures was found at 8 hours (Table 5) Because of the considerable number of post metaphase figures at 8 hours, it was felt that a confirmatory test should be done on the second day, seeking a peak at 6 hours (Table 5), which also was found

[illegible] treated at the time of giving [illegible] s of 1 000 R were given to a [illegible] [illegible] regress on of the whole mass, equal in the two areas, with total clinical regression four months after treatment

Comment The uncertainty of the peak is a disquieting feature, and there appeared to be no advantage in the use of Colcemid

Case 5 A Cape coloured woman, 63 years old, presented with a two year history of an unpigmented lump on her *right foot*, with progressive enlargement On examination, this

Table 6

Case 5. Serial biopsies after 3 mg Colchicine intravenously

Time (hours)	Mitotic cells/10^3 cells	Metaphase figures/10^3 cells
0	17 (9–27)	9 (4–17)
2	9 (4–17)	5 (1–11)
4	8 (3–15)	5 (1–11)
6	23 (14–34)	12 (6–20)
8	10 (4–18)	5 (1–11)
10	12 (6–20)	6 (2–13)
12	12 (6–20)	8 (3–15)
14	15 (8–24)	8 (3–15)
16	21 (13–31)	15 (8–24)
18	23 (14–34)	16 (9–25)
20	13 (7–22)	8 (3–15)
22	19 (11–29)	15 (8–24)
24	11 (5–19)	7 (2–14)
26	3 (0– 8)	3 (0– 8)
28	5 (1–11)	2 (0– 7)
30	10 (4–18)	6 (2–13)
32	9 (4–17)	6 (2–13)
34	16 (5–19)	11 (5–19)
36	7 (0– 8)	3 (0– 8)

Table 7

Case 5 Serial biopsies after 2 mg Vincristine intravenously

Time (hours)	Mitotic cells/10^3 cells	Metaphase figures/10^3 cells
0	13 (7–22)	6 (2–13)
2	25 (16–36)	17 (9–27)
4	34 (23–47)	26 (17–37)
6	60 (46–76)	41 (29–55)
8	48 (35 63)	31 (21–43)
10	43 (31–57)	31 (21–43)
12	40 (28 54)	28 (18–40)

It was decided to give palliative treatment to the epigastric mass It was also decided to determine the time of the Colcemid induced peak and treat half the lesion at the time of the peak and half when the dose of Colcemid was given The results are shown in Table 4. There was a clear peak at 6 hours and accordingly, treatment following the usual plan was started T[illegible]
Cu HVL, [illegible]
was given orally, and the left six hours later to coincide with the metaphase peak Two doses only were given to each area over 8 days and treatment was then abandoned because of the relief of pain and the poor general condition of the patient No difference in the regression

It is probable, as the tumour becomes more and more disorganised by the irradiation, that the ability of a significant fraction of cells to respond to a spindle drug, is prejudiced. In Cases 1 and 2, about 8 per cent of the cells in the tumour as a whole, were affected. This is similar to levels obtained by GRIEM & MALKINSON (1962, 1966) and SUTTON (1965). This percentage represents a good peak, but it is unlikely that a marked clinical reponse would be seen, since the numbers involved in the peak are insignificant, even with the marked increase in sensitivity. If however, the great majority of the cells in the growth fraction of the tumour could be blocked in metaphase by the use of a more powerful agent or one given intra arterially, the situation might be different. This deserves further consideration.

These results do not suggest that the use of metaphase inducing agent and radiation out of phase are of no value. It might be that repeated doses of agents of this kind would destroy, progressively, the cells in the growth fraction of the tumour and induce those in GO, or the resting phase, to move into the cycle and thus be more available for assault with either radiation or the metaphase inducing agent.

Acknowledgements

This work was supported by the Medical Research Council, the Cancer Research Trust and the Radiotherapy Research Fund of the University of Cape Town.

SUMMARY

The literature concerning the use of metaphase inducing agents as clinical sensitisers to radiation is briefly reviewed and five cases are reported, which suggest that under ordinary clinical conditions these agents are not likely to be of value. These results accord with animal experiments and a possible reason is suggested.

ZUSAMMENFASSUNG

Es wird die Literatur über den Gebrauch von Metaphasen induzierender Substanzen als klinische Sensibilisatoren bei der Bestrahlung kurz dargestellt und über fünf Fälle berichtet, welche zur Vermutung veranlassen dass unter gewöhnlichen klinischen Verhältnissen diese Substanzen wahrscheinlich nicht von Wert sind. Die Ergebnisse stimmen mit Ergebnissen an Tiereexperimenten überein und es wird eine mögliche Erklärung gegeben.

RÉSUME

Les auteurs passent brièvement en revue la littérature concernant l'utilisation d'agents inducteurs de la métaphase comme sensibilisateurs cliniques aux radiations, ils présentent 5 cas qui font penser que dans les conditions cliniques habituelles ces agents ne présentent vraisemblablement pas d'intérêt. Ces résultats sont en accord avec l'expérimentation animale, les auteurs en donnent une raison possible.

was found to be a ...
oedema and cellulitis ...
showed a poorly diff...
Three mg Colchicine ... hourly
intervals for a period of thirty-six hours

The results appear in Table 6 No significant peak was obtained It was therefore decided to try another metaphase inducing agent Three days later 2 mg Vincristine was given intravenously and serial biopsies were taken every two hours for 12 hours A clearly significant peak was obtained at six hours (Table 7)

The tumour was then divided into two halves, one half to be treated at the time of administration of the Vincristine (T = 0, *off peak*) and the other half to be treated *six hours* later (T = 6, on peak) In view of the fact that in Case 2, the peaking was lost after two days of treatment, it was felt that weekly fractions may allow the peaking to be maintained for a longer period Therefore weekly fractions of 700 R were given to a total dose of 4 550 R over 35 days Biopsies were taken from the mass during treatment The peaking was again early lost in the course of treatment One month after treatment, there was no clinical improvement The mass remained the original size Because of the patient s cardiac condition, surgery was thought to be inadvisable and the patient returned home without any further treatment

Comment In this case, Vincristine induced a significant peak, whereas Colchicine did not although both drugs were given intravenously As in Case 2, the peaking was again lost after the first two fractions, and this could be a reason that there appeared to be no advantage in using Vincristine in combination with radiation

Discussion

The increase of sensitivity to radiation at the metaphase as shown by TERASIMA & TOLMACH (1961) is of the order of decrease in mean lethal dose from D_0 100–120 rad to D_0 59–82 rad Accordingly, if a peak of mitoses is obtained after the use of a metaphase blocking agent, regardless of how the drug was administered, radiation must be given at the time of the peak

GRIEM and co-workers have used four and sixteen hours as the time interval between drug administration and radiation, because this is the time interval they found between administration of the drug and occurrence of the peak However, this was in dysplastic mouse hairs and mycosis fungoides In the present five cases, it was found that the peak occurred at four to six hours after drug administration Therefore, this is the time interval that has been allowed between giving the drug and the radiation Apart, perhaps, from Case 1, there is no evidence in these five patients of any value in timing radiation to coincide with the peak It would appear difficult to do this in practice for a number of reasons It seems that one drug may induce a significant peak, while another may not in the same patient (Case 5) In this case, both drugs were given intravenously but only Vincristine produced a significant peak

It was thought that the loss of the peaking as seen in Case 2, after two fractions, might have been a result of the fractionation Therefore, case 5 was treated with weekly fractions, but again the peaking was lost after two treatments

It is probable, as the tumour becomes more and more disorganised by the irradiation, that the ability of a significant fraction of cells to respond to a spindle drug, is prejudiced In Cases 1 and 2, about 8 per cent of the cells in the tumour as a whole, were affected This is similar to levels obtained by GRIEM & MALKINSON (1962, 1966) and SUTTON (1965) This percentage represents a good peak, but it is unlikely that a marked clinical reponse would be seen, since the numbers involved in the peak are insignificant, even with the marked increase in sensitivity If however, the great majority of the cells in the growth fraction of the tumour could be blocked in metaphase by the use of a more powerful agent or one given intra arterially, the situation might be different This deserves further consideration

These results do not suggest that the use of metaphase inducing agent and radiation out of phase are of no value It might be that repeated doses of agents of this kind would destroy, progressively, the cells in the growth fraction of the tumour and induce those in GO, or the resting phase, to move into the cycle and thus be more available for assault with either radiation or the metaphase inducing agent

Acknowledgements

This work was supported by the Medical Research Council, the Cancer Research Trust and the Radiotherapy Research Fund of the University of Cape Town

SUMMARY

The literature concerning the use of metaphase inducing agents as clinical sensitisers to radiation is briefly reviewed, and five cases are reported, which suggest that under ordinary clinical conditions these agents are not likely to be of value These results accord with animal experiments and a possible reason is suggested

ZUSAMMENFASSUNG

Es wird die Literatur uber den Gebrauch von Metaphasen induzierender Substanzen als klinische Sensibilisatoren bei der Bestrahlung kurz dargestellt und uber funf Falle berichtet, welche zur Vermutung veranlassen dass unter gewohnlichen klinischen Verhaltnissen diese Substanzen wahrscheinlich nicht von Wert sind Die Ergebnisse stimmen mit Ergebnissen an Tierexperimenten uberein, und es wird eine mogliche Erklarung gegeben

RESUME

Les auteurs passent brièvement en revue la littérature concernant l utilisation d agents inducteurs de la métaphase comme sensibilisateurs cliniques aux radiations, ils presentent 5 cas qui font penser que dans les conditions cliniques habituelles ces agents ne presentent vraisemblablement pas d intéret Ces résultats sont en accord avec l experimentation animale, les auteurs en donnent une raison possible

REFERENCES

BONOMINI B and FIORENTINO M Spindle poisons in radiotherapy Prog Biochem Pharmacol 1 (1965) 674

BRUES A M, MARBLE B B and JACKSON E B Effects of Colchicine and radiation on growth of normal tissues and tumours Amer J Cancer 38 (1940), 159

CONSTANTIN R Faut il associer les injections de Colchicine à la radiothérapie dans le traitement du cancer? J Radiol Électrol 27 (1946), 466

GIRGIS A, MARTIN J F, ORSONI D et PONTHUS P Resultats de l association Colchicine radiothérapie dans le traitement des tumeurs malignes J Radiol Électrol 27 (1946), 244

GRIEM M L and MALKINSON F D Modification of radiation response of tissue by Colchicine *Preliminary clinical evaluation* 8th International Cancer Congress (1962) p 241

— — Modification of radiation response of tissue by Colchicine Amer J *Roentgenol* 97 (1966), 1003

— — and MORSE P H Modification of radiation response of tissue by Colchicine Radiology 77 (1961), 486

GUYER M F and CLAUS P E Irradiation of cancer following injection of Colchicine Proc Soc exp Biol 42 (1939), 565

HIRSHFIELD J W TENNANT R and OUGHTERSON A W The effect of Colchicine and X ray on a transplantable mammary carcinoma in mice Yale J Biol Med 13 (1940) 51

HUANT E (a) Action de la Colchicine sur la radio sensibilité des tumeurs malignes Gaz Hôp Paris 117 (1944) 55

— (b) Nouvelles considérations quant à l action de la Colchicine sur la radiosensibilité des tumeurs Gaz Hop Paris 117 (1944) 230

HUGEUNIN R TRUHART R et SARACINO R Premiers résultats de l utilisation en chimiothérapie anticancéreuse d un dérivé de la Colchicine La N Desacétyl Thiocolchicine Bull Ass franç Cancer 42 (1955) 308

KEIBL E und LOETSCH A Beobachtungen uber eine kombinierte Colchicin Rontgentherapie bei Leukamie Schweiz med Wschr 30 (1950) 288

MALLET L et LECAMUS H Poisons caryoclasiques et radiothérapie dans le traitement du cancer Presse med 52 (1944) 230

REVIGLIO J M A propos de l association Colchicine Roentgenthérapie dans le traitement *des tumeurs malignes Radiol Clin (Basel) 17 (1948)* 149

SUTTON M Superior mediastinal obstruction treated with Demecolcine followed by radiotherapy Brit med J 1 (1965) 495

TARNOWSKI G S BANE H N CONRAD J NICKSON J J STOCK C C and SUGIURA K Effects of combination of radiation and chemotherapeutic agents against experimental animal tumours Cancer Res (1957) Suppl No 3

TERASIMA T and TOLMACH J L Changes in X ray sensitivity of He La cells during the division cycle Nature (London) 190 (1961) 1210

FROM THE DEPARTMENT OF RADIOLOGY, THE UNIVERSITY OF TEXAS MEDICAL BRANCH, GALVESTON, TEXAS 77550, U S A

EFFECT OF THERAPEUTIC RADIATION ON PERIPHERAL BLOOD LYMPHOCYTES IN PATIENTS WITH CARCINOMA OF THE BREAST

V K JENKINS, M H OLSON, H N ELLIS and R N COOLEY

There is increasing evidence that immunologic mechanisms are important in detecting and destroying malignant cells (ALEXANDER & FAIRLEY 1967, GOOD & FINSTAD 1969, HELLSTRÖM et coll 1971) These immune mechanisms, including the thymus dependent lymphocyte (T-cell) system, have been demonstrated in both animal and human tumors and may also operate in human carcinoma of the breast (CATALONA et coll 1973), however, specific immunologic evidence has not been demonstrated An intact, vigorous cell mediated immune mechanism may be of therapeutic advantage to patients with malignant neoplasms, particularly when the bulk of their primary tumor has been eradicated by irradiation (DEODHAR et coll 1972, EILBER & MORTON 1970) There is considerable concern that the methods of treating neoplasms of the breast, including radiation therapy, may reduce this immune function and adversely affect natural immunity (DEODHAR et coll, DAO & KOVARIC 1962, FISHER 1971, MEYER 1970, STJERNSWÄRD et coll 1972) affording an increased chance for growth of residual or metastatic tumor cells On the other hand, some evidence has been presented indicating that local radiation therapy for carcinoma of the breast does not impair overall cellular immunity (GROSS et coll 1973, MCCREDIE et coll 1972)

Submitted for publication 25 June 1974

The present investigation was designed to evaluate the initial effects of cancericidal irradiation for carcinoma of the breast on lymphocyte responses in patients at different clinical stages of disease and in relation to whether or not patients had experienced a mastectomy before radiation therapy For this purpose peripheral blood samples from patients before, during and immediately after radiation treatment were examined to determine the effects of the treatment on the number and responsiveness to mitogens of lymphocytes Cultures of whole blood or of purified lymphocytes from patients were stimulated with non specific mitogens and the response determined by measuring tritiated thymidine (^{3}HTdR) incorporation into newly synthesized DNA

Materials and Methods

Irradiation procedures The patients were staged clinically according to the international classification of carcinoma of the breast (COPELAND 1965) and placed in one of two irradiation categories dependent on whether mastectomy had been performed Patients irradiated after mastectomy received 5000 to 6000 rad to the chest wall through 2 tangential fields, 5 000 rad to axillary tissues and 4 500 rad to the internal mammary chain and supraclavicular areas during a 5 to 6 week period Patients without mastectomy before radiation therapy received 5 000 to 6 000 rad tumor dose through 2 tangential breast fields in 5 to 6 weeks and doses to the axillary, internal mammary, and supraclavicular tissues similar to those used for patients treated after mastectomy

Culture techniques A total of 136 blood samples from 82 patients with carcinoma of the breast and 93 blood samples from 65 healthy individuals were used Blood samples were tested from patients at different stages of treatment, 42 patients were tested only once, 14 twice, and 26 were tested before, during and at the end of treatment Control samples were taken from relatives of the patients or laboratory personnel in normal health

For preparation of whole blood cultures, 5 ml of peripheral blood were withdrawn by venous puncture from patients and control individuals on the same day Clotting was prevented by addition of preservative free heparin Total white cell and differential counts were performed by standard methods (WINTHROP 1967) Blood cells were diluted, cultured, and the lymphocytes stimulated to undergo blastic transformation according to methods previously described (JENKINS et coll 1973, PAULY & SOKAL 1972) Briefly, the whole blood was diluted 1 20 with RPMI 1640 and 3 ml aliquots of the cell suspension containing 150 μl of blood were set up in triplicate in 16 mm × 125 mm plastic culture tubes for each mitogen used No heterologous serum was added to the cultures Cultures were routinely incubated for 7 days at 37°C, except in one experiment designed to determine responses at different culture periods The stimulated cultures contained 10 μg of purified phytohemagglutinin (PHA) in which the mitogenic/hemagglutinating activity ratio was

Table 1

Mean numbers of white blood cells in peripheral blood of patients with carcinoma of the breast in relation to clinical staging

Clinical stage	No of patients	Mean No of blood cells ±SE/mm³		
		Total leukocytes	Granulocytes	Lymphocytes
I	7	6 756±835	4 284+565	2 277±635
II	11	6 732±834	4 403±759	1 901±239
III	12	6 909+620	4 057±579	2 326±152
IV	9	6 696±473	4 623±373	1 734±241
I through IV	39	6 782±328	4 326+289	2 061 +142
Healthy controls	36	6 693+280	4 114±240	2 319±105

increased to approximately 100 1 during purification, 300 μg of pokeweed mitogen (PWM) or 10 μg of concanavalin A (CCA)

For cultures of purified lymphocytes, samples of approximately 30 ml each of peripheral blood were withdrawn in heparinized syringes from patients and healthy controls The lymphocytes were separated from the other blood cells by a nylon-column filtration method (DANIELS et coll 1970) The lymphocytes were suspended in culture media (TC 199) containing 20 per cent fetal calf serum to obtain a final concentration of 5×10^5 cells/ml in a total volume of 2 ml/culture For stimulation of the lymphocytes, 0 1 ml of PHA-M or 0 016 ml PHA P per 10^6 cells were added to duplicate culture bottles and the cultures were incubated at 37°C, for 3 days

Evaluation of lymphocyte transformation

Whole blood cultures Lymphocyte responses to the mitogens were determined by a ³HTdR incorporation method (PAULY & SOKAL 1972), 1 0 μCi of ³HTdR (2 0 Ci/mM) in 0 2 ml of media was added to each culture 24 h before harvest At the end of culture the cells were sedimented by centrifugation, washed twice with cold 3 per cent acetic acid, decolorized with hydrogen peroxide, and digested in one normal KOH (JENKINS et coll) The number of disintegrations per min from the labeled DNA of each culture was determined from counts made in a liquid scintillation spectrophotometer

Purified lymphocyte cultures For isotope incorporation 2 5 μCi of ³HTdR (2 0 Ci/mM) in 0 05 ml were added to each culture 2 hours before harvest At harvest the cells were centrifuged and washed in balanced salt solution containing unlabeled thymidine Two ml of 10 per cent trichloroacetic acid (TCA) were added to each tube to precipitate the DNA The precipitate was centrifuged and washed twice with 5 ml of 5 per cent TCA The precipitate was finally washed with methanol,

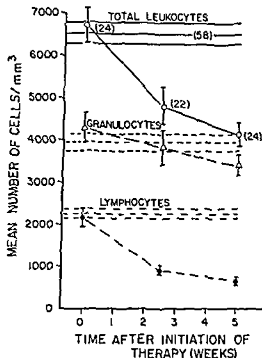


Fig 1 Effect of radiation therapy for carcinoma of the breast on numbers of total white blood cells (○), granulocytes (△), and lymphocytes (●) The mean values ±SE are given for patients before, during and at the end of treatment Means ±SE for healthy controls are indicated by solid or broken lines The number of patients or samples from healthy controls are given in parentheses

centrifuged and dried at 100°C for 5 minutes The precipitate was finally digested in KOH and prepared for determination of activity as described for whole-blood cultures

Results

Effects on peripheral blood counts Numbers of lymphocytes, granulocytes and total leukocytes were determined in 39 patients with carcinoma of the breast presenting at different clinical stages for irradiation (Table 1) There was no evidence that the mean numbers of peripheral blood cells were different in groups of patients with advanced disease as compared to the numbers in patients at earlier stages The effects of radiation treatment on the numbers of white cells in the peripheral blood of 24 of the patients tested before and after treatment are shown in Fig 1 The mean numbers of leukocytes in the patients were decreased during treatment by 2561 cells/mm³ or 38 per cent (p 0 001) During treatment the mean number of lymphocytes in the patients also decreased, to 31 per cent of the pre-treatment value ($p<0\ 001$), a loss of 1481 cells/m³ The mean number of granulocytes in the treated patients were also less by 877 cells/mm³ ($p<0\ 05$)

Effects on lymphocyte response in whole-blood cultures Stimulation of lymphocytes by PHA in whole-blood cultures of 5 patients tested at the end of radiation (5 000 rad) was less than the stimulation in cultures of healthy controls of similar age (Fig 2) The responses of cultures from patients and controls were greater after 5 to 7 days of incubation than the response of corresponding cultures harvested after 3 days For additional analysis of the responsiveness of peripheral blood cul-

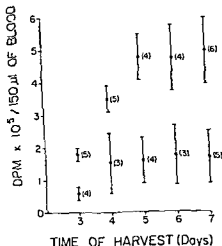


Fig. 2. Response of cultures containing 150 μl of blood in 3 ml media to PHA stimulation at different times of culture harvest. ○ mean value ±SE for healthy controls ● mean value ±SE for patients with carcinoma after 5 000 rad tumor dose The numbers of patients or controls tested at each time are given in parentheses

tures to all 3 mitogens, the 7-day harvest time was selected on the basis of these data (Fig 2) and the report by PAULY & SOKAL (1972), also indicating an optimum response after 5 to 7 days of growth

The responses of whole-blood cultures of 26 patients tested before, during and at the end of radiation treatment are given in Table 2. There were no significant differences between responses of cultures prepared before initiation of radiation therapy and samples from a heterogeneous group of individuals in normal health who were tested at the same time as the patients During treatment the mean responses of the patients decreased significantly and at the end of treatment the mean response to PHA was reduced to 39 per cent of the pre-treatment response ($p<0\ 01$) and responses to PWM and CCA were reduced to 15 per cent ($p<0\ 01$) and 34 per cent ($p<0\ 01$) of pre treatment values

Comparisons of lymphocyte responsiveness in patients who were treated by mastectomy 2 to 6 weeks before initiation of radiation therapy with the responsiveness of patients who were not operated upon are made in Table 3 Responses to the mitogens determined immediately before, during or at the end of radiation treatment were not significantly different in the 2 groups of patients The responses to all 3 mitogens were less in patients during radiation therapy (Table 2), but both groups of patients revealed similar decreases

Further comparisons of the lymphocyte responses of patients in relation to clinical staging are given in Table 4 Before radiation therapy the responses of patients in the more advanced stages III and IV were not significantly less than the responses of patients in the earlier stages I or II After radiation therapy the responses of lymphocytes in the cultures were less than the responses pre-treatment as found previously (Table 2), but values for the few patients tested were not significantly less in the stage III and IV patients than in the stage I and II patients

Table 2

Effect of therapeutic radiation for carcinoma of the breast on lymphocyte response to mitogenic stimulation in whole blood cultures 150 μl blood in 3 ml cultures grown for 7 days

Mitogens	^{3}HTdR incorporation (mean DPM ±SE × 10^3/culture)			
	Healthy individuals	Patients (No given in parentheses)		
		Pre-treatment	2 000–2 800 rad	5 000–6 000 rad
PHA (10 μg/culture)	331±16 (93)	280±30 (26)	189±33 (26)	108±23 (26)
PWM (300 μg/culture)	48±5 (76)	59±10 (23)	23±8 (22)	9±3 (23)
CCA (10 μg/culture)	70±6 (80)	58±12 (23)	27±5 (21)	20±8 (23)

Table 3

Lymphocyte response to mitogenic stimulation in whole-blood cultures from patients with carcinoma of the breast as related to surgery before radiation treatment Mastx, patients with simple or radical mastectomy

Mitogens	^{3}HTdR incorporation (mean DPM ±SE × 10^3/culture) No of patients given in parentheses					
	Pre-treatment		2 000–2 800 rad		5 000–6 000 rad	
	No mastx	mastx	No mastx	mastx	No mastx	mastx
PHA (10 μg/culture)	257±49 (17)	296±27 (24)	185±34 (17)	175±34 (24)	113±35 (12)	94±20 (25)
PWM (300 μg/culture)	54±12 (16)	67±11 (22)	17±8 (13)	22±8 (21)	13±4 (9)	11±5 (21)
CCA (10 μg/culture)	61±16 (14)	76±15 (21)	21±5 (15)	24±5 (21)	21±8 (10)	9±2 (18)

Effects on lymphocyte response in purified lymphocyte cultures The responses to PHA of cultures of 1×10^6 purified lymphocytes from irradiated patients as compared with cultures of an equal number of cells from healthy controls appear in Table 5 Although lymphocytes from 10 of the 23 patients responded poorly (5 to 45 per cent of control values), cells of 6 of the remaining patients responded much greater than controls (145 to 279 per cent) resulting in mean values that were not significantly different from mean values of controls

Discussion

Advantages suggested for the whole-blood method of measuring lymphocyte response are (1) 5 ml of blood is more easily obtained than larger volumes (30 to

Table 4

Lymphocyte responses to mitogens in whole-blood cultures from patients with carcinoma of the breast in relation to clinical staging

Radiation treatment	Mitogens	³HTdR incorporation (mean DPM ±SE × 10³/culture) (No of patients given in parentheses) Clinical stage			
		I	II	III	IV
Pre treatment	PHA	294±54 (7)	282±47 (13)	284±53 (12)	261±61 (9)
	PWM	67±13 (7)	51±16 (11)	80±18 (11)	54±15 (8)
	CCA	84±27 (6)	81±26 (10)	73±20 (11)	41±16 (8)
5 000–6 000 rad	PHA	53+10 (7)	103±33 (14)	144±40 (10)	67±36 (6)
	PWM	4±1 (5)	10+6 (9)	11±4 (10)	6±2 (4)
	CCA	8±4 (5)	10±4 (11)	22±9 (9)	10±4 (4)

50 ml) from patients under treatment, (2) greater reproducibility and better correlation with skin test data than observed with an isolated lymphocyte technique (PAULY & SOKAL), (3) avoidance of variables such as degree of cell damage during isolation of lymphocytes, (4) indication (theoretically) of quantitative response of the individual rather than the qualitative response of a given number of lymphocytes which may vary in number and heterogeneity (PARK & GOOD 1972) and, (5) more cultures may be tested from a single blood sampling, especially from patients with fewer peripheral blood lymphocytes following radiation therapy (JENKINS et coll)

Some criticisms of the whole-blood technique are (1) augmentation of lymphocyte response by erythrocytes, (2) alteration of response by polymorphonuclear cells, and (3) a long culture period relative to generation cycle It has been demonstrated that erythrocyte membranes did not increase lymphocyte transformation induced by the purified form of PHA (JOHNSON et coll 1972) Purified PHA was used in the present investigation, therefore it is unlikely that the presence of erythrocytes in cultures was a serious problem Polymorphonuclear leukocytes were reported to increase transformation of lymphocytes by PHA (GOUGH 1964), but PARK & GOOD did not find any major effect of granulocytes on stimulation of lymphocytes in whole-blood cultures The 7-day harvest time used in this investigation was previously shown to be within the peak of T cell response for cultures of whole blood from healthy individuals (PAULY & SOKAL) Similarly, cultures of blood from healthy controls and irradiated patients in the present investigation had higher responses to PHA after 5 to 7 days of cultures than after 3 days of culture (Fig. 2), but differences in responses of patients and controls was evident at all time periods tested

The whole blood results indicate that the irradiated patients have reduced responsiveness to all 3 mitogens used (Table 2) PHA and CCA are considered mainly T-cell mitogens, although CCA may also stimulate B-cells (ANDERSSON et coll 1972),

Table 5

Lymphocyte transformation in cultures of purified lymphocytes (1×10^6) from patients with carcinoma of the breast and healthy individuals in response to PHA as measured by ^3HTdR incorporation into DNA

Mitogens	^{3}HTdR incorporation (mean DPM $\times 10^3$ $\pm$SE culture) (No of patients or controls given in parentheses)	
	Healthy individuals	Patients (after 5 000 rad)
PHA-M	48 ± 5 (7)	62 ± 27 (7)
PHA-P	308 ± 50 (12)	227 ± 54 (16)

therefore a similar decrease in responses to these 2 mitogens is consistent with decreased numbers of T-cells capable of blastogenic transformation However, PWM activates both B- and T-cells (JANOSSY & GREAVES 1971) and the decrease in response to PWM was even greater than the decreases in response to PHA and CCA, therefore it seems unlikely that the change can be ascribed exclusively to a selective loss in T cells In contrast, the mean responses to PHA in cultures of purified lymphocytes from 23 irradiated patients were not significantly less than the mean responses of the same number of lymphocytes from 19 healthy controls (Table 5) Thus, a group of patients could have an overall radiation induced lymphocyte deficiency and still have normal or near normal qualitative responses for a given number of purified lymphocytes

Reduced T cell responses confirm the data of STJERNSWARD et coll (1972) that 15 of 18 patients irradiated for carcinoma of the breast had a more than 20 per cent decrease in isotope incorporation in cultures stimulated with PHA and COSIMI et coll (1973) that 10 of 12 irradiated patients had a decrease of more than 20 per cent One or more mechanisms might explain the decrease in the lymphocyte responses observed in patients after radiation therapy One possibility is that some inhibitory factor, as described by CATALONA et coll (1973) and by WHITTAKER et coll (1971) is being released into the patient s serum during irradiation and interferes with lympho cyte proliferation in vitro If such a factor is operative, it probably inhibits both T-cell and B cell response since responses to PHA, PWM, and CCA were all depressed during irradiation Another possibility is that the depressed response may reflect sublethal damage to the genetic mechanism of the lymphocytes during radia tion therapy that may render them incapable of mitotic activity in response to any of the mitogens However, in view of the radiation induced lymphopenia in these patients, and the evidence that purified lymphocytes from more than half the irradiated patients were capable of near normal or greater response to PHA, it is likely

that the responses noted in whole blood cultures reflect a decrease in the number of circulating lymphocytes capable of blastogenic transformation

Although the mean responses in whole blood cultures were reduced, there was no evidence to suggest that patients who had undergone mastectomy before radiation therapy responded differently than patients without mastectomy The implication that the ability of the blood lymphocytes to respond to mitogens is not overtly correlated with tumor burden is further supported by comparison of responsiveness related to clinical staging of the neoplasm Patients with larger primary tumors or extensive nodal involvement (stage III) and patients with metastatic lesions (stage IV) had responses before and after radiation therapy, comparable to patients with small primary lesions and no clinical evidence of nodal involvement

An adverse role on tumor immunity by radiation treatment has been suggested for patients with carcinoma of the breast (FISHER, MEYER) In contrast are 2 reports, one stating that delayed hypersensitivity reaction to dinitrochloro-benzene was not impaired in the majority of patients tested 3 and 9 months after initiation of therapy (GROSS et coll 1973) and another stating that PHA responsiveness of lymphocytes did not change or was increased in patients for 11 months after treatment with radiation (MCCREDIE et coll) Differences between our data indicating an initial depression in lymphocyte response and reports of increased or no effect on the lymphocyte response at delayed time periods after treatment may result from changes taking place in the lymphocyte pool during the months following therapy

Whether the in vitro correlate of cell mediated immunity, as measured by mitogenic stimulation in whole blood cultures, indicates capacity of patients to react immunologically to specific tumor antigens and whether these indications are significant in predicting clinical outcome are conjectural Proof that radiation therapy is adverse to natural tumor immunity resulting in worsened prognosis can only be obtained by a correlation of the clinical progression with in vitro or in vivo lymphocyte analyses Without such proof, it seems reasonable that means should be sought to protect as many lymphocytes as possible during treatment

Acknowledgement

This investigation was supported by Public Health Service Research Grant No CA 13435 from the National Cancer Institute.

SUMMARY

Effects of radiation therapy for carcinoma of the breast on responsiveness to mitogens of blood lymphocytes of patients at different clinical stages were analysed Patients at different clinical stages had comparable numbers and responses of lymphocytes During therapy the mean lymphocyte numbers decreased to 31 per cent of the pre treatment value and mean responses to mitogens in whole blood cultures decreased to 15 to 39 per cent of pre treatment values. Similar decreases occurred whether or not mastectomy was performed

ZUSAMMENFASSUNG

Die Wirkung der Strahlentherapie wegen eines Brustkarzinoms auf die Wirksamkeit von mitogenen Substanzen auf die Blut-Lymphozyten von Patienten in verschiedenen klinischen Stadien wurde analysiert Patienten in verschiedenen klinischen Stadien hatten vergleichbare Anzahl und Reaktionen der Lymphozyten Wahrend der Therapie fiel die mittlere Leukozytenzahl auf 31 Prozent der Ausgangswerte und die durchschnittliche Reaktion gegenüber mitogenen Substanzen auf 15 bis 39 Prozent der Ausgangswerte in Vollblut-Kulturen Ein ähnlicher Abfall trat unabhangig davon auf, ob eine Mastektomie vorgenommen wurde oder nicht

RÉSUMÉ

Les auteurs ont étudié les effects du traitement par les radiations pour le cancer du sein sur la capacité de réponse aux mitogènes des lymphocytes sanguins de malades à différents stades cliniques Chez des malades à différents stades cliniques le nombre et les réponses des lymphocytes sont comparables Au cours du traitement le nombre moyen des lymphocytes diminue jusqu'à 31 pour cent de la valeur avant le traitement et les réponses moyennes aux mitogènes dans des cultures de sang complet diminuent jusqu'à 15 à 39 pour cent de la valeur avant traitement On observe es diminutions semblables en l'absence ou en la présence d'une mastectomie

REFERENCES

ALEXANDER P and FAIRLEY G H Cellular resistance to tumors Brit med Bull 23 (1967), 86

ANDERSSON J, MÖLLER G and SJÖBERG O B lymphocytes can be stimulated by Concanavalin A in the presence of humoral factors released by T cells Europ J Immunol 2 (1972), 99

CATALONA W J, SAMPLE W F and CHRETIEN P B Lymphocyte reactivity in cancer patients Correlation with tumor histology and clinical stage Cancer 31 (1973), 65

COPELAND M M American joint committee on cancer staging and end results reporting Cancer 18 (1965), 1637

COSIMI A B, BRUNSTETTER F H, KEMMERER W T and MILLER B N Cellular immune competence of breast cancer patients receiving radiotherapy Arch Surg 107 (1973), 531

DANIELS J C, SAKAI H, COBB E K, REMMERS JR A R, SARLES H E, FISH J C, LEVIN W C and RITZMANN S E Altered nucleic acid synthesis in lymphocytes from patients with chronic uremia Amer J med Sci 259 (1970), 214

DAO T L and KOVARIC J Incidence of pulmonary and skin metastases in women with breast cancer who received post-operative irradiation Surgery 52 (1962), 203

DEODHAR S D, CRILE JR G and ESSELSTYN JR C B Study of the tumor cell lymphocyte interaction in patients with breast cancer Cancer 29 (1972), 1321

EILBER F R and MORTON D L Impaired immunologic reactivity and recurrence following cancer surgery Cancer 25 (1970), 362

FISHER B The present status of tumor immunology Adv Surg 5 (1971), 189

GOOD R A, and FINSTAD J Essential relationship between the lymphoid system, immunity and malignancy Nat Cancer Inst Monogr 31 (1969), 41

GOUGH J, ELVES M M and ISRAELS M G G The formation of macrophages from lymphocytes in vitro Exp Cell Res 38 (1964), 467

GROSS L, MANFREDI O L and PROTOS A A *Effect of Cobalt-60 irradiation upon cell mediated immunity* Radiology 106 (1973), 653

HELLSTROM I, HELLSTROM K E, SJOGREN H O and WARNER G A Demonstration of cell mediated immunity to human neoplasms of various histological types Int J Cancer 7 (1971) 1

JANOSSY G and GREAVES M F Lymphocyte activation I Response of T and B lymphocytes to phytomitogens Clin exp Immunol 9 (1971), 483

JENKINS V K, OLSON M H and ELLIS H N *In vitro* methods of assessing lymphocyte transformation in patients undergoing radiotherapy for bronchogenic cancer Tex Rep Biol Med 31 (1973) 19

JOHNSON R A, SMITH T K and KIRKPATRICK C H Augmentation of phytohemagglutinin mitogenic activity by erythrocyte membranes Cell Immunol 3 (1972), 186

MCCREDIE J A, INCH W R and SUTHERLAND R M Effect of postoperative radiotherapy on peripheral blood lymphocytes in patients with carcinoma of the breast Cancer 29 (1972) 349

MEYER K K Radiation induced lymphocyte-immune deficiency A factor in the increased visceral metastases and decreased hormonal responsiveness of breast cancer Arch Surg *101 (1970), 114*

PARK B H and GOOD R A A new micromethod for evaluating lymphocyte responses to phytohemagglutinin Quantitative analysis of the function of *thymus-dependent cells.* Proc nat Acad Sci 69 (1972), 371

PAULY J L and SOKAL J E A simplified technique for in vitro studies of lymphocyte reactivity Proc Soc exp Biol 140 (1972), 40

STJERNSWARD J, JONDAL M, VANKY F, WIGZELL H and SEALY R Lymphopenia and change in distribution *of human B and T lymphocytes in peripheral blood* induced by irradiation for mammary carcinoma Lancet 1972, p 1352.

WHITTAKER M G REES K and CLARK C G Reduced lymphocyte transformation in breast cancer Lancet 1971, p 892.

WINTHROP M N N Enumeration of white corpuscles *In* Clinical hematology 6th edition p 425. *Lea & Febiger, Philadelphia 1967*

FROM THE GENERAL DEPARTMENT (DIRECTOR PROF J EINHORN), RADIUMHEMMET, KAROLINSKA SJUKHUSET, S-104 01 STOCKHOLM, SWEDEN

EFFECTS OF ^{131}I THERAPY ON BLOOD BORNE LEUCOCYTES IN HYPERTHYROID PATIENTS

G LUNDELL

Patients with hyperthyroidism exhibit a decreased number of peripheral basophilic granulocytes compared with euthyroid individuals (TURIN 1910, INAGAKI 1957), but these cells increase following ^{131}I therapy (FERLIN & MANTERO 1968) In some cases of hyperthyroidism increased levels of circulating lymphocytes have also been found (BISTROM 1946) In this report the number of different types of leucocytes before and after ^{131}I therapy are compared

Material and Methods

The number of peripheral leucocytes and their percentage differential were examined in 54 hyperthyroid patients, of these 35 with nodular glands, immediately before and 2 to 4 months after ^{131}I therapy 49 women and 5 men, varying from 42 to 83 years of age (mean age 60 2 years)

The evaluation of thyroid function before and following therapy as well as the principles for the treatment have been reviewed elsewhere (LARSSON 1955, BELING & EINHORN 1961, LUNDELL & JONSSON 1973)

The leucocytes were stained with May–Grunwald–Giemsa and the total number of leucocytes and their percentage differential were determined For practical reasons it was not possible to have all the blood tests in the morning with the patients

Submitted for publication 27 February 1975

Table 1

Leucocyte values in 54 hyperthyroid patients before therapy

Cell type	No of cells		Per cent of total	
	Mean	SE	Mean	SE
Juvenile neutrophils	229	24	3 7	0 3
Segmented neutrophils	3 188	165	51 7	1 3
Eosinophils	112	16	1 8	0 2
Basophils	22	5	0 3	0 1
Monocytes	431	30	7 0	0 4
Lymphocytes	2 189	119	35 5	1 4
Total	6 171	266	100 0	

fasting In each single case, however, the tests before and after treatment were performed at the same time of the day in order to minimize changes in the leucocyte count occurring during the day The statistical method used was the Student's *t* test

Results

Following the ^{131}I treatment 11 patients were still hyperthyroid after 2 to 4 months, 2 patients were hypothyroid and the remaining 41 patients euthyroid

The leucocyte values before therapy are given in Table 1 and were within the range of normal values obtained at this hospital in healthy individuals

In the 41 euthyroid and 2 hypothyroid patients the number of juvenile neutrophils and also of the eosinophils and basophils increased significantly The total number of cells was not significantly altered (Table 2) A comparison based on the percentage differential in these patients gave the same results as for the absolute values In the 11 patients, still hyperthyroid, the total number of leucocytes did not differ significantly for the pre treatment values, nor the different types of leucocytes (Table 3)

Discussion

Previously it has been shown that ^{131}I treatment of hyperthyroidism is followed by an increase in the number of basophilic granulocytes In the present material, it was found that the number of juvenile neutrophils and eosinophilic granulocytes also increased, but that the number of other cells remained unchanged The reason for the observed increase is unclear

External irradiation is followed by reduction of the absolute numbers of lymphocytes and segmented neutrophils (LAWRENCE et coll 1948, JACOBSON et coll 1949, GLAS & WASSERMAN 1974) As for the percentage differential leucocyte counts, a

Table 2

Changes in the absolute numbers of leucocytes in 43 patients without signs of thyroid hyperfunction 2–4 months after ^{131}I therapy for hyperthyroidism

Cell type	No of cases			Mean of individual leucocyte differences		Level of significance for the difference, p
	Increase	Decrease	Unchanged	Mean	SE	
Juvenile neutrophils	27	16	0	+ 99	36	<0 01
Segmented neutrophils	28	15	0	+356	224	—
Eosinophils	27	13	3	+ 39	15	<0 05
Basophils	21	10	12	+ 22	8	<0 01
Monocytes	20	23	0	+ 4	38	—
Lymphocytes	25	18	0	+ 37	140	—
Total	25 cases	17 cases	1 cases	+557	342	—

Table 3

Changes in the absolute numbers of leucocytes in 11 patients remaining hyperthyroid 2–4 months after ^{131}I therapy for hyperthyroidism

Cell type	No of cases			Mean of individual leucocyte differences		Level of significance for the difference, p
	Increase	Decrease	Unchanged	Mean	SE	
Juvenile neutrophils	3	8	0	−154	84	—
Segmented neutrophils	4	7	0	496	353	—
Eosinophils	3	8	0	+ 6	47	—
Basophils	5	3	3	+ 11	10	—
Monocytes	6	5	0	13	67	—
Lymphocytes	4	7	0	− 39	325	—
Total	3 cases	8 cases	0 cases	−685	721	—

relative increase has been noted in juvenile and segmented neutrophils, monocytes, eosinophils and basophils (LUNDELL 1974) In those patients who remained hyperthyroid after ^{131}I therapy, no tendency was seen suggesting an increase in the number of juvenile segmented neutrophils, basophilic or eosinophilic granulocytes The 11 patients, hyperthyroid 2 to 4 months after the ^{131}I treatment, received a mean dose of 5 0 mCi, while the 43 patients without signs of hyperthyroidism after the treatment received a mean dose of 7 9 mCi This difference is not statistically significant

and the main reason for the difference between these groups was that one patient in the latter group had a very large goitre requiring a total of 70 mCi It therefore seems unlikely that the changes observed in patients rendered euthyroid were due to the treatment as such On the other hand, the number of patients who remained hyperthyroid was small, and therefore the results are somewhat less conclusive

SUMMARY

The different types of circulating leucocytes were examined in 54 patients before and 2 to 4 months after ^{131}I therapy for hyperthyroidism An absolute and differential percentage increase in the number of juvenile segmented neutrophils, eosinophilic and basophilic granulocytes was demonstrated in the patients free from signs of hyperthyroidism after therapy This increase was statistically significant No changes occurred in the 11 patients remaining hyperthyroid

ZUSAMMENFASSUNG

Die verschiedenen Typen von zirkulierenden Leukozyten wurden bei 54 Patienten vor und 2 bis 4 Monate nach ^{131}J Therapie wegen Überfunktion der Thyreoidea untersucht Bei Patienten, die frei von Zeichen einer Thyreoidea-Überfunktion nach der Therapie waren, wurden ein absoluter und relativer prozentueller Anstieg in der Zahl der jungen segmentförmigen Neutrophilen, der eosinophilen und basophilen Granulozyten nachgewiesen Dieser Anstieg was statistisch signifikant Es traten keine Veränderungen bei 11 Patienten, die hyperthyreoid verblieben waren, auf

RESUMÉ

Les différents types de leucocytes circulants ont été examines chez 54 malades avant et de 2 à 4 mois apres traitement par ^{131}I pour hyperthyroïdie L'auteur a mis en evidence une augmentation absolue et différentielle du pourcentage du nombre des neutrophiles segmentes jeunes, des granulocytes éosinophiles et basophiles chez les malades ne presentant plus de signes d hyperthyroïdie après le traitement Cette augmentation est statistiquement significative Il n y a pas eu de modification chez les 11 malades qui restaient hyperthyroïdiens.

REFERENCES

BELING U and EINHORN J Incidence of hypothyroidism and recurrences following ^{131}I treatment of hyperthyroidism Acta radiol 56 (1961), 275

BISTROM O On the morphology of blood and bone marrow in thyrotoxicosis Acta chir. scand 94 (1946) Suppl No 114

FERLIN G e MANTERO F Il comportamento dei granulociti basofili nel morbo di Basedow in corso di terapia con radioiodio (I^{131}) (In Italian) Acta isotopica 8 (1968), 134

GLAS U and WASSERMAN J Effect of radiation treatment on cell mediated immune response in carcinoma of the breast Acta radiol Ther Phys. Biol 13 (1974), 83

INAGAKI S The relationship between the level of circulating basophil leucocytes and thyroid function Acta endocr (Kbh) 26 (1957), 477

JACOBSON L O, MARKS E K and LORENZE E The hematological effects of ionizing radiations Radiology 52 (1949), 371

LARSSON L G Studies on radioiodine treatment of thyrotoxicosis Acta radiol (1955), Suppl No 126

LAWRENCE J S, DOWDY A H and VALENTINE W N Effects of radiation on hemopoiesis Radiology 51 (1948) 400

LUNDELL G Effects of radiation therapy on blood borne leucocytes in patients with mammary carcinoma Acta radiol Ther Phys Biol 13 (1974), 307

— and JONSSON J Thyroid antibodies and hypothyroidism in ^{131}I therapy for hyperthyroidism Acta radiol Ther Phys Biol 12 (1973), 443

TURIN M Blutveränderungen unter dem Einfluss der Schilddrüse und Schilddrüsensubstanz Dtsch Z Chir 107 (1910), 343

ACTA RADIOLOGICA

OFFICIAL ORGAN OF THE RADIOLOGICAL SOCIETIES OF DENMARK, FINLAND, NORWAY AND SWEDEN

Vol 14 Fasc 5 | THERAPY PHYSICS BIOLOGY | 1975 October

GENETIC EFFECTS OF ACUTE AND CHRONIC IRRADIATION WITH 14 MeV NEUTRONS

I. Genetic aspects

K-G LUNING, C RÖNNBÄCK and W SHERIDAN

II. Technique of neutron irradiation

M HOLMBERG

I GENETIC ASPECTS

The genetic effects of chronic exposure to neutrons were found by SEARLE et coll (1964) to be much higher than those occurring after acute exposure The neutrons used had a mean energy of 0 7 MeV Previously, RUSSELL et coll (1954) had reported that with acute exposure monoenergetic 14 MeV neutrons gave much lower effectiveness than those with energies around 1 MeV With this background, it was of interest to make further comparisons of the effects of acute and chronic exposure to 14 MeV neutrons on spermatogonia The results are described in the present report

Material and Methods

Animals from an inbred CBA strain were used The male mice were 60 to 70 days old at the start of the experiment Due to technical difficulties the experiment was

From the Laboratory of Radiation Genetics, S-171 64 Solna, and the Research Institute of National Defence S-172 04 Sundbyberg, Sweden

Submitted for publication 16 October 1974

divided into two parts In the first part, acute irradiation only was given These males were divided into three groups according to the dose· 150 rad (30 P males), 250 rad (46), and an unirradiated control group (74 P males)

The second part of the experiment was started before the results of the first part had been evaluated As the most appropriate dose was uncertain a large sample of males was used, divided into five groups 75 rad acute (45 P males), 150 rad acute (45), 250 rad acute (45), 250 rad chronic (103), fractionated, with about 8 h a day for 5 days per week through 11 weeks, and an unirradiated control group (75 P males) (The irradiation technique is described and discussed on page 412)

In the first experiment the three groups of males were mated shortly after irradiation with 3 virgin CBA females each, with new females for each of the first 3 weeks The females were killed and examined for intra-uterine deaths on the 17th day after the beginning of mating This gives information about the effect on post-meiotic stages The males were assumed to enter a sterile period and were left without females for 2 weeks After this period they were again given virgin females, which remained until pregnancy occurred These females were isolated to give birth to their litters and were replaced by new females For each irradiated male it was thus possible to observe when the first litter was born, which was indicative of regained fertility The offspring were retained for use in the analysis of recessive lethals

In the second experiment the males given acute exposure were kept without females until those chronically exposed showed the first indication of regained fertility The latter were immediately mated with 3 females each in three subsequent weeks As all males turned out to be sterile the third group of females were allowed to stay with the males for 5 to 6 weeks The females were then replaced with new females every 4th week until the males had regained fertility Females were then successively replaced when pregnant ones were isolated

By this time it was evident from the first part of the experiment that a comparison between the group given 250 rad acute, and the chronically exposed males, was of great importance Furthermore, it was evident that the control group could be excluded This will be further discussed in the presentation of the results Offspring were thus obtained from the males given 250 rad acute, and chronic irradiation, respectively, and male animals were sampled from the progeny, at weaning, for further breeding tests

In both the first and the second parts of the experiment the F_1 males, when about 60 days old, were mated with 3 CBA females to produce daughters When these females were ready to deliver, the F_1 males were present for a couple of days to use the post-partum oestrus for a new pregnancy About 12 F_2 females from each F_1 male were necessary for the test While waiting for the sexual maturity of the F_2 females, the F_1 males were mated with 3 fresh CBA females, which 17 days after the beginning of mating were killed and analysed for the number or dead and live implants in the uterus Semi-sterile males could thus be identified and excluded from the back-cross to daughters

Table 1

Effects of acute exposure to 14 MeV neutrons on postmeiotic stages (spermatozoa and spermatides)

Series		Implants	Dead	Per cent
Control	1st week	893	85	9 52
	2nd week	696	59	8 48
	3rd week	816	68	8 33
150 rad*	1st week	289	61	21 11
	2nd week	308	78	25 32
	3rd week	193	73	37 82
250 rad*	1st week	359	84	23 40
	2nd week	293	95	32.42
	3rd week	109	54	49 54

* ±8%. See Technique of neutron irradiation, page 412.

F_1 males with normal fertility were subsequently mated with 1 to 3 F_2 daughters each for 7 days These females were killed 17 days after the beginning of mating and the uterine content was examined

The F_1 males which in the back-cross test gave rise to an excessive rate of intra-uterine death, indicating that they might be lethal bearers, were mated with 3 CBA females per week to produce F_2 offspring which could be used in tests to confirm the lethal heterozygosity

Results

The main purpose was to analyse the possible differences in the mutagenic effectiveness of acute and chronic neutron irradiation This may be done either by examining dominant lethals or transmissible mutations The latter have the advantage that at least theoretically they may be followed through successive generations Among transmissible mutations recessive lethals were chosen, as by back-crossing F_1 males to their daughters the analysis of the whole genome may be covered The recessive lethals are identified by causing excessive intra uterine death in the back-crossing

Another type of mutational event which also results in excessive intra uterine death is translocations resulting in semi sterility All F_1 males were mated with females from the CBA strain to identify the semi steriles Such F_1 males gave in the offspring from these crosses an excessive rate of intra uterine death Thus a second type of transmissible effect identified as semi sterile was obtained as a by product

Effects on post meiotic stages The irradiated P males in the first part of the experiment were used in matings during the first 3 weeks after irradiation to gain preliminary information about the effect of 14 MeV neutrons using post meiotic cells (Table 1)

divided into two parts In the first part, acute irradiation only was given These males were divided into three groups according to the dose 150 rad (30 P males), 250 rad (46), and an unirradiated control group (74 P males)

The second part of the experiment was started before the results of the first part had been evaluated As the most appropriate dose was uncertain a large sample of males was used, divided into five groups 75 rad acute (45 P males), 150 rad acute (45), 250 rad acute (45), 250 rad chronic (103), fractionated, with about 8 h a day for 5 days per week through 11 weeks, and an unirradiated control group (75 P males) (The irradiation technique is described and discussed on page 412)

In the first experiment the three groups of males were mated shortly after irradiation with 3 virgin CBA females each, with new females for each of the first 3 weeks The females were killed and examined for intra-uterine deaths on the 17th day after the beginning of mating This gives information about the effect on post meiotic stages The males were assumed to enter a sterile period and were left without females for 2 weeks After this period they were again given virgin females, which remained until pregnancy occurred These females were isolated to give birth to their litters and were replaced by new females For each irradiated male it was thus possible to observe when the first litter was born, which was indicative of regained fertility The offspring were retained for use in the analysis of recessive lethals

In the second experiment the males given acute exposure were kept without females until those chronically exposed showed the first indication of regained fertility The latter were immediately mated with 3 females each in three subsequent weeks As all males turned out to be sterile the third group of females were allowed to stay with the males for 5 to 6 weeks The females were then replaced with new females every 4th week until the males had regained fertility Females were then successively replaced when pregnant ones were isolated

By this time it was evident from the first part of the experiment that a comparison between the group given 250 rad acute, and the chronically exposed males, was of great importance Furthermore, it was evident that the control group could be excluded This will be further discussed in the presentation of the results Offspring were thus obtained from the males given 250 rad acute, and chronic irradiation, respectively, and male animals were sampled from the progeny, at weaning, for further breeding tests

In both the first and the second parts of the experiment the F_1 males, when about 60 days old, were mated with 3 CBA females to produce daughters When these females were ready to deliver the F_1 males were present for a couple of days to use the post-partum oestrus for a new pregnancy About 12 F_2 females from each F_1 male were necessary for the test While waiting for the sexual maturity of the F_2 females, the F_1 males were mated with 3 fresh CBA females, which 17 days after the beginning of mating were killed and analysed for the number or dead and live implants in the uterus Semi-sterile males could thus be identified and excluded from the back cross to daughters

Table 1

Effects of acute exposure to 14 MeV neutrons on postmeiotic stages (spermatozoa and spermatides)

Series		Implants	Dead	Per cent
Control	1st week	893	85	9.52
	2nd week	696	59	8.48
	3rd week	816	68	8.33
150 rad*	1st week	289	61	21.11
	2nd week	308	78	25.32
	3rd week	193	73	37.82
250 rad*	1st week	359	84	23.40
	2nd week	293	95	32.42
	3rd week	109	54	49.54

* ±8 %. See Technique of neutron irradiation, page 412.

F_1 males with normal fertility were subsequently mated with 1 to 3 F_2 daughters each for 7 days. These females were killed 17 days after the beginning of mating and the uterine content was examined.

The F_1 males which in the back-cross test gave rise to an excessive rate of intra-uterine death, indicating that they might be lethal bearers, were mated with 3 CBA females per week to produce F_2 offspring which could be used in tests to confirm the lethal heterozygosity.

Results

The main purpose was to analyse the possible differences in the mutagenic effectiveness of acute and chronic neutron irradiation. This may be done either by examining dominant lethals or transmissible mutations. The latter have the advantage that at least theoretically they may be followed through successive generations. Among transmissible mutations recessive lethals were chosen, as by back-crossing F_1 males to their daughters the analysis of the whole genome may be covered. The recessive lethals are identified by causing excessive intra-uterine death in the back-crossing.

Another type of mutational event which also results in excessive intra-uterine death is translocations resulting in semi sterility. All F_1 males were mated with females from the CBA strain to identify the semi steriles. Such F_1 males gave in the offspring from these crosses an excessive rate of intra-uterine death. Thus a second type of transmissible effect identified as semi-sterile was obtained as a by-product.

Effects on post-meiotic stages. The irradiated P males in the first part of the experiment were used in matings during the first 3 weeks after irradiation to gain preliminary information about the effect of 14 MeV neutrons using post meiotic cells (Table 1).

Table 2

Time to regain fertility

Series	Numer of P males	Mean time ± SE (days)
150 rad acute	29	54 90 ± 0 29
250 rad acute	28	72 29 ± 1 51
250 rad chronic	74	86 54 ± 1 17

It is evident that acute neutron irradiation, like roentgen irradiation (BATEMAN 1958), had an effect which varied with dose and also with the spermatogenic stages

As no parallel experiments with roentgen irradiation were performed the RBE cannot be estimated By comparison with previous experiments with the same CBA strain (FRÖLEN 1965) it may, however, be concluded that the RBE seems to lie between 1 and 2

Time to regain fertility This time was measured to get further information about the injury to the irradiated testes such as that described by RUSSELL et coll (1954) Each P male was allowed to have 3 females from the 6th week after irradiation The regaining of fertility was estimated as the time from irradiation to the birth of its first offspring minus 20 days (the pregnancy) In the second part of the experiment similar estimates were obtained from the males given chronic irradiation (Table 2)

Obviously the lower acute dose affected the males to a lesser degree than the higher dose Also the variance was smaller in the series with the lower dose The chronic irradiation indicated a longer time before regaining fertility than did the corresponding acute dose

Production of F_1 males When the P males had regained fertility they were mated with CBA females which eventually gave birth to litters At weaning the F_1 males were sampled The drafting of F_1 males in the first part of this experiment has been described by LÜNING (1971) In the second part the same procedure was used The mean number of F_1 males per P males was 3 4 in the chronic series and 3 8 in the acute series

Test of recessive lethals The first part of this experiment has been presented by LÜNING (1971) but the results will be summarized here The comparison of acute and chronic neutron irradiation concerns a more extensive analysis of suspected lethal heterozygotes

The analysis of the experiments performed with a mean of 4 F_1 sons from each P male made it evident that the method used was not satisfactory The lack of effectiveness was due to the presence of spontaneous mutations in inbred strains and the variation in their occurrence (LÜNING 1975 a) In that report a model is presented

allowing calculation of the distribution of dead implants from lethal free (normal death rate 8 per cent) and lethal heterozygotes This gives an opportunity to identify lethal free and lethal heterozygous mice

The proportion of lethals may be estimated in two ways One is to compare the observed distribution with the model, the other to evaluate the excess of intra uterine death assuming that the excess is due to recessive lethals LÜNING & SEARLE (1971) calculated that each per cent recessive lethals caused a reduced survival of 0 125 per cent

A tendency exists among lethal heterozygotes to have a slightly lower mating capacity than lethal free males (LÜNING 1969, 1975 b) Such an effect would lead to an underestimation of the frequency of recessive lethals based on the total material For that reason the present data from each individual F_1 male is divided in such a way (LÜNING 1975 a) that the first group includes the first examined females which brought the sum of implants up to or just beyond 50 (mean 53 83, compare the model = 53) If there were additional data they were referred to the second group ir respective of the size A few F_1 males never reached the minimum level of 50 implants They are presented separately The results of the pregnancies and the intra uterine death are given in Tables 3 and 4

The number of dead in offspring to individual males appear in Table 5, based on the material in group 1 in Tables 3 and 4

Confirmation of recessive lethals It was assumed that recessive lethals would show up as families with excessive prenatal death in the back-cross tests

In the presentation of the first part of this experiment LÜNING (1971) outlined a method to confirm suspected recessive lethals The idea was to mate suspected lethal-carriers with females of the strain used, to produce F_2 offspring If the F_1 male was heterozygous for a recessive lethal, half of both his male and female offspring should be expected to carry the same lethal By mating the F_2 sons with their sisters results simulating the back-cross test performed in the main test would be obtained Ideally at least 7 F_2 sons and more than 50 daughters from each F_1 male should be encountered

This method would with satisfactory precision confirm lethality, but disproving suspected lethal heterozygosity would be more difficult The main object was to try to confirm lethality, however

From the second part of the test 36 F_1 males were taken out for further breeding As the F_1 males were about 8 to 9 months old some of them did not breed, or too little material was obtained and failed to include any F_2 males that could confirm the lethal heterozygosity

Among the F_1 males which in the test significantly deviated from the control level F_2 offspring from 6 males were obtained In Table 6 the number of F_2 males tested is presented as well as the number with excessive death in their offspring and consequently supposed to be lethal carriers

Table 3

The results from backcrossing F_1 males to their daughters Group 1 includes the first analysed females which brought the number of implants to or just beyond 50 implants Group 2 contains the remaining data from each male A few males never reached the limit 50 implants They are presented separately

Series	No of impl /male	No. of F_1 ♂♂	No of mated ♀♀	No of pregn ♀♀	Group 1			
					Dead		Impl	Per cent dead
					Early	Late		
Control								
	< 50	2	12	8				
	⩾ 50	73	928	784	278	35	3 955	7 91
150 rad								
	< 50	3	19	10				
	⩾ 50	92	1 198	1 040	358	49	4 993	8 15
250 rad								
	< 50	8	93	38				
	⩾ 50	84	1 047	902	342	65	4 564	8 92

Table 4

Data from chronic and acute irradiations with 250 rad

Series	No of impl /male	No of F_1 ♂♂	No of mated ♀♀	No of pregn ♀♀	Group 1			
					Dead		Impl	Per cent dead
					Early	Late		
Chronic								
	50	18	154	76				
	> 50	156	2 242	1 892	631	135	8 332	9 19
Acute								
	50	13	104	58				
	50	85	1 244	987	336	105	4 533	9 73

Among the F_1 males most strongly suspected of being lethal heterozygotes 7 were confirmed, while 2 were not These latter gave only 2 and 3 F_2 males respectively to examine The next lower significance class had 6 F_1 males tested of which 5 were confirmed Although 7 F_2 males from F_1 male No 138 were tested no confirmation was obtained

The F_1 males which deviated from the control with a degree of significance of 95 to 99 per cent had only 4 confirmed out of 11 This result agrees well with expectation

Finally it may be mentioned that among the 36 F_1 males which were further tested,

Table 3 (*cont*)

Group 2				Total		
Dead		Impl	Per cent dead	Dead		Impl
Early	Late			Early	Late	
				5	—	55
145	22	2 048	8 15	423	57	6 003
				4	—	51
209	34	3 130	7 76	567	83	8 123
				24	2	232
166	37	2 412	8 42	508	102	6 976

Table 4 (*cont*)

Group 2				Total		
Dead		Impl	Per cent dead	Dead		Impl
Early	Late			Early	Late	
				40	12	514
475	82	5 862	9 50	1 106	217	14 194
				25	3	386
245	36	2 757	10 19	581	141	7 290

10 were included which had not reached the significance level but still showed high rates of dead implants or excess of foetuses dying late in development Among these 2 were confirmed to carry lethals This is also in agreement with the expectation that up to about 1/3 of the lethal heterozygous F_1 males would fail to be detected

The presence of recessive lethals has thus been proved among the group called suspected lethals The data (Group 1 in Tables 3, 4) from the back-cross test may thus be used to calculate the rate of lethals

Test of allelism From the P males 4 F_1 males were taken as a mean If the P ge

Table 5

The number of dead from individual F_1 males, data from group I (Tables 3, 4)

Series	No of dead implants																				Total
	0	1	2	3	4	5	6	7	8	9	10	11	12	13	14	15	16	17	18	19	
Control		7	11	8	16	16	5	4	4		1						1				73
150 rad	2	5	7	16	16	26	10	3	1	2	4										92
250 rad, I		5	7	12	17	20	4	10	4	1	1		1	1	1						84
250 rad, II	1	4	11	4	17	14	11	10	5	3	2		1		1		1				85
Chronic	2	13	12	24	29	19	19	16	7	6	3		4	1							1 156

Table 6

Confirmation of suspected lethal heterozygous F_1 males by matings $F_2♂ \times F_2♀♀$ The F_1 males are arranged according to how strongly lethal heterozygosity was suspected The number of tested and confirmed F_2 males are given for individual F_1 males

F_1 No	F_2 males*		F_1 No	F_2 males**		F_1 No	F_2 males***	
	Tested	Conf		Tested	Conf		Tested	Conf
39	4	0	145	4	1	6	3	2
85	4	0	150	5	1	71	2	0
86	2	0				74	2	1
94	6	1				147	3	0
151	2	0				148	3	1
161	2	1						
174	6	0				149	7	2
308	5	0						
126	3	1	61	3	1	65	2	1
183	4	0	138	7	0	66	1	1
325	2	1	186	5	1	131	4	1
			199	7	1			

* $0.01 < p < 0.05$
** $0.001 < p < 0.01$
*** $p < 0.001$

neration carried a spontaneous lethal 2 or more sons could carry the same lethal When 2 F_1 brothers are suspected lethal heterozygotes it is consequently of interest to decide whether they ar allelic or not LÜNING (1969) pointed out that test of allelism was technically simple if sufficient females were available

Among the confirmed lethals 4 pairs of brothers from the chronic series were found of which 3 could be tested for allelism All three pairs turned out to be allelic Whether the same allele appeared in two or three groups of brothers could not be tested due to shortage of females

The origin of these three pairs of F_1 males may either be clusters of new mutations or some of the parents may have been carrying a preexisting (*spontaneous*) recessive lethal The probability of the former is, however, very low For that reason it was assumed that they represent *spontaneous mutations*.

Estimation of the rate of lethals It has thus been shown (1) that the rate of intra uterine death is slightly higher in back-cross tests of irradiated series than in controls (Tables 3, 4), (2) that several F_1 males giving high rates of intra uterine death had sons with similar excessive intra uterine death in their offspring (in mating with sisters) and thus confirms the suspected lethal heterozygosity in the F_1 males

From point 2 support may be found for the working hypothesis that the difference in point 1 is due to recessive lethals

In the control 2 suspected lethals were obtained of which one was further tested and confirmed and used in a test of dominance effects (LÜNING 1975 b) In the chronic series it was found from the allelism test that of 3 pairs of brothers that were suspected lethal heterozygotes all three turned out to be alleles inter se It is improbable that they should be induced mutations and it must be assumed that they were introduced from heterozygous parents and thus preexisting spontaneous mutations in the inbred strain This indicates that the chronic series may have included more spontaneous lethals than the control Thus comparison with the control to estimate the proportion of lethals in the experimental series may be fallacious The arguments by LÜNING (1975 a) when presenting the model may be pertinent It was stated that when 4 or less dead occurred among the first 50 implants in back-cross of F_1 males to their daughters those males could be considered lethal free Additional material from such males would give information about the rate of intra uterine death in lethal free males From data in group 1 (Tables 3, 4) lethal free males were selected and from them were taken data from group 2 In the present experiment 8 66 per cent (623/7 197) was obtained Over the last 8 years 14 experiments have been run resulting in ten corresponding data There was no detectable heterogenity and therefore these data were combined with the present data giving $8\,11 \pm 0\,18$ per cent (1 908/23 516) This figure agrees well with the 8 per cent used for the model

By using this figure for the 'normal rate of death the degree of inferiority in survival in the experimental series may be estimated

This method may also allow an estimation of the total proportion of recessive lethals (preexisting and new spontaneous + induced) The results are given in Table 7

Table 5 presents the distribution of F_1 males according to the number of dead among the first 50 implants and by comparison with the model the proportion of lethals may be estimated Assuming that the proportion of lethals is x and of lethal-free (l-x) the proportion expected to have for instance 8 or more dead may be estimated from the model The model gives the coefficients for an equation For the limit 8 it is $0\,066724(1-x) + 0\,760713x$ = observed proportion (Table 7)

The proportion of lethals in the chronic series is similar to that in the acute (Table

Table 7

From data in Group 1 (Tables 3, 4) the survival is compared with survival in lethal free. Each per cent decrease corresponds to 8 per cent lethals (A). The proportion of lethals in (B) is estimated from the distribution of lethals in Table 5

Series	A		B
	Ratio surviving irr / lethal free	Per cent lethals	Distribution per cent lethals
Control	1.0021	—	2.2
Acute 150 rad	0.9995	0.4	1.3
Acute 250 rad, I	0.9912	7.0	5.8
Acute 250 rad, II	0.9824	14.1	12.4
Chronic 250 rad	0.9882	9.4	10.7
Acute 250 rad (I + II)	0.9868	10.6	9.1
250 rad (Ac. I + II) + Chr	0.9875	10.0	9.9

7). The chronic series had 3 pairs of lethal-heterozygous brothers assumed to carry spontaneous mutations. Thus, there are no indications of an excessive proportion of lethals induced by chronic as compared to acute exposure.

Comparison of the data in Table 7 of 250 rad acute (I + II) versus chronic exposure does not indicate any difference in the distribution. All three series given 250 rad may thus be combined to estimate the proportion of lethals (see Table 7). The two different estimates on this larger material are fairly congruent. As they are the sum of spontaneous and induced mutations they give an overestimate of the mutagenic effectiveness of neutrons. However, the test performed did not allow a proper estimate of the spontaneous mutation rate. LUNING & SEARLE (1971) describe three control series with varying results. This is in fact what may be expected (LÜNING 1975 c). Data from further control experiments, using the same procedure, have allowed two estimates of the load of spontaneous mutations, i.e. 4.2 and 6.2 per cent, respectively. The former is in comparison to lethal free and the latter from the distribution of dead in the first 50 implants. These estimates are close to those given by LUNING & SEARLE. Using these means of spontaneous mutations as a correction factor an estimate of the induced mutation rate in the neutron test will lie around 5 to 6 per cent at 250 rad. This is about twice that estimated from acute roentgen radiation tests. The material does not allow more accurate calculations, and no further speculation has therefore been attempted.

Semisterility and sterility. Excessive intra-uterine death in offspring of F_1 males back-crossed to their daughters was used to detect recessive lethals. As semisterility will have similar, although more obvious, effects all F_1 males were, before the start

Table 8

The proportion of fertile, semisterile sterile and dead among the F_1 males

Series	Fertile		Semi sterile	Sterile	Dead
	< 50 impl	~ 50 impl			
I Control	2	73	—	4	1
Acute 150 rad	3	92	1	5	—
Acute 250 rad	8	84	1	5	—
II Chronic 250 rad	18	156	3	8	—
Acute 250 rad	13	85	1	3	—

of the back crossing, mated with females from the inbred CBA strain F_1 males with 30 per cent or more dead implants in these matings were mated with further CBA females to confirm suspected semisterility Thus semisterile males could be excluded from taking part in the further test

With this test information on the proportion of semisterile as well as of sterile males was obtained The figures for fertile, semisterile and sterile males appear in Table 8 The proportion of sterile animals was about the same in all series The number of semisteriles was low and did not indicate any difference between acute and chronic exposure

Discussion

The effect of 14 MeV neutrons on post meiotic cells measured as dominant lethals and on the peri and pre meiotic cells was analysed by examining the time required for males to regain fertility The test of dominant lethals could only be performed with acute exposure as the chronic exposure had made the males temporarily sterile Comparison of these results with those of RUSSELL indicate similar effects, viz. that the effects of 14 MeV neutrons are similar to those of roentgen radiation This is contrary to the results from neutrons with a spectrum of energies with a mean around 1 and 0 7 MeV indicating higher effectiveness (RUSSELL et coll 1954, SEARLE & PHILIPS 1964) The main interest concentrated on the comparison of acute and chronic exposure of spermatogonia, using recessive lethals and semisterility among F_1 males as criteria The results have in both cases pointed in the same direction, viz that no detectable difference existed between acute and chronic exposure to 14 MeV neutrons This result differs from that gained by SEARLE and his group in observations of specific locus mutations using neutrons with a mean of 0 7 MeV from the GLEEP reactor They found a manifold excess of effectiveness of chronic exposure The reason for these diverging results might be the use of neutrons with different energies On the other hand, RUSSELL using reactor neutrons with a mean energy of 1 MeV observed no difference between acute and chronic exposure

The three experiments differ in some crucial points besides the source and the energy of neutrons· In the present test the exposure called 'chronic' was in fact fractionated with a low dose rate (7 to 8 h/day, 5 days/week, 11 weeks) while RUSSELL and SEARLE administered nearly continuous irradiation with short interruptions for technical service The dose rate in RUSSELL's test was at lowest 0 17 rad/min while in SEARLE's it ranged from 0 0024 to 0 0014 rad/min (BATCHELOR et coll 1966) In our test the dose rate was 0 01 rad/min The total dose also differed, being in RUSSELL's test 63 rad, in SEARLE's 214 neutrons + 93 rad γ, and in the present test 250 rad including 10 to 12 per cent γ radiation From this it is evident that the total dose in the test of SEARLE and his group and in the present one are fairly similar

The main differences lie in the energy level and the dose rate, being a 4 to 6 times higher rate in the present test, and a fractional irradiation A comparison of RUSSELL's and SEARLE's data indicates a similar level of energy and mode of irradiation but difference in the dose, and a 70 to 120 times higher dose rate in RUSSELL's test

From these comparisons it appears that the dose rate, when comparing RUSSELL's and SEARLE's data, may be the possible cause of the different results In addition it is obvious from a comparison of the present data and SEARLE's experiments, that energy and therefore the LET also may be of great importance for the effect of chronic neutron exposure

The relation to dose rate, neutron energy and effect of fractionated versus chronic exposure were beyond the scope of the present projects The investigation has indicated, however, that the question of possible genetic hazards of chronic exposure to neutrons is extremely complex

II TECHNIQUE OF NEUTRON IRRADIATION

The neutron irradiation was performed at the 300 kV accelerator at the Research Institute of National Defence, Dept 4 The neutrons were produced by the D(T, n) ^{4}He reaction in adsorbed, water-cooled tritium targets at 160 kV The target thickness was infinite at the used voltage implying that neutrons were produced in an energy interval from 14 2 to 14 8 MeV The cross-section for the D(T, n) ^{4}He reaction has a marked resonance at 110 keV and by using the reaction cross-section, the kinematics of the reaction and the cross-section for the slowing down of the deutrons in the target the mean energy with its half-width could be calculated to be (14 5 $\pm$ 0 1) MeV

The ion beam was deflected with a magnet after the accelerator tube to eliminate other ions than the single charged deutrons This essentially increased the lifetimes of the targets but gave also a low background when determining the neutron flux by monitoring the ^{4}He-particles which are simultaneously produced with the neutrons

For the chronic irradiation the mice were kept in cages which were mounted in two rows along the circumference of a circle with a radius of 1 m Only angles smal-

ler than 90° were used, i e the cages occupied ±75° of the circumference The target and the cages with mice were situated 1 8 m above the concrete floor, hence the contribution from room scattered neutrons was small

For the acute exposures the irradiation conditions were not quite as good as in the chronic case The mice were contained in a cage with the form of a circular arc (270°) with an inner radius of 10 cm and an outer radius of 15 cm The target was at the centre of the cage This arrangement had two disadvantages Firstly, angles equal to and greater than 90° had to be used and for these angles neutron scattering in material surrounding the tritium target is greater than in the forward directions Secondly, the short distance between the cage and the target caused a spread of the neutron intensity across the cage Some of these disadvantages were probably eliminated by the movements of the mice during the irradiation However, the dose spread is given as estimated from geometrical and physical conditions

For the chronic exposure the dose rate was about 0 70 rad/h with the dose delivered for about two and a half months since no irradiations were made during weekends Because of the stability of the accelerator no operator had to keep a continuous watch An alarm system was used which indicated if the dose rate deviated with more than 10 per cent from the preset value and the neutron flux was then adjusted, which seldom happened The running schedule was followed with the exception of an interruption of one day (the third irradiation day) due to troubles with the ion source

Neutron dose measurement The dosimetry used in neutron irradiations is in general based on direct measurements of the absorbed dose, i e by measuring on the charged secondary particles (recoil protons, α particles etc) which are produced in the neutron interaction with tissue The commonly used detector is an *ionization chamber with its gas and walls* consisting of tissue equivalent material The reason for using this method is that many neutron sources (e g nuclear reactors) give neutrons with continuous energy spectra and in such cases other methods are not particularly reliable

In the present irradiation, however, it was preferred to measure the neutron flux, and the absorbed dose was then determined by the use of the transformation tables between neutron flux and absorbed dose This method gives reliable results for *mono-energetic* neutrons, furthermore any *discussion* about the dose determination could be based on a knowledge about the *neutron flux*

Neutron flux The neutron flux was determined in two ways

a) *Associated α particles counting* The Q value for the reaction D(T, n) ^{4}He is +17 6 MeV and this energy is shared between the neutron and the particle The energy of the ^{4}*He particle is* angle dependent and is 4 8 MeV in the forward direction and 2 7 MeV *in* the backward *direction* The ^{4}*He* particle was detected by a stilbene crystal, which was placed *in the* backward direction, 1 cm below the deutron

beam, and at a distance of 80 cm from the target The crystal with the dimensions 2 54 cm × 2 54 cm was enclosed in a foil which was equipped with a thin Al-window with an area of 0 81 cm² through which the ^{4}He-particles could pass without any considerable loss of energy The light output from the crystal was taken via a light pipe to a photomultiplier tube (AVP 56) After amplification the pulses in the ^{4}He peak were selected with a single channel analyzer and fed to fast scalers and also to a ratemeter The number of counts registered by the fast scaler for each irradiation day was used as a measure of the integrated neutron flux The pulse-height spectrum from the crystal and the position of the single channel analyzer window were frequently checked on a multichannel analyzer during all the runs

The neutron flux was calculated from the number of registered ^{4}He-particle counts, the solid angle of the detection area of the stilbene crystal and the angular distribution of the ^{4}He-particle as taken from FEWELL (1968) A total error of 10 per cent was estimated for this determination of the neutron flux

b) Neutron induced fission counting The neutron flux was also measured with two fission chambers containing ^{235}U and ^{238}U A good separation between pile-up of α particle pulses and fission pulses was obtained since the amount of fissile material was rather small (16 and 31 3 mg, respectively) The fission chambers were situated at different distances and angles from the target and the number of fission pulses was counted simultaneously as the pulses from the ^{4}He-detector system The neutron flux was calculated from the known amount of fissile material and the fission cross-sections of ^{235}U and ^{238}U The values for the fission cross-sections given in the evaluation by DAVEY (1966) averaged over the actual energy interval were used The error in the neutron flux determination was estimated to be 12 per cent

The neutron fluxes as determined from (a) and (b) agree within 10 per cent, i e within the estimated uncertainties The mean value of the two different determinations was used, allowing for an error of 8 per cent

Absorbed dose The transformation tables of BACH & CASWELL (1968) were used to obtain the absorbed dose from the measured neutron flux These tables make use of the nuclear cross sections for the different reactions occurring with neutrons around 14 5 MeV and the energies of the secondary particles The value 6.5×10^{-9} rad/n cm^{-2} was used for the first collision dose

The contribution of gamma rays to the absorbed dose was estimated from measurements with thermo-luminescent dosimeters The gamma-ray contribution was 10 to 12 per cent of the dose Corrections were also estimated for the dose contributions from thermal neutrons and for multiple scattering of the primary neutrons These corrections increased the first collision neutron dose by the order of 5 per cent

Radiation quality The radiation quality for 14 5 MeV neutrons is rather complex since several nuclear reactions contribute to the dose and each reaction gives a

radiation quality quite different from the others The main dose contribution, however, is due to the recoil protons and this contribution is about 70 per cent Compared with a reactor neutron spectrum the 14 5 MeV neutrons give rise to recoil protons with much higher energies and consequently lower LET values However, these 14 5 MeV neutrons also give rise to dense ionization tracks because of the neutron elastic collisions with O, N and C nuclei as well as tracks from (n, α) reactions A calculation of the track average LET distributions for different neutron spectra has been made by BEWLEY (1968) This calculation shows that for a reactor neutron spectrum the distribution of LET values are not too different from a Gaussian shape, but the 14 5 MeV neutrons give a distribution with low LET-values for the recoil protons but high LET-values for other secondary particles It is thus necessary to be careful if using a mean LET-value for the 14 5 MeV neutrons, since the LET distribution from these neutrons has two components which are very different

Acknowledgements

The authors are indebted to Mr L Eriksson and Mr I Lindgren who were responsible for the special constructions in the accelerator facility which were needed for the present irradiation They were also responsible for the drift running of the accelerator The two authors, K G Luning and W Sheridan, wish to express their gratitude for support from Statens Råd for Atomforskning

SUMMARY

Male CBA mice were exposed to 14 5 MeV neutron, either in an acute (150 or 250 rad) or a chronic dose (250 rad) and the genetic effects of the irradiations were compared No detectable difference in the rate of mutations existed between acute and chronic exposure, with these neutrons

ZUSAMMENFASSUNG

Mannliche CBA Mause wurden mit 14,5 MeV V Neutronen, entweder mit akuten Dosen (150 oder 250 rad) oder einer chronischen Dosis (250 rad) bestrahlt und die genetischen Effekte der Bestrahlung verglichen Es bestanden keine nachweisbaren Unterschiede in der Frequenz von Mutationen zwischen akuter und chronischer Bestrahlung mit den verwendeten Neutronen

RESUMÉ

Des souris males CBA ont eté exposées à des neutrons de 14,5 MeV, soit à une dose brève (150 ou 250 rad) soit à une dose prolongee (250 rad) et on a comparé les effets génétiques de ces irradiations On n a pas constaté de différence décelable sur le taux des mutations entre les expositions aigues et chroniques à ces neutrons

REFERENCES

BACH R L and CASWELL R S Energy transfer to matter by neutrons Radiat Res 35 (1968), 1

BATCHELOR A L, PHILLIPS R J S and SEARLE A G A comparison of the mutagenic effectiveness of chronic neutron- and γ irradiation of mouse spermatogonia Mutat Res 3 (1966), 218

BATEMAN A J Mutagenic sensitivity of mature germ cells in the male mouse Heredity 12 (1958), 213

BEWLEY D R Calculated LET distributions of fast neutrons Radiat Res 34 (1968) 437

DAVEY W G An analysis of the fission cross sections of ^{232}Th, ^{233}U, ^{234}U, ^{235}U, ^{236}U, ^{237}Np, ^{238}U, ^{239}Pu, ^{240}Pu, ^{241}Pu and ^{242}Pu from 1 keV to 10 MeV Nucl Sci Engn 26 (1966), 149

FEWELL T R An evaluation of the alpha counting technique for determining 14 MeV neutron yields Nucl Instr and Methods 61 (1968), 61

FRÖLÉN H The effect on the length of life in the offspring of X irradiated male mice Mutat Res 2 (1965), 287

LÜNING K G Dominant effects of recessive lethals in mice II Viability and mating ability Mutat Res 8 (1969), 573

— Testing for recessive lethals in mice Mutat Res 11 (1971), 125

— (a) Test of recessive lethals in the mouse Mutat Res 27 (1975) 357

— (b) Analysis of the dominance effect of a spontaneous recessive lethal in the mouse on homozygous and heterozygous genetic background Mutat Res 27 (1975), 257

— (c) Spontaneous recessive lethal mutations in the mouse Mutat Res 27 (1975) 367

— and SEARLE A G Estimates of the genetic risks from ionizing irradiation Mutat Res 12 (1971), 291

RUSSELL W L Studies in mammalian radiation genetics Nucleonics 23 (1965) 53

— RUSSELL L B and KIMBALL A W The relative effectiveness of neutrons from a nuclear detonation and from a cyclotron in inducing dominant lethals in the mouse Amer Nat 88 (1954), 269

SEARLE A G and PHILIPS R J S Genetic effects of neutron irradiation in mice *In* Biological effects of neutron and proton irradiations Edited by P I Smirnov Vol I IAEA, Vienna 1964, pp 361–370

FROM PETROV RESEARCH INSTITUTE OF ONCOLOGY, LENINGRAD 188646, USSR

LASER THERAPY OF HUMAN BENIGN AND MALIGNANT NEOPLASMS OF THE SKIN

R I WAGNER, A P KOZLOV, K G MOSKALIK, L M KHACHATURYAN and O L PERTSOV

The development of new methods for the treatment of tumours is one of the most urgent problems of oncology It is, therefore, natural that optical quantum generators which feature such useful properties as generation of highly monochromatic, coherent, precisely directed beams and, particularly, the enormous density of energy, should attract general attention as a possible means of therapy of malignant tumours Promising results of numerous experimental investigations (McGUFF 1966, GOLDMAN 1966, 1967, KAVETSKY et coll 1969, GAMALEYA 1972, KOZLOV et coll 1973) have suggested the application of laser radiation in oncologic clinic

This report deals with the results of laser therapy of human precancerous lesions, benign and malignant tumours of the skin

A powerful laser installation of the Pulsar 1000 type specially designed for oncologic therapy was used The installation comprises a solid neodymium-doped glass optical quantum generator It is provided with a light guide for focusing the beam on the exposed spot A light simulation system is supplied for visual checking on the beam setting Radiation wavelength 10 600 Å, maximum pulse energy 1 000 J, beam divergence angle not more than 12°, pulse duration 10^{-3} s, variation of beam diameter within 3 to 30 mm

Submitted for publication 16 October 1974

Table

Precancerous lesions and tumours of the skin treated by laser radiation

	Tumour size (larger diameter, cm)				
	up to 0 9	1–1 9	2–2 9	3 and more	Total
Papilloma	114	27	2	—	143
Keratoma, hyperkeratosis	7	3	—	—	10
Contagious mollusces	11	1	—	—	12
Angioma, angiofibroma, pyococcal granuloma	44	13	—	—	57
Epithelioma	3	1	2	2	8
Pigmented naevus	15	11	1	—	27
Basal cell carcinoma	45	24	5	—	74
Squamous cell carcinoma	1	—	1	—	2
Melanoblastoma	4	8	1	—	13
Metastatic melanoblastoma in the skin	59	—	—	—	59
Total	303	88	12	2	405

A total of 405 precancerous lesions and cutaneous tumours in 235 patients (157 women and 78 men, aged 15 to 80 years) has been treated, of these 257 were precancerous lesions and benign tumours and 148 malignant tumours Of the patients 230 were treated in an out patient clinic and 5 in hospital

The diagnoses and size of the lesion are given in the Table It appears that the majority of the lesions were epithelial neoplasms and that the size was less than 2 cm in diameter in most cases The lesions were distributed all over the body, i e head, neck, thorax, abdomen and extremities The 59 melanoblastoma metastases were encountered in 5 patients

Type of pathology was ascertained on the basis of clinical data, cytologic assay of imprints obtained from the ulcerated surface of the tumour and microscopy of biopsy material Morphologic confirmation of diagnosis was obtained in 70 per cent of cases

The precise measurement of the pulse density of radiation energy is essential in laser therapy, since it determines the depth and extent of tumour destruction The magnitude of energy density was selected for each individual case, the type of neoplasm, its area and height, consistence, pigmentation and localization being taken into consideration

Small, soft, highly pigmented and considerably vascularized neoplasms were exposed to beams of lower density A higher density of energy was used in the treatment of compact light-coloured tumours and those covered with thick keratin-layers In the therapy of precancerous lesions and benign tumours, the pulse density

of radiation energy varied within 200 to 450 J/cm², basal and squamous cell carcinomas 400 to 600 J/cm², melanoblastomas and their metastases in the skin 800 to 1 000 J/cm² As a rule, one exposure was sufficient in precancerous lesions and benign tumours Depending on the size, shape, thickness and localization, a malignant tumour was treated by 1 to 30 pulses The surrounding tissues were not exposed in the treatment of precancerous lesions and benign tumours

The treatment of malignant tumours started with an exposure of an 0 5 to 1 cm wide annular zone of normal tissue round the visible periphery of the tumour, then, the tumour itself was exposed This method serves to reduce the transport of neoplastic cells by the blood and lymphatic vessels and to prevent local recurrences In most cases, one exposure was sufficient but in large tumours it could be impossible to expose the entire neoplastic mass and, particularly, its deeper layers, and therefore several exposures were needed

The irradiation was usually slightly painful but in some cases there were no complaints at all The exposure of the tumour was less painful than that of the surrounding normal tissues Since pain was not acute, therapy was conducted without local anesthesia

The laser irradiation causes destruction of tumour and normal tissues, followed by the development of a coagulation necrosis The necrotic area is generally 1 to 2 mm wider than the light spot diameter The epidermis peels off around the necrotic area After the crust has fallen off, a granulating surface is revealed which, gradually, becomes covered with epithelium within the following 2 to 5 weeks A pink soft scar remains on the tumour site, which subsequently obtains the colour of the skin When necrosis does not develop, the granulating surface is covered with epithelium without scarring Wounds always heal without suppuration, no untoward side-effects, either general or local, have been observed

All patients have been regularly examined during 2 to 30 months after therapy There have been two cases of recurrence—in patients with cutaneous papillomatosis and a pigmented naevus on the skin of the abdominal wall six and eight weeks after treatment, respectively These relapses are thought to have been due to inadequate treatment (failure to expose the entire mass of tumour), which was inevitable at the initial stages of laser therapy No recurrences of carcinoma or melanoblastoma of the skin have been observed

Some illustrative cases may be reported

Case 1 Female, aged 65, with a dark brown mole 0 5 cm in diameter in the frontonasal region. The mole began to grow and converted to an 18 mm × 15 mm × 13 mm partially ulcerated node within 6 months before the treatment The diagnosis of melanoblastoma was

patient has been kept under observation for 22 months A pink soft scar is slightly visible on the tumour site (Fig. 1)

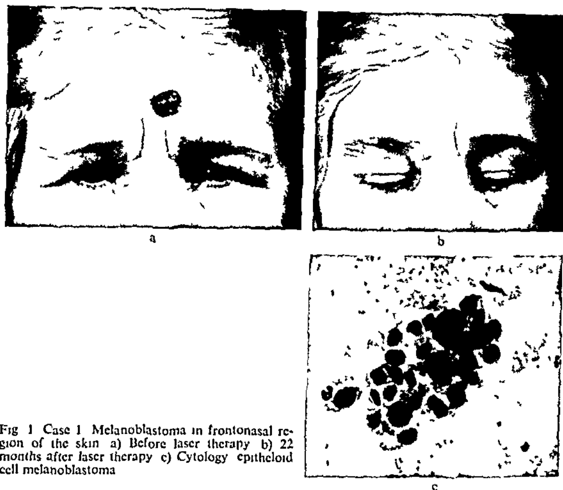


Fig 1 Case 1 Melanoblastoma in frontonasal region of the skin a) Before laser therapy b) 22 months after laser therapy c) Cytology epitheloid cell melanoblastoma

Case 2 Male, aged 53, with a black patch 1 cm in diameter on the skin of the bregma for 15 years Two years before the treatment, it gradually increased in size to 1 5 cm in diameter and became lighter in colour Within the last months, it ulcerated, bled, and a brown tumour node measuring 0 6 cm × 0 4 cm × 0 1 cm appeared on its surface The diagnosis melanoblastoma was confirmed by cytology of the imprints from the ulcerated surface of the tumour The melanoblastoma and a 1 cm wide annular zone of the surrounding normal tissues were exposed to 16 pulses in one session, energy density 800 to 1 000 J/cm² The patient has been observed for 1 year A pink soft scar is hardly visible on the tumour site (Fig 2)

Thus, the results of laser irradiation of human precancerous lesions and neoplasms of the skin should be considered useful and the cosmetic effect quite satisfactory

Similarly good results of laser therapy of human skin tumours are reported by others (GOLDMAN et coll 1964, HELSPER et coll 1964, MCGUFF 1966, MCGUFF et coll 1966, PARSONS et coll 1968, LAGUNOVA et coll 1971, LAZAREV *et coll* 1971, WAGNER et *coll* 1974)

However, small cutaneous neoplasms only, lend themselves easily to laser therapy The extension of the tumour must not exceed 2 0 to 2 5 cm With larger lesions, its application is not advisable, because of rough scarring

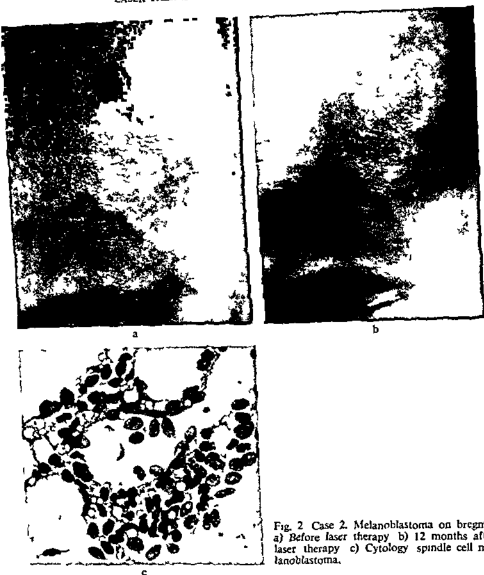


Fig. 2 Case 2. Melanoblastoma on bregma. a) Before laser therapy b) 12 months after laser therapy c) Cytology spindle cell melanoblastoma.

One of the components of a successful las~r therapy of human cutaneous tumours is to ensure that the whole mass of tumour is exposed both its entire surface area and all deeper layers To prevent local recurrences, the treatment should begin with an exposure of an annular zone of normal tissue round the lesion and thereafter, the tumour its~lf

It should be pointed out that laser therapy offers some advantages as compared with other methods of skin tumour treatment Laser therapy is conducted, as a rule, in out patient clinic, in one session, and does not require local anesthesia The pro

cedure does not take long time The wound heals quickly, without being infected Laser radiation does not exert any deleterious effect on the organism On the contrary, some authors point out that a laser beam may stimulate, to a certain degree, the protective response of the organism and, hence, accelerate regenerative processes (KAVETSKY et coll 1969, KORYTNY & ZAZULEVSKAYA 1971, MOSKALIK et coll 1974)

The results gained suggest that the radiation of the neodymium pulsed laser may be effectively used *not only in the therapy of human precancerous lesions and benign* tumours of the skin but also, in principle, in the therapy of cutaneous carcinoma and melanoblastoma

SUMMARY

Radiation of a powerful neodymium doped glass pulsed laser, Pulsar-1000 type, has been used for therapy of 235 patients with a total of 257 precancerous lesions and benign tumours, 76 basal and squamous cell carcinomas, 13 melanoblastomas and 59 metastatic melanoblastomas in the skin Energy density used in the treatment of precancerous lesions and benign tumours was 200–450 J/cm², in basal and squamous cell carcinomas 400–500 J/cm², in melanoblastomas and their skin metastases 800–1 000 J/cm² The results have been satisfactory

ZUSAMMENFASSUNG

Die Strahlung eines kraftigen, aus Neodymium Glas hergestellten Puls Lasers, Pulsar-1000 Typ, wurde zur Therapie von 235 Patienten mit zusammen 257 prakanzerosen Veranderungen und benignen Tumoren, 76 Basal und Schuppenzellkarzinomen, 13 Melanoblastomen und 59 metastatischen Melanoblastomen der Haut verwendet Die bei der Behandlung verwendete Energiedichte betrug fur die benignen Tumoren 200 bis 450 J/cm², *für die Basal- und Schuppenzellkarzinonome 400 bis 500 J/cm² und fur die Melanoblastome* und deren Haut Metastasen 800 bis 1 000 J/cm² Die Ergebnisse waren zufriedenstellend

RÉSUMÉ

La radiation d un puissant laser pulsé en verre dopé au néodyme du type Pulsar 1 000, a été utilisée pour le traitement de 235 malades présentant un total de 257 lésions pré cancéreuses et de tumeurs bénignes, 76 carcinomes baso cellulaires et à cellules épidermoïdes, 13 mélanoblastomes et 59 mélanoblastomes métastatiques dans la peau La den sité d énergie utilisée dans le traitement des lésions pré cancéreuses et tumeurs bénignes était de 200–450 J/cm², dans les carcinomes baso cellulaires et à cellules épidermoïdes 400–500 J/cm², dans les mélanoblastomes et leurs métastases cutanées 800–1 000 J/cm² Les résultats ont été *satisfaisants*

REFERENCES

GAMALEYA N Lasers in experiments and clinic (In Russian) Medizina, Moscow 1972
GOLDMAN L Laser cancer research Springer Verlag, Berlin, Heidelberg, New York 1966
— Biomedical aspects of the laser *Springer Verlag, New York 1967*

— IGELMAN J and RICHFIELD D Impact of the laser on nevi and melanomas Arch Derm. 90 (1964) 71
HELSPER J, SHARP G, WILLIAMS H and FESTER W The biological effect of laser energy on human melanoma. Cancer 17 (1964), 1299
KAVETSKY R, TCHUDAKOV V, SIDORIK E, GAMALEYA N and KOGUT T Lasers in biology and medicine (In Russian) Zdorovye, Kiev 1969
KOZLOV A, MOSKALIK K and AKIMOV A On the influence of the pulse energy and irradiation rhythm on the antitumor effect of laser radiation (In Russian.) Vop Onkol 6 (1972), 65
— AKIMOV A., MOSKALIK K and PERTSOV O Antitumour effect of laser radiation. Acta radiol Ther Phys Biol 12 (1973), 241
KORYTNY D and ZAZULEVSKAYA L. Stimulation of phagocytosis by local radiation of laser beams (In Russian) *In* All Union Symposium on Biological and Oncolytic Effect of Laser, p 35 Moscow 1971
LAGUNOVA L, VICHNEVSKY A, LIHOVETSKYA L, ROSENFELD E and RAZIGRIN B On the possibility of treating the melanoma metastasis by laser radiation (In Russian) Ehsp Khir Anestez. 5 (1971), 50
LAZAREV I, POLISHTSHUK E, ALPATYEVA S, BARATOV H, ISAKOV V and POPOV YA Application of laser radiation in oncological clinic *In*. All Union Symposium on Biological and antitumour effect of laser radiation, p 39 Moscow 1971
MCGUFF P (a) Surgical application of laser Springfield, Boston 1966
— (b). Laser radiation for basal cell carcinoma. Dermatologica 133 (1966), 379
— DETERLING R. and GOTTLIEB L. Laser radiation for metastatic malignant melanoma J Amer med Ass 195 (1966), 393
MOSKALIK K, SKACHOV A and ILCHENKO A The effect of laser radiation on some characteristics of responsiveness of laboratory animals with tumours (In Russian) Patologicheskaya Physiologia i experimentalnaya therapia 1 (1974), 76
PARSONS R, CAMPBELL J and THOMLEY M Carcinoma of the penis treated by the ruby laser J Urol 100 (1968), 38
WAGNER R., KOZLOV A., MOSKALIK K. and KHACHATURYAN L On the therapy of precancerous lesions and tumours of the skin by laser Pulsar 1000 radiation (In Russian.) Vop Onkol 4 (1974) 11

FROM THE SECTION OF PREVENTIVE MEDICINE, COUNTY COUNCIL, THE DEPARTMENTS OF RADIATION THERAPY AND DIAGNOSTIC RADIOLOGY, CENTRALLASARETTET, S-801 30 GÄVLE, AND RADIUMHEMMET, KAROLINSKA SJUKHUSET, S-104 01 STOCKHOLM, SWEDEN

MASS-SCREENING OF A FEMALE POPULATION FOR DETECTION OF EARLY CARCINOMA OF THE BREAST

S JAKOBSSON, B LUNDGREN, O MELANDER and T NORIN

The size of a malignant tumour of the breast and the presence of axillary nodal involvement are highly correlated to prognosis (BLOOM *1965*, FISCHER et *coll 1969*, RENNAES 1970) A correlation between tumour size and nodal metastases also exists Tumours with more than 10 mm diameter are from a biologic point of view to be regarded as large When smaller they are difficult, if not impossible to palpate unless they are localized adjacent to the skin

As there is no absolute correlation between tumour size and tumour age, the term 'early mammary carcinoma' should be replaced by the term 'preclinical and presymptomatic carcinoma', defined as a clinically occult malignancy without symptoms Malignant tumours at that stage must by definition be detected by technical means

Most reports on thermography in breast screening deal with populations of a selective bias in one way or another (DAVEY et coll 1970, FURNIVAL et coll 1970, HOFFMAN 1967, ISARD et coll 1969, LILIENFIELD et coll 1969, NATHAN et coll 1972, SHAWE 1969, STRAX 1971) Opinions on thermography as a screening instrument differ, but the method is mostly recommended for use only in combination with clinical examination and mammary radiography (BERNETT et coll 1970, FURNIVAL et coll , GERSHON-COHEN 1970, HOFFMAN, LILIENFIELD et coll , SHAWE)

Submitted for publication *13 August 1974*

Table 1

Women invited to and participating in general health screening

Age groups	Number invited	Participating number	Per cent
35–39	1 041	918	88
40–44	1 278	1 148	90
45–49	1 452	1 254	86
50–54	1 317	1 151	87
55–59	1 214	1 044	86
60–64	1 181	976	83
65–69	1 019	753	74
70–74	858	555	65
75–	1 102	368	33
Total	10 462	8 167	78

The present investigation is part of a research project concerning evaluation of multiphasic screening performed in the city of Gavle, under auspices of the National Board of Health and Welfare and the County Council The screening programme includes urine tests, blood-chemical and haematologic analyses, a comparison of several ECG methods with automated evaluation, Odelca chest radiography with heart size measurement included, and breast tumour screening by thermography and a questionnaire

The aim of the breast programme was to test whether it is possible to detect presymptomatic malignant tumours, using a questionnaire and thermography as screening methods Women selected by these means were referred to a thorough examination comprising mammary radiography and clinical examination All routines were adapted for automated data processing

Material The material comprised those who at the beginning of August 1969 were domiciled in one of the two parishes in the city and were born 1944 or earlier, in all 24 171 subjects Breast examination was offered all women 35 years of age and older, altogether 10 462 women (Table 1) This report concerns only results of the first screening period from October 1969 to October 1970

Methods

Screening A self administered questionnaire with 24 questions and an information folder with instructions on self examination were distributed to all subjects Women answering 'yes' to one or more of the following three questions were selected to the secondary examination (1) Previous treatment for breast tumour, (2) detection

Table 2

Mammary carcinoma found at secondary examination
The rate given is per thousand subjects examined

Age groups	Abnormal group		Control group	
	Number	Rate	Number	Rate
35–44	4	6 7	0	0
45-64	18	13 6	2	5 2
65–	12	29 3	0	0
Total	34	14 6	2	2 3

of a lump, not varying in size with the menstrual cycle, or (3) dark discharge from the nipple The technical equipment for thermography were AGA (Thermovision) and Bofors IR-Camera Grey-tone thermograms, 11 per subject, were recorded by technical assistants with limited previous medical experience The thermograms were later examined by an experienced radiologist, who also had access to questionnaire Subjects with abnormal thermograms and a control group of women with normal thermograms were selected to the secondary examination

Secondary examination The roentgen unit was a Senographe made by CGR, the film used was Kodak's Industrex C, developed in a Pakorol unit with a 9 minute turn-over time Three views of each breast were obtained—cranio caudal, medially oblique and lateral When necessary, additional views were taken The radiation dose to the skin with this procedure was measured to 2 rad per exposure

Clinical examination (inspection and palpation) was performed with the subjects sitting as well as lying down Fine-needle aspiration biopsy (FRANZEN & ZAJICEK 1968) was performed in cases of possible malignancy

At the time of the examination neither the radiologist nor the clinical examiner (an oncologist) had access to any information about the subject, except name and date of birth Palpation was not performed by the radiologist

Reports on mammary radiography and clinical examination, as well as on thermography, were made separately and independently, and were recorded as follows, with one digit for each breast

(1) Normal, (2) *borderline abnormal, considered benign,* (3) *borderline abnormal,* possibly malignant, (4) abnormal, probably malignant, and (5) abnormal, typical carcinoma

The code 1–5 would thus signify 'normal right breast, carcinoma in the left' It was not possible to use this classification method in the evaluation of the thermography The intention was to select only subjects coded 3 and higher, but many belonging to group 2 were regarded as borderline, possibly malignant, and therefore also selected

Table 3

Clinical staging

Stage	No cases	
T0N0M0		14
T1N0M0	7	
T2N0M0	4	13
T3N0M0	2	
T2N1M0	3	
T3N1M0	3	7
T2N1M1	1	

In cases of probable carcinoma, patients were referred to the local surgical clinic for biopsy, when positive cytology, curative treatment was started immediately

Among those who passed the secondary examination (selected at the screening), 614 subjects were taken under further close surveillance Assigned to this group were those with code 3–5 at thermography, with code 3 or 4 at mammary radiography and code 3 or 4 at clinical examination

Only two cases with code 5 at mammary radiography were found to have benign tumours after surgical biopsy Clinical examination had no false code 5

Results

In the screening participated 8 167 women, or 78 per cent of all invited From this group, 2 331 subjects were selected to the secondary examination At this stage 172 women refused, i e 2 159 were actually examined The control group selected among 5 836 subjects with normal screening reports comprised 876 invited, of which 844 were examined

On secondary examination 34 cases of malignancy were detected in the abnormal group (Table 2) and two cases among the controls The difference in carcinoma prevalence between selected and controls is statistically significant ($p<0\ 01$) Table 3 demonstrates the tumours classified according to the TNM-system (American Joint Committee 1962) Of the 34 carcinoma cases, 27 had no clinical signs of nodal metastases Fourteen malignant tumours were detected with mammary radiography, 4 at clinical examination and 15 at both modalities By mistake one case was not examined by mammary radiography In 7 cases the history alone was sufficient for selection, 4 of these also had abnormal thermograms Objective signs of tumours were observed by the technical assistants in 2 cases with abnormal thermograms, 25 cases were selected because of abnormal thermograms only However, 8 of them had abnormal thermograms of one breast, whereas their tumours were detected in the other which was without thermographic abnormalities

Of the 34 carcinoma cases with an average age of 58 years, 14 were both preclinical and presymptomatic and detected at mammary radiography only. The average age of these 14 women was 64 years Presymptomatic tumours were clinically detected in 15 other subjects with an average age of 56 years Only 5 women were symptomatic with clinically detectable tumours The average age of these 5 was 52 years

During the first year after the screening, a further 19 cases of carcinoma were detected in the target population, 6 of them appeared among women with abnormal screening reports, 13 among those with normal reports

Discussion

When trying to compare evaluations of the accuracy of different screening methods, it is difficult to explain the varying results One reason for such inconsistencies might be that populations examined are not clearly defined, nor the criteria used for classifying a finding as positive or negative Comparisons would be greatly simplified if some general categories of populations could be accepted (1) Patients with clinically evident malignancy, (2) patients with vague breast complaints but without clinical signs of malignant tumour as well as patients in medical care for other reasons than breast complaints, and (3) non selected populations participating in screening programmes

The inexact and not clearly defined meaning of words like 'preclinical', 'occult', etc also makes comparisons of different reports difficult This also applies to mammary radiography and thermography where results are highly dependent on a multitude of technical factors, i e equipment, exposure data, film and developing process Even more difficult is to standardize positioning and compression techniques A final influence has the ability and experience of the examiners The clinical examinations of the present material were performed by three oncologists with long experience All radiologic films were analysed by the same radiologist, who, though with several years of general roentgenologic experience, might be considered as inexperienced in mammary radiography at the beginning of the project Thermograms were interpreted by a radiologist with several years of experience in that field The screened population was a selected one only with respect to age, and covers all social strata typical for a medium-sized Swedish city

In this material no more than 2 per cent of those who participated in the primary examination had abnormal breast history, which corresponds to 6 per cent of all selected subjects Two thirds of these had been previously treated for carcinoma of the breast Among women with an abnormal history, 8 cases of carcinoma were found of which two had no symptoms at the time of screening, but were selected because of their previous breast tumour Thus less than one fifth of the patients with malignancies had symptoms before detection Self-examination can without doubt be ruled out as a useful means towards early detection Concerning early detection this

Table 4

Temperature differences of 1°C or more between corresponding areas in the two breasts, abnormal heat areas, irregular vessels and hot spot appearing among malignant cases and among randomly selected women

	No	Drop outs %	Temperature differences		Abnormal heat area %	Irregular vessels %	Hot spot %
			Coldest areas %	Warmest areas %			
Abnormal group	232	6	14	22	40	78	19
Normal group	583	0	2	3	1	35	1
Malignant cases	34	0	6	21	47	56	27

statement is also valid for clinical examination On the other hand, clinical examination seems to pick up some tumours missed by mammary radiography and thermography

The following criteria were considered as potentially important for the diagnosis of carcinoma of the breast with thermography (BOURJAT & GAUTHERIE 1972, GERSHON-COHEN et coll 1970, JONES 1969) (1) Temperature differences between corresponding areas in the two breasts, (2) irregular vessels, (3) abnormal heat regions, and (4) hot spot

Of special interest are temperature differences because of their possible use in automatic screening of malignant breast tumours Efforts were made to assess the validity of these criteria by analysing their frequency in random samples of subjects without malignancy in one normal group and one abnormal group and in carcinoma cases (Table 4)

A difference in temperature between coldest areas, considered to be of much more importance than that between warmest areas, occurred more frequently among abnormal subjects without malignancies than among those with carcinoma Considering that only 2 out of 34 subjects with malignant tumour had a temperature difference of 1°C or more between the coldest areas, a simple measurement of the temperature would not seem to be useful as a criterion for automatic screening Irregular vessels in at least one breast appeared in 78 per cent of the abnormal group and in 19 of the 34 breasts with malignancy (56 per cent) Regarding the other criteria no difference could be found between their occurrence among selected subjects with and without malignancy

Thermography is not a fast screening method Peak examination capacity was 320 women per day with two cameras running for eight hours Four assistants were at work three days a week with the cameras, the other two days one of them was needed for sorting of films and records Mean unit capacity per week was 180 examinations However, the limiting factor in routine screening is the interpretation

capacity, to which examination capacity must be adapted The experience is that about 60 to 70 examinations a day is hard work even for a very experienced interpreter

A high selection rate at thermographic screening is reported in literature (DOWDY et coll 1971, GERSHON-COHEN, ISARD et coll NATHAN et coll) In the present material 29 per cent of the population were selected by thermography or a positive history This rate is high in a screening procedure and calls for a very expensive follow-up organisation Another drawback is that women react with apprehension and anxiety to being selected The invitation letter to the secondary examination, though carefully worded, often made the receiver feel certain that she had a malignant tumour This was right only in 1 5 per cent of all cases Fear was in fact not unusual even when subjects were recalled to examination, though they were clearly told that the reason was technical, for instance a film accident in the development procedure Reactions of this kind must be taken into account when a method with a high selection rate is considered

The eight carcinoma cases found in the 'wrong' breast are also considered as a negative factor Because of the high selection rate, the low examination and interpretation capacity and the generally vague diagnostic criteria, the conclusion is that thermography is not a suitable method for breast screening, at least not in the present stage of development

In accordance with previously published works, the present investigation has shown that early diagnosis is possible by technical means On the other hand, it will take many years before a final evaluation can be made There is still no definitive evidence for the hypothesis that breast screening has an influence on mortality Evidence to that effect has in fact only recently begun to appear for other screening programmes that have been in action for many years, for instance regarding carcinoma of the uterine cervix

Conclusions

The definition 'early carcinoma of the breast' should be a 'clinically occult tumour with no symptoms' which calls for detection by technical means The opinions on thermography as a screening instrument are inconsistent In the Swedish screening trial, questionnaire and thermography were used for selection to a secondary examination with mammary radiography, clinical examination and in some cases thin-needle aspiration biopsy, 8 167 women were screened In spite of having achieved early detection in many cases, and a statistically significant enrichment of malignant cases in the selected group when compared to controls, thermography was found to have considerable disadvantages as a screening method because of high selection rate and a low interpretation capacity, which makes the total screening procedure expensive

Acknowledgements

The Gavle study is being carried out by Gavleborg County Council and the National Board of Health and Welfare, Sweden The project is supervised by Gunnar Malmstrom,

National Board of Health and Welfare and by Åke Sjostrom, director of the Statistical Division, National Board of Health and Welfare, Sweden The investigation has been supervised by Professor Jerzy Einhorn Radiumhemmet, Karolinska Sjukhuset, Stockholm

SUMMARY

In 1969–1970 a breast mass screening was undertaken in Gavle, with thermography and questionnaire Mammary radiography and clinical examination of subjects with abnormal screening reports and of a group of normal subjects were performed In spite of having achieved early detection of malignant tumours in many cases with a preponderance of carcinoma cases in the abnormal group, thermography was found to have considerable drawbacks as a screening method

ZUSAMMENFASSUNG

Wahrend der Jahre 1969–1970 wurde ein Brust Massen Screening in Gavle mit Thermographie und Befragung durchgefuhrt Rontgenuntersuchung der Brust und klinische Untersuchung von Personen mit anomalen Screening Rapporten und einer Gruppe normaler Personen wurden vorgenommen Obwohl in vielen Fallen mit einem Überwiegen von Karzinom Fallen in der anomalen Gruppe eine fruhzeitige Entdeckung von malignen Tumoren erreicht wurde zeigte sich, dass die Thermographie wesentliche Nachteile als Screening Methode hat

RÉSUME

En 1969 1970, les auteurs ont entrepris à Gavle, un dépistage systematique de tumeurs du sein par la thermographie et par un questionnaire Ils ont fait aussi une radiographie mammaire et un examen clinique aux femmes présentant des anomalies au dépistage et à un groupe de femmes normales Bien que la thermographie ait permis la detection précoce de tumeurs malignes dans de nombreux cas, avec une préponderance de cas de cancer dans le groupe anormal elle présente des inconvenients considérables comme méthode de dépistage

RÉFÉRENCES

American Joint Committee Clinical Staging System for Cancer of the Breast (1962)

BERNETT P, VAILLANT W und FISCHER T Fruherkennung des Brustkrebses Langenbecks Arch klin Chir 327 (1970) 1217

BLOOM H J G The influence of delay on the natural history and prognosis of breast cancer Brit J Cancer 19 (1965), 228

BOURJAT P und GAUTHERIE M Thermographie der Mammakarzinome Electromedizin 1 (1972) 17

... or cancer worth while? ... J 3 (1970), 696

... H, BARKER W F, LAGASSE L. D, SPERLING L, ZELDIS L J and LONGMIRE W P Jr Mammography as a *screening* method for the examination of large populations Cancer 28 (1971), 1558

FISCHER B, SLACK N H and BROSS I D J Cancer of the breast Size of neoplasm and prognosis Cancer 24 (1969), 1071

FRANZÉN S and ZAJICEK J Aspiration biopsy in diagnosis of palpable lesions of the breast Acta radiol Ther Phys Biol 7 (1968), 241

FURNIVAL I G, STEWART H J, WEDDELL J M, DOVEY P, GRAVELLE J H, EVANS K T and FORREST A P M Accuracy of screening methods for the diagnosis of breast disease Brit med J 4 (1970), 461

GERSHON COHEN J Breast cancer Roles of mammography and thermography Industr Med Surg 39 (1970), 330

— HERMEL M B and MURDOCK M G Thermography in detection of early breast cancer Cancer 26 (1970), 1153

HOFFMAN R L Thermography in the detection of breast malignancy Amer J Obstet Gynec 98 (1967), 681

ISARD H J, OSTRUM B J and SHILO R Thermography in breast carcinoma Surg Gynec Obstet 128 (1969), 1289

JONES C H Interpretation problems in thermography of the female breast Bibl radiol 5 (1969), 96

LILIENFIELD A M, BARNES J M, BARNES R B, BRASFIELD R, CONNELL J F, DIAMOND E, GERSHON COHEN J, HABERMAN J, ISARD H J, LANE W Z, LATTES R, MILLER J SEAMAN W and SHERMAN R An evaluation of thermography in the detection of breast cancer Cancer 24 (1969), 1206

NATHAN B E, IAN BURN J and MACERLEAN D P Value of mammary thermography in differential diagnosis Br med J 2 (1972), 316

PRINCE J L Screening for breast cancer Lancet 2 (1970), 927

RENNAES S Cancer of the breast in women Acta chir scand Suppl 266 (1970)

SHAWE G D H Experience with thermography in the mass screening of breast tumors Bibl radiol 5 (1969), 109

STRAX P New techniques in mass screening for breast cancer Cancer 28 (1971) 1563

FROM THE DEPARTMENT OF RADIATION THERAPY (DIRECTOR PROF G NOTTER) SAHLGRENSKA SJUKHUSET, S 413 45 GOTHENBURG, SWEDEN

HORMONAL TREATMENT OF MAMMARY CARCINOMA WITH PROGYNON-DEPOT AND DEPOSTAT

G NOTTER and G BERNDT

In patients with carcinoma of the breast objective regression of the primary tumour and metastases may be achieved by hormonal treatment in about 30 to 40 per cent of the cases The efficiency of hormonal treatment varies for different hormones according to the age of the patient, the presence of specific hormone receptors in the breast tissue, the type and dissemination of the tumour and to the previous treatment Androgens usually are less effective and have more side effects than oestrogens (Breast Cancer Group 1961, 1962, 1964, Report to the Council on Drugs 1960), anabolic steroids (NOWAKOWSKI 1967, KENNEDY & YARBRO 1968), cortisone (LEMON 1959, VAN GILSE 1962) and gestagens (GOLDENBERG 1959, CROWLEY & MCDONALD 1962 COLSKY et coll 1963, CURWEN 1963, 1964, JONES 1970, BERNDT & STENDER 1970) have also been used with comparable clinical efficiency

The first experiences with combined oestrogen progesterone treatment in experimental carcinoma of the breast in rats were published by HUGGINS et coll (1962) These hormones have been used since in humans (CROWLEY & MCDONALD 1962, 1965)

Combined treatment with oestradiolvalerianate (Progynon Depot) and 17 α-hydroxy-19 norprogesteroncapronate (Depostat) were used previously and objective

Submitted for publication 25 September 1974

FISCHER B, SLACK N H and BROSS I D J Cancer of the breast Size of neoplasm and prognosis Cancer 24 (1969), 1071

FRANZÉN S and ZAJICEK J Aspiration biopsy in diagnosis of palpable lesions of the breast Acta radiol Ther Phys Biol 7 (1968), 241

FURNIVAL I G, STEWART H J, WEDDELL J M, DOVEY P, GRAVELLE J H, EVANS K T and FORREST A P M Accuracy of screening methods for the diagnosis of breast disease Brit med J 4 (1970), 461

GERSHON COHEN J Breast cancer Roles of mammography and thermography Industr Med Surg 39 (1970), 330

— HERMEL M B and MURDOCK M G Thermography in detection of early breast cancer Cancer 26 (1970), 1153

HOFFMAN R L Thermography in the detection of breast malignancy Amer J Obstet Gynec 98 (1967), 681

ISARD H J, OSTRUM B J and SHILO R Thermography in breast carcinoma Surg Gynec Obstet 128 (1969), 1289

JONES C H Interpretation problems in thermography of the female breast Bibl radiol 5 (1969), 96

LILIENFIELD A M, BARNES J M, BARNES R B, BRASFIELD R, CONNELL J F, DIAMOND E, GERSHON COHEN J, HABERMAN J, ISARD H J, LANE W Z, LATTES R, MILLER J, SEAMAN W and SHERMAN R An evaluation of thermography in the detection of breast cancer Cancer 24 (1969), 1206

NATHAN B E, IAN BURN J and MACERLEAN D P Value of mammary thermography in differential diagnosis Br med J 2 (1972), 316

PRINCE J L Screening for breast cancer Lancet 2 (1970), 927

RENNAES S Cancer of the breast in women Acta chir scand Suppl 266 (1970)

SHAWE G D H Experience with thermography in the mass screening of breast tumors Bibl radiol 5 (1969), 109

STRAX P New techniques in mass screening for breast cancer Cancer 28 (1971), 1563

FROM THE DEPARTMENT OF RADIATION THERAPY (DIRECTOR PROF G NOTTER) SAHLGRENSKA SJUKHUSET, S-413 45 GOTHENBURG, SWEDEN

HORMONAL TREATMENT OF MAMMARY CARCINOMA WITH PROGYNON-DEPOT AND DEPOSTAT

G NOTTER and G BERNDT

In patients with carcinoma of the breast objective regression of the primary tumour and metastases may be achieved by hormonal treatment in about 30 to 40 per cent of the cases The efficiency of hormonal treatment varies for different hormones according to the age of the patient, the presence of specific hormone receptors in the breast tissue, the type and dissemination of the tumour and to the previous treatment Androgens usually are less effective and have more side effects than oestrogens (Breast Cancer Group 1961, 1962, 1964, Report to the Council on Drugs 1960), anabolic steroids (NOWAKOWSKI 1967, KENNEDY & YARBRO 1968), cortisone (LEMON 1959, VAN GILSE 1962) and gestagens (GOLDENBERG 1959, CROWLEY & MCDONALD 1962, COLSKY et coll 1963, CURWEN 1963, 1964 JONES 1970, BERNDT & STENDER 1970) have also been used with comparable clinical efficiency

The first experiences with combined oestrogen progesterone treatment in experimental carcinoma of the breast in rats were published by HUGGINS et coll (1962) These hormones have been used since in humans (CROWLEY & MCDONALD 1962, 1965).

Combined treatment with oestradiolvalerianate (Progynon Depot) and 17 α hydroxy 19 norprogesteroncapronate (Depostat) were used previously and objective

---

Submitted for publication 25 September 1974

Table I

Effect of SH 834 in 117 patients with 171 metastases at different sites Remission rate 48/117 (41 %)

Site of metastases	Incidence of metastases	SH 834-effect	
		Remissions	Failures
Lung	34	16	18
Pleura	22	12	10
Liver	14	1*	13
Bone	57	15	42
Soft tissue	44	22	22

* Liver scan and liver function test, no microscopy

regression was observed in more than 40 per cent of the patients (NOTTER & KAIGAS 1966, BERNDT & STENDER 1970)

The present report summarises further experiences

Material

Between April 1966 and July 1974, 157 patients with microscopically verified inoperable or disseminated carcinoma of the breast were treated by intramuscular injections of a mixture of 90 mg oestradiolvalerianate and 300 mg 17-α-hydroxy-19-norprogesteroncapronate/week (SH 834, Schering AG, Berlin) Only women with progressive disease were treated and only patients with well observable metastases or primary tumours, not simultaneously receiving other treatment, such as irradiation or cytostatic drugs, were evaluated

For evaluating the responses the criteria of the Cooperative Breast Cancer Group (National Cancer Institute) were applied Objective remission was therefore accepted only if (1) all demonstrable tumour masses diminished measurably in size, (2) more than 50 per cent of non-osseous lesions decreased in size although all bone lesions remained static, (3) more than 50 per cent of total lesions improved while the remainder were static Only regressions of at least three months duration were classified as remission

Forty of the 157 patients could not be evaluated 17 with inoperable tumours were irradiated simultaneously, 1 was treated simultaneously with a cytostatic agent and 22 were treated with SH 834 less than 4 weeks In 7 of the latter the treatment had to be discontinued because of undesirable side effects, mostly circulatory disturbances such as thrombosis or thrombophlebitis, 9 patients were lost during the follow-up, 6 died (2 of brain metastases, 1 of cardiac infarction, 1 of apoplexy and 2 of unknown cause)

Table 2

Remissions by SH 834 in relation to site and to menopausal age Pre menopausal patients and those previously treated excluded (Objective remission/patients treated)

Predominant site of metastases	Menopausal age				Total
	<1 year	1–5 years	5–10 years	>10 years	
Breast	0/0	0/2	2/6	10/15	12/23
Osseous	0 0	0/5	1/6	4/15	5/26
Visceral	0 0	0/3	4/14	11/28	15/45*
Total	0/0	0/10	7/26	25/58	32/94

* Remissions in 12/23 lung metastases, 2/6 pleural metastases, 1/13 liver metastases and 0/3 brain metastases

Thus, 117 patients remained for evaluation All but 2 patients were in natural or artificial menopause

Results

Treatment with SH 834 The results of the hormonal treatment appear in Table 1 Regression occurred in 48 of the 117 patients (41 %) If the 40 patients, who were treated less than 4 weeks or could not be evaluated for other reasons, are classified as failures, the 48 remissions represent 30 per cent of the whole group of 157 patients

Tumour growth in soft tissue (inoperable primary tumours, local recurrences, skin and lymph node metastases) reacted well to the hormonal treatment in 22 out of 44 cases Lung metastases diminished or disappeared in 16/34 cases, pleural effusions in 12/22 cases but bone metastases only in 15/57 cases Liver metastases remained unchanged by the treatment except in 1 out of 14 cases In this case a pathologic liver scan was partially normalized and a total remission of pleural carcinomatosis occurred

If, according to the suggestion of the U S A Cooperative Breast Cancer Group (1961) premenopausal women and those with previous hormonal treatment, are excluded, and the material then classified according to menopausal age and localizations of the dominant lesion (12 groups), 32/94 patients (34 %) remain with remissions (Table 2)

The generally low therapeutic result in patients with visceral metastases (lung, pleura, liver, brain) depends on the fact that 30 per cent were liver and brain metastases

The frequency of remissions increased significantly with the time elapsed since the menopause, but not with the age of the patient (Tables 2, 3) The mean age of all the 157 patients was 62 3 years (range 29 to 90), of those with remissions 64 1 (48 to 87) and of those without response, 60 6 years (29 to 90) there was therefore no

Table 3

Remissions with SH 834 in relation to menopausal age and free interval (Objective remission/patients treated)

Menopausal age	Free interval		Total
	0–1 year	>1 year	
<5 years	0/8	1/8	1/16
>5 years	12/34	34/66	46/100
Total	12/42	35/74	47/116

1 premenopausal remission with free interval >1 year

significant difference between these two groups In >5 year menopausal women the remissions were much higher (46/100) than in the <5 year menopausal group (1/10) (Table 3) One of the best parameters for hormone sensitivity of the tumour was, as in other series, the length of the free interval (time elapsing between diagnosis and recurrence) The best results were obtained in >5 year menopausal women with free interval >1 year Objective remissions occurred only in 12/34 patients with metastases appearing during the first year following the diagnosis of the tumour, as opposed to 35/64 patients with a longer recurrence-free interval (Table 3) The average remission time was 8 months (range 3 to 36) Lung metastases reacted most favourably, averaging 10 months (3 to 36)

Treatment with other hormones When other hormones were given following SH 834 (in cases of failure or following temporary remission), only 1/34 patients improved On the other hand, remissions were encountered in 16/37 patients when SH 834 was given following initial therapy with testosterone ananthate, methenolone enanthate, drostanolon propionate or norethisterone acetate

In 10 patients with remissions the SH 834 injections had to be discontinued because of a temporary supply difficulty, and the patients were given norethisterone acetate Five of them developed recurrences within 1 to 2 months, 2 within 5 and 12 months, and one died Following subsequent treatment of the remaining 7 patients with SH 834, a further remission of the tumour was obtained in 6 A continuous regression of malignant growth was obtained in two other patients by a combination of Progynon-Depot 100 mg/week i m and Norethisterone 40 mg daily by mouth

Side effects Undesirable side effects during the treatment with SH 834 occurred in 30/157 patients, the treatment had to be discontinued in 12 cases (Table 4) Peripheral thrombosis and thrombophlebitis were observed in 17/157, i e 11 per cent of the patients, 5 of these developed severe thrombotic complications, and 3 of them died However, all of them had severe secondary diseases such as diabetes, heart failure and advanced metastases which may have contributed to the complications.

Table 4

Side effects during SH 834 treatment in 157 patients

Type of complication	No of cases	SH 834 therapy stopped	Deaths
Thrombosis and thrombophlebitis	17	7	3
of these			
heart infarction	1	—	1
pulmonary embolism	1	—	1
gangrene of the toe	1	1	—
apoplexy	2	1	1
Jaundice	5	2	—
Hypercalcemia	1	1	—
Oedema heart failure	6	1	—
Retrosternal pains	1	1	—
Total	30	12	3

Casuistic One patient aged 66 with diabetes mellitus and angina pectoris died from a heart infarct 6 weeks after the beginning of the SH 834 treatment with good regression of the tumour A 79 year-old patient with cardiac failure and varicose veins died of pulmonary embolism after 6 months treatment A 60-year-old woman with multiple cranial metastases died of apoplexy after 2 weeks treatment A 65 year old patient with cerebral sclerosis and cardiac insufficiency developed signs of cerebral infarction after 13 months treatment with SH 834 and therefore the treatment was discontinued A 57 year-old patient had to have a toe amputated because of gangrene following crural embolism Five patients (all with liver metastases) developed jaundice after 2 to 4 weeks treatment with SH 834 Hepatotoxic reactions without jaundice occurred in 6 other patients with liver metastases

Pathologic changes in liver function due to SH 834 were not observed in patients without liver metastases One patient with bone metastases developed hypercalcemia after the first injection Serum calcium levels increased from 5 4 to 8 mEq/l and the treatment had to be abandoned

Some patients complained of tension in the remaining breast during treatment When SH 834 injections were discontinued, withdrawal bleedings occurred after 4 to 8 weeks

One patient reacted extremely well on the combination of SH 834 and cytostatics The effect of the hormones is in this case naturally difficult to evaluate The patient had a total regression of a 12 cm × 10 cm inoperable breast tumour with axillary and supraclavicular metastases after 25 months treatment with 5 Fu and Sendoxan (62 g of each) and 105 injections of SH 834 (315 ml)

Discussion

The patients in this series were not selected randomly with another group of patients treated by other hormones There was no exclusion of patients with very advanced diseases and bad prognosis Many patients who had previously failed to respond to other hormones have been included in this material, and these were cer-

Table 5

Therapeutic efficiency of SH 834 compared with androgens and oestrogens in menopausal women with disseminated carcinoma of the breast (Objective remission/patients treated)

Predominant site of metastases	Retrospective analysis*		Prospectively randomised material**		SH 834 present material
	Androgens	Oestrogens	Androgens	Oestrogens	
Breast	6/33	33/81	9/36	14/41	12/23
Osseous	25/80	7/32	8/86	10/78	5/26
Visceral	3/10	8/25	8/121	20/121	15/45
Total	34/123	48/138	25/243	44/240	32/94

* Report to the Council on Drugs J Amer med Ass 172 (1960), 1271
** Breast Cancer Group Cancer Chemother Reports, Suppl 41 (1964), 1

tainly less hormone sensitive with a worse prognosis than those not previously treated

Although it is difficult to compare results of different therapeutic measures in tumour patients from different centres because of differences in clinical staging, grading of malignancy, menopausal age and previous treatment, the results of the *SH 834* seem at least as good as those of testosterone propionate and diethylstilbestrol *(Table 5)* The present results are not as good as those reported by KENNEDY & YARBRO (1968) However, in their series, injections of high doses of methenolone enanthate (Primobolan-Depot) 3 × 400 mg/week i m were given Among the patients with pulmonary and pleural metastases remissions occurred in 13/27 (50 %) Liver and brain metastases, however, were refractory (Tables 1, 2) It is therefore not adequate to group these different types of visceral metastases together without regard to their individual influences on the patients' prognosis DAO & NEMOTO (1965) also observed this fact when comparing the therapeutic effects of adrenalectomy with hormonal treatment with 'reference androgens' (fluoxymesterone and 2-α methyl-dihydrotestosterone) They achieved 21/47 remissions by adrenalectomy in lung and pleural metastases, but in none of 5 cases with liver metastases nor in 1 case of brain metastases, compared with 2/39, 1/5 and 0/2 remissions in the 'reference androgens' group

The effect of SH 834 on lung and pleural metastases in the present material is comparable with those after adrenalectomy in postmenopausal patients, and the oestrogen-gestagen-combination may therefore be tried as the first treatment of choice

The therapeutic results with SH 834 are somewhat better than those with gestagen alone, by which 10 to 20 per cent remissions could be achieved (TAYLOR & MORRIS 1951, JONSSON et coll 1959, JONES et coll 1970) The results are also superior to those

obtained with norethisterone acetate treatment alone (Primolut Nor) in a dosage of (CURWEN 1963, 1964, NOTTER & KAIGAS 1966) Only CURWEN

gens and progestin, compared with a single agent, observed in 6/22 cases by CROWLEY & McDONALD (1965) has been verified in the present material in 11/21 patients The duration of the remissions obtained by SH 834 is the same as for testosterone and oestrogens (Breast Cancer Group 1964, KENNEDY 1965), and norethisterone acetate (NOTTER & WICKLUND 1967) The relatively high risk of side effects, especially the risk of thrombosis and embolism should be stressed However, tumour patients have a high incidence of infarction and thrombo-embolism due to their age and secondary diseases such as heart failure, atherosclerosis, diabetes mellitus and venous stasis It is, therefore, difficult to estimate the potential risk of a specific hormonal agent, but the causal relation between the hormonal treatment and the complication in some patients seems to be certain Thromboprophylaxis should therefore be given in patients with a history of previous thrombosis or thrombophlebitis In the cases of thrombosis in the present material this complication generally developed during the first 3 to 4 weeks of treatment and the patients should, therefore, be observed particularly carefully during this period However in out patients without a previous history of thrombo-vascular complications or heart failure the risk of side effects seems to be low Clinically latent or manifest circulatory insufficiency should be treated by digitalization and dehydration as is usual in steroid therapy

Temporary increases of the liver serum enzymes during oestrogen–gestagen treatment may be observed (BERNDT & STENDER 1970) but usually have little clinical significance and disappear spontaneously However, in cases with liver metastases, long-standing alterations, jaundice and bile stasis may occur and compel discontinuation of the therapy The combination of norethisterone acetate and ethinylestradiol is most dangerous in this respect (NOTTER 1966)

Conclusions

Combined treatment of disseminated mammary carcinoma with oestrogens and gestagens of SH 834-type seems to be effective in post menopausal women and also more effective than androgens, oestrogens and gestagens used as single therapeutic agents Careful consideration, however, has to be taken of the potential risk of thrombosis in patients with cardio-vascular decompensation and in patients with a history of previous thromboembolic diseases Combination therapy with oestrogens and gestagens may also be used with good effect as second choice hormone therapy when other hormones have failed or are no longer effective

Acknowledgement

The drug SH 834 was kindly supplied by Schering AG, Berlin

SUMMARY

The results of combined treatment with 90 mg estradiol valerianate and 300 mg 17 α-hydroxy-19-norprogesterone-capronate (SH 834) (3 ml once a week i m) in 117 cases with disseminated or inoperable mammary carcinoma are reported Objective remissions of 3 to 36 months were obtained in 48 patients Soft tissue, lung and pleura metastases responded more favourably than bone metastases Liver and brain metastases were unaffected

ZUSAMMENFASSUNG

Es wird uber die Ergebnisse von kombinierter Behandlung mit 90 mg Estradiol Valerianat und 300 mg 17-α Hydroxy-19-Norprogesteron Capronat (SH 834) (3 ml einmal wochentlich i m) bei 117 Fallen mit disseminierten oder inoperablen Mamma Karzinomen berichtet Es wurden objektiven Remissionen von 3 bis 36 Monaten bei 48 Patienten erhalten Weich-Gewebe-, Lungen- und Pleura-Metastasen reagierten besser als Knochenmetastasen Leber und Gehirnmetastasen waren unbeeinflusst.

RÉSUMÉ

Présentation des resultats dans 117 cas de cancer du sein disséminé ou inopérable d un traitement associant 90 mg de valérianate d'estradiol et 300 mg de capronate de 17-α-hydroxy-norprogestérone (SH 834) (à raison de 3 ml par semaine i m) Les auteurs ont obtenu des rémissions objectives de 3 à 36 mois chez 48 malades Les métastases des tissus mous, des poumons et de la plèvre ont repondu de façon plus favorable que les métastases osseuses Les métastases hépatiques et cérébrales n'ont pas été améliorées

REFERENCES

BERNDT G und STENDER H St Die Östrogen–Gestagen Kombinationsbehandlung des metastasierenden Mammakarzinoms mit SH 834 Dtsch med Wschr 95 (1970), 2399

Breast Cancer Group Progress report Results of studies by the cooperative breast cancer group 1956–60 Cancer Chemother Rep 11 (1961), 109

— Testosterone proprionate therapy of breast cancer A Progress Report Cancer Chemother Rep 16 (1962), 273

— Results of studies of the cooperative breast cancer group 1961–63 Cancer Chemother Reports (1964) Suppl No 41

— Testosterone proprionate therapy in breast cancer J Amer med Ass 188 (1964), 1069

COLSKY J, SHNIDER B, JONES R JR, NEVINNY STICKEL H B, HALL T, REGELSON W, SELAWRY O S, OWENS A JR, BRINDLEY C O, FREI E and UZER Y A comparative study of 9 alpha bromo-11-beta-ketoprogesterone and prednisolone in the treatment of advanced carcinoma of the female breast Cancer (Philad) 16 (1963), 502

CROWLEY L G and MCDONALD J Clinical trial of Delalutin in the treatment of advanced mammary carcinoma in post menopausal women Cancer (Philad) 15 (1962), 1218

— — Delalutin and estrogens for the treatment of advanced mammary carcinoma in the post-menopausal women Cancer (Philad) 18 (1965), 436

CURWEN S The value of norethisterone acetate in the treatment of advanced carcinoma of the breast Clin Radiol 14 (1963), 445
— Use of norethisterone acetate (SH 820, Schering AG Berlin) in treatment of advanced carcinoma of the breast J Endocr 28 (1964), 3
DAO TH L and NEMOTO T An evaluation of *adrenalectomy and androgen in disseminated* mammary carcinoma Surg Gynec Obstet 121 (1965), 1257
VAN GILSE H A Long term treatment with cortico-steroids of patients with metastasic breast cancer Cancer Chemother Rep 16 (1962), 293
GOLDENBERG I S and HAYES M A Hormonal therapy of metastatic female breast carcinoma I 9 alpha bromo 11 ketoprogesterone Cancer (Philad) 12 (1959), 738
HALL TH C DEDERICK M M, NEVINNY H B and MUENCH H Prognostic value of response of patients with breast cancer to therapeutic castration Cancer Chemother Rep 31 (1963), 47
HUGGINS C, MOON R C and MORII S Extinction of experimental mammary cancer. I Estradiol 17 beta and progesterone Proc nat Acad Sci 48 (1962), 379
JONES V A prospective trial of estrogens, androgens and progestogens for treatment of advanced breast cancer *In* The clinical management of advanced breast cancer, p 24 Edited by C A F Joslin and E N Gleave Tenovus Workshop Publications, Cardiff 1970
JONSSON U, COLSKY J, LESSNER H E, ROATH O S, ALPER R G and JONES R JR Clinical and pharmacological observations of the effects of 9-alpha bromo-11 ketoprogesterone in patients with carcinoma of the breast Cancer (Philad) 12 (1959), 509
KENNEDY B J Hormone therapy for advanced breast cancer Cancer (Philad) 18 (1965), 1551
— and BROWN H J Combined estrogenic and androgenic hormone therapy in advanced breast cancer Cancer (Philad) 18 (1965), 431
— and FORTUNY I E Therapeutic castration in the treatment of advanced breast cancer Cancer (Philad) 17 (1964), 1197
— and FRENCH L Hypophysectomy in advanced breast cancer Amer J Surg 110 (1965), 411
— and YARBRO J W Effect of methanolone enanthate (NSC 64967) in advanced cancer of the breast Cancer (Philad) 21 (1968), 197
LEMON H M Prednisone therapy of advanced mammary cancer Cancer (Philad) 12 (1959), 93
LEWISON E F Prophylactic versus therapeutic castration in the total treatment of breast cancer Obstet gynec Surg 17 (1962), 769
— Castration in the treatment of advanced breast cancer Cancer (Philad) 18 (1965), 1558
McDONALD J Endocrine ablation in disseminated mammary carcinoma Surg Gynec Obstet 115 (1962), 215
NOTTER G Toxiska biverkningar av gestagena och estrogena hormoner vid brostcancer (In Swedish) Lakartidningen 63 (1966) 3577
[illegible] mmakarzinoms
[illegible] 966), 1920
[illegible] Mammakarzi-
[illegible] mit gestagenen Hormonen Munch med Wschr 109 (1967), 2602
NOWAKOWSKI H Moglichkeiten und Grenzen der endokrinen Therapie des metastasierenden Mammakarzinoms Verh dtsch Ges inn Med 73 (1967), 505
PEARSON O H and RAY B S Hypophysectomy in the treatment of metastatic mammary cancer Amer J Surg. 99 (1960), 544

SUMMARY

The results of combined treatment with 90 mg estradiol valerianate and 300 mg 17-α hydroxy-19 norprogesterone-capronate (SH 834) (3 ml once a week i m) in 117 cases with disseminated or inoperable mammary carcinoma are reported Objective remissions of 3 to 36 months were obtained in 48 patients Soft tissue, lung and pleura metastases responded more favourably than bone metastases Liver and brain metastases were unaffected

ZUSAMMENFASSUNG

Es wird uber die Ergebnisse von kombinierter Behandlung mit 90 mg Estradiol Valerianat und 300 mg 17-α-Hydroxy-19-Norprogesteron Capronat (SH 834) (3 ml einmal wochentlich i m) bei 117 Fallen mit disseminierten oder inoperablen Mamma Karzinomen berichtet Es wurden objektiven Remissionen von 3 bis 36 Monaten bei 48 Patienten erhalten Weich-Gewebe-, Lungen- und Pleura-Metastasen reagierten besser als Knochenmetastasen Leber und Gehirnmetastasen waren unbeeinflusst

RÉSUMÉ

Présentation des résultats dans 117 cas de cancer du sein disséminé ou inopérable d un traitement associant 90 mg de valérianate d estradiol et 300 mg de capronate de 17-α-hydroxy norprogestérone (SH 834) (à raison de 3 ml par semaine i m) Les auteurs ont obtenu des rémissions objectives de 3 à 36 mois chez 48 malades Les métastases des tissus mous, des poumons et de la plèvre ont répondu de façon plus favorable que les métastases osseuses Les métastases hépatiques et cérébrales n'ont pas été ameliorées

REFERENCES

BERNDT G und STENDER H St Die Östrogen–Gestagen Kombinationsbehandlung des metastasierenden Mammakarzinoms mit SH 834 Dtsch med Wschr 95 (1970), 2399

Breast Cancer Group Progress report Results of studies by the cooperative breast cancer group 1956–60 Cancer Chemother Rep 11 (1961), 109

— Testosterone proprionate therapy of breast cancer A Progress Report Cancer Chemother Rep 16 (1962), 273

— Results of studies of the cooperative breast cancer group 1961–63 Cancer Chemother Reports (1964) Suppl No 41

— Testosterone proprionate therapy in breast cancer J Amer med Ass 188 (1964), 1069

COLSKY J, SHNIDER B, JONES R JR, NEVINNY-STICKEL H B, HALL T, REGELSON W, SELAWRY O S, OWENS A JR, BRINDLEY C O, FREI E and UZER Y A comparative study of 9 alpha bromo 11-beta-ketoprogesterone and prednisolone in the treatment of advanced carcinoma of the female breast Cancer (Philad) 16 (1963), 502

CROWLEY L G and MCDONALD J Clinical trial of Delalutin in the treatment of advanced mammary carcinoma in post menopausal women Cancer (Philad) 15 (1962), 1218

— — Delalutin and estrogens for the treatment of advanced mammary carcinoma in the post-menopausal women Cancer (Philad) 18 (1965), 436

ROM THE GUSTAF WERNER INSTITUTE, UNIVERSITY OF UPPSALA, S-750 20 UPPSALA,
DEPARTMENT OF NEUROSURGERY, UPPSALA UNIVERSITY HOSPITAL, S-750 14 UPPSALA,
WEDEN AND NASA AMES RESEARCH CENTRE, MOFFETT FIELD, CALIFORNIA 94035, U S A

HIGH-ENERGY PROTONS IN THE POSTOPERATIVE TREATMENT OF MALIGNANT GLIOMA

S GRAFFMAN, W HAYMAKER, R. HUGOSSON and B JUNG

The reduced tolerance of normal brain tissue to radiation when large volumes are irradiated (demonstrated experimentally by BERG & LINDGREN 1963) and the indeterminable extent of neoplastic growth have evoked two principles for the irradiation of glioblastoma multiforme TODD (1963) suggested that the target volume should include a marginal zone of only 2 to 3 cm around the apparent site of the tumour, whereas CONCANNON et coll (1960), BOUCHARD (1966) and LEGRÉ et coll (1969) recommend that 50 to 100 per cent of the brain be included in the irradiation field Because of the slow growth rate, low sensitivity and the risk of late radiation effects on normal brain tissue, the usefulness of postoperative irradiation of astrocytoma I and II (KERNOHAN *et coll* 1949) has been questioned, e g. by ZULCH (1969) On the other hand, the *rationale* for irradiation of astrocytoma III and IV is well documented (BOUCHARD) However, the results are almost exclusively palliative Tumours diagnosed as astrocytoma III and IV are often composed of cells of varying differentiation Poorly differentiated or anaplastic cells in the central region are frequently surrounded by a broad zone of more highly differentiated astrocytoma cells (SCHERER 1940, RUSSELL & RUBENSTEIN 1960)

Hypothetically, greater palliation may be achieved when the central tumour

Submitted for publication 14 November 1974

RAY B S and PEARSON O H Hypophysectomy in treatment of disseminated breast cancer Surg Clin N Amer 43 (1962), 419

Report to the Council on Drugs Androgens and estrogens in the treatment of disseminated mammary carcinoma Retrospective study of 944 patients J Amer med Ass 172 (1960), 1271

SEGALOFF A, WEETH J B, RONGONE E L, MURISON P L and BOWERS C Y Hormonal therapy in cancer of the breast XVI The effect of delta-1 testololactone on clinical course and hormonal excretion Cancer (Philad) 13 (1960), 1017

TAYLOR S G III and MORRIS R S JR Hormones in breast metastasis therapy Med Clin N Amer 35 (1951), 51

Table

Irradiation data

Case	1	2	3	4	5	6	7
Period of irradiation (days)	60	36	31	25	32	28	28
Number of fractions	11	10	10	8	10	9	9
Dose (rad)	5 000	5 100	5 100	3 900	5 100	5 200	5 100
(reu)	1 850	2 000	2 000	1 650	2 000	2 100	2 100
Diameter of field (cm)	6	8	8	8	8	9	9
Depth of field (cm)	6 4	5 4	7 5	7 6	9 2	7 9	7 7

cubes of polystyrene arranged in a two-dimensional matrix The beam was monitored by nitrogen flushed ion chambers of transmission type which on each occasion were calibrated with ^{11}C activation tests A plateau in the depth dose distribution was obtained, after monitoring, by passing the beam through a ridge filter which modulated the proton energy spectrum (LARSSON 1961, KARLSSON 1964, GRAFFMAN et coll 1965, JUNG et coll, (to be published)

A special skull table was constructed which allowed precise alignment of the patient to the beam axis and the restriction of movements during irradiation (Fig 1) A moulage of thin sticks of Perspex was used to compensate for the curvature of the skull

A diagnostic roentgen generator and an image intensifier were used to observe indicators placed on the resection surfaces during the operation These served in the determination of the radiation field for the first treatment Subsequently only external indicators (on each side of the head) were used, together with optical pointers, for the alignment of the patient Possible displacements of midline structures, which might be an early sign of an acute oedematous reaction in the irradiated brain tissue, were checked by repeated echoencephalography In addition, movements of the internal indicators were sought on orthogonal films exposed before each irradiation session The internal indicators and the dose distribution in one of the patients appear in Fig 2

Irradiation data A circular field was used In cases 6 and 7 a small segment of the field was excluded in order to avoid irradiation of the eyes A single field was used for all patients and the beam was directed to the side of the head The total dose administered was 5 000 to 5 200 rad, in 9 to 11 fractions given over about 4 weeks The individual irradiation data are given in the Table In order to avoid an acute oedematous reaction the first dose was 300 rad for all patients The doses were then successively increased to a maximum of 700 rad, the latter dose given late in each

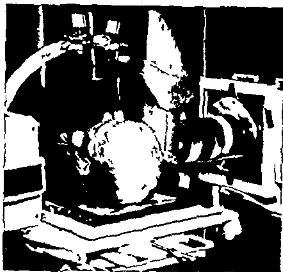


Fig 1

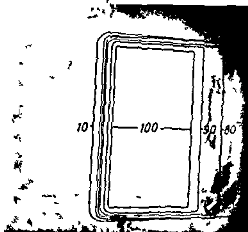


Fig 2

Fig 1
located
collima
temporal region

Fig 2 Isodose curves in a central plane of a beam 8 cm in diameter, superimposed on a film of case 3

region, containing more rapidly growing cells, is exposed to a high dose, even though not all tumour cells are included in the irradiated volume In cases of limited tumour extent this might also increase the cure rate

The principles recommended by TODD, allowing relatively large tumour doses, have been used in the present investigation Whether this procedure justifies the higher risk of part of the tumour escaping irradiation is questionable, but probably can only be evaluated by the use of a homogeneous and sharply defined radiation beam The geometrical properties of a ridge-filtered, high-energy proton beam meet this requirement

Seven patients with malignant glioma given post-operative proton irradiation, and the microscopic findings of four brains examined subsequently, are now reported The aim was to elucidate the following problems (1) the practicability of fractionated irradiation of brain tumours with high energy protons, (2) the risk involved in such therapy of early reactions, late necrosis and any unforeseen complications, (3) the effects of high energy protons on normal and neoplastic brain tissue, (4) the optimum field size and tumour dose, and (5) the clinical results

Methods of irradiation The irradiation was carried out with the 185 MeV external proton beam from a synchrocyclotron The shaping of the beam was accomplished with collimators and sweeping magnets which gave a sharply defined beam with a transverse homogeneity better than ± 5 per cent Before each irradiation the transverse homogeneity was controlled by measurement of ^{11}C-activity induced in small

tion Al
autopsy
be obtained for further analysis

diagnosed At operation the lobe was resected and an macro...
removed The tumour was an astrocy
the patient s general condition deterior
ued At autopsy, large tumour masses were found in ...
large irradiated region of the brain The brain could not be obtained for further analysis

Case 5 A 58 year old male with a short history of severe memory disturbances and one epileptic episode A sparsely vascularized tumour was found in the left frontal lobe, macroscopically all tumour tissue was removed Irradiation was begun 2 months after operation. The depth of the irradiated region was 9 2 cm, or about 2 2 cm beyond the midline of the brain The memory disturbances persisted during the following months, after which the patient s general condition deteriorated gradually Death occurred 10 months after operation and autopsy was performed (vide infra)

Case 6 A 61 year old female who had headache, drowsiness, slight hemiparesis and aphasia for one week before admission to hospital At angiography, a large tumour with abnormal vessels was found in the left temporal lobe A lobectomy was carried out Tissue extensively infiltrated by tumour in the region of the basal ganglia was left in situ Irradiation was commenced 21 days later Depth of penetration of the protons was 7 9 cm, or about 0 9 cm beyond the midline of the brain The neurologic signs disappeared and the patient remained well for 6 months, after which she deteriorated progressively She died 10 months after surgery and autopsy was performed (vide infra)

begun 22 days after operation The depth of the irradiated region was 7 7 cm, or about 0 7 cm beyond the midline of the brain During the period of radiation therapy and for the following 5 months the patient remained well Death occurred 11½ months after operation and autopsy was performed (vide infra)

Post morten examinations Four brains were obtained for detailed microscopy (cases 1, 5, 6 and 7) Before sectioning the brain the site of the field of irradiation was established Using the skull films on which the irradiation field was indicated as a guide a probe was placed at the point on the side of the brain corresponding to the centre of the field The field was outlined with indian ink dots on the brain surface

The brain was then sectioned in the sagittal plane at about 1-cm intervals, the brain blocks reassembled, and a probe pushed, in the coronal plane, through the brain thus establishing the centre point of the radiation beam in each brain block. The field was then indicated on each block by dots The brain blocks were embedded in paraffin and cut at 6 to 10 μm Various stains were used luxol fast blue PAS-

series Each session required about 20 min, in which the irradiation time varied between 3 and 15 min depending on the dose, field size and beam condition For practical reasons a conventional fractionation scheme with five treatments per week could not be followed and the irradiation was delivered in two fractions per week

The LET-distribution of high-energy protons is nominally low The biologic effect of the protons should be similar to that of ^{60}Co radiation (c f STENSON 1969, JOHANSSON 1972) Recoil protons as well as nucleons and nuclei emitted in nuclear reaction add a small high-LET component In the last few millimeters of their range the protons have themselves a high LET The ridge filter modifies the proton energy spectrum so that protons stop everywhere in the plateau region More protons stop in the deeper part of the irradiated tissue, and the high LET-proton component thus increases with depth The increase in RBE is probably of importance only in the last few millimeters of the field and is estimated to be about 10 per cent (GRAFFMAN et coll 1967, GRAFFMAN & JUNG 1970) In order to compensate for this increase the maximum penetration depth of the radiation beam was reduced at one or two of the treatment sessions Figures giving maximum depth of penetration of the beam refer to the maximum depth of the 100 per cent isodose

Case reports

Case 1 A 28 year old male with a 3 year history of temporal lobe epileptic seizures Angiography revealed a large tumour with abnormal vessels in the right temporal lobe A lobe resection was carried out A small part of the tumour had to be left in the insular region Irradiation was begun 47 days postoperatively After the first fraction a transient psychotic state developed, probably due to meningitis, incidental to the continuous registration of the intracranial pressure Treatment was recommenced 30 days later and completed without further complications For 9 months after the last irradiation the patient was well and able to work He died 14 months after the operation and autopsy was performed (*vide infra*)

Case 2 A 54 year old male with headache, fatigue and dizziness of insidious onset, followed 3 months later by slight hemiparesis A large tumour in the right temporal lobe was disclosed At operation a malignant glioma with abnormal vessels was found and partially excised The medial extent of the tumour was uncertain At microscopy the tumour was found to be an astrocytoma, grade III Irradiation was delayed until 2½ months after the operation The patient's general symptoms ameliorated and the neurologic deficits quickly disappeared Except for some neurotic traits, the patient's condition was satisfactory for about one year after which he deteriorated and death occurred 14 months postoperatively No autopsy was performed

Case 3 A 25 year old female with a 6-month history of headache blurred vision and memory disturbances Angiography revealed a large tumour in the left temporal lobe A lobectomy was carried out The main bulk of the tumour was tough and yellow, its central part was grey, friable and bled easily The same kind of tissue extended into the insular cortex, and since medial infiltration of the tumour was also obvious, total removal of neoplastic tissue was not attempted Microscopy revealed an astrocytoma, grade III Irradiation was started one month later The patient resumed her former occupation 4½ months after opera-

tion About 3 years later she gradually deteriorated and died 50 months after operation At autopsy, tumour tissue was found in the left frontal and parietal lobes The brain could not be obtained for further analysis

Case 4 A 62 year old male who presented with minor epileptic fits, aphasia, and changes in personality over a period of 3 months A tumour involving the left temporal lobe was diagnosed At operation the lobe was resected and all macroscopically visible tumour tissue removed The tumour was an astrocytoma, grade IV Radiation therapy was begun but the patient s general condition deteriorated so rapidly that the treatment had to be discontinued At autopsy, large tumour masses were found in both hemispheres far beyond the large irradiated region of the brain The brain could not be obtained for further analysis

Case 5 A 58 year old male with a short history of severe memory disturbances and one epileptic episode A sparsely vascularized tumour was found in the left frontal lobe, macroscopically all tumour tissue was removed Irradiation was begun 2 months after operation The depth of the irradiated region was 9 2 cm, or about 2 2 cm beyond the midline of the brain The memory disturbances persisted during the following months, after which the patient s general condition deteriorated gradually Death occurred 10 months after operation and autopsy was performed (vide infra)

Case 6 A 61 year old female who had headache, drowsiness, slight hemiparesis and aphasia for one week before admission to hospital At angiography, a large tumour with abnormal vessels was found in the left temporal lobe A lobectomy was carried out Tissue extensively infiltrated by tumour in the region of the basal ganglia was left in situ Irradiation was commenced 21 days later Depth of penetration of the protons was 7 9 cm, or about 0 9 cm beyond the midline of the brain The neurologic signs disappeared and the patient remained well for 6 months, after which she deteriorated progressively She died 10 months after surgery and autopsy was performed (vide infra)

Case 7 A 61 year old male with headache, dizziness and memory disturbances for 3 months A large highly vascularized tumour of the right frontal lobe was revealed The tumour could not be totally removed because the corpus callosum was infiltrated Irradiation was begun 22 days after operation The depth of the irradiated region was 7 7 cm, or about 0 7 cm beyond the midline of the brain During the period of radiation therapy and for the following 5 months the patient remained well Death occurred 11½ months after operation and autopsy was performed (vide infra)

Post morten examinations Four brains were obtained for detailed microscopy (cases 1, 5, 6 and 7) Before sectioning the brain the site of the field of irradiation was established Using the skull films on which the irradiation field was indicated as a guide, a probe was placed at the point on the side of the brain corresponding to the centre of the field The field was outlined with indian ink dots on the brain surface

The brain was then sectioned in the sagittal plane at about 1-cm intervals, the brain blocks reassembled, and a probe pushed, in the coronal plane, through the brain, thus establishing the centre point of the radiation beam in each brain block The field was then indicated on each block by dots The brain blocks were embedded in paraffin and cut at 6 to 10 μm Various stains were used luxol fast blue-PAS-

series Each session required about 20 min, in which the irradiation time varied between 3 and 15 min depending on the dose, field size and beam condition For practical reasons a conventional fractionation scheme with five treatments per week could not be followed and the irradiation was delivered in two fractions per week

The LET-distribution of high-energy protons is nominally low The biologic effect of the protons should be similar to that of ^{60}Co radiation (c f STÉNSON 1969, JOHANSSON 1972) Recoil protons as well as nucleons and nuclei emitted in nuclear reaction add a small high-LET component In the last few millimeters of their range the protons have themselves a high LET The ridge filter modifies the proton energy spectrum so that protons stop everywhere in the plateau region More protons stop in the deeper part of the irradiated tissue, and the high LET-proton component thus increases with depth The increase in RBE is probably of importance only in the last few millimeters of the field and is estimated to be about 10 per cent (GRAFFMAN et coll 1967, GRAFFMAN & JUNG 1970) In order to compensate for this increase the maximum penetration depth of the radiation beam was reduced at one or two of the treatment sessions Figures giving maximum depth of penetration of the beam refer to the maximum depth of the 100 per cent isodose

Case reports

Case 1 A 28 year old male with a 3 year history of temporal lobe epileptic seizures Angiography revealed a large tumour with abnormal vessels in the right temporal lobe A lobe resection was carried out A small part of the tumour had to be left in the insular region Irradiation was begun 47 days postoperatively After the first fraction a transient psychotic state developed, probably due to meningitis, incidental to the continuous registration of the intracranial pressure Treatment was recommenced 30 days later and completed without further complications For 9 months after the last irradiation the patient was well and able to work He died 14 months after the operation and autopsy was performed (vide infra)

Case 2 A 54 year old male with headache, fatigue and dizziness of insidious onset, followed 3 months later by slight hemiparesis A large tumour in the right temporal lobe was disclosed At operation a malignant glioma with abnormal vessels was found and partially excised The medial extent of the tumour was uncertain At microscopy the tumour was found to be an astrocytoma grade III Irradiation was delayed until 2½ months after the operation The patient s general symptoms ameliorated and the neurologic deficits quickly disappeared Except for some neurotic traits, the patient's condition was satisfactory for about one year after which he deteriorated and death occurred 14 months postoperatively No autopsy was performed

Case 3 A 25 year old female with a 6 month history of headache, blurred vision and memory disturbances Angiography revealed a large tumour in the left temporal lobe A lobectomy was carried out The main bulk of the tumour was tough and yellow, its central part was grey, friable and bled easily The same kind of tissue extended into the insular cortex, and since medial infiltration of the tumour was also obvious, total removal of neoplastic tissue was not attempted Microscopy revealed an astrocytoma, grade III Irradiation was started one month later The patient resumed her former occupation 4½ months after opera-

face (right temporal polar region) the tumour measured 6 0 cm × 3 5 cm becoming gradually smaller with increasing depth (Fig 3 a) There was no indication that the tumour extended into the left hemisphere The proton beam did not penetrate (6 4 cm) quite as deep as the tumour tissue

Near the surface practically all the tumour was within the irradiated region, while at deeper levels most of the tumour lay outside

The tumour within the irradiated region was friable, intensely hemorrhagic and contained accumulations of coagulated fluid These features were less prominent elsewhere Furthermore, much of the tumour was sharply defined inside but not outside the irradiation area (Fig 3 a) The lateral ventricles were somewhat enlarged Irradiated tissues not infiltrated by tumour appeared unaffected

Microscopy The tumour was an astrocytoma grade IV A representative view of the tumour within the irradiated region appears in Fig 3 b There seemed to be as many multinucleated giant cells per unit area outside the field of irradiation, as inside Vessels within the tumour both inside and outside the irradiated area were hypertrophic and hyperplastic and, in numerous areas, extraordinarily large telangiectasies were present Areas of necrosis together with occluded vessels were observed throughout but the areas of necrotic tumour within the irradiated region were larger than outside P T A H preparations demonstrated fibrinous material around the vessels at both sites, only in focal areas within necrotic tumour was fibrillary gliosis of moderate degree revealed The irradiated tumour tissue was permeated by coagulated fluid and, in places (including the leptomeninges), pools of the fluid, such pools, but smaller, also occurred outside the irradiated tissue

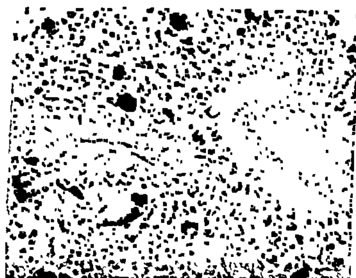
In the irradiated tumour tissue near the body of the lateral ventricle there was an area, about 1 5 cm in diameter, in which all the vessels were necrotic and most of the tissue was amorphous and spongy, small aggregates of neoplastic cells were present around rather numerous recognizable vessels Furthermore, there were clusters of occluded vessels with greatly thickened, hyalinized and laminated walls Such tissue was considered to be tumour tissue which had been completely destroyed by the proton radiation except for small islands of perivascular neoplastic cells

Around the mass of tumour tissue, particularly in the non irradiated region there was a corona of neoplastic cells together with hypertrophied and hyperplastic vessels Irradiated tissue not containing tumour cells was not altered except that the myelin was pale in some areas as a result of oedema

Comment Parts of the neoplastic tissue within the irradiated region were destroyed but in between these regions were viable tumour cells The reactive changes in the blood vessels, leading to their occlusion clearly represented a radiation effect The extraordinary amount of plasma exudate, which was much more marked within the irradiated area than outside, is considered an indication of alterations in the blood-brain barrier induced by radiation



a



b

Fig 3. a) Case I The radiation area is indicated by dots The head of the caudate nucleus is occupied by hemorrhagic tumour, for the most part sharply outlined In the centrum semiovale, less hemorrhagic tumour tissue exists outside the irradiated area b) Section from irradiated part of the tumour Characteristic features of glioblastoma multiforme X190 Luxol fast blue-PAS-haematoxylin

haematoxylin, haematoxylin-eosin, Van Gieson-haematoxylin, cresyl echt violet, and phosphotungstic acid haematoxylin (P T A H.)

Case I. A 6-cm field of brain of the right side received 5 000 rad in 11 fractions over a period of 60 days (Table) Death occurred 12½ months after the beginning of irradiation.

Gross examination. The tumour was located in the temporo-parieto-frontal region on the right side, occupying *the centrum semiovale, and infiltrating the corpus* callosum, gyrus cinguli, and the head of the caudate nucleus On the presenting sur-

10 fractions over a period of 32 days (Table) Death occurred 8 months after radiation therapy was commenced

Gross examination The depth reached by the proton beam was 9 2 cm, or about 2 2 cm beyond the midline of the brain Tumour tissue was found 2 5 cm beyond the midline The tumour, except for a small portion most distant from the irradiation port lay within the irradiated area

In the median plane the rostrum of the corpus callosum was greatly expanded by tumour (Fig 4 a) The adjacent right gyrus cinguli also contained tumour A section 2 5 cm to the right of the midline revealed a small amount of tumour tissue in the lateral part of the corpus callosum, the head of the caudate nucleus and in the adjacent white matter

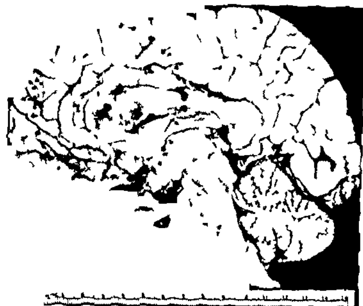
The main bulk of the tumour was located in the rostral half of the left frontal lobe Two of the gyri of the frontal pole were decidedly abnormal The white matter in these gyri was softened and atrophic Contiguous with these atrophic gyri was a large mass 4 to 6 cm in diameter

Microscopy The main part of the tumour (bilaterally) was an astrocytoma grade IV On the irradiated side a sizable tumour mass continuous with the glioblastoma *extended into the leptomeninges Although resembling a meningeal sarcoma,* this growth was regarded as a part of the original tumour which had acquired reticulum from invaded meninges

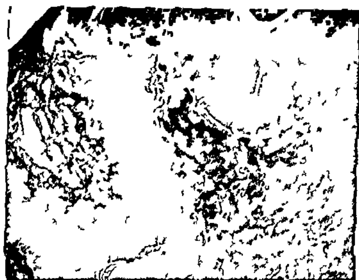
On the left side relatively large areas of white matter contained sinuous cords of necrotic tumour separated by viable neoplastic tissue (Fig 4 b) The necrotic tissue was permeated by extravasated plasma like material Viable tumour cells were also found perivascularly within such cords which commonly contain fibrinous material The viable cells between the cords of necrotic tumour cells were mainly astroglia, many of which were anaplastic and multinucleated Vessels within the necrotic tumour and brain tissue shared in the necrosis and many vessels were thrombosed and exhibited very thickened, laminated and hyalinized walls At the border of the mass fairly sharp in places, tongues of necrotic tumour tissue projected as a corona into the adjacent normal tissue All the tumour excepting the meningeal mass was confined to the white matter In addition, as seen in P T A H preparations, there were focal areas of advanced fibrillary gliosis throughout the badly injured tumour tissue

White matter near the main tumour mass, within the irradiated area, was intact but was invaded by anaplastic astrocytes Reduced myelin staining was found in some tissues in the vicinity of vessels

In the corpus callosum the appearance of the tumour was similar but contained less necrosis Plasma like material occurred in smaller quantities than in the main tumour mass In the *gyrus cinguli, on the other hand,* there were small areas of tumour which appeared necrotic



a



b

Fig. 4. a) Case 5. The perimeter of the radiation area is indicated by dots. The tumour has considerably expanded the corpus callosum. b) Section from the superior part of frontal lobe. *Largely necrotic tu*mour tissue (darker stained) inter

Whether tumour cells existed outside the irradiated region before irradiation or represented tumour spread afterwards was impossible to determine and therefore no conclusion could be reached about whether radiation had influenced tumour spread. However, the sharp lower border of the main mass of the tumour within the irradiated region (Fig. 3 a) *might indicate a restrictive influence of the radiation on* tumour spread. Of particular interest was the lack of effect of radiation on the normal tissue at a distance from the tumour but well within the irradiated area.

Case 5. An 8 cm region of brain on the left side was exposed to 5 100 rad given in

It was also well circumscribed In addition, small tumour nodules projected from the wall of the fourth and lateral ventricles

The temporal lobe mass lay partly within the irradiated region and partly ventral to it Much of the tumour in the paracentral lobule was in the irradiated region and appeared largely necrotic The remaining part, dorsal to the irradiated region, did not seem to be necrotic The frontal lobe tumour, partly in the irradiation field and partly outside, was uniform in appearance and without evident necrosis

The irradiated white matter was not altered The right hemisphere appeared free from change

Microscopy The periventricular nodules as well as small tumours in the meninges surrounding the upper brain stem and located in the base of the hypothalamus as well as over the convex surface of the cerebrum proved to be composed of malignant ependymoma (ependymoblastoma), reminiscent in places of glioblastoma multiforme The tumour in the paracentral lobule (Fig 6 a) and that in the frontal pole had the same structure Grossly the tumour in the paracentral lobule was more necrotic in the portion in the irradiated area (Fig 6 b) This was confirmed microscopically Fairly large pools of coagulated plasma existed in both parts of the tumour, but were largest in the irradiated part Hyperplastic leptomeningeal fibroblastic cells penetrated the tumour to considerable depths as cords or broad masses Vessels in the non irradiated part of the tumour in the paracentral lobule were distended and had uniform, thin walls, and here and there a vessel contained a thrombus In the irradiated part, however, most of the vessels within necrotic tumour tissue were necrotic, others displayed intimal thickening or had marked hyperplastic adventitia, one relatively large thrombosed aneurysm and numerous intact thrombosed vessels also appeared

Tumour tissue, forming isolated aggregates or large cell masses, was found along the dorsal and ventral aspects of the brain stem and in the interpeduncular fossa There was a tendency to form lobules and the cells were fairly uniform in appearance with elongated or oval nuclei and distinct polar processes of varying thickness and length lying parallel with one another There was a tendency to pseudorosette formation Giant cells with bizarre nuclei were encountered in some areas, but no tumour necrosis The neoplastic tissue in these regions had all the characteristics of malignant ependymoma

The mass in the temporal lobe, deep to the excision, was almost totally necrotic Because of the amorphous character of the necrotic tissue it was not possible to decide in what extent the tissue had previously contained tumour Many necrotic vessels within the necrotic tissue were surrounded by extravasated plasma Along the periphery of the necrotic mass, and extending for different distances from the mass, were anaplastic tumour cells located either in disrupted tissue (Fig. 6 c) or in relatively intact tissue P T A H preparations revealed extreme fibrillary astrogliosis throughout the mass



Fig 5 Case 6 Left hemisphere The perimeter of the radiation area indicated by dots The white matter of the temporal lobe appears indurated and clearly distinguishable from the white matter of the remainder of the hemisphere One tumour is present in the paracentral gyrus, and another in the frontal pole

The rest of the brain tissue within the irradiated area, including that near the limit of the range of the protons, appeared unaltered and was indistinguishable from the tissue outside the area Part of the lenticular nucleus was within the irradiation area and part outside, both appeared relatively unaltered

Comment The extensive necrosis in a sizable proportion of the tumour indicated the effect of radiation It is possible that the viable tumour cells in between the cords of necrotic tumour represented newly formed cells The degree of plasma exudation in the tumour mass was greater than is usually found in non-irradiated anaplastic glioma A radiation induced alteration in the blood-brain-barrier system thus seems likely Tumour tissue in the corpus callosum and the adjacent part of the right hemisphere might represent spread following irradiation No changes were found in brain tissue distant from the tumour mass but within the irradiated region

Case 6 A 9-cm field of the left side of the brain was exposed to 5 200 rad given in 9 fractions over a period of 28 days (Table) Death occurred 9 months after irradiation was begun The irradiated volume extended 7 9 cm deep to the surface of the head, i e about 0 7 cm into the right hemisphere

Gross examination One extensive area of tissue necrosis and two tumours were found in sagittal sections of the left hemisphere (Fig 5) The area of the tissue necrosis was located in the temporal lobe in the region of the surgical resection and extended deeply into the white matter It was a solid, opaque white mass with a jagged border One of the tumours, which was a discrete mass, occupied the paracentral lobule of the parietal lobe It replaced cortex and extended into the meninges The second tumour, small but similar in appearance, was found in the frontal pole

It was also well circumscribed In addition, small tumour nodules projected from the wall of the fourth and lateral ventricles

The temporal lobe mass lay partly within the irradiated region and partly ventral to it Much of the tumour in the paracentral lobule was in the irradiated region and appeared largely necrotic The remaining part, dorsal to the irradiated region, did not seem to be necrotic The frontal lobe tumour, partly in the irradiation field and partly outside, was uniform in appearance and without evident necrosis

The irradiated white matter was not altered The right hemisphere appeared free from change

Microscopy The periventricular nodules as well as small tumours *in the meninges surrounding the upper brain stem and located in the base of the hypothalamus* as well as over the convex surface of the cerebrum proved to be composed of malignant ependymoma (ependymoblastoma), reminiscent in places of glioblastoma multiforme The tumour in the paracentral lobule (Fig 6 a) and that in the frontal pole had the same structure Grossly the tumour in the paracentral lobule was more necrotic in the portion in the irradiated area (Fig 6 b) This was confirmed microscopically Fairly large pools of coagulated plasma existed in both parts of the tumour, but were largest *in the irradiated part Hyperplastic leptomeningeal fibroblastic cells* penetrated the tumour to considerable depths as cords or broad masses Vessels in the non irradiated part of the tumour in the paracentral lobule were distended and had uniform, thin walls, and here and there a vessel contained a thrombus In the irradiated part, however, most of the vessels within necrotic tumour tissue were necrotic others displayed intimal thickening or had marked hyperplastic adventitia one relatively large thrombosed aneurysm and numerous intact thrombosed vessels also appeared

Tumour tissue forming isolated aggregates or large cell masses, was found along the dorsal and ventral aspects of the brain stem and in the interpeduncular fossa There was a tendency to form lobules and the cells were fairly uniform in appearance with elongated or oval nuclei and distinct polar processes of varying thickness and

ependymoma

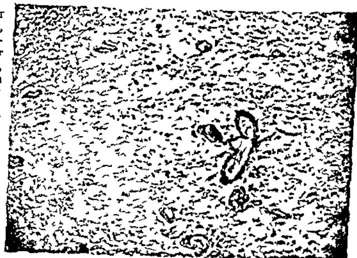
The mass in the temporal lobe, deep to the excision, was almost totally necrotic Because of the amorphous character of the necrotic tissue it was not possible to decide in what extent the tissue had previously contained tumour Many necrotic vessels within the necrotic tissue were surrounded by extravasated plasma Along the periphery of the necrotic mass, and *extending for different distances from the mass*, were anaplastic tumour cells located either in disrupted tissue (Fig 6 c) or in relatively intact tissue P T A H preparations revealed extreme fibrillary astrogliosis throughout the mass



a



b



c

Fig 6 a) Same case as in Fig 5 From non-irradiated part of tumour in paracentral lobule Narrow, elongated cells are aligned perpendicular to the surface of the vascular adventitia (to the left) Elsewhere, some cell clusters tend to form pseudorosettes Vessel walls appear relatively normal × 190 Luxol fast blue-PAS-haematoxylin b) Tumour in paracentral lobule The lower half of the tumour in the radiated area, where a greater degree of tumour necrosis is evident × 4 5 Luxol fast blue-PAS-haematoxylin c) Irradiated temporal lobe area Anaplastic tumour cells in a column in between tissue which is partially or totally necrotic × 100 Luxol fast blue-PAS-haematoxylin

No abnormality was observed in transirradiated white or grey matter in the area in between the three neoplasms

Comment The tumour undoubtedly originated from an ependymal site in the region of the fourth ventricle and spread by seedlings through the cerebrospinal fluid

The radiation appeared to have totally destroyed much of the tissue in the temporal lobe but since viable tumour cells were found at the periphery of the mass, it would be reasonable to assume the presence of pre existing tumour in the necrotic mass Damage to nutrient vessels at the time of operation, or vascular compression subsequently, could have been partly responsible for the advanced degree of necrosis both in the irradiated and non irradiated areas A considerable part of the tumour in the irradiated area of the paracentral lobule had also been rendered necrotic, presumably by the radiation The aneurysm could well have been radiation induced

Brain substance intervening between the tumours, and occupying the more central part of the irradiated region, presented no change that could be attributed to radiation injury

Case 7 A 9 cm field of the right side of the brain was exposed to 5 100 rad given in 9 fractions over a period of 28 days (Table) Death occurred 11 months after the commencement of irradiation

Gross examination Tumour tissue was first encountered in the right frontal lobe about 3 cm deep to the convex cerebral surface All the tumour at this level, as well as most others was within the irradiated volume At deeper levels the tumour occupied much of the frontal lobe Tumour tissue in this region blended with a solid tumour mass situated just in front of the lamina terminalis (Fig 7 a) Neoplastic tissue was also found in the septal region, the rostral half of the corpus callosum, and the corresponding part of the gyrus cinguli The entire thalamus was also densely infiltrated by tumour continuous with the mass in front of the lamina terminalis Only the rostral half of the thalamus was irradiated (Fig 7 a)

Tumour extended across the midline into the white matter of the left frontal lobe via the corpus callosum, occupying an area about 2 5 cm in diameter At its farthest limit the tumour extended about 3 cm from the midline The lateral and third ventricles were somewhat enlarged but not the fourth ventricle

No abnormality was observed in irradiated tissue free from tumour The effects of the proton irradiation extended 7 7 cm from the surface of the right side of the head and across the midline but fell somewhat short of the growth in that hemisphere

Microscopy The tumour was classed as an astrocytoma grade IV on the basis of cellular anaplasia, evident over a wide area Tumour giant cells were relatively few in most areas, numerous in others



a



b

Fig. 6 a) Same case as in Fig. 5 From non irradiated part of tumour in paracentral lobule Narrow elongated cells are aligned perpendicular to the surface of the vascular adventitia (to the left) Elsewhere some cell clusters tend to form

ted temporal lobe area Anaplastic tumour cells in a column in between tissue which is partially or totally necrotic ×100 Luxol fast blue PAS haematoxylin



c

from its periphery *a florid growth* of anaplastic cells with an even wider distribution than in the previous section

A parasagittal section on the right side revealed a dense infiltration of tumour cells in the thalamus and *hypothalamus* both *within* and without the irradiated region Tumour necrosis was minimal in both structures, no vascular abnormalities present at site of irradiation

The large solid tumour situated *in front of the lamina terminalis (Fig 7 b)* was necrotic centrally, and vessels in this region were thrombosed and also necrotic Surrounding this solid tumour and extending from the base of the frontal lobe to the septal region (in the irradiated region) was a broad zone in *which much of the tumour* tissue was totally necrotic The same was true for the tumour tissue in the corpus callosum and adjacent white matter

In a parasagittal section from a level just to the left of the midline rampant glioblastoma *multiforme* was *again* observed The head of the caudate nucleus was also densely infiltrated by tumour cells

P T A H preparations demonstrated fibrillary gliosis of moderate degree sparsely *scattered around the vessels in tumour tissue*

A survey of white matter in regions unoccupied by tumour cells, yet within the irradiated area revealed no evidence of necrosis

Comment There was a wide dissemination of tumour cells both inside and outside the irradiated region A small proportion of tumour in the more central part of this area was *apparently* rendered *necrotic* by the *radiation* No evidence was found that tissue not occupied by tumour had undergone delayed necrosis

Discussion

1) The equipment used was fully capable of delivering irradiation in all 67 sessions, safely and with minimal side effects Sedation was unnecessary and no patient objected to head fixation *Checking of the position of the patient s head after each session* showed that the entrance and exit points of the central beam axes did not shift more than two millimeters

2) No evidence of an acute *cerebral oedema* was *observed in any of the seven* patients The position of the indicators on the resection surfaces, as observed on films remained unchanged It appears that the sharply demarcated proton beam allows as much as 700 rad *to be administered twice a week* without risk of an undue reaction provided that the treatment is given postoperatively and provided that the initial exposure to 300 rad evokes no signs of an oedematous reaction

3) Microscopy *of the four cases revealed that the* irradiated brain tissue free from tumour was unaltered except for minor changes attributable to oedema The latter might be due to circulatory disturbances brought about by the presence of tumour

With respect to the effects of *high-energy* protons on neoplastic tissue in the



a



b

Fig 7 a) Case 7 Midsagittal section The perimeter of the radiation area indicated by dots Tumour in front of the lamina terminalis The thalamus is expanded as a result of tumour growth The hemorrhagic septal area also contains tumour as does the corpus callosum b) Cerebral white matter in the irradiated area Nerve fibers are widely separated from one another and necrotic Anaplastic tumour cells have infiltrated the tissue ×250 Luxol fast blue PAS haematoxylin

In the irradiated part of the brain at a superficial level there were large areas of white matter in which the fibers were demyelinated and widely separated from one another although oedema fluid was not observed however anaplastic tumour cells were seen among these fibers (Fig 7 b) numerous rostrally and less frequent caudally Tumour cells of the same kind infiltrated the entire width of the basal frontal cortex in several regions no neoplastic cells were found in non irradiated tissue

On the section through the level of the hippocampus and the temporal horn of the lateral ventricle a similar appearance was found but here anaplastic cells were ubiquitous having densely infiltrated the tissue both white and grey far beyond the irradiated area The brain tissue immediately above adherent hyperplastic dura surrounding the frontal pole was largely necrotic

A little deeper solid tumour was encountered in the white matter and radiating

The use of high-energy protons in the postoperative treatment of malignant glioma will probably not increase the mean survival time drastically. In future series the same principles with respect to the selection of irradiation field will probably be adhered to, whereas the effective tumour dose might be increased. If the relative vulnerability of tumour cells could be increased, the field size might be enlarged to increase the chance that all neoplastic tissue would be irradiated.

Acknowledgements

The authors are greatly indebted to the staff of the Gustaf Werner Institute, making the treatment possible, and to Professor B. Nohrman, former head of the Department of Radiation therapy, Uppsala University, for valuable clinical advice.

For technical work in the preparation of the brain sections we wish to express appreciation to Nancy Call and Katherine Surı.

SUMMARY

Fractionated irradiation with high-energy protons was given postoperatively to seven patients with malignant glioma. In four cases in which detailed microscopic examinations were performed, radiation induced tumour necrosis was evident but in all four cases viable tumour cells were also observed. No abnormalities that could be attributed to radiation were observed in brain tissue free from tumour. The therapeutic results were comparable to the results achieved by other modern therapies. The results support the view that the RBE of high-energy protons is similar to that for ^{60}Co radiation. It is suggested that a larger radiation dose, delivered by a homogeneous, well-defined proton field could possibly result in an improved therapeutic result without undue risk of injury to normal brain tissue.

ZUSAMMENFASSUNG

Eine fraktionierte Bestrahlung mit hochenergetischen Protonen wurde sieben Patienten mit Glioma multiforme postoperativ gegeben. In vier Fallen, bei denen detaillierte mikroskopische Untersuchungen durchgefuhrt wurden, fanden sich eine Strahleninduzierte Tumornekrose, es wurden jedoch auch in allen vier Fallen viable Tumorzellen beobachtet. Keine Veranderungen, die der Bestrahlung zugeschrieben werden konnten, wurden im Tumor freien Gehirngewebe beobachtet. Die therapeutischen Ergebnisse waren denjenigen, die mit anderen modernen Therapien erhalten werden, vergleichbar. Die Ergebnisse stutzen die Auffassung, dass die RBE hochenergetischer Protonen der von ^{60}Co Strahlung ahnlich ist. Es wird vermutet, dass eine hohere Strahlendosis, die durch ein homogenes, gutdefiniertes Protonenfeld gegeben wird, moglicherweise zu einem besseren therapeutsichen Ergebnis ohne Risiko einer Schadigung normalen Gehorngewebes fuhren mag.

RESUME

Sept malades atteints de glioblastome multiforme ont subi une irradiation post opératoire fractionnee au moyen de protons de haute energid. Dans 4 cas ou on a fait des exa-

present material, there was clear evidence of radiation induced tumour necrosis in three of the cases, and probable necrosis of minor degree in the fourth (case 7) The fibrillary gliosis observed (in P T A H preparations) in partly necrotic tumour and brain tissue in three of the cases, but particularly in case 3, is considered to be a reaction of astroglial cells to vascular and tissue changes induced by the radiation A similarly intense reaction has been observed previously (HAYMAKER et coll 1972) Both the malignant ependymoma and the anaplastic astrocytomas were sensitive to radiation

NIELSEN et coll (1972) reported on the effects of large single doses of high energy protons on human brain tissue They found that the RBE of these protons was much the same as for conventional roentgen rays The doses used in the present investigation, when expressed in normal tissue CRE (KIRK et coll 1971), were approximately 2 000 reu (range 1 800–2 125 reu) The dosage involving a great risk of cerebral necrosis corresponds to a CRE of about 2 200 reu and the lowest dosage known to produce such a sequela corresponds to about 1 500 reu (LINDGREN 1958)

The relevance of the CRE concept in this context may be questionable but is included for reference purpose No attempts were made to compensate for differences in irradiated volumes

The small autopsy material and the relatively short observation period in the present cases do not allow any definite conclusions to be drawn regarding the proton RBE Several factors influence the response to radiation, such as the state of vessels of the brain (HOPEWELL et coll 1970) and the volume of tissue irradiated The integral doses used, with reference to maximum tumour dose, were 50 to 75 per cent lower than are usually given This was partly due to the well defined irradiated volume The importance of the dose volume relationship in radiation therapy was emphasized by JONES (1963) in connection with the assumed absence of collateral circulation in the cerebral hemisphere Considering these factors, it would seem to follow that there are no findings that would contradict the view that the RBE of high energy protons is about the same as for ^{60}Co photons In agreement with this assumption is the degree of skin reaction At the portal of entry area, the irradiation dose which was 80 to 100 per cent of the tumour dose, caused a dermatitis sicca, some exudative dermatitis with much epilation

4) Choice of optimum field size poses the problem of how best to suppress reproductive capacity of the tumour cells and still avoid appreciable injury to the normal tissue With a small field the risk of tumour cells lying outside the irradiated area must be weighed against the advantages of a larger tumour dose In all four autopsied brains was not only necrotic tumour tissue, but also viable tumour cells, found within the volume considered to have been irradiated The reasons why tumour was present at autopsy are not evident

5) The survival period of the proton-irradiated patients was similar to that reported from other types of irradiation The quality of life during this period was also found to be comparable to that reported by others (BETTY 1964, BOUCHARD 1966)

LEGRÉ J, AMALRIC R et PADAUT J L irradiation des glioblastomes multiformes. Acta radiol Ther Phys Biol 8 (1969), 118

LINDGREN M On tolerance of brain tissue and sensitivity of brain tumours to irradiation. Acta radiol (1958) Suppl No 170

NIELSEN S L, KJELLBERG R M, ASBURY A K and KOEHLER A M Neuropathologic effects of proton beam irradiation in man I Dose response relationships after treatment of intracranial neoplasm. Acta neuropath (Berl) 20 (1972) 348

RUSSELL D S and RUBINSTEIN L J Pathology of tumours of the nervous system Edward Arnold Ltd, London 1960

SCHERER H J The forms of growth in gliomas and their practical significance Brain 63 (1974) 2

rgans and malignant tumours.

supratentorial gliomas. Brit J Radiol 36 (1963) 645

ZULCH K J Roentgen sensitivity of cerebral tumours Acta radiol Ther Phys. Biol 8 (1969) 92

mens microscopiques détaillés, on a trouvé des signes de nécrose tumorale due aux radiations, mais dans ces 4 cas on a aussi observé des cellules tumorales viables Les auteurs n ont pas observé d anomalie pouvant etre attribuée aux radiations dans le tissu cérébral non tumoral Les résultats thérapeutiques ont été comparables à ceux des autres méthodes modernes de traitement Ces resultats confirment l opinion que l EBR des protons de haute énergie est semblable à celle du rayonnement du ^{60}Co Les auteurs pensent qu une dose de rayonnement plus importante, délivrée par un champ de protons homogène bien limité pourrait ameliorer le désultat thérapeutique sans risque inacceptable de lésion du tissu cérébral normal

REFERENCES

BERG N O and LINDGREN M Relation between field size and tolerance of rabbit s brain to roentgen (200 kV) irradiation via slit-shaped field Acta radiol Ther Phys Biol 1 (1963), 147

BETTY M J Quality of survival in treated patients with supratentorial glioma J Neurol Neurosurg Psychiat 27 (1964), 556

BOUCHARD J Radiation therapy of tumours and diseases of the nervous system Lea & Febiger, Philadelphia 1966

CONCANNON J P, KRAMER S and BERRY R The extent of intracranial gliomata at autopsy and its relationship to techniques used in radiation therapy of brain tumours Amer J Roentgenol 34 (1960), 99

GRAFFMAN S and JUNG B Clinical trials in radiotherapy and the merits of high energy protons Acta radiol Ther Phys Biol 9 (1970), 1

— — NOHRMAN B A and BERGSTRÖM R Supplementary treatment of nasopharyngeal tumours with high energy protons Acta radiol Ther Phys Biol 6 (1967), 361

— HUGOSSON R, JUNG B and NOHRMAN B A High energy protons in postoperative treatment of glioblastoma multiforme *In* Progress in Radiology Proc XI Int Congress of Radiology, Rome 1965

HAYMAKER W, RUBINSTEIN L J and MIQUEL J Brain tumors in irradiated monkeys Acta neuropath (Berl) 20 (1972) 267

HOPEWELL J W and WRIGHT E A The nature of latent cerebral irradiation damage and its modification by hypertension Brit J Radiol 43 (1970), 161

JOHANSSON K I Deoxyribonucleic acid metabolism in the small intestine in vivo and in vitro A study of the normal and 180 MeV proton or ^{60}Co gamma irradiated mouse Abstracts of Uppsala Dissertations from the Faculty of Science 204, 1972

JONES A Radiotherapy of gliomata Clinical and biological factors Proc roy Soc Med 53 (1963), 673

JUNG B, RIKNER H G and SJOGREN O On the production and monitoring of broad, homogeneous radiation fields of high energy protons with special reference to the spatial and temporal dose distribution To be published in a Suppl to Acta radiol

KARLSSON B Methoden zur Berechnung und Erzielhung einiger fur die Tiefentherapie mit Protonen gunstigen Dosisverteilungen Strahlentherapie 124 (1964) 481

KERNOHAN J W, MABON R F, SVIEN H J and ADSON A W Symposium on a new and simplified concept of gliomas Astrocytomas Proc Mayo Clin 24 (1949), 71

KIRK J, GRAY W M and WATSON R R Cumulative radiation effect Part 1 Fractionated treatment regimes Clin Radiol 22 (1971) 145

LARSSON B Pre therapeutic physical experiment with high energy protons Brit J Radiol 34 (1961), 143

Material and Methods

The material consisted of three groups

(1) Seven patients with thyroid malignancy, cytologically or histologically confirmed 3 with anaplastic, 2 with follicular and 2 with papillary carcinomas One of the patients with follicular carcinoma had a bone metastasis, in the others the malignancy was confined to the thyroid gland In addition, two patients with a cytologically confirmed recurrence of papillary thyroid carcinoma in the lymph glands of the neck subsequent to surgical thyroidectomy and modified neck dissection were included

(2) Three patients with benign thyroid adenoma, microscopically confirmed

(3) Six patients with diffuse or nodular goitre, the diagnosis was based upon the clinical findings and ^{131}I or $^{99}Tc^{m}$-pertechnetate scintigraphy

In all cases scintigraphy of the neck and upper thoracic region with $^{99}Tc^{m}$-Solcocitran and ^{131}I or $^{99}Tc^{m}$-pertechnetate was performed before therapy In the patient with a bone metastasis, this area was also examined using ^{131}I and $^{99}Tc^{m}$-Solcocitran

One mCi of $^{99}Tc^{m}$ pertechnetate or 50 μCi of ^{131}I were administered 1 and 24 hours, respectively, before the scanning procedure When using $^{99}Tc^{m}$-Solcocitran, 10 mCi were injected intravenously and the scanning procedure was performed 2 and 4 hours after the injection, in a few instances also 30 min after the administration The rectilinear scanner Picker Magnascanner III with a 7 6 cm (3 inch) crystal and a focusing thyroid collimator was used In order to exclude any remaining activity from a previous examination with $^{99}Tc^{m}$-pertechnetate, an interval of at least 3 days was introduced before the $^{99}Tc^{m}$-Solcocitran examination By the use of a pulse height analyzer, the $^{99}Tc^{m}$-Solcocitran scan was found not to be influenced by a previous ^{131}I examination

The preparation of $^{99}Tc^{m}$ Solcocitran was made in strict accordance with the instructions supplied by the manufacturer, and each preparation was checked for radiochemical purity by thin layer chromatography These chromatograms were developed on Silica gel (Gelman ITLC SG, Stockholm), the solvents used were 0 9 per cent sodium chloride and 100 per cent methylethylketone No free $^{99}Tc^{m}$ pertechnetate or reduced $^{99}Tc^{m}$ contaminants could be demonstrated

Results

The uptake of ^{131}I or $^{99}Tc^{m}$ pertechnetate was decreased in all primary tumours compared with the one in normal thyroid tissue Also in the bone metastasis from the follicular carcinoma, an uptake of ^{131}I was found In the lymphoglandular metastases in the two cases with recurrence of papillary carcinoma no uptake of ^{131}I was recorded

The relative uptake of $^{99}Tc^{m}$ Solcocitran was neither decreased nor increased in any of the areas examined, regardless of the interval between the injection of the substance and the scanning procedure

FROM THE GENERAL DEPARTMENT, RADIUMHEMMET (DIRECTOR PROF J EINHORN) AND THE DEPARTMENT OF CLINICAL RADIATION PHYSICS, THE NATIONAL INSTITUTE OF RADIATION PROTECTION (DIRECTOR: PROF. R WALSTAM), S-104 01 STOCKHOLM, SWEDEN

TRIALS TO DIFFERENTIATE THYROID TUMOURS BY THE USE OF $^{99}Tc^{m}$-SOLCOCITRAN

G LUNDELL and SUSANNA CASSEBORN

The value of ^{131}I and $^{99}Tc^{m}$-pertechnetate is well documented in the examination of thyroid disease Patients with a decreased uptake in a nodule, as compared to normal thyroid tissue, are usually regarded as having a malignant lesion until otherwise proven

Several attempts to use other substances in the differential diagnosis of thyroid tumours have been made, among these ^{75}Se-methionine (THOMAS et coll 1969), ^{131}Cs-chloride (ALEVIZAKI et coll 1973) and ^{67}Ga-citrate (KOUTRAS et coll 1973) have been tried However, a definite differentiation of malignant from benign lesions using any of these substances has not been possible

Recently, a citrate-tin compound (Solcocitran, Solco Nuclear Inc, Birsfelden, Switzerland) has been introduced which, after labelling with $^{99}Tc^{m}$, is advocated for the detection of malignant lesions in bone and brain It is stated (Solco Nuclear 1974), that $^{99}Tc^{m}$-Solcocitran has a high and selective uptake in neoplastic tissue and that no false positive or false negative cases have been found in examined groups with bone or brain lesions

Therefore it seemed of interest to investigate the value of $^{99}Tc^{m}$-Solcocitran in the differentiation of thyroid lesions

Submitted for publication 12 May 1975

Material and Methods

The material consisted of three groups

(1) Seven patients with thyroid malignancy, cytologically or histologically confirmed 3 *with anaplastic*, 2 *with follicular* and 2 with papillary carcinomas One of the patients with follicular carcinoma had a bone metastasis, in the others the malignancy was confined to the thyroid gland In addition, two patients with a cytologically confirmed recurrence of papillary thyroid carcinoma in the lymph glands of the neck subsequent to surgical thyroidectomy and modified neck dissection were included

(2) Three patients with benign thyroid adenoma, microscopically confirmed

(3) Six patients with diffuse or nodular goitre, the diagnosis was based upon the clinical findings and ^{131}I or ^{99}Tc^{m}-pertechnetate scintigraphy

In all cases scintigraphy of the neck and upper thoracic region with ^{99}Tc^{m} Solcocitran and ^{131}I or ^{99}Tc^{m}-pertechnetate was performed before therapy In the patient with a bone metastasis, this area was also examined using ^{131}I and ^{99}Tc^{m}-Solcocitran

One mCi of ^{99}Tc^{m}-pertechnetate or 50 μCi of ^{131}I were administered 1 and 24 hours, respectively, before the scanning procedure When using ^{99}Tc^{m}-Solcocitran, 10 mCi were injected intravenously and the scanning procedure was performed 2 and 4 hours after the injection, in a few instances also 30 min after the administration The rectilinear scanner Picker Magnascanner III with a 7 6 cm (3 inch) crystal and a focusing thyroid collimator was used In order to exclude any remaining activity from a previous examination with ^{99}Tc^{m}-pertechnetate, an interval of at least 3 days was introduced before the ^{99}Tc^{m}-Solcocitran examination By the use of a pulse height analyzer, the ^{99}Tc^{m} Solcocitran scan was found not to be influenced by a previous ^{131}I examination

The preparation of ^{99}Tc^{m}-*Solcocitran was made in strict accordance with the instructions* supplied by the manufacturer, and each preparation was checked for radiochemical purity by thin layer chromatography These chromatograms were developed on Silica gel (Gelman ITLC SG, Stockholm), the solvents used were 0 9 per cent sodium chloride and 100 per cent methylethylketone No free ^{99}Tc^{m}-pertechnetate or reduced ^{99}Tc^{m} contaminants could be demonstrated

Results

The uptake of ^{131}I or ^{99}Tc^{m}-pertechnetate was decreased in all primary tumours compared with the one in normal thyroid tissue Also in the bone metastasis from the follicular carcinoma, an uptake of ^{131}I was found In the lymphoglandular metastases in the two cases with recurrence of papillary carcinoma no uptake of ^{131}I was recorded

The relative uptake of ^{99}Tc^{m}-Solcocitran was neither decreased nor increased in any of the areas examined, regardless of the interval between the injection of the substance and the scanning procedure

FROM THE GENERAL DEPARTMENT, RADIUMHEMMET (DIRECTOR PROF J EINHORN) AND THE DEPARTMENT OF CLINICAL RADIATION PHYSICS, THE NATIONAL INSTITUTE OF RADIATION PROTECTION (DIRECTOR PROF R WALSTAM), S-104 01 STOCKHOLM, SWEDEN

TRIALS TO DIFFERENTIATE THYROID TUMOURS BY THE USE OF $^{99}Tc^{m}$-SOLCOCITRAN

G LUNDELL and SUSANNA CASSEBORN

The value of ^{131}I and $^{99}Tc^{m}$-pertechnetate is well documented in the examination of thyroid disease Patients with a decreased uptake in a nodule, as compared to normal thyroid tissue, are usually regarded as having a malignant lesion until otherwise proven

Several attempts to use other substances in the differential diagnosis of thyroid tumours have been made, among these ^{75}Se methionine (THOMAS et coll 1969), ^{131}Cs chloride (ALEVIZAKI et coll 1973) and ^{67}Ga citrate (KOUTRAS et coll 1973) have been tried However, a definite differentiation of malignant from benign lesions using any of these substances has not been possible

Recently, a citrate-tin compound (Solcocitran, Solco Nuclear Inc, Birsfelden, Switzerland) has been introduced which, after labelling with $^{99}Tc^{m}$, is advocated for the detection of malignant lesions in bone and brain It is stated (Solco Nuclear 1974), that $^{99}Tc^{m}$-Solcocitran has a high and selective uptake in neoplastic tissue and that no false positive or false negative cases have been found in examined groups with bone or brain lesions

Therefore it seemed of interest to investigate the value of $^{99}Tc^{m}$-Solcocitran in the differentiation of thyroid lesions

Submitted for publication 12 May 1975

FROM THE INSTITUTE OF PATHOLOGY, THE E N T DEPARTMENT AND THE RADIUM CENTRE, MUNICIPAL HOSPITAL, UNIVERSITY OF ÅRHUS, DK 8000 ÅRHUS, DENMARK

EPIDERMOID CARCINOMA OF THE LIP

Histologic grading in the clinical evaluation

C LUND H SOGAARD, O ELBROND, K JORGENSEN and A P ANDERSEN

The prognosis of epidermoid carcinoma of the lip is usually favourable An exception consists of cases of recurrence or residual tumour after the primary treatment and in particular the occurrence of regional lymph node metastases, initially or later

A correlation between the clinical assessment and standardized graded histologic examination is the object of the present report in order to distinguish the potential risk group of patients in whom recurrence or metastases were particularly likely to occur Such a group would require special therapeutic measures, e g frequent follow-up examinations and possibly elective neck dissections

This series consists of a part of the major material of 869 patients treated for carcinoma of the lip previously analysed clinically (JORGENSEN et coll 1973) The present part comprises 438 patients treated during the period 1955–1966, since continuous microscopic material for evaluation was not available before 1955

Clinical aspects Among the 438 patients with microscopically confirmed epidermoid carcinoma of the lip recurrence or residual tumour after the primary treatment occurred in 53 (12 1 per cent), lymph node metastases in 33 (7 6 per cent), of these 10 (2 3 per cent) were primary and 23 (5 3 per cent) secondary, distant metastases

Submitted for publication 25 April 1974

The ^{99}Tc^{m}-Solcocitran was thus of no value in the differentiation of benign from malignant thyroid lesions. Furthermore, no increased uptake was found in the bone metastasis from the follicular carcinoma.

Acknowledgement

Solcocitran was supplied by AB Atomenergi, Nykoping, Sweden

SUMMARY

The uptake of ^{99}Tc^{m}-Solcocitran was examined in 16 patients with thyroid disease The relative uptake could not be used to distinguish between malignant and benign thyroid tumours

ZUSAMMENFASSUNG

Die Aufnahme von ^{99}Tc^{m}-Solcocitran wurde bei 16 Patienten mit Erkrankung der Thyreoidea untersucht Die relative Aufnahme konnte nicht verwendet werden, um zwischen malignen und benignen Thyreoideatumoren zu unterscheiden.

RÉSUMÉ

Les auteurs ont étudié chez 16 malades atteints d'affection thyroid enne la fixation du ^{99}Tc^{m}-Solcocitran La fixation relative ne permet pas de distinguer entre les tumeurs thyroidiennes bénignes et malignes

REFERENCES

ALEVIZAKI C D, GHEORGHIADIS N, GONTICAS S S, IKKOS D D, KATSAS A and TSIALAS S Diagnostic value of ^{131}Cs scanning in thyroid malignancy 11 Internationale Jahrestagung der Gesellschaft fur Nuklearmedizin, Athens (1973), 28

KOUTRAS D A, PANDOS P, SFONTOURIS J, KOUKOULOMMATI-SPENTZA A and MALAMOS B Thyroid scanning with ^{67}Ga and ^{131}I 11 Internationale Jahrestagung der Gesellschaft für Nuklearmedizin E V, Athens (1973), 89

Solco Nuclear, Birsfelden, Switzerland Solcocitran®–^{99m}Tc, a tumour scanning agent Preliminary report, 1974

THOMAS JR C G, PEPPER F D and OWEN J Differentiation of malignant from benign lesions of thyroid gland using complementary scanning with 75-selenomethionine and radioiodide Ann Surg 170 (1969), 396

Table 3

Microscopic grading

	Points 1	2	3	4
Appearance	Exophytic papillomatous	Inverted papillomatous	Small cords and groups of cells	Marked cellular dissociation
Cytoplasmic differentiation (keratinization)	High >50% keratinized	Moderate 20–50% keratinized	Poor 5–20% keratinized	None 0–5%
Nuclear differentiation (BRODERS)	High >75% mature	Moderate 75–50% mature	Poor 50–25% mature	None 0–25% mature
Mitosis*	Single 0–1	Moderate number 0–3	Great number 0–5	Numerous >5
Mode of invasion (modus)	Well defined borderline	Cords, less marked borderline	Groups of cells. No dist. borderline	Diffuse growth
Stage of invasion (depth)**	Possible invasion	Microinvasion (few cords)	Nodular into submucosa	Invasion deeper than submucosa
Vascular invasion	None	Possible	Lymph. vessels	Blood vessels
Cellular response (plasma-lymphocytic)	Marked (continuous rim)	Moderate (many large patches)	Slight (a few small patches)	None

* Minimum evaluation on 5 fields, 250 ×

** 'No invasion' may constitute preinvasive lesion

Table 4

Microscopy of 463 biopsies

Total series	Structures	Cytopl diff	Nuclear diff	Mitosis	Mode	Depth	Vasc invasion	Cell response	Average score
Estimated parameters	461	463	463	462	451	196	449	457	
Number of points	1 008	843	1 009	829	916	570	829	777	
Microscopic score	2.2	1.8	2.2	1.8	2.0	2.9	1.9	1.7	2.1

Table 1

Treatment in 33 cases with regional lymph node metastases

	No of cases	Died of		Alive without recurrence at 5 years
		carcinoma of the lip	other causes	
Surgery	19	5	2	12
Irradiation	14	13		1
Total	33	18	2	13

developed in 4 (0 9 per cent) Secondary lymph node metastases are defined as metastases which do not manifest themselves until after the primary treatment of the tumours and constituted 23/33 (70 per cent) of the total metastases

The regional lymph node metastases were treated either by surgery or by irradiation (Table 1). Eighteen of the patients (55 per cent) died of carcinoma of the lip, indicating the prognostic importance of the metastases The T classification (UICC 1968) in relation to the frequency of secondary metastases is given in Table 2

The frequency of the secondary metastases, the local recurrences and the residual tumours increases from the T1 to the T3 groups (Table 2, col 2). An evident increased frequency of secondary metastases is also encountered in patients with local recurrence or residual tumour (23 per cent), most marked in the T3 group (46 per cent) (Table 2, col 4).

Histology. Carcinoma of the lip is almost invariably of the epidermoid type of a varying differentiation and growth Thus, the classification and grading must consider both the tumour cell population and the tumour–host relationship

The grading system used (Table 3) is based upon principles given by JACOBSSON et coll. (1973) and JACOBSSON (1973) in their investigation on glottic carcinoma Each of the 8 parameters is graded from 1 to 4, each grade being strictly defined to obtain reproducible results, comparable also with the evaluation of other pathologists

Table 2

Frequency of secondary metastases in relation to T-classification and occurrence of local recurrence and residual tumour

	No recurrence	Frequency of secondary metastases	Local recurrences and residual tumours	Frequency of secondary metastases
T1	207	4 (2 %)	14	1 (7 %)
T2	143	3 (2 %)	20	4 (20 %)
T3	31	5 (16 %)	13	6 (46 %)
T4	0	0	0	0
Total	381	12 (3 %)	47	11 (23 %)

Table 3

Microscopic grading

	Points 1	2	3	4
Appearance	Exophytic papillomatous	Inverted papillomatous	Small cords and groups of cells	Marked cellular dissociation
Cytoplasmic differentiation (keratinization)	High >50% keratinisized	Moderate 20–50% keratinisized	Poor 5–20% keratinisized	None 0–5%
Nuclear differentiation (BRODERS)	High >75% mature	Moderate 75–50% mature	Poor 50–25% mature	None 0–25% mature
Mitosis*	Single 0–1	Moderate number 0–3	Great number 0–5	Numerous >5
Mode of invasion (modus)	Well defined borderline	Cords, less marked borderline	Groups of cells. No dist. borderline	Diffuse growth
Stage of invasion (depth)**	Possible invasion	Microinvasion (few cords)	Nodular into submucosa	Invasion deeper than submucosa
Vascular invasion	None	Possible	Lymph vessels	Blood vessels
Cellular response (plasma-lymphocytic)	Marked (continuous rim)	Moderate (many large patches)	Slight (a few small patches)	None

* Minimum evaluation on 5 fields, 250×

** 'No invasion' may constitute preinvasive lesion

Table 4

Microscopy of 463 biopsies

Total series	Structures	Cytopl diff	Nuclear diff	Mitosis	Mode	Depth	Vasc. invasion	Cell response	Average score
Estimated parameters	461	463	463	462	451	196	449	457	
Number of points	1 008	843	1 009	829	916	570	829	777	
Microscopic score	2 2	1 8	2 2	1 8	2 0	2.9	1 9	1 7	2 1

Fig 1 Distribution of total series of 438 patients including 33 cases with regional lymph node metastases (black bars) in relation to score value

Fig 2 Frequency of regional lymph node metastases in relation to score value ▭ primary metastases ▭ secondary metastases

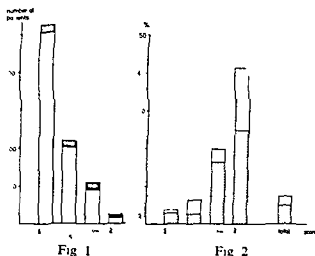


Fig 1 Fig 2

The microscopy was performed by two pathologists, both unaware of the clinical findings

Each specimen can obtain a maximum sum of 32 (4 × 8) It was not always possible to assess all parameters, because of defective specimens Hence, a score value, defined as the total sum divided by the number of parameters assessed, was used The

Table 5

Relationship between clinical state and microscopic grading

	No of cases	Structure	Cytopl diff	Nuclear diff	Mitosis	Mode (type)	Depth	Vasc invasion	Cell response	Average score
Total material	(463)	2 2	1 8	2 2	1 8	2 0	2 9	1 9	1 7	2 1
Material with rec and metastases excluded	(393)	2 1	1 8	2 1	1 7	2 0	2 8	1 8	1 7	2 0
Rec or metastases	70	2 4	2 2	2 6	2 2	2 3	3 6	2 2	1 9	2 4
Recurrences only	37	2 0	2 0	2 5	1 9	2 2	3 5	2 1	1 9	2 3
Metastases only	17	2 2	2 0	2 4	2 4	2 1	3 7	1 9	1 9	2 3
Rec and metastases	16	2 8	2 7	3 1	2 8	2 7	3 5	3 7	2 1	2 8
Prim metastases	10	2 6	2 3	2 7	2 5	2 3	4 0	2 4	2 2	2 6
Sec. metastases	23	2 5	2 2	2 8	2 5	2 3	3 6	2.3	1 9	2 5
Died of carcinoma	18	2 7	2 5	2 9	2 5	2 6	4 0	2 4	2 2	2.7

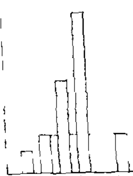


Fig 3

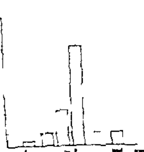


Fig 4

Fig. 3 Frequency of residual tumours and recurrences in relation to score value

Fig. 4 Frequency of deaths from carcinoma of the lip in relation to score value.

microscopic material consisted of 463 biopsies (438 patients), some being from a *residual tumour, a recurrence* or *a new primary* neoplasm The clinical histologic correlation includes only the score values for the primary biopsy The growth into the depth could only be assessed in 196 specimens, i e 41 per cent (Table 4), thus creating an inaccuracy also of other parameters which often have a higher score value in the depth of an infiltrating lesion

Clinical and microscopic correlation The score values were correlated with the group of patients with (1) metastases, (2) residual tumour or recurrence, (3) metastases and residual tumour or recurrence, (4) fatal cases, and (5) T classifiaction

Table 5 presents the correlation of clinical assessment and microscopic score values for the first 4 groups The nuclear differentiation and the growth in the depth contribute quite particularly to a higher score value in groups with recurrence and metastases, whereas the number of mitoses exerts its influence mainly in the group with metastases The parameter cellular response is somewhat higher in the four groups as in the report by BENNETT et coll (1971)

Arbitrary classification of the 438 patients by score value (Fig 1) reveals that 263 (60 per cent) belong to the group with the lowest grade of malignancy Metastases occur in all groups, but with a significantly increased frequency ($p < 0\ 05$) at a score value exceeding 2 5 (Fig. 2)

Table 6

Relationship between T grouping and score value

	2	2 1 2 5	2 6–3 0	≤ 3 1
T1	146 221 66 %	56 221 25 %	15/221 7 %	4/221 2 %
T2	97/165 59 %	39/165 24 %	23/165 14 %	6/165 4 %
T3	18/50 36 %	13/50 26 %	16/50 32 %	3/50 6 %

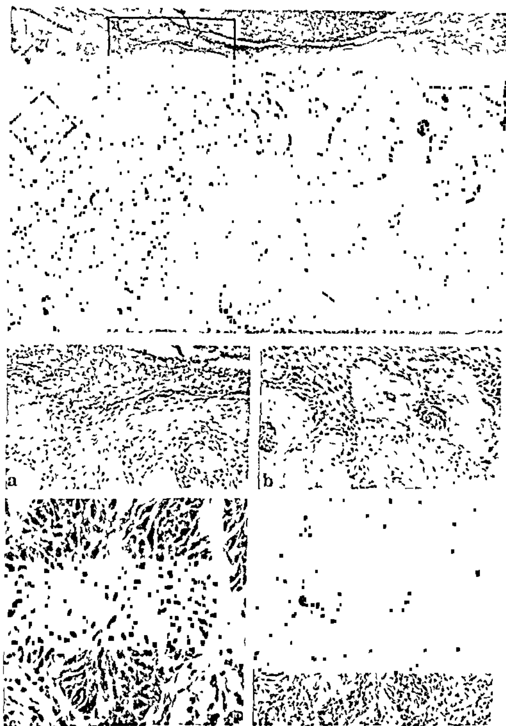


Fig 6 Photomicrograph A relatively highly differentiated epidermoid carcinoma (general view) may vary from surface to depth (insets)

The present analysis of the results of a multifactorial microscopic grading (Table 3) of the primary tumours in a TNM classified series of epidermoid carcinoma of the lip reveals a statistically significant correlation between the microscopic grading and (1) the frequency of local residual tumours and recurrences (2) the frequency of metastases and (3) mortality (Fig 5) These results agree with those of JACOBSSON in his report on laryngeal carcinoma However, it was found that microscopic grading was significantly correlated to the TNM classification Although it was not possible within each T stage to demonstrate a statistically significant correlation between the microscopic grading and the frequency of residual tumour or recurrence and lymph node metastases, the tendency seems to be beyond doubt The absence of significance may be due to clinical or microscopic uncertain evaluation of the lesion or to inexact calculation Radium intubation may afford uncertain dosage, and possibly some residual tumour and recurrences may be ascribed to this factor It may also be emphasized (Table 4) that only 41 per cent of the biopsies allowed microscopic evaluation of all parameters Uncertain calculation was caused by the numerically small T groups (Tables 7, 8)

Conclusion The microscopic grading proved correlated to the TNM system and gave, in addition, supplementary prognostic information It seems justified to suggest that the system should primarily be applied to other highly differentiated epidermoid carcinomas

A superficial biopsy is not satisfactory for a thorough evaluation of a neoplasm In a case of a tumour of the lip this means a wedge-shaped biopsy into the centre and bottom of the tumour (Fig 6)

A prospective investigation including a correlation analysis between microscopic grading and therapeutic principles may possibly elucidate whether this may have consequence with respect to the primary treatment

SUMMARY

A retrospective microscopic evaluation of primary biopsies was carried out in a material of 438 patients with carcinoma of the lip A multifactorial grading system consisting of 8 parameters each sub-divided into 4 grades, was used The degree of malignancy showed a statistically significant correlation to the frequency of metastases frequency of recurrence or residual tumour, mortality and T classification This grading system may allow a separation of risk groups in which special treatment and follow up should be applied

ZUSAMMENFASSUNG

Es wurde eine retrospektive mikroskopische Bewertung der primaren Biopsien eines Materials von 438 Patienten mit Karzinomen der Lippe vorgenommen Ein Multifaktoren Gradierungssystem jedes in 4 Grade aufgeteilt, wurde verwendet Der Umfang der Malignitat zeigte eine statistisch signifikante Korrelation zur Frequenz von Metastasen, zur Fre-

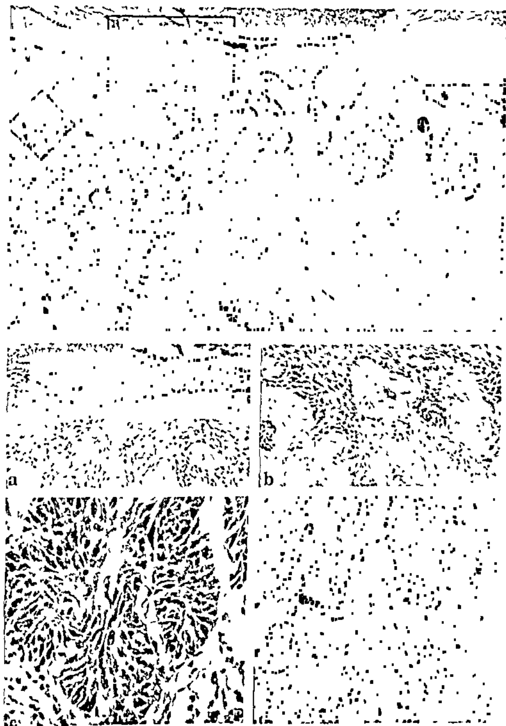
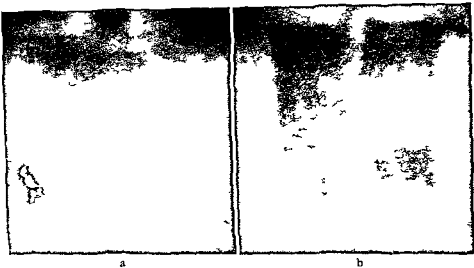


Fig. 6. Photomicrograph. A relatively highly differentiated epidermoid carcinoma (general view) may vary from surface to depth (insets).



F g 7 Sk n react on at end of treatment a) $T = 29$ days and b) max mal reaction 10 days later $T = 39$ days Fract onation schedules R ght f eld 5 267 rad p r week and $RD = 5\,500$ rad left field 2×500 rad p r week and RD 4 500



F g 8 P gmentat on n one of the pat ents five months after treatment Fract onat on schedules as in F g 7

quenz von Rezidiven oder Resttumoren, der Mortalität und der T Klassifikation Das Gradierungssystem mag eine Absonderung von Risiko Gruppen erlauben, bei welchen eine spezielle Behandling und Nachuntersuchung angewandt werden sollten

RÉSUMÉ

Les auteurs ont fait une étude microscopique rétrospective de biopsies primaires sur une serie de 438 malades atteints de cancer de la lèvre Ils ont utilisé un système de gradation multifactorielle comprenant 8 paramètres chacun subdivisé en 4 grades Le degré de malignité est corrélé de façon statistiquement significative à la fréquence des métastases, à la frequence des récidives ou des tumeurs résiduelles, à la mortalité et à la classification T Ce système de gradation peut permettre de séparer des groupes à risque différent auxque' on devrait appliquer un traitement spécial et une surveillance spéciale

REFERENCES

BENNETT S H, FUTRELL J W, ROTH J A, HOVE R C and KETCHAM A S Prognostic significance of histologic host response in cancer of the larynx or hypolarynx Cancer 28 (1971), 1255

BRODERS A C Squamous cell epithelioma of the lip J Amer med Ass 74 (1920), 656

— Carcinoma grading and practical application Arch of Path (Chic) 2 (1926), 376

— The microscopic grading of cancer *In* Treatment of cancer and allied diseases Chapter IV, p 19 Edited by G T Porch and E M Livingstone Harper and Brothers, New York, London 1940

JAKOBSSON P Å Glottic carcinoma of the larynx Thesis, Stockholm 1973

— ENEROTH C M, KILLANDER D, MOBERGER G and MÅRTENSSON B Histologic classification and grading of malignancy in carcinoma of the larynx Acta radiol Ther Phys Biol 12 (1973), 1

JORGENSEN K, ELBROND O and ANDERSEN A P Carcinoma of the lip A series of 869 cases Acta radiol Ther Phys Biol 12 (1973), 177

LEVER W F Histopathology of the skin J B Lippincott, Philadelphia Toronto 1967

UICC Union Internationale Contre le Cancer, Geneva 1968

ERRATA

Acta radiol Ther Phys Biol 14 (1975), 475

Due to a technical error the colour prints, Fig 7 a and b, have been placed up side down

The CRE formula is also defined at the subtolerance level unlike the NSD formula (ELLIS 1969) The CRE and NSD values are therefore only numerically comparable at the limit of normal connective tissue tolerance We have chosen to use the CRE concept because it allows more straight forward handling The CRE instead of the NSD is therefore referred to in the present report although the discussion below is valid for both systems

Before using formulae like the CRE system in clinical routine it is necessary to prove their reliability experimentally under controlled clinical conditions The present work reports such a test comparing the biologic effect of 2 different treatment sched ules with 2 and 5 irradiations respectively per week under otherwise identical conditions

Material and Methods

Thirteen patients with mammary carcinoma were irradiated postoperatively in the parasternal region bilaterally field size 5 cm × 12 cm The series was designed to give identical CRE values of 1 835 for both fields although they were irradiated with different types of fractionation On the left side 2 irradiations were given per week totally 9 × 500 = 4 500 rad (reference dose) i e N = 9 and T 29 days The right side was irradiated daily 5 times per week during the same time period (29 days) i e 21 irradiations The dose per fraction d for equivalent CRE values to the two areas of irradiation was calculated by means of the equation

$$\left(\frac{29}{9}\right)^{0\,11} 500 \quad 9^{0\,65} \quad \left(\frac{29}{21}\right)^{0\,11} d \quad 21^{0\,65} \qquad d = 262\ rad$$

The total dose given to the right hand field was 21 × 262 rad = 5 500 rad (reference dose) i e N 21 and T 29 days (Fig 1)

The biologic effect of the irradiation was estimated by measuring the skin erythema and pigmentation Both were recorded by means of a photoelectric reflection meter (Photovolt Model 670) An area of approximately 2 5 cm² was illuminated with light of wavelength 578 nm width 8 nm at half maximum received by interference filter (CHU et coll 1960) Light of this wavelength is absorbed by oxyhaemaglobin The reflected light was read (in scale divisions) The increase of pigmentation resul ting from the treatment was registered in the same manner but with light of wave lengths above 660 nm received by a gelatin filter with cut of at 660 nm Meas urements were performed twice weekly commencing before the first treatment In addition the patients were photographed once a week Previous investigations had shown that radiation erythema is generally more marked above the second intercostal space than below it due to a difference in sympathetic tone in this region (ADAMS-RAY 1952 NOTTER et coll 1965) The measurements were therefore performed at 4 points, numbered 1 to 4 (Fig 1) thus enabling comparison of the anatomically equi valent regions 1 and 2 3 and 4 respectively

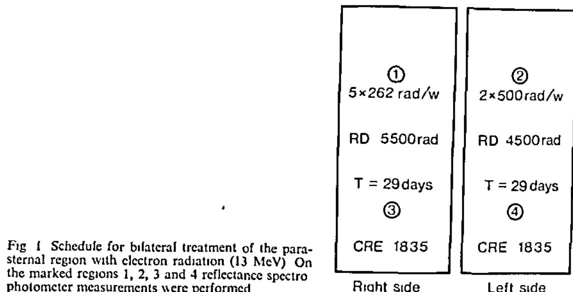


Fig 1 Schedule for bilateral treatment of the parasternal region with electron radiation (13 MeV) On the marked regions 1, 2, 3 and 4 reflectance spectrophotometer measurements were performed

$$CRE = \left(\frac{T}{N}\right)^{0\ 11} d\ N^{0\ 65}$$

where N is the number of treatments of d rad evenly distributed over T days In the formula above ^{60}Co radiation is considered as reference and thus the relative biologic effectiveness, RBE, is equal to 1 (The dimension of CRE is rad days $^{0\ 11}$, which has been called 'reu', the radiation effect unit The unit has been excluded from this report pending a new proposal from ICRU) In the formula, N is assumed to represent the influence of repair of sublethal damage and T the influence of cell repopulation The CRE value corresponding to the tolerance level is considered to be constant for a given type of normal tissue and a given volume, originally proposed by ELLIS in the NSD model (1968) These CRE levels may, however, vary between different centers due to variations in criteria of tolerance

Table 1

Variations in reflectance spectrophotometer measurements in 3 different series 10 measurements in each series

Skin	Wavelength nm	Mean value scale divisions
Non irradiated	578	33 9 + 0 9
(series A)	660	58 8 ± 0 5
Irradiated	578	24 1 ± 0 8
(series B)	660	55 3 ± 0 4
Non irradiated	578	34 4 ± 1 0
(series C)	660	58 3 + 0 3

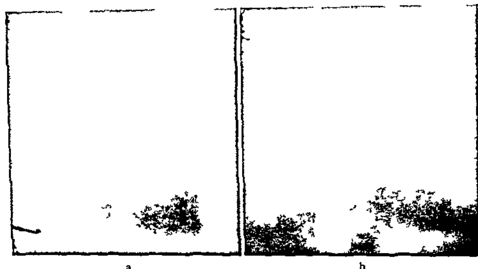


Fig. 7 Skin reaction at end of treatment a) T = 29 days and b) maximal reaction 10 days later T = 39 days Fractionation schedules Right field 5×262 rad per week and RD = 5 500 rad left field 2×500 rad per week and RD = 4 500 rad



Fig. 8 Pigmentation in one of the patients five months after treatment Fractionation schedules as in Fig. 7

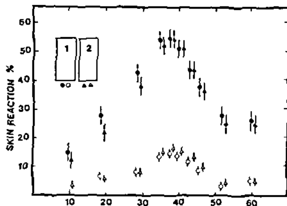


Fig 3

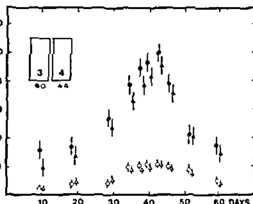


Fig 4

Fig 3 Results of reflectance spectrophotometer measurements of skin erythema (wavelength 578 nm) and pigmentation (wavelength 660 nm) in a patient, in the upper parasternal region Measurement point 1, 5 × 262 rad per week and RD = 5 500 rad, measurement point 2, 2 × 500 rad per week and *RD* = *4 500* rad The treatment series were completed at 29 days Black symbols indicate erythema, white symbols pigmentation

er parasternal region in the same patient as in fig 3
and RD = 5 500 rad, measurement point 4, 2 × 500 rad
n Fig 3)

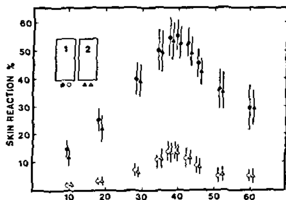


Fig 5

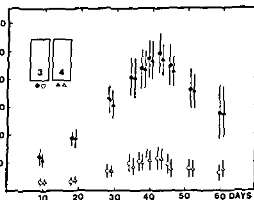


Fig 6

ie patients as in Fig 5
, 2 × 500 rad and RD =
4 500 rad (·)

the type of fractionation (Fig 5) In the lower region (Fig 6) erythema did not become maximal until 11 to 16 days after the completion of treatment i e 40 to 45 days after commencement of the irradiation

The limits of error in the diagram are mainly due to variations in the response to radiation from patient to patient All patients developed a dry erythema, bordering on an exudative reaction, in the center of the field where the dose was approximately



r 12 Sk n react on at the end of treatment

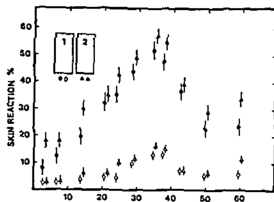


Fig 10

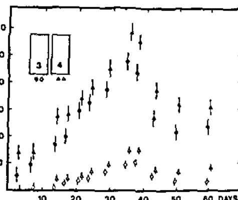


Fig 11

Fig 11 Results of measurements in the lower parasternal region in the same patient as in fig 10 Measurement point 3, 2 × 475 rad per week and RD = 4 275 rad, measurement point 4, 2 × 500 rad per week and RD = 4 500 rad (Symbols as in Fig 3)

five fractions weekly, thus given in T = 9 to 10 days CRE 1 410 corresponds to N = 6 and N = 14 respectively, when T = 19 to 20 days However, equal CRE values during the radiation treatment are not simultaneously related to identical kin reactions as these are delayed It is therefore difficult to compare the reactions during the period of treatment itself and to assess the results at the last occasion of treatment It is important that this be borne in mind when drawing conclusions from retrospective investigations

In order to gain an impression of the variation of the skin reactions with dosage, the right and left parasternal regions of 2 patients were treated as follows right field 2 × 475 rad per week to a total dose of 4 275 rad, left field 2 × 500 rad per week to a total dose of 4 500 rad, which means a deliberate difference in dosage of 5 per cent The dosage difference determined in one patient was only 3 per cent and the reaction was the same in both fields The results of reflectance measurements in the other patient (Figs 10, 11) illustrate the effect of a measured dosage difference of 6 to 7 per cent Visually, the difference in reaction between the fields was obvious and greater than in any of the patients in the CRE test (Fig 12) This result together with the more marked reaction in the center of the field at approximately 5 per cent higher dose suggests the dose-dependence of the effect on the skin and also indicates the precision with which it is possible to verify the CRE model The method of measurement is highly reproducible and the sensitivity is fully comparable with that of the eye It is therefore considered that reflectance spectrophotometer measurement offers a useful method for quantification of erythema and pigmentation Whether or not these early reactions are relevant for calculations of late effects in the skin and connective tissue is, however, a different question and cannot at the moment be decisively answered (ARCANGELI et coll 1974, ELLIS 1968, FOWLER 1969)

The hypothesis that the capillary endothelium as a common target in different organs perhaps is most important for the determination of the radiation tolerance is [illegible] more accented This opinion has experimental support in an [illegible] ent structures depending on the metabolic activity or need for [illegible] hemic interchange The functional tolerance levels for different organs may well be strongly related to the tolerance of parenchymal cells to injury of their microcirculation exemplified with the low tolerance dose of the kidney If this is true, then the tolerance levels of specific normal tissues could be expressed with different CRE levels

The NSD formula, probably better known than the CRE formula, has been criticized for being based on an extrapolation of too few and uncertain clinical data. Increased experimental and clinical investigations of the CRE model are therefore indicated The present investigation exemplifies how the CRE formula may be used for prospective calculation of biologically equivalent doses for different treatment schedules This enables objective description and comparison of differences in radiation effect between normal and malignant tissue in various fractionation schedules. Although the tumour effect cannot be calculated it is possible in both retrospective and prospective investigations to correlate the therapeutic results of irradiated tumours to the CRE for the normal tissues within the target volume

SUMMARY

The CRE formula was used for calculation of biologically equivalent radiation doses with different fractionation schedules The early radiation effects, skin erythema and pigmentation were measured with a reflectance spectrophotometer at wavelengths 578 and 660 nm The course and maximum for both erythema and pigmentation agreed well with the two types of fractionation The results seem to justify further use of this simple formula.

ZUSAMMENFASSUNG

Die CRE Formel wurde fur Berechnungen der biologisch aquivalenten Strahlendosen bei verschiedenen Fraktionierungs-Schemata verwendet Die fruhzeitigen Strahleneffekte, Haut-Erythem und Pigmentierung wurden mit einem reflektierenden Spektrophotometer bei einer Wellenlänge von 578 und 660 nm gemessen Verlauf und Maximum fur sowohl Erythem und Pigmentierung stimmten gut mit den beiden verwendeten Fraktionierungs-Typen uberein Die Ergebnisse durften den weiteren Gebrauch dieser einfachen Formel rechtfertigen

RÉSUMÉ

La formule CRE a eté utilisee pour calculer les doses de radiation biologiquement equivalentes avec differents schemas de fractionnement Les effets precoces des radiations, l erytheme cutané et la pigmentation ont ete mesures avec un spectrophotometre à reflectance

The hypothesis that the capillary endothelium as a common target in different organs perhaps is most important for the determination of the radiation tolerance is becoming more and more accepted This opinion has experimental support in an electron microscopic investigation of heart, skeletal muscle, lung and kidney in rats (PHILLIPS et coll 1972) The microcirculation is more or less well developed in different structures depending on the metabolic activity or need for an effective and rapid hemic interchange The functional tolerance levels for different organs may well be strongly related to the tolerance of parenchymal cells to injury of their microcirculation exemplified with the low tolerance dose of the kidney If this is true, then the tolerance levels of specific normal tissues could be expressed with different CRE levels

The NSD formula, probably better known than the CRE formula, has been criticized for being based on an extrapolation of too few and uncertain clinical data. Increased experimental and clinical investigations of the CRE model are therefore indicated The present investigation exemplifies how the CRE formula may be used for prospective calculation of biologically equivalent doses for different treatment schedules This enables objective description and comparison of differences in radiation effect between normal and malignant tissue in various fractionation schedules Although the tumour effect cannot be calculated it is possible in both retrospective and prospective investigations to correlate the therapeutic results of irradiated tumours to the CRE for the normal tissues within the target volume

SUMMARY

The CRE formula was used for calculation of biologically equivalent radiation doses with different fractionation schedules The early radiation effects, skin erythema and pigmentation were measured with a reflectance spectrophotometer at wavelengths 578 and 660 nm The course and maximum for both erythema and pigmentation agreed well with the two types of fractionation The results seem to justify further use of this simple formula

ZUSAMMENFASSUNG

Die CRE Formel wurde fur Berechnungen der biologisch aquivalenten Strahlendosen bei verschiedenen Fraktionierungs Schemata verwendet Die fruhzeitigen Strahleneffekte, Haut Erythem und Pigmentierung, wurden mit einem reflektierenden Spektrophotometer bei einer Wellenlange von 578 und 660 nm gemessen Verlauf und Maximum fur sowohl Erythem und Pigmentierung stimmten gut mit den beiden verwendeten Fraktionierungs-Typen uberein Die Ergebnisse durften den weiteren Gebrauch dieser einfachen Formel rechtferti gen

RESUMÉ

La formule CRE a été utilisée pour calculer les doses de radiation biologiquement équi valentes avec différents schémas de fractionnement Les effets précoces des radiations, l érythème cutane et la pigmentation ont éte mesures avec un spectrophotometre à réflectance

FROM THE DIVISION OF RADIATION BIOLOGY, THE SWEDISH RESEARCH INSTITUTE OF NATIONAL DEFENCE, S-172 04 SUNDBYBERG, SWEDEN

INFLUENCE OF OESTROGEN ON THE EXCRETION OF STRONTIUM-90 AND -85 IN MICE

C RÖNNBÄCK and A NILSSON

In mice treated with oestrogenic hormones in combination with ^{90}Sr, a highly significant increased number of osteosarcomas occurred as well as a shortened mean tumour induction time as compared to animals treated with strontium only (NILSSON & RÖNNBACK 1973) This seems to confirm the general idea that proliferative stimulation of irradiated cell populations—in this case osteoblasts and their precursors—is an important link in a possible multistep mechanism of irradiation induced malignancies

The purpose of the present report is to give quantitative comparison of retention and excretion of ^{90}Sr in mice treated with oestrogen in combination with ^{90}Sr and with ^{90}Sr only

Material and Methods

Four hundred male CBA mice, aged 65–70 days and weighing about 25 g at the start of the investigation were divided into two main experiment series as follows

Experiment series I

Group	No of mice	Oestrogen treatment (mg animal/inj)	Relation between ^{85}Sr and oestrogen injections
I	50	1 0 + 0 5 + 0 25	^{85}Sr inj 1 week before first oestrogen inj
II	50	1 0 + 0 5 + 0 25	^{85}Sr inj 1 week after first oestrogen inj.
III	50	1 0 + 0 5 + 0 25 + 0 25 + 0 25	^{85}Sr administered 1 week after last oestrogen inj
IV	50	None	No oestrogen ^{85}Sr administered at the same time as in group III

Submitted for publication 21 January 1975

pour des longueurs d'ondes 578 et 660 nm L'évolution et le maximum de l'érythème et de la pigmentation sont en bonne concordance avec les deux types de fractionnement Ces resultats semblent justifier qu'on continue à utiliser cette formule simple

REFERENCES

ADAMS RAY J Differences in redness between the fourth cervical and the thoracic segments on the anterior surface of the trunk following irritation with mustard oil Acta derm - venereol 32 (1952), 10

ARCANGELI G, FRIEDMAN M and PAOLUZI R A quantitative study of late effect on normal skin and subcutaneous tissues in human beings Brit J Radiol 47 (1974), 44

CHU F C H, CONRAD J T, BANE H N, GLICKSMAN A S and NICKSON J J Quantitative and qualitative evaluation of skin erythema Radiology 75 (1960), 406

ELLIS F Fractionation in radiotherapy *In* Modern trends in radiotherapy Edited by T J Deely and C A P Wood Butterworths, London 1 (1967), 34

— The relationship of biological effect to dose time fraction factors in radiotherapy *In* Current topics in radiation research (Edited by M Ebert and A Howard North Holland Publishing Company, Amsterdam 4 (1968), 359

— Dose, time and fractionation a clinical hypothesis Clin Radiol 20 (1969) 1

— Nominal standard dose and the ret Brit J Radiol 44 (1971), 101

FOWLER J F The estimation of total dose for different numbers of fractions in radiotherapy Brit J Radiol 38 (1965), 365

— Time dose relationship in radiotherapy Europ J Cancer 6 (1969), 207

— Effects of radiation exposure in therapeutic range Truncated doses and dose fractionation *In* Late effects of radiation, p 65 Edited by R M Fry, D Grahn, M Griem and J Rust Taylor & Francis Ltd, London 1970

KIRK J, GRAY W M and WATSON R Cumulative Radiation Effect Part I Fractionated treatment regimes Clinical Radiology 22 (1971), 145

LINDSKOUG B Automated thermoluminescence reader II Experiments and theory Acta radiol Ther Phys Biol 14 (1975), 347

MARKUS B Problems of high energy electron dosimetry in radiobiological experiments *In* Annals of the New York Academy of Sciences 161 (1969), 282

NOTTER G, TSIOULIAS T and ÅSARD P E Erythema differences between the cranial and caudal parasternal regions at 12 MeV electron irradiation Acta radiol Ther Phys Biol 3 (1965), 177

PHILLIPS L, BENAK S and ROSS G Ultrastructural and cellular effects of ionizing radiation *In* Frontiers of Radiation Therapy and Oncology Ed Vaeth (S Karger, Basel Munchen, Paris, London, New York, Sydney) 6 (1972), 21

STRANDQVIST M Studien uber die kumulative Wirkung der Rontgenstrahlen bei Fraktionierung Acta radiol (1944) Suppl No 55

WINSTON B, ELLIS F and HALL E The Oxford NSD calculator for clinical use Clin Radiol 20 (1969), 8

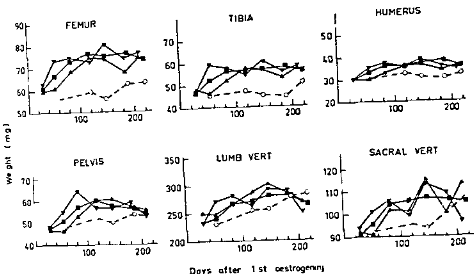


Fig. 1 Absolute weight of skeleton parts ▲ Group I, ▼ Group II, ■ Group III, O Group IV

increased significantly ($p<0.001$) compared to the controls A marked increase was found in the pelvis and both vertebrae during a period beginning about 60 days after injection up to approximately 200 days, when the difference between the treated and control animals had been nearly eliminated

For the second experiment series the weight of the skeleton parts related to the corresponding controls with the latter given the value of 1 00 appears in Fig 2. In the diagram the abscissa starts on day 0, the day for strontium administration, i e 7 days after the first oestrogen injection

The tendency of increasing bone weight is clear also for animals treated with oestrogen together with ^{85}Sr (group VII) The weight of the femurs again increased strongly (Fig 2 b) with the increase beginning about 1 month after the oestrogen administration

In the other two groups (VI and VIII) the strontium treatment consisted of ^{90}Sr combined with ^{85}Sr, and the results appeared different from that in group VII (Fig 2 a, c) In group VI no oestrogen was administered An overall weight decrease appeared during the first 30-day period, followed by an increase up to 2 months from injection From that time on, the weight of all examined skeleton parts was less than that of corresponding controls In group VIII, where the ^{90}Sr was administered to oestrogen pretreated animals, the bone weights, when related to the control values, were about the same The result seems analogous to that in group VI (Fig 2 a), but the general weight level between 1 and 3 months after injection was higher than in the control group and also higher than that of group VI The combined treatment of oestrogen together with ^{90}Sr shortened the life span and no animals in that group survived 150 days after the strontium injection

The oestrogen (Estradurin) was subcutaneously injected with 4-week intervals between the injections

The four main groups (I–IV) were divided into two subgroups with 15 and 35 males, respectively

All animals were injected intraperitoneally with 0 1 ml of a ^{85}Sr-chloride solution, diluted with physiologic saline This dose (about 1 μCi per animal) gave to each animal, within the first five minutes following the injection, an initial counting rate of approximately 90 000 counts per minute when measured in a Small Animal Counter The animals in the first subgroup were used for repeated measurements of the strontium retention which was expressed as per cent of the initial measurement for each animal, giving the mean and standard error for the treatment groups

In the second subgroup five randomly selected animals were killed at 1 month after the first oestrogen injection and after 2, 3, 4, 5, 6 and 7 months in order to prepare femur, tibia, humerus, one pelvic bone, one lumbar and one sacral vertebra The weights of these were noted and the strontium retention was measured by means of a conventional well crystal

Experiment series 2

Group	No of mice	Oestrogen treatment (mg/animal/inj)	Radiostrontium-treatment
V	50	None	None
VI	50	None	(^{90}Sr + ^{85}Sr) on day 0
VII	50	1 0 + 0 5 + 0 25	^{85}Sr on day 0
VIII	50	1 0 + 0 5 + 0 25	(^{90}Sr + ^{85}Sr) on day 0

The oestrogen injections were given with 4-week intervals, the first one 7 days before day 0, 0 8 μCi ^{90}Sr/g body weight, together with about 1 μCi ^{85}Sr/animal was administered in groups VI and VIII

In this second experiment series the oestrogen (Estradurin) injections in groups VII and VIII started one week before the administration of strontium as in group II In this part of the experiment the strontium was administered either as a tracer dose of ^{85}Sr alone, group VII (as in groups I–IV), or as ^{90}Sr together with ^{85}Sr, the former as a solution of $^{90}Sr(No_3)_2$ The nuclide solutions were in all cases given intraperitoneally, the hormone solution subcutaneously

In each of the groups V–VIII five randomly selected animals were killed at 7, 14, 28, 56, 84, 112, 140, 168 and 196 days after the day of strontium administration For those animals the weight and strontium retention was noted for femur, sternum, pelvis and lumbar vertebrae

Results

One effect of the oestrogen administration is reflected by the increase of the weight of the skeleton parts examined in experiment series 1 (Fig 1) In mice treated with oestrogen in combination with ^{85}Sr the weight of especially the tubular bones had

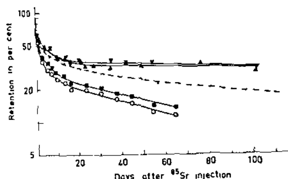


Fig. 3 Whole body retention of ^{85}Sr ▲ Group I, ▼ Group II, ■ Group III, ○ Group IV, --- ^{85}Sr-excretion in not hormone treated mice

received all oestrogen injections, i e in animals more than four months older than those in groups I and II It is evident that the non-oestrogen treated animals had a lower retention than the hormone treated even at this high excretion rate In the second experiment series only a few whole body countings were performed, which however, confirmed the excretion pattern given

From the well crystal measurements on the six skeleton parts it was evident that animals having received ^{85}Sr one week after the first oestrogen injection (group II) had higher retention values in all skeleton parts except for the pelvis than the animals to which strontium was administered before the hormones (Fig 4) The differences between groups I and II were significant during a period up to 2 months after injection, but decreased after that time

In groups III and IV there was a still more evident difference in retention (up to a factor of 2) with the lower values for the non-oestrogen treated mice In both of these groups much higher excretion rates were observed, with almost parallel slopes of the excretion curves within the observation period, i e the first hundred days after the injection of ^{85}Sr

In the second experiment series activity measurements were performed on femur, sternum, pelvis and lumbar vertebrae from mice in groups VI–VIII These results were not contradictory to those from the measurements in experiment series 1 on mice treated with oestrogen in combination with ^{85}Sr The retention as well as the excretion rates were of the same order of magnitude

In animals treated with ^{90}Sr combined with ^{85}Sr no difference in the excretion rate was observed in femur and sternum whether the animals were hormone treated or not (groups VI versus VIII) On the other hand the pelvis and lumbar vertebrae from hormone treated animals had a significantly lower retention than those not oestrogen treated (Fig 5) From approximately 2 months after strontium injection these excretion curves were rather parallel

Except for the shortened life span increased osteoporosis also occurred in animals in group VIII

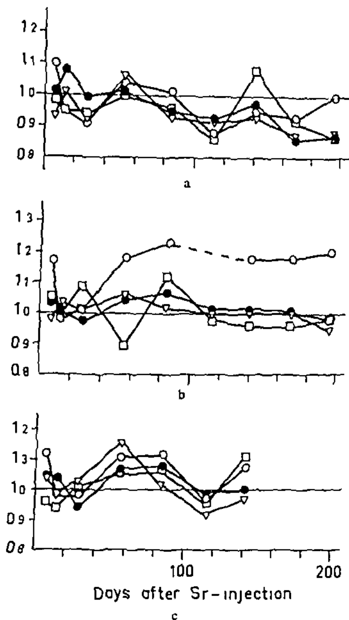


Fig 2 Weight of skeleton parts related to controls (=1 00) a) ^{90}Sr + ^{85}Sr b) oestrogen + ^{85}Sr c) oestrogen + (^{90}Sr + ^{85}Sr) ○ femur □ sternum △ pelvis ● lumbar vertebrae

The results of the activity measurements by whole body counting in experiment series I appear in Fig 3, where the dotted line indicates a normal excretion rate for ^{85}Sr in mice, aged 75 days when injected and not treated with any other agent The retention in groups I and II clearly deviated from this line indicating a slower excretion rate On the other hand there was no significant difference between groups I and II The overall excretion rate in the latter groups seems not to be influenced by the time of the oestrogen distribution (one week before or after the strontium) The lower two lines in that diagram show the excretion rate for animals in groups III and IV The strontium was here administered when the animals in group III had

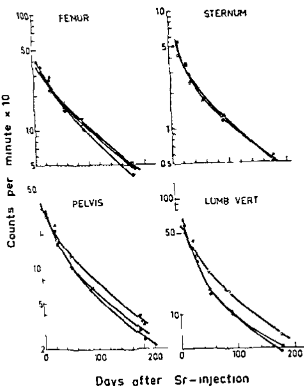


Fig. 5 Retention of strontium in the skeleton parts (experiment series 2) ▽ $^{90}Sr+^{85}Sr$, ● oestrogen + ^{85}Sr, ▲ oestrogen + ($^{90}Sr+^{85}Sr$)

suppressive effect on the bone cells followed by an increased activity and proliferation leading to induction of osteosarcomas (NILSSON 1962, 1970) (Fig. 6) In the second experiment series, where ^{90}Sr was administered to the animals in groups VI and VIII, the bone weights consequently should be lower in the former, not hormone treated group, compared to the controls (group V) About 2 months after injection the bone weights decreased (Fig 2 a)

In mice treated with both oestrogen and ^{90}Sr the decrease in weight during the first 30 days was somewhat lesser than in animals treated with ^{90}Sr alone The following period during which the formation of new bone occurred with an intensity that seemingly counterbalanced the destruction caused by the nuclide, lasted for another two months At the end of that period, i e 90 to 100 days after injection, the weight of the examined skeleton parts became lower than in non-treated controls This observation agrees completely with microscopic findings, i e ^{90}Sr considerably induces lysis and break down of the bone built up by the influence of oestrogen (Figs 7, 8)

The general increase of the bone weight, especially that of femur and sternum, at the end of the observation period (140 days) for the animals treated with both oestrogen and ^{90}Sr, could probably be an indication of an increasing frequency of tumour

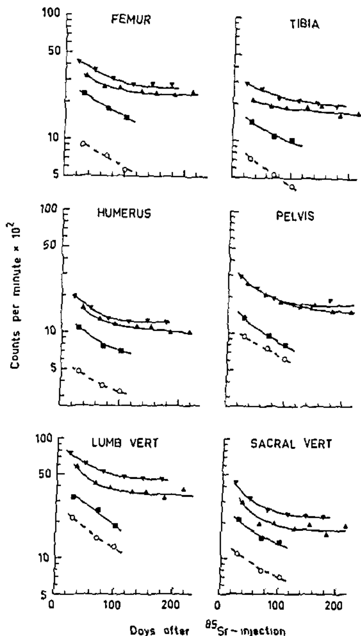


Fig 4 Retention of ^{85}Sr in the skeleton parts (experiment series 1) ▲ Group I, ▼ Group II, ■ *Group III*, ○ *Group IV*

Discussion

Oestrogen hormones which cause a marked formation of new endosteal bone in mice by stimulation of osteoblasts (SIMMONS 1962) have, as shown in the first experiment series, caused an evident increase of the weight of especially the tubular bones, but also, to a lesser degree, in other parts of the skeleton There was no evidence, however, for a correlation between the amount of oestrogen administered to the animals and the degree of increased bone weight

On the other hand, when given in doses which induce bone tumours, ^{90}Sr has a

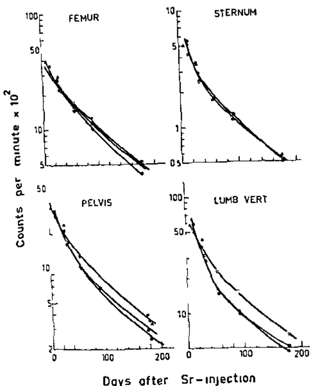


Fig. 5 Retention of strontium in the skeleton parts (experiment series 2) ▽ $^{90}Sr+^{85}Sr$, ● oestrogen + ^{85}Sr, ▲ oestrogen + ($^{90}Sr+^{85}Sr$)

suppressive effect on the bone cells followed by an increased activity and proliferation leading to induction of osteosarcomas (NILSSON 1962, 1970) (Fig 6) In the second experiment series, where ^{90}Sr was administered to the animals in groups VI and VIII, the bone weights consequently should be lower in the former, not hormone treated group, compared to the controls (group V) About 2 months after injection the bone weights decreased (Fig 2 a)

In mice treated with both oestrogen and ^{90}Sr the decrease in weight during the first 30 days was somewhat lesser than in animals treated with ^{90}Sr alone The following period during which the formation of new bone occurred with an intensity that seemingly counterbalanced the destruction caused by the nuclide, lasted for another two months At the end of that period i e 90 to 100 days after injection, the weight of the examined skeleton parts became lower than in non treated controls This observation agrees completely with microscopic findings, i e ^{90}Sr considerably induces lysis and break down of the bone built up by the influence of oestrogen (Figs 7, 8)

The general increase of the bone weight especially that of femur and sternum, at the end of the observation period (140 days) for the animals treated with both oestrogen and ^{90}Sr, could probably be an indication of an increasing frequency of tumour

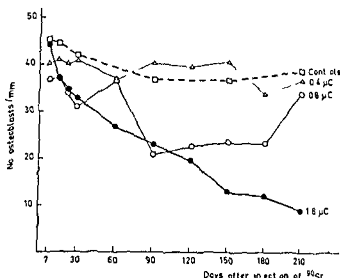


Fig 6 Number of osteoblasts per mm endosteum of distal metaphysis of femur related to dose and time (Open circles the actual dose of 0 8 μCi per g body weight) (From NILSSON 1970)

buds This hypothesis has, however, not been analysed microscopically in this investigation Shortly after this time, a great proportion of the animals treated with oestrogen together with ^{90}Sr died, often with signs of haemorrhagic diathesis This phenomenon and the reduced mean survival time was also observed by NILSSON & RÖNNBACK, who found that a combination of oestrogen and ^{90}Sr significantly potentiated the cancerogenic effect in mice and also caused a decreased survival time as compared to treatment with ^{90}Sr alone

The femur from a mouse treated with oestrogen only and examined 45 days after the first hormone injection is illustrated in Fig 7 a The femur was more or less filled with newly formed bone Fig 7 b reveals the different appearance at 45 days of a femur from a mouse also treated with ^{90}Sr 1 week after the start of the hormone administration

The formation of new bone was decreased and practically no typical osteoblasts were observed along the endosteal linings of the bone at microscopy

In mice killed 121 days after the first hormone injection these differences were still more accentuated In the mice treated with hormones only, the whole medullary cavity had become almost filled with new bone (Fig 8 a) In animals also treated with ^{90}Sr this bone formation had decreased and the newly formed bone was broken down, mainly distally and proximally (Fig 8 b)

Besides these microscopic findings, the frequencies of tumours in four bones (NILSSON & RÖNNBACK) were compared with results from activity measurements on femur and pelvis in the present report (Table)

The ratio of the activities are below 1 00 indicating a lower longterm strontium retention (and -dose) in the bones from mice treated with both oestrogen and ^{90}Sr It is suggested that this depends on the procedure where the initially active oestrogen bone successively is broken down influenced by ^{90}Sr and thus releasing the nuclide

This gives a strong evidence that the higher tumour rate found in these experi-

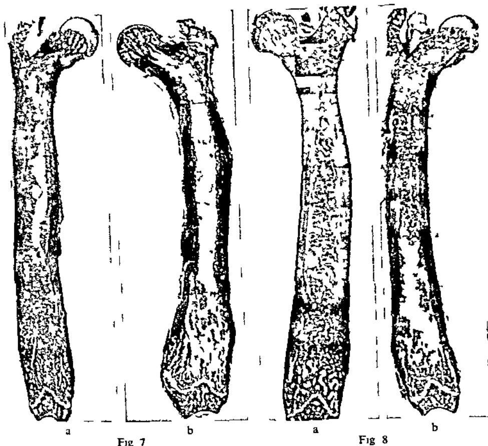


Fig 7 a) Femur of mouse 45 days after injection of oestrogen (van Gieson approx × 6) b) Femur of mouse 45 days after injection of oestrogen and 38 days after injection of ^{90}Sr (van Gieson, approx × 6) (From NILSSON & RONNBACK 1973)

Fig 8 a) Femur of mouse 121 days after first injection of oestrogen (van Gieson approx × 6) b) Femur of mouse 121 days after first injection of oestrogen and 114 days after ^{90}Sr injection (van Gieson, approx × 6) (From NILSSON & RONNBACK 1973)

ments is not to be correlated to a higher strontium dose It rather supports the theories that at the same time irradiated and stimulated cell populations are exposed to a larger risk for tumour induction

It was instead supposed that the oestrogenic hormones with their stimulating effects on bone cells and their precursors to proliferation was the main reason for the increased tumour frequency However, the hormones would, as it was anticipated, change the skeletal turnover of strontium to a considerable degree

It must, however, be recognized that the contradictory observations as regards the bone metabolism in the two present experiment series were dependent on the fact that different isotopes of strontium were used In the first part a low dose of

Table 1

Frequency of tumours at different sites compared to corresponding activity measurements

Bone	Oestrogen + ^{90}Sr (A)		^{90}Sr only (B)		Ratio			
	No of tumours	Mean No of tumours/bone	No of tumours	Mean No of tumours/bone	Mean No (A) / Mean No (B)	cpm in (A) / cpm in (B) 56	92	177 days after ^{90}Sr injection
Femur	86	0 878	57	0 504	1 74	0 976	0 923	0 975
Tibia	57	0 582	38	0 336	1 73	—	—	—
Humerus	83	0 847	38	0 336	2 52	—	—	—
Pelvis	33	0 337	14	0 124	2 72	0 825	0 776	0 664
Total (in all examined bones)	414 tumours in 90 tumour bearing mice		264 tumours in 113 tumour bearing mice					

the 'harmless' ^{85}Sr was administered and its retention curves might only be regarded as reflecting the changes in the bone metabolism caused by the oestrogen In the second series the animals were given about 20 μCi of ^{90}Sr together with oestrogen, an amount of the nuclide that, contrary to ^{85}Sr caused an enhanced destruction of the bone tissue (Figs 7, 8)

The higher retention found by whole body countings as well as well crystal measurements on the skeleton parts from mice treated with both oestrogen and ^{85}Sr (groups I, II, VII) compared to not oestrogen treated ones of the same age, might be explained by the increased rate of bone apposition

The retention was higher in animals pretreated with oestrogen, even if the time interval between oestrogen and nuclide injections was as short as one week Out of the six examined bone types only the pelvis had another retention pattern

It was impossible to evaluate whether or not the higher amount of oestrogen given in group III influenced the turnover rate for ^{85}Sr compared to groups I and II because of the different ages of the animals at the time for strontium injection Previously it was found that the excretion rate was faster in older mice than in younger ones as in reports by SPECKMAN & NORRIS (1964), GUSMANO et coll (1968) The latter authors stated that the slope of the plasma specific activity curves in rats after injection of ^{85}Sr decreased with the age of the animals A high value of the rate of transfer between plasma, extracellular fluid and soft tissue to exchangeable bone could reflect a larger available surface concomitant with the high accretion rate in young, actively metabolizing bone, thus reflecting a more rapid uptake of the nuclide in the compartment of slowly exchanging bone in younger animals

It was also found that the distribution of ^{85}Sr was not uniform in the skeleton of young pigs (ANDERSON 1968) When injected 2 days after birth and on the basis of

the per cent of strontium retained between 24 and 50 days after injection, the highest uptake was found in the skull and mandible, followed by the long bones and vertebrae, ribs and sternum He also stated that bones having greater turnover or renewal rates lost a larger portion of their radiation activity between 24 and 50 days after injection than did bones with lower turnover rates Extrapolating these results to man, he implicated the bones mentioned together with their blood forming tissues as the most likely to receive the highest radiation dose from fall out ^{90}Sr

Previously have been emphasized the different effects on the bone tissues and metabolism caused by ^{90}Sr compared to ^{85}Sr, and also the potentiating effects caused by the oestrogenic hormones in combination with ^{90}Sr Because of the destructive effect of ^{90}Sr in the bone tissues, there was supposed to be a lower retention in the group treated with both ^{90}Sr and ^{85}Sr compared to the retention found in animals in addition treated with oestrogen with its bone apposition effects

Contradictory to this hypothesis it was evident (cf Fig 5) that the strontium retention in the non hormone treated animals (group VI) in no case was lower than in mice treated with both oestrogen and ^{90}Sr Concerning femur and sternum there was no difference depending on treatment, in pelvis and lumbar vertebrae the retention in non oestrogen treated animals was evidently higher In the hormone treated animals there should consequently be a lower irradiation dose to the bones and thus less irradiation injured tissues (Table)

It has, however, been shown that the effect of this lower dose in combination with oestrogenic hormones was more deleterious for the animals NILSSON & RÖNNBÄCK stated that mice given oestrogenic hormones combined with ^{90}Sr had a significantly shorter survival time than mice given ^{90}Sr only In spite of this, the number of bone tumours per mouse was approximately a factor of 2 greater in the hormone treated ^{90}Sr mice than in only ^{90}Sr treated Also the induction time was shorter in the mice treated both with oestrogen and ^{90}Sr As there was a higher rate of tumours also in the femur of the mice treated with both oestrogen and ^{90}Sr, though the retention was of the same order of magnitude whether the animals were hormone treated or not (Fig 5), it must be stated that the irradiation injury not solely can be referred to the irradiation dose in a physical sense Great attention must be payed to the internal} environmental conditions under which the irradiation occurs, in this case particularly to the proliferative stimulus to the bone cells induced by oestrogens

SUMMARY

Groups of male CBA-mice were treated with oestrogenic hormones alone or in combination with ^{85}Sr and ^{90}Sr The strontium retention was measured in special skeleton parts and also by means of whole body counting After a period of increasing bone weight in mice treated with oestrogen and ^{90}Sr, there were signs of a serious breakdown of that newly formed oestrogenic' bone tissue. The strontium retention was in no case found higher in animals treated with both the hormones and ^{90}Sr when compared to those treated with ^{90}Sr alone The life span was shortened in mice given the combined treatment The results

support the theories that at the same time irradiated and stimulated cell populations are exposed to a larger risk for induction of tumours and that the irradiation injury cannot be referred entirely to the irradiation dose in a physical sense

ZUSAMMENFASSUNG

Gruppen von mannlichen CBA-Mäusen wurden mit Oestrogenen Hormonen alleine oder in Kombination mit ^{85}Sr und ^{90}Sr behandelt Die Strontium Retention wurde in besonderen Skelett Teilen und auch mittels Gesamtkorper Messung bestimmt Nach einer Periode stiegenden Knochengewichts bei Mausen, die mit Oestrogen und ^{90}Sr behandelt wurden traten Zeichen eines schweren Abbaus dieses neugebildeten „oestrogenen" Knochengewebes auf Die Strontium Retention war in keinem Fall hoher bei Tieren die mit sowohl Hormonen als auch ^{90}Sr behandelt worden waren verglichen mit solchen die nur mit ^{90}Sr behandelt worden waren Die Lebenslange war bei den Mausen, denen eine kombinierte Behandlung gegeben worden war, herabgesetzt Die Ergebnisse stutzen die Theorien, dass Zell-Populationen, die gleichzeitig bestrahlt und stimuliert werden, ein grosseres Risiko unterlaufen, Tumoren zu entwickeln, und dass der Strahlenschaden nicht ausschliesslich auf die Strahlendosis im physikalischen Sinn zuruckgefuhrt werden kann

RÉSUMÉ

Des groupes de souris mâles CBA ont ete traités par des hormones oestrogènes seules ou en association avec du ^{85}Sr et du ^{90}Sr La fixation du strontium a eté mesuree dans cer taines parties du squelette et aussi par comptage de tout le corps Après une période d aug mentation du poinds du squelette chez les souris traitées par les oestrogènes et le ^{90}Sr, on observe des signes de détérioration grave de ce tissu osseux « oestrogenique » nouvellement forme La fixation de strontium chez les animaux traités par les hormones et par le ^{90}Sr n'a été dans aucun cas supérieure à celle des animaux traites seulement par le ^{90}Sr La durée de vie a éte raccourcie chez les souris qui ont reçu le traitement associe Ces résultats viennent à l'appui des théories d'après lesquelles les populations cellulaires qui subissent en meme temps une stimulation et une irradiation sont exposées à un risque plus grand d'induction de tumeur et d'après lesquelles les dommages dus à l irradiation ne peuvent pas etre attribues entièrement à la dose d'irradiation au sens physique

REFERENCES

ANDERSON J J B Effect of time on distribution of injected radiostrontium in the skeleton of young pigs Hlth Phys 15 (1968), 237

GUSMANO E A, CONCANNON J N BOZZO S R and COHN S H Evaluation of the para meters of strontium metabolism in the rat as a function of age Radiat Res 33 (1968), 540

NILSSON A Histogenesis of ^{90}Sr-induced osteosarcomas Acta vet scand 3 (1962) 185

— Pathologic effects of different doses of radiostrontium in mice Dose effect relationship in ^{90}Sr-induced bone tumours Acta radiol Ther Phys Biol 9 (1970), 155

— and RONNBÄCK C Influence of oestrogenic hormones on carcinogenesis and toxicity of radiostrontium Acta radiol Ther Phys Biol 12 (1973), 209

SPECKMAN Th W and NORRIS W P The age dependence of strontium retention in rats and mice Radiat Res 23 (1964), 461

ACTA RADIOLOGICA

OFFICIAL ORGAN OF THE RADIOLOGICAL SOCIETIES OF DENMARK, FINLAND, NORWAY AND SWEDEN

Vol 14
Fasc 6

THERAPY PHYSICS BIOLOGY

1975
December

LOW DOSE IRRADIATION IN ADVANCED TUMOURS OF HEAD AND NECK

B PIERQUIN, F BAILLET and C H BROWN

The increasing interest in continuous low dose rate irradiation seems to justify a report on the results of a second series of patients treated between December 1971 and August 1973 at this hospital In the first series, 6 cases with head and neck neoplasms were treated at L Institut Gustave Roussy between January and December 1970 (PIERQUIN & BAILLET 1971) and the results were sufficiently encouraging for a second series to be begun Only the 19 cases with more than 9 months follow-up are reported here an account of the results of the entire series is in preparation

No definite conclusions can yet be drawn regarding the place of low dose rate irradiation in the management of advanced head and neck tumours, but certain trends seem clear, as well as certain effects associated with this technique alone

The clinical staging used is that described by PIERQUIN et coll (1970), this TNM classification is based essentially on the apparent dimensions of the tumour T1 1 cm, T2 1 to 2 cm T3a 3 to 4 cm, T3b 4 to 5 cm T4a 5 to 7 cm, T4b more than 7 cm The staging is also influenced by the type of the tumour growth, i e exophytic, infiltrative or ulcerative

From Service de Cancérologie Radiotherapeutique du CHU Henri Mondor F 94000 Creteil, France Submitted for publication 9 December 1974

Table 1

The material of 19 patients with tumours of the mouth and pharynx

Case No	Age	Sex	Tumour Site	Extension	Stage
1	57	M	*Tonsil*	*Palate, tongue*	T4a N3
2	78	M	Vallecula	Posterior 2/3 tongue	T3b N3
3	60	M	Base of tongue	Complete fixation	T4b N1
4	67	M	Base of tongue	Mid 1/3 tongue and floor	T4a N0
5	48	F	Mobile tongue	Tonsil and post 1/3	T4a N3
6	51	M	Laryngo-pharynx	Tongue	T4b N0
7	60	M	Soft palate	Uvula, tonsil	T3a N3
8	85	M	Base of tongue	Pyriform sinus	T3b N0
9	50	M	Tonsil	Tongue	T4a N2
10	47	M	Floor of mouth	Gingiva, tongue	T4a N3
11	62	M	Base of tongue	Fauces, floor of mouth	T4a N0
12	51	M	Tonsil	Post 2/3 of tongue	T4a N0
13	44	M	Tonsil and tongue*	Post 1/3 of tongue	T4b N3
14	46	M	Epiglottis	Pharyngal walls	T3b N0
15	48	M	Base of tongue	Tonsil, mid 1/3	T4a N0
16	49	M	Mobile tongue	Post 1/3	T4a N3
17	77	M	Base of tongue	Post 1/3	T3b N3
18	60	M	Hypopharynx	Vallecula, larynx	T4b N1
19	66	M	Tonsil and tongue	Vallecula, larynx	T3b N3

* This patient had two tumours on opposite sides

Material and Methods On admission all 19 patients had advanced tumours of the upper respiratory and alimentary tracts, which would have had a grave prognosis if treated by conventional radiation therapy (CHASSAGNE 1958, PIERQUIN et coll 1966) The site of origin of the tumours and their clinical extension and staging are given in Table 1, as well as the age and sex of the patients With few, if any, exceptions the major aetiologic factor was alcohol, closely followed by tobacco (WYNDER et coll 1957), and the general condition of most patients was poor

All patients were treated by a Theratron junior, whose source had been replaced by a small industrial source with a cross-sectional area of 0 78 cm², and at installation in December 1971 had an activity of 45 Ci

The patients were treated lying down with the head held gently by calipers or sandbags. In the first series it was found that rigid immobilisation was neither tolerable nor necessary.

Irradiation was given by two direct, parallel opposed, horizontal beams of equal size for 7 to 8 hours per day. At a source to skin distance of 55 cm, this gave a daily tumour fraction of 800 to 1 000 rad (range of output, 103 to 139 rad/h) A minimum

Table 2

Treatment and results

Case No	Dose (rad)	Treatment		Survival (months)	Recurrence	Necrosis	Condition in March 1974
		Time (days)	No of fractions				
1	7 000	10	8	6 5	Probable	No	Dead following tracheostomy
2	7 000	10	8	6	No	No	Dead of bronchial carcinoma
3	7 000	10	8	25	No	Large	Alive
4	7 000	9	7	18	No	Small	Dead of prostatic carcinoma
5	7 000	13	11	24	No	Large	Alive
6	7 000	10	8	8	Not known	Large	Dead following gastrostomy
7	7 000	13	11	23	No	No	Well
8	7 000	10	8	21	No	No	Well
9	7 000	10	8	8	Yes	No	Dead of recurrence at site of treated area
10	7 000	16	12	19	Yes	Yes	Alive
11	6 500	13	11	10	Yes	No	Dead of persistent disease
12	3 500 3 500	35	5 5	14	No	Yes	Dead of gastro-intestinal haemorrhage
13	3 500 3 500	47	5 5	13	Yes	No	Dead of primary tumour
14	4 500 2 500	45	6 4	15	No	No	Well
15	4 500 2 500	48	7 4	14	No	No	Well
16	4 500 2 500	51	6 4	8 5	Yes	No	Dead of primary tumour outside treated area
17	4 500 2 500	67	6 5	12	No	No	Well
18	7 000	18	14	11	Possible	Yes	Alive
19	4 500 2 500	44	5 4	11	No	No	Well

of 5 treatments were given per week but weekends, holidays and staffing arrangements sometimes caused gaps between one or two sessions Provided that an opportunity for refreshment and to walk about was given every hour or two the long immobilisation was well tolerated

Apart from 7 patients who underwent split-course irradiation, the midpoint axial dose received was 7 000 rad in 8 to 11 fractions This represents 6 300 rad to the 90 per cent isodose, which encompassed the tumour volume

be a risk of necrosis in extensive tumours, and the effect on the tumour was greater than that of conventional fractionated irradiation, with a total regression of tumour in the treated volume within 2 to 3 months

The present series has confirmed and amplified those conclusions The technique was entirely feasible The patient tolerated 7 or 8 hours irradiation per day and the treatment set-up was easily and simply maintained for that period of time without elaborate immobilisation techniques

The dose, 7 000 rad maximum, seems to have been right Although the mucosal reactions were severe, they were no more severe than is seen in the short radical course of fractionated irradiation of head and neck tumours, and many patients have maintained their nutrition at home The skin reaction, however, is markedly less than that encountered following a fractionated course given in a cast or jig

A dose of 7 000 rad seemed to have an effect on the tumour in nearly all cases In one patient (No 11), however, the necrotic tumour did not regress completely, nor did the skin or the mucosa show more than slight signs of having been irradiated Retrospectively the technical factors were controlled and found satisfactory and the failures to respond remain unexplained

Of 4 recurrences, 2 occurred outside or at the limit of the treated volume and the remaining 2 followed the split course treatment

On the other hand it may be that the dose of 7 000 rad is marginally too high Seven necroses (6 extensive) in 19 patients is a high rate but all of the patients with necrosis had T4 tumours It must be emphasised that there has been no recurrence and no necrosis in any of the 6 uncomplicated T3 tumours up to the present time (July 1974)

It seems that the RBE of continuous low dose rate external irradiation cannot be the same as that of high rate irradiation since daily doses of 1 000 rad given at the usual rate would undoubtedly be unsupportable for more than a very few treatments The time relationships of the reactions and the effect on the tumour closely resemble those of implantation which is not merely a reflection of a small volume, but is due also in part to the low rate of irradiation Furthermore, the remarkable efficacy of the irradiation in treating extensive, ulcerating tumours suggests that it may have a lower oxygen enhancement ratio than conventionally fractionated irradiation

In a third series, just started, the effectiveness of low-output irradiation will be compared prospectively with conventional cobalt-therapy in a controlled trial of treatment of T3 head and neck tumours This stage has been chosen since T3 tumours are more narrowly defined than T4 tumours which develop complications that are attributable more to destruction of normal tissue than to the treatment

A word of caution is necessary, however Late necrotic complications may develop after the present period of observation and for this reason a split course therapy will be used in the third series (3 500 rad × 2, with a three week interval) accepting the higher risk of recurrence

Conclusion

A second series of 19 patients with T3 and T4 tumours of the mouth and pharynx has been treated by fractionated low dose rate irradiation The results have confirmed the conclusions tentatively drawn from a first series of head and neck tumours, that such treatment is feasible, tolerable and highly effective Regression occurred in a large proportion of tumours, though at the expense of a rather high necrosis rate complications, however, were only encountered in the T4 cases Further improvement in results are expected from a closer selection of patients in a planned comparative trial

SUMMARY

A material of 19 patients with T3 and T4 tumours of the mouth and pharynx was treated by fractionated low dose rate irradiation Regression occurred in a large proportion of tumours but at the expense of a high rate of necrosis.

ZUSAMMENFASSUNG

Neunzehn Patienten mit T3 und T4 Tumoren des Mundes und Pharynx wurden mit fraktionierter Bestrahlung mit niedriger Dosis Leistung behandelt Eine Regression war bei einem grossen Teil der Tumoren zu verzeichnen, jedoch auf Kosten einer hohen Frequenz von Nekrosen

RÉSUMÉ

Dix neuf malades atteints de cancers ORL largement etendues (T3 et T4) ont ete irradies par telecobaltherapie a faible debit La regression tumorale a éte totale dans la grande majorite des cas les necroses au sein du volume tumoral ont éte relativement frequentes

REFERENCES

CHASSAGNE D Etude de 44 *cas de tumeurs de la base de langue traitees par le Betatron* (22 MeV) Memoire pour le CES d Electroradiologie Paris 1958

PIERQUIN B et BAILLET F La téleradiotherapie continue et de faible debit Ann Radiol 14 (1971) 617

— — La teléradiotherapie continue et de faible debit Deuxième rapport J Radiol 55 (1974) 757

be a risk of necrosis in extensive tumours, and the effect on the tumour was greater than that of conventional fractionated irradiation, with a total regression of tumour in the treated volume within 2 to 3 months

The present series has confirmed and amplified those conclusions The technique was entirely feasible The patient tolerated 7 or 8 hours irradiation per day and the treatment set-up was easily and simply maintained for that period of time without elaborate immobilisation techniques

The dose, 7 000 rad maximum, seems to have been right Although the mucosal reactions were severe, they were no more severe than is seen in the short radical course of fractionated irradiation of head and neck tumours, and many patients have maintained their nutrition at home The skin reaction, however, is markedly less than that encountered following a fractionated course given in a cast or jig

A dose of 7 000 rad seemed to have an effect on the tumour in nearly all cases In one patient (No 11), however, the necrotic tumour did not regress completely, nor did the skin or the mucosa show more than slight signs of having been irradiated Retrospectively the technical factors were controlled and found satisfactory and the failures to respond remain unexplained

Of 4 recurrences, 2 occurred outside or at the limit of the treated volume and the remaining 2 followed the split course treatment

On the other hand it may be that the dose of 7 000 rad is marginally too high Seven necroses (6 extensive) in 19 patients is a high rate but all of the patients with necrosis had T4 tumours It must be emphasised that there has been no recurrence and no necrosis in any of the 6 uncomplicated T3 tumours up to the present time (July 1974)

It seems that the RBE of continuous low dose rate external irradiation cannot be the same as that of high rate irradiation since daily doses of 1 000 rad given at the usual rate would undoubtedly be unsupportable for more than a very few treatments The time relationships of the reactions and the effect on the tumour closely resemble those of implantation which is not merely a reflection of a small volume, but is due also in part to the low rate of irradiation Furthermore, the remarkable efficacy of the irradiation in treating extensive, ulcerating tumours suggests that it may have a lower oxygen enhancement ratio than conventionally fractionated irradiation

In a third series, just started, the effectiveness of low-output irradiation will be compared prospectively with conventional cobalt-therapy in a controlled trial of treatment of T3 head and neck tumours This stage has been chosen since T3 tumours are more narrowly defined than T4 tumours which develop complications that are attributable more to destruction of normal tissue than to the treatment

A word of caution is necessary, however Late necrotic complications may develop after the present period of observation and for this reason a split course therapy will be used in the third series (3 500 rad $\times$ 2, with a three week interval) accepting the higher risk of recurrence

FROM THE RADIOTHERAPY CENTER, DIVISION OF THE DEPARTMENT OF RADIOLOGY, UNIVERSITY OF WISCONSIN HOSPITAL, MADISON, WISCONSIN 53706, AND THE DIVISION OF RADIOTHERAPY, UNIVERSITY OF ARIZONA SCHOOL OF MEDICINE, TUCSON, ARIZONA 85702, U S A

TREATMENT OF GLIOBLASTOMA MULTIFORME

A review

W L CALDWELL and S A ARISTIZABAL

Of the various types of brain tumors, there is none with as ominous an outlook as glioblastoma multiforme Since the tumor is almost without exception limited to its site of origin in the brain, a situation rare with other malignant tumors, local treatment can be envisaged as being potentially curative Yet, cure is rarely the result, even in major treatment centers Resection alone results in limited survival and most treatment series indicate that the addition of postoperative irradiation, although yielding an occasional survivor, increases the median survival only several months

In an effort to investigate whether local irradiation could better supplement operative resection split-course therapy was tried, and the results were compared with those of regularly fractionated irradiation regimens Beginning in 1966, doses approximately corresponding to 1 820 ret, which perhaps exceed the usually accepted central nervous system tolerance, were used for the split-course technique (2 800 rad in 10 fractions in 11 to 13 days, rest of 21 to 24 days, and then another 2 800 rad in 10 fractions in 11 to 13 days, Table 1) This dose subsequently was reduced to approximately 5 200 rad (substituting the 280 rad increments with 260 rad/fraction), however, in order to be more in line with the conventional dose level of 5 250 to 5 600 rad in 25 to 28 fractions in 33 to 38 days used after 1966 for the regularly fractioned treatment regimens

Submitted for publication 2 December 1974

— RAYNAL M ENNUYER A et BATAINI P Etude comparative des résultats concernant les épithéliomas de la région amygdalienne traités Institut Gustave Roussy et à la Fondation Curie Ann Radiol 9 (1966) 815

— CHASSAGNE D CACHIN Y BAILLET F et FOURNELLE LE BUIS F Carcinomes épidermoides de la langue mobile et du plancher buccal Acta radiol Ther Phys Biol 9 (1970) 465

WYNDER E L BROSS I J and FELDMAN R J A study of the aetiological factors in cancer of the mouth Cancer 10 (1957) 1300

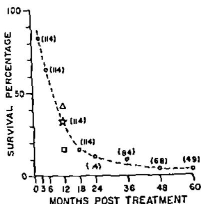


Fig 2. Survival curve for the series At 1 year effect of treatment on survival is indicated (number of cases in parentheses) □ high dose split course, ★ low dose split course, △ continuous irradiation

therapy (5 600 rad) the one-year survival was 17 per cent and none survived at two years For moderate dose split-course therapy (5 000 to 5 300 rad) the one-year survival was 33 per cent and the two year survival 19 per cent Although it cannot be stated with certainty that case selection between the three treatment techniques was similar, there was no intentional bias

Treatment volumes depended basically upon the location and size of the tumor as defined by angiography or brain scan or as delineated at craniotomy Also, during the first 2½ years, the treatment policy was generally to use small fields Subsequently, the approach changed to larger treatment portals, a 13 cm × 11 cm field (143 cm²) encompasses a major portion of the brain (Fig 3), but does spare some of the scalp and parts of the brain at low risk The whole brain was irradiated in only 3 patients

The distribution of one-year survivors according to age at the initiation of therapy appears in Fig 4 The median age of one-year survivors was 47 years, slightly less than for the entire series (53 years) The patients in ages 50 to 69 years had a particularly

Table 1

Treatment regimens used most frequently (6 patients did not complete treatment 2 conventional, 4 split-course)

	Approx NSD (ret)	No of patients
Conventional fractionation		
4 500/22 Rx/30 days } 2 64–8 66	1 470	16
4 000 20 Rx/26 days } 2 64–8 66	1 370	12
5 600 28 Rx/38 days 9 66–8/68	1 700	6
5 250 25 Rx/33 days 9 68–9/71	1 650	30
Split course		
5 600 20–21 Rx/45–50 days 9/66–8/68	1 820	23
5 000–5 300 20–21 Rx/45–50 days 9 68–9/71	1 640	21

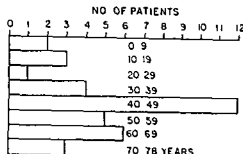


Fig 1 Age distribution of patients included in the entire series

Material and Methods

Between February 1, 1964, and September 30, 1971, 114 patients with glioblastoma multiforme were treated with megavoltage radiations (^{60}Co gamma rays and 6 MV linear accelerator, roentgen radiation) at the Vanderbilt University Hospital Virtually all patients with glioblastoma multiforme seen at this hospital during this period were irradiated, postoperative death or severe neurologic deficit postoperatively were the usual causes for exclusion Eighty males and thirty-four females with ages ranging from 4 to 78 years comprised this series The median age at start of treatment was 53 years (Fig 1) Histologic confirmation of the diagnosis was obtained in all but the six patients in whom the tumor position precluded biopsy or resection, all of these latter patients are dead

The patients were irradiated by several treatment schemes (Table 1) The majority of patients were treated with doses of either 4 000 to 4 500 rad or 5 250 to 5 600 rad for conventional, uninterrupted fractionation (5 days per week) and 5 000 to 5 600 rad for the split-course regimens Doses discussed are maximum doses to the primary tumor volume

Irradiation was performed through opposed lateral fields Early in this series the fields averaged approximately 100 cm² with only one field being irradiated daily However, after 1966, field sizes were increased to an average of 135 cm² and each field was irradiated daily In some patients the final 500 to 1 000 rad of irradiation were from fields reduced in size The size of the field was determined by tumor location and its apparent volume Generous margins were the rule, but in only three instances was the whole brain irradiated for even a part of the treatment

Results

Survival results for the entire series are given in Table 2 Only 2 of the 49 patients available for five-year survival analysis are living and well, and 3 of 68 survive at four years The one-year survival for the entire group, including the 6 patients who did not complete their planned course of treatment and 1 patient lost to follow up (considered dead), is 33 per cent and at two years the survival is 12 per cent

Conventional therapy was associated with a one-year survival of 40 per cent and a two-year survival of 15 5 per cent (Fig 2, Table 3) With high dose split-course

Table 2

Survival, post irradiation

Months post irradiation	No alive/total	Per cent survival
3	95/114	83
6	73/114	64
12	37/114	33
18	18/114	16
24	14/114	12
36	8 84	10
48	3/68	4 5
60	2/49	4

Table 3

Survival and its relationship to technique of treatment

Survival (months)	Split course		Conventional fractionation
	5 600 rad	5 000–5 300 rad	4 000–5 600 rad
6	15/23	15/21	41/64
12	4/23 (17%)	7/21 (33%)	26 64 (40%)
(17%)	(33%)		(40%)
18	0/23	5/21 (24%)	13/64 (20%)
24	0/23	4/21 (19%)	10 64 (15 5%)

of 4 000 rad in 21 fractions over 7 days or 63 fractions over 21 days gave survivals similar to those with conventional fractionation (21 fractions daily for 21 days) to a dose of 4 000 rad SIMPSON, of course, had hoped that treating with multiple small fractions would permit a significant improvement in the curative ratio (obtaining improvement in local control without adversely affecting normal tissue tolerance) Perhaps the optimal utilization of this approach has not been obtained

The effect of field size on survival is difficult to evaluate because of biases involved in selection of field sizes Perhaps the data show an advantage to medium-sized fields, but small tumors have a relatively good prognosis and these tumors, according to the treatment policy, were treated with smaller fields than were the larger tumors For the small tumors treated with medium-sized fields, an even better survival with larger field therapy might have resulted Whole brain irradiation was used rarely (in three patients only), so the role of extended field therapy cannot be assessed accurately

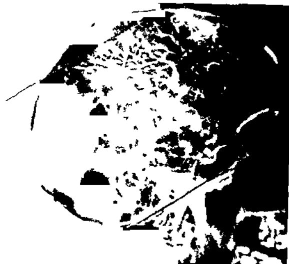


Fig 3 A patient with a parieto occipital glioblastoma multiforme with a lateral treatment portal measuring 13 cm × 11 cm

low survival rate, only 11 of 60 (18 per cent) being one-year survivors The females had a better survival rate than the males, 30 per cent of the entire group was com posed of females, but 39 per cent of the one year survivors were females

Site of origin of glioblastoma multiforme has been considered important in sur vival (RAMSEY & BRAND 1973) Included in the seven survivors at 3 years post therapy in this series are 2 patients with frontal lesions, 2 with fronto parietal tumors 2 with parieto occipital tumors, and 1 with a cerebellar tumor Four of these patients were female, the age ranged from 4 to 65 years Details of the treatment in these patients is included in Table 4

There was no microscopic documentation of brain necrosis amongst any of the autopsied patients, even in those receiving the high dose split course therapy Residual tumor, usually in the center of the irradiated volume, was found in every instance again even with the high dose split course therapy

Discussion

The results do not suggest that high dose irradiation is necessary to obtain maximal survival However, evaluation does show a probable benefit from treatment with doses of approximately 5 000 rad 42 per cent of the patients treated with conventional fractionation with doses ranging from 4 000 to 5 600 rad survived one year

The use of the split course therapy, at least with the schemes described in the present series, is of no apparent advantage as far as survival is concerned, in fact, at both dose levels the patients treated by split course techniques had lower one-year survival rates than those treated with conventional fractionation The explanation for this is not apparent

Results of attempts to improve survival by drastically altering treatment fractionation have been reported by SIMPSON (1970) Treatments every 8 hours with total doses

Table 4

Treatment details on the eight 3 year survivors

Case	Age	Sex	Location	Date of initiation of irradiation	Treatment regimen	Field size (cm)	Current status
1	65	M	R frontal	8/64	205 rad/22 Rx/29 days	8 × 10	D 10 67
2	13	F	L fronto parietal	9 66	200 rad/28 Rx/40 days	10 × 12	A & W
3	37	M	L parietal	12/66	250 rad/16 Rx 28 days	12 × 12	D 9/70
4	33	M	R parieto-occipital	6 68	250 rad/22 Rx/36 days	10 10	A & W
5	4	F	Cerebellar	4/70	200 rad/25 Rx/36 days	8 8	A & W
6	41	M	R parieto occipital	8/70	260 rad/19 Rx/40 days (split)	11 12	A & W
7	48	F	R fronto-parietal	1/71	200 rad/20 Rx/27 days	6 × 6	A & W
8	65	F	L frontal	3/71	250 rad/21 Rx/32 days	8 × 8	A & W

a better response to treatment and this factor should influence the therapy decision as well

Optimum radiation therapy, with dose and fractionation as well as volume being important factors, combined with chemotherapy may result in significantly improved palliation and perhaps even better survival Controlled investigations to document conclusively the significant parameters affecting results of irradiation, in particular, are urged

Acknowledgements

National Cancer Institute, Wisconsin Clinical Cancer Training in Radiotherapy Physics, and

SUMMARY

Experience in irradiating 114 patients with glioblastoma multiforme is reviewed The split course therapy utilized in this series even to high doses (approximately 5 600 rad in 20 fractions over 45 to 50 days) was not associated with an improved survival and does not seem of benefit over conventional fractionation Adding BCNU (or perhaps tri iodothyronine) to medium field (less than 135 cm²) and moderate dose irradiation (5 000 rad in 25 treatments in 33 days) may improve the outlook for patients with glioblastoma multiforme An expanded controlled clinical trial to assess this promise of improved treatment results seems indicated

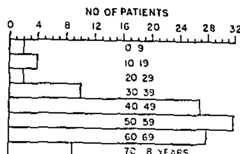


Fig 4 Age distribution of patients surviving 1 year post irradiation

Nevertheless, the one year survival rate of 33 per cent is similar to the 34 per cent reported by KRAMER (1973) with whole brain irradiation (±a boost to the primary tumor) to a dose of at least 6 000 rad in 6 to 7 weeks, the five year survival rates also are not dissimilar Our present feeling is that fields in excees of 150 cm² usually are not necessary However, a randomized prospective trial would be required to verify this opinion

WALKER (1973) has reported an improved median survival of glioblastoma patients irradiated in association with BCNU (1 3-bis(chloroethyl)-1-nitrosourea) administration (80 mg/m² daily for 3 days, repeated subsequently every two months) Median survival for a series of 223 patients now is available for evaluation with follow up times of one to four years Twenty-three of the patients are still alive The median survival of the randomized patients given supportive therapy alone after resection is 14 weeks, treated with BCNU alone 21 weeks, and irradiated without adjuvant BCNU 34 weeks With irradiation and BCNU the median survival is extended to 40 weeks, in addition the results suggest a greater percentage of long-term survivors with this approach There also is interest in the use of BuDR intra-arterially in conjunction with irradiation (HOSHINO & SANO 1969) and more recently in other reports, imidazole carboxamide with either BCNU or meCCNU have been utilized (HORTON & CUNNINGHAM)

YUNG et coll (1973) reported on a group of 18 patients treated in the early 1960 s These patients were treated with a tumor dose of 4 000 rad in 4 weeks while the patients were maintained hyperthyroid (with a BMR of at least +30 per cent) by the administration of tri-iodothyronine Patients treated with surgery alone had a mean survival of 12 weeks, irradiation alone 18 weeks, surgery together with irradiation 29 weeks, and surgery, irradiation and tri-iodothyronine 102 weeks Based on these preliminary results, further investigation of this approach to the treatment of glio blastoma multiforme is indicated

Selection of suitable patients for treatment obviously is important KRAMER has recommended that patients with significant postoperative neurologic deficits or elderly patients should not be subjected to radiation therapy Patients with gliomas grade 3 have a better prognosis than those for grade 4 and, therefore, these patients should be approached with somewhat more optimism Females and young patients also have

FROM THE INSTITUTE OF PATHOLOGY, THE E N T DEPARTMENT, AND THE RADIUM CENTRE, MUNICIPAL HOSPITAL, UNIVERSITY OF ÅRHUS, DK-8000 ÅRHUS, DENMARK.

EPIDERMOID CARCINOMA OF THE TONGUE

Histologic grading in the clinical evaluation

C Lund, H Sogaard, O Elbrond, K Jorgensen and A P Andersen

Epidermoid carcinoma of the tongue generally has a poor prognosis This is due partly to the high frequency of recurrence or residual tumour after the primary treatment and partly to the even higher frequency of regional lymph node metastases, initially or later

A comparison between a clinical evaluation and a standardized, graduated microscopy was performed to find out the potential risk group of patients in whom recurrence, residual tumour or metastases would be most likely to occur

The material constitutes part of a larger series of 96 patients treated for carcinoma of the anterior two thirds of the tongue Previously a clinical analysis of this series has been published (Elbrond et coll 1973) The present report comprises 49 patients treated during the period 1955 to 1966, histologic material was not available for evaluation before 1955

Clinical aspects A recurrence or residual tumour was observed after the primary treatment in 28 patients (57 %), 35 (71 %) developed regional lymph node metastases ((13 primary (26 %), 22 secondary (45 %)) and in 14 patients (29 %) no metastases were observed In 7 cases (14 %) distant metastases were diagnosed during the follow-

Submitted for publication 20 September 1974

ZUSAMMENFASSUNG

Die Erfahrungen bei 114 bestrahlten Patienten mit einem Glioblastoma multiforme werden vorgelegt Die Split-Course-Therapie, die bei dieser Serie verwendet wurde, war, auch mit hohen Dosen (etwa 5 600 rad in 20 Fraktionen wahrend 45 bis 50 Tagen), nicht mit einer verbesserten Überlebensrate verbunden und scheint gegenuber konventioneller Fraktionierung ohne Vorteil zu sein Eine Kombination von Bestrahlung und BCNU (oder auch Tri-Jodthyronin) bei einer mittleren Feldgrosse (weniger als 135 cm²) und massigen Dosen (500 rad in 25 Behandlungen und 33 Tagen) konnen die Aussichten fur Patienten mit Glioblastoma multiforme verbessern Eine ausgedehntere kontrollierte klinische Versuchsserie, um diese Hoffnung auf verbesserte Behandlungsresultate festzustellen, scheint angezeigt zu sein

RÉSUMÉ

Les auteurs presentent l'irradiation de 114 malades atteints de glioblastome multiforme Le traitement en 2 temps utilisé dans cette série, meme à des doses élevées (approximativement 5 600 rad en 20 fractions sur 45 à 50 jours) n a pas entrainé une amélioration de la survie et ne semble pas supérieur au fractionnement habituel L'association de BCNU (ou peut-etre de tri iodothyronine) à un champ de dimension moyenne (inférieure à 135 cm²) et une dose d irradiation modérée (5 000 rad en 25 seances en 33 jours) peut améliorer l'avenir des malades atteints de glioblastome multiforme Il semble indiqué de procéder à un large essai clinique controlé pour apprécier cet es poir d'amélioration des résultats du traitement

REFERENCES

ARISTIZABAL S A and CALDWELL W L Time dose-volume relationships in the treatment of glioblastoma multiforme Radiology 101 (1971), 201

HORTON J and CUNNINGHAM T Unpublished data from Albany Medical College

HOSHINO T and SANO K Radiosensitization of malignant brain tumors with bromouridine (thymidine analogue) Acta radiol Ther Phys Biol 8 (1969), 15

KRAMER S Radiation therapy in the management of malignant gliomas *In* Proceedings of the Seventh National Cancer Conference, p 823 J B Lippincott Co, Philadelphia and Toronto 1973

ORTON C G and ELLIS F A simplification in the use of the NSD concept in practical radiotherapy Brit J Radiol 46 (1973), 529

RAMSLY R G and BRAND W N Radiotherapy of glioblastoma multiforme J Neurosurg 39 (1973), 197

SIMPSON W J Discussion of Split course techniques paper by Holsti, L R *In* Time and dose relationships in radiation biology as applied to radiotherapy, p 301, Brookhaven National Laboratory 50203 (C 57), 1970

WALKER M D Chemotherapy of malignant glioma *In* Proceedings of the Seventh National Cancer Conference p 817 J B Lippincott Co Philadelphia and Toronto 1973

YUNG W K, GRIEM M L STEWARD W and MARKS J E Glioblastoma Analysis of treatment with radiation and tri iodothyronine Invest Radiol 8 (1973), 270

Table 3

Microscopic grading

	Points			
	1	2	3	4
Appearance	Exophytic papillomatous	Inverted papillomatous	Small cords and groups of cells	Marked cellular dissociation
Cytoplasmic differentiation (keratinization)	High >50 % keratinisized	Moderate 20–50 % keratinisized	Poor 5–20 % keratinisized	None 0–5 %
Nuclear differentiation (BRODERS)	High 75 % mature	Moderate 75–50 % mature	Poor 50–25 % mature	None 0–25 % mature
Mitosis*	Single 0–1	Moderate number 0–3	Great number 0–5	Numerous 5
Mode of invasion (modus)	Well defined borderline	Cords less marked borderline	Groups of cells No dist borderline	Diffuse growth
Stage of invasion (depth)**	Possible invasion	Microinvasion (few cords)	Nodular into submucosa	Invasion deeper than submucosa
Vascular invasion	None	Possible	Lymph vessels	Blood vessels
Cellular response (plasma lymphocytic)	Marked (continous rim)	Moderate (many large patches)	Slight (a few small patches)	None

* Minimum evaluation on 5 fields 250

** No invasion is recorded as carcinoma in situ

The microscopy was performed without knowledge of the clinical evaluation Only the primary biopsy from the 49 patients was analysed

Each specimen can attain a maximum score of 32 (8 × 4) As it was not always possible to assess all parameters usually because of defective specimens, a score value was set up defined as the score divided by the number of parameters assessed

The growth in depth could be evaluated in only 69 per cent (34/49) of the biopsies (Table 4) This might influence the evaluation of the other parameters which often gives a higher score value at the depth of an infiltrating lesion (Fig 5)

Correlation between microscopic and clinical evaluation The score value was correlated to (1) the entire material, (2) the group with recurrence or residual tumour,

Table 1

Frequency of regional lymph node metastases

No	Primary metastases	Secondary metastases	Metastases total	No metastases
49	13 (27 %)	22 (44 %)	35 (71 %)	14 (29 %)

Table 2

Recurrences of primary tumour, residues and regional lymph node metastases in relation to T classification

No of patients		No of recurrences of primary tumour or residues	No of regional lymph node metastases
T1	6	1 (17 %)	1 (17 %)
T2	8	3 (38 %)	4 (50 %)
T3	25	14 (56 %)	20 (80 %)
T4	10	10 (100 %)	10 (100 %)
Total	49	28 (57 %)	35 (71 %)

up period Secondary lymph node metastases are defined as metastases manifesting themselves after the primary treatment of the tumour

The results of treating the regional lymph node metastases have been extremely discouraging, the 5-year survival rate being only 9 per cent (3/35) Accordingly, the occurrence of regional metastases has a decisive prognostic influence Out of 14 patients without regional metastases only 3 died of carcinoma of the tongue, 6 died of intercurrent diseases without recurrence, and 5 were alive after 5 years without signs of recurrence

The T classification in relation to the frequency of local recurrences or residual tumours and regional metastases appears in Table 2 As might be expected, their frequency was highest in the T3 and T4 groups in the latter 100 per cent Thus, also a TNM classification gave relevant prognostic information

Microscopy Carcinoma of the tongue is almost invariably of the epidermoid type, but of a varying degree of differentiation and varying growth This affords a multifactorial grading, comprising partly the tumour cell population and partly the tumour host relationship

A grading system (Table 3) is used, based in principle upon a system applied by Jakobsson (1973) to a series of glottic carcinomas and by Lund et coll (1975) to a series of carcinomas of the lip This system comprises 8 parameters, each of which is graded from 1 to 4 Each parameter is accurately defined making it possible to reproduce the results and obtain comparable values

Table 4

Microscopic grading of primary biopsies

Total series	Structures	Cytopl diff	Nuclear diff	Mitosis	Mode	Depth	Vasc invasion	Cell response	Mean score
Estimated parameters	48	49	49	49	48	34	46	46	
Number of points	128	110	135	119	127	115	103	96	
Mean score	2.7	2.2	2.8	2.4	2.6	3.4	2.2	2.1	2.6

Table 5

Relationship between T grouping and score value

	0–2.5	2.6–4
T1	4/6 67%	2/6 33%
T2	3/8 38%	5/8 62%
T3	9/25 36%	16/25 64%
T4	4/10 40%	6/10 60%

of carcinoma (Fig. 4). However, this difference is significant ($p < 0.05$) only in the group with regional metastases.

The T classification in relation to score grouping appears in Table 5. There seems to be a tendency for the T2, T3, and T4 groups, assessed microscopically, to be more malignant than the T1 group. However, the numbers involved are small, not allowing a definite evaluation. On the other hand a significant ($p < 0.05$) relationship existed between the frequency of regional lymph node metastases and the score values within the T1 and T2 groups (Table 6). The same applies to the cases with recurrence or residual tumour.

Discussion

The importance of a microscopic grading of epidermoid carcinomas has been discussed by Broders (1920, 1926, 1940), primarily as a monofactor system based upon cellular differentiation. A generally accepted bifactorial system has been

Fig 1 Distribution of total series and cases with regional lymph node metastases in relation to score value ☐ 14 patients without metastases, ☐ 35 patients with metastases

Fig 2 Frequency of residual tumours and recurrences in relation to score value

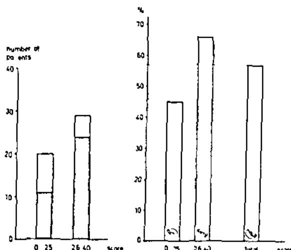


Fig 1 Fig 2

Fig 3 Frequency of regional lymph node metastases in relation to score value ☐ primary metastases, ☐ secondary metastases

Fig 4 Frequency of deaths from carcinoma of the tongue in relation to score value

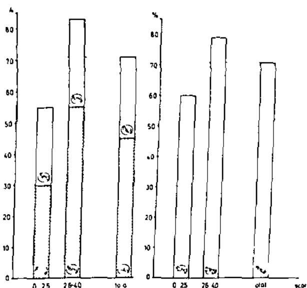


Fig 3 Fig 4

(3) the group with metastases, (4) the group dying of carcinoma, (5) the T classification

Due to the relatively small number of patients, two sub-groups only were used with a high and a low score value, respectively, arbitrarily separated at a score value =2 5

The grouping of the entire material by score value is presented in Fig 1 The figure reveals that 59 per cent (29/49) were in the group with the higher score values The recurrences or residual tumours occurred with an increased frequency at score values exceeding 2 5 (Fig 2) A similar increase in the frequency in relation to score value was seen for the cases with metastases (Fig 3) and the group of patients dead

Table 4

Microscopic grading of primary biopsies

Total series	Structures	Cytopl diff	Nuclear diff	Mitosis	Mode	Depth	Vasc. invasion	Cell response	Mean score
Estimated parameters	48	49	49	49	48	34	46	46	
Number of points	128	110	135	119	127	115	103	96	
Mean score	2.7	2.2	2.8	2.4	2.6	3.4	2.2	2.1	2.6

Table 5

Relationship between T grouping and score value

	0–2.5	2.6–4
T1	4/6 67 %	2/6 33 %
T2	3/8 38 %	5/8 62 %
T3	9/25 36 %	16/25 64 %
T4	4/10 40 %	6/10 60 %

of carcinoma (Fig. 4). However, this difference is significant ($p<0.05$) only in the group with regional metastases.

The T classification in relation to score grouping appears in Table 5. There seems to be a tendency for the T2, T3, and T4 groups, assessed microscopically, to be more malignant than the T1 group. However, the numbers involved are small, not allowing a definite evaluation. On the other hand a significant ($p<0.05$) relationship existed between the frequency of regional lymph node metastases and the score values within the T1 and T2 groups (Table 6). The same applies to the cases with recurrence or residual tumour.

Discussion

The importance of a microscopic grading of epidermoid carcinomas has been discussed by BRODERS (1920, 1926, 1940), primarily as a monofactor system based upon cellular differentiation. A generally accepted bifactorial system has been

Table 6

Relationship between frequency of regional lymph node metastases and score value in the T-groups

T1 group			
Score	0–2.5	2.6–4.0	total
number	0/4 (0 %)	1/2 (50 %)	1/6 (17 %)
T2 group			
Score	0–2.5	2.6–4.0	total
number	0/3	4/5 (80 %)	4/8 (50 %)
T3 group			
Score	0–2.5	2.6–4.0	total
number	7/9 (78 %)	13/16 (81 %)	20/25 (80 %)
T4 group			
Score	0–2.5	2.6–4.0	total
number	4/4 (100 %)	6/6 (100 %)	10/10 (100 %)

advocated by inter alios LEVER (1967) It comprises, besides the degree of cellular differentiation, also an evaluation of the growth in depth JAKOBSSON (1973) elaborated these two factors to comprise 4 parameters each Applying this multifactorial system to a series of laryngeal carcinomas, he demonstrated a clearly significant relation between a summation of the 8 parameters and prognosis

A correlation between TNM stage and prognosis is evident in all TNM classified series of tumours in the head- and neck-area Application of a well-defined multifactorial microscopic system to TNM classified series is of considerable interest as a supplement to the prognostic assessment In a series of epidermoid carcinomas of the lip (LUND et coll 1975) it has given relevant prognostic data, there being a significant relation ($p < 0.05$) between microscopic grading and the frequency of (1) local recurrences and residual tumours, (2) regional lymph node metastases, (3) mortality, and (4) the T classification

In the present series of carcinomas of the tongue a significant correlation ($p < 0.05$) was found between microscopic grading and the frequency of regional lymph node metastases No statistical significance was found between recurrence or residual tumour cases, mortality and T classification on the one hand and the score value on the other Within the individual T groups (Table 6), however, it is of importance that all 5 cases with metastases in the T1 and T2 groups were among the tumours with a score value exceeding 2.5 This gives a metastatic frequency of 71 per cent (5/7) in the biopsies with a high score value against 0 per cent (0/7) in the biopsies with a low score value in the T1 and T2 groups, which is statistically significant ($p < 0.05$) The same applies to the cases with recurrence or residual tumour





Fig. 5 A relatively highly differentiated epidermoid carcinoma (general view) may vary from surface to depth (insets)

The absence of further statistical significance may be due to uncertain clinical or microscopic evaluation or to the calculation Three different modes of primary treatment (radium intubation external irradiation surgery) were used and the TNM classification may be uncertain in a retrospective assessment The quality of the

specimen, and especially its representativeness (Table 4), may include factors of uncertainty and the calculation may be uncertain due to the small numerical quantities in the individual T groups

Conclusion

A well defined, multifactorial microscopic grading system applied to a clinically well-investigated series of patients with *epidermoid carcinoma of the tongue* gave relevant data retrospectively All 5 metastatic cases in the T1 and T2 groups occurred in patients with tumours of a high score value (degree of malignancy), whereas no metastases occurred within these two groups with a low score value (Table 6) This may be said to be an important supplement in the evaluation of the prognosis

The results suggest that the clinical TNM classification be supplemented by microscopic grading of the primary tumour to facilitate the separation of special risk groups in which regional metastases may be expected A biopsy representative of the tumour growth in the depth is necessary in cases where the tumour is small (Fig 5)

SUMMARY

In a series of 49 patients with epidermoid carcinoma of the tongue microscopy of the primary biopsy was performed, using a multifactorial grading system consisting of 8 para meters, each of 4 grades The score value (degree of malignancy) revealed a statistically significant correlation with the frequency of regional metastases As this was particularly marked in the T1 and T2 groups, it seems to be an important supplement to the clinical evaluation of risk groups

ZUSAMMENFASSUNG

Bei einer Serie von 49 Patienten mit einem Epidermoid Karzinom der Zunge wurde die primare Biopsie unter Verwendung eines Multifaktorgradierungssystems bestehend aus 8 Parametern, von welchen jeder in 4 Grade aufgeteilt war, mikroskopisch untersucht Der Markierungs Wert (Grad von Malignitat) ergab eine statistisch signifikante Korre lation zur Frequenz der regionalen Metastasen Da dieses besonders markiert bei den T1 und T2 Gruppen war, scheint dieses ein bedeutungsvolles Supplement bei der klinischen Feststellung von Risikogruppen zu sein

RÉSUMÉ

Sur une série de 49 malades atteints de carcinome épidermoïde de la langue l examen microscopique de la biopsie primaire a été fu en utilisant un systeme de gradation multi factoriel consistant en 8 parametres ayant chacun 4 grades Le nombre de points (degré de malignité) s est montré en corrélation statistiquement significative avec la fréquence des métastases régionales Etant donné que ceci était particulièrement marqué dans les groupes T1 et T2 cette cotation paraît etre un complément important à l appréciation clinique des groupes de risque

REFERENCES

BRODERS A C Squamous cell epithelioma of the lip J Amer med Ass 74 (1920), 656
— Carcinoma grading and practical application Arch Path (Chic) 2 (1926), 376
— The microscopic grading of cancer *In* Treatment of cancer and allied disease, p 19 Edited by G T Porch and E M Livingstone Harper and Brothers, New York and London 1940 p 19
ELBRØND O, ANDERSEN A P and JØRGENSEN K Carcinoma linguae A series of 96 patients Acta radiol Ther Phys Biol 12 (1973), 465
JAKOBSSON P Glottic carcinoma of the larynx Thesis, Stockholm 1973
LEVER W F Histopathology of the skin J B Lippincott Philadelphia and Toronto 1967
LUND C, SØGAARD H, ELBRØND O, JØRGENSEN K and ANDERSEN A P Carcinoma of the lip Prognostic evaluation Acta radiol Ther Phys Biol 14 (1975), 465
UICC Union Internationale Contre le Cancer, Geneva 1968

FROM THE DEPARTMENTS OF RADIATION THERAPY (DIRECTOR PROF I KAZEM), AND OTOLARYNGOLOGY (DIRECTOR PROF W BRINKMAN), SINT RADBOUD ACADEMIC HOSPITAL, CATHOLIC UNIVERSITY, NIJMEGEN, THE NETHERLANDS

PRE-OPERATIVE SHORT INTENSIVE RADIATION THERAPY OF T3–T4 LARYNGEAL CARCINOMA

I KAZEM, P VAN DER BROEK, W BRINKMAN, M TUREK and B J M BOSBOOM

Surgery or irradiation may be used in the treatment of advanced carcinoma of the larynx The overall results, however, of either modality applied separately is rather disappointing Pre operative radiation therapy followed by radical surgery for the treatment of advanced but resectable carcinoma of the larynx and laryngopharynx was first introduced by GOLDMAN & SILVERSTONE (1961) Similar approaches were later suggested by HENDRICKSON & LIEBNER (1968) and OGURA & BILLER (1970 a) and it is now generally accepted that pre operative irradiation significantly improves the results at least in supraglottic and laryngopharyngeal carcinoma However, a controversy still exists in respect to the dose and the timing of the pre operative radiation therapy GOLDMAN et coll (1970 1972), supported by WANG et coll (1972) and CONSTABLE et coll (1972) recommend high doses 5 500 rad is given to the tumour bearing volume in 5 to 6 weeks followed by surgery within a rest period of three to six weeks HENDRICKSON (1970) and OGURA & BILLER (1970 b) on the other hand suggested a low dose therapy HENDRICKSON employed a dose of 2 000 R delivered in 8 treatments over 10 days followed promptly by surgery OGURA & BILLER ad-

Submitted for publication 6 November 1974

Table 1

Summary of all cases of T3–T4 laryngeal carcinoma treated in the period 1968 to 1972

Region		Treatment modality			Total
		Radiation therapy only	Pre oper R.T + surg.	Surgery only	
Glottic	T3	19	10	2	
	T4	0	1	0	32
	All	19	11 (2N+)	2 (1N+)	(3N+)
Supraglottic	T3	18	14	1	
	T4	18	6	1	58
	All	36 (17N+)	20 (8N+)	2	(25N+)
Subglottic	T3	2	1	1	
	T4	0	1	0	5
	All	2	2	1	
Total		57	33	5	95 (28N+)

N palpable cervical nodes

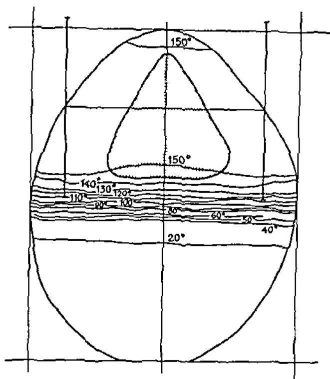
ministered a dose ranging between 1 500 and 3 000 R over two to three weeks followed by surgery three to four weeks later The experiences of short intensive pre-operative irradiation of T3–T4 laryngeal carcinomas is now reported

Material and Methods

In the period 1968 to 1972, 95 patients with T3–T4 laryngeal carcinoma were treated 57 patients received radiation therapy only, 33 pre-operative irradiation followed by surgery, and 5 patients were primarily treated by surgery only (Table 1)

All patients had microscopically confirmed squamous cell carcinoma Clinical, endoscopic and radiographic examinations were performed in all patients Site and primary tumour classification were assigned according to the international TNM classification recommended for the period 1963 to 1972 Three patients of the 32 with glottic carcinoma had palpable cervical nodes, two of these were in the pre-operative group and one was treated primarily with surgery In the supraglottic group 25 patients had palpable nodes, 17 of these were in the group irradiated only (48 per cent) and eight in the pre-operative irradiation group (40 per cent)

Radiation therapy only The irradiation is administered to the tumour bearing volume using two parallel opposing fields Telecobalt gamma radiation is utilized with an additional diaphragm applied to the beam (Figure) The field size ranges from 6 cm 8 cm to 7 cm × 9 cm depending on the extent of the tumour and the presence of palpable nodes. A total tumour dose of 6 000 to 6 500 rad is delivered in 6 to 7 weeks



Radiation treatment plan of an illustrative case of *laryngeal carcinoma* to demonstrate the isodose summation lines of two parallel opposing fields Telecobalt gamma radiation used with additional tungsten diaphragm Field size 8 cm × 8 cm

Pre-operative radiation therapy The same planning procedure field sizes and radiation quality as in the former group are employed A total dose of 2 500 rad in 5 equal sessions on five successive days is given This is usually administered on Monday through Friday, and surgery is performed the following Monday with the week end between the end of radiation therapy and operation

Surgery Total laryngectomy is performed, neck dissection only when lymph nodes with possible metastases are encountered Horizontal incisions are always employed If a neck dissection is indicated, the incision is drawn up to the mastoid tip and down to the acromion Three point junctions are avoided The larynx is mobilised and removed together with the hyoid bone, and in case of subglottic extension together with part of the thyroid gland Tracheostomy is made through a separate incision *The pharyngeal defect is closed in one line avoiding three point junctions* The pharynx is closed in three layers with continuous stitches using dexon, a synthetic suture material which is slowly resorbed

Results

All patients were evaluated for at least one year To enhance the meaning of the results over the rather short period of observation only tumour free survival is reported for one year, two years and three years The following categories of patients are

Table 2

Overall one-year tumour free survival, T3–T4 laryngeal carcinoma

Treatment modality	Total number treated	Number alive	Per cent
Radiation therapy only	57	23	40
Pre-operative irradiation + surgery	33	23	64
Surgery only	(5)	(3)	(60)

Table 3

One-year tumour free survival, T3–T4 glottic carcinoma

Treatment modality	Total number treated	Number alive	Per cent
Radiation therapy only	19	11	57
Pre-operative irradiation + surgery	11	7	64

Table 4

Two-year tumour free survival, T3–T4 glottic carcinoma

Treatment modality	Total number treated	Number alive	Per cent
Radiation therapy only	16	8	50
Pre-operative irradiation + surgery	8	4	50

counted as failures and are not included in the tumour free survival (1) Patients dead of causes related or unrelated to their laryngeal carcinoma, and (2) patients alive with local or distant metastases

Table 2 gives the overall one-year tumour free survival for all regions grouped according to treatment modality The number of patients in this series treated with surgery only is too small to allow any conclusions The group treated with combined pre-operative radiation therapy shows an overall higher rate (64 per cent) compared with the group irradiated only (40 per cent) When patients were grouped according to regions an obvious difference was noted in glottic tumours compared to supraglottic tumours The one-year tumour free survival of T3–T4 glottic tumours appears in Table 3 There is a slightly higher survival rate (64 per cent) in the pre-operative group compared to the survival rate (57 per cent) in the group irradiated only However, the two-year tumour free survival rate for both treatment modalities is identical (50 per cent, Table 4)

Table 5

One-year tumour free survival, T3–T4 supraglottic carcinoma

Treatment modality	Total number treated	Number alive	Per cent
Radiation therapy only	36	11	31
Pre-operative irradiation + surgery	20	15	75

Table 6

Two- and three-year tumour free survival, T3–T4 supraglottic carcinoma

Treatment modality	2-year survival		3 year survival	
	No	Per cent	No	Per cent
Radiation therapy only	11/32	34	6/20	30
Pre-operative irradiation + surgery	11/13	84	8/9	88

The tumour free survival rates for supraglottic tumours are given in Tables 5 and 6 The group receiving pre-operative radiation therapy demonstrates significantly superior results after one year (75 per cent), two years (84 per cent), and three years (88 per cent) In comparison the group of patients with T3–T4 supraglottic tumours irradiated only yielded 31 per cent, 34 per cent and 30 per cent for the one-year, two-year and three-year tumour free survival, respectively

Complications There is no operative mortality in this series No significant complications attributed to the pre-operative radiation was observed in any of the patients All wounds healed promptly and no incidence of fistulas was recorded

Discussion

The results confirm published data about the value of pre-operative radiation therapy combined with surgery for the treatment of advanced supraglottic carcinoma The data, however, demonstrate no advantage of such treatment in the case of advanced glottic carcinoma Almost identical results in terms of tumour free survival may be obtained with radiation therapy only

The short, intensive pre operative irradiation used, offers the advantage of an effective radiation dose in a short treatment interval This saves the patient and hospital several weeks of treatment time as well as avoids the delay of surgical treatment

It seems that the controversy regarding high or low dose for pre operative irradiation of advanced laryngeal carcinoma may be settled by employing the short, intensive treatment schedule The nominal standard dose (NSD) equivalent to 2 500 rad in 5 days calculated according to the formula proposed by ELLIS is 1 423 ret This amounts to about 77 per cent of the normal tissue tolerance estimated at an NSD of 1 800 ret A dose of 2 500 rad given in 5 equal successive daily fractions is probably biologically equivalent to a dose of 4 500 rad given in a period of 4 to 5 weeks *The treatment schedule* proposed in this report thus combines the efficacy of the high dose schedule with the convenience of the low dose schedule Further, short intensive radiation therapy is well tolerated and surgery *is usually performed before* the onset of reaction

Acknowledgement

The technical assistance of Miss R v d Loo is gratefully acknowledged

SUMMARY

A group of 33 patients with T3 T4 laryngeal carcinomas received in the period *1968* to 1972 pre operative irradiation with ^{60}Co followed by surgery A total dose of 2 500 rad was

only In glottic tumours the results were similar in both groups, but significantly superior in supraglottic tumours receiving pre operative radiation therapy The treatment schedule proposed is well tolerated and surgery is usually performed before the onset of reaction

ZUSAMMENFASSUNG

Eine Gruppe von 33 Patienten mit T3 T4 Larynxkarzinomen erhielt während der Periode zwischen 1968 und 1972 praoperative Bestrahlung mit ^{60}Co gefolgt von Chirurgie Eine Gesamtdosis von 2 500 rad wurde in 5 gleichgrossen Fraktionen gegeben Die Tumor freie Überlebensfrequenz dieser Patienten wurde mit derjenigen einer vergleichbaren Gruppe von 57 Patienten die lediglich Strahlentherapie erhalten hatte verglichen Die Gesamt resultate der praoperativen Gruppe (64 %) sind gegenuber derjenigen der Gruppe die nur bestrahlt worden war uberlegen Bei Glottistumoren waren die Ergebnisse bei beiden Gruppen ahnlich aber signifikant uberlegen bei Supraglottistumoren die praoperative Strahlentherap e erhalten hatten Das vorgeschlagene Behandlungsschema wird gut vertragen und Chirurgie wird gewohnlicherweise vor dem Einsetzen der Reaktionen ausgefuhrt

RÉSUME

Un groupe de 33 malades atteints de cancer larynge T3 T4 ont été traités au cours de la période 1968 a 1972 par une irradiation pre-opératoire au ^{60}Co suivie d intervention chirurgicale Une dose totale de 2 500 rad a eté donnee en 5 seances egales Le taux de survie sans tumeur de ces malades est comparé à celui d un groupe comparable de 57 malades traités

uniquement par les radiations Les resultats d'ensemble dans le groupe des malades irradiés avant l opération (64%) sont superieurs à ceux des malades qui n'ont eu que l irradiation Dans les tumeurs glottiques les résultats sont similaires dans les 2 groupes mais ils sont significativement supérieurs dans les tumeurs supra glottiques ayant eu une irradiation pré opératoire Le schéma de traitement proposé est bien toléré et l intervention chirurgicale est habituellement exécutée avant le début de la réaction

REFERENCES

CONSTABLE W, MARKS R D, ROBBINS J and FITZ HUGH G S High dose pre operative radiotherapy and surgery for cancer of the larynx Laryngoscope 82 (1972), 1861

GOLDMAN J L and SILVERSTONE S M Combined radiation and surgical therapy for cancer of the larynx and laryngopharynx Trans Amer Acad Ophthal Otolaryngol 65 (1961), 496

GOLDMAN J, GUNSBERG M, FRIEDMAN W, RYAN J and BLOOM B Combined therapy for cancer of the laryngopharynx Arch Otolaryng 92 (1970), 221

— SILVERSTONE S, ROFFMAN J and BIRKEN E High dosage pre operative radiation and surgery for carcinoma of the larynx and laryngopharynx A 14 year program Laryngo scope 82 (1972), 1869

HENDRICKSON F R The results of low dose pre operative radiotherapy for advanced carcinoma of the larynx *In* Front Radiation Ther Onc, Volume 5, p 123 Karger, Basel, Munchen, Paris, New York 1970

— and LIEBNER E Results of pre operative radiotherapy for supraglottic larynx cancer Ann Otol (St Louis) 77 (1968), 222

OGURA J and BILLER H (a) Pre operative irradiation for laryngeal and laryngopharyngeal cancers Laryngoscope 80 (1970), 802

— — (b) Planned pre operative irradiation for laryngeal and laryngopharyngeal carcinomas *In* Front Radiation Ther Onc, Volume 5, p 100 Karger, Basel, Munchen, Paris, New York 1970

WANG C C, SCHULTZ M D and MILLER P Combined radiation therapy and surgery for carcinoma of the supraglottis and pyriform sinus Laryngoscope 82 (1972), 1883

FROM THE DEPARTMENT OF RADIATION ONCOLOGY, CLAIRE ZELLERBACH SARONI TUMOR INSTITUTE, MOUNT ZION HOSPITAL AND MEDICAL CENTER SAN FRANCISCO, CALIFORNIA 94120, U.S.A.

EVALUATION OF TIME-DOSE FACTORS IN GLOTTIC TUMORS

KENNETH H LUK and JOSEPH R CASTRO

Experience has shown excellent tumor control and functional results following radiation therapy for limited squamous carcinoma of the vocal cords (BUSCHKE & VAETH 1963, FLETCHER & KLEIN 1964, GOFFINET et coll. 1973) Most treatment schemes have been based on five or six fractions per week with a range of 6 000 to 7 000 rad (super-voltage) given over a period of five to seven weeks ARISTIZABAL & CALDWELL (1972) in reviewing a number of reports have recommended a tumor dose biologically equivalent to 1960 ret, utilizing the nominal standard dose formula of ELLIS (1968) The basic dose recommended for ^{60}Co therapy by FLETCHER & KLEIN (1964) is 6 000 rad in five-and-one-half weeks (27 fractions) for minimal disease, plus an additional boost of 500 to 1 000 rad in 2 to 5 fractions for bulky disease Control rates for T1 and T2 tumors approximate 80 to 90 per cent with a very low rate of severe edema or cartilage necrosis unless a dose biologically equivalent to 2 000 ret is exceeded Because of a sigmoid curve relationship of tumor control to dose, a control rate of 90 per cent is probably as high as can be obtained in vocal cord carcinoma without an unacceptably high level of necroses

Despite the very abrupt changes in tumor control rates and necrosis rates with different fractionation schemes in other tumor sites, changes in fractionation from 5 days per week to 3 or 4 days per week do not appear to show similar effects in

This research was supported in part by National Institutes of Health, USPHS, Grant CA-5203
Submitted for publication 5 May 1975

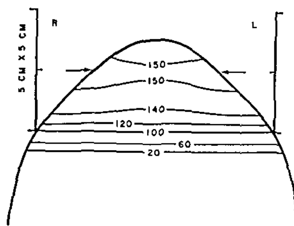


Fig 1 Opposed lateral fields with compensators ^{60}Co, 1 25 MeV, SSD 80 cm

treatment of vocal cord tumors The reasons for this are unclear but may be related to the small volume of normal tissues included in the treatment field It has been emphasized by FLETCHER & KLEIN (1964) that partial sparing of the arytenoid cartilages for tumors localized to the anterior part of the vocal cords results in a lower incidence of arytenoid edema and subsequent voice dysfunction Thus the proportion of the vital structure included in the radiation beam may be more important than the total volume of normal tissues irradiated

At least one randomized clinical trial is underway to evaluate 3 days per week versus 5 days per week treatment of vocal cord tumors (ELLIS et coll 1969, WIERNIK et coll 1972), with no apparent differences in results as yet Completely erroneous or inadequate localization of vocal cord tumors is rare, so that failure of control or complication ordinarily is a function of the time dose-volume parameters Thus vocal cord tumors form a good model for evaluation of time-dose-volume relationships

Material and Method Sixty patients with localized squamous cell carcinoma of the vocal cord without nodal or distant metastases were irradiated with 4 fractions per

Table 1

Distribution of patients by T stage All patients N0, M0

Stage	Vocal cord carcinoma		
	No of patients	Patients excluded	Patients examined
T1	46	3	43
T2	12	1	11
T3	2	1	1
T4	—	—	—
Total	60	5	55

Table 2

Local control by T stage with minimum 2 years follow-up

Stage	Vocal cord carcinoma	
T1	34/43	80%
T2	9/11	81.5%
T3	1/1	—
T4	—	—

week Five patients were excluded from analysis because of death from intercurrent diseases within 12 months from completion of radiation therapy At least a 24-month follow up period was available for 55 patients All patients were clinically staged according to the TNM system (Table 1)

Dose schedule and treatment technique The technique ordinarily used was ^{60}Co irradiation through opposed portals, with compensating or wedge filters placed in the radiation beam An example of a typical dose distribution for such a treatment plan is illustrated in Fig 1

Patients with T1 and T2 vocal cord lesions commonly received 6 000 rad in six-and-one half weeks with 4 treatment fractions per week utilizing 5 cm × 5 cm opposed portals as measured by the 50 per cent isodose line For the few patients with T3 vocal cord lesions the dose was 7 000 rad in 8 weeks, 4 fractions per week, through 7 cm × 8 cm portals

Results

The interest was directed both to local control (Tables 2, 3) and complication rates (Table 4) in the 4 fraction/week patients The control rate in T1 lesions is slightly lower than in the best reported series (Table 5) as is the average ret dose calculated directly from Ellis' formula without taking into account the concept of partial tolerance The control rates for T2 lesions, however, are comparable to other reported series

Table 3

Analysis of local control according to NSD (ret) of local cord carcinoma

Stage	1 600–1 700	1 700–1 800	1 800–1 900	1 900–2 000	Average ret value
T1	4/4	4 6	24/31	2/2	1 800
T2	—	1/1	7/9	1/1	1 850
T3	—	—	—	1/1	1 950
Total	4/4	5/7	31/40	4 4	

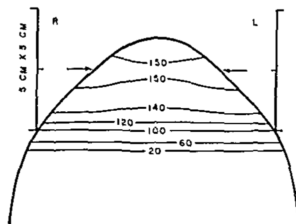


Fig 1 Opposed lateral fields with compensators ^{60}Co, 1 25 MeV, SSD 80 cm

treatment of vocal cord tumors The reasons for this are unclear but may be related to the small volume of normal tissues included in the treatment field It has been emphasized by FLETCHER & KLEIN (1964) that partial sparing of the arytenoid cartilages for tumors localized to the anterior part of the vocal cords results in a lower incidence of arytenoid edema and subsequent voice dysfunction Thus the *proportion of the vital structure included in the radiation beam may be more important* than the total volume of normal tissues irradiated

At least one randomized clinical trial is underway to evaluate 3 days per week versus 5 days per week treatment of vocal cord tumors (ELLIS et coll 1969, WILRNIK et coll 1972), with no apparent differences in results as yet Completely erroneous or inadequate localization of vocal cord tumors is rare, so that failure of control or complication ordinarily is a function of the time-dose-volume parameters Thus vocal cord tumors form a good model for evaluation of time-dose-volume relationships

Material and Method Sixty patients with localized squamous cell carcinoma of the vocal cord without nodal or distant metastases were irradiated with 4 fractions per

Table 1

Distribution of patients by T stage All patients N0, M0

Stage	Vocal cord carcinoma		
	No of patients	Patients excluded	Patients examined
T1	46	3	43
T2	12	1	11
T3	2	1	1
T4	—	—	—
Total	60	5	55

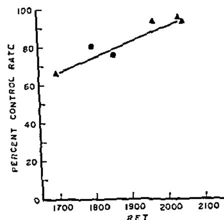


Fig 2 Dose-response curve for T1N0 vocal cord carcinoma using NSD Cf Table 5 ● 4 fractions/week ▲ 5 fractions/week

voices Sixteen patients had mild or intermittent hoarseness, six of whom continued to smoke and drink excessively after the course of radiation therapy Only one patient developed necrosis of the arytenoid which slowly healed with conservative care

Twelve patients were followed for more than five years, and no severe late radiation injuries could be demonstrated

Table 6

Procedures after local irradiation Failure in true vocal cord tumors

Patient	Stage	Ret	Time after *irradiation* therapy	Procedure	Comment
1	T1	1 789	8 months	None	Expired 15 months obstruction of larynx
2	*T1s*	*1 821*	*8 months*	*Partial laryngectomy*	*75 month NED*
3	T2	1 810	3 months	Total laryngectomy Neck dissection negative	24 month NED
4	T1	1 810	4½ months	Hemilaryngectomy	48 month NED
5	T2	1 852	5 months	Total laryngectomy Neck dissection negative	36 month NED
6	T1	1 810	5½ months	Hemilaryngectomy Neck dissection 6/21 nodes	26 month NED
7	T1	1 859	5 months	Total laryngectomy	50 month NED
8	T1	1 810	6 months	Hemilaryngectomy	45 month NED
9	T1	1 841	28 *months*	Cord stripping for microinvasive carcinoma	39 month NED
10	T1	1 810	7 months	Hemilaryngectomy	66 month NED
11	T1	1 734	64 months	Tracheostomy Direct laryngoscopy and biopsy	Expired of massive hemorrhage from tracheostomy

Table 4

Evaluation of voice quality after treatment minimum follow up time was 24 months

	No of patients
Good speaking voice	26
Mild or intermittent hoarseness*	16
Persistent hoarseness with necrosis of arytenoid**	1
No data available for analysis	8
Early failure followed by surgery	9
Total	60

*Six of these patients documented to continue to smoke and drink

**The ulceration slowly healed with conservative treatments Biopsy No malignancy

Eleven of the 55 patients were radiation therapy failures with recurrence of disease locally Among the local radiation failures, one patient expired of obstruction by recurrent tumor, three patients had total laryngectomy, five patients had hemilaryngectomy and one patient had stripping of the vocal cord only (Table 6) Four patients had radical neck dissection one such patient had clinically obvious neck node metastasis, 2 patients had primary recurrence but no palpable nodes, and one was planned for surgery although there was no evidence of primary recurrence or nodal metastasis Only the patient with clinically palpable neck nodes yielded a positive specimen Of the 11 patients with local failures, 10 had an attempt at surgical salvage, 9 successfully The average time of recurrence after radiation therapy was seven-and-one-half months

Complications Twenty-six of the 51 patients who had control of their tumors and were available for follow-up examination were documented to have excellent speaking

Table 5

Dose response of T1N0 vocal cord carcinoma

	Ret value	Patient controlled	Rate
Morris & Deeley (1962	1 700	21/32	66 %
Present material*	1 800	34/43	80 %
Aristizabal & Caldwell (1972)*	1 860	15/20	75 %
Fletcher & Klein (1964)	1 920–2 020	108/118	92 %
Hibbs & Hendrickson (1966)	2 000–2 100	115/125	92 %
Stewart (1966)	1 950–2 130	114/122	94 %

* Treatment schedule of 4 fractions per week

ZUSAMMENFASSUNG

Sechzig Patienten mit einem *lokalisierten Schuppenzellkarzinom* des Stimmbands ohne Metastasen wurden mit vier Fraktionen wochentlich behandelt Es traten keine schwerwiegenden Komplikationen bei dem verwendeten Dosierungs- und Fraktionierungsschema auf Die Qualitat der Stimme war nach der Bestrahlung *zufriedenstellend Nach einer* Nachuntersuchungsperiode von wenigstens zwei Jahren waren die Kontrollraten fur T1 and T2 Tumoren 80% bzw 81,5% Alle Versager bei der Strahlentherapie wurden chirurgisch geheilt Es wurde eine Dosisresponskurve fur T1 Schäden unter Verwendung der Ellis'schen Formel aufgestellt, um die NSD von Daten der verschiedenen therapeutischen Zentra herzuleiten *Keine Unterschiede fur die untersuchten* Parameter zwischen dem vier mal und funf mal wochentlichen Behandlungsschema scheinen vorzuliegen Eine ret-Dosis von etwa 1 800 erscheint etwas niedrig fur optimale Kontrollraten bei T1 und T2 Tumoren

RÉSUME

Soixante malades atteints de carcinome epidermoide localisé de la corde vocale sans atteinte lymphatique ou métastatique ont eté traites par quatre fractions par semaine La dose et le fractionnement decrits n'ont pas entraines de complications serieuses La qualite de la voix apres traitement a ete satisfaisante Apres un minimum d'observations de *deux ans, les taux de guerison pour les tumeurs T1 et T2 sont respectivement de 80 et 81,5%.* Tous les echecs du traitement par les radiations ont eté gueris chirurgicalement Les auteurs ont établi une courbe de réponses en fonction de la dose pour les lesions T1 utilisant la formule d Ellis pour en deduire la NSD, à partir de donnees provenant de différents centres de traitement Ils concluent qu il n'y a pas de differences dans les paramètres etudies entre les schemas de traitement hebdomadaire par quatre et cinq fractions Une dose ret d'environ 1 800 parait un peu faible pour un taux de guerison optimale des tumeurs T1 et T2

REFERENCES

ARISTIZABAL S A and CALDWELL W L Radiation tolerance of the normal tissue of the larynx Radiology 103 (1972), 419

BACLESSE F Comparative study of results obtained with conventional radiotherapy (200 kV) and cobalt therapy in the treatment of cancer of the larynx Clin Radiol 18 (1967), 292

BUSCHKE F and VAETH J M Radiation therapy of carcinoma of the vocal cord without mucosal reaction Amer J Roentgenol 89 (1963), 29

ELLIS F Time, fractionation and dose rate in radiotherapy *In* Frontiers in radiation therapy and oncology, p 131 S Karger, New York 1968

— BRINDLE J, CHURCHILL-DAVIDSON J F J et coll *Interim progress report (1969) on* the British Institute of Radiology fractionation study on 3 fractions/week or 5 fractions/week treatment of larynx and pharynx (1969)

FLETCHER G H and KLEIN R Dose-time volume relationship in squamous cell carcinoma of the larynx, Radiology 82 (1964), 1032

GOFFINET D R, ELTRINGHAM J R, GLATSTEIN E. and BAGSHAW M A Carcinoma of the larynx, results of radiation therapy in 213 patients Amer J Roentgenol 117 (1973), 553

HIBBS G G and HENDRICKSON F R Telecobalt therapy of early malignant tumors of vocal cord Radiology 86 (1966), 447

Table 7

Radiation therapy for vocal cord carcinoma Local control at 24 months

Authors	Stage T1N0		T2N0		T3N0	
Aristizabal & Caldwell (1972)	15/20	75%	—		—	
Bablesse (1967)	17/18	94%	34/59	58%	13/36	36%
Morrison & Deeley (1962)	21/32	66%	—		—	
Fletcher & Klein (1964)	108/118	92%	24/30	80%	1/3	33%
Hibbs & Hendrickson (1966)	115/125	92%	30/39	76%	—	
Stewart (1969)	114/122	94%	66/90	73%	—	
Present material	34/43	80%	9/11	81%	1/1	—

Discussion

An important test of an altered treatment fractionation schedule is the tumor response to radiation and local control of disease by such treatment technique Such a treatment schedule cannot be justified because of convenience alone, rather it must promise an equal rate of control as well as an acceptable degree of normal tissue reaction and complication rate

In Tables 5 and 7 several series of reported results are summarized for vocal cord tumors A dose-response curve can be constructed from the data derived from these series of patients Fig 2 demonstrates a linear relationship between dose and local control of T1N0 vocal cord carcinomas treated by different techniques The ret value for patients treated at 4 fractions per week falls along this dose-response curve at a lower level of control It appears, despite the decreased fractionation schedule, that the control rate in this current group is somewhat low for patients with T1 tumors The complication rate, however, is within the acceptable range Voice quality was also satisfactorily preserved in these patients

SUMMARY

Sixty patients with localized squamous cell carcinoma of the vocal cord without nodal or metastatic disease were treated with four fractions per week No serious complications occurred with the dose and fractionation schedule as outlined Voice quality after treatment has been satisfactory After a minimum of two years follow up the control rates for T1 and T2 tumors are 80% and 81 5%, respectively All radiation therapy failures were cured surgically A dose-response curve was constructed for T1 lesions, utilizing the Ellis' formula to derive the NSD, from data from different therapy centers There appears to be no differences in the parameters studied between four and five fractions per week treatment schedules A ret dose of approximately 1800 appears somewhat low for optimal control rates in T1 and T2 tumors

FROM THE RADIATION PHYSICS DEPARTMENT (DIRECTOR PROFESSOR G HETTINGER),
UNIVERSITY OF UMEA S-901 85 UMEA, SWEDEN

ELECTRON DEPTH ABSORBED DOSES FOR SMALL PHANTOM DEPTHS

Comparison between different accelerators

G HULTEN and H SVENSSON

Electron depth absorbed dose distribution in the build up region is not as well known as that for depths beyond the absorbed dose maximum The first parts of the depth dose curves are thus not included in the tables given by NACP (1971) and HPA (1971) in spite of their greater significance for the choice of a suitable treatment technique

Published depth dose distributions show great discrepancies at small phantom depths (SVENSSON & HETTINGER 1967 ORCHARD & MARTIN SMITH 1971, HVOLBY 1972 DAHLER et coll 1972, ALMEIDA & ALMOND 1974) The discrepancies may depend on differences in either the dosimetry or the electron beam qualities Therefore measurements were performed with a uniform technique at different accelerators to analyse the background of the observed discrepancies

Method

Accelerators Depth dose curves in the build up region were measured at a linear accelerator a microtron and at four betatrons (Table) Originally the BBC 35 MeV betatrons had perspex tubes to delimit the beam and a transmission chamber as

Submitted for publication 29 Apr l 1975

MORRISON R and DEELEY T J The treatment of the larynx by supervoltage radiotherapy Clin Radiol 13 (1962), 145

STEWART J G Late effects of radiation—the radiotherapist s problem Brit J Radiol 42 (1969), 797

WIERNIK G , BLEEHEN N M , BRINDLE J et coll Fifth progress report on the British Institute of Radiology fractionation trial of 3F/week or 5F/week treatment of larynx and pharynx Brit J Radiol 45 (1972), 754

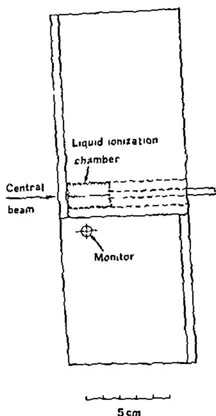


Fig. 1 The polystyrene phantom used for absorbed dose measurements in the build up region

Phantom The phantom consists of two parts, one lower fixed block into which the monitor chamber was placed and one upper moveable part containing the liquid ionization chamber (Fig 1) Polystyrene slabs of different thickness were placed in front of the liquid ionization chamber to achieve different measuring depths The two detectors did not disturb each other

Depth absorbed dose curves for small depths, with water and polystyrene as phantom material, have been compared at 10 MeV for accelerators 5 and 6 The relative depth absorbed dose curves coincide within 0 5 per cent This indicates, that compared with water, which is usually taken as reference material, the higher electron density and the lower scattering power in polystyrene seem to cancel out

Results and Discussions

Dose build-up at different accelerators Depth absorbed dose curves were measured for field sizes close to 6 cm × 6 cm and 13 cm × 13 cm Depth dose distributions for 10 MeV electrons appear in Fig 2. The build-up ratio, BUR, defined here as the ratio between the absorbed dose at 0 5 mm depth and the absorbed dose at maxi-

Table

Accelerator number	Accelerator	Centre in Sweden
1	MEL SL 75/10 linear accelerator	Uppsala
2	Siemens 18 MeV betatron	Jonkoping
3	Siemens 42 MeV betatron	Malmo
4	BBC 35 MeV betatron	Uppsala
5	BBC 35 MeV betatron	Umeå
6	Scanditronix MM-10 microtron	Uppsala*

* The measurements were performed at the manufacturer The accelerator is now installed in Brescia, Italy

monitor The betatron in Umeå has since been modified and is now equipped with a different collimating, monitoring and scattering system (SVENSSON 1971) In Uppsala a modified collimating system is ordinarily used However, during these measurements the original system was used and the results for this accelerator are therefore more representative of the primary performance The applied SSD and scattering foil for a given field size were in accordance with the local practice for treatment Accelerators 3 and 4 (Table) were not ordinarily used for electron treatments at energies above 25 MeV but some experiments for these energies are included in this report

Detector A small and energy independent detector is required for measurements in electron fields where the absorbed dose gradient is steep and the spectral distribution of the electrons is changing A small parallel plate liquid ionization chamber has been used (WICKMAN 1974 a) The present chamber does not allow measurements in water Therefore, all measurements were performed in a polystyrene phantom The chamber walls were made of a styrene co-polymer coated with a semitransparent beryllium layer and as the mass collision-stopping power ratio for polystyrene and liquid varies only one per cent in the energy interval 100 keV to 40 MeV (WICKMAN 1974 a, 1974 b), the detector should be almost energy independent for measurements of the absorbed dose In the energy range 8 to 30 MeV the energy independence has been verified in a comparison between the liquid ionization and the ferro sulphate dosimeters (SVENSSON et coll 1973) The precision for the detector has been determined with a Co 60 unit and the standard deviation for one single measurement was 0 2 per cent

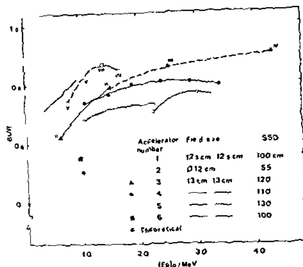


Fig. 3 The build up ratio, BUR, in the central beam for the investigated accelerators If different scattering foils were used the foil number is given in the diagram with roman letters

ferent processes, namely energy transfer to secondary electrons and increase in spherical fluence with phantom depth due to scattering of primary electrons (HARDER 1965 BOAG 1972) The former process is slightly energy dependent while the latter strongly decreases with energy

BUR values that increase with energy must therefore be expected BUR values can be estimated from the theoretical central axis depth dose curves for water (published by BERGER & SELTZER 1969) These BUR values increase with energy from approximately 0 69 at 10 MeV to 0 91 at 40 MeV These two figures include a correction of SSD from infinite SSD to 100 cm carried out by the method of BURNS (1972) The experimental BUR values do not increase so evidently with energy (Fig 3) as seems to be explained by the broad spectral distribution of the electron beams from the accelerators and also, in the high energy range, from the contamination of the electron beams with roentgen radiation generated in the scattering foil and tube window An increase of the roentgen contamination thus decreases the BUR as the build up is larger for such a radiation than for electron radiation

Depth absorbed dose curves for BBC 35 MeV betatrons measured with thermoluminescence dosimetry differ somewhat from our results The BUR values from HVOLBY is thus nearly constant 0 92 for all energies in the energy range 10 to 35 MeV and DAHLER et coll measured a BUR of 0 91±4 % for 10 MeV, 0 86±3 % for 15 MeV

BUR at different field sizes Generally, the experimental BUR values decreased with an increase of the field size The decrease was in the range 2 to 4 per cent for the two field sizes investigated A larger build-up is also to be expected for the large fields (BREITLING & VOGEL 1965) A deviation was obtained, however, at accelerator I

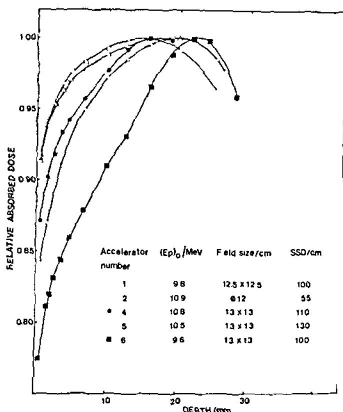


Fig 2 Measured absorbed dose distributions at small phantom depths in polystyrene for five different accelerators at about 10 MeV

mum depth is determined from these curves In Fig 2 the depth absorbed dose distributions imply BUR-values from 0 77 to 0 92 These discrepancies were not influenced appreciably by differences in SSD and energy, except for accelerator 2 (SSD = 55 cm) where the divergence of the beam decreased the electron fluence by about 6 per cent for the first 15 mm in the phantom (about 3 per cent decrease for the other accelerators)

The discrepancies are mainly explained by differences in spectral and angular distribution of the electrons A small difference between the accelerators may also be due to the various degrees of roentgen contamination of the beams However, this contamination is more important at higher energies The BUR values for the two BBC betatrons differ by about 3 per cent The higher build-up at accelerator 5 is explained by the differences in the collimating and scattering system Accelerator 6, the microtron, produces a clean electron beam with a small contribution from scattered and low-energy electrons (BRAHME et coll 1975)

Absorbed dose build-up at different energies BUR values in the central beam for different accelerators and energies are given in Fig 3 for field sizes close to 13 cm × 13 cm In Fig 4 the depth for absorbed dose maximum has been plotted versus energy for similar irradiation geometries

The absorbed dose build up for electron radiation depends mainly on two dif-

coll.), which explain why the result from this accelerator differs from the rest. Corresponding observations have been made by DE ALMEIDA & ALMOND, who compared the results from a scanning beam linear accelerator with those from betatrons. The former accelerator also has a very clean beam and the depth of absorbed dose maximums at large depths. It may thus be necessary to use other reference depths for these accelerators than those recommended by ICRU.

Acknowledgement

We wish to thank Prof. Gunnar Hettinger and Dr Goran Wickman for valuable discussions.

SUMMARY

Depth dose distributions at small phantom depths in polystyrene were measured with a liquid ionization chamber at six different accelerators. The absorbed dose at 0.5 mm depth relative to the absorbed dose maximum in the central beam varied between 0.77 and 0.92 for 10 MeV electrons. Generally the surface absorbed dose increased with increasing energy or decreasing field size. Results from measurements off axis indicate small differences from the data available for the central beam.

ZUSAMMENFASSUNG

Tiefendosisverteilungen bei geringen Phantomtiefen wurden in Polystyren mit einer Flussigkeits Ionisationskammer bei sechs verschiedenen Acceleratoren gemessen. Die absorbierte Dosis bei 0,5 mm Tiefe relativ zum absorbierten Dosismaximum im Zentralstahl variierte zwischen 0,77 und 0,92 fur 10 MeV Elektronen. Im Ganzen gesehen stieg die absorbierte Oberflächendosis mit steigender Energie oder abnehmender Feldgrosse. Die Ergebnisse von Messungen ausserhalb der Achse ergaben geringe Differenzen von den zugänglichen Daten fur den Zentralstrahl.

RÉSUMÉ

Les distributions de doses en profondeur a de petites profondeurs sur des fantomes en polystyrene ont éte mesurées avec une chambre d'ionisation liquide pour 6 accelerateurs différents. La dose absorbee a 0.5 mm de profondeur a varie entre 0.77 et 0.92 de la dose absorbee maximale sur le rayon central pour des electrons de 10 MeV. En géneral, la dose absorbee en surface augmente avec l'augmentation de l'energie ou avec la diminution des dimensions du champ. Les resultats des mesures faites en dehors de l'axe sont peu différents des résultats obtenus pour le rayon central.

REFERENCES

DE ALMEIDA C. E. and ALMOND P. R.: Comparison of electron beams from the Siemens betatron and the Sagittaire linear ac[illegible]

[illegible] at the 12th International Congress of Radiology, Tokyo, Japan, Oct. 1969.

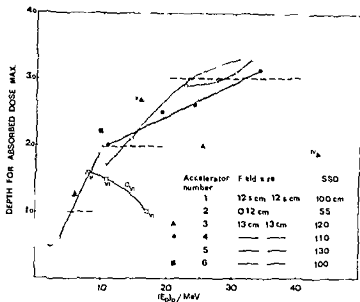


Fig 4 The depth for absorbed dose maximum in polystyrene measured under the same irradiation geometries as in Fig 3 For energies above 20 MeV where the absorbed dose close to maximum is nearly constant over several cm the depth is uncertain within some mm

For the small field the BUR was thus 7 per cent lower at 3 6 MeV and 3 per cent lower at 10 MeV than for the large one This result seems to be explained from the collimating construction of accelerator 1 The large radiation fields are contaminated with electrons that have been scattered in the collimating systems The small field applicator shields the central beam from most of these electrons and therefore gives a smaller BUR

BUR off axis Measured BUR values off axis indicate small differences from those in the central beam The values are always higher, about 2 per cent, except close to the field boundary where the increase is up to 5 per cent No significant discrepancies were found for the different accelerators

The depth for absorbed dose maximum The depth of absorbed dose maximum varies at a given electron energy for different accelerators (Fig 4) An increase of this depth with energy for broad electron beams is to be expected (BERGER & SELTZER) and this is also found for most of the accelerators An opposite energy dependence is observed for accelerators 2 and 3 Most of the depths for dose maximum agree well with the reference depths given for various energies by ICRU (1972) and NACP (1972), (broken line in Fig 4) ICRU has stated 'The reference depth must be sufficiently great that the contribution of scattered electrons is not serious, but close enough to the maximum so that there is a slow variation of absorbed dose with depth' The latter part of this statement is thus in agreement with our investigations for most of the irradiation geometries An exception is the result from accelerator 6, the microtron The recommended reference depth is 1 cm The absorbed dose varies rapidly near this depth (Fig 2) The microtron has a very clean electron beam, narrow spectral distribution and small angular spread of the electrons (BRAHME et

ROM THE DEPARTMENT OF RADIATION THERAPY, SAHLGRENSKA SJUKHUSET, S-413 45
GÖTEBORG, SWEDEN

TREATMENT OF DISSEMINATED CARCINOMA OF THE BREAST BY METENOLONE ENANTHATE

G Notter

Androgenic and oestrogenic hormones have been used in the treatment of disseminated carcinoma of the breast for many years Prospective analyses have demonstrated that oestrogens are usually more effective than androgens (Council on Drugs 1960, Kennedy 1965) Both hormones have undesirable side effects, sometimes necessitating discontinuation of treatment Androgen treatment in high doses for 4 to 6 weeks leads to obvious virilisation, increased libido and hoarseness, side effects unpleasant to most female patients Sodium and water retention also occurs, increasing the risk of complications such as oedema and thrombo-vascular lesions Stimulation of the bone marrow may cause polyglobuli, plethora and chest pains simulating angina pectoris

Metenolone Enanthate has a less virilising effect than testosterone propionate and is in addition not converted to oestrogens Kennedy & Yarbro (1968) used this preparation in a hitherto unusually high dosage of 3 × 400 mg/week in a prospectively randomised trial together with testosterone propionate in the treatment of disseminated carcinoma of the breast In their series objective remissions were observed in 13 out of 27 patients In the present material an attempt has been made to reproduce this result in a larger number of cases

Submitted for publication 29 November 1974

BOAG J W Surface ionization ratios for electrons in the energy range 3 to 11 MeV Brit J Radiol 45 (1972), 229

BRAHME A, HULTÉN G and SVENSSON H Electron depth absorbed dose distribution for a 10 MeV clinical microtron Phys in Med Biol 20 (1975), 39

BREITLING G und VOGEL K H Über den Einfluss des Streuung auf den Dosisverlauf schneller Elektronen *In* Symposium on High-Energy Electrons, Montreaux 1964, p 20 Edited by A Zuppinger and G Poretti Springer Verlag, Berlin 1965

BURNS J E Conversion of percentage depth dose from one SSD to another and calculation of tissue/air ratios *In* Central axis depth dose data for use in radiotherapy Brit J Radiol (1972) Suppl No 11, p 101

DAHLER A, BENGTSSON B E and LINDSKOUG B Skin doses for electrons in the energy range 10 to 33 MeV Acta radiol (1972) Suppl No 313, p 48

HARDER D Durchgang schneller Elektronen durch dicke Materialschichten Habilitationsschrift, Wurzburg 1965

Hospital Physicists' Association (HPA) A practical guide to electron dosimetry (5–35 MeV) Report Series No 4, London 1971

HVOLBY J Depth dose near the surface by fast electron irradiation Acta radiol Suppl No 313 (1972) p 60

International Commission on Radiological Units and Measurements (ICRU) Report No 21 Radiation Dosimetry Electrons with initial energies between 1 and 50 MeV ICRU, Washington 1972

Recommendations of the Nordic Association of Clinical Physics (NACP) Procedures in radiation therapy dosimetry with 5 to 50 MeV electrons and roentgen gamma rays with maximum photon energies between 1 MeV and 50 MeV Acta radiol Ther Phys Biol 11 (1972), 603

ORCHARD P G and MARTIN-SMITH P Surface ionization ratios for electrons in the energy range 3–11 MeV and the implications for treatment of superficial lesions Brit J Radiol 44 (1971), 817

SVENSSON H Influence of scattering foils, transmission monitors and collimating system in the absorbed dose distribution from 10 to 35 MeV electron radiation Acta radiol Ther Phys Biol 10 (1971), 443

— and HETTINGER G Measurement of doses from high energy electron beams at small phantom depths Acta radiol Ther Phys Biol 6 (1967) 289

— HULTÉN G, HETTINGER G and WICKMAN G Determination of absorbed dose conversion factors of an air ionization chamber for 10–33 MeV electron and photon beams with the aid of a liquid ionization chamber Paper presented at the XIII International Congress of Radiology, Madrid 1973

WICKMAN G (a) A liquid ionization chamber with high spatial resolution Phys in Med Biol 19 (1974), 66

— (b) Radiation quality independent liquid ionization chamber for dosimetry of electron radiation from medical accelerators Acta radiol Ther Phys Biol 13 (1974), 37

Only regression of at least 3 months' duration has been evaluated as remission No simultaneous treatment with other hormones or cytostatic agents has been given during the period

Initially the dose schedule recommended by KENNEDY & YARBRO of 3×400 mg/week during a period of 3 months was planned Marked virilisation occurred with this high dose and, as a good clinical effect was observed with 2×200 mg/week, the treatment further commenced on this lower dose

A total of 43 patients were treated, 2 of these for less than 3 months, they have not been evaluated In both these cases treatment was discontinued because of progression of the tumour Thus, 41 patients were treated regularly for at least 3 months with doses of not less than 400 mg/week 18 patients initially with 3×400 mg/week for 3 months, 2 initially with 3×400 mg/week for 2 months, 1 patient with 2×400 mg/week for 2 months, 2 patients with 2×400 mg/week for 1 month, and 18 patients with 2×200 mg/week for 3 months

Following the initial treatment the patients received regular maintenance doses of 1×400 mg, 1×200 mg and 1×100 mg/week intra muscularly, respectively

Result

The result appears in Table 1 Regressions occurred in 8 of the 41 (8/41) evaluated patients, 33 failed In the failure group 12 patients were included whose disease remained static, or regression of less than 50 per cent occurred, thus not fulfilling the criteria for remission

In the group of remissions, total regression of the tumour occurred in 2 patients and more than 50 per cent regression in 6 The mean remission time was 12 months (3–27), the mean treatment time was 15 months (93–810 days) and the mean Primobolan Depot dose was 20 4 g (5 8–37 3)

In the 12 patients of the failure group with static disease or less than 50 per cent regression the mean duration of this relative therapeutic effect was 10 months (4–25) The mean treatment time was 11 months (124–892 days) and the mean dose of Primobolan Depot was 14 6 g (4 4–42 8)

In the 21 patients without any therapeutic effect the mean treatment time was 170 days (90–450) and the mean hormone dose 12 g (5 6–28)

If the 2 patients who were treated less than 3 months are included in the failure group there remain 8 remissions out of 43 (19 per cent), which is in agreement with the generally observed remission rate for androgenic hormones in the treatment of carcinoma of the breast

Tumour growth in soft tissue (inoperable primary tumours, local recurrences, skin and lymph node metastases) reacted relatively well to the hormonal treatment, totally in 10/24 cases

Osseous metastases reacted less well only in 2/29 cases However, in 11/29 cases the disseminated osseous metastases remained static during the treatment time

Table 1

The effect of Metenolone Enanthate on different sites of metastases Number in brackets indicate static disease

Site of metastases	Incidence of metastases	Therapeutic effect	
		Remission	Failure
Breast	2	2	—
Soft tissue			
cutis, subcutis lymph nodes	22	8	14 (4)
Osseous	29	2	27 (11)
Visceral			
liver	4	—	4
lung	7	—	7 (1)
pleura	3	1	2
brain	—	—	—
Total	67	13	54

Objective remission in 8/41 patients
Static disease in 12/48 patients (evaluated as failures)

Methods and Material

During the period January 1972 to July 1974, 43 patients with microscopically verified inoperable or disseminated carcinoma of the breast have been treated by intramuscular injections of Metenolone Enanthate Schering AG, Berlin, have supplied a specially manufactured solution with a concentration twice as high as that in the generally available Primobolan Depot, i e 200 mg/ml (SH 6 0601 F)

All patients were post-menopausal Only women with progressive disease have been treated Previously 11 patients had been treated with other hormones, e g oestrogens, gestagens, prednisolone, without evident therapeutic effect It was ensured that all previous hormone treatment had been withdrawn at least 1 month before the administration of Metenolone Enanthate Measurable tumours or metastates were controlled regularly once a month Roentgen examinations of the skeleton were carried out at 3 monthly periods or in the case of progressive symptoms or signs earlier Blood counts and serum electrolytes and liver function tests were controlled once a month for 3 months and thereafter every second month

For the evaluation of response the criteria of U S A Cooperative Breast Cancer Group (National Cancer Institute) were applied Objective remissions were therefore, only accepted if (a) *all demonstrable tumour masses diminished measurably in size,* (b) more than 50 per cent of non-osseous lesions decreased in size although all bone lesions remained static, and (c) more than 50 per cent of total lesions improved while the remainder were static

Table 3

The effect of Metenolone Enanthate in relation to post menopausal age and the free interval Objective remissions patients treated The numbers in brackets indicate static disease

Post menopausal age	Free interval		Total
	0–1 year	> 1 year	
< 5 years	0/3 (1)	1/4	1/7 (1)
> 5 years	2/11 (2)	5/23 (9)	7/34 (11)
Total	2/14 (3)	6/27 (9)	8/41 (12)

increased libido, developing in almost all patients when Metenolone Enanthate is given in high doses of 400 mg/week for a period of 3 to 5 months

If higher doses are used, as in 23 of our patients, virilisation developed as early as 2 to 3 months after the beginning of treatment Cramps in the limbs, particularly in the legs, occurred in 18 patients, and in one even in the facial muscles The cause of this side effect is uncertain No electrolyte disturbance was established The symptoms disappeared rapidly after discontinuation of treatment, or with reduction in dosage to 100–200 mg/week or every other week

Of the 41 patients, 29, with marked virilisation, developed in addition a facial flush similar to that seen in polycythaemia, probably due to a dilation of skin capillaries and to increased erythrocytes Most patients increased in weight by a few kilograms, mainly due to sodium and water retention In elderly patients with latent cardiac decompensation this could easily lead to cardio-vascular failure, and careful control of these patients is essential Symptoms such as dyspnoea and retrosternal pains simulating angina pectoris occurred in 10/41 patients All symptoms regressed completely a few weeks after the treatment had been discontinued

Hypercalcaemia developed in one patient, but this rapidly returned to normal levels after the treatment with Primobolan Depot had been discontinued and phosphate solution administered No disturbance of liver function was observed during treatment with large doses

Discussion

The patients in the present material were not randomized with another group of patients treated by other hormones There was no selection of patients in relation to the grade or type of dissemination of the disease

In 30/41 patients Primobolan Depot was the first choice of hormonal treatment, in 11 patients it was the second one One of the 8 objective remissions only, belonged to the second group

Four patients had liver metastases with slightly increased transaminases but otherwise normal liver function None of them reacted to the hormonal treatment

Table 2

The effect of Metenolone Enanthate in 30 patients in relation to the site of metastases and post-menopausal age Patients treated previously by other agents are not included Remissions/patients treated Numbers in brackets indicate static disease

Dominant site of metastases	Menopausal age				Total
	1 year	1–5 years	5–10 years	10 years	
Breast		1/1		1/1	2/2
Soft tissue					
cutis, subcutis					
lymph nodes	0/1 (1)		1/1	4/5	5/7 (1)
Osseous	0/3	0/2 (1)	0/1	0/13 (7)	0/19 (8)
Visceral					
liver			0/1		0/1
lung				0/1	0/1
pleura					
brain					
Total	0/4 (1)	1/3 (1)	1/3	5/20 (7)	7/30 (9)

Visceral metastases regressed in only 1/14 cases Liver and lung metastases remained unchanged

If, according to the suggestion of the U S A Cooperative Breast Cancer Group, the pre-menopausal women and those who had received hormonal treatment earlier are excluded, and the material is classified according to the post-menopausal age and localization of the dominant lesion, 7/30 patients (23 per cent) remained as remissions (Table 2)

The number of remissions increased significantly with the duration of the menopause and the age of the patient (Tables 2, 3) The mean age of the patients with remissions was 71 years (51 to 83), of those without remissions 61 (38 to 84) years No difference could be observed within the group of failures, i e between those in whom the disease remained static and those completely without hormonal effect

The same relationship existed concerning the post-menopausal age and the therapeutic effect The mean post-menopausal age of the patients with remissions was 24 (3 to 43) years and that of the other patients 11 (1 to 29) years

In the more than 5 year post-menopausal women the remission rate was higher (7/34) than in the less than 5 year post-menopausal group (1/7) The best therapeutic results were obtained in the more than 5 year post-menopausal women with more than 1 year free interval (Table 3)

Side effects The most common and unpleasant side effects during the treatment with androgenic hormones are those of virilisation such as hirsutism, hoarseness and

evaluable patients Soft tissue metastases responded best Liver and brain metastases were unaffected The therapeutic efficiency of Primobolan Depot is comparable to that of testosterone propionate but the agent is less virilising

ZUSAMMENFASSUNG

Dreiundvierzig Patienten mit disseminierten oder inoperablen Karzinomen der Brust wurden mit Metonolone Enanthate (Primobolan Depot) mit Dosen von 400 bis 1 200 mg/ Woche mindestens 3 Monate lang behandelt Objektive Remissionen, die länger als 3 Monate anhielten, traten in 8 von 41 Patienten, die beurteilt werden konnten, auf Weichgewebemetastasen reagierten am besten Leber und Gehirnmetastasen wurden nicht beeinflusst Die therapeutische Wirksamkeit von Primobolan Depot ist der von Testosteron Propionat vergleichbar, hat jedoch geringeren virilisierenden Effekt

RÉSUMÉ

Quarante trois malades atteintes de cancer du sein disseminé ou inoperable ont eté traitees par le Metenolone Enanthate (Primobolan Dépot) à des doses allant de 400 a 1 200 mg par semaine pendant au moins 3 mois On a observé des rémissions objectives durant plus de 3 mois dans 8 des 41 cas utilisables Ce sont les metastases dans les tissus mous qui ont le mieux répondu Les metastases hépatiques et cérebrales n'ont pas ete influencees L'effet therapeutique du Primobolan Depot est comparable à celui du propionate de testosterone mais cet agent est moins virilisant

REFERENCES

ADAIR F E, MELLORS R C, FARROW J H, WOODARD H Q, ESCHER G C and URBAN J A The use of Estrogens and Androgens in advanced Mammary Cancer Clinical and Laboratory Study of one hundred and five Female Patients J Amer med Ass 40 (1949), 1193

American Medical Association Committee on Research Androgens and estrogens in the treatment of disseminated mammary carcinoma J Amer med Ass 172 (1960), 1271

GOLDENBERG I S and HAYES M A Hormonal therapy of metastatic female breast carcinoma *II 2-x methyl-dihydrotestosterone* propionate Cancer 14 (1961), 705

KENNEDY B J Hormonal control of breast cancer Ann intern Med 63 (1965), 329

— and YARBRO J W Effect of Metenolone enanthate (MSC-64967) in advanced cancer of the breast Cancer 21 (1968), 197

STOLL B A Androgen, Corticosteroid and Progestin *therapy In* Endocrine *therapy in* malignant disease Chapter 8, p 167 Edited by W B Saunders, London 1972

WATERS M N RAVDIN R S, ANSFIELD F J and SEGALOFF A Androgenic Therapy for advanced Breast Cancer in Women A report of the Cooperative Breast Cancer Group J Amer med Ass 223 (1973), 1267

The remission rate of 19 per cent is comparable with the usual response to androgenic hormonal treatment in breast carcinoma, which is inferior to that of oestrogenic hormones The results were less favourable than those of KENNEDY & YARBRO who reported a remission rate of 48 per cent with Metenolone Enanthate 1 200 mg/week It is also less than the effect of the nonandrogenic steroid Calusterone (17β-hydroxy-7β, 17α-dimethylandrost-4-en-3-one), obtained by GOLDENBERG et coll (1973) in a prospective investigation Objective remission was observed in about 28 per cent of 109 patients with approximately equal effect on local, osseous and visceral metastases However, it is very difficult to compare results of different therapeutic regimes in tumour patients from various centres because of the differences in regard to assessment of clinical parameters The virilising effect of Metenolone Enanthate is less than that of testosterone propionate but it is quite obvious after treatment with about 5 to 10 g during 2 to 4 months The frequently troublesome cardio-vascular side effects and virilisation means an enforced reduction in the hormone dose after a few months of treatment Experience from this material shows that an initial dose of 2×400 mg weekly is adequate in achieving a full therapeutic effect in 6 to 8 weeks

Should there be no signs of regression at this time, continuation of treatment is contraindicated with regard to the side effects In cases with regression, treatment may be continued at a lower dose of 100 to 200 mg/week This dose is tolerated by most patients for a long period of time

A surprising feature was the low therapeutic effect on osseous lesions in this series Objective remission was found in only 2 out of 29 cases, in contrast to the usually observed 20 to 25 per cent This may depend on the definition of remission and the fact that it is difficult to assess remission with over 50 per cent cases with only osseous metastases, especially if some areas had been irradiated previously However, 11/29 cases with disseminated osseous metastases classified as failures, remained static during the treatment with Primobolan Depot with a mean time of 10 months, which may be considered as a partial therapeutic effect

As in all hormone treatment, careful control of patients on treatment with Metenolone Enanthate is necessary, particularly during the initial months of treatment, with regard to possible hypercalcaemia and cardio-vascular failure

Apart from the anti-tumour effect, the anabolic and bone marrow stimulation activity of Primobolan is very useful in long term treatment of patients with carcinoma with a depressed bone marrow due to metastases, irradiation or earlier cytostatic therapy Doses of 100 to 200 mg/week seem to delay or prohibit pancytopenia in cases simultaneously treated with cytostatic agents

SUMMARY

Forty three patients with disseminated or inoperable carcinoma of the breast were treated with Metenolone Enanthate (Primobolan Depot) with doses of 400 to 1 200 mg/week for at least 3 months Objective remissions lasting longer than 3 months occurred in 8 out of 41

be induced in experimental animals by the administration of thyrotrophic or thyroid hormones (GREGOIRE 1942, REINHARDT & WAINMAN 1942, GYLLENSTEN 1953, LUNDIN 1958, ERNSTRÖ[illegible] & GYLLENSTEN 1959 ERNSTRÖM 1963)

These findin [illegible]
cytes in vivo [illegible]
hormones induced DNA-synthesis of human lymphoid cells in vitro

Material and Methods

Separation of lymphoid cells Venous blood was obtained from healthy euthyroid individuals It was defibrinated by gentle agitation in a beaker containing glass pearls Separation of nucleated cells was performed according to the method described by COULSON & CHALMERS (1964) The number of lymphoid cells was determined in a Burker chamber after crystal violet staining The cell-suspensions used for the experiments contained a minimum of 60 per cent of lymphocytes

Thyroid hormones The sodium salts of levo-triiodothyronine (L-T_3) and levo-thyroxine (L-T_4) were obtained from Nyegaard and Co AB, Stockholm, Sweden, sodium dextro thyroxine (D-T_4) from Travenol Laboratories Inc, Ill, USA, and sodium dextro-triiodothyronine (D-T_3) from E Merck Svenska AB, Stockholm, Sweden The thyroid hormones were suspended in sterile water, the pH was adjusted to 11 9 with sodium hydroxide, and after millipore filtration were immediately used Thyroid hormones in twofold dilution starting with 0 1 mg (dilution 1/1) were added to the cell cultures In a few experiments, higher concentrations of the hormones were used In each case, however, the added volume was 0 1 ml In some experiments (Tables 1, 2) sodium hydroxide was added to control cultures at a dose equivalent to that present at a hormone dilution of 1/1

Sodium iodide In order to test the eventual influence upon the lymphoid cell responsiveness to iodide liberated through a possible decomposition of the thyroid hormones, sodium iodide (pro analysi, E Merck AG, Darmstadt, Germany) was added to the cell cultures as described for the thyroid hormones

Cell cultures 2 0 × 10^6 lymphoid cells were cultured in screw cap glass tubes with an inner diameter of 15 5 mm and with rounded bottoms (Johnson & Jorgensen Ltd, London, England) Each contained 1 0 ml of Eagle's Minimal Essential Medium supplemented with Earle's salts (MEM) supplemented with 100 units of penicillin and 150 μg of streptomycin per ml and 10 per cent human serum from AB-positive blood donors The serum was made complement deficient by incubation at 56°C for 30 minutes before use, and stored at −20 C Varying amounts of thyroid hormone served as controls After 4 days incubation at 37°C in a humidified atmosphere containing 5 per cent CO_2, each culture received 0 1 ml of MEM containing 0 4

FROM RADIUMHEMMET, GENERAL DEPARTMENT (DIRECTOR PROF J EINHORN), S-104 01 STOCKHOLM, SWEDEN

THYROID HORMONES AND LYMPHOID CELLS

G LUNDELL and H BLOMGREN

Hyperplasia of the peripheral lymphatic tissue, thymic enlargement and lymphocytosis of the bone marrow have been observed in patients with hyperthyroidism and thyroiditis (CROTTI 1922, BALDRIDGE & PETERSON 1927, MARGOLIS 1931, HAMMAR 1936, AXELROD & BERMAN 1951, DOUGHERTY 1952, IRVINE & SUMERLING 1965 MICHIE et coll 1967) Similar changes were, however, not observed in the lymphatic system of patients with non-toxic goitres (MICHIE et coll) Since the amount of thymic tissue decreased following antithyroid drug therapy, it is conceivable that hyperplasia of the thymus was a direct consequence of raised levels of circulating thyroid hormones (MICHIE et coll)

Recently it has been shown that the incorporation of ^{14}C-thymidine of lymphoid cells in vitro is increased in patients with hyperthyroidism as compared with euthyroid individuals, and that these increased values were normalized after ^{131}I therapy (LUNDELL et coll 1976) The increased levels of ^{14}C-thymidine incorporation by lymphoid cells in vitro were not caused by a shift in the proportion of thymus dependent lymphocytes (T-cells) and non-T-lymphocytes (mainly B-cells) in hyperthyroid as compared with euthyroid individuals (LUNDELL et coll 1975) Moreover, there is documentation demonstrating that the peripheral lymphocytes in some patients with hyperthyroidism have increased size (HERNBERG 1954) and increased RNA-content (SMITH et coll 1971) Thymolymphatic hyperplasia may also

This investigation was supported by the Cancer Society in Sweden Submitted for publication 23 July 1975

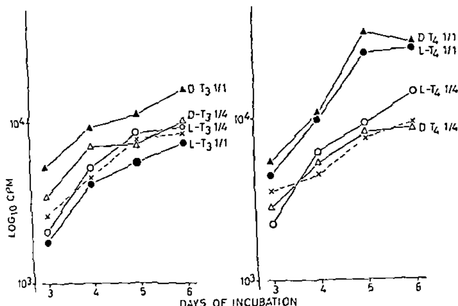


Fig. 1 Increment of ^{14}C thymidine uptake of lymphoid cells by thyroid hormones in relation to the incubation period ×---× control, without hormone (quadruplicate determinations)

μCi of ^{14}C thymidine (specific activity 54 mCi/mM, Radiochemical Centre, Amersham England) Twenty-four hours later the cultures were completed by centrifugation in the cold and by the addition of trichloroacetic acid The amount of incorporated isotope, expressed as counts per minute (cpm), was determined by a Packard Scintillation Counter Details concerning culture conditions and measurements of activity have been given previously (GLAS & WASSERMAN 1974) Unless otherwise stated, duplicate cultures were performed

Statistical methods Mean values and standard errors (SE) were calculated on an arithmetical basis and plotted on semilogarithmic scales Statistical significance of mean values was calculated using the Student's t-test

Results

Lymphoid cells from euthyroid donors were cultured 6 days in the absence and in the presence of thyroid hormones Thymidine incorporations were determined on days 3, 4, 5 and 6 The results of two such experiments using the same cell donor appear in Fig 1 It is seen that ^{14}C-thymidine uptake of control cultures, without hormones, increased during the incubation period The presence of the highest concentration of D-T_3 (left diagram) and D-T_4 and L-T_4 (right diagram) enhanced the thymidine uptake as compared to the control cultures

Table 1

Influence of thyroid hormones on the ^{14}C-thymidine incorporation of lymphoid cells. Mean values ± standard errors (S.E.) were calculated from 10 cultures. Dilution 1/1 corresponds to 0.1 mg of L-T_4 or D-T_4 per tube, The number of cpm for the control tubes without added NaOH, was 18 173 ± S.E. 1 308

Hormone	Dilution	Incorporation of thymidine, No. of counts/min		Level of significance for the difference to control, p
		Mean	S.E.	
L-T_4	1/1	27 498	1 741	<0.001
L-T_4	1/2	20 060	1 298	—
L-T_4	1/4	17 292	1 144	—
D-T_4	1/1	26 950	1 128	<0.001
D-T_4	1/2	22 276	1 035	<0.01
D-T_4	1/4	17 995	1 281	—
Control, no hormone, NaOH added	—	17 072	1 354	

Table 2

Influence of thyroid hormones on the ^{14}C-thymidine incorporation of lymphoid cells. Mean values ± standard errors (S.E) were calculated from 10 cultures. Dilution 1/1 corresponds to 0 1 mg of L-T_3 or D-T_3 per tube The number of cpm for the control tubes without added NaOH, was 2 022 ± S E 210

Hormone	Dilution	Incorporation of thymidine, No. of counts/min		Level of significance for the difference to control, p
		Mean	S E	
L-T_3	1/1	3 211	188	<0.01
L-T_3	1/2	4 433	345	<0.001
L-T_3	1/4	3 151	313	<0.05
L-T_3	1/16	2 411	288	—
D-T_3	1/1	6 875	443	<0.001
D-T_3	1/2	5 554	551	0.001
D-T_3	1/4	3 702	305	0.001
D-T_3	1/16	2 785	352	—
Control, no hormone, NaOH added	—	1 959	287	

hypofunction (FABRIS et coll 1971 a) Treatment of such animals with somatotrophic hormone and thyroxine can induce maturation of the lymphoid system (FABRIS et coll 1971 b, 1972) In contrast, adrenal and gonadal steroids inhibit proliferation of lymphocytes, and the adrenal steroids may exert a direct cytolytic effect on lymphoid cells (DOUGHERTY)

For the present investigation of the impact of thyroid hormones on lymphoid cell proliferation in vitro, thyroxine and triiodothyronine in both racemic forms (D and L) have been used *In clinical practice* $D\text{-}T_3$ *has only a slight activity* as compared to $L\text{-}T_3$ in goitre prevention (GROSS & PITT RIVERS 1953) and $L\text{-}T_4$ is reported to possess some 8 to 10 times the activity of D T_4 in the treatment or human myxoedema (SALTER 1950) Large quantities of D T_4 reduce the level of circulating thyrotropin and serum lipids in both hypothyroid and euthyroid patients (GORMAN et coll 1974)

In the present in vitro experiments, however, no main differences were observed when comparing the L- and the D isomers, which could indicate that the demonstrated effect of the thyroid hormones is not confined to their hormonal activity, but rather a reflection of a nonspecific mitogenic acivity This is uncertain, however, since experimental conditions prevailing in vitro are different from those in vivo It is therefore of interest that D T_4 in vitro is as potent as L T_4 in uncoupling oxidative phosphorylation (LARDY & MALEY 1954), causing mitochondrial swelling (TAPLEY & HATFIELD 1962) and affecting amino acid incorporation into protein (SOKOLOFF & KAUFMAN 1961) L T_3, which is at least as potent as L T_4 in all multiple physiologic actions, has little effect upon this amino acid incorporation Furthermore, SHAPIRO et coll (1971) support the possibility originally proposed by TAPLEY et coll (1959), that differences in the peripheral distribution between D T_4 and $L\text{-}T_4$ may contribute to the observed differences in their over all hormonal potency in vivo, enhanced binding of D T_4 by liver and kidney appears to divert the hormone from critical effector sites in other tissues

The concentrations of thyroid hormones required to detect lymphoid cell stimulation in vitro were non physiologically high This is in agreement with the results of other investigations of the effects of thyroid hormones in vitro, for example in experiments concerning the oxidative phosphorylation and swelling of mitochondria *Thyroid hormones are relatively insoluble* at the pH of the cell cultures, however, and furthermore it is reasonable to assume that thyroid hormones are at least partially bound to plasma proteins in these cell cultures It is therefore possible that the concentrations of thyroid hormones that affect the lymphoid cells in the present experiments are in reality closer to the physiologic conditions in man than it would seem from the amounts added to the test tubes

One of the explanations of the stimulatory *effect of thyroid hormones* upon the DNA synthesis of lymphoid cells might be that iodide had been degraded from the hormones *However, no significant* change in the DNA synthesis was observed when adding sodium iodide to the cell cultures in corresponding quantities used for the

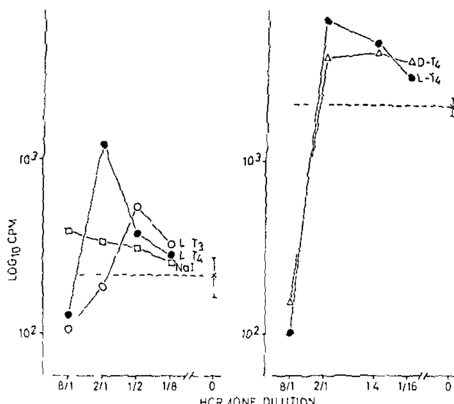


Fig 2 Effects of thyroid hormones and NaI on DNA-synthesis of lymphoid cells x --- x control, without hormone (quadruplicate determinations)

The ^{14}C-thymidine uptake of lymphoid cells cultured for 4 days in the presence or absence of the L- and D-forms of T_4 and T_3, respectively appears in Tables 1, 2 Two different cell donors were used in these experiments The tables show that both the L- and D-forms of the hormones caused significantly enhanced DNA-synthesis of the cells, and that this effect was dose dependent The same results were obtained in other experiments with several different cell donors

Additional experiments were conducted to assess the optimum hormone concentrations for stimulation of cells Two such experiments are presented in Fig 2 using two different blood donors It is seen that hormone concentrations of 0 8 mg per tube reduced the thymidine uptake in comparison to control cultures without hormone Lower concentrations stimulated the lymphocytes to increased DNA-synthesis In one of the experiments (left diagram), the presence of NaI was tested with regard to enhancement of ^{14}C-thymidine uptake by the cells High concentrations slightly enhanced DNA-synthesis of the cells, but not to the same extent as the hormones

Discussion

The development and maintenance of the lymphoid system is influenced by hormonal forces A general lymphoid tissue atrophy developed in mice with pituitary

REFERENCES

AXELROD A R and BERMAN L The bone marrow in hyperthyroidism and hypothyroidism Blood 6 (1951), 436

BALDRIDGE C W and PETERSON F R Splenic enlargement in hyperthyroidism J Amer med Ass 88 (1927) 1701

COULSON A S and CHALMERS P G Separation of viable lymphocytes from human blood Lancet 1 (1964), 468

CROTTI A Thyroid and thymus Lea and Febiger, Philadelphia, Ed 2 (1922), p 750

DOUGHERTY T F Effect of hormones on lymphatic tissue Physiol Rev 32 (1952), 379

ERNSTRÖM U Thyroxin induced changes in cell composition of lymph node tissue, spleen and thymus Acta path microbiol scand 59 (1963), 145

— a) Influence of the thymus on thyroxin-induced lymphatic hyperplasia in young guinea-pigs Acta path microbiol scand 64 (1965), 304

— b) Influence of neonatal thymectomy on the lymphatic system and on its reaction to exogenous thyroxin in guinea pigs Acta path microbiol scand 65 (1965), 192

— and GYLLENSTEN L The histologic picture in thyroxin-induced lymphatic hyperplasia Acta path microbiol scand 47 (1959), 243

— and HEDBACK A L Mitotic studies in thyroxin stimulated thymo-lymphatic tissue Acta path microbiol scand 65 (1965), 215

— and LARSSON B Thyroxin stimulated venous output of small lymphocytes from the thymus Acta path microbiol scand 65 (1965), 203

FABRIS N, PIERPAOLI W and SORKIN E a) Hormones and the immunological capacity III The immunodeficiency disease of the hypopituitary Snell Bagg dwarf mouse Clin exp Immunol 9 (1971), 209

— — — b) Hormones and the immunological capacity IV Restorative effects of developmental hormones or of lymphocytes on the immunodeficiency syndrome of the dwarf mouse Clin exp Immunol 9 (1971) 227

— — — Lymphocytes, hormones and ageing Nature 240 (1972), 557

GLAS U and WASSERMAN J Effect of radiation treatment on cell mediated immune response in carcinoma of the breast Acta radiol Ther Phys Biol 13 (1974), 83

GREGOIRE Ch Influence de L hyperthyroïdie Experimentale (Thyroxine, hormone thyreo trope antéhypophysaire) sur la regenération du thymus consecutive a une involution aigue Arch int Pharmacodyn 67 (1942), 173

GORMAN C A, DARGAVILLE R M, JIANG N S and ELLEFSON R D Comparative effects of d T_4 and l T_4 on h-TSH, serum lipids BMR, and thyroid hormone concentration American Thyroid Association, Fifth Meeting 1974

GROSS J and PITT RIVERS R 3 5 3'-triiodothyronine 2 Physiological activity Biochem J 53 (1953) 652

GYLLENSTEN L Influence of thymus and thyroid on the postnatal growth of the lymphatic tissue in guinea pigs Acta anat Suppl No 18 (1953)

HAMMAR J A Die Normal Morphologische Thymusforschung in letzen Vierteljahrhundert Barth Verlag, Leipzig (1936)

HERNBERG C A Thyrotoxicosis and the size of the lymphocytes. Acta med scand 149 (1954) 37

IRVINE W J and SUMERLING M D Radiological assessment of the thymus in thyroid and other diseases Lancet 1 (1965), 996

LARDY H A and FELDOTT MALEY G Metabolic effects of thyroid hormones in vitro Progr Hormone Res 10 (1954), 129

LUNDELL G WASSERMAN J, EINHORN N and GRANBERG P O DNA synthesis of

thyroid hormones Moreover, the slight changes in the pH of the cell cultures due to the different amounts of thyroid hormones added, were not found to influence the DNA-synthesis

Since the granulocytes of the cell cultures are not likely to survive for the culture period used, they are not expected to influence the results obtained with the thyroid hormones in vitro As for the monocytes, the influence of thyroid hormones on the in vitro DNA-synthesis is not known Preliminary in vitro experiments with highly purified lymphocyte suspensions, analyzing the effect of L-T_3 and L-T_4, support the present results

The results indicate that lymphocytes are stimulated to cell division by thyroid hormones, which thus could be one of the factors responsible for the hyperplasia of the lymphoid system in hyperthyroid individuals The hyperplasia of extra lymphatic tissue observed in animals treated with thyroxine is probably due to both an accelerated migration of cells from the thymus which seed to these organs (ERNSTROM & LARSSON 1965), and to an increased proliferation in situ (ERNSTRÖM 1965 a, 1965 b) The present in vitro experiments correspond with the conclusion that thyroxine causes lymphoid tissue hypertrophy by stimulating the division of lymphocytes, and not by a prolongation of their life span (ERNSTRÖM & HEDBACK 1965)

Acknowledgement

The skilful technical assistance of Mrs Kerstin Håkansson is gratefully acknowledged

SUMMARY

The impact of D- and L-forms of triiodothyronine and thyroxine on DNA-synthesis of human lymphoid cells was tested in vitro The incorporation of [14]C thymidine into DNA was increased by addition of large quantities of both types of hormone in either racemic form

ZUSAMMENFASSUNG

Der Einfluss der D- und L Formen von Trijodothyronin und Thyroxin auf die DNS Synthese menschlicher lymphoider Zellen wurde in vitro getestet Die Inkorporation von [14]C-Thymidin in die DNS wurde durch Zusatz grosser Mengen beider Typen von Hormonen in ihren beiden racemischen Formen gesteigert

RESUMÉ

Les auteurs ont etudié l impact des formes D et L de triiodothyronine et de thyroxine sur la synthèse de l'ADN des cellules lymphoides humaines in vitro L incorporation de [14]C-thymidine dans l'ADN est augmentée par l addition de grandes quantités de ces 2 types d hormone dans l'une ou l'autre de leurs formes racémiques

REFERENCES

AXELROD A R and BERMAN L The bone marrow in hyperthyroidism and hypothyroidism *Blood* 6 (1951), 436.

BALDRIDGE C W and PETERSON F R Splenic enlargement in hyperthyroidism J Amer med Ass 88 (1927), 1701

COULSON A S and CHALMERS P G Separation of viable lymphocytes from human blood Lancet 1 (1964), 468

CROTTI A. Thyroid and thymus Lea and Febiger, Philadelphia, Ed 2 (1922), p 750

DOUGHERTY T F Effect of hormones on lymphatic tissue Physiol Rev 32 (1952), 379

ERNSTROM U Thyroxin induced changes in cell composition of lymph node tissue, spleen and thymus Acta path microbiol scand 59 (1963), 145

— a) *Influence of the thymus on thyroxin induced lymphatic hyperplasia in young guinea-pigs* Acta path microbiol scand 64 (1965) 304

— b) Influence of neonatal thymectomy on the lymphatic system and on its reaction to exogenous thyroxin in guinea pigs Acta path microbiol scand 65 (1965) 192

— and GYLLENSTEN L The histologic picture in thyroxin induced lymphatic hyperplasia Acta path microbiol scand 47 (1959), 243

— and HEDBACK A -L Mitotic studies in thyroxin stimulated thymo-lymphatic tissue Acta path microbiol scand 65 (1965), 215

— and LARSSON B Thyroxin stimulated venous output of small lymphocytes from the thymus Acta path microbiol scand 65 (1965), 203

FABRIS N PIERPAOLI W and SORKIN E a) Hormones and the immunological capacity III *The immunodeficiency disease of the hypopituitary Snell Bagg dwarf mouse* Clin exp Immunol 9 (1971), 209

— — — b) Hormones and the immunological capacity IV Restorative effects of developmental hormones or of lymphocytes on the immunodeficiency syndrome of the dwarf mouse Clin exp Immunol 9 (1971) 227

— — — Lymphocytes, hormones and ageing Nature 240 (1972) 557

. . .

secutive a une involution

Go. .. D *Comparative effects* or d T_4 and l-T_3 on h TSH, serum lipids, BMR, and thyroid hormone concentration American Thyroid Association Fifth Meeting 1974

GROSS J and PITT RIVERS R 3 5 3 triiodothyronine 2 Physiological activity Biochem J 53 (1953) 652

GYLLENSTEN L. Influence of thymus and thyroid on the postnatal growth of the lymphatic tissue in guinea pigs Acta anat Suppl No 18 (1953)

HAMMAR J A *Die Normal* Morphologische Thymusforschung in letzen Vierteljahrhundert Barth Verlag, Leipzig (1936)

HERNBERG C A Thyrotoxicosis *and the size of the lymphocytes* Acta med scand 149 (1954), 37

IRVINE W J and SUMERLING M D Radiological assessment of the thymus in thyroid and *other diseases* Lancet 1 (1965), 996

LARDY H A and FELDOTT MALEY G Metabolic effects of thyroid hormones in vitro Progr Hormone Res 10 (1954), 129

LUNDELL G, WASSERMAN J, EINHORN N and GRANBERG P O DNA synthesis of

lymphocytes in hyperthyroid and euthyroid subjects Effect of ^{131}I therapy for hyperthyroidism To be published in Acta radiol Ther Phys Biol (1976)

— — GRANBERG P-O and BLOMGREN H Lymphocyte populations in peripheral blood in hyperthyroid and euthyroid subjects To be published in Clin exp Immunol (1975)

LUNDIN P M Anterior pituitary gland and lymphoid tissue growth Acta endocr 28 (1958) Suppl No 40

MARGOLIS H M The possible significance of the thymus gland in the syndrome of hyperthyroidism Ann intern Med 4 (1931), 1112

MICHIE W, SWANSON BECK J, MAHAFFY R G, HONEIN E F and FOWLER G B Quantitative radiological and histological studies on the thymus in thyroid disease Lancet 1 (1967), 691

REINHARDT W O and WAINMAN P Effect of thyroidectomy, castration, and replacement therapy on thymus, lymph nodes, spleen in male rats Proc Soc exp Biol 49 (1942), 257

SALTER W T Chemical developments in thyroidology Charles C Thomas, Springfield, Illinois (1950)

SHAPIRO H C, SURKS M I and OPPENHEIMER D H Cellular and plasma protein determinants in the differential distribution and metabolism of D- and L-thyroxine in the rat Endocrinology 88 (1971), 93

SMITH J F B, GLEN A C A and GREIG W R The nucleic acid content of lymphocytes in thyrotoxicosis Clin exp Immunol 8 (1971), 911

SOKOLOFF L and KAUFMAN S Thyroxin stimulation of amino acid incorporation into protein J biol Chem 236 (1961), 795

TAPLEY D F and HATFIELD W B The peripheral action of thyroxine Vitamins Hormones 20 (1962), 251

— DAVIDOFF F F, HATFIELD W B and ROSS J E Physiological disposition of D- and L-thyroxine in the rat Amer J Physiol 197 (1959), 1021

FROM THE CLAIRE ZELLERBACH SARONI TUMOR INSTITUTE, MOUNT ZION HOSPITAL AND MEDICAL CENTER, SAN FRANCISCO, CALIFORNIA 94120, AND THE LAWRENCE BERKELEY LABORATORY, UNIVERSITY OF CALIFORNIA, BERKELEY, CALIFORNIA 94720, U S A

PROTECTION OF THE SKIN OF MICE AGAINST IRRADIATION WITH CYCLOTRON-ACCELERATED HELIUM IONS BY 2-MERCAPTOETHYLAMINE

D G BAKER and J T LEITH

The availability of megavoltage radiation as a modality for cancer therapy has largely reduced the significance of skin tolerance as a limiting factor in treatment planning There remain two circumstances in which the risk of complications from excessive radiation injuries to the skin may limit the use of this modality These occur when the adjacent radiation fields must be matched and therefore risk overlap, and when the skin must be in the radiation field in order to re treat for recurrent disease

Currently, the use of high linear energy transfer (LET) radiation (ARCHAMBEAU et coll 1974, BROWN et coll 1973, WITHERS 1973) as a treatment modality is being actively explored Due to the higher RBE associated with these radiation qualities, it seems likely that this would also be a situation in which the skin tolerance could become an important, perhaps limiting, consideration Local protection of the skin would, under some circumstances, permit higher doses of radiation to be delivered to the tumor volume

Among the first to demonstrate that a local protective effect could be obtained was FORSSBERG (1950) who found that a subcutaneous injection of 2-Mercaptoe-

Submitted for publication 9 September 1974

thylamine (MEA) in guinea pigs could prevent radiation induced epilation DARCIS & GILSON (1967) and DARCIS & HATTERBECK (1958) irrigated the vaginal mucosa and rectum of mice with an MEA solution before irradiation and observed that the number of abnormal exfoliated cells produced by the radiation was significantly diminished, presumably due to the protective effect of MEA

FOGH (1960) observed a significant degree of protection when a 1 per cent suspension of MEA in Vaseline was applied topically to a small area of rabbit skin two hours before irradiation BACQ et coll (1961) found that percutaneous injection of MEA would provide local protection of mouse skin from epilation GOEPP et coll (1967 a, b, 1968, 1969), have demonstrated that a single drop of saturated aqueous solution of MEA applied to the tongue of a mouse before irradiation produced a significant protection (dose reduction factor of 1 35) to the mucosal surfaces The possibility that a topical application of MEA would protect the oral mucosa of mice *against repeated exposures to roentgen irradiation was also investigated by* ANTONE & GIBBS (1973)

LOWY & BAKER (1972, 1973) reported that the topical application of a 10 percent suspension of MEA applied to the skin of mice 15 minutes before irradiation with 250 keV roentgen rays resulted in a dose reduction factor of 1 6, 1 4 and 1 2, using an acute dry desquamation, moist desquamation, and necrosis, respectively, as end points The same authors observed that topical MEA also seemed to reduce some of the late sequelae of radiation injury to the skin

In view of these data, investigations were undertaken to determine whether any local protection from radiation injury to the skin from high LET radiation by the topical application of MEA could be demonstrated

Materials and Methods

Female mice (C_3H/HeJ, Jackson Laboratories, Bar Harbor, Me) were used The mice were housed five per cage and offered food (Simonsen Laboratories, Gilroy, Ca) and water ad libitum They were 9 to 10 weeks of age and 20 to 24 gram in weight at the time of irradiation

For high LET radiation, the 184-inch cyclotron of the Lawrence Radiation Laboratory, Berkeley, California, was used The cyclotron produces a beam of helium ions of 910 MeV initial energy The quality of the radiation was modified as previously described (RAJU et coll 1969, 1972) resulting in the depth dose distribution appearing in Fig 1 An oval brass aperture 20 mm 18 mm placed immediately in front of the mouse leg provided the collimation The dose rate at the skin surface was 350 rad per minute

The MEA for topical application was prepared as follows 2 g of the drug (Cal Biochem, Los Angeles, Ca) was mixed with 1 ml of distilled water and a sufficient volume of saturated sodium bicarbonate solution to bring the pH to 6 5 to 7 5 Approximately 1 ml was required Unibase (Parke, Davis & Co Detroit Mich)

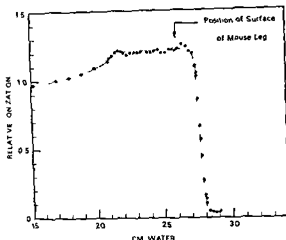


Fig. 1 Schematic of modified Bragg curve used in irradiation of mouse legs The position of the surface of the leg for the extended Bragg peak experiments is indicated in the figure The points indicate actual ionization chamber readings and a smooth curve has been drawn through the points.

was added to bring the drug concentration to 10 per cent by weight The mixture was blended to a smooth paste A placebo for the control animals was prepared in which the MEA was omitted Fifteen minutes before irradiation, the right legs were covered by either the protective or nonprotective (placebo) creams

Table 1

Grading system for skin irradiation reactions

Tissue grades and appearance in acute injury phase	Tissue grades and appearance in recovery phase
1 0 no difference from controls	1 0 no difference from controls
1 5 slight erythema	1 5 limb appears normal except for presence of hair depigmentation
2.0 distinct erythema	2 0 hair is depigmented and there is sparse regrowth of hair
2 5 suggestion of dry desquamation	2 5 sparse regrowth of hair probably no edema the skin does not appear as thin as in a 3 0 recovery state
3 0 dry desquamation powdery appearance of skin on close observation with small cracks and flaking of skin usually edematous	3 0 marked epilation, skin is thin appearing and presents a tight appearance may be a reduction in the size of the limb
3 5 dry desquamation with suggestion of incipient skin breakdown	3 5 very thin shiny skin usually edematous
4 0 moist desquamation of moderate extent patchy appearance	4 0 focal areas of moist desquamation with extensive scab formation
4 5 major percent of limb is involved in moist desquamation may find small areas of necrosis	4 5 small nonhealing areas
5 0 significant amount of necrosis with loss of dermis, similar to a third degree burn	5 0 open, but nondraining wound

thylamine (MEA) in guinea pigs could prevent radiation induced epilation DARCIS & GILSON (1967) and DARCIS & HATTERBECK (1958) irrigated the vaginal mucosa and rectum of mice with an MEA solution before irradiation and observed that the number of abnormal exfoliated cells produced by the radiation was significantly diminished, presumably due to the protective effect of MEA

FOGH (1960) observed a significant degree of protection when a 1 per cent suspension of MEA in Vaseline was applied topically to a small area of rabbit skin two hours before irradiation BACQ et coll (1961) found that percutaneous injection of MEA would provide local protection of mouse skin from epilation GOEPP et coll (1967 a, b, 1968, 1969), have demonstrated that a single drop of saturated aqueous solution of MEA applied to the tongue of a mouse before irradiation produced a significant protection (dose reduction factor of 1 35) to the mucosal surfaces The possibility that a topical application of MEA would protect the oral mucosa of mice against repeated exposures to roentgen irradiation was also investigated by ANTONE & GIBBS (1973)

LOWY & BAKER (1972, 1973) reported that the topical application of a 10 percent suspension of MEA applied to the skin of mice 15 minutes before irradiation with 250 keV roentgen rays resulted in a dose reduction factor of 1 6, 1 4 and 1 2, using an acute dry desquamation, moist desquamation, and necrosis, respectively, as end points The same authors observed that topical MEA also seemed to reduce some of the late sequelae of radiation injury to the skin

In view of these data, investigations were undertaken to determine whether any local protection from radiation injury to the skin from high LET radiation by the topical application of MEA could be demonstrated

Materials and Methods

Female mice (C_3H/HeJ, Jackson Laboratories, Bar Harbor, Me) were used The mice were housed five per cage and offered food (Simonsen Laboratories, Gilroy, Ca) and water ad libitum They were 9 to 10 weeks of age and 20 to 24 gram in weight at the time of irradiation

For high LET radiation, the 184 inch cyclotron of the Lawrence Radiation Laboratory, Berkeley, California, was used The cyclotron produces a beam of helium ions of 910 MeV initial energy The quality of the radiation was modified as previously described (RAJU et coll 1969, 1972) resulting in the depth dose distribution appearing in Fig 1 An oval brass aperture 20 mm 18 mm placed immediately in front of the mouse leg provided the collimation The dose rate at the skin surface was 350 rad per minute

The MEA for topical application was prepared as follows 2 g of the drug (Cal Biochem, Los Angeles, Ca) was mixed with 1 ml of distilled water and a sufficient volume of saturated sodium bicarbonate solution to bring the pH to 6 5 to 7 5 Approximately 1 ml was required Unibase (Parke, Davis & Co , Detroit, Mich)

Table 2

Values for average early (one to 30 days postirradiation) skin reactions in unprotected and MEA protected mice

Dose level (rad)	Condition	
	MEA protected	Unprotected
1 250	1 31*	1 36
	(8)**	(8)
1 750	1 42	1 67
	(8)	(8)
2 500	1 89	2.84
	(8)	(9)
3 000	2.54	3 30
	(7)	(4)

* indicates the mean value of the average early skin reaction

** the number in parentheses indicates the number of animals from which the mean value of the average early skin reactions were obtained

factors (DMF) for selected levels of injury response For average one to 30-day postirradiation scores of 1 5, 2 0, and 2 5, the DMF values are

$$DMF_{(1\ 5)} = \frac{1\ 890 \text{ rad MEA}}{1\ 530 \text{ rad placebo}} = 1\ 24$$

$$DMF_{(2\ 0)} = \frac{2\ 590 \text{ rad MEA}}{2\ 070 \text{ rad placebo}} = 1\ 25$$

$$DMF_{(2\ 5)} = \frac{2\ 960 \text{ rad MEA}}{2\ 370 \text{ rad placebo}} = 1\ 25$$

Although the dose response curves in Figs 2 and 3 give indications of the protection afforded by topically applied MEA, it has been suggested by KELLERER & BRENOT (1973) that difficulties can arise in derivation of modifying factors such as DMF from uncertainties in interpolation and curve-fitting of dose effect relations, particularly since evaluation of skin reactions is based on a numerical grading system having an inherent subjectivity Effects measured using an ordinal scale may therefore be analyzed using nonparametric statistics, such as the Mann-Whitney rank order test (SIEGEL 1956) It is suggested that this test will allow estimation of the skin responses after helium ion irradiation with MEA protection which are most similar to the helium ion skin reactions after different doses without chemoprotection In Table 4, this test has been used to compare mice protected either with topical MEA or placebo This allows establishment of the dose comparisons which are not otherwise statistically acceptable as being equivalent If such dose comparisons are not valid, the ratio of doses (and therefore DMF) has no relevance In these comparisons the 5 per cent level of significance for discrediting the null hypothesis was chosen

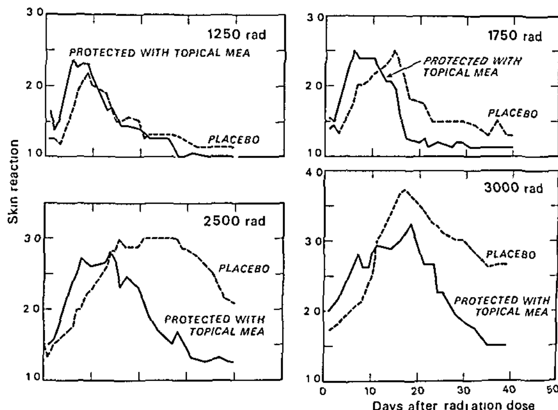


Fig 2 Development of acute skin reactions after different doses of cyclotron accelerated helium ions

One day before irradiation, the hair on the right leg was removed using a depilatory agent (LOWY & BAKER 1973) For irradiation, the animals were anesthesized with sodium Pentobarbital injected intraperitoneally (35 mg/kg) and the leg placed in the center of the radiation beam as previously described (RAJU et coll 1969, LEITH et coll 1974)

The acute skin reactions were observed daily and graded by a numerical system (Table 1) to which the skin reactions could be related

Results

The dose response curves for the protected and for the unprotected skin reactions of helium ion irradiated mouse leg are shown in Fig 2 These two irradiation conditions were compared by using the areas underneath the skin reaction curves (days one to 30 after irradiation) as an index of the dose dependent total skin reactions The area underneath the curve divided by the number of days gives the average skin reaction per day (FOWLER 1967, DENEKAMP et coll 1966, HEGAZY & FOWLER 1973) Tables 2 and 3 list average skin reactions for the MEA-protected and unprotected mice In Fig 3, these values have been used to obtain dose-modifying

Table 4

Comparisons of skin reactions over the period of one to 30 days postirradiation

	Dose (rad)				Range of unacceptable DMF	
	3 000 control	2 500 control	1 750 control	1 250 control		
1 250 MEA	*	*	*	NS	0 7	—
1 750 MEA	*	*	NS	NS	0 7	—
2 500 MEA	*	*	NS	*	1 0	2 0
3 000 MEA	*	NS	*	*	1 0	1 7

An asterisk indicates that comparison of the total skin reactions over the period of one to 30 days postirradiation are significantly different at the 5 per cent level of confidence using the Mann-Whitney rank-order test As a corollary, the ratio of doses of MEA protected placebo protected mice is excluded from the limits of acceptable DMF values
NS indicates a comparison of dose effect responses which are not statistically different at the 5 per cent level of confidence and therefore indicate an acceptable DMF comparison

irritating action of the MEA or depilatory agent A similar effect may be produced by plucking the hair immediately before irradiation (HEGAZY et coll 1973) Such irritation decreases the cell cycle time and skin reactions appear somewhat earlier than in nonstimulated skin One result of the irritating action of the chemical agents is to increase the area under the 30-day dose–response curve and therefore effectively decrease the DMF estimate The real protection afforded by the topical MEA is therefore probably 15 per cent greater than indicated by the DMF of 1 25

Because of the extension of the Bragg curve by interposition of a ridge filter, the modified Bragg curve (Fig 1) represents a family of curves of varying energy and, consequently, varying LET Therefore, the LET at the surface of the skin may not be expressed as a single LET value, but rather should be expressed as dose per unit interval of LET spectrum The LET distribution at the surface of the mouse skin is not currently available, however, the modal LET is probably approximately 15 keV/micron

In their investigations of skin reactions of mice, YUHAS & STORER (1969) found a DMF of 2 4 for production of ulceration in 50 per cent of an irradiated skin field after systemic protection by intraperitoneal injection of WR 2721 In agreement with LOWY & BAKER (1973), a diminished severity of skin reaction was found in the present investigation and also a more rapid repair of the clinically demonstrable skin injury in the protected animals, even after irradiation with helium ions where the modal LET is increased by a factor of 7 over the 250 keV roentgen rays (JOHNS 1956)

It is assumed that the protective effect of MEA is asserted by influencing the

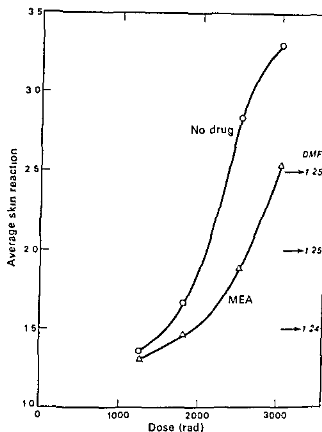


Fig 3 Dose response curves of the average one- to 30 day post irradiation skin reactions for mice irradiated with single doses of modified Bragg peak helium ions, either unprotected (placebo) or protected by topical application of MEA The DMF for various levels of effect is indicated

Discussion

The data indicate that a dose-modifying factor of approximately 1 25 may be obtained in single dose exposures to cyclotron-accelerated helium ions by the use of topically applied MEA The skin reactions of the protected animals all show an early peak in the gradings at 7 to 9 days, several days before the development of the skin reactions in the non-protected animals This is a transient response due to the

Table 3

Values of maximum skin reaction and time after irradiation when maximum reaction is first attained

Dose level (rad)	MEA protected		Unprotected	
	Maximum skin reaction	First day of maximum skin reaction	Maximum skin reaction	First day of maximum skin reaction
1 250	2 3	6	2 2	9
1 750	2 5	6	2 5	14
2 500	2 8	14	3 0	16
3 000	3 2	18	3 7	17

SUMMARY

Mouse skin was exposed to doses of 1 250 to 3 000 rad using a helium ion beam with modal LET of 15 keV per micron The skin reactions were evaluated for mice treated with a topical application of 10 per cent MEA in a cream base or a placebo 15 minutes before irradiation A comparison of the skin reactions indicated that the MEA treatment resulted in a *DMF* of at least 1 2. The implication for radiation therapy was discussed

ZUSAMMENFASSUNG

Mausehaut wurde mit Dosen von 1 250 bis 3 000 rad unter Verwendung eines Helium Ion Strahls mit einer modalen LET von 15 keV per Mikron bestrahlt Die Haut-Reaktionen wurden bei Mausen, die mit einer lokalen Applikation von 10% MEA in einer Krem-Base oder einem Placebo 15 Minuten vor der Bestrahlung behandelt worden waren, festgestellt Ein Vergleich der Hautreaktionen deutet darauf hin, dass die MEA Behandlung zu einer DMF von mindestens 1,2 fuhrt Die Bedeutung fur die Strahlentherapie wird diskutiert

RÉSUMÉ

La peau des souris est exposee à des doses entre 1 250 et 3 000 rad au moyen d'un faisceau d ions d helium avec un modal de LET de 15 keV par micron La reaction de la peau est mesuree dans les souris traitees avec une application locale de creme de MEA à 10% et

REFERENCES

ARCHAMBEAU J O, BENNETT G W, LEVINE G S, COWEN R and AKANUMA A Proton radiation therapy Radiology 110 (1974), 445

BACQ Z M, DECHAMPS G, FISCHER P, HERVE A, LEBIHAN H, LECOMTE J, PIROTTE M and RAYER P X rays and therapy of radiation sickness with 2 mercaptoethylamine Science 117 (1953), 633

BIANCHI E e GASPARINI S L'aumentata resistenza tissulare cutanea alle radiazioni x in rapporto alla somministrazione di beta-mercaptoetilamina al 0 5% per infiltrazione sottocutanea nel tratto da irradiare (In Italian) Radiologia 11 (1955), 1137

BROWN D Q, SEYDEL H G and TODD P Inactivation of cultured human cells and control of C3H mouse mammary tumors with accelerated nitrogen ions Cancer 32 (1973), 541

COHEN L and COHEN A Experimental evaluation of systemic modification (cysteamine, menadione, flavonoids and corticocoids) modifying reactions to radiotherapy Brit J Radiol 32 (1959), 18

DARCIS L et GILSON G Application vaginale de cystamin et radioprotection locale Experientia 13 (1957), 242

— et HATTERBECK P De l'action radioprotectrice exercée sur la muqueuse rectale par la cystéamine administrée par voie générale et par la cystéamine administree par voie intrarectale Experientia 14 (1958), 18

indirect mechanisms If the spectrum of LET values of the accelerated helium ions is similar to the LET spectrum for neutrons described by Rossi (1964), then the proportion of high energy events (expected to produce injury by direct action) would not be expected to change significantly with dose

Rossi, however, found that the LET spectrum for the γ-radiation of ^{60}Co (low LET) showed an increase in the frequency of high energy events (proportion of damage by direct action) as the dose increased These observations may explain why Lowy & Baker (1972, 1973) found a decrease in the protective effect of MEA as the roentgen-ray dose increased, while in the present investigation, with a higher modal LET value, a constant DMF over the range of doses used was found It has been shown (Leith et coll 1974) that recovery between equal size fractions of helium ions, in the modified Bragg peak region of ionization, split over a 24-hour period, is about 80 per cent of the comparable recovery occurring between equal-sized fractions of 230 keV roentgen rays

It is interesting that a differential (cell cycle dependent) protective action of MEA for cell lethality in Chinese hamster cells has been demonstrated by Sinclair (1968, 1969) He found that cells in radiation sensitive stages (G_2 and M) of the cell cycle were most protected Mouse skin has approximately 10 to 15 per cent of epidermal basal cells in the G_2 phase (Gelfant 1965), which may suggest that topical protection of skin by MEA may be achieved even with radiations of relatively high LET

It is of interest to consider the possible beneficial effects of topically applied MEA with regard to a tumor response after heavy particle radiation For example, the data of Rockwell & Kallman (1973) show that, at a single roentgen ray dose of 2 500 rad, which in our helium-ion irradiated mice causes a maximum skin reaction just below the threshold for moist desquamation (Fig 2), approximately 30 per cent of EMT6 solid sarcoma tumors will be cured If the skin is protected (DMF = 1 25), this means that a biologically equivalent dose of 3 125 rad to the skin could be given If this were done, it should increase the percentage of cures of the solid tumor to about 65 per cent The RBE of these accelerated helium ions in the modified Bragg peak region relative to 230 keV roentgen rays is about 1 2 to 1 3 (Leith et coll 1974, Raju et coll 1971, 1972) Therefore, in the care of the tumor this increase in RBE would further increase the therapeutic ratio

It seems reasonable to suggest that topically applied MEA may be clinically useful to obtain a skin sparing effect in those circumstances in which excessive irradiation of the skin is unavoidable The clinical implications of the comparison deserve further consideration

Acknowledgements

This research was supported by USPHS Research Grants CA11412 and CA05203 and GRS RR05472 from the National Institutes of Health (DGB) and by the United States Atomic Energy Commission and the National Aeronautics and Space Administration (JTL) The authors acknowledge with thanks the assistance of Mary Krier

SUMMARY

Mouse skin was exposed to doses of 1 250 to 3000 rad using a *helium ion beam with modal* LET of 15 keV per micron The skin reactions were evaluated for mice treated with a topical application of 10 per cent MEA in a cream base or a placebo 15 minutes before irradiation A comparison of the skin reactions indicated that the MEA treatment resulted in a DMF of at least 1 2. The implication for radiation therapy was discussed

ZUSAMMENFASSUNG

Mausehaut wurde mit Dosen von 1250 bis 3000 rad unter Verwendung eines Helium Ion Strahls mit einer modalen LET von 15 keV per Mikron bestrahlt Die Haut-Reaktionen wurden bei Mäusen, die mit einer lokalen Applikation von 10% MEA in einer Krem Base oder einem Placebo 15 Minuten vor der Bestrahlung behandelt worden waren, festgestellt Ein Vergleich der Hautreaktionen deutet darauf hin, dass die MEA Behandlung zu einer *DMF von mindestens 1 2 fuhrt Die Bedeutung fur die Strahlentherapie wird diskutiert*

RESUMÉ

La peau des souris est exposee a des doses entre 1 250 et 3 000 rad au moyen d'un faisceau d ions d helium avec un modal de LET de 15 keV par micron La réaction de la peau est mesuree *dans les souris traitees avec une application* locale de crème de MEA à 10% et avec un placebo, 15 minutes avant l irradiation Après comparaison des réactions de la peau, on remarque que le traitement par MEA résulte en un DMF d au moins 1,2. On en discute l implication en radiothérapie

REFERENCES

ARCHAMBEAU J O, BENNETT G W, LEVINE G S, COWEN R and AKANUMA A Proton

117 (1953) 633

BIANCHI E e GASPARINI S L aumentata resistenza tissulare cutanea alle radiazioni x in rapporto alla somministrazione di beta mercaptoetilamina al 0 5% per infiltrazione sottocutanea nel tratto da irradiare (In Italian) *Radiologia 11 (1955), 1137*

BROWN D Q, SEYDEL H G and TODD P Inactivation of cultured human cells and control of C3H mouse mammary tumors with accelerated nitrogen ions Cancer 32 (1973) 541

COHEN L. and COHEN A Experimental evaluation of systemic modification (cysteamine menadione, *flavonoids* and corticocoids) modifying reactions to radiotherapy *Brit J* Radiol 32 (1959), 18

DARCIS L. et GILSON G Application vaginale de cystamin et radioprotection locale Experientia 13 (1957), 242

— et HATTERBECK P De l'action radioprotectrice exercee sur la muqueuse rectale par la cystéamine administrée par voie générale et par la cystéamine administree par voie intrarectale Experientia 14 (1958), 18

indirect mechanisms If the spectrum of LET values of the accelerated helium ions is similar to the LET spectrum for neutrons described by ROSSI (1964), then the proportion of high energy events (expected to produce injury by direct action) would not be expected to change significantly with dose

ROSSI, however, found that the LET spectrum for the γ-radiation of ^{60}Co (low LET) showed an increase in the frequency of high energy events (proportion of damage by direct action) as the dose increased These observations may explain why LOWY & BAKER (1972, 1973) found a decrease in the protective effect of MEA as the roentgen-ray dose increased, while in the present investigation, with a higher modal LET value, a constant DMF over the range of doses used was found It has been shown (LEITH et coll 1974) that recovery between equal size fractions of helium ions, in the modified Bragg peak region of conization, split over a 24-hour period, is about 80 per cent of the comparable recovery occurring between equal-sized fractions of 230 keV roentgen rays

It is interesting that a differential (cell cycle dependent) protective action of MEA for cell lethality in Chinese hamster cells has been demonstrated by SINCLAIR (1968, 1969) He found that cells in radiation sensitive stages (G_2 and M) of the cell cycle were most protected Mouse skin has approximately 10 to 15 per cent of epidermal basal cells in the G_2 phase (GELFANT 1965), which may suggest that topical protection of skin by MEA may be achieved even with radiations of relatively high LET

It is of interest to consider the possible beneficial effects of topically applied MEA with regard to a tumor response after heavy particle radiation For example, the data of ROCKWELL & KALLMAN (1973) show that, at a single roentgen ray dose of 2 500 rad, which in our helium-ion irradiated mice causes a maximum skin reaction just below the threshold for moist desquamation (Fig 2), approximately 30 per cent of EMT6 solid sarcoma tumors will be cured If the skin is protected (DMF = 1 25), this means that a biologically equivalent dose of 3 125 rad to the skin could be given If this were done, it should increase the percentage of cures of the solid tumor to about 65 per cent The RBE of these accelerated helium ions in the modified Bragg peak region relative to 230 keV roentgen rays is about 1 2 to 1 3 (LEITH et coll 1974, RAJU et coll 1971, 1972) Therefore, in the care of the tumor this increase in RBE would further increase the therapeutic ratio

It seems reasonable to suggest that topically applied MEA may be clinically useful to obtain a skin sparing effect in those circumstances in which excessive irradiation of the skin is unavoidable The clinical implications of the comparison deserve further consideration

Acknowledgements

This research was supported by USPHS Research Grants CA11412 and CA05203 and GRS RR05472 from the National Institutes of Health (DGB) and by the United States Atomic Energy Commission and the National Aeronautics and Space Administration (JTL) The authors acknowledge with thanks the assistance of Mary Krier

STRAUBE R L, PATT H M, SMITH D E and TYREE E. B Influence of cysteine on the radiosensitivity of Walker rat carcinoma 256 Cancer Res 10 (1950), 243

WILSON C W Effect of pre irradiation intraperitoneal injection of cysteamine upon the skin and depilatory reactions produced by X rays in the legs of mice Brit J Radiol 31 (1958), 100

WITHERS H R Biological basis for high LET radiotherapy Radiology 108 (1973), 131

YUHAS J M and STORER J B Differential chemoprotection of normal and malignant tissues J nat Cancer Inst 42 (1969), 331

DENEKAMP J D, FOWLER J F, KRAGT K, PARNELL C J and FIELD S D Recovery and repopulation in mouse skin after irradiation with cyclotron neutrons as compared with 250 kv X-rays or 15 MeV electrons Radiat Res 29 (1966), 71

FOGH B Local chemical protection of the skin against roentgen radiation injury Acta radiol 53 (1960), 49

FORSSBERG A On the possibility of protecting the living organism against roentgen rays by chemical means Acta radiol 33 (1950), 296

FOWLER J F Kinetics of injury and repair to mammalian tissue by high LET radiation Radiat Res Suppl 7 (1967), 276

GELFANT S Patterns of cell division the demonstration of discrete cell populations *In* Methods in cell physiology, p 359 Edited by D Prescott Academic Press, New York 1966

GOEPP R A and FITCH F W Topical chemical protection against oral radiation death in mice Radiat Res 34 (1968), 36

HARRIS J W and PHILLIPS T L Radiobiological and biochemical studies of thiophosphate radioprotective compounds related to cysteamine Radiat Res 46 (1971), 362

HEGAZY M A H and FOWLER J F Cell population kinetics and desquamation skin reactions in plucked and unplucked mouse skin Cell Tissue Kinet 6 (1973), 587

IRIE H and YOSHIHARA H Influence of radiation protective agents on the therapeutic effects of radiations for malignant tissues Chemotherapia (Basel) 3 (1961), 176

JOHNS H E Radiation fields and their dosimetry *In* Radiation dosimetry, p 591 Edited by G J Hine and G L Brownell Academic Press, New York 1956

KELLERER A M and BRENOT J Nonparametric determination of modifying factors in radiation therapy Radiat Res 56 (1973), 28

LEITH J T, LYMAN J T, HOVORD J, SCHILLING W A and BAKER D G Comparison of skin responses of mice after single or fractionated exposure to cyclotron-accelerated helium ions and 230 kv X-irradiation Submitted to Radiat Res 1974

LOWY R O and BAKER D G Effect of radioprotective drugs on the therapeutic ratio for a mouse tumor system Acta radiol Ther Phys Biol 12 (1973), 425

— — Protection against local irradiation injury to the skin by locally and systemically applied drugs Radiology 105 (1972), 425

RAJU M R, LYMAN J T, BRUSTOD T and TOBIAS C A Heavy-charged particle beams *In* Radiation Dosimetry, Vol III, p 151 Edited by F H Attix and E Tochilin Academic Press, New York 1969

— GNANAPURANI M, MADHVANATH U, HOWARD J and LYMAN J T Relative biological effectiveness and oxygen enhancement ratio at various depths of a 910 MeV helium ion beam Acta radiol Ther Phys Biol 10 (1971), 353

— — MARTINS B, HOWARD J and LYMAN J T Measurement of OER and RBE of a 910 MeV helium ion beam using cultured cells (T-1) Radiology 102 (1972), 425

ROCKWELL S and KALLMAN R F Cellular radiosensitivity and tumor radiation response in the EMT6 tumor cell system Radiat Res 53 (1973) 281

ROSSI H H Correlation of radiation quality and biological effect *In* Physical factors and modification of radiation injury Edited by H E Whipple and L D Hamilton Ann N Y Acad Sci 114 (1964) 4

SCHWARTZ E E, SHAPIRO B and KILLMANN G Selective chemical protection against radiation in tumor-bearing mice Cancer Res 24 (1964), 90

SIEGEL S Nonparametric statistics McGraw-Hill, New York 1956

SINCLAIR W K Cysteamine differential X ray protective effect on Chinese hamster cells during the cell cycle Science 159 (1968), 442

— Protection by cysteamine against lethal X ray damage during the cell cycle of Chinese hamster cells Radiat Res 39 (1969), 135

Material and Methods

Clinical material Multiple bone metastases had been revealed by radiography in 7 female patients with disseminated mammary carcinoma They were treated with cytostatic drugs and corticosteroids One patient with a Ewing s sarcoma of the left femur was also included in the material

All patients were examined by gamma camera after administration of both $^{99}Tc^m$-Diphosphonate and $^{99}Tc^m$ Solcocitran, the time interval between the examinations was at least two days $^{99}Tc^m$-Diphosphonate was given first to 4 patients and $^{99}Tc^m$-Solcocitran was given first to the remaining The time interval between the injection of the compounds and commencement of the gamma camera examination was 4 hours as recommended by the manufacturers Both compounds were injected intravenously with an activity of 10 mCi $^{99}Tc^m$

Six recordings were made from each patient posterior view of the head and neck, thorax, lower thoracic and lumbar region, and the pelvis supplemented with an anterior view of the pelvis In the patient with the Ewing s sarcoma the whole skeleton was examined

Animal experiments Four mongrel dogs, weighing 8 to 11 kg and 8 to 15 months old, with no clinical signs of disease were used, the youngest had growing epiphyseal cartilages Osteotomy at the middle of the left ulna was performed under general anaesthesia No fixation was applied during healing A fracture of the ulna alone seems to cause the dog little discomfort and has the advantage of being easy to examine Callus formation was demonstrated radiographically two weeks after the osteotomy

At 2 16 and 36 days after the osteotomy, the nuclides were given and the distribution of activity in both fore legs was recorded by gamma camera under general anaesthesia Three dogs were given $^{99}Tc^m$-Solcocitran and one dog $^{99}Tc^m$ Diphosphonate The nuclides were injected intravenously with an activity of 0 4 mCi/kg body weight 4 hours before the gamma camera recording

Since it became clear that both compounds were taken up at the osteotomy sites, the possibility that this accumulation was due to increased blood flow was investigated in the dog with the largest callus formation Immediately following the gamma camera recording of the $^{99}Tc^m$ Solcocitran uptake, 100 μCi of ^{131}I labelled RIHSA was administered

Recording equipment The distribution of activity was recorded with a gamma camera (Pho Gamma HP, Nuclear Chicago, Chicago, Illinois, USA) connected with an image data processing system (Med II, Nuclear Data Instruments AB, Uppsala, Sweden) The number of counts from the osteotomy site and a region proximal to this were determined and compared In all $^{99}Tc^m$ examinations a 140 keV converging collimator was used, in the RIHSA recording this was exchanged for a 1 000 hole parallel

FROM THE GENERAL DEPARTMENT (DIRECTOR: PROF. J. EINHORN), RADIUMHEMMET, S-104 01 STOCKHOLM, THE DEPARTMENTS OF SURGERY (DIRECTOR: PROF. N. OBEL) AND CLINICAL RADIOLOGY (DIRECTOR: PROF. S.-E. OLSSON), ROYAL VETERINARY COLLEGE, S-104 05 STOCKHOLM, AND THE DEPARTMENT OF CLINICAL RADIATION PHYSICS (DIRECTOR: PROF. R. WALSTAM), THE NATIONAL INSTITUTE OF RADIATION PROTECTION, S-104 01 STOCKHOLM, SWEDEN.

$^{99}Tc^m$-SOLCOCITRAN IN THE DETECTION OF BONE MALIGNANCY

G. LUNDELL, L. GARMER, SUSANNA CASSEBORN and B.-I. RUDÉN

Certain phosphate compounds labelled with $^{99}Tc^m$ are used in the detection of bone malignancy in man (SUBRAMANIAN et coll. 1972, DUNSON et coll. 1973). Unfortunately, any state of increased bone turnover seems to cause a high uptake of these compounds and therefore their diagnostic value is somewhat limited. A stannous-citrate compound, Solcocitran, for labelling with $^{99}Tc^m$ was recently introduced by Solco Nuclear (Birsfelden, Switzerland). The manufacturers state that $^{99}Tc^m$-Solcocitran has a high and selective uptake in neoplastic tissue in bone and brain and that no false positive or false negative results occur (Solco Nuclear 1974). It was therefore considered of value to compare $^{99}Tc^m$-Solcocitran with $^{99}Tc^m$-Diphosphonate in the detection of human bone malignancy and also to determine if an increased uptake of $^{99}Tc^m$-Solcocitran occurred in fractures.

Submitted for publication 19 June 1975.

Material and Methods

Clinical material Multiple bone metastases had been revealed by radiography in 7 female patients with *disseminated mammary* carcinoma They were treated with cytostatic drugs and corticosteroids One patient with a Ewing's sarcoma of the left femur was also included in the material

All patients were examined by gamma camera after administration of both $^{99}Tc^m$-Diphosphonate and $^{99}Tc^m$-Solcocitran, the time interval between the examinations was at least two days $^{99}Tc^m$-Diphosphonate was given first to 4 patients and $^{99}Tc^m$-Solcocitran was given first to the remaining The time interval between the injection of the compounds and commencement of the gamma camera examination was 4 hours as recommended by the manufacturers Both compounds were injected intravenously with an activity of 10 mCi $^{99}Tc^m$

Six recordings were made from each patient posterior view of the head and neck, thorax, lower thoracic and lumbar region, and the pelvis supplemented with an anterior view of the pelvis In the patient with the Ewing's sarcoma the whole skeleton was examined

Animal experiments Four mongrel dogs, weighing 8 to 11 kg and 8 to 15 months old, with no clinical signs of disease were used, the youngest had growing epiphyseal cartilages Osteotomy at the middle of the left ulna was performed under general anaesthesia No fixation was applied during healing A fracture of the ulna alone seems to cause the dog little discomfort and has the advantage of being easy to examine Callus formation was demonstrated radiographically two weeks after the osteotomy

At 2, 16 and 36 days after the osteotomy, the nuclides were given and the distribution of activity in both fore legs was recorded by gamma camera under general anaesthesia Three dogs were given $^{99}Tc^m$ Solcocitran and one dog $^{99}Tc^m$-Diphosphonate The nuclides were injected intravenously with an activity of 0 4 mCi/kg body weight 4 hours before the gamma camera recording

Since it became clear that both compounds were taken up at the osteotomy sites, the possibility that this accumulation was due to increased blood flow was investigated in the dog with the largest callus formation Immediately following the gamma camera recording of the $^{99}Tc^m$-Solcocitran uptake, 100 μCi of ^{131}I-labelled RIHSA was administered

Recording equipment The distribution of activity was recorded with a gamma camera (Pho Gamma HP, Nuclear Chicago, Chicago, Illinois, USA) connected with an image data processing system (Med II, Nuclear Data Instruments AB, Uppsala, Sweden) The number of counts from the osteotomy site and a region proximal to this were determined and compared In all $^{99}Tc^m$ examinations a 140 keV converging collimator was used, in the RIHSA recording this was exchanged for a 1 000 hole parallel



Fig 1

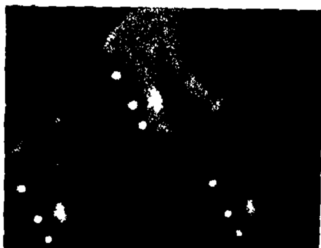


Fig 2

Fig 1 Film of the radius and ulna 16 days after osteotomy of the ulna dog No 4

Fig 2 Gamma camera recording of both fore legs of the same dog as in Fig 1 after administration of $^{99}Tc^{m}$ Solcocitran 16 days after osteotomy Middle marker indicates the osteotomy site

collimator After adjustment of the pulse height analyser no influence of the previous administration of $^{99}Tc^{m}$-Solcocitran was detected

At different times after the administration of $^{99}Tc^{m}$-Solcocitran to the dogs, blood samples were drawn and the blood activity determined in a well counter with a pulse height analyser

The nuclides were obtained from AB Atomenergi, Nykoping, Sweden The $^{99}Tc^{m}$-compounds were labelled in strict accordance with the instructions provided by the manufacturers, and each preparation was tested for chemical purity by thin layer chromatography The chromatograms were developed on Silica-gel (Gelman Instrument Co, Ann Arbor, Michigan, USA) Two solvents were used 0 9 per cent sodium chloride and 100 per cent methyl ethyl ketone

Results

Clinical material Gamma camera examination of the patients with secondary bone malignancy using $^{99}Tc^{m}$-Diphosphonate disclosed all metastatic lesions that had been

Table

Results of gamma camera examinations in dogs

Dog No	Compound	Days after osteotomy	Total No. of counts	Collimator	Ratio of counts from osteotomy site/normal tissue
1	$^{99}Tc^m$ Diphosphonate	16	300 000	Converging	2.4
		36	300 000	Converging	1.8
2	$^{99}Tc^m$-Solcocitran	16	40 000	Converging	1.4
		36	40 000	Converging	1.4
3	$^{99}Tc^m$ Solcocitran	16	40 000	Converging	1.3
		36	40 000	Converging	1.3
4	$^{99}Tc^m$-Solcocitran	16	40 000	Converging	2.2
		36	40 000	Converging	3.2
		36	40 000	Parallel	2.7
	RIHSA	36	20 000	Parallel	0.9

previously detected by radiography and usually several more. In the patient with Ewing's sarcoma, the nuclide was accumulated in a larger area than indicated by the previous radiography.

However, when using $^{99}Tc^m$-Solcocitran the number of metastases that could be observed was actually less than that demonstrated radiographically. The extension of the Ewing's sarcoma corresponded to that found with $^{99}Tc^m$-Diphosphonate. Whenever $^{99}Tc^m$-Solcocitran was used less difference existed between the activity recorded from the bone lesions and the surrounding tissue than with $^{99}Tc^m$-Diphosphonate.

Two hours after the injection of $^{99}Tc^m$-Solcocitran, 3 patients complained of headache of moderate intensity, which lasted for about 8 hours. These patients were examined on the same day with the same preparation. The chromatograms revealed a peak, corresponding to an unknown contamination, when 100 per cent methyl ethyl ketone was used as solvent. This peak was estimated to contain 5 per cent of the total activity and was separated from the $^{99}Tc^m$-Solcocitran fraction. No chromatographic abnormality was found in any other preparation.

Animal experiments. Increased uptake of $^{99}Tc^m$ was evident at the osteotomy site in all dogs at each examination (Figs 1, 2). The numerical results of the examinations on all dogs at 16 and 36 days appear in the Table. No increased activity at the osteotomy site was found following the administration of RIHSA.

The results of the blood activity measurements are given in Fig. 3. No animal showed any signs of illness.



Fig 1



Fig 2

Fig 1 Film of the radius and ulna 16 days after osteotomy of the ulna, dog No 4

Fig 2 Gamma camera recording of both fore legs of the same dog as in Fig 1 after administration of $^{99}Tc^{m}$-Solcocitran, 16 days after osteotomy Middle marker indicates the osteotomy site

collimator After adjustment of the pulse height analyser no influence of the previous administration of $^{99}Tc^{m}$-Solcocitran was detected

At different times after the administration of $^{99}Tc^{m}$-Solcocitran to the dogs, blood samples were drawn and the blood activity determined in a well counter with a pulse height analyser

The nuclides were obtained from AB Atomenergi, Nykoping, Sweden The $^{99}Tc^{m}$-compounds were labelled in strict accordance with the instructions provided by the manufacturers, and each preparation was tested for chemical purity by thin layer chromatography The chromatograms were developed on Silica-gel (Gelman Instrument Co , Ann Arbor, Michigan, USA) Two solvents were used 0 9 per cent sodium chloride and 100 per cent methyl ethyl ketone

Results

Clinical material. Gamma camera examination of the patients with secondary bone malignancy using $^{99}Tc^{m}$-Diphosphonate disclosed all metastatic lesions that had been

Table

Results of gamma camera examinations in dogs

Dog No	Compound	Days after osteotomy	Total No of counts	Collimator	Ratio of counts from osteotomy site normal tissue
1	^{99}Tc^{m} Diphosphonate	16	300 000	Converging	2 4
		36	300 000	Converging	1 8
2	^{99}Tc^{m} Solcocitran	16	40 000	Converging	1 4
		36	40 000	Converging	1 4
3	^{99}Tc^{m}-Solcocitran	16	40 000	Converging	1 3
		36	40 000	Converging	1 3
4	^{99}Tc^{m} Solcocitran	16	40 000	Converging	2.2
		36	40 000	Converging	3 2
		36	40 000	Parallel	2 7
	RIHSA	36	20 000	Parallel	0 9

previously detected by radiography and usually several more In the patient with Ewing s sarcoma, the nuclide was accumulated in a larger area than indicated by the previous radiography

However, when using ^{99}Tc^{m} Solcocitran the number of metastases that could be observed was actually less than that demonstrated radiographically The extension of the Ewing s sarcoma corresponded to that found with ^{99}Tc^{m}-Diphosphonate Whenever ^{99}Tc^{m} Solcocitran was used less difference existed between the activity recorded from the bone lesions and the surrounding tissue than with ^{99}Tc^{m}-Diphosphonate

Two hours after the injection of ^{99}Tc^{m} Solcocitran, 3 patients complained of headache of moderate intensity, which lasted for about 8 hours These patients were examined on the same day with the same preparation The chromatograms revealed a peak, corresponding to an unknown contamination, when 100 per cent methyl ethyl ketone was used as solvent This peak was estimated to contain 5 per cent of the total activity and was separated from the ^{99}Tc^{m}-Solcocitran fraction No chromatographic abnormality was found in any other preparation

Animal experiments Increased uptake of ^{99}Tc^{m} was evident at the osteotomy site in all dogs at each examination (Figs 1, 2) The numerical results of the examinations on all dogs at 16 and 36 days appear in the Table No increased activity at the osteotomy site was found following the administration of RIHSA

The results of the blood activity measurements are given in Fig 3 No animal showed any signs of illness



Fig 1



Fig 2

Fig 1 Film of the radius and ulna 16 days after osteotomy of the ulna, dog No 4

Fig 2 Gamma camera recording of both fore legs of the same dog as in Fig 1 after administration of $^{99}Tc^{m}$ Solcocitran 16 days after osteotomy Middle marker indicates the osteotomy site

collimator After adjustment of the pulse height analyser no influence of the previous administration of $^{99}Tc^{m}$-Solcocitran was detected

At different times after the administration of $^{99}Tc^{m}$ Solcocitran to the dogs, blood samples were drawn and the blood activity determined in a well counter with a pulse height analyser

The nuclides were obtained from AB Atomenergi, Nykoping, Sweden The $^{99}Tc^{m}$-compounds were labelled in strict accordance with the instructions provided by the manufacturers, and each preparation was tested for chemical purity by thin layer chromatography The chromatograms were developed on Silica-gel (Gelman Instrument Co, Ann Arbor, Michigan, USA) Two solvents were used 0 9 per cent sodium chloride and 100 per cent methyl ethyl ketone

Results

Clinical material Gamma camera examination of the patients with secondary bone malignancy using $^{99}Tc^{m}$-Diphosphonate disclosed all metastatic lesions that had been

Table

Results of gamma camera examinations in dogs

Dog No	Compound	Days after osteotomy	Total No of counts	Collimator	Ratio of counts from osteotomy site normal tissue
1	$^{99}Tc^{m}$ Diphosphonate	16	300 000	Converging	2.4
		36	300 000	Converging	1 8
2	$^{99}Tc^{m}$ Solcocitran	16	40 000	Converging	1 4
		36	40 000	Converging	1 4
3	$^{99}Tc^{m}$ Solcocitran	16	40 000	Converging	1 3
		36	40 000	Converging	1 3
4	$^{99}Tc^{m}$ Solcocitran	16	40 000	Converging	2 2
		36	40 000	Converging	3 2
		36	40 000	Parallel	2 7
	RIHSA	36	20 000	Parallel	0 9

previously detected by radiography and usually several more In the patient with Ewing s sarcoma, the nuclide was accumulated in a larger area than indicated by the previous radiography

However, when using $^{99}Tc^{m}$ Solcocitran the number of metastases that could be observed was actually less than that demonstrated radiographically The extension of the Ewing s sarcoma corresponded to that found with $^{99}Tc^{m}$-Diphosphonate Whenever $^{99}Tc^{m}$ Solcocitran was used less difference existed between the activity recorded from the bone lesions and the surrounding tissue than with $^{99}Tc^{m}$-Diphosphonate

Two hours after the injection of $^{99}Tc^{m}$-Solcocitran, 3 patients complained of headache of moderate intensity, which lasted for about 8 hours These patients were examined on the same day with the same preparation The chromatograms revealed a peak, corresponding to an unknown contamination, when 100 per cent methyl ethyl ketone was used as solvent This peak was estimated to contain 5 per cent of the total activity and was separated from the $^{99}Tc^{m}$ Solcocitran fraction No chromatographic abnormality was found in any other preparation

Animal experiments Increased uptake of $^{99}Tc^{m}$ was evident at the osteotomy site in all dogs at each examination (Figs 1, 2) The numerical results of the examinations on all dogs at 16 and 36 days appear in the Table No increased activity at the osteotomy site was found following the administration of RIHSA

The results of the blood activity measurements are given in Fig 3 No animal showed any signs of illness

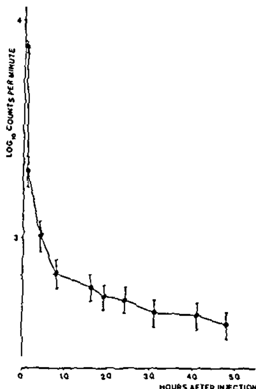


Fig. 3. Relative activity of $^{99}Tc^{m}$ per ml of blood after administration of $^{99}Tc^{m}$-Solcocitran. Each value represents the mean of 3 dogs ± the standard error of the mean.

Discussion

The main impression gained from the present material was that $^{99}Tc^{m}$-Solcocitran was a less sensitive indicator of secondary bone malignancy than $^{99}Tc^{m}$-Diphosphonate, and provided even less diagnostic information than conventional radiography. One reason for this discrepancy seems to be the low uptake of $^{99}Tc^{m}$-Solcocitran in the metastases as compared with that measured in the surrounding bone. An improvement would probably be attained by prolonging the time interval between the administration of $^{99}Tc^{m}$-Solcocitran and the gamma camera recording, as suggested by the elimination curve in Fig. 3. A higher activity of $^{99}Tc^{m}$ would then be required, however, thus increasing the absorbed dose to the patient.

Since all the patients with mammary carcinoma had been receiving cytostatic and corticosteroid therapy for several months, the results of our examinations could be disputed on grounds of changes produced by this therapy. KAMPFFMEYER et coll. (1967) reported that following introduction of hormonal therapy or chemotherapy the uptake of ^{18}F in bone metastases remained unchanged during the first 4 months. It is reasonable to assume that any influence of treatment would have affected the results obtained with $^{99}Tc^{m}$-Solcocitran and $^{99}Tc^{m}$-Diphosphonate in equal proportion.

Contrary to expectations, $^{99}Tc^{m}$-Solcocitran activity was high in healing fractures in dogs, and thus the compound can hardly be claimed to be selective for neoplastic tissue. The high activity of $^{99}Tc^{m}$-Solcocitran in the fracture which was also examined

with RIHSA, was not caused by increased blood flow in this region as indicated by the negative RIHSA scan This finding is interesting in the light of MCLAUGHLIN's hypothesis (1975) that $^{99}Tc^m$-phosphate compounds have an affinity for the hydroxyapatite crystals of newly formed bone

SUMMARY

A new $^{99}Tc^m$-labelled compound, $^{99}Tc^m$-Solcocitran, has been introduced for detection of

pounds accumulated in fractures in dogs $^{99}Tc^m$ Solcocitran seems to offer no advantage over existing techniques in the detection of bone malignancy

ZUSAMMENFASSUNG

Eine neue $^{99}Tc^m$ gezeichnete Substanz, $^{99}Tc^m$-Solcocitran, ist zur Darstellung von Knochen- und Gehirn Malignitaten eingefuhrt worden Diese wird als fur maligne Gewebe spezifisch bezeichnet Im vorliegenden Material war jedoch $^{99}Tc^m$-Solcocitran zur Darstellung von metastatischen Knochen Läsionen von Patienten weniger empfindlich als $^{99}Tc^m$-Diphosphonat oder konventionelle Rontgendarstellung Beide $^{99}Tc^m$-Verbindungen sammelten sich in Frakturen von Hunden an $^{99}Tc^m$-Solcocitran scheint keinen Vorteil gegenuber befindlichen Verfahren zur Entdeckung von Knochenmalignitat zu bieten

RÉSUME

Nouveau produit marque au $^{99}Tc^m$, le $^{99}Tc^m$ Solcocitran a éte propose pour la detection des tumeurs malignes osseuses et cerebrales Il est presente comme etant specifique des tissus neoplastiques Cependant, dans la presente serie, le $^{99}Tc^m$ Solcocitran a eté moins sensible pour la mise en evidence de lesions osseuses métastatiques chez les malades que n etait le $^{99}Tc^m$ Diphosphonate ou la radiographie classique Ces deux composes marques au $^{99}Tc^m$ se fixent dans les fractures chez les chiens Le $^{99}Tc^m$ Solcocitran semble ne pas presenter d avantage sur les techniques existantes pour la détection des tumeurs malignes osseuses

REFERENCES

DUNSON G L STEVENSON J S, COLE C M, MEILOR M K and HOSAIN F Preparation and comparison of Technetium-99m Diphosphonate, Polyphosphate and Pyrophosphate nuclear bone imaging radiopharmaceuticals Drug Intell clin Pharm 7 (1973), 471

KAMPFFMEYER H G, DVORKIN H, CARR E A and BULL F E The effect of drug therapy on the uptake of radioactive fluorine by osseous metastases Clin Pharmacol Ther 8 (1967), 647

MCLAUGHLIN A F Uptake of ^{99m}Tc bone scanning agent of lungs with metastatic calcification J nucl Med 16 (1975), 322

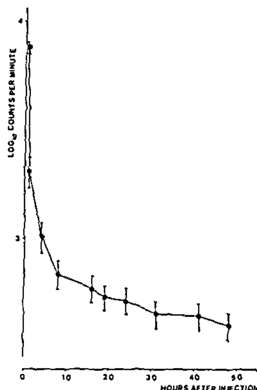


Fig 3 Relative activity of $^{99}Tc^{m}$ per ml of blood after administration of $^{99}Tc^{m}$-Solcocitran Each value represents the mean of 3 dogs ± the standard error of the mean

Discussion

The main impression gained from the present material was that $^{99}Tc^{m}$-Solcocitran was a less sensitive indicator of secondary bone malignancy than $^{99}Tc^{m}$-Diphosphonate, and provided even less diagnostic information than conventional radiography One reason for this discrepancy seems to be the low uptake of $^{99}Tc^{m}$-Solcocitran in the metastases as compared with that measured in the surrounding bone An improvement would probably be attained by prolonging the time interval between the administration of $^{99}Tc^{m}$-Solcocitran and the gamma camera recording, as suggested by the elimination curve in Fig 3 A higher activity of $^{99}Tc^{m}$ would then be required, however, thus increasing the absorbed dose to the patient

Since all the patients with mammary carcinoma had been receiving cytostatic and corticosteroid therapy for several months, the results of our examinations could be disputed on grounds of changes produced by this therapy KAMPFFMEYER et coll. (1967) reported that following introduction of hormonal therapy or chemotherapy the uptake of ^{18}F in bone metastases remained unchanged during the first 4 months It is reasonable to assume that any influence of treatment would have affected the results obtained with $^{99}Tc^{m}$-Solcocitran and $^{99}Tc^{m}$-Diphosphonate in equal proportion.

Contrary to expectations, $^{99}Tc^{m}$-Solcocitran activity was high in healing fractures in dogs, and thus the compound can hardly be claimed to be selective for neoplastic tissue The high activity of $^{99}Tc^{m}$-Solcocitran in the fracture which was also examined

with RIHSA, was not caused by increased blood flow in this region as indicated by the negative RIHSA scan This finding is interesting in the light of McLAUGHLIN's hypothesis (1975) that ^{99}Tc^{m}-phosphate compounds have an affinity for the hydroxyapatite crystals of newly formed bone

SUMMARY

A new ^{99}Tc^{m} labelled compound ^{99}Tc^{m}-Solcocitran, has been introduced for detection of bone and brain malignancy It is claimed to be specific for neoplastic tissue In the present material however ^{99}Tc^{m} Solcocitran was less sensitive in indicating metastatic bone lesions in patients than was ^{99}Tc^{m}-Diphosphonate or conventional radiography Both ^{99}Tc^{m} compounds accumulated in fractures in dogs ^{99}Tc^{m} Solcocitran seems to offer no advantage over existing techniques in the detection of bone malignancy

ZUSAMMENFASSUNG

Eine neue ^{99}Tc^{m} gezeichnete Substanz, ^{99}Tc^{m} Solcocitran, ist zur Darstellung von Knochen- und Gehirn Malignitaten eingefuhrt worden Diese wird als fur maligne Gewebe spezifisch bezeichnet Im vorliegenden Material war jedoch ^{99}Tc^{m} Solcocitran zur Darstellung von metastatischen Knochen Lasionen von Patienten weniger empfindlich als ^{99}Tc^{m}-Diphosphonat oder konventionelle Rontgendarstellung Beide ^{99}Tc^{m}-Verbindungen sammelten sich in Frakturen von Hunden an ^{99}Tc^{m} Solcocitran scheint keinen Vorteil gegenuber befindlichen Verfahren zur Entdeckung von Knochenmalignitat zu bieten

RESUMÉ

Nouveau produit marque au ^{99}Tc^{m}, le ^{99}Tc^{m} Solcocitran a été propose pour la detection des tumeurs malignes osseuses et cerebrales Il est présenté comme etant specifique des ... té moins ... ades que ... que Ces deux composes marques au ^{99}Tc^{m} se fixent dans les fractures chez les chiens Le ^{99}Tc^{m}-Solcocitran semble ne pas presenter d avantage sur les techniques existantes pour la detection des tumeurs malignes osseuses

REFERENCES

DUNSON G L STEVENSON J S, COLE C M MELLOR M K and HOSAIN F Preparation and comparison of Technetium 99m Diphosphonate Polyphosphate and Pyrophosphate ... Drug Intell clin Pharm 7 (1973) 471

... and BULL F E The effect of drug therapy ... by osseous metastases Clin Pharmacol Ther 8 (1967) 647

McLAUGHLIN A F Uptake of ^{99m}Tc bone scanning agent of lungs with metastatic calcification J nucl Med 16 (1975) 322

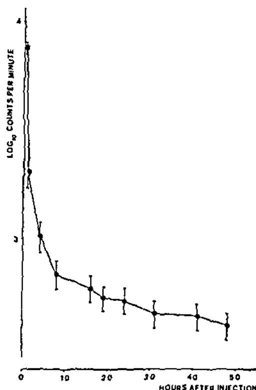


Fig 3 [illegible]
after ac[illegible]
value re[illegible]
error of the mean

Discussion

The main impression gained from the present material was that ^{99}Tc^{m}-*Solcocitran* was a less sensitive indicator of secondary bone malignancy than ^{99}Tc^{m}-*Diphosphonate*, and provided even less *diagnostic information* than conventional radiography One reason for this discrepancy seems to be the low uptake of ^{99}Tc^{m}-Solcocitran in the metastases as compared with that measured in the surrounding bone An improvement would probably be attained by prolonging the time interval between the administration of ^{99}Tc^{m}-Solcocitran and the gamma camera recording, as suggested by the elimination curve in Fig 3 A higher activity of ^{99}Tc^{m} would then be required, however, thus increasing the absorbed dose to the patient

Since all the patients with mammary carcinoma had been receiving cytostatic and corticosteroid therapy for several months, the results of our examinations could be disputed on grounds of changes produced by this therapy KAMPFFMEYER et coll (1967) reported that following introduction of hormonal therapy or chemotherapy the uptake of ^{18}F in bone metastases remained unchanged during the first 4 months It is reasonable to assume that any influence of treatment would have affected the results obtained with ^{99}Tc^{m}-Solcocitran and ^{99}Tc^{m}-Diphosphonate in equal proportion.

Contrary to expectations, ^{99}Tc^{m}-Solcocitran activity was high in healing fractures in dogs, and thus the compound can hardly be claimed to be selective for neoplastic tissue The high activity of ^{99}Tc^{m}-Solcocitran in the fracture which was also examined

DE HOPITAL HENRI MONDOR, SERVICE DE CARCINOLOGIE RADIOTHERAPIQUE (PROFESSEUR B PIERQUIN), F 94100 CRETEIL ET, INSTITUT GUSTAVE ROUSSY. DEPARTMENT DES RADIATIONS (PROFESSEUR M TUBIANA) F-94800 VILLEJUIF, FRANCE

DETERMINATION DE LA FONCTION DE DIFFUSION DE RAYONS X DE 25 MV DANS UN MILIEU EQUIVALENT-TISSU

GINETTE MARINELLO et ANDREE DUTREIX

Lorsque l on veut connaitre la distribution de la dose dans un champ de forme complexe la methode la plus precise (CUNNINGHAM et coll 1965) consiste a calculer separement en chaque point la contribution a la dose du rayonnement primaire et du rayonnement diffusé Ce calcul necessite la connaissance en tout point de l espace du rayonnement diffuse par un pinceau elementaire La première etape de ce calcul est la determination de la fonction de diffusion en fonction de la profondeur dans le milieu et des dimensions du faisceau C'est cette fonction de diffusion que nous avons cherche a determiner experimentalement pour des rayons X de 25 MV

Caracteristiques du faisceau

Pour effectuer cette étude, nous avons utilise un faisceau de rayons X de 25 MV produit par un accélerateur lineaire de type Sagittaire (CSF) dont nous avons determine la qualite en étudiant son attenuation en « faisceau etroit » dans differents materiaux

Soumis à la redaction le 14 fevrier 1975

Solco Nuclear, Birsfelden, Switzerland Solcocitran®-^{99m}Tc, a tumour scanning agent Preliminary report, 1974

SUBRAMANIAN G, MCAFEE J G and BELL E G ^{99m}Tc labeled polyphosphate as a skeletal imaging agent *Radiology 102 (1972), 701*

DE HÔPITAL HENRI MONDOR, SERVICE DE CARCINOLOGIE RADIOTHÉRAPIQUE (PROFESSEUR B. PIERQUIN) F 94100 CRETEIL ET, INSTITUT GUSTAVE ROUSSY DEPARTMENT DES RADIATIONS (PROFESSEUR M TUBIANA) F 94800 VILLEJUIF, FRANCE

DETERMINATION DE LA FONCTION DE DIFFUSION DE RAYONS X DE 25 MV DANS UN MILIEU EQUIVALENT-TISSU

GINETTE MARINELLO et ANDRÉE DUTREIX

Lorsque l on veut connaitre la distribution de la dose dans un champ de forme complexe la méthode la plus précise (CUNNINGHAM et coll 1965) consiste a calculer séparement en chaque point la contribution a la dose du rayonnement primaire et du rayonnement diffuse Ce calcul nécessite la connaissance en tout point de l espace du rayonnement diffuse par un pinceau elementaire La premiere étape de ce calcul est la determination de la fonction de diffusion en fonction de la profondeur dans le milieu et des dimensions du faisceau C est cette fonction de diffusion que nous avons cherche a determiner experimentalement pour des rayons X de 25 MV

Caracteristiques du faisceau

Pour effectuer cette étude nous avons utilisé un faisceau de rayons X de 25 MV produit par un accelerateur lineaire de type Sagittaire (CSF) dont nous avons determine la qualite en étudiant son attenuation en « faisceau etroit » dans différents matériaux

---

Soumis à la rédaction le 14 février 1975

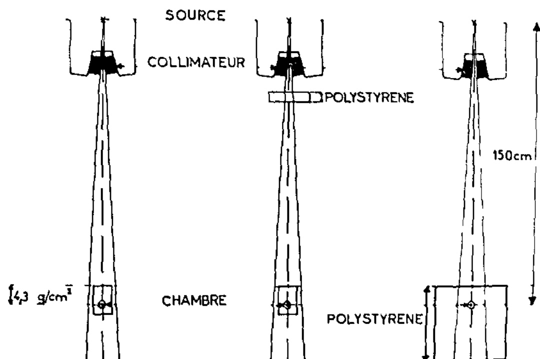


Fig. 1. Dispositifs expérimentaux utilisés pour mesurer: a) la dose due au rayonnement primaire en l'absence de toute atténuation; b) la dose due au rayonnement primaire après atténuation par un écran; c) la dose en profondeur dans le milieu équivalent tissu.

Générateur de rayons X. Les rayons X de 25 MV sont obtenus en projetant un faisceau d'électrons monoénergétique de 25 MeV sur une cible de tungstène de 4 mm d'épaisseur au centre. Le faisceau de rayons X obtenu par le processus de freinage traverse ensuite un cone égalisateur en plomb de 2,9 cm d'épaisseur au centre et une chambre d'ionisation moniteur à quatre quadrants dont les électrodes en kapton métallisé ont une épaisseur négligeable.

Un système de collimation, constitué par deux paires de machoires mobiles en plomb de 20 cm d'épaisseur, permet d'obtenir des faisceaux d'irradiation dont les dimensions varient de 2 cm × 2 cm à 37 cm × 37 cm au niveau de l'axe de rotation de l'appareil, c'est à dire à 105 cm de la source.

Qualité du faisceau. Nous l'avons déterminée expérimentalement en étudiant son « atténuation en faisceau étroit » dans le polystyrène, l'acier, le laiton et le plomb.

La Fig. 1 a représente les conditions expérimentales choisies de manière à réduire le plus possible la contribution du rayonnement diffusé à la dose (Voir paragraphe suivant).

Les différentes courbes d'atténuation en « faisceau étroit » obtenues en plaçant des épaisseurs croissantes d'un matériau donné à la sortie du collimateur (Fig. 1 b) sont représentées sur la Fig. 2. Elles correspondent à des fonctions exponentielles; aussi avons nous caractérisé le faisceau par sa couche de demi-atténuation (CDA) dans les différents matériaux (Tableau 1).

Tableau 1

Valeur de la couche de demi-atténuation (CDA) du faisceau de rayons X de 25 MV utilisé en fonction de la nature du matériau

Nature de l'écran	Masse volumique (g × cm⁻³)	CDA (cm)	CDA (g × cm⁻²)
Polystyrène	1,03	21 85	22,5
Acier	7,7	2 66	20 5
Laiton	8 6	2,33	20,0
Plomb	11,2	1,26	14,1

Conditions de diffusion minimale

Ce travail nécessite une mesure précise de la dose due aux photons primaires pour étudier par exemple l'atténuation du faisceau dans les différents matériaux ou le coefficient de diffusion à l'entrée B_0

Pour effectuer cette mesure, nous entourons une chambre d'ionisation de petites dimensions (chambre BALDWIN 0,2 cm³) d'un petit bloc de plexiglas cylindrique de 4 6 cm de diamètre et de 6 cm de hauteur, le centre de la chambre étant situé sous 4,3 g × cm⁻² de plexiglas Les dimensions et la forme de ce « capuchon » dit minimal sont très proches de celles de la région irradiée de laquelle provient la majorité des électrons arrivant au centre de la chambre et assure un bon équilibre électronique latéral et longitudinal DUTREIX et ses collaborateurs estiment qu'un tel volume de milieu équivalent tissu est suffisant pour assurer l'équilibre électronique à au moins 90 % de sa valeur (DUTREIX et coll 1965)

Nous plaçons cette chambre entourée du « capuchon minimal » à grande distance du collimateur (distance source chambre égale à 150 cm) de manière à ce qu'elle soit le moins sensible possible au rayonnement diffusé par le collimateur (Fig 1 a)

Dans ces conditions, le détecteur enregistre les électrons secondaires mis en mouvement par les photons primaires dans le « capuchon minimal » auxquels viennent s'ajouter quelques électrons secondaires mis en mouvement par des photons diffusés par le collimateur ou nés dans les parois du capuchon Les électrons secondaires provenant du collimateur quant à eux, sont d'une part dispersés du fait de la grande distance et, d autre part, arrêtés en grande partie par le capuchon de plexiglas

Nous avons ainsi un moyen de mesure de la dose due au rayonnement primaire seul $D_p(m, l)$ en notant la réponse de la chambre, pour une même indication de la chambre moniteur de l'accélérateur, en fonction des dimensions du faisceau mesurées à la distance de la chambre

En toute rigueur, cette mesure ne permet pas de déterminer la dose due au rayonnement primaire seul puisqu'il se produit une atténuation et une diffusion des photons dans le « capuchon minimal » Notre but n'étant pas la détermination absolue

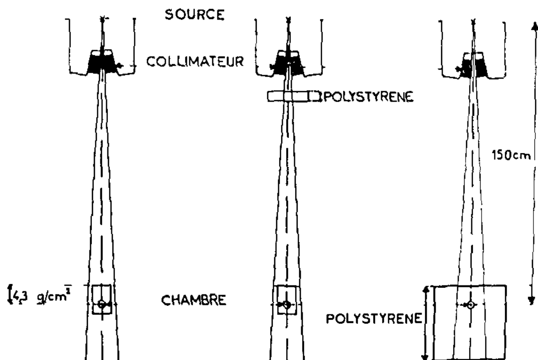


Fig 1 Dispositifs expérimentaux utilisés pour mesurer a) la dose due au rayonnement primaire en l absence *de toute attenuation b)* la dose due au rayonnement primaire apres atténuation par un ecran c) la dose en profondeur dans le milieu équivalent tissu

Generateur de rayons X Les rayons X de 25 MV sont obtenus en projetant un faisceau d electrons monoenergetique de 25 MeV sur une cible de tungstene de 4 mm d epaisseur au centre Le faisceau de rayons X obtenu par le processus de freinage traverse ensuite un cone egalisateur en plomb de 2 9 cm d epaisseur au centre et une chambre d ionisation moniteur a quatre quadrants dont les electrodes en kapton metallise ont une epaisseur negligeable

Un système de collimation constitué par deux paires de machoires mobiles en plomb de 20 cm d epaisseur permet d obtenir des faisceaux d irradiation dont les dimensions varient de 2 cm 2 cm a 37 cm × 37 cm au niveau de l axe de rotation de l appareil c est a dire a 105 cm de la source

Qualite du faisceau Nous l avons determinee experimentalement en etudiant son « attenuation en faisceau etroit » dans le polystyrene l acier le laiton et le plomb

La Fig 1 a represente les conditions experimentales choisies de maniere a réduire le plus possible la contribution du rayonnement diffusé a la dose (Voir paragraphe suivant)

Les differentes courbes d attenuation en « faisceau etroit » obtenues en plaçant des epaisseurs croissantes d un materiau donne a la sortie du collimateur (Fig 1 b) sont représentées sur la Fig 2 Elles correspondent a des fonctions exponentielles aussi avons nous caracterise le faisceau par sa couche de demi atténuation (CDA) dans les differents materiaux (Tableau 1)

Tableau 1

Valeur de la couche de demi-atténuation (CDA) du faisceau de rayons X de 25 MV utilisé en fonction de la nature du matériau

Nature de l'écran	Masse volumique ($g \times cm^{-3}$)	CDA (cm)	CDA ($g \times cm^{-2}$)
Polystyrène	1 03	21 85	22,5
Acier	7 7	2 66	20 5
Laiton	8 6	2,33	20 0
Plomb	11 2	1 26	14 1

Conditions de diffusion minimale

Ce travail nécessite une mesure précise de la dose due aux photons primaires pour étudier par exemple l'atténuation du faisceau dans les différents matériaux ou le coefficient de diffusion à l'entrée B_0

Pour effectuer cette mesure nous entourons une chambre d'ionisation de petites dimensions (chambre BALDWIN 0 2 cm^3) d'un petit bloc de plexiglas cylindrique de 4 6 cm de diamètre et de 6 cm de hauteur le centre de la chambre étant situé sous 4 3 $g \times cm^{-2}$ de plexiglas Les dimensions et la forme de ce « capuchon » dit *minimal* sont très proches de celles de la région irradiée de laquelle provient la majorité des électrons arrivant au centre de la chambre et assure un bon équilibre électronique latéral et longitudinal DUTREIX et ses collaborateurs estiment qu'un tel volume de milieu équivalent tissu est suffisant pour assurer l'équilibre électronique à au moins 90 % de sa valeur (DUTREIX et coll 1965)

Nous plaçons cette chambre entourée du « capuchon minimal » à grande distance du collimateur (distance source-chambre égale à 150 cm) de manière à ce qu'elle soit le moins sensible possible au rayonnement diffusé par le collimateur (Fig 1 a)

Dans ces conditions le détecteur enregistre les électrons secondaires mis en mouvement par les photons primaires dans le « capuchon minimal » auxquels viennent s'ajouter quelques électrons secondaires mis en mouvement par des photons diffusés par le collimateur ou nés dans les parois du capuchon Les électrons secondaires provenant du collimateur quant à eux sont d'une part dispersés du fait de la grande distance et d'autre part arrêtés en grande partie par le capuchon de plexiglas

Nous avons ainsi un moyen de mesure de la dose due au rayonnement primaire seul D_p(m l) en notant la réponse de la chambre pour une même indication de la chambre moniteur de l'accélérateur en fonction des dimensions du faisceau mesurées à la distance de la chambre

En toute rigueur cette mesure ne permet pas de déterminer la dose due au rayonnement primaire seul puisqu'il se produit une atténuation et une diffusion des photons dans le « capuchon minimal » Notre but n'étant pas la détermination absolue

du kerma, nous avons neglige cette correction qui consiste en un facteur constant par lequel il faudrait multiplier toutes les valeurs de la fonction de diffusion

Determination du coefficient de diffusion a l'entree d'un milieu equivalent-tissu

Les mesures ont eté effectuees au point de l'axe du faisceau dans le milieu materiel, où l'equilibre electronique de régime serait atteint si seuls, les photons diffuses par des photons primaires contribuaient a la fluence energétique totale des electrons secondaires

En pratique, ce point est situe a la profondeur m égale a 4,3 $g \times cm^{-2}$ et ne correspond pas au point de l'axe du faisceau ou la valeur de la dose absorbee est maximale (maximum) En effet, par suite de la contribution non négligeable des photons diffuses et des electrons secondaires provenant du collimateur et de l'air separant la source de la surface du milieu, le maximum est d'autant plus proche de la surface que les dimensions du faisceau sont plus grandes Il est par exemple situe a 3,5 $g \times cm^{-2}$ pour un faisceau de section 30 cm × 30 cm a 150 cm de la source (MARINELLO & DUTREIX 1973)

Le coefficient de diffusion a l'entree B_0 est defini comme étant la valeur de la dose à la profondeur m, exprimee par rapport a la dose due au rayonnement primaire en ce point, c'est-a-dire pour un champ carre de côte l

$$B_0(l) = \frac{D_p(m\ l) + D_s(m, l)}{D_p(m, l)} \qquad (1)$$

en designant respectivement par D_p et D_s les doses dues au rayonnement primaire et au rayonnement diffuse

Ce coefficient B_0 n'est pas egal a un coefficient de retrodiffusion car les photons diffuses vers l'avant et provenant de points situes a une epaisseur plus faible que m contribuent a la dose

La mesure de la dose due au rayonnement primaire $D_p(m, l)$ est decrite dans le paragraphe precedent

Pour mesurer la dose $D_p(m, l) + D_s(m, l)$ a la profondeur m nous avons place la chambre d'ionisation dans un fantome de milieu equivalent tissu (polystyrène de densite 1,03) en conservant une distance source-chambre egale a 150 cm (Fig 1 c) et nous avons note sa reponse pour une même indication de la chambre moniteur de l accelérateur en fonction des dimensions du faisceau Dans ces conditions, le detecteur enregistre les électrons secondaires mis en mouvement dans le milieu par les photons primaires et les photons diffuses par le milieu a la profondeur m, ainsi que quelques electrons secondaires mis en mouvement par les photons diffuses par le collimateur

En premiere approximation, nous obtenons la valeur du coefficient B_0 en com-

Tableau 2

Variation du coefficient de diffusion à l'entrée d'un milieu équivalent tissu en fonction des dimensions du faisceau

Dimensions du faisceau (cm × cm)	B_0	
	RX de 25 MV*	Cobalt 60**
0	1	1
5 × 5	$1{,}00_4$	$1{,}01_7$
7 × 7	$1{,}00_8$	$1{,}02_3$
10 × 10	$1{,}01_1$	$1{,}03_8$
15 × 15	$1{,}01_3$	$1{,}05_3$
20 × 20	$1{,}01_8$	$1{,}06_1$
25 × 25	$1{,}01_8$	$1{,}07_3$
30 × 30	$1{,}01_9$	$1{,}08_0$
38 × 38	$1{,}02_1$	$1{,}08_3$

* d'après nos mesures

** d'après GUPTA et CUNNINGHAM (1966)

parant la réponse du détecteur entouré du « capuchon minimal » à celle du détecteur placé dans le fantôme

$$B_0 = \frac{\text{réponse du détecteur placé dans le fantôme}}{\text{réponse du détecteur placé dans le « capuchon minimal »}}$$

L'atténuation des photons primaires est en effet la même dans les deux cas et nous pouvons considérer que l'augmentation de la dose enregistrée quand le détecteur est placé dans le milieu est due essentiellement aux photons diffusés dans le milieu. En réalité les photons du faisceau dont l'énergie est comprise entre 0 et 25 MeV donnent certainement naissance à un petit nombre d'électrons secondaires dont le parcours maximal est supérieur à 4,3 $g \times cm^{-2}$, électrons secondaires dont nous ne tenons pas compte dans nos mesures. Nous commettons donc une petite erreur que nous ne pouvons pas évaluer.

Le Tableau 2 montre la variation du coefficient de diffusion à l'entrée B_0 en fonction des dimensions du faisceau pour des rayons X de 25 MV comparée aux valeurs publiées pour les rayons γ du Cobalt 60 (GUPTA & CUNNINGHAM 1966, Brit. J. Radiol. Suppl. No. 11).

Comme nous pouvions nous y attendre, la contribution du rayonnement diffusé à la dose est peu importante à la profondeur m pour ces rayonnements d'énergie élevée puisqu'elle ne dépasse pas 2 % pour un champ de 38 cm × 38 cm.

Détermination de la fonction de diffusion en profondeur

La fonction de diffusion F à la profondeur x, définie comme la dose due au rayonnement diffusé à cette profondeur exprimée par rapport à la dose due au rayonne

du kerma, nous avons neglige cette correction qui consiste en un facteur constant par lequel il faudrait multiplier toutes les valeurs de la fonction de diffusion

Determination du coefficient de diffusion a l'entree d'un milieu equivalent-tissu

Les mesures ont ete effectuees au point de l'axe du faisceau dans le milieu materiel, où l'equilibre électronique de régime serait atteint si seuls, les photons diffuses par des photons primaires contribuaient a la fluence energetique totale des electrons secondaires

En pratique, ce point est situé a la profondeur m égale a 4,3 g × cm^{-2} et ne correspond pas au point de l'axe du faisceau ou la valeur de la dose absorbee est maximale (maximum) En effet, par suite de la contribution non negligeable des photons diffuses et des electrons secondaires provenant du collimateur et de l'air separant la source de la surface du milieu, le maximum est d'autant plus proche de la surface que les dimensions du faisceau sont plus grandes Il est par exemple situé a 3,5 g × cm^{-2} pour un faisceau de section 30 cm × 30 cm a 150 cm de la source (MARINELLO & DUTREIX 1973)

Le coefficient de diffusion à l'entree B_0 est defini comme etant la valeur de la dose à la profondeur m, exprimée par rapport à la dose due au rayonnement primaire en ce point, c'est a dire pour un champ carre de cote l

$$B_0(l) = \frac{D_p(m, l) + D_s(m, l)}{D_p(m, l)} \tag{1}$$

en designant respectivement par D_p et D_s les doses dues au rayonnement primaire et au rayonnement diffuse

Ce coefficient B_0 n est pas égal a un coefficient de rétrodiffusion car les photons diffuses vers l avant et provenant de points situés a une epaisseur plus faible que m contribuent a la dose

La mesure de la dose due au rayonnement primaire $D_p(m, l)$ est decrite dans le paragraphe precedent

Pour mesurer la dose $D_p(m, l) + D_s(m, l)$ à la profondeur m nous avons place la chambre d'ionisation dans un fantome de milieu équivalent-tissu (polystyrene de densite 1,03) en conservant une distance source chambre egale a 150 cm (Fig 1 c) et nous avons note sa reponse pour une meme indication de la chambre moniteur de l accelerateur en fonction des dimensions du faisceau Dans ces conditions, le detecteur enregistre les electrons secondaires mis en mouvement dans le milieu par les photons primaires et les photons diffusés par le milieu a la profondeur m ainsi que quelques électrons secondaires mis en mouvement par les photons diffuses par le collimateur

En premiere approximation, nous obtenons la valeur du coefficient B_0 en com-

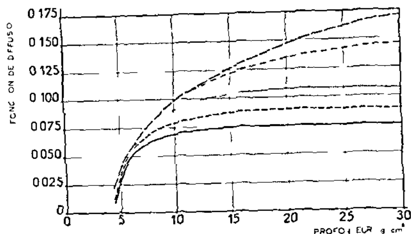


Fig. 3 Variation de la fonction de diffusion F en fonction de la profondeur dans le milieu équivalent tissu et des dimensions du faisceau 5 cm × 5 cm (——) 7 cm × 7 cm (-) 10 cm × 10 cm ( ) 20 cm × 20 cm ( ) et 38 cm × 38 cm (— —)

Tableau 3

Variation de la fonction de diffusion F en fonction des dimensions du faisceau et de la profondeur dans le milieu

Profondeur ($g\ cm^{-2}$)	Fonction de diffusion						
	5 cm × 5 cm	7 cm × 7 cm	10 cm × 10 cm	15 cm × 15 cm	20 cm × 20 cm	30 cm × 30 cm	38 cm × 38 cm
4.3	0.007	0.009	0.012	0.016	0.019	0.024	0.028
5	0.032	0.033	0,033	0.034	0.035	0.038	0.039
6	0.051	0.054	0.055	0.057	0.057	0.058	0.058
7	0.059	0.064	0.067	0.069	0.069	0.069	0.069
8	0.064	0.072	0.077	0.080	0.080	0.080	0.080
9	0.067	0.077	0.085	0.089	0.089	0.089	0.089
10	0.069	0.079	0.091	0.098	0.099	0.099	0.099
12	0.072	0.084	0.099	0.107	0.110	0.111	0.111
14	0.073	0.087	0.103	0.115	0.119	0.120	0.122
16	0.074	0.088	0.105	0.121	0.126	0.129	0.132
18	0.075	0.089	0.107	0.125	0.130	0.136	0.139
20	0.076	0.089	0.108	0.127	0.135	0.142	0.147
22	0.076	0.089	0.108	0.129	0.137	0.146	0.154
24	0.076	0.089	0.108	0.132	0.141	0.151	0.159
26	0.076	0.089	0.108	0.134	0.143	0.156	0.164
28	0.076	0.089	0.108	0.134	0.145	0.158	0.168
30	0.076	0.089	0.108	0.135	0.146	0.160	0.171

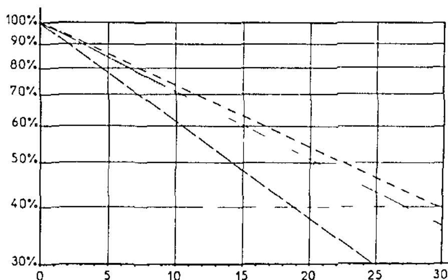


Fig 2 Courbes d'attenuation en « faisceau etroit » des rayons X de 25 MV emis par un accelerateur linéaire de type Sagittaire dans differents matériaux polystyrène (- -), acier (——), laiton ( ) et plomb (-·-)

ment primaire a la profondeur m, permet d'exprimer facilement l'importance de la diffusion dans le milieu

Pour des raisons de simplicite, nous l'avons mesuree sur l'axe du faisceau et nous avons admis qu'elle était valable en tout point du milieu

Pour un champ carre de côte l, elle est égale a

$$F = \frac{D_s(x, l)}{D_p(m, l)} \tag{2}$$

en designant respectivement par $D_s(x, l)$ la dose due au rayonnement diffuse a cette profondeur x et $D_p(m, l)$, la dose due au rayonnement primaire à la profondeur m La distance source chambre est maintenue constante pour éliminer l'influence de la divergence du faisceau

Si nous designons par R(x, l) la valeur de la dose en un point situe a la profondeur x dans le milieu irradie par un faisceau de section carrée de côte l, exprimée par rapport a la dose a la profondeur m

$$R(x, l) = \frac{D_p(x, l) + D_s(x, l)}{D_p(m, l) + D_s(m, l)} \tag{3}$$

et si nous exprimons la dose a la profondeur m en fonction de $B_0(l)$, d'après (1) nous obtenons

$$R(x, l) = \frac{D_p(x, l) + D_s(x, l)}{B_0(l) \; D_p(m, l)} \tag{4}$$

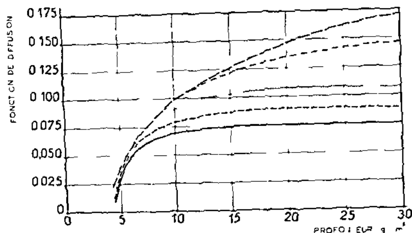


Fig. 3 Variation de la fonction de diffusion F en fonction de la profondeur dans le milieu equivalent tissu et des dimensions du faisceau 5 cm 5 cm (——) 7 cm 7 cm ( ) 10 cm × 10 cm ( ) 20 cm 20 cm ( ) et 38 cm 38 cm (— —)

Tableau 3

Variation de la fonction de diffusion F en fonction des dimensions du faisceau et de la profondeur dans le milieu

Profondeur (g cm ²)	Fonction de diffusion						
	5 cm *5 cm*	7 cm × *7 cm*	10 cm × *10 cm*	15 cm × *15 cm*	20 cm *20 cm*	30 cm *30 cm*	38 cm *38 cm*
4 3	0 007	0 009	0 012	0 016	0 019	0 024	0 028
5	0 032	0 033	0 033	0 034	0 035	0 038	0 039
6	0 051	0 054	0 055	0 057	0,057	0 058	0 058
7	0 059	0 064	0 067	0 069	0 069	0 069	0 069
8	0 064	0 072	0 077	0 080	0 080	0 080	0 080
9	0 067	0 077	0 085	0 089	0 089	0 089	0 089
10	0 069	0 079	0 091	0 098	0 099	0 099	0 099
12	0 072	0 084	0,099	0 107	0 110	0 111	0 111
14	0 073	0 087	0 103	0 115	0 119	0 120	0 122
16	0 074	0 088	0 105	0 121	0,126	0 129	0 132
18	0 075	0 089	0 107	0 125	0 130	0 136	0 139
20	0 076	0 089	0 108	0 127	0 135	0 142	0 147
22	0 076	0 089	0 108	0 129	0 137	0 146	0 154
24	0 076	0 089	0 108	0 132	0 141	0 151	0 159
26	0 076	0 089	0 108	0 134	0 143	0 156	0 164
28	0 076	0 089	0 108	0 134	0 145	0 158	0 168
30	0 076	0 089	0 108	0 135	0 146	0 160	0 171

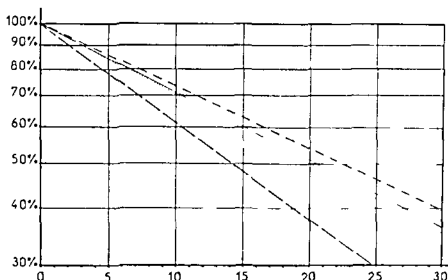


Fig 2 Courbes d'atténuation en « faisceau étroit » des rayons X de 25 MV émis par un accélérateur linéaire de type Sagittaire dans différents matériaux polystyrène (- -), acier (——) laiton ( ) et plomb (---)

ment primaire à la profondeur m, permet d'exprimer facilement l'importance de la diffusion dans le milieu

Pour des raisons de simplicité, nous l'avons mesurée sur l'axe du faisceau et nous avons admis qu'elle était valable en tout point du milieu

Pour un champ carré de coté l, elle est égale à

$$F = \frac{D_s(x, l)}{D_p(m, l)} \tag{2}$$

en désignant respectivement par $D_s(x, l)$ la dose due au rayonnement diffusé à cette profondeur x et $D_p(m, l)$, la dose due au rayonnement primaire à la profondeur m La distance source-chambre est maintenue constante pour éliminer l influence de la divergence du faisceau

Si nous désignons par $R(x, l)$ la valeur de la dose en un point situé à la profondeur x dans le milieu irradié par un faisceau de section carrée de coté l, exprimée par rapport à la dose à la profondeur m

$$R(x, l) = \frac{D_p(x, l) + D_s(x, l)}{D_p(m, l) + D_s(m, l)} \tag{3}$$

et si nous exprimons la dose à la profondeur m en fonction de $B_0(l)$, d après (1) nous obtenons

$$R(x, l) = \frac{D_p(x, l) + D_s(x, l)}{B_0(l) \; D_p(m \; l)} \tag{4}$$

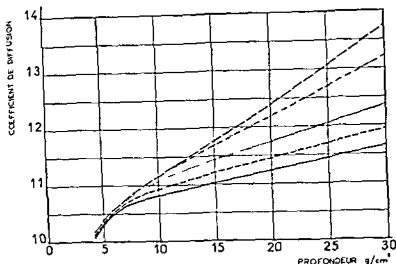


Fig 4 Variation du coefficient de diffusion à la profondeur x B_x en fonction de la profondeur dans le milieu et des dimensions du faisceau 5 cm × 5 cm (——) 7 cm × 7 cm (---), 10 cm × 10 cm ( ) 20 cm × 20 cm (-) et 38 cm × 38 cm (— —)

Les resultats presentes dans ce travail correspondent a des faisceaux de section carree mais peuvent etre etendus a des faisceaux de section rectangulaire ou circulaire Nous avons en effet montre dans une etude precedente (MARINELLO & DUTREIX) que les regles ou les tables d equivalence etablies pour le rayonnement γ du Cobalt 60 (Brit J Radiol 1972) s'appliquaient aussi aux rayons X de 25 MV

Determination du coefficient de diffusion a la profondeur x

Il peut etre interessant dans certains cas d exprimer la dose a la profondeur x en fonction de la dose due au rayonnement primaire a cette profondeur C est la raison pour laquelle on definit B_x coefficient de diffusion a la profondeur x, comme etant egal a

$$B_x = \frac{D_p(x, 1) + D_s(x, 1)}{D_p(x, 1)} \qquad (6)$$

D apres (2) ce coefficient peut encore s exprimer de la maniere suivante

$$B_x \quad 1 + F \quad \frac{D_p(m, 1)}{D_p(x \ 1)} \qquad (7)$$

et donc se calculer a partir de la fonction de diffusion F et du rapport $D_p(x, 1)/D_p(m\ 1)$ lu sur la courbe d attenuation des photons primaires dans le milieu équi valent tissu (Fig 2)

Nos resultats, consignes dans le Tableau 4 et la Fig 4, montrent la variation de ce coefficient B_x avec la section du faisceau et la profondeur du point dans le milieu

Tableau 4

Variation du coefficient de diffusion B_x en fonction des dimensions du faisceau et de la profondeur dans le milieu

Profondeur $g \times cm^{-2}$	Coefficient de diffusion						
	5 cm × 5 cm	7 cm × 7 cm	10 cm × 10 cm	15 cm × 15 cm	20 cm × 20 cm	30 cm × 30 cm	38 cm × 38 cm
4,3	1,007	1,009	1,012	1,016	1,019	1,024	1,028
5	1,033	1,034	1,034	1,035	1,036	1,039	1,040
6	1,054	1,057	1,058	1,060	1,060	1,061	1,061
7	1,064	1,069	1,073	1,075	1,075	1,075	1,075
8	1,071	1,080	1,086	1,089	1,089	1,089	1,089
9	1,077	1,088	1,098	1,102	1,102	1,102	1,103
10	1,082	1,094	1,108	1,116	1,117	1,117	1,118
12	1,091	1,106	1,125	1,135	1,139	1,140	1,140
14	1,098	1,117	1,138	1,154	1,160	1,161	1,164
16	1,106	1,126	1,150	1,173	1,180	1,185	1,189
18	1,115	1,136	1,163	1,191	1,198	1,208	1,212
20	1,123	1,144	1,175	1,205	1,218	1,230	1 238
22	1,131	1,153	1,186	1,222	1,236	1,251	1,265
24	1,139	1,163	1,198	1,242	1,258	1,277	1,291
26	1,148	1,173	1,210	1,261	1,279	1,302	1 320
28	1,157	1,184	1,224	1,278	1,300	1,327	1,348
30	1,167	1,196	1,238	1,298	1,322	1,353	1,377

La fonction de diffusion F peut donc s'exprimer par

$$F = R(x, l) \quad B_0(l) - \frac{D_p(x, l)}{D_p(m, l)} \tag{5}$$

Le terme $D_p(x, l)/D_p(m, l)$ représente l'atténuation du rayonnement primaire entre la profondeur m et la profondeur x et se déduit facilement de la courbe d'attenuation des photons primaires dans le milieu équivalent-tissu (Fig 2) Le terme $B_0(l)$ vient d'être determine expérimentalement (Tableau 2) et il suffit donc de mesurer R(x, l) pour en déduire la valeur de la fonction de diffusion F

Dans ce but, nous avons repris le montage expérimental utilisé pour mesurer la dose a l'entrée du milieu equivalent-tissu (Fig 1 c) et nous avons ajoute des epaisseurs croissantes de polystyrene devant le detecteur Nous en avons déduit la variation de R(x, l) en fonction de la profondeur du point dans le milieu et des dimensions du faisceau au niveau du détecteur

Les valeurs de la fonction de diffusion F ainsi obtenues sont presentees sur la Fig 3 et le Tableau 3 Elles sont assez proches de celles qui avaient eté obtenues théoriquement par DUTREIX (1956) pour des rayons X de 22,5 MV, les écarts observes pouvant être attribués au fait que seuls les photons diffusés du premier ordre avaient été pris en considération dans ses calculs

— DUTREIX A et TUBIANA M Electronic equilibrium and transition stages Phys in Med Biol 10 (1965), 177

GUPTA S K and CUNNINGHAM J R Measurement of tissue air ratios and scatter functions for large field sizes, for Cobalt 60 gamma radiation Brit J Radiol 39 (1966), 7

MARINELLO G et DUTREIX A Etude dosimetrique d un faisceau de rayons X de 25 MV J Radiol Electrol 12 (1973), 951

MEREDITH W J and NEARY G J The production of isodose curves and the calculation of energy absorption from standard depth dose data Brit J Radiol 17 (1944), 75

On sous-estime generalement l'importance de la contribution du rayonnement diffuse a la dose pour les rayonnements de tres haute energie Pourtant cette contribution represente 12 % de la dose due au rayonnement primaire a 20 cm de profondeur pour un champ de 5 cm × 5 cm et 23 % pour un champ de 30 cm × 30 cm La diffusion ne peut donc être négligee dans les calculs de distribution de dose effectués dans les conditions habituelles de la radiotherapie

RÉSUMÉ

Les auteurs ont détermine expérimentalement la fonction de diffusion de rayons X de 25 MV dans un milieu equivalent tissu en fonction des dimensions du faisceau et de la profondeur dans le milieu Au préalable, ils ont effectué une étude de l atténuation du faisceau dans différents matériaux pour le caracteriser Les resultats présentés dans ce travail montrent l importance de la contribution du rayonnement diffuse à la dose pour les rayonnements de très haute énergie

SUMMARY

The diffusion function of 25 MV Roentgen rays in a tissue equivalent material was determined experimentally as a function of the size of the beam and of the depth into the material In order to characterize the beam, the attenuation of the beam in various materials was previously investigated The results of the investigation demonstrate the important contribution of diffused radiation to the dose when using very high energy radiation

ZUSAMMENFASSUNG

Es wurde die Streuungsfunktion von 25 MV Rontgenstrahlen in einem Gewebeaquivalenten Material experimentell als Funktion der Weite des Strahlenbundels und der Tiefe im Material untersucht Um das Strahlenbundel zu charakterisieren, war zuvor die Abschwachung der Strahlen in verschiedenen Materialen untersucht worden Die Ergebnisse der Untersuchung zeigten die Bedeutung des Beitrags gestreuter Strahlung zur Dosis wenn sehr hohe Strahlenenergie verwendet wird

REFERENCES

British Journal of Radiology Suppl II, Londres 1972 Depth dose tables for use in radio therapy

CLARKSON J R A note on depth doses in fields of irregular shapes Brit J Radiol 14 (1941), 265

CUNNINGHAM J R Scatter air ratios Phys in Med Biol 17 (1972) 42

— GUPTA S K and JOHNS H E A computer method for the calculation of isodose curves for wedge fields Brit J Radiol 38 (1965) 637

DUTREIX J Etude de la diffusion des photons émis par un bétatron de 22 5 MeV dans un milieu de dimensions finies et composé d éléments de faible numéro atomique Thèse de Docteur Ingenieur, Faculte des sciences de Paris, 1956

... to the necessity of making the use of units as simple as possible for non specialists,

[illegible]

Explanatory note *The gray is the SI unit of absorbed dose* The gray can also be used with other physical quantities expressed in joules per kilogram provided these quantities belong to the field of ionizing radiation

Thus the SI unit the joule per kilogram when used for ionizing radiation (absorbed dose, kerma, specific energy imparted, etc) is given the name *gray* with the symbol Gy, 1 Gy = 100 rad = 1 J/kg And the SI unit the reciprocal second (one per second) for activity is given the name *becquerel*, symbol *Bq* 1 Bq = 1 s^{-1} ≈ 2.703 × 10^{-11} Ci

Antoine Henri Becquerel (1852–1908) discovered radioactivity in 1896 ('rayons de Becquerel') and was given the Nobel Prize in physics in 1903 together with Marie and Pierre Curie.

Louis Harold Gray (1905–1965) made one of the most fundamental contributions to radiation dosimetry, the principle now known as the Bragg Gray Principle

The ICRU did not recommend to the International Committee of Weights and Measures that a special name be given to the SI unit of exposure to replace the currently used rontgen (R)

The ICRU now recommends that the special units the rad, the rontgen and the curie be gradually abandoned over a period not less than about 10 years and replaced by the SI units the gray (Gy), the coulomb per kilogram (C/kg) and the becquerel (Bq), respectively *It is desirable that preparatory steps be taken as soon as possible by various national and* international bodies in order to facilitate a smooth, safe and efficient transition

In its report, Supplement to ICRU Report 19, Dose Equivalent, (1973) the ICRU published its decision that the physical dimension of the quantity *dose equivalent* should be the same as for absorbed dose From the radiation protection point of view the availability of a proper set of quantities and units in this field is of paramount importance The formulation (for selection) of a suitable unit for dose equivalent is therefore a special problem which will be thoroughly discussed by ICRU

On behalf of the International Commission on Radiation Units and Measurements

H O Wyckoff	*A Allisy*	*K Liden*
Chairman	Vice Chairman	Scientific Secretary Radiation Physics Department *University Hospital* S-221 85 Lund, Sweden

References

LIDÉN K SI units in radiology and radiation measurement *Acta radiol Ther Phys Biol* 12 (1973), 81

— Special radiation units SI units, or both Acta radiol Ther Phys Biol 13 (1974), 95

— SI Units in biomedical dosimetry *In Biomedical dosimetry*, p 451 IAEA, Vienna 1975

INTERNATIONAL COMMISSION ON RADIATION UNITS AND MEASUREMENTS Dose Equivalent, Suppl to Report 19 ICRU, Washington, D C, 1973

THE NEW SPECIAL NAMES OF SI UNITS IN THE FIELD OF IONIZING RADIATION

At the meeting of the International Commission on Radiation Units and Measurements (ICRU) in July 1974, the extensive worldwide response to the previous correspondence on SI units (Lidén 1973, 1974) was discussed in considerable detail. A statement on SI units was then prepared and sent to the International Committee of Weights and Measures, CIPM, for consideration. In this statement the ICRU recommended the adoption of special names for the SI unit the joule per kilogram, J/kg, when applied to absorbed dose and related quantities, and for the SI unit the reciprocal second, s^{-1}, when applied to the quantity activity as a measure of the rate of spontaneous nuclear transformation of radioactive nuclides. The ICRU statement was also discussed at the IAEA symposium on Advances in Biomedical Dosimetry, March 10 to 14, 1975 (Lidén 1975). The CIPM treated the ICRU proposals with expedience and drafted two resolutions for consideration by the 15th General Conference of Weights and Measures, CGPM, at its meeting in May–June 1975. At this meeting, which celebrated the 100 year anniversary of the Meter Convention, the CGPM adopted the following resolutions:

Resolution H 1

The Fifteenth Conférence Générale des Poids et Mesures,

— owing to the urgency, expressed by the International Commission on Radiation Units and Measurements (ICRU) to extend the use of the International System of Units to research work and applications in radiology,

— owing to the necessity of making the use of units as simple as possible for non specialists,

— taking into account the seriousness of the risk of errors in therapy,

Adopts the following special name of SI unit for activity: the becquerel, symbol Bq, equal to the second to the power minus one.

Resolution H 2

The Fifteenth Conférence Générale des Poids et Mesures

— owing to the urgency, expressed by the International Commission on Radiation Units and Measurements (ICRU) to extend the use of the International System of Units to research work and applications in radiology,

— owing to the necessity of making the use of units as simple as possible for non specialists,

the gray, sy[illegible]

Explanatory note The gray is the SI unit of absorbed dose The gray can also be used with other physical quantities expressed in joules per kilogram provided these quantities belong to the field of ionizing radiation

Thus the SI unit the joule per kilogram when used for ionizing radiation (absorbed dose, kerma, specific energy imparted, etc) is given the name *gray* with the symbol *Gy*, 1 Gy = 100 rad = 1 J/kg And the SI unit the reciprocal second (one per second) for activity is given the name *becquerel* symbol *Bq* 1 Bq 1 s^{-1} ≈ 2 703 × 10^{-11} Ci

Antoine Henri Becquerel (1852–1908) discovered radioactivity in 1896 (rayons de Becquerel) and was given the Nobel Prize in physics in 1903 together with Marie and Pierre Curie

Louis Harold Gray (1905–1965) made one of the most fundamental contributions to radiation dosimetry, the principle now known as the Bragg Gray Principle

The ICRU did not recommend to the International Committee of Weights and Measures that a special name be given to the SI unit of exposure to replace the currently used rontgen (R)

The ICRU now recommends that the special units the rad the rontgen and the curie be gradually abandoned over a period not less than about 10 years and replaced by the SI units *the gray (Gy), the coulomb per kilogram (C/kg) and the becquerel (Bq), respectively* It is desirable that preparatory steps be taken as soon as possible by various national and international bodies in order to facilitate a smooth, safe and efficient transition

In its report, Supplement to ICRU Report 19, Dose Equivalent, (1973) the ICRU published its decision that the physical dimension of the quantity *dose equivalent* should be the same as for absorbed dose From the radiation protection point of view the availability of a proper set of quantities and units in this field is of paramount importance The formulation (for selection) of a suitable unit for dose equivalent is therefore a special problem which will be thoroughly discussed by ICRU

On behalf of the International Commission on Radiation Units and Measurements

H O Wyckoff	*A Allisy*	*K Liden*
Chairman	Vice Chairman	Scientific Secretary Radiation Physics Department University Hospital S 221 85 Lund, Sweden

References

LIDÉN K SI units in radiology and radiation measurement Acta radiol Ther Phys Biol 12 (1973) 81

— Special radiation units SI units or both Acta radiol Ther Phys Biol 13 (1974), 95

— SI Units in biomedical dosimetry *In* Biomedical dosimetry, p 451 IAEA, Vienna 1975

INTERNATIONAL COMMISSION ON RADIATION UNITS AND MEASUREMENTS Dose Equivalent, Suppl to Report 19 ICRU Washington, D C , 1973

Books received

We acknowledge with thanks under this heading books received for review, we trust this will be regarded as a sufficient mark of appreciation of the courtesy of the sender Reviews of selected items will appear as soon as an opportunity affords

ADVANCES IN CHEMICAL RADIOSENSITIZATION International Atomic Energy Agency, Vienna 1974

(THE) BIOLOGICAL AND CLINICAL BASIS OF RADIOSENSITIVITY Edited by M Friedman Charles C Thomas, Springfield, Illinois 1974

FRONTIERS OF RADIATION THERAPY AND ONCOLOGY Primary bone cancer The multidiscipline disease Vol 10 Edited by J M Vaeth S Karger AG, Basel 1975

FROST D and JAMMET H Manual on radiation protection in hospitals and general practice Vol 2 Unsealed Sources World Health Organization, Geneva 1975

MAYNEORD W V and CLARKE R H Carcinogenesis and radiation risk A biomathematical reconnaissance British Journal of Radiology, Supplement Number 12 The British Institute of Radiology, London 1975

NEW TECHNIQUES IN TUMOR LOCALIZATION AND RADIO-IMMUNOASSAY Edited by M N Croll L W Brady, T Honda and R J Wallner John Wiley & Sons Ltd , London 1974

NORWOOD W D Health protection of radiation workers Charles C Thomas, Springfield, Illinois 1975

NUCLEAR MEDICINE Edited by H N Wagner H P Publishing Co , Inc New York 1975

NUCLEAR MEDICINE IN CLINICAL PEDIATRICS Edited by H Handmaker and J M Lowenstein The Society of Nuclear Medicine Publishing Sciences Group Inc Acton Mass 1975

POPULATION DOSE EVALUATION AND STANDARDS FOR MAN AND HIS ENVIRONMENT International Atomic Energy Agency Vienna 1974

SELF-ASSESSMENT OF CURRENT KNOWLEDGE IN THERAPEUTIC RADIOLOGY Edited by N B Hornback Medical Examination Publishing Company, New York 1975

SMITH E E Radiation Science at the National Physical Laboratory 1912–1955 National Physical Laboratory, Her Majesty s Stationary Office, London 1975

(A) STUDY GUIDE IN NUCLEAR MEDICINE Edited by F Ashkar A Miale and W Smoak Charles C Thomas Springfield Illinois 1975

Subject index to Volume 14 — THERAPY PHYSICS BIOLOGY

Radiation therapy

Chemotherapy

Radioactive isotopes

Radiation physics

Technique

Radiation biology

Radiation protection

List of Authors

List of Supplements to Acta Radiologica

Nos 173-346

(Issued December 1975)

For Suppl Nos 1-172 inclusive, see list issued December 1960, in Vol 54, fasc 6

The supplements are published from time to time and are not included in the subscription rate. Prices and year of publication of numbers already issued are detailed below

173 ERIK ODEBLAD, BJÖRN WESTIN and SVEN ERIK ENGLUND Disappearance measurements Theoretical, technical biological and medical aspects 1959 *Price Sw Kr 30*

174 LARS BILLING and ERIK SEVERIN Slipping epiphysis of the hip A roentgenological and clinical study based on a new roentgen technique 1959 *Price Sw Kr 35*

175 ÅKE HANNGREN Studies on the distribution and fate of C^{14}- and T-labelled p-aminosalicylic acid (PAS) in the body 1959 *Price Sw Kr 25*

176 LARS BJORK Cineradiographic studies on the Fallopian tubes in rabbits 1959 *Price Sw Kr 25*

177 PEKKA VUORINEN The roentgenographic slit methods A survey and analysis of procedures based on the use of a narrow bundle of roentgen rays (scanography) 1959 *Price Sw Kr 25*

178 BENGT H O ROSENGREN Determination of cell mass by direct X-ray absorption 1959 *Price Sw Kr 25*

179 S HULTBERG, O DAHL, R THORAEUS, K J VIKTERLOF and R WALSTAM *Kilocurie* cobalt 60 therapy at the Radiumhemmet Equipment technique and dose measurements 1959 *Price Sw Kr 35*

180 BENGT LILJA Motor activity of the stomach 1959 *Price Sw Kr 25*

181 PER AMUNDSEN The diagnostic value of conventional radiological examination of the heart in adults (Appendix by R G CARPENTER An account of the statistical analysis of the relative heart volumes of 755 patients in various disease groups) 1959 *Price Sw Kr 20*

182 H M TRUBY Acoustico-cineradiographic analysis considerations with especial reference to certain consonantal complexes 1959 *Price Sw Kr 35*

183 ERIK BOIJSEN Angiographic studies of the anatomy of single and multiple renal arteries. 1959 *Price Sw Kr 30*

184 GUSTAF NOTTER A technique for destruction of the hypophysis using Y^{90} spheres A radiologic, endocrine and histologic study 1959 *Price Sw Kr 35*

185 BENGT LILIEQUIST The subarachnoid cisterns An anatomic and roentgenologic study 1959 *Price Sw Kr 35*

186 BENGT LILIEQUIST Pontine angle tumour Encephalographic appearances 1959 *Price Sw Kr 30*

187 HOLGER SKÖLDBORN On the design, physical properties and practical application of small condenser ionization chambers 1959 *Price Sw Kr 30*

188 JENS NIELSEN Anno Actatis Suae LX Papers dedicated to Jens Nielsen, professor of radiotherapy at the University of Copenhagen, on his sixtieth anniversary December 19, 1959 *Price Sw Kr 40*

189 OLOV DAHL and KARL JOHAN VIKTERLOF Attainment and value of precision in deep radiotherapy Some fundamentals with special reference to moving beam therapy with 200 to 250 kV roentgen rays and cobalt 60 gamma radiation 1960 *Price Sw Kr 35*

214 BENGT TJERNBERG Lymphography An animal study on the diagnosis of V×2 carcinoma and inflammation 1962 *Price Sw Kr 35*

215 PAAVO KLAMI Periarthrosis calcarea of the shoulder joint Its differentiation from other stiff and painful shoulders 1962 *Price Sw Kr 30*

216 P EDHOLM, I FERNSTROM K LINDBLOM and S I SELDINGER Roentgen television in practice with special regard to puncture examinations 1962 *Price Sw Kr 35*

217 FOLKE EDSMYR Carcinoma of the vulva An analysis of 560 patients with histologically verified squamous cell carcinoma 1962 *Price Sw Kr 30*

218 P SOILA M GRÖNROOS O KAUPPILA und L PYYKÖNEN Wasserlosliche, viskosierte wasserlosliche und jodolige Kontrastmittel in der Hysterosalpingographie Vergleichende Untersuchungen 1962 *Price Sw Kr 25*

219 STIG SANDMARK Hiatal incompetence Studies on mechanics and principles of examination for hiatus hernia and gastro-oesophageal reflux 1963 *Price Sw Kr 25*

220 MAX LUNDBERG Free movements in the temporomandibular joint A cineradiographic study 1963 *Price Sw Kr 30*

221 ÅKE NORHAGEN Selective angiography of the hepatic veins Experimental investigations of basal circulatory dynamics 1963 *Price Sw Kr 35*

222 ERLING HAMMER JACOBSEN Genetically significant radiation doses in diagnostic radiology 1963 *Price Sw Kr 35*

223 ASTRID BROHULT Alkoxyglycerols and their use in radiation treatment An experimental and clinical study 1963 *Price Sw Kr 30*

224 CARL OLOF OVENFORS Pulmonary interstitial emphysema—An experimental roentgen diagnostic study 1964 *Price Sw Kr 35*

225 GEORG THEANDER Variation in shape of gallbladder during cholecystography 1964 *Price Sw Kr 30*

226 HUGO BOGREN The composition and structure of human gallstones 1964 *Price Sw Kr 30*

227 LARS NORDQVIST The sagittal diameter of the spinal cord and subarachnoid space in different age groups—A roentgenographic post mortem study 1964 *Price Sw Kr 25*

228 LENNART WICTORIN Bone resorption in cases with complete upper denture — A quantitative roentgenographic photogrammetric study 1964 *Price Sw Kr 30*

229 ARNFINN ENGESET Irradiation of lymph nodes and vessels—Experiments in rats with reference to cancer therapy 1964 *Price Sw Kr 30*

230 LARS HOLLENDER Determining the elements of the interior orientation in roentgenography 1964 *Price Sw Kr 30*

231 HANS HENRIK HOLM The hydrodynamics of micturition—Examination by means of micro manometer and uroflowmeter of the hydrodynamic conditions in normal subjects and in patients suffering from obstruction in the posterior part of the urethra 1964 *Price Sw Kr 30*

232 EBBE CEDERQUIST Clinical application of whole body counting of ^{85}Sr and ^{47}Ca in patients with and without widespread malignant skeletal disease 1964 *Price Sw Kr 30*

233 SVEN PAULIN Coronary angiography—A technical anatomic and clinical study 1964 *Price Sw Kr 40*

234 TROELS MUNKNER The influence of para aminosalicylic acid on the I^{131} metabolism 1965 *Price Sw Kr 30*

235 ANDERS LUNDERQUIST Angiography in carcinoma of the pancreas 1965 *Price Sw Kr 35*

236 RUNE WALSTAM Studies on therapeutic short-distance and intracavitary gamma beam techniques—Physical considerations with special reference to radiation protection 1965 (Out of print)

261 Kai Setälä, Björn Lindroos and Otto Nyyssönen Cancer chemotherapy studies *cytoplasmic barrier in malignant epidermal cells against the effect of colchicine*—An [illegible] 1966 *Price Sw Kr 25*

263 [illegible]

264 [illegible] and bacteriological follow up study on a pediatric series and on animals with [illegible] pneumonia 1967 *Price Sw Kr 30*

265 Kai Setälä, Otto Nyyssönen and Björn Lindroos Ultrastructural changes in benign and malignant epidermal states in mice after topical beta radiation 1967 *Price Sw Kr 30*

266 Göran Nylander Vascular response to vasopressin as reflected in angiography—An experimental study in the dog. 1967 *Price Sw Kr 35*

267 Johan Folin Angiography in renal tumours—Its value in diagnosis and differential diagnosis as a complement to conventional methods 1967 *Price Sw Kr 35*

268 Eero Tala Carcinoma of the lung—A retrospective study with special reference to pre diagnosis period and roentgenographic signs 1967 *Price Sw Kr 35*

269 Carl O Henrikson Iodine 125 as a radiation source for odontological roentgenology 1967 *Price Sw Kr 35*

270 Cations in intravascular contrast media and development of specific metrizoate formulas — Pharmacologic and clinical studies Proc Symposia at Copenhagen, November 1964, and Sandefjord, September 1966 1967 *Price Sw Kr 40*

271 Erna Tarkiainen Intracostal vein meningorachidography—A technical, anatomic and clinical study 1967 *Price Sw Kr 35*

272 Allan Lunderquist Arterial segmental supply of the liver—An angiographic study 1967 *Price Sw Kr 35*

273 Kai Setälä, Max Sickala, Otto Nyyssönen and Erna Tarkiainen Quantitative three-dimensional scintillography of the stomach with technetium (^{99m}Tc) 1967 *Price Sw Kr 30*

274 Per Bergsjö Radiation induced early changes in size and vascularity of cervical carcinoma—A colpophotographic and clinical study 1968 *Price Sw Kr 35*

275 Sune Ericson The parotid gland in subjects with and without rheumatoid arthritis 1968 *Price Sw Kr 40*

276 Rolf Jensen Anterior teeth relationship and speech—Studies using cineradiography synchronized with speech recording. 1968 *Price Sw Kr 35*

277 Sven Ahlbäck Osteoarthrosis of the knee—A radiographic investigation 1968 *Price Sw Kr 35*

278 Irene Sjögren Kjell Bergström and Herman Lodin Echoencephalography in infants and children Comparison with cerebral pneumography in measuring ventricular size 1968 *Price Sw Kr 35*

279 Bertil Jarplid Radiation induced asymmetry and lymphoma of thymus in mice 1968 *Price Sw Kr 35*

280 Erkki M Laasonen Information transmission in roentgen diagnostic chains—Experimental and clinical studies 1968 *Price Sw Kr 35*

281 Rasmus Stenström Arthrography of the knee joint in children—Roentgenologic anatomy diagnosis and the use of multiple discriminant analysis 1968 *Price Sw Kr 35*

282 Karl Karlstedt Carcinoma of the uterine corpus—Factors bearing on the curability 1968 *Price Sw Kr 35*

283 Leo Stjernvall Pharmacodynamic response of epidermal hyperplasias to topical vinblastine treatment 1968 *Price Sw Kr 35*

309 LAURI PATOMAKI A mathematical model for radiation fields of telecobalt treatment units—With special reference to the isodoses of Rocus 1971 *Price Sw Kr 35*

310 RADIOBIOLOGIC INVESTIGATIONS Edited by Erik Lindgren and Bernhard Tribukait 1971 *Price Sw Kr 45*

311 HALVOR VERMUND Enhancement of radiation effects by chemotherapy 1971 *Price Sw Kr 35*

312 PERTTI KASKI Osteomedullography of the tibia 1971 *Price Sw Kr 40*

313 PROCEEDINGS OF THE SIXTH CONFERENCE OF THE NORDIC ASSOCIATION OF CLINICAL PHYSICS held in Århus Denmark 1970 Edited by C B Madsen and K Liden 1972 *Price Sw Kr 45*

314 BIRGER HELIN Heart volume in human kidney transplantation 1972 *Price Sw Kr 25*

315 UNO WEGELIUS Angiography of the hand Clinical and postmortem investigations 1972 *Price Sw Kr 35*

316 P E S PALMER Haemangiosarcoma of Kaposi 1972 *Price Sw Kr 35*

317 JUHANI RAUSTE Lymphographic findings in granulomatous inflammations and connective tissue diseases—Differential diagnosis between these diseases and lymphomas 1972 *Price Sw Kr 30*

318 OVE MATTSSON Formation of the tomographic image—With special reference to blurring 1972 *Price Sw Kr 35*

319 PROGRESS IN VETERINARY RADIOLOGY Proceedings of the 2nd International Conference of Veterinary Radiologists held in Stockholm 1970 Edited by Sten Erik Olsson 1972 *Price Sw Kr 45*

320 TJAKKO KUIPERS Carcinoma of the uterine cervix Aspects of clinical oncology in patients referred for radiation therapy 1972 *Price Sw Kr 50*

321 BO LUNDSTROM Angiographic abnormalities following percutaneous needle biopsy of the kidney 1972 *Price Sw Kr 40*

322 LARS BLOMQUIST Mode of accumulation of iodophenylalanines in the exocrine pancreas and certain tumours 1972 *Price Sw Kr 40*

323 INGER BROLIN Radiologic reporting 1973 *Price Sw Kr 40*

324 TIMO TELARANTA The role of host tissue in skin carcinogenesis—An investigation with skin tumor resistant and skin tumor susceptible mice 1973 *Price Sw Kr 35*

325 NILS GUNNAR LINDQUIST Accumulation of drugs on melanin 1973 *Price Sw Kr 40*

326 JOHN ERIK JOHNSSON Hysterography and diagnostic curettage in carcinoma of the uterine body 1973 *Price Sw Kr 40*

327 ERIC BERGQUIST Tentorial notch and adjacent major vessels in carotid angiography 1973 *Price Sw Kr 45*

328 O HASSLER and S O HILTALA Angiographic abnormalities in the urinary bladder wall after irradiation Part I Animal experiments Part II Clinical investigation 1973 *Price Sw Kr 45*

329 OLOF ECKERDAL Tomography of the temporomandibular joint—Correlation between tomographic image and histologic sections in a three dimensional system 1973 *Price Sw Kr 40*

330 JORMA RANTANEN Radiation injury of connective tissue—A biochemical investigation with experimental granuloma 1973 *Price Sw Kr 40*

331 FRANZ PAUL PROBST Congenital defects of the corpus callosum—Morphology and encephalographic appearances 1973 *Price Sw Kr 50*

332 GUDRUN ALM CARLSSON Dosimetry at interfaces—Theoretical analysis and measurements by means of thermoluminescent LiF 1973 *Price Sw Kr 40*

333 MATTI VALLE Postoperative coronary angiography 1973 *Price Sw Kr 40*

334 I JOELSSON A SANDRI and H L KOTTMEIER Carcinoma of the uterine corpus—A retrospective survey of individualized therapy 1973 *Price Sw Kr 40*

335 METRIZAMIDE A NON IONIC WATER SOLUBLE CONTRAST MEDIUM—Experimental and preliminary clinical investigations 1973 *Price Sw Kr 50*

336 SVEN SCHELLER and LARS MÅRTENSON Traumatic dislocation of the patella A radiographic investigation 1974 *Price Sw Kr 50*

337 OSSI KORHOLA Myocardial scintigraphy and estimation of regional blood flow with xenon 133 1974 *Price Sw Kr 40*

338 KURT ÅSTRAND and SVEN REICHMANN Optimised tomography Theoretical and practical analyses of the elimination of depiction errors in tomography 1974 *Price Sw Kr 40*

339 ILKKA SURAMO Lymphography in tuberculosis 1974 *Price Sw Kr 40*

340 EEVA NORDMAN ^{75}Se sodium selenite scintigraphy in diagnosis of tumours 1974 *Price Sw Kr 45*

341 ILPO LAUTEALA Pelvimetry with image intensifier camera A low radiation dose method *1974 Price Sw Kr 50*

342 ANDERS MOLLER Pneumography in paraventricular and intraventricular tumours of the posterior fossa 1974 *Price Sw Kr 60*

343 HÅKAN JORULF Roentgen diagnosis of intraperitoneal fluid A physical, anatomic and clinical investigation *1975 Price Sw Kr 55*

344 Skeletal development, growth rate and hip dysplasia Experimental investigations with special reference to the effect of estrogens, growth hormone and nutrition Edited by Sten Erik Olsson 1975 *Price Sw Kr 70*

345 HANS KUISK and FAIZ M KHAN Nominal standard dose and tumor standard dose Tables for radiation therapy planning and analysis 1975 *Price Sw Kr 65*

346 Computer tomography of brain lesions Edited by Erik Lindgren 1975 *Price Sw Kr 73*